

Graduate Schools Yearbook **2014**



Editors:

Kim Dam-Johansen

Peter Szabo

Aliff H. A. Razak

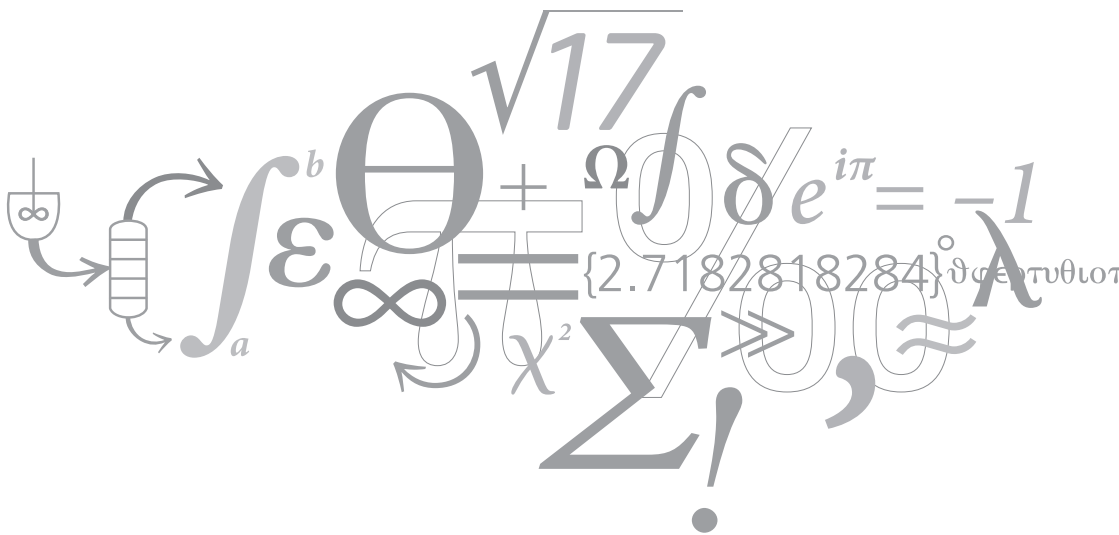
Graduate Schools Yearbook **2014**

Editors:

Kim Dam-Johansen

Peter Szabo

Aliff H. ARazak



Address: Department of Chemical and Biochemical Engineering
Søltofts Plads, Building 229
Technical University of Denmark
DK-2800 Kgs. Lyngby
Denmark

Telephone: +45 4525 2800
Fax: +45 4588 2258
E-mail: kt@kt.dtu.dk
Internet: www.kt.dtu.dk

Print: J&R Frydenberg A/S
København
January 2015

Cover: Troels Glismann

Cover photo: Christian Ove Carlsson

ISBN-13: 978-87-93054-51-6

Preface

In this Graduate Schools Yearbook 2014, the PhD students of DTU Chemical and Biochemical Engineering present their research projects. Some of the students have only just initiated their research, whereas others are close to concluding their work and present their most significant results. We hope that you will find the Yearbook interesting, and we invite you to contact us in case you would like to know more about the projects or topics described in the following pages.

The PhD projects in this Yearbook cover all areas in which our Department is active including areas in product design, process design and production in the chemical, biotechnological, pharmaceutical, food technology and energy technology industry.

This year, we have managed to consolidate our level of activity at the Department, meaning that we have kept our total number of PhD students significantly higher than 100.

In 2015, we will still focus on increasing the number of PhD students shared with enterprises and research partners around the world. In this connection, we are increasing our activities in China with a new PhD agreement with the Institute of Process Engineering (IPE) at the Chinese Academy of Sciences.

We wish you a pleasant reading.

Yours Sincerely

Kim Dam-Johansen
Professor, Head of Department

Peter Szabo & Aliff H. ARazak
Editors

Contents

A

Improving dielectric permittivity by incorporating PDMS-PEG multi block copolymer into PDMS network <i>A Razak, Aliff H.</i>	1
Process Considerations for Systems Biocatalysis <i>Abu, Rohana</i>	3
Modeling of gas-solid cyclones <i>Ahli-Gharamaleki, Mohammad</i>	5
Modeling of Enhanced Oil Recovery by Low Salinity Waterflooding <i>Alexeev, Artem</i>	7
Predictive Modeling of Gas Diffusion and Solubility in Polymers for Offshore Pipelines <i>Almeida, Susana</i>	9
Generic Model-Based Tailor-Made Design and Analysis of Biphasic Reaction Systems <i>Anantpinijwatna, Amata</i>	13
New Catalysts for Hydrodeoxygenation of Biomass Pyrolysis Oil <i>Arndal, Trine Marie Hartmann</i>	15
Modeling of Asphaltene System with Association Model <i>Arya, Alay</i>	17
Interconnected fluidized bed technology <i>Azizaddini, Seyednezamaddin</i>	19
B	
Modelling, Synthesis and Analysis of Biorefinery Networks <i>Bertran, Maria-Ona</i>	21
Operation and Design of Diabatic Processes <i>Bisgaard, Thomas</i>	23
CO ₂ -Hydrates - Challenges and Possibilities <i>Bjørner, Martin Gamel</i>	25
Plant-wide modelling and control for nitrous oxide emissions from wastewater treatment plants <i>Boiocchi, Riccardo</i>	29
Fermentation processes at small scale <i>Bolic, Andrijana</i>	31

An Optimization Based Framework for Design and Retrofit of Municipal Wastewater Treatment Plants: Case study on side-stream nitrogen removal technologies <i>Bozkurt, Hande</i>	35
Partitioning between Heterotrophic and Autotrophic Forest Respiration by Means of Stable Isotopes <i>Brændholt, Andreas</i>	37
C	
Design of Hydrophilic Polymers for Activated non-Fouling Coatings <i>Camos Noguer, Albert</i>	39
Continuous Crystallization and Filtration of Active Pharmaceutical Ingredients and Intermediates for Pharmaceutical Production <i>Capellades Méndez, Gerard</i>	41
Microscopic simulation of wettability alteration during smart water flooding on chalk reservoirs <i>Chakravarty, Krishna Hara</i>	43
Synthesis and design of integrated-intensified chemical/biochemical processes <i>Cheali, Peam</i>	45
Computer-aided Mixture and Blend Design <i>Cignitti, Stefano</i>	47
Consistent thermodynamic properties of lipids systems <i>Cunico, Larissa Peixoto</i>	49
D	
Development of Highly Efficient Solid Oxide Electrolyzer Cell Systems <i>Duhn, Jakob Dragsbæk</i>	51
F	
Characterization of Microbial Consortia for Keratin Degradation Processes <i>Falco, Francesco Cristino</i>	53
Systematic Methods and Tools for Computer Aided Modelling <i>Fedorova, Marina</i>	55
Micro Scale Reactor System Development with Integrated Advanced Sensor Technology <i>Fernandes, Ana Carolina Oliveira</i>	57
Risk Associated With the Decompression of High Pressure High Temperature (HP/HT) Fluids - Study on Pure Liquid Water <i>Figuerola Murcia, Diana Carolina</i>	59
Sustainable Process Design with Process Intensification <i>Frauzem, Rebecca</i>	61

Computer-aided molecular design and property prediction models for working fluids of thermodynamic cycles <i>Frutiger, Jérôme</i>	63
G	
Investigation of oxygen-blown biomass gasification <i>Gadsbøll, Rasmus Østergaard</i>	65
Sustainable design of Biorefinery Systems for Biorenewables <i>Gargalo, Carina Lira</i>	67
A Dynamic Mathematical Model for Packed Columns in Carbon Capture Plants <i>Gaspar, Jozsef</i>	69
Enzyme enhanced carbon dioxide absorption <i>Gladis, Arne</i>	71
Optical Spectroscopy for Gas Analysis in Biomass Gasification <i>Grosch, Helge</i>	73
Evaluating Enzymatically Assisted CO ₂ Removal from Flue-Gas with Carbonic Anhydrase <i>Gundersen Deslauriers, Maria</i>	75
H	
Investigation of <i>Aspergillus niger</i> aggregation behavior and its relationship to industrial fermentation <i>Hagemann, Timo</i>	77
Microbial Enhanced Oil Recovery for North Sea Oil Reservoir <i>Halim, Amalia Yunita</i>	79
A Simultaneous Approach for Synthesis and Design of Process and Water Networks <i>Handani, Zainatul Bahiyah</i>	83
Deposition Build-Up in Grate and Suspension Boilers Firing Biomass <i>Hansen, Stine Broholm</i>	85
Development of New Automotive Diesel Oxidation and NH ₃ Slip Catalysts <i>Hansen, Thomas Klint</i>	87
Combustion Characterization of Bio-derived Fuels and Additives <i>Hashemi, Hamid</i>	89
Dispersion of Carbon Nanotubes in Polydimethylsiloxane and the Influence on the Mechanical and Electrical Properties <i>Hassouneh, Suzan Sager</i>	93
A miniaturized experimental platform for development of recovery processes <i>Heintz, Søren</i>	95

Relaxation Mechanism Study of Polymer Blends by Rheological Experiments <i>Hengeller, Ludovica</i>	99
Modification of polymer surfaces to enhance enzyme activity and stability <i>Hoffmann, Christian</i>	101
J	
Biomass Burners for Biodust Combustion <i>Johansen, Joakim Myung</i>	103
K	
VPPD Lab – A Computer Aided Tool for Product-Process Design <i>Kalaku, Sawitree</i>	105
Sustainability Assessment of Integrated Food & Bioenergy Systems in Ghana <i>Kamp, Andreas</i>	107
Controlled Release from PMMA Microcapsules Triggered by Gamma Irradiation <i>Kostrzewska, Malgorzata</i>	111
L	
Modeling Mass Transfer in Small Scale Reactors using Computational Fluid Dynamics <i>Larsson, Hilde</i>	113
Biorefining of Wheat Straw: Distribution of mineral element deposits in pretreated biomass <i>Le, Duy Michael</i>	115
Catalytic Materials for Combined Particulate and NO _x Removal from Diesel Vehicles <i>Linde, Kasper</i>	117
Fuel Efficiency and Fouling Control Coatings in Maritime Transport <i>Lindholdt, Asger</i>	119
Hemp Fibers: Enzymatic Effect of Microbial Processing on Fiber Bundle Structure <i>Liu, Ming</i>	121
Bioprocess Engineering for the Application of P450s <i>Lundemo, Marie Therese</i>	125
M	
Design, Control and Analysis of Intensified Processes <i>Mansouri, Seyed Soheil</i>	127
Reactive Separation Technology: Biomimetic Enzyme Immobilization on Polymeric Membrane <i>Marpani, Fauziah</i>	131

Novel encapsulation technique for incorporation of high permittivity fillers into silicone elastomers <i>Mazurek, Piotr Stanislaw</i>	133
Novel Strategies for Control of Fermentation Processes <i>Mears, Lisa</i>	135
Enzymatic Hydrolysis of Xylan Integrated With Membrane Technology: Free Enzyme System <i>Mohd Sueb, Mohd Shafiq</i>	137
Acid and Abrasive Resistant Coatings for the Heavy Duty Industry <i>Møller, Victor Buhl</i>	139
N	
Ash Chemistry in Circulating Fluidized Bed <i>Narayan, Vikas</i>	141
Synthesis of novel biobased binders for alkyd paint systems <i>Nguyen, Hiep</i>	144
Robustness of Phytase Catalysis for Improved Iron Bioavailability <i>Nielsen, Anne Veller Friis</i>	147
Liquid Fuel Production from Lignin Solvolysis by 2-Propanol <i>Nielsen, Joachim Bachmann</i>	149
Agglomeration in Dual-Fluidized Bed Gasification <i>Nordby, Mads Willemoes</i>	151
Mixing and oxygen transfer processes in bioreactors <i>Nørregaard, Anders</i>	153
O	
Deactivation of Selective Catalytic Reduction Catalysts in Biomass Fired Power Plants <i>Olsen, Brian Kjærgaard</i>	155
P	
Modeling and Synthesis of Pharmaceutical Processes: Moving from batch to continuous manufacturing <i>Papadakis, Emmanouil</i>	157
Inhibition of Gas Hydrate Formation by Antifreeze Proteins <i>Perfeldt, Christine Malmos</i>	159
Model of Stickiness in Spray Drying <i>Petersen, Thomas</i>	161

Q

Morphology, Rheology and Mass Transfer in Fermentation Processes
Quintanilla, Daniela 163

R

Selective and Efficient Synthesis of Ethanol from Dimethyl Ether and Syngas
Rasmussen, Dominik Bjørn 165

μ -Tools for Development of ω -Transaminase Processes
Ringborg, Rolf Hoffmeyer 169

Shape optimization of a microreactor for biocatalytic synthesis of optically pure chiral amines
Rosinha, Inés Pereira 171

S

Biochar Fraction Needed on Willow Gasification to Be a Carbon Neutral Bioenergy: Offsetting Direct and Indirect Land Use Changes
Saez de Bikuña, Koldo 175

Development of the Electrolyte Cubic-Plus-Association Equation of State
Schlaikjer, Anders 177

Modelling of Gasification of Biomass in Dual Fluidized Beds
Seerup, Rasmus 181

Bioprocess Evaluation Tools
Seita, Catarina Sanches 183

Development of advanced mathematical data interpretation methods for application in microbioreactors
Semenova, Daria 185

The influence of hydrogen bonding on nonlinear extensional rheology of supramolecular poly(n-butyl acrylate)
Shabbir, Aamir 187

Practical Application of Models in the Urban Water System: Simulation Based Scenario Analysis
Snip, Laura Johanna P. 189

T

Low Temperature Thermal Gasification of marginal biomass and waste resources – coproduction of energy and fertilizer
Thomsen, Tobias 193

Biooxidation – Reactor and Process Design
Toftgaard Pedersen, Ashbjørn 195

Novel Clay/Nanocellulose Biocomposite Films and Coatings in the Context of New Packaging Materials <i>Trifol Guzman, Jon</i>	197
Single Biomass Particle Combustion and Fuel Characterization <i>Trubetskaya, Anna</i>	199
Process synthesis and design using process group contribution methodology <i>Tula, Anjan Kumar</i>	203
An experimental and theoretical study of CO ₂ hydrate formation systems <i>Tzirakis, Fragkiskos</i>	205
W	
On the Correlation Between Youngs Modulus and Melt Flow in Fiber Spinning Operations <i>Wingstrand, Sara Lindeblad</i>	209
Z	
The electrical breakdown strength of prestretched elastomers with and without sample volume conservation <i>Zakaria, Shamsul</i>	211
Fast Pyrolysis of Lignin and Direct Upgrading of the Pyrolysis Vapor via H-ZSM-5 <i>Zhou, Guofeng</i>	213
Å	
Modeling the Automotive SCR system <i>Åberg, Andreas</i>	215



Aliff Hisyam A Razak

Phone: +45 4525 6819

E-mail: ahis@kt.dtu.dk

Supervisors: Anne Ladegaard Skov
Peter Szabo

PhD Study

Started: December 2013

To be completed: November 2016

Improving dielectric permittivity by incorporating PDMS-PEG multi block copolymer into PDMS network

Abstract

Polydimethylsiloxanes (PDMS) are well-known to cause hydrophobic surfaces due to their low surface energy as well as they possess low permittivity and low conductivity. On the other hand, polyethyleneglycols (PEG) behaves hydrophilic and is a highly permittivity and conductive polymer. Combination of both polymers as a block copolymer depicts a possibility for substantial improvement of properties such as high permittivity and non-conductivity – if carefully designed. The objective is to synthesize PDMS-PEG multi block copolymer assembling into different morphologies such as lamellar, cylinder, gyroid and spheres based on variation of volume fractions of PDMS and PEG. Different volume fractions of PDMS and PEG introduce different properties in terms of contact angles, dielectric permittivity and rheological behaviour. All morphologies of PDMS-PEG block copolymer in this study exhibit high storage permittivity but at the same time the loss permittivity is high. By incorporating conductive PDMS-PEG block copolymer into commercial PDMS elastomer from Wacker Chemie (MJK), the storage permittivity is significantly enhanced by 60% with 20% of PDMS-PEG block copolymer incorporated in the PDMS network.

Introduction

A novel dielectric electroactive polymer (DEAP) material which is often associated with high storage and low loss permittivity has been extensively studied [1]. As one of the promising dielectric elastomer, silicone elastomers such as polydimethylsiloxane (PDMS) exhibit low permittivity, but show large actuation strain due to the inherent softness [2]. On the contrary, polyethyleneglycol (PEG) possess high permittivity, but is not capable of actuating. Combining both polymers as a block copolymer depicts a possibility for substantial improvement of properties such as high permittivity and non-conductivity.

In principal, block copolymers assemble into different morphologies such as spheres, cylinder, gyroid and lamellar [3]. Different morphologies can be obtained by altering the volume fraction of the constituents in the block copolymer, for instance varying the number average molecular weight (\bar{M}_n) of 'A' polymer in 'AB' diblock copolymer as depicted in figure 1. On the other hand, morphologies for triblock copolymer are more complex and up to 30 different morphologies can be obtained [4]. Thus, we can predict that the morphologies for multiblock copolymer would increase the level of complexity with phases depending on the degree of polymerization, number of distinct polymers in the block copolymer, temperature and the sequence of distinct

polymers [4, 5]. Matsushita et.al have reported that for lamellar morphology of styrene (S)-isoprene (I) block copolymer (SI)_n, domain spacing is reduced as number of repeating units (*n*) is increased [6]. The aim is to have the morphologies such as sphere so that the conductive polymer (PEG) will be in the discontinuous phase which will lead to an interruption of current flow from one side of the film to the other.

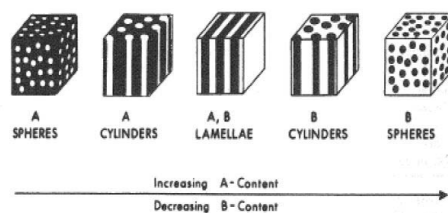


Figure 1: Different morphologies obtained when varying the volume fraction of one constituent in a diblock copolymer [3].

The applied synthesis of PDMS-PEG multi block copolymer is based on hydrosilylation reaction occurring at specific temperature with presence of platinum (II) complex catalyst as depicted in figure 2.

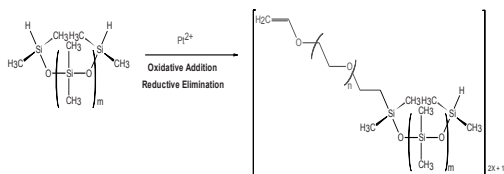


Figure 2: Hydrosilylation reaction of PDMS-PEG multi block copolymer with presence of platinum II catalyst.

Results and Discussion

Asymmetrical morphologies in PDMS-PEG multi block copolymer were investigated by varying chain lengths of PDMS while sustaining the equivalent chain length of PEG (250 g/mol). In order to obtain varying volume fractions the chain lengths of PDMS chains were varied. The chain lengths were 3, 7, 14 and 81 repeating units for SiH, H03 and H11 and H21 respectively. Figure 3 shows that the loss permittivity for all PDMS-PEG multi block copolymer is higher than the storage permittivity causing the loss factors are extremely high compared to the standard where the aim is to be as low as possible below 1 so that these materials are able to store energy in terms of charge separation. None of the morphologies obtained from these PDMS-PEG multi block copolymer caused a discontinuous phase for PEG such that a non-conductive nature of the developed elastomers was obtained.

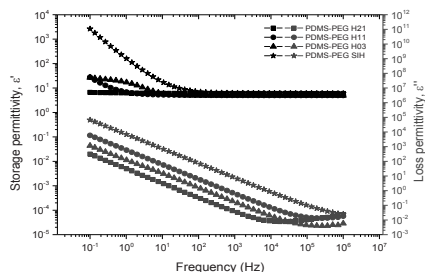


Figure 3: Storage and loss permittivity for all PDMS-PEG block copolymer.

Therefore the PDMS-PEG block copolymer was further diluted with commercial PDMS elastomer (MJK) in a binary polymer blend, the storage permittivity of the matrix is expected to increase. Among the results of PDMS-PEG block copolymer blended with MJK, the polymer blend with PDMS-PEG (H03) depicts the most promising result with low loss permittivity. The plots in figure 4 show that the addition of conductive PDMS-PEG (H03) block copolymer significantly increases the storage permittivity of the silicone elastomer (3.5) to 5.2 for 20 wt% PDMS-PEG (H03) while maintaining a loss permittivity below 0.6. This shows that the obtained morphology holds a continuous phase for PDMS and discontinuous phase for conductive PDMS-PEG block copolymer. In terms of conductivity, there is no sign of plateau region at lower frequencies in a conductivity

versus frequency plot as shown in figure 5 and this supports the conclusion above.

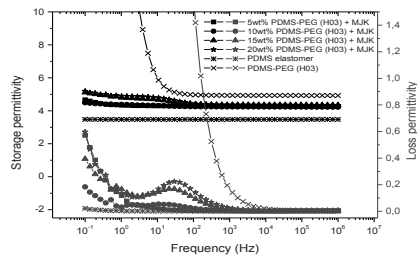


Figure 4: Storage and loss permittivity for 5 to 20 wt% of PDMS-PEG (H03) block copolymer blended in PDMS network.

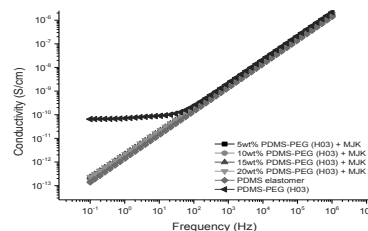


Figure 5: Conductivity for 5 to 20 wt% of PDMS-PEG (H03) block copolymer blended in PDMS network.

Conclusion

Incorporating 20 wt% of conductive PDMS-PEG block copolymer (\bar{M}_n of 550 g/mol) in to a silicone elastomer increases the storage permittivity up to 60% compared to commercial PDMS elastomer. While this polymer blend behaves as amphiphilic, the viscoelastic properties are maintained and enhanced permittivity and low loss permittivity and conductivity are obtained.

References

- Madsen FB, Dimitrov I, Daugaard AE, Hvilsted S, Skov AL (2013) Novel cross-linkers for PDMS networks for controlled and well distributed grafting of functionalities by click chemistry. *Polym Chem* 4:1700
- Brochu P, Pei Q (2010) Advances in dielectric elastomers for actuators and artificial muscles. *Macromol Rapid Commun* 31:10-36
- Khandpurj AK, Farster S, Bates FS, Hamley IW, Ryan AJ (1995) Diblock Copolymer Phase Diagram near the Order-Disorder Transition. *Macromolecules* 28:8796-8806
- Zheng W, Wang ZG (1995) Morphology of ABC triblock copolymers. *Macromolecules* 28:7215-7223
- Mai Y, Eisenberg A (2012) Self-assembly of block copolymers. *Chem Soc Rev* 41:5969-85
- Matsushita Y, Mogit Y, Mukai H, Watanabe J (1994) Preparation and morphology of multiblock copolymers of the (AB)_n type. *Polymer (Guildf)* 35:246-249



Rohana Abu
Phone: +45 4525 2926
E-mail: roha@kt.dtu.dk

Supervisors: John M. Woodley
Krist V. Gernaey

PhD Study
Started: October 2013
To be completed: September 2016

Process Considerations for Systems Biocatalysis

Abstract

“Systems Biocatalysis” is a concept for constructing multi-enzyme processes *in vitro* for the synthesis of chemical products. Each constructed artificial metabolism is controlled in an efficient way in order to achieve a sufficiently favourable conversion for the target product. However, biocatalytic processes are thermodynamically and kinetically controlled reactions and often have low productivity compared to the chemical processes under the conditions necessary for industrial operation. Thus, it is necessary to evaluate the potential for each multi-enzyme system in order to identify its feasibility, so that the concept can be successfully applied. To date, numerous promising multi-enzyme cascades have been reported in scientific literature and will continue to increase in the future as a useful approach for industrial practice in many different applications. The objective of this work is to build models for evaluation of multi-enzyme cascades and to develop a systematic framework for assisting process decision making in process development of such systems.

Introduction

Numerous scientific papers have been published on the role of multi-enzyme cascades in the synthesis of chemicals, from fine chemical products to pharmaceutical drugs. The study of multi-enzyme cascades is expected to increase in the future as a useful approach for many different types of applications, including in biofuel and biomedical processing. Enzymes work efficiently under mild reaction conditions and often a low concentration of reactants are required to selectively catalyse reactions. However, these conditions are far from the conditions necessary in industrial chemical processes, thus a lower product yield is frequently achieved which limits the applicability of biocatalytic reactions.

Currently, a concept of “Systems Biocatalysis” for constructing multi-enzyme cascades *in vitro* for the synthesis of chemical products has been introduced¹. The objective is to control the constructed artificial metabolism efficiently in order to achieve a sufficiently favourable conversion for the valuable product. This concept leads to a design of the additional toolbox for biocatalytic transformations that consists of multi-enzyme cascade, for instance, a self-sufficient redox cascade that capable to regenerate nicotinamide cofactors *in situ* as shown in Fig. 1. Such cascade is beneficial for industrial practice, as the use of cofactors is generally expensive and the use of external source of

an hydride from glucose or formate is eliminated.

Multi-enzyme cascades as illustrated in Fig. 1 are principally controlled by thermodynamic and kinetic of the whole system. The primary enzyme often has thermodynamic uphill, such as ω -transaminase (EC.2.6.1.X) as in Fig. 1(a). The equilibrium yield can be improved by coupling with the energetically favourable reactions (energy-releasing reactions such as, alanine dehydrogenase-catalysed reaction, EC1.4.1.1) that is successfully achieved >99% conversion^{2,3}. If the reaction is thermodynamically improved, further study of enzyme kinetic in cascades will be useful and significant for control strategies⁴. Therefore, there is a need to evaluate the feasibility of multi-enzyme cascade, so that the concept of “systems biocatalysis” can be successfully applied on an industrial scale.

Process considerations

Systems Biocatalysis – In order to design multi-enzyme cascades, there is a need to identify the raw materials/functional group of the starting substrates. This can be done by determining the interaction matrix that shows the relationship among the components involved in the cascades. This is also important to avoid the crossover interaction/inhibition among components for enabling continuous high efficiency. It is also required to identify the enzyme selectivity towards its substrate as to ensure the enzymes act at their optimal

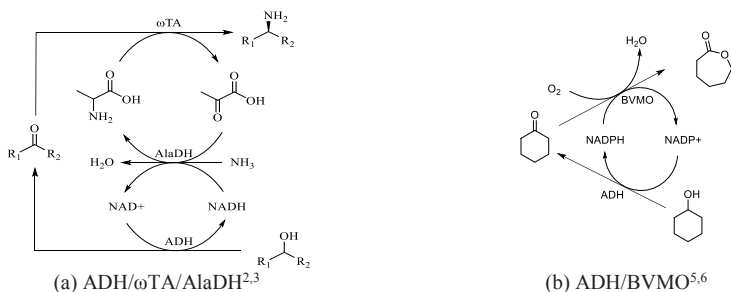


Figure 1: Enzymatic toolbox of self-sufficient redox cascades. (a) ADH/ ω -TA/AlaDH coupled system and (b) ADH/BVMO. ADH: alcohol dehydrogenase, ω -TA: ω -transaminase, AlaDH: alanine dehydrogenase, BVMO: Baeyer-Villiger monoxygenases.

activities. The novel biocatalytic modules have been currently established where each constructed module consists of cascades, allowing the use of different raw material as the starting substrate. These modules can run on its own based on the substrate availability, showing the flexibility concept of systems biocatalysis⁷.

Thermodynamic study – In order to design systems biocatalysis efficiently, the thermodynamic properties such as the Gibbs free energy and equilibrium constant are required for each biocatalytic reaction so that the favourability of the reaction and the maximum theoretical yield of the cascades can be determined. The most common tools that are available for obtaining thermodynamic properties are the group contribution (GC) method and *ab initio* quantum mechanics (QM) method. To date, Jankowski-GC method⁸ (the updated version from Mavrovouniotis⁹) is used to estimate the Gibbs free energy for biotransformation. In QM method, the total energy of reaction could be calculated based on the optimal energy of molecular structure of the components involved¹⁰. The commercial QM software is available to quickly estimate the thermodynamic properties, such as the Spartan¹⁴. However, unclear definition of the standard state condition for biocatalytic reactions significantly increases error in calculating equilibrium data using the tools. Jankowski-GC method refers the apparent equilibrium constant as concentration-based rather than activity-based equilibrium constant, considering the aqueous phase at 298.15 K. QM method uses the standard state of gas-phase (298.15 K, 1 atm) to estimate the total energy of a reaction. As an alternative, the mathematical modelling might be a useful tool to evaluate thermodynamic data for specific case studies.

Kinetic study – a mathematical model of multi-enzyme cascades is constructed based on the kinetic mechanism of individual enzymes¹¹. The important parameters to perform such calculation are:

- Michealis-Menten kinetics (k_m , V_{max})
- substrate/product inhibition (k_i)
- biocatalyst activity (turnover frequency, $1/k_{cat}$)

- biocatalyst stability (deactivation rate constant, k_d)

In most cases, Michaelis–Menten parameters vary in the literature reports, due to different types of host organisms and experimental conditions (temperature, pH, ionic strength, buffer, and etc.). Thus, mathematical modelling often developed based on specific case studies and the robustness of the models is still questionable especially for multi-enzyme cascades. However, mechanistic modelling is still a good tool to understand the behaviour of enzymatic reaction, especially in the multi-enzyme cascades as the interaction between enzyme and components are of importance.

References

1. Servi, S.; Wohlgenuth, R.; Fessner, W. D. http://www.cost.eu/domains_actions/cmst/Actions/CM1303 (accessed Aug 26, 2014).
2. Tauber, K.; Fuchs, M.; Sattler, J. H.; Pitzer, J.; Pressnitz, D.; Koszelewski, D.; Faber, K.; Pfeffer, J.; Haas, T.; Kroutil, W. *Chemistry* 2013, 19, 4030–4035.
3. Sattler, J. H.; Fuchs, M.; Tauber, K.; Mutti, F. G.; Faber, K.; Pfeffer, J.; Haas, T.; Kroutil, W. *Angew. Chem. Int. Ed. Engl.* 2012, 51, 9156–9159.
4. Xue, R.; Woodley, J. M. *Bioresour. Technol.* 2012, 115, 183–195.
5. Staudt, S.; Bornscheuer, U. T.; Menyes, U.; Hummel, W.; Gröger, H. *Enzyme Microb. Technol.* 2013, 53, 288–292.
6. Mallin, H.; Wulf, H.; Bornscheuer, U. T. *Enzyme Microb. Technol.* 2013, 53, 283–287.
7. Sattler, J. H.; Fuchs, M.; Mutti, F. G.; Grischek, B.; Engel, P.; Pfeffer, J.; Woodley, J. M.; Kroutil, W. *Angew. Chemie* 2014, 126, 1–6.
8. Jankowski, M. D.; Henry, C. S.; Broadbelt, L. J.; Hatzimanikatis, V. *Biophys. J.* 2008, 95, 1487–1499.
9. Mavrovouniotis, M. L. *J. Biol. Chem.* 1991, 266, 14440–14445.
10. Hehre, W. J. *A Guide to Molecular Mechanics and Quantum Chemical Calculations*; Wavefunction, Inc.: Irvine, California, 2003.
11. Santacoloma, P. A.; Sin, G.; Gernaey, K. V.; Woodley, J. M. *Org. Process Res. Dev.* 2011, 15, 203–212.



Mohammad Ahli-Gharamaleki
Phone: +45 4525 2952
E-mail: moag@kt.dtu.dk
Discipline: CHEC research Center

Supervisors: Kim Dam-Johansen
Weigang Lin

PhD Study
Started: December 2013
To be completed: December 2016

Modeling of gas-solid cyclones

Abstract

Gas-solid cyclones are well known due to their various applications in the industries for separation of solid particles from gas stream. In addition, cyclones also have the ability to be applied as a reactor for reactions with short reaction time that can enhance the conversion of the reactants for different applications. This project focuses on Computational Particle Fluid Dynamics (CPFD) modelling of cyclone reactor gas solid systems to obtain a new understanding of particle behavior inside the reactor, and study on the coupling of fluid dynamics and chemical reactions. The developed model will be validated with pilot scale experiments for flow patterns and performance parameters.

Introduction

Gas-solid cyclones are widely applied in various industries for separation of solid particles from gas stream, through vortex flow. In cyclone separators, a strong swirling turbulent flow is formed to separate phases with different densities applying rotational effects and gravity. As in many confined swirling flow systems, the hydrodynamics in a cyclone can be of a complex nature. Flow reversal, quasi-periodic fluctuations and strongly anisotropic turbulence are some of the characteristics.

Examples for application of cyclones are preheaters in cement industry, catalyst recovery from the reacting gases in Fluid Catalytic Cracking (FCC) and removing particles from gas streams in power industry for particulate emission control. The latter application has important environmental impact, since particulate emission regulations are getting stricter as high-concentrations of fine particles in the atmosphere form a serious threat to human health. Cyclones are energy efficient and low-maintenance separation devices and contribute in a very economical manner to reduction of the particulate emission [1].

Some investigations have been carried out on describing fine particles moving with a carrier gas inside the cyclones. However, less study was focused on considering a cyclone as a gas-solid reactor.

The potential applications of this type of reactor have been considered to various chemical reactions such

as reduction of iron, coal pyrolysis, combustion, gasification and fluid catalytic cracking [2]–[6].

When used as a gas-solid reactor, this type of device can enhance the conversion of the reactants by increasing the residence time of the solid reactants due to swirling motion. With this approach, residence time distribution (RTD) of solid particles becomes a challenging parameter. Calculation of the performance parameters of cyclone reactors needs generally accurate information on the flow pattern, the heat/mass transfer and kinetics of the chemical reactions occurring in the process.

The lack of fundamental understanding of the fluid dynamics and chemical reactions for cyclone reactors is due to the fact that the fluid dynamics within a cyclone is complex. Moreover, inclusion of parameters, such as residence time, particle-particle collision, particle size distribution and particle concentrations, as well as other relevant physical properties, add further complexities to the conservation equations. Computational fluid dynamics (CFD) simulations of the fluid and particle flows in cyclones provides an effective tool for understanding on the details of the flow and reaction within the cyclones [7]. However, the system to be used for the simulations is very complicated and the computation is time consuming even with powerful computers. To reach a reasonable computational time, system needs to be simplified. One of the solutions is to consider a balance between fluid dynamics and chemical reaction in simplified model. The latter is a

core point of this study to provide reliable results for better understanding and knowledge on design, scale up and optimization.

The main aim of this project is to map the relative importance of fluid dynamics and chemical reactions in different high temperature gas-solid processes with involvement of flow pattern, transport phenomena and chemical reactions and to propose a methodology for process simplification. The methodology may be applied to the systems such as mineral processing or biomass conversion.

Objectives

The specific objectives of this project are:

- To improve the understanding of gas-solid fluid dynamics and reaction kinetics within a cyclone through a comprehensive literature review
- Application of CPFD model to simulate the flow pattern in a gas-solid cyclone
- Experimental calibration and validation of the CPFD model
- Optimization of high dust loading cyclone and possible applications of a cyclone to solid fuel conversion process

Methodology

Different modelling studies have been performed on the common gas-solid reactors by basic fluid dynamics and detailed reaction schemes, resulting in an unnecessary complexity for understanding of the main mechanisms. To avoid unnecessary complexity of gas- solid reactors, and also access more reliable models, a balance between fluid dynamics and chemical reaction is important. This issue is apparently of a critical importance for cyclone reactors as well. CPFD is an approach to simplify design and analysis when both fluid dynamic and chemical reactions are involved with relatively high solid concentrations.

Residence time of particles in cyclones is short, lower than a few seconds. Also, heat transfer efficiency between carrier gas and solid particles is high. Consequently, it can be anticipated that cyclones would be well suited for carrying out fast reactions of solid particles requiring high heat fluxes.

It is essential to know particle behavior inside reactor in order to predict the relationship of fluid dynamics and chemical reactions on the particle behavior.

Therefore, the first step of this project is to model the solid and gas flow pattern in cyclone on cold mode to obtain the basic knowledge of gas and particle flows inside the reactor without considering any reaction. The model will be calibrated and validated by experimental studies.

The experimental set up used in the study will consider all the practical and theoretical demands. Special efforts have been done to provide sufficient measurements for obtaining the system parameters.

Based on the validated model and the flow patterns, the reaction model will be implemented for a high temperature system with mass and heat transfer taken into consideration.

The developed model would then be used to predict the performance parameters of the cyclone reactors, such as pressure drop, efficiency, temperature profile and conversion, with respect to variations in system properties (such as solid loading, cyclone geometry, inlet gas velocity, and gas/solid inlet temperature and particle size)

Acknowledgements:

The author acknowledges the financial support from Department of Chemical and Biochemical Engineering, Technical University of Denmark.

References

1. A. C. Hoffmann and L. E. Stein, *Gas Cyclones and Swirl Tubes*, Second Edi. Berlin Heidelberg, New York: Springer, 2008.
2. J. Lede, F. Verzaro, and B. Antoine, "Flash Pyrolysis of Wood in a Cyclone Reactor," pp. 309–317, 1986.
3. J. Lede, H. Z. Li, F. Soullignac, and J. Villermaux, "Measurement of Solid Particle Residence Time in a Cyclone Reactor: A Comparison of Four Methods," vol. 22, pp. 215–222, 1987.
4. S. K. Kang, T. W. Kwon, and S. D. Kim, "Hydrodynamic characteristics of cyclone reactors," *Powder Technol.*, vol. 58, no. 3, pp. 211–220, Jul. 1989.
5. S. Luidold, H. Antrekowitsch, and R. Ressel, "Production of niobium powder by magnesiothermic reduction of niobium oxides in a cyclone reactor," *Int. J. Refract. Met. Hard Mater.*, vol. 25, no. 5–6, pp. 423–432, Sep. 2007.
6. G. Manenti and M. Masi, "Simulation study of production of fine ceramic powders in a cyclone reactor," *Chem. Eng. Process. Process Intensif.*, vol. 50, no. 2, pp. 151–159, Feb. 2011.
7. V. V. Ranade, *Computational Flow Modeling for Chemical Reactor Engineering*. California: ACADEMIC PRESS, 2002.



Artem Alexeev
 Phone: +45 4525 2886
 E-mail: arta@kt.dtu.dk
 Discipline: AT CERE

Supervisors: Alexander Shapiro
 Kaj Thomsen

PhD Study
 Started: September 2012
 To be completed: August 2015

Modeling of Enhanced Oil Recovery by Low Salinity Waterflooding

Abstract

Low salinity waterflooding is one of the modern applied enhanced oil recovery (EOR) techniques. The process involves a number of physico-chemical fluid-rock interactions which in a complex manner depend on the external conditions and component composition of brine and are not very well understood. In this paper we describe the mathematical model based on the wettability alteration mechanism caused by ion exchange. The model is applied to simulate the process of low salinity waterflooding; results obtained match qualitatively laboratory observations.

Introduction

EOR by means of low salinity waterflooding, has been experimentally proved in a great number of laboratory tests by different research groups. Some of the well tests performed confirm the laboratory observations. The interest in low salinity waterflooding has been growing during the past decade; as a result a number of mechanisms were proposed to explain the physico-chemical mechanisms behind the effect [1]. However, none of the mechanisms have been generally accepted. Only a minor part of the papers addresses the numerical modeling of low salinity waterflooding [2,3]. The modeling approach is based on a widely agreed mechanism that injection of low salinity water results in the wettability alteration of the rock surface from oil-wet to water-wet conditions.

Physic-Chemical Model

In this paper we focus on the effect of low salinity flooding in sandstone rocks. It is required, according to accumulated knowledge, that the sandstone rock contains clays and oil contains polar components. Importance of clay is explained by its high specific surface. Under reservoir conditions clays surfaces bear negative charge and strongly interact with the ions in the brine. The presence of the clays may result in two different mechanisms to benefit the. The first possibility is that exposure of the rock to the brine with low salinity results in clays swelling with a subsequent mobilization of fines. Another mechanism is that ionic composition on the clay surface can significantly affect its wettability. EOR by means of low salinity waterflooding has been proven for the rocks that don't

allow migration of fines. Thus we concentrate on the second possible mechanism in order to understand the chemical interactions involved.

The wettability of the surface is altered due to a ion exchange process, which occurs on the surface of the clay and can be viewed as substitution of one type of particles by another bearing the same overall charge. The overall amount of equivalents that can be held by the clay is called the cation exchange capacity (CEC). The reaction of cation exchange is represented by:



where $>X$ is used to denote adsorbed ions. The substitution of monovalent cations by divalent cations is expected on the exposure of clay surface to low salinity brines [4], this process is to reduce the concentration of divalent cations below their concentration in the injected brine. This was observed in laboratory experiments [5] and also correlated with the increase in recovery which allowed to assume that concentration of divalent cations on the surface controls the wettability of clays and thus can be used as an interpolation variable for the parameters governing the two-phase flow.

The equilibrium concentrations in the bulk c_i and on the surface σ_i are related by means of mass action law:

$$K_{eq} = \frac{c_{Na}^2 \sigma_{Ca}}{\sigma_{Na}^2 c_{Ca}} \quad (2)$$

$$2\sigma_{Ca} + \sigma_{Na} = CEC \quad (3)$$

The re-equilibration can be relatively slow, which may require introducing kinetics of the ion exchange.

Mathematical Model

The governing system of equations consists of material balance equations for brine and chemical species presented:

$$\partial_t(\phi s) + \partial_x f(s, \sigma_j) = 0, \quad (4)$$

$$\partial_t(\phi s c_i + \sigma_i) + \partial_x (f(s, \sigma_j) c_i) = 0, \quad (5)$$

where ϕ is porosity, s is saturation and $f(s, \sigma_j)$ is the fractional flow function determined by the relative permeability curves. Generally Corey-type relative are used, that include 6 parameters. Given the two sets for high salinity (HS) and low salinity (LS) the values of the parameters for intermediate salinities can be calculated using the surface concentrations as interpolation variable as discussed above:

$$s_{or} = H(\sigma_j) s_{or}^{HS} + (1 - H(\sigma_j)) s_{or}^{LS}, \quad (6)$$

where s_{or} is the residual oil saturation and $H(\sigma_j)$ is the interpolating function; the rest parameters are interpolated in the same manner.

Numerical Model

In order to gain high accuracy we implemented primitive-variable-based MUSCL-Hancock scheme used to solve the hyperbolic part of the flow equations [6]. This approach allows constructing high-resolution schemes in the presence of shocks characteristic for the hyperbolic problems.

Results and Discussion

We present the results of simulation of secondary recovery by means of low salinity waterflooding. The primary recover, - injection of 3 pore volumes (PV) of formation water (FW), is followed by the injection of low salinity water (LSW) for 3 more PV. The residual oil saturation changes from 0.4 for FW to 0.2 for LSW.

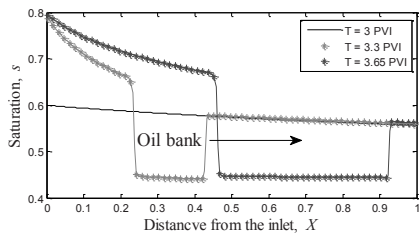


Figure 1: Saturation profiles after injection of 3 PV of FW (black), continued with injection of LSW for 0.3 PV (red) and 0.65 PV (blue).

Fig. 1 illustrates the saturation profiles. After 1 PVI most of the mobile oil has been displaced resulting in slow increase in recovery with time. It can be seen from Fig. 1 that the injection of low salinity brine leads to formation of the oil bank, which is gradually displaced. At around 3.7 PVI the oil bank reaches the effluent resulting in increase of oil production. Analysis of the effluent on the Fig. 2 shows that arrival of the oil bank

coincides with the production of brine with significantly lowered Ca^{2+} concentrations.

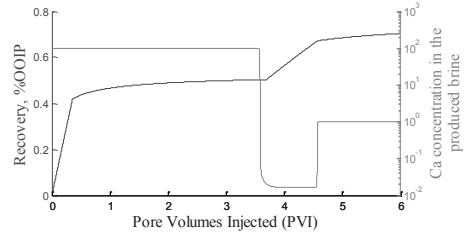


Figure 2: Accumulated recovery (blue) and Ca concentration in the produced brine normalized by the Ca^{2+} concentration in the injected LSW (red)

It may seem that low Ca^{2+} zone is responsible for the low salinity effect, however it is not the case: main effect comes from the low salinity water itself.

Even though the model was claimed to be able to match accurately the laboratory observations, it has a number of weak sides. Firstly, it does not explain the mechanism by which divalent cations change the wettability of the surface. Secondly, it does not require a specific model for oil, and cannot explain why presence of polar components is required for EOR process.

Recently a more complex analysis has been proposed to describe chemical equilibrium of ions in the brine and polar oil components on the surface of the clay [7]. Polar components in oil can be attached to the surface directly or through formation of complexes with divalent cations. Incorporating this chemical model into numerical simulation will allow covering the questions that were put forward above. However question of the model applicability remains opened.

Acknowledgements

This PhD study is part of the Smart Water project which is funded by industrial partners: DONG Energy and Mærsk, the Danish EUDP under the Danish Energy Agency and by the Danish research councils.

References

1. T. Austad, A. RezaeiDoust, T. Puntervold, SPE 129767 (2010).
2. V. Omekeh, S. Evje, H. A. Friis, Int. J. Numer. Anal. Model., 4(2) (2012), 95-128
3. C. T. Q. Dang, Q. P. Nguyen, Z. J. Chen, L. X. Nghiem, SPE 166447 (2013).
4. J. Appelo, D. Postma. Geochemistry, groundwater and pollution. CRC Press, 2005.
5. S. Pieterse, M. B. Pingo-Almada, Van M. Haasterecht, H. van der Linde, N. Brussee, F. Marcellis, SPE 165180 (2013).
6. P. Brady, J. Krumhansl, SPE 153744 (2013).
7. D.E. van Odyck, S. Lovett, F. Monmont, N. Nikiforakis, R. Soc. Lond. Proc. Ser. A Math. Phys. Eng. Sci., (2012)

**Susana Almeida**

Phone: +45 4525 2863
E-mail: susal@kt.dtu.dk
Discipline: AT-CERE

Supervisors: Nicolas von Solms
Georgios Kontogeorgis
Adam Rubin, NOV Flexibles
Christian Wang, NOV Flexibles
Jacob Sonne, NOV Flexibles

PhD Study

Started: December 2013
To be completed: November 2016

Predictive Modeling of Gas Diffusion and Solubility in Polymers for Offshore Pipelines

Abstract

The transport of carbon dioxide (CO₂) between the capture and storage point is matter of great importance for the oil and gas industry, although it is not as often debated. National Oilwell Varco (NOV) manufactures flexible pipelines for offshore transport of fluids in deep water conditions. Flexible pipelines are a good alternative to fixed installations, mainly because of the advantages of easier storage and transport, lower operating costs, simpler maintenance and higher chemical and mechanical resistance [1]. A flexible pipeline consists of several layers, where the so-called inner polymer liner provides the barrier to the egress of the gas being transported. Inside the pipeline the gas is often transported at extreme conditions of temperature and pressure, for a gas often well beyond supercritical.

Introduction

Flexible pipes are used as a key component in the oil and gas industry, especially for offshore applications. The design of a flexible pipeline consists of different layers of material, most of them metallic. But there are two types of polymeric materials of crucial importance, the first located at the outer-shell of the pipe which has the main function of protecting from sea water corrosion the inner metallic surfaces; the second polymeric layer is in permanent contact with the transported fluid and therefore reinforces from the inner side the isolation of the metal layers. Moreover, this polymeric inner layer needs to have special mechanical and chemical properties compatible with the transported fluid to avoid leakages and guarantee high safety levels. Due to its critical importance to effective transport, the inner polymer is the main object of this study. Inside the pipeline the gases are transported at high temperature and pressure, well above supercritical [2]. The critical properties of CO₂ are: $T_c = 30.98$ °C and $P_c = 73.77$ bar [3]. There are two main issues regarding the contact of supercritical fluids with polymers: a swelling phenomenon of the polymer of variable extension depending of the type of polymer used, which could lead to rupture of the pipeline; and the gradual degradation of the polymer that can lead to a loss of some key barrier properties of the polymer.

The study and optimization of the transport properties of supercritical fluids in these pipeline systems is an experimental challenge that requires the acquisition of some thermodynamics and transport properties, such as solubility and permeability. This can be achieved using equipment, such as a Magnetic Suspension Balance (MSB) and a 2-D permeation cell for measuring the solubility and the permeability, respectively. These properties are dependent on pressure, temperature, and composition of the gas, but also on the interactions with the chain group in the polymer. Also, a particular matter to take into account is the change of the polymers physical properties during the transport at extreme conditions, such as the density, diffusivity, swollen volume and even the free volume of the polymers [2].

Transport Phenomena

The phenomena of gas transport through a polymer can be decomposed into 5 steps, which can be summarized as follows:

- Diffusion through the limit layer on the side corresponding to the higher partial pressure (upstream side);
- Absorption of the gas (mainly due to chemical affinity or solubility) in the polymer;
- Diffusion of the gas inside the membrane polymer;

- Desorption of the gas at the side of lower partial pressure;
- Diffusion through the limit layer of the downstream side [4].

The transport phenomena can be grouped into three transport coefficients: diffusion, solubility, and permeability, where the permeability coefficient is obtained by multiplying the other two coefficients.

Another important factor for gas transport in polymers to be taken into account is the crystallinity. The crystallinity fraction of polymer is attributed to the region where the molecules are well arranged, in a regular order. If in one hand the sorption and diffusion phenomena take place in the amorphous regions, on the other hand the crystalline regions act as barriers for diffusion and are not included in the sorption process. However, the existence of crystalline regions seems to not influence the sorption mode in the amorphous regions [2].

Temperature dependence

A common approach in the literature is to use an Arrhenius equation as a descriptor of the temperature influence in the different coefficients. For example, for permeability the equation should be:

$$Pe = Pe_0 \exp\left(\frac{-E_p}{RT}\right) \quad (1)$$

Where Pe_0 represents the limit value of permeability for the infinite molecular agitation ($T \rightarrow \infty$), E_p is the apparent activation energy of permeation, T is the absolute temperature and R is the universal gas constant. Through a linearization of Eq. 1 is possible to obtain the unknown variables using the slope and the ordinate from the trendline of the experimental data [4]-[7]

Specific Objectives

The purpose of this study is:

1. Experimental measurements of solubility and permeability of pure CO₂ and its mixture with methane (90/10) in different types of polymers – PVDF, XLPE and PA11 - up to 110 °C and pressures up to 650 bar;
2. Modelling the above properties based on the equation of state sPC-SAFT. It is an objective the inclusion of the volumetric properties of the polymer (such as polymer swelling) in the model.

Measurements and Modeling of Solubility

The MSB can be simply described as a balance that enables the weighing of the samples in almost all environments at controlled temperature and pressure conditions. The operational conditions can go up to 350 bar and 200 °C. The sample is placed in a sample container which is connected to a permanent magnet. Under the balance there is an electromagnet that attracts the magnet whenever there is an electric current passing through it. Thus, it is possible to find the mass of the

polymer with the absorbed gas. The density of the gas at the current pressure and temperature conditions is acquired by MSB and after a buoyancy correction the solubility coefficient is obtained. A scheme of the set-up is represented in Figure 1.

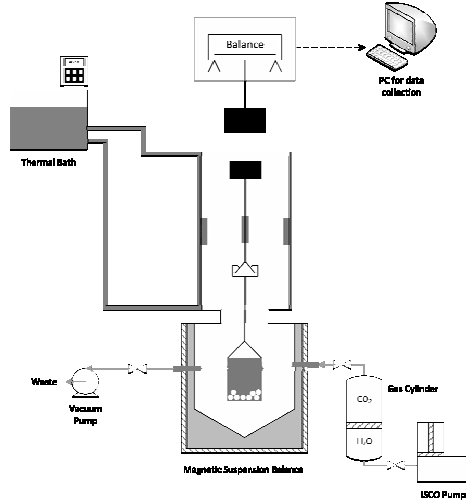


Figure 1: Schematic diagram of the MSB set-up.

The most versatile and successful models for predicting and correlating the thermodynamic properties (solubility and swelling) of gas/polymer mixtures, especially at elevated pressures, are equations of state [8]. In particular, the equation of state sPC-SAFT, suitable for polymers and developed at DTU [9] has been successfully applied to these and other similar systems— see Figures 2 and 3.

As a main conclusion, it was observed that the solubility is higher while increasing pressure and temperature parameters, for both polymers.

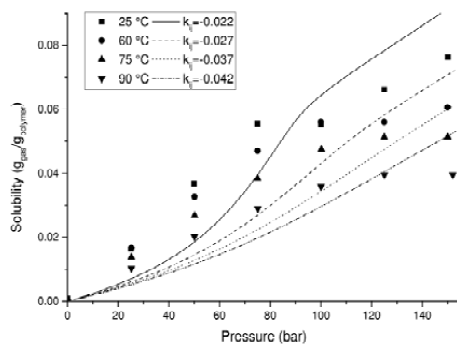


Figure 2: sPC-SAFT correlations for CO₂ solubility in PVDF at 45, 60, 75 and 90 °C. The crystallinity of the polymer used in the model prediction was estimated to

be 45%. The binary interaction parameter needs to be temperature dependent in order to capture the experimental data.

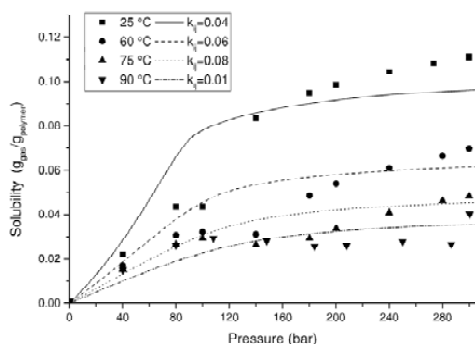


Figure 3: sPC-SAFT correlations for CO₂ solubility in XLPE at 45, 60, 75 and 90 °C. The crystallinity of the polymer used in the model prediction was estimated to be 50%. The binary interaction parameter reveals to be temperature dependent.

Around 80 bar a significant increase of the solubility is observed; one possible explanation for this phenomena is that the swelling of the polymer (caused by the passage of CO₂ from gas to supercritical stage) is more affected – the volume of the sample contributes for the buoyancy correction to the solubility calculation – than the change in weight caused by the gas solubility itself.

Measurements and Modelling of Permeability

As already mentioned, the permeability is obtained from a 2-D permeation cell. The high pressure 2-D permeation cell was designed and manufactured by the Department of Chemical and Biochemical Engineering at Technical University of Denmark. The operating conditions of the cell are up to 150 °C and 700 bar. The set-up of the equipment is shown in Figure 4. The cell consists of two stainless steel chambers: a high-pressure chamber – or primary chamber – and a low pressure chamber – or secondary chamber.

Predictive theories for diffusion in polymers are rare, although Vrentas and Duda [5] have proposed a model based on the concept of free volume in a polymer, where the free volume is divided into interstitial free volume and “hole” free volume, where only the hole free volume is available for solvent diffusion. This is usually taken from a model such as Flory-Huggins, although an equation of state such as sPC-SAFT can also be used [6].

The effect of the temperature was studied in the permeability coefficient between 45 and 90 °C and a significant variation of the permeability is observed with the increasing of temperature. These results are expected because the increase of temperature causes

mobility of the polymer chain, resulting in an enhancement of the gas molecules diffusion [6].

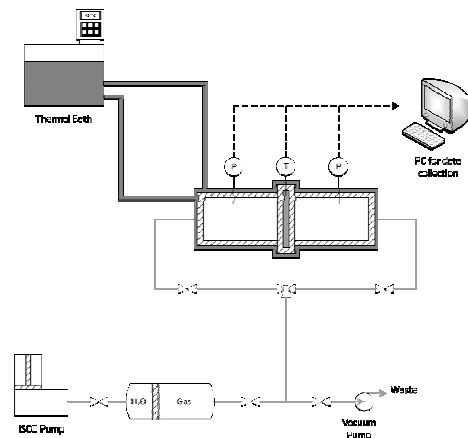


Figure 4 - Schematic diagram of the 2-D permeation cell set-up

Figures 5, 6 and 7 present the permeability of CO₂ in the three studied polymers as function of temperature and pressure, which allows to apply the Arrhenius equation linearization.

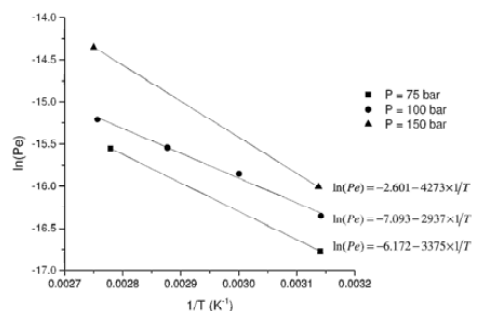


Figure 5 – Logarithm of the permeability coefficient as function of the inverse of the temperature for CO₂ in PVDF and respective Arrhenius equation for the different studied pressures.

The variation of permeability with pressure was observed to be dependent of the type of polymer – for instance PVDF has higher permeability while increasing the pressure (Figure 5); contrarily to this, XLPE shows a lower permeability with the pressure increase (figure 6), this former behavior can be explained by a compression of the polymer chains at higher pressures, decreasing the free space and thus limiting gas passage. PA11 shows a peculiar behavior (see Figure 7), attributed to the loss of mass that polymer experienced along the measurement due to the release of the plasticizer. The loss of mass was even more significant for higher

pressures and temperatures were it reached a decrease of 3.5%.

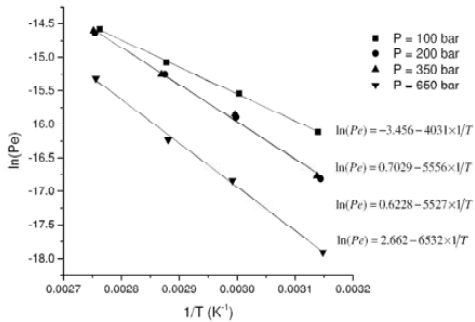


Figure 6 - Logarithm of the permeability coefficient as function of the inverse of the temperature for CO₂ in XLPE and respective Arrhenius equation for the different studied pressures.

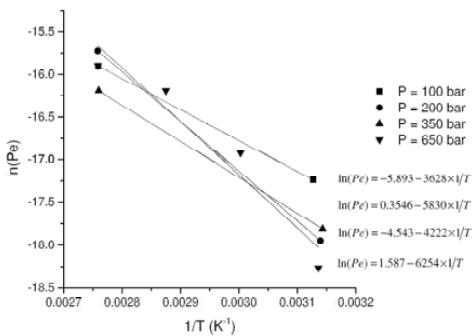


Figure 7 - Logarithm of the permeability coefficient as function of the inverse of the temperature for CO₂ in PA11 and respective Arrhenius equation for the different studied pressures.

Future Work

- Further experiments with MSB and 2-D permeation cell to measure the solubility and permeability, respectively, at different temperatures, pressures and gases mixtures;
- Determination of the polymer swelling at different temperatures and pressures;
- Investigate the change of the crystallinity fraction in the studied pressures and temperatures;
- Develop of a model that combines a SAFT model for solubility with a novel model for transport phenomena of gases in polymers integrating the work done before.

Acknowledgements

The author gratefully acknowledges NOV Flexibles and DTU for funding the project.

References

1. A. Rubin, C. Wang, Qualifications of Flexible Dynamic Risers for Supercritical CO₂, Offshore Technology Conference, Houston, USA, 2012
2. S. Almeida, Measurement and Modeling of Supercritical CO₂ Solubility and Permeability in Polymers for Offshore Applications, M.Sc. thesis, DTU Chemical Engineering (2012).
3. REFPROP, NIST, version 8.
4. M. Klopffer, B. Flaconnèche, Transport Properties of gases in polymers: Biographic Review, Oil & Gas Science and Technology, 56, (2001), 223-244.
5. J.S. Vrentas, J.L. Duda, Free-Volume Interpretation of Influence of Glass-Transition on Diffusion in Amorphous Polymers, J. Appl. Polym. Sci., 22, (1978), 2325.
6. J. K. Adewole, L. Jensen, U. A. Al-Mubaiyedh, N. von Solms, and I. A. Hussein, "Transport properties of natural gas through polyethylene nanocomposites at high temperature and pressure," J. Polym. Res., vol. 19, no. 2, p. 9814, Feb. 2012.
7. B. Flaconneche, J. Martin, and M. H. Klopffer, "Permeability, Diffusion and Solubility of Gases in Polyethylene, Polyamide 11 and Poly (Vinylidene Fluoride)," *Oil Gas Sci. Technol.*, vol. 56, no. 3, pp. 261–278, May 2001.
8. N. von Solms, M. L. Michelsen, G. M. Kontogeorgis, Prediction and Correlation of High-Pressure Gas Solubility in Polymers with Simplified PC-SAFT, Ind. Eng. Chem. Res. 44, (2005), 3330.
9. N. von Solms, M. L. Michelsen, and G. M. Kontogeorgis, Computational and Physical Performance of a Modified PC-SAFT Equation of State for Highly Asymmetric and Associating Mixtures, Ind. Eng. Chem. Res. 42, (2003), 1098.



Amata Anantpinijwatna
Phone: +45 4525 2912
E-mail: amatana@kt.dtu.dk

Supervisors: Rafiqul Gani
John M. Woodley

PhD Study
Started: August 2013
To be completed: July 2016

Generic Model-Based Tailor-Made Design and Analysis of Biphasic Reaction Systems

Abstract

Biphasic reaction system offers possibility of making novel synthesis routes, flexible or easier operation and separation, as well as, higher production yield; hence, it has broad application range from organic reactions in pharmaceutical and agro-bio industries to CO₂ capture. Though, framework and generic model for modelling of biphasic reaction systems had already been developed, there are still rooms for improvements. In this study, a framework for modelling biphasic reaction systems is extended to facilitate the model development in support of model-based process design-analysis. A more recent thermodynamic model is implemented to broadening the applicability.

Introduction

Biphasic reacting systems have a broad application range from organic reactions in pharmaceutical and agro-bio industries to CO₂ capture [1,2]. In these systems, phases are created by two immiscible liquids such as aqueous-organic solvents, ammonium-organic solvents, supercritical carbon dioxide-ionic liquid, or membrane-separated. Reactants, catalysts (including biocatalysts and enzymes), and products can exist in different liquid phases, allowing novel synthesis path as well as enhancing selectivity and conversion through regulating phases composition with solvent selection or operation conditions. Moreover, by manipulating reactor conditions, reactants, catalysts and products may end up in different phases, leading to lessening the separation tasks.

In order to efficiently develop, design, analyse and optimize the process, mathematical modelling which collectively describe physical and chemical equilibrium, reaction mechanism, and unit operation must be generated. Previously, a framework for modelling of the biphasic reaction system has been proposed [3] together with a generic model. The framework has been applied successfully to reaction systems with PTC and pseudo PTC. In this work, extension of previous work has been done to get more predictive and wider range of applicability of the generic model and framework; as well as a more recent thermodynamic model is implemented to broadening the applicability.

Objectives

- To propose a framework for modeling biphasic reaction systems.
- To develop a model of interested biphasic reaction systems.
- To use developed models for designing, optimizing, and analyzing the system.

Framework and Generic Model

Figure 1 shows our extended framework for modelling biphasic reaction systems. The first step is the problem definition followed by articulation of the assumptions used and collection of the relevant data. Normally, the model is represented by three set of equations: balance, constitutive and conditional equations [4]. In this work, the constitutive and conditional equations are combined into modules for describing physical equilibrium and chemical reactions (kinetics, equilibrium and/or diffusion). Problem-specific models are then generated from different combinations of the equations from the three modules.

In module 1, the physical equilibrium equations are formulated. In particular, the partition coefficient is defined as a distribution of each heterogeneous species between the two co-existing phases related by equations 1 and 2.

$$K_i^E = \frac{\gamma_i^\alpha}{\gamma_i^\beta}$$

1

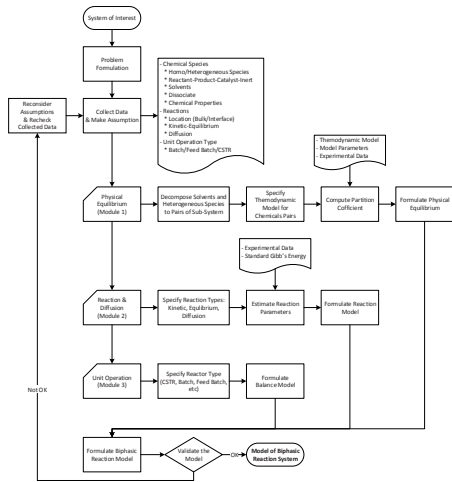


Figure 1: Extended framework for modelling of biphasic reaction systems

$$x_i^\alpha = K_i^E x_i^\beta \quad 2$$

The activity coefficients are calculated from an appropriate thermodynamic model, where the model parameters, if not available, will need to be obtained. When parameters have not been established, experimental data need to be measured for parameter regression. The intention is to develop a model with parameters that can be used for other systems.

In module 2, the reaction mechanisms are established. The generic reaction model is formulated as non-elementary reaction rate law, shown in equation 3.

$$R_j = k_j \left(\prod_i C_i^{\alpha_{ij}} - \frac{\prod_i C_i^{\beta_{ij}}}{K_j^{Eq}} \right) \quad 3$$

The balance equations (module 3) depend on the reactor geometry and the biphasic description. Generic mass balance equation is related with other module through extent of reaction concept shown in equations 4 and 5.

$$\frac{d\xi_j}{dt} = R_j \quad 4$$

$$N_i = N_{i,0} + \sum_j \nu_{ij} \xi_j + F_{i,0} - F_i \quad 5$$

Application of Segment Activity Model

In order to predict partition coefficient (K_i^E) of heterogeneous species such as phase transfer catalysts (PTC), the species and solvents are decomposed into pairs, and activity coefficient of each pair is calculated by appropriate thermodynamic model.

NRTL segment activity coefficient model (NRTL-SAC) and extension version for electrolytes systems [5,6] offer wide range of applicability for a system with limited experimental data.

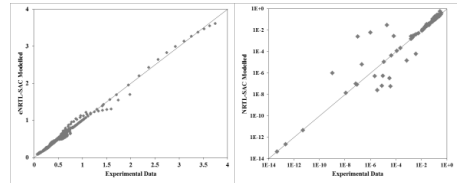


Figure 2: Comparison of experimental data and eNRTL-SAC modelled activity coefficients of 24 PTCs (left) and experimental data and NRTL-SAC modelled maximum solubility of 11 PTCs (right)

The model is initially applied to PTC activity coefficients and solubility calculation in both aqueous and organic phases. The results show an acceptable agreement between experimental data and model prediction as shown in Figure 2.

Conclusion and Future Perspective

Extension of the framework for modelling biphasic reaction systems for more flexibility has been done. It is successfully applied to various cases which highlight the flexibility and model generation-solution features of the framework. The generic model is also modified to effectively and uncomplicatedly deal with complex systems.

The segment activity coefficient (NRTL-SAC/eNRTL-SAC) model implementation should help reducing number of experimental data needed for parameters regression, hence, widening range of applicable systems. It shows promising prediction capability and requires further investigation.

We plan to add energy balances feature to the framework since some of the systems are highly exothermic. Such a model could then be used to design the full process operation and apply the framework to more case studies.

Acknowledgements

I'd like to thank Professor Felipe Lopez-Isunza, Professor John P. O'Connell, and Professor Alfonso Mauricio Sales-Cruz for great advices. I'd like to thank Syngenta AG for interesting cases study. I also would like to thank Thai's OCSC for a financial support.

References

1. H. Nowothnick, A. Rost, T. Hamerla, R. Schomäcker, C. Müller, D. Vogt, Catal. Sci. Technol. 3 (2013) 600.
2. E. Santacesaria, A. Renken, V. Russo, R. Turco, R. Tesser, M. Di Serio, Ind. Eng. Chem. Res. 51 (2012) 8760.
3. A. Anantpinijwatna, G. Sin, J. O'Connell, R. Gani, in: Proc. 8th Int. Conf. Found. Comput. Process Des., Elsevier, 2014.
4. I.T. Cameron, R. Gani, Product and Process Modelling: A Case Study Approach, Elsevier, 2011.
5. C. Chen, P. Crafts, Ind. Eng. Chem. Res. (2006) 4816.
6. C.-C. Chen, Y. Song, Ind. Eng. Chem. Res. 44 (2005) 8909.



Trine Marie Hartmann Arndal
Phone: +45 4525 2809
E-mail: trina@kt.dtu.dk
Discipline: Catalysis and Reaction Engineering

Supervisors: Prof. Anker Degn Jensen, DTU-KT
Dr. Martin Høj, DTU-KT
Prof. Jan-Dierk Grunwaldt, KIT
Dr. Jostein Gabrielsen, Haldor Topsøe A/S

PhD Study
Started: April 2014
To be completed: April 2017

New Catalysts for Hydrodeoxygenation of Biomass Pyrolysis Oil

Abstract

Hydrodeoxygenation (HDO) is a promising technique to convert biomass pyrolysis oil (bio-oil) into low oxygen and high fuel grade oil. To support the process development, this project targets a systematic study of possible catalysts in terms of activity and stability of different catalyst systems, reaction mechanisms of different bio-oil model compounds and optimization of operating conditions. The project is part of the project "H2CAP - Hydrogen assisted catalytic biomass pyrolysis for green fuels".

Introduction

Pyrolysis of biomass produces a high yield of condensable oil at moderate temperature and low pressure. This bio-oil has adverse properties such as high oxygen and water contents, high acidity and immiscibility with fossil hydrocarbons [1]. Catalytic hydrodeoxygenation (HDO) is a promising technology that can be used to upgrade the crude bio-oil to fuel-grade oil [2]. The development of the HDO process is challenged by rapid catalyst deactivation, instability of the pyrolysis oil, poorly investigated reaction conditions and a high complexity and variability of the input oil composition [2]. However, continuous catalytic hydroxyprolysis coupled with downstream HDO of the pyrolysis vapors before condensation shows promise.

Specific Objectives

The objective of this project is to develop suitable catalysts for the catalytic hydroxyprolysis and the downstream HDO processes having high activity, high stability and a favorable cost and to improve the understanding of the HDO process. This will be done through experimental and theoretical investigations of the HDO reaction under well-defined conditions using bio-oil model compounds, and possibly, at a later stage, partly converted (stabilized) pyrolysis oil. The project objectives cover:

- A literature survey on hydroxyprolysis and HDO with emphasis on the latter in terms of bio-oil composition, catalyst formulation, proposed reaction mechanisms, deactivation

mechanisms and recent technological advances.

- Preparation of HDO catalysts in the laboratory.
- Test of prepared catalysts in a high pressure experimental setup along with investigation of process conditions. Different bio-oil model compounds will be applied.
- Detailed characterization of prepared catalysts (fresh and spent).
- Selection of HDO catalysts for hydroxyprolysis and downstream deep HDO. Investigation of catalyst stability, reaction mechanisms and deactivation mechanisms.
- Experiments with real bio-oil.

Results and Discussion

Experimental HDO is carried out in a Pyrolysis Oil Converter (POC) setup consisting of a fixed bed catalytic reactor with a typical bed volume of 6-7 cm³. The setup is capable of operation up to 120 bar and 550 °C. It is possible to connect five unique gasses and two unique liquids to the reactor feed. Liquids and gasses are separated downstream of the reactor and are analyzed by GC-MS (FID, liquids) and GC (FID/TCD, gasses).

Different classes of both noble and non-noble catalysts have shown promising activity in the HDO of bio-oil model compounds; e.g. sulfides, oxides, reduced species and phosphides [2,3]. Different bio-oil model compounds comprising a wide range of functionalities

such as polyols, phenols, aldehydes and ketones will be applied individually and in mixtures in order to investigate reaction mechanisms of individual compounds and interactions such as competitive inhibition. Special attention is paid to operating conditions (e.g. temperature, H_2 partial pressure, residence time) and to tolerance against water, sulfur, chlorine and potassium which are abundant in bio-oil.

Initial experiments: Activity of bulk MoO_3

MoO_3 has been reported to be active in the HDO of oxygenates at low hydrogen partial pressure through a reverse Mars–van Krevelen mechanism [4,5]. The conversion of acetone – a simple bio-oil model ketone – has been investigated over MoO_3 at 350–400 °C and near ambient pressure. Selected results are shown in Figure 1. Blank experiments have shown that acetone does not undergo gas phase reactions at the applied conditions.

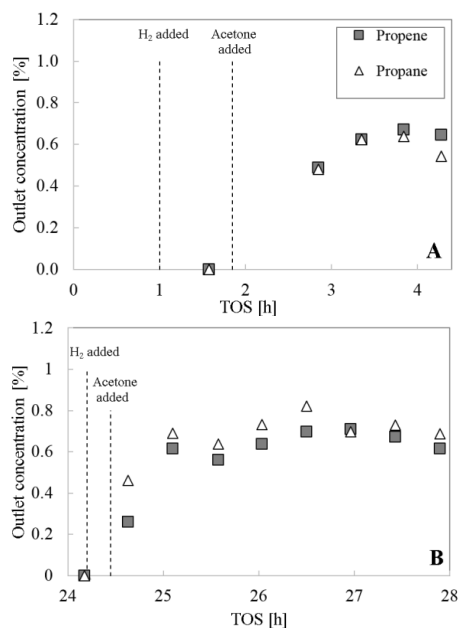


Figure 1: Acetone conversion over bulk MoO_3 at 400°C with a total feed of 60 mmol/min and a partial pressure of acetone of 0.05 bar ($\approx 3\%$ in the feed). Partial pressure of H_2 in bar A) 1.08 and B) 1.85. The catalyst has been flushed with N_2 in between A and B.

Acetone is readily converted to the HDO products propene and propane, the latter in contradiction with the common perception that MoO_3 does not possess hydrogenation activity [4,5]. An acetone conversion up to approximately 50 % has been observed in the initial experiments.

No significant cracking activity occurred and only a negligible amount of condensation products were detected. It has been proposed that MoO_3 is activated through a mild surface reduction introducing oxygen

vacancies that act as sites for oxygenate adsorption [4,5]. An activation period has been detected after introducing acetone into the feed stream – independent on the previous time on stream with hydrogen. This indicates that the catalyst could be activated through a carburization process.

Returning to the initial conditions at the end of an experiment has shown severe catalyst deactivation. Reactivation of the spent catalyst by oxidation in diluted air (10 % O_2) at 400 °C was not possible. This could be explained by coke deposition, which would require higher temperatures for regeneration. To evaluate the stability of MoO_3 further, experiments will be carried out with water and sulfur in the feed. Also, a series of supported MoO_3 samples on different supports (Al_2O_3 , ZrO_2 , TiO_2) will be prepared and tested. Finally, other bio-oil model compounds will be included in the investigation.

Density Functional Theory (DFT) calculations at Stanford University and X-ray Absorption Fine Structure (XAFS) characterization at Karlsruhe Institute of Technology will aid the understanding of the different catalyst systems investigated.

Conclusions

HDO of bio-oil is a complex process due to the complex nature of pyrolysis oil. Development of active and stable catalysts for the hydroxyprolysis and downstream HDO requires a systematic investigation and understanding of the conversion of individual and mixed model compounds over different catalysts at different operating conditions. Initial experiments for conversion of acetone over bulk MoO_3 show interesting results, with an acetone conversion up to approximately 50 % into the HDO products propane and propene. Future work will further evaluate the performance of bulk MoO_3 and other catalyst systems.

Acknowledgements

This work is part of the Combustion and Harmful Emission Control (CHEC) research center at The Department of Chemical and Biochemical Engineering at DTU. The project is funded by The Danish Council for Strategic Research, The Programme Commission on Sustainable Energy and Environment.

References

1. A.V. Bridgwater, *Biomass and Bioenergy* 38 (2012) 68–94.
2. P. M. Mortensen, J.-D. Grunwaldt, P.A. Jensen, K.G. Knudsen, A.D. Jensen, *Applied Catalysis A: General* 407 (2011) 1–19.
3. P. M. Mortensen, J.-D. Grunwaldt, P.A. Jensen, A.D. Jensen, *ACS Catalysis* 3 (2013) 1774–1785.
4. T. Prasomsri, T. Nimmanwudipong, Y. Román-Leshkov, *Energy and Environmental Science* 6 (2013) 1732–1738.
5. T. Prasomsri, M. Shetty, K. Murugappan, Y. Román-Leshkov, *Energy and Environmental Science* 7 (2014) 2660–2669.



Alay Arya
Phone: +45 4525 2864
E-mail: alaya@kt.dtu.dk
Discipline: Centre for Energy Resources Engineering

Supervisors: Georgios Kontogeorgis
Nicolas von Solms

PhD Study
Started: January 2014
To be completed: December 2016

Modeling of Asphaltene System with Association Model

Abstract

Asphaltene precipitation is calculated using Cubic Plus Association (CPA) equation of state (EoS) following specific modeling approach and oil characterization. It is found that temperature dependent cross-association energy correlates asphaltene phase envelope quite well in agreement with experimental data. Effect of gas injection on asphaltene precipitation is also correlated with experimental data by tuning only single binary interaction parameter.

Introduction

Asphaltene is normally present in the reservoir oil and for industry it is analogous to “cholesterol” since its precipitation stops the entire production and causes the loss of millions of dollars. It is an “ill defined” component of high molecular weight (around 500-4000 gm/mol), which is considered most polar part in the oil compared to the other components. This polar nature of asphaltene is believed to be imparted by heteroatoms (O, S, N, vanadium, nickel) present in its structure. Because of this polar nature asphaltenes associate with each other and precipitate at certain temperature, pressure and composition. However, prediction of these conditions, where asphaltene precipitates, is quite uncertain and detailed thermodynamic model and appropriate oil characterization is required. Asphaltenes can easily precipitates as pressure is reduced but also if the oil is diluted by light hydrocarbons eg. gas such as methane, CO₂ or nitrogen. Ever since the introduction of enhanced oil recovery (EOR) method with gas this problem has become even worse. Moreover, oil with little amount of asphaltene (say, 0.1 mol %) may show precipitation problem than the oil with moderate amount of it (say 1 mol %) and vice versa. Different EoSs with different modeling approach have been used to predict asphaltene phase equilibria; however, there is no single convincing model for industries to use.

Specific Objective

The purpose of this project is to use EoS based on association theory and develop an approach to predict asphaltene precipitation at different conditions of temperature, pressure and composition. We plan to use CPA [4] and Perturbed Chain Statistical Associating

Fluid Theory (PC-SAFT) EoS [6,7] models to compare the results.

Discipline

Engineering Thermodynamics.

Modeling Approach

There could be different ways to characterize oil with asphaltenes, however, in this report we characterize oil based on SARA (Saturates Aromatics Resins Asphaltene) analysis. Ideally, we should have separator gas and heavy oil molar compositional analysis, gas to oil ratio and SARA analysis to back calculate the composition of reservoir oil by combining separator gas and heavy oil. SARA analysis gives composition of heavy oil into weight fraction. To convert it into molar fraction, we need molecular weight information of each fraction, which is generally not available. In addition, asphaltenes has tendency to cross associate with resins and aromatics, which entails to determine cross associating energies for asphaltenes-resins and asphaltenes-aromatics pairs. Asphaltenes molecules are self-associating, which entails to determine one more parameter that is self-associating energy for asphaltene-asphaltene pair. To reduce degree of freedoms (number of unknown parameters to be determined) and also inspired from Zhidong et al [5], we merge three different fractions (Saturates, Aromatics, Resins) into single fraction (Heavy component). Asphaltenes are considered as monomeric molecules and its molecular weight is assumed to be 750 DA [2,3]. Critical properties of asphaltenes are also fixed assuming its solubility parameter to be 18 MPa^{1/2}. Self-association energy ($\epsilon^{AA}/R=3000$ K) and association volume fraction

of asphaltene molecules ($\beta^{AA}=0.050$) are also fixed. For heavy component, normal boiling point is calculated from Pedersen relationship. Critical parameters of heavy component are calculated from Kesler –Lee relationship. Critical pressure of heavy component is tuned with respect to bubble points of reservoir oil. Cross-association energy (ϵ^{AH}/R) between heavy component and asphaltene is temperature dependent and calculated from experimental data of upper onset pressures at two different temperatures. Cross-association volume fraction ($\beta^{AH}=0.050$) is also fixed.

Results and Discussion

Asphaltene Phase Envelope

Asphaltene phase envelope is calculated for reservoir oil presented in Jamaluddin [1]. Critical pressure of heavy component is tuned with respect to bubble points. Only two points of upper onset pressure are used to regress the ϵ^{AH}/R and rest of the trend points are pure calculation. From Figure 1, one can observe that CPA model can correlate upper onset points and bubble points. Lower onset pressure curve is pure prediction, which is in good agreement with experimental data.

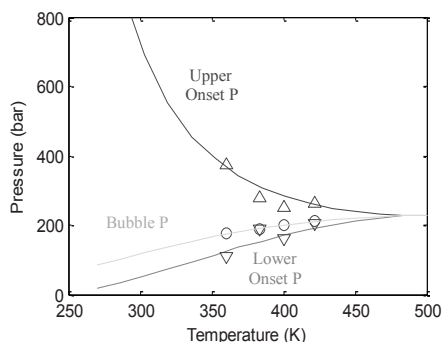


Figure 1: Asphaltene Phase Envelope for reservoir oil. Solid lines represent CPA model calculation. Symbols represent experimental data from Jamaluddin [1].

Effect of Gas Injection

Once we have calculated the temperature dependent ϵ^{AH}/R and critical pressure of heavy component, we can calculate the effect of gas injection on asphaltene precipitation. Figure 2 shows the effect of N_2 injection on the upper onset pressure of the same oil considered above. CPA can accurately correlate the experimental data but only after tuning the binary interaction parameter for asphaltene- N_2 pair.

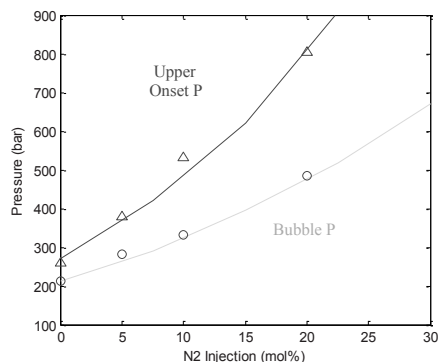


Figure 2: Asphaltene Upper Onset Pressure and Bubble pressure as a function of amount of N_2 injection. Solid lines represent CPA model calculation. Symbols represent experimental data from Jamaluddin [1].

Conclusion

The asphaltene modeling approach with CPA EoS is very simple to use since it involves only two unknown parameters. Model is able to correlate the asphaltene phase envelope with experimental data after regressing critical pressure of heavy component and temperature dependent cross-association energy. Effect of gas injection can also be correlated after tuning only one binary interaction parameter. However, model is not completely predictive and need minimum experimental data for tuning.

Acknowledgments

The financial contribution to this project is partly from BP.

References

1. A.K.M. Jamaluddin, N. Joshi, F. Iwere, O. Gurpinar, Society of Petroleum Engineering, 74393, 2002.
2. L. Buch, H. Groenzin, E. B. Gonzalez, A.I. Simonn, L.G. Carlos, C.M. Oliver, Fuel 82 (2003) 1075-1084.
3. B. Sophie, C.G. Cristiane, N. Koyo, G. Gale, C.M. Oliver, Fuel 85 (2006) 1-11.
4. G.M. Kontogeorgis, G.K. Folas, "Thermodynamic Models for Industrial Applications – from classical and advanced mixing rules to association theories", Wiley 2010, 262.
5. L. Zhidong, A. Firoozabadi, Fuels 2010, 24, 1106-1113.
6. J. Gross, G. Sadowski, Ind. Eng. Chem. Res. 40 (2001) 1244-1260.
7. J. Gross, G. Sadowski, Ind. Eng. Chem. Res. 41 (2002) 5510-5515.



Seyednezamaddin Azizaddini
Phone: +45 4525 2890
E-mail: seaz@kt.dtu.dk

Supervisors: Kim Dam-Johansen
Weigang Lin
Peter Arendt Jensen

PhD Study **Gas-Solid reactions and reactor systems**
Started: December 2012
To be completed: November 2015

Interconnected fluidized bed technology

Abstract

Interconnected fluidized bed (IFB) systems are applied for gas-solid processes with two steps, two reactors operating at different reaction atmospheres or conditions. Solids are recirculated between the fluidized beds typically through loop-seals which can control the solid circulation rate and prevent backflow of gases. Depending on the characteristics of the process, different particle types, mostly particles in Geldart group A and B, were already applied in IFB systems. There may be demands for application of fine particles with very large surface area (Geldart group C) in IFB systems. Such particles may cause channeling and agglomeration in the traditional loop-seals. In this project, a new loop-seal configuration for IFB systems is studied in order to facilitate use of interconnected fluidized bed systems operating with fine cohesive Geldart group C particles.

Introduction

IFB system is typically composed of two parallel fluidized bed reactors with separate gas atmospheres and with the solid material circulating between the reactors through so-called loop-seals. Such reactor systems may be used for different kind of reactions, i.e. fluid catalytic cracking of hydrocarbons – where the cracking is carried out in one reactor under reducing conditions where the solid catalyst is gradually deactivated by coke formation. The poisoned catalyst particles are then transferred to the second reactor for regeneration under mild oxidizing conditions to avoid high temperature sintering.

Another example is chemical looping combustion where oxygen carrier particles, mostly metal oxides, carry oxygen from the combustion air to a gaseous fuel. The metal oxide particles gain oxygen from the air in the first reactor. Then particles are transported to the other reactor where the metal oxide reacts with the gaseous fuel. In this way the fuel and air are never mixed which can be a significant advantage for some applications.

In a chemical looping hydrogen production process, metal oxide (MeO) particles are transported to the reducer in contact with fuel, e.g. syngas or methane. Afterwards, metal (Me) particles are transported to the H₂ generator reactor in contact with water vapor to produce hydrogen.

Low temperature gasification of biomass in the presence of calcium oxide particles may be used for production of syngas with high content of hydrogen and separation of carbon dioxide. Calcium carbonate particles formed by reaction of calcium oxide with CO₂ are transported to a calciner, to be calcined back to calcium oxide.

In the examples mentioned above, circulation of solids between two fluidized beds operating under very different conditions is realized by different types of non-mechanical valves, such as J-valves, U-valves and L-valves [1].

Literature studies reveal that utilization of fine particles in various industrial applications – such as catalysts, sorbents, drugs, cosmetic, bio-materials, food, etc. tends to increase [2]. IFB systems have the potential to be applied as one of the unit operations which facilitates handling and reaction of two-phase gas-solid processes. Two relevant sequent processes, like oxidation-reduction, carbonation-calcination or absorption-desorption, could be implemented separately in each reactor of an IFB system, where each fluidized bed is operated under its own controlled pressure, temperature and gaseous atmosphere.

Loop-seals are one of the crucial parts which play an important role in operation of an IFB system. Loop-seals control the solid circulation between fluidized beds and prevent mixing of gaseous product of connected fluidized beds. Conventional loop-seals have

difficulties handling the fine particles due to operational issues which occur for fine particles, e.g. channeling, cracking and formation of large agglomerates.

Specific objectives

This study will deal with a new type of loop-seals dedicated for operations of interconnected fluidized bed systems with the particles containing large amount of Geldart group C particles.

The new loop-seal comprises of a part which is operated under fast fluidization or pneumatic transport regime [4], and other part is a dense moving bed. Within the transport section, fine particles are transported individually or in form of agglomerates out by elutriation. High gas velocity in the outlet section of this device transports the particles and prevents backflow of gases.

Primarily, the new design is analyzed under cold flow conditions to characterize hydrodynamic of the system and disclose design parameters.

The studies are being carried out experimentally under different operating conditions for various types of particles. Additionally, mathematical modeling will be performed to understand hydrodynamic of solid and gas flow in the loop-seal. The new loop-seal is expected to be applied in an IFB system to make the operation of fine group C particles feasible.

Loop-seal for fine particles

Conventional loop-seals are operated with Geldart group A and B particles under superficial gas velocities close to the minimum fluidization velocity of the particles. Application of the conventional loop-seals for operation of Geldart group C particles is a significant challenge. In order to study and optimize the pattern and structure of the loop-seal used for fine particles, a cold loop-seal simulator is designed and constructed.

The test rig consists of two sections, dilute phase in the draft tube and dense phase in the annulus section. Considering the particles properties (e.g. size and density) and operating conditions (e.g. gas feeding rate and draft tube diameter), the draft tube is operated under fast/turbulent fluidization or pneumatic transport regime.

Particles are accelerated after being in contact with the high velocity upward gas stream and regarding their momentum, reach a specific height above the draft tube outlet. Particles in the formed fountain are deposited down into the annulus section. At the bottom of the annulus section, gap between draft tube and bottom of the device, particles are sucked into the gas stream and transported upward. In the annulus section, a downward moving dense bed is observed.

Considering particles flow pattern, solid particles are internally circulated in the device. And higher gas flow rates increases the height of the fountain even to the outlet section which leads to transportation of particles out of the device.

Fine particles experience difficulties to move down through the annulus section and flow to the high gas

flow stream at the bottom section. So, experiments were performed on larger particle sizes while individual operation of fine particles, in this device, seems impossible.

Moreover, supplementary experiments were performed by changing the geometric parameters and operating conditions. Summary of the results from operation of set-up are represented in Table 1. It shows if the geometric or operational parameter increase, how the pressure drop, internal solid circulation rate and flow fraction distribution change. Trend of acquired results from corresponding parameters are in a good agree with other studies on similar set-up [5].

Table 1. Summary of the experimental results

Parameters (if increases)	Pressure drop	Internal solid circulation rate	Flow fraction distribution
Particle size	↓	-	↑
Gap of draft tube	↑	↑	↑
Draft tube diameter	↓	↑	↓
Total gas flow rate	↓	↑	↓

New set-up was designed and constructed based on the observed issues from operation of fine particles in the first version. Some modifications and fundamental changes on were applied on configuration of the device. Next phase of this project is to check the feasibility of handling the fine particles in the new test rig which is expected to act as a loop-seal for fine particles.

Conclusion and future works

Construction, modification and development of a device for a new loop-seal which can handle Geldart Group C particles were performed. The experiences from the preliminary studies of the device were conducted to the modification and design of the new version. New structural configuration was proposed with the new port for feeding of fine particles.

Experimental studies on operation of the new test rig with coarse particles and also fine particles are implemented. Modifications and corrections are applied to achieve handling of fine particles by means of new device.

Acknowledgements

The author would like to thank the Technical University of Denmark for financing the project.

References

1. T.M. Knowlton, Particulate Solid Research (2012) 25-49.
2. J. Shabaniyan, R. Jafari, J. Chaouki, Int. Review Chem. Eng., 4 (1) (2012) 16-50.
3. D. Geldart, Powder Tech., 7 (1973) 285-292.
4. J. Grace, Can. J. Chem. Eng., 64 (3) (1986) 353-363.
5. T. Nagashima, H. Ishikura, and K. Ide, Korean J. Chem. Eng., 15 (3) (1998), 683-698.



Maria-Ona Bertran

Phone: +45 4525 2817
E-mail: marber@kt.dtu.dk

Supervisors: Rafiqul Gani
John M. Woodley
Anker D. Jensen

PhD Study
Started: September 2014
To be completed: August 2017

Modelling, Synthesis and Analysis of Biorefinery Networks

Abstract

The production of fuels and chemicals is primarily based on crude oil. The use of biomass as raw material represents a sustainable alternative. In order to establish a new industrial system on the basis of biomass, a systematic approach to generating, evaluating and selecting biorefinery processing networks is needed. In this PhD study, a systematic methodology for synthesis and design of biorefinery networks will be developed, along with the associated methods and tools.

Introduction

Petroleum is currently the primary raw material for the production of fuels and chemicals. Consequently, our society is highly dependent on fossil non-renewable resources. Recently, renewable raw materials are receiving increasing interest for the production of chemicals and fuels, so a new industrial system based on biomass is being established with sustainability as the main driving force [1].

A biorefinery is a processing facility for the production of multiple products (including biofuels and chemicals) from biomass, an inexpensive, abundant and renewable raw material [2].

The optimal synthesis of biorefinery networks problem is defined as: *given* a set of biomass derived feedstock and a set of desired final products and specifications, *determine* a flexible, sustainable and innovative processing network with the targets of minimum cost and sustainable development taking into account the available technologies, geographical location, future technological developments and global market changes.

The synthesis and design of processing networks involves the selection of raw materials, processing technologies/configurations and product portfolio compositions among a number of alternatives. A common approach to the formulation and solution of this class of decision-making problems is mathematical programming, in which the problem is decomposed into: (i) representation of the superstructure of alternatives, (ii) formulation of the mathematical optimization problem, and (iii) solution of the

optimization problem to determine the optimal design according to the defined criteria and constraints [3].

Compared to crude oil feedstock, biomass has lower quality and its processing cost is higher. Also, the quality and quantity of biomass is affected by the region and climate [4]. Therefore, unlike the optimal petrochemical refinery, the optimal biorefinery network problem should have location-dependent solutions.

Table 1: Methods and applications for optimal synthesis of biorenewables [4]

Author/s	Method	Application
Karrupiah et al. [5]	MINLP	Corn-based ethanol production
Drobez et al. [6]	MINLP	Biogas production
Harwardt et al. [7]	MINLP	Butyl-levulinate separation
Zondervan et al. [8]	MINLP	Production of ethanol, butanol
Martin and Grossmann [9]	MINLP	FT-diesel production
Voll and Marquardt [10]	RNFA; MIP	Production of 3-MTHF
Ponce-Ortega et al. [11]	Disjunctive programming	Production of bioalcohols
Rizwan et al. [12]	MINLP	Production of biodiesel

The mathematical programming approach has already been applied to the case of biorefinery networks for specific applications; some of them are shown in Table 1 [4]. However, a generic systematic methodology for biorefineries is still not at hand.

Process systems engineering (PSE) methods and tools have been widely used in the petrochemicals and fuels sectors. In order to identify the optimal biorefinery network, existing PSE methods and tools will prove essential.

Discipline

The research conducted in this project is primarily within the field of process systems engineering (PSE).

Objectives

The objective of this project is to develop a systematic method and associated tools to synthesize, design and analyze innovative biorefinery networks based on chemical and biological approaches to convert biomass feedstock into valuable chemicals and biofuels. The project comprises two main tasks: (i) the development of a generic synthesis methodology for biorefinery networks and (ii) the establishment of generic methods and tools for synthesis, design and evaluation of biorefinery networks and their integration in a computer-aided framework.

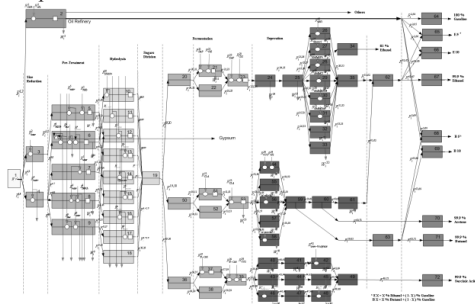


Figure 1: Biorefinery superstructure [8].

In the first task, the possible biorefinery networks will be represented as a superstructure of alternatives. Figure 1 shows a biorefinery superstructure developed by Zondervan et al. [8]. In this project, this will be expanded with other alternatives thus increasing the scope and significance of the superstructure.

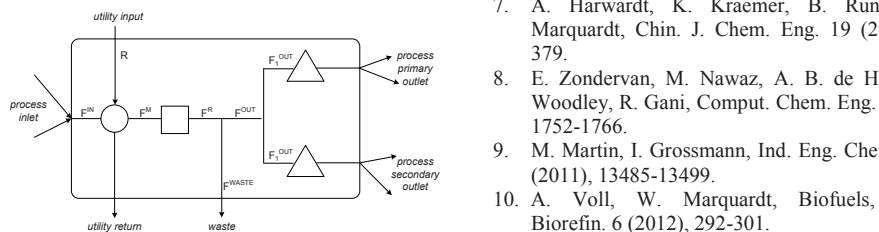


Figure 2: Generic process interval scheme [13].

Each processing interval in the superstructure is modelled with a generic model based on the scheme in Figure 2 [13]. The complete biorefinery model will be solved to determine the optimal network for each considered scenario.

In the second task, computer-aided methods and tools will be developed. A knowledge base of biorefinery raw material, processing technologies and products will be built where all necessary data for the problem solution are to be stored. The knowledge base should include information such as component properties, utility and capital cost data, product specifications, prices of chemicals, transportation data and reaction stoichiometry and conversion.

The developed method is expected to identify the optimal route for a given set of biomass and products while satisfying the sustainability criteria and taking into account the geographical and supply chain constraints. The method will be applied to different case studies in order to show its application.

Conclusions

The problem of systematic synthesis and design of biorefinery networks will be addressed in this project. A systematic methodology is to be developed, which should include the problem formulation, analysis and solution using a mathematical programming approach. Moreover, supporting computer-aided methods and tools will be created and integrated with the methodology, which is expected to determine optimal biorefinery networks for different scenarios.

References

1. M. Hechinger, A. Voll, W. Marquardt, *Comput. Chem. Eng.* 34 (2010), 1909-1918.
2. B. Kamm, M. Kamm, *Appl. Microbiol. Biotechnol.* 64 (2) (2004), 137-145.
3. A. Quaglia, C. L. Gargalo, S. Chairawongsa, G. Sin, R. Gani, *Comput. Chem. Eng.* 72 (2015), 68-86.
4. Z. Yuan, B. Chen, R. Gani, *Comput. Chem. Eng.* 49 (2013), 217-229.
5. R. Karrupiah, A. Peschel, I. E. Grossmann, M. Martin, W. Martinson, L. Zullo, *AIChE J.* 54 (2008), 1499-1525.
6. R. Drobez, Z. N. Pintaric, B. Pahor, Z. Kravanja, *Asia-Pacific J. of Chem. Eng.* 6 (5) (2011), 1932-2143.
7. A. Harwardt, K. Kraemer, B. Rungeler, W. Marquardt, *Chin. J. Chem. Eng.* 19 (2011), 371-379.
8. E. Zondervan, M. Nawaz, A. B. de Haan, J. M. Woodley, R. Gani, *Comput. Chem. Eng.* 35 (2011), 1752-1766.
9. M. Martin, I. Grossmann, *Ind. Eng. Chem. Res.* 50 (2011), 13485-13499.
10. A. Voll, W. Marquardt, *Biofuels, Bioprod. Biorefin.* 6 (2012), 292-301.
11. J. M. Ponce-Ortega, V. Pham, M. El-Halwagi, *Ind. Eng. Chem. Res.* 51 (2012), 3381-3400.
12. M. Rizwan, J. H. Lee, R. Gani, *Comput. Chem. Eng.* 58 (2013), 305-314.
13. A. Quaglia, B. Sarup, G. Sin, R. Gani, *Comput. Chem. Eng.* 38 (2012), 213-223.



Thomas Bisgaard

Phone: +45 4525 2811
E-mail: thbis@kt.dtu.dk

Supervisors: Jens Abildskov
Jakob Kjøbsted Huusom
Nicolas von Solms
Kim Pilegaard

PhD Study
Started: September 2012
To be completed: January 2016

Operation and Design of Diabatic Processes

Abstract

Separation of mixtures by distillation is an energy intensive task, but yet, amongst one of the cheapest. Due to increasing attention paid on environmental footprint and sustainability, new intensified configurations are appearing with the goal of reducing utility consumption. Meanwhile, conventional equipment is continuously improved to enhance resource utilization. Because of various competing technologies, a better understanding must be collected in order to identify strengths and weaknesses in novel distillation configurations. As it is today, no full-scale diabatic distillation columns are currently operating in the industry. The aim of this PhD project is to shed light on the potential benefits of diabatic operation and to handle some of the barriers for industrial application/acceptance of diabatic distillation columns.

Introduction

Multi-stage distillation has been known since the 16th century and is the most common unit operation in the chemical industry. At present, multi-stage distillation is considered a mature technology; however, alternative intensified configurations have appeared recently. Reactive distillation, dividing-wall columns, and mechanical vapor recompression column are examples of industrially proven, intensified configurations.

The heat-integrated distillation column (HIDiC) is considered a potential alternative to the conventional distillation column (CDiC). These configurations are illustrated in Figure 1. In the HIDiC, gradual condensation occurs along the rectifying section and gradual boil-up occurs along the stripping section as heat is exchanged between the sections, realized by operating the rectifying section at a higher pressure using a compressor above the feed stage.

Various studies concern benchmarking of the HIDiC but the overall conclusion is contradictory due to numerical dissimilarities and different basis of comparisons. This issue has been addressed by several authors recently, and it appears that the economic advantage of any of the configuration is a complex function of mixture identity, whereas correlations between optimality and relative volatility have been shown for ideal mixtures. Furthermore, several studies have already proven the operability of the HIDiC by simulation and experimentally in bench-scale

experiments, but more work has to be done to simulate real industrial applications.

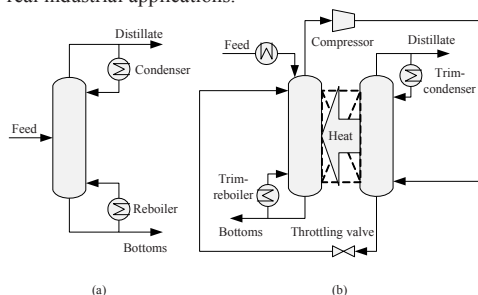


Figure 1: (a) Conventional distillation column (CDiC) and (b) Heat-Integrated Distillation Column (HIDiC).

Specific Objectives

Design of conventional distillation columns is a well-known task. The most common approach is the graphical McCabe-Thiele method, which in principal is restricted to binary mixtures with components with similar heats of vaporization and columns with adiabatic stages. However, for diabatic distillation columns such as the HIDiC, more advanced methods are needed. Different HIDiC design methods have been appearing in literature as e.g. the Extended Ponchon-Savarit Method [1,2] which graphically combines phase equilibria and energy balances in one diagram, and the Thermo-Hydraulic Approach [3] which takes into account

physical realization of adding heat transfer area inside the column. The weakness of all methods are that they all require many design decisions that are crucial to the economic feasibility of the design. Recently, the design issue has been addressed, and a systematic design methodology has been proposed accounting for both economical and hydraulic feasibility and has been tested on several industrial relevant, binary mixtures.

Results and Discussion

The proposed design method is illustrated on the separation of 83 mol/s equimolar, saturated liquid feed mixture of methanol/ethanol at atmospheric pressure. The separation specifications are 99.5% methanol in top and 0.5% ethanol in bottom.

Two measures are used as design criteria: The relative annualized cost and the hydraulic feasibility indicator. The relative annualized cost is the ratio of the annualized cost of a HiDiC to that of a CDiC:

$$RTAC = TAC_{HiDiC} / TAC_{CDiC} \quad (1)$$

Hydraulic feasibility indicator is the ratio of available heat transfer area to installed heat transfer area:

$$HFI = A_{available} / A_{installed} \quad (2)$$

The available heat transfer area is based on a concentric design with the stripping section as the outer shell [3]. A feasible design satisfies following constraints:

$$RTAC < 1 \text{ and } HFI \geq 1 \quad (3)$$

The methodology is illustrated in Figure 2 as the evolution of capital expenditures (CAPEX) and TAC, where each point represent an intermediate column design given by:

- A base case design for a CDiC method is obtained using the McCabe-Thiele method
- An economic optimum of a CDiC is obtained by varying the number of stages maintaining same relative feed location leading to 33/33 stages in rectifying/stripping sections. The CAPEX is increased because of more stages required, while TAC is reduced due to reduced utility consumption
- The pressure of the rectifying section is increased until a specified minimum temperature gradient is obtained (here 5 K). This design is not heat integrated and thus the TAC is significantly increased because of the addition of a compressor. A compression ratio of 2.09 is required.
- It is proposed to thermally couple as many stages as possible. Furthermore, the coupling should take place as far away from the feed stage as possible. In this example, the sections are equally sized and thus the couplings 1-34, 2-35, ..., 33-66 is adopted, counting from top. The heat exchange area is increased until external reflux-free or external boil-up-free operation is obtained, giving a heat exchange area of 48 m²/stage while maintaining minimum 5 K driving force. The CAPEX of this design is significantly increased compared to optimum CDiC in point B, because of a compressor and 33 internal heat exchangers, but the TAC is lower as RTAC=0.76 and HFI=0.17.

- In order to increase HFI to satisfy Eq. 3, the number of heat-integrated stages is increased as long as TAC is decreased simultaneously, resulting in 41/41 stages (all heat-integrated). The external reflux/boil-up-free operation leads to 34.8 m²/stage heat transfer area and a compression ratio of 2.121. HFI is increased to 0.23.
- The remaining option for increasing HFI is to decrease heat transfer area until HFI=1, leading to 18.8 m²/stage at a cost of a RTAC of 1.00.

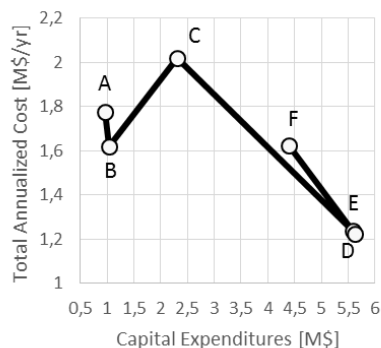


Figure 2: Illustration of proposed design algorithm for the separation of methanol/ethanol.

Conclusion

Diabatic distillation is an attractive technology from economical and an environmental point of view. The barrier for industrial acceptance of the HiDiC is the complexity associated with integration and investment of the internal heat exchangers. The significance of considering the physical available space for heat exchangers has been demonstrated by the presented case study. As shown, a methodology is developed. Now the remaining task is to relate the techno-economic feasibility of the HiDiC to classes of mixtures, in order to close a gap for industrial implementation.

References

- T.-J. Ho, C.-T. Huang, L.-S. Lee, C.-T. Chen, *Ind. Eng. Chem. Res.* 49 (1) (2010) 350-358.
- T. Wakabayashi, S. Hasebe, *Comput. Chem. Eng.* 56 (2013) 174-183.
- M. Gadalla, L. Jiménez, Z. Olujić, P.J. Jansens, *Comput. Chem. Eng.* 51 (2007) 1346-1354.

List of Publications

- T. Bisgaard, J.K. Huusom and J. Abildskov, *Proceedings of ACD2012*, 2012, Denmark.
- T. Bisgaard, J.K. Huusom and J. Abildskov, *Proceedings of ESCAPE*, 2013, Finland.
- T. Bisgaard, J.K. Huusom and J. Abildskov, *Proceedings of DYCOPS* 2013, India.
- T. Bisgaard, J.K. Huusom, J. Abildskov, *Proceedings of the 10th international conference on distillation & absorption* 2014, Germany.



Martin Gamél Bjørner

Phone: +45 4525 2886
E-mail: mgabi@kt.dtu.dk
Discipline: Applied Thermodynamics

Supervisors: Georgios Kontogeorgis

PhD

Started: June 2012
To be completed: August 2015

CO₂-Hydrates - Challenges and Possibilities

Abstract

Despite its importance, accurate modeling of carbon dioxide (CO₂) and in particular mixtures of CO₂ is still a challenge. Popular approaches model CO₂ either as an inert or as a solvating molecule. In principle, however, CO₂ is a quadrupolar molecule and should rigorously be modeled as one. In this PhD project, in an attempt to obtain a more physically correct model, a quadrupolar contribution to the Helmholtz energy, inspired by recent advances within the statistical association fluid theory (SAFT), is proposed and combined with the well-known cubic plus association (CPA) equation of state (EoS). The new model has successfully been applied to the prediction of derivative properties of CO₂ and the prediction of binary vapor-liquid (VLE) and liquid-liquid equilibria (LLE).

Introduction

In recent years CO₂ has received a significant amount of negative attention due to its contribution to the global warming and the fact that the amount of CO₂ in the atmosphere continues to rise. This is believed to be largely due to the high amounts of CO₂ emitted to the atmosphere as a result of e.g. electricity production from the combustion of fossil fuels. Alone in Denmark more than 40 million tons of CO₂ are emitted each year [1]. The reduction of the CO₂ emission is considered a high priority.

To understand the problems caused by CO₂, high quality experimental data and accurate models, valid over a wide range of conditions and chemicals, are necessary. For example a novel technique for CO₂ capture using gas hydrates has recently been patented [2]. The operation pressure of the technique, however, is currently too high to be economically profitable. It is believed that this pressure could be reduced by specific additives. Such a screening process, however, is expensive and time consuming, and accurate models for CO₂ in mixtures would greatly facilitate this process.

Mixtures of CO₂ and gas hydrates are also a nuisance in the petroleum industry, where the phase equilibrium of mixtures of CO₂ in hydrocarbons, water and glycols are of particular importance [3].

In this work, in an effort to improve current models and obtain a more physically correct model, a quadrupolar term, inspired by recent advances within SAFT, is proposed and combined with the well-known CPA EoS (Kontogeorgis et al. [4]). In this contribution

the new model is compared to other popular approaches for the prediction of binary VLE and LLE.

Specific Objectives

The purpose of the overall FTP project is to acquire a solid experimental and theoretical basis for understanding and addressing the problems of CO₂ and CO₂ hydrates, for the possible utilization of hydrate formation as a CO₂ capture technology.

More specifically a molecular thermodynamic model for CO₂ has been developed, based on the CPA EoS. The model includes a quadrupolar term which is based on a modification of expressions developed from statistical thermodynamics [5]. For the pure compounds a similar quadrupolar expression has been employed previously by Karakatsani et al. [6] while mixing and combining rules resemble those employed by e.g. Gubbins and Twu [7] as well as Jog et al. [8].

The model has first been tested for various pure compound bulk properties such as liquid densities, heat capacities, and the speed of sound. Secondly the model has been tested for binary mixtures containing CO₂ and alkanes, water and alcohols.

The model will also be tested for its ability to reproduce the experimentally observed excess properties such as the excess enthalpy and volume from binary mixtures and its ability to model ternary and possible quaternary mixtures of CO₂.

Finally the model will be incorporated in a van der Waals-Platteeuw theory for describing CO₂ hydrates.

Results and Discussion

Despite the importance of CO₂ containing mixtures, most equations of state still struggle with the predictions of the phase equilibrium of such mixtures [3]. A reason for this may be that traditional approaches such as the Soave-Redlich-Kwong (SRK) [9] EoS treat CO₂ as an inert. Even in modern equations of state such as the Statistical Association Fluid Theory (SAFT) only dispersive forces are usually considered. The continued use of such procedures may be attributed to the fact that the mixture behavior is (mostly) captured quite well when the model is adjusted with a relatively large interaction parameter (k_{ij}). The predictive nature of the models is lost in this way, however, and it is uncertain how well such procedures work when extended to mixtures with more than two components.

Other more pragmatic approaches tend to treat CO₂ as a self-associating (hydrogen bonding) or solvating molecule, such procedures often works well resulting in better correlations with smaller interaction parameters [3]. Unfortunately the improvement is obtained at the cost of additional pure component parameters and, in some cases, an extra parameter for the binary mixtures.

Rigorously, however, CO₂ has a large quadrupole moment (i.e. a concentration of charges at four separate points in the molecule). Quadrupolar forces are small short ranged forces relative to regular van der Waals forces; they may become important, however, for molecules with a significant quadrupole. This is believed to be the reason for the unusual phase behavior of mixtures of CO₂.

For these reasons several quadrupolar terms have been included within the SAFT framework, e.g. the quadrupolar models suggested by Gross [5] and Karakatsani et al. [6]. These terms are mainly based on the statistical mechanical theories for quadrupolar fluids developed by Stell and coworkers [5, 10, 11].

Inspired by the advances seen within the SAFT framework we have recently developed a new quadrupolar term which is directly applicable in equations of state such as the CPA EoS. The term is essentially a combination of the approach employed by Karakatsani et al. [6] for pure compounds with mixing rules similar to those employed by Jog et al. [8]. The form of the new term employed in this work does not add any additional adjustable parameters compared to CPA without association.

The CPA is an equation of state, which combines the simplicity of the SRK EoS with the association term from Wertheim's theory. The model is set in the Helmholtz energy as a summation of independent contributions from the SRK and association term respectively. Consequently the Helmholtz energy term of the CPA EoS is coupled with the quadrupolar term assuming that the energy terms are additive:

$$A^{res} = A^{SRK} + A^{Assoc} + A^{quad} \quad (1)$$

Equation 1 is used to combine the quadrupolar terms within the CPA framework.

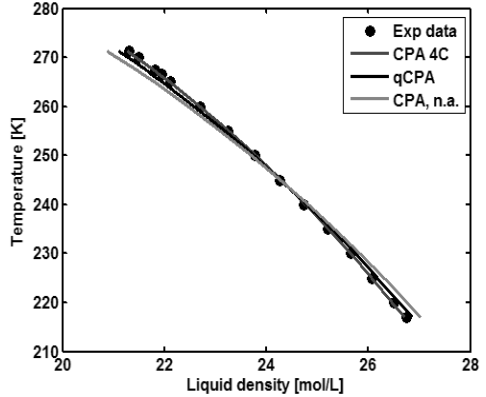


Figure 1: Model correlations to the experimental liquid density of CO₂. Circles are experimental data from [12].

In this contribution we compare three approaches to CO₂ using CPA; namely when CO₂ is treated as either an inert species (only A^{SRK} in Eq. 1 is non-zero), a self-associating species using the 4C association scheme ($A^{quad}=0$ in Eq. 1) or as a quadrupolar molecule employing the new quadrupolar term ($A^{Assoc}=0$ in Eq. 1). Typically pure compound parameters are fitted to saturated liquid densities and saturated vapor pressures. However, as Figure 1 illustrates the correlations to liquid density are almost equally good using the three different approaches to CO₂. CPA without association (n.a.) captures the data quite well, it does, however, deviate systematically at either endpoints Superior correlations are obtained when CO₂ is treated as an associating compound, but at the cost of two extra highly correlated adjustable parameters, on the other hand the quadrupolar term offers some improvement too, without the need for additional adjustable parameters. Table 1 shows the regressed parameters of the three approaches, and Table 2 shows their deviation from experimental data. The experimental value of the quadrupolar moment of CO₂ (4.3DÅ) is employed.

Table 1: Estimated pure compound parameters of the CPA using three different approaches for CO₂. Reduced temperature range: $T_r=[0.7-0.9]$.

Type	Γ [K]	b [mL /mol]	c_1	β	ϵ/R [K]	Ref
n.a.	1552	27.2	0.76	-	-	3
4C	1389	28.4	0.69	29.7	471	3
Quad	1318	27.9	0.68	-	-	This work

Obviously the improvement is most significant for the liquid density where deviations are reduced almost by an order of magnitude when CO₂ is treated as either an associating or quadrupolar species. However, we should keep in mind that the improvement is obtained at the cost of two extra adjustable parameters when CO₂ is

assumed to be self-associating. As the CPA EoS already correlates the data quite well, identification of ‘unique’ parameters may be an issue, since the data used for parameter estimation is sparse in relation to the model. That is, good agreement between correlated and experimental pure compound properties is not a sufficient condition for a good predictive model, but certainly a necessary one.

Table 2: Percentage absolute average deviations (AAD) from experimental data for CO₂ with the CPA using three different approaches for CO₂.

Type	%AAD in p^{liq}	%AAD in P^{sat}	Ref
n.a.	0.80	0.20	3
4C	0.10	0.07	3
Quad	0.07	0.12	This work

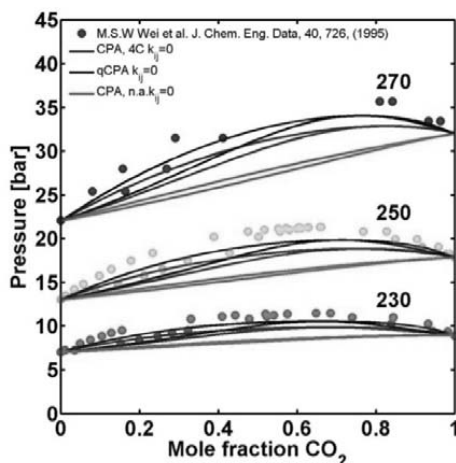


Figure 2 - Predicted ($k_{ij}=0$) VLE of CO₂+ethane at three temperatures (in Kelvin). Circles are experimental data from [13].

To evaluate the predictive capability of the quadrupolar term the VLE of a number of CO₂+hydrocarbon mixtures have been predicted based on the pure compound parameters only. That is, no interaction parameter is employed.

Using the three approaches for CO₂ Figure 2 and Figure 3 compares the predicted VLEs of the binary mixtures CO₂+ethane and CO₂+propane with experimental data.

It is clear from Figure 2 and Figure 3 that significant improvements can be obtained using either a quadrupolar term or CPA with association compared to the CPA without association. That is, without the quadrupolar term an almost ideal Raoult's law type VLE is predicted in Figure 2, while both other approaches predict the azeotrope, although at slightly lower pressures than experimentally observed.

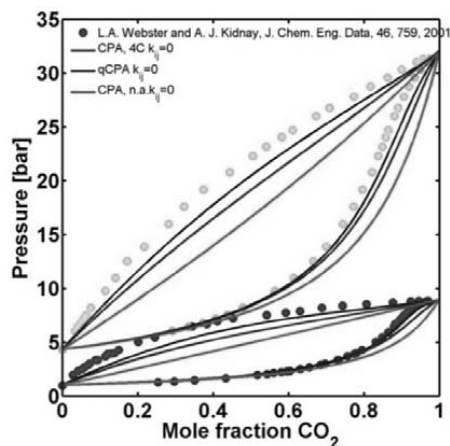


Figure 3: Predicted ($k_{ij}=0$) VLE of CO₂+propane at two different temperatures. Circles are experimental data from [14].

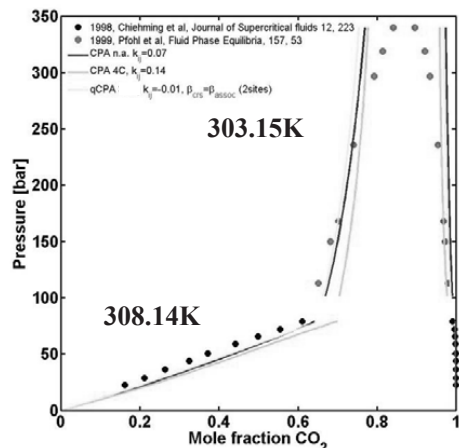


Figure 4 - Vapor liquid (308.14K) and liquid-liquid equilibrium (303.15K) of CO₂+nananol. Circles are experimental data from [15,16].

It is worth noting that in both cases CPA with the quadrupolar term results in slightly better predictions than CPA with association. That is, better predictions are obtained with a quadrupolar CPA although this model employs only 3 pure compound parameters, compared to the 5 parameters in the associating case. Another rigorous test for any equation of state is how well it can correlate liquid-liquid equilibria. Figure 4 show the vapor-liquid and liquid-liquid equilibrium of CO₂+nananol at two almost identical temperatures. A single interaction parameter has been correlated to the liquid-liquid equilibrium data for each model approach. It can be seen from the figure that all models correlate both the vapor-liquid equilibrium and the liquid-liquid equilibrium quite well, however, an interaction

parameter of almost zero is employed when CO₂ is correctly treated as a quadrupolar fluid, suggesting that the model can almost predict the equilibrium behavior of the system. When CO₂ is treated as an associating species, however, a very large interaction parameter is needed.

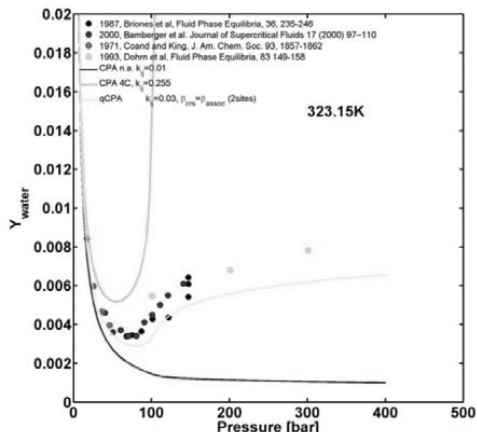


Figure 5 - Vapor and liquid equilibrium phases of the CO₂ rich phase of the mixture CO₂+water as a function of pressure (at 323.15K). Circles are experimental data from [17-20].

Another difficult but well-known binary is the VLE and LLE of CO₂+water. Figure 5 show the VLE and LLE of the CO₂-rich water+CO₂ phase (the water rich phase is correlated well for all approaches with the same interaction parameter). Again we see that the quadrupolar model is capable of representing this system using a single interaction parameter, whereas none of the other models are capable of this.

Conclusions

In an effort to improve the predictive capabilities of classic thermodynamic models for mixtures containing CO₂ a novel quadrupolar term have been proposed and combined with the CPA EoS. It has been found that the model may significantly improve the prediction of binary VLE of CO₂+hydrocarbon mixtures.

It has furthermore been found that the quadrupolar term is capable of accurately representing the LLE between CO₂ and higher alcohols, using a much smaller interaction parameter than the other approaches, suggesting that it represents a more physically realistic model.

Finally preliminary investigations suggests that the model is capable of modelling the CO₂-rich phase of the CO₂+water system using only a single, small, interaction parameter, something which is not possible with the other approaches without the addition of a second parameter.

Future work will focus on further validation of the model on multicomponent mixtures as well as in the prediction of excess properties.

Acknowledgements

The author is grateful to the Danish Research Council for Independent Research – Technology and Production Sciences and DTU for funding this project.

References

- O.-K. Nielsen, M.S. Plejdrup, M. Winther, M. Nielsen, S. Gyldenkærne, M.H. Mikkelsen, R. Albrektsen, M. Thomsen, K. Hjelgaard, L. Hoffmann, P. Fauser, H.G. Bruun, V.K. Johannsen, T. Nord-Larsen, L. Vesterdal, I.S. Møller, O.H. Caspersen, E. Rasmussen, S.B. Petersen, L. Baunbæk, M.G. Hansen, Denmark's National Inventory Report 2014, No. 101, Aarhus University, DCE – Danish Centre for Environment and Energy, 2014.
- D.F. Spencer, Methods of selectively separating CO₂ from a multicomponent gaseous stream, US Patent 5700311 (1997) and 6106595 (2000).
- I. Tsvintzelis, G.M. Kontogeorgis, M.L. Michelsen, E.H. Stenby, Fluid Phase Equilibria 306 (1) (2011) 38-56.
- G.M. Kontogeorgis, E.C. Voutsas, I.V. Yakoumis D.P. Tassios, Ind. Eng. Chem. Res 35(11) (1996) 4310-4318.
- B. Larsen, J. C. Rasaiah, G. Stell, Mol. Phys 33(4) (1977) 987-1027.
- E.K. Karakatsani, T. Spyriouni, I.G. Economou, AIChE Journal 51 (8) (2005) 2328-2342.
- K.E. Gubbins, C.H. Twu, Chem. Eng. Sci. (33) (1978) 863-878.
- P.K. Jog, S.G. Sauer, J. Blaesing, W. G. Chapman, Ind. Eng. Chem. Res. 40 (21) (2001) 4641-4648.
- G. Soave, Chem. Eng. Sci. (27) (1972) 1197-1203.
- G. Stell, J.C. Rasaiah, H. Narang, Mol. Phys. 27 (5) (1974) 1393-1414.
- G.S. Rushbrooke, G. Stell, J.S. Høye, Mol. Phys. 26 (5) (1973) 1199-1215.
- W. Duschek, R. Kleinrahm, W. Wagner, J. Chem. Thermodyn 22, (1990) 841-864.
- M.S. -W Wei, T.S. Brown, A.J. Kidnay, E.D. Sloan, J. Chem. Eng. Data, 40 (1995) 726-731.
- L.A. Webster, A.J. Kidnay, J. Chem. Eng. Data 46 (2001) 759-764.
- C. Chiehming, C. Kou-Lung, D. Chang-Yih, J. Supercrit. Fluids, 12 (1998) 223-237.
- O. Pfohl, A. Pagel, G. Brunner, Fluid Phase Equilib 157 (1999) 53-79.
- J.A. Briones, J.C. Mullins, M.C. Thies, B.-U. Kim, Fluid Phase Equilib, 36 (1987) 235-246.
- A. Bamberg, G. Sieder, G. Maurer, J. Supercrit. Fluids, 17, (2000) 97-110.
- A.D. King, C.R. Coan, J. Am. Chem. Soc. 93 (1971), 1857-1862.
- R. Dohrn, A.P. Büinz, F. Devlieghere, D. Thelen, Fluid Phase Equilibria, 83, (1993), 149-158.



Riccardo Boiocchi
Phone: +45 4525 2910
E-mail: ricca@kt.dtu.dk

Supervisors: Gürkan Sin
Krist V. Gernaey

PhD Study
Started: 01/10/2013
To be completed: September 2016

Plant-wide modelling and control for nitrous oxide emissions from wastewater treatment plants

Abstract

There is an increasing number of evidences showing that nitrous oxide (N_2O), a greenhouse gas with a global warming potential (GWP) 300 times larger than the one of carbon dioxide (CO_2) and an ozone-depleting substance, is emitted in a considerable amount from domestic wastewater treatment plants (WWTPs). For this reason, development of WWTP control strategies is nowadays focused on finding strategies that can accomplish the legal effluent quality standards while minimizing greenhouse gas emissions as well.

Introduction

Nitrous oxide (N_2O) is well-known as the dominant ozone-depleting substance and a harmful greenhouse gas with a global warming potential 300 times larger than the one of carbon dioxide [1]. In literature there is a substantial number of published evidences demonstrating that wastewater treatment plants treating mainly wastewater from households contribute considerably to the global N_2O emissions [2]. In particular, biochemical studies have shown that N_2O can be produced in the liquid phase during the biochemical processes responsible for biological nitrogen removal. These processes are: heterotrophic denitrification [3] and autotrophic nitrification [4, 5]. The first is the oxidation of the organic biodegradable matter with nitrogen compounds such as nitrate and nitrite as electron acceptors [6], whereas the latter is the oxidation of total ammonia nitrogen to nitrate with oxygen as electron acceptor [7]. There are many environmental parameters which affect the N_2O production during these two processes. For instance, with regard to heterotrophic denitrification it is well-known that a too high concentration of dissolved oxygen can lead to incomplete reduction of the previously-mentioned nitrogen compounds. As a consequence, an accumulation of N_2O , an intermediate in the reduction of nitrate to nitrogen gas, can occur [8]. Moreover, low availability of organic biodegradable carbon can lead to the same negative consequence [9]. With regard to autotrophic nitrification, oxygen is one of the main factors [10]. As a matter of fact, a lack of oxygen during autotrophic nitrification is shown to force ammonia-

oxidizing bacteria (AOB) to use nitrogen compounds as electron acceptors for ammonia nitrogen oxidation. In this case, N_2O is formed simply as a consequence of nitrogen compound reduction.

As can be deduced, accomplishing environmental conditions in the WWTPs that minimize the formation of N_2O is the route towards mitigating the emissions of N_2O . Process control is widely used to support achieving the legal effluent quality requirements of the WWTP. Up to now, several control strategies have been designed with control objectives such as maintaining the oxygen concentration at a set point, or maintaining the internal recycle proportional to the influent flow rate (ratio control), or keeping the ammonium effluent concentration below effluent limits. However, no specific control strategies have been designed for the minimization of the amount of N_2O emitted as the control objective. This PhD project aims at filling this gap.

Methodology

The development of control strategies will be performed on an extension of the Benchmark Simulation Model n°2 (BSM2). As a consequence, the preliminary step to be done before the control design will be to extend the BSM2. This extension will regard both the plant configuration and the description of the biochemical processes. In particular, the plant configuration will be extended with side-stream systems such as partial nitrification/Anammox process by Vangsgaard [11]. The Activated Sludge Model for Greenhouse gases n°1 by Guo and Vanrolleghem [12] will be used to include N_2O

production by both denitrifying heterotrophs and AOB. The new BSM will be used as reference for the development of the control strategies mentioned in the introduction. The first step for the design of a control strategy is to define its objectives and constraints. Here, the objective is the minimization of N_2O emitted. The definition of constraints has to deal with boundaries such as legal limits for the effluent and economic management chances. Afterwards, a process review has to be performed, which consists mainly in identifying, among the system inputs, the disturbances to be overcome through the control and the possible manipulated variables. A global sensitivity analysis is the next step, to analyze the effect of operating conditions on the system. Moreover, if the control strategy will involve more than one controlled variable, an analysis of the loop interactions will be made. Once the open loop assessment has been performed, the closed loop(s) control structure will be decided. It is worth to mention that there exist different kinds of controllers which can be used. There are for example Proportional Integral Derivative (PID) and fuzzy-logic controllers (FLCs). PID controllers provide a single control action on the basis of the predicted effect of the disturbances on the process. There are different tuning strategies which provide optimal values of PID controller parameters such as the Internal Model Control (IMC) which requires a linearization of the process model. The FLC design is based on expert knowledge and in this case there are no deterministic rules to tune the different parameters for an optimal control performance. However, for specific process systems it is important to determine the effect of the different tuning choices on the control performance, and to define the criteria to follow when making decisions during the fuzzy-logic control design. There is evidence showing that in cases such as wastewater control a fuzzy-logic controller can have better performance and has a better chance to be realizable compared to a PID controller [13]. For this reason, during this PhD project the fuzzy-logic control approach has been taken into consideration.

A fuzzy-logic control strategy has been recently developed and tested on a sequencing-batch reactor for single-stage partial nitrification/Anammox [14]. Based on a combination of measurements of the nitrogen species concentration in the influent and in the effluent on the one hand, and insights into the activities of three distinctive microbial groups on the other hand, the diagnosis provides information on: nitrification, nitration, anaerobic ammonium oxidation and overall autotrophic nitrogen removal. These four results give insight into the state of the process and are used as inputs for the controller that manipulates the aeration to the reactor. The diagnosis tool was first evaluated using 100 days of real process operation data obtained from a lab-scale single-stage autotrophic nitrogen removing reactor. This evaluation revealed that the fuzzy logic diagnosis is able to provide a realistic description of the microbiological state of the reactor with process

engineering insight analysis. An evaluation of both the diagnosis tool and the controller was done by simulating a disturbance in the influent concentration. High and steady nitrogen removal efficiency was achieved thanks to the diagnosis and control system. Finally, development of the diagnosis and control as two independent systems provided further insight into the operation performance, gives transparency towards the operator and makes the system flexible for future maintenance or improvements. Although the choice of some parameters is more intuitive and experience-based than mechanistic, it is important to note that wrong design decisions can lead to instances of low sensitivity or instability of the control system itself. For this reason, in order to improve the awareness of FLC designers regarding the impact of their decisions on the control response to disturbances, a study investigating the effect of FLC parameters on the control response has recently been started up. In particular, the FLC design parameters are being systematically modified in order to address how they affect the response of the controller. The results of this study will provide the FLC designers with relevant instructions regarding the decisions that need to be taken on certain parameters in order to achieve the desired control system response. N_2O control will be performed using the same structure of this FLC strategy.

References:

1. A. R. Ravishankara, J. S. Daniel and R. W. Portmann, *Science* 326 (2009) 123-125.
2. M. J. Kampschreur, H. Temmink, R. Kleerebezem, M. S.M. Jetten, M. C. M. van Loosdrecht, *Water Research* 43 (2009) 1093-1103.
3. K. Hanaki, Z. Hong, T. Matsuo, *Water Science and Technology* 26(5) (1992) 1027-1036.
4. L. J. Shaw, G. W. Nicol, Z. Smith, J. Fear, J. I. Prosser, E. M. Baggs, *Environmental Microbiology* 8(2) (2006) 214-222.
5. H. Zheng, K. Hanaki, T. Mtsuo, *Water Science and technology* 30(6) (1994) 133-141.
6. Knowles R. *Microbiological reviews* 46 (1) (1982) 43-70.
7. U. Wiesmann: *Advances in Biochemical Engineering Biotechnology* 51 (1994) 114-153.
8. S. Otte, N.G. Grobden, L. A. Robertson, m.S. Jetten, J. G. Kuenen, *Applied and Environmental Microbiology* 62(7) (1996) 2421-2426.
9. H. Itokawa, K. Hanaki, T. Matsuo *Water Research* 35 (3) (2001) 657-664.
10. M. J. Kampschreur, N.C.G. Tan, R. Kleerebezem, C. Picioreanu, M. S. M. Jetten, M.C: M. van Loosdrecht, *Environmental Science and Technology* 42 (2) (2008) 429-435.
11. A. K. Vangsgaard, PhD thesis (2013).
12. L. Guo and P. Vanrolleghem, *Bioprocess and Biosystem Engineering* 37 (2014) 151-163.
13. R. M. Tong, M. B. Beck, A. Latten, *Automatica* 16 (1980) 659-701.
14. R. Boiocchi, M. Mauricio-Iglesias, A. K. Vangsgaard, K. V. Gernaey and G. Sin, *Journal of Process Control*, accepted, (2014).



Andrijana Bolic
Phone: +45 4525 2958
E-mail: anb@kt.dtu.dk

Supervisors: Krist Gerneay
Anna Eliasson Lantz

PhD Study
Started: March 2010
To be completed: June 2015

Fermentation processes at small scale

Abstract

At present, research in bioprocess science and engineering requires fast and accurate analytical data (rapid testing) that can be used for investigation of the interaction between bioprocess operation conditions and the performance of the bioprocess. Miniaturization could result in a set of attractive tools necessary for obtaining a vast amount of experimental data in a short time. The main objective of this project is to develop a microbioreactor platform for continuous cultivations of *Saccharomyces cerevisiae*, where NIR spectroscopy could be further implemented for rapid on-line measurement of process variables like substrate and biomass.

Introduction

Conventional microbial cell cultivation techniques are not sufficient anymore considering the fast development of tools for genetic manipulation of biological systems resulting in large numbers of strains and conditions that need to be screened. Usually bench-scale reactors, flasks and tubes are used for obtaining relevant experimental data of microbial cultivations. Although bench-scale reactors have efficient control of process variables and yield valuable data, they are expensive, labor intensive and they provide a relatively small amount of data.

Beside the above-mentioned vessels, today, microtiter plates are increasingly used for screening experiments considering that they provide easy handling, low cost and high throughput. Nevertheless, the process control in microtiter plates is often not reliable enough to provide realistic numbers in view of later scale up which is affecting the overall value of data. Different reactor configurations and their positioning according to throughput and data quality are presented in Figure 1.

There is a big driving force and interest in the last decade for development of new techniques which could provide both high quality data and also a high quantity of experimental data. In recent years microbioreactors and other small scale systems have been researched intensely due to their clear advantages like small volume, little or no need for cleaning (one time usage), high throughput (multiple bioreactors in parallel), high information content and control capabilities [1]. Small scale systems together with analytical methods are providing the opportunity for a potentially automated and well defined experimental system, which can deliver results that are more comparable to bench-scale reactors in comparison to e.g. a shake flask.

Even though microbioreactors have many advantages, it is important to bear in mind that they also have issues related to their size and handling. Evaporation, proper and reliable stirring, interconnections between micro-scale features and the 'macro world' are just some of the burning problems that need to be solved. In addition, measurements of several process variables at small scale are not straightforward to implement. They rely on analytical

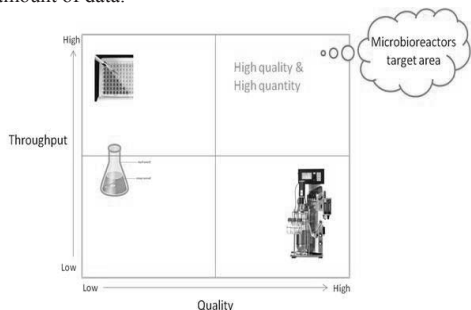


Figure 1: Different vessels (microtiter plates, flasks and bench-scale bioreactor) and their positioning according to throughput and data quality.

Regarding microbial cultivations in flasks and tubes, there is a general lack of control and the amount of data collected per experiment is usually not sufficient.

methods, which are not sufficiently developed for such a small scale at this point. If the measurements are possible, they are not cheap either.

Another important issue that needs to be addressed is determining the optimal working volume while keeping in mind the final objective – application. Does one need a sample or not? Does one talk about cells in suspension or adhered to a substrate? The final microbioreactor design should thus strongly depend on the goal of a specific microbioreactor application.

Micro- and milliliter scale reactor design

To address some of the previously mentioned questions, a bioreactor platform with 1-2 ml working volume is developed. Considerable effort is placed in development a system that could provide reproducibility and easy handling at a reasonable cost.

Platform

The reactor surrounding is equally important as the reactor itself. Keeping this in mind, a platform with gas connections, optical fibers for sensing, a specially designed heater and standard temperature sensor was designed and fabricated. It can be seen in Figure 2.

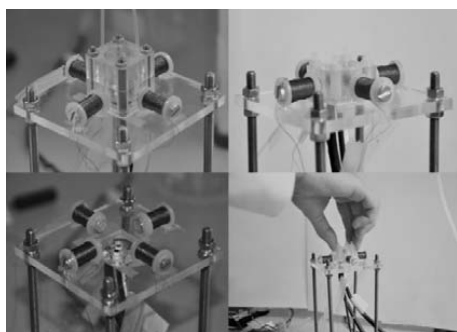


Figure 2: Microbioreactor together with platform

The reactor can be placed on a platform using a ‘Lego’ approach, which ensures reproducibility in sensing and establishing connections. Furthermore, this configuration lowers the cost per microbioreactor, considering that expensive parts of the system are reusable and placed in the platform, while the bioreactor is mostly made from cheap PMMA and has one magnetic ring and two sensor spots.

Reactor and stirrer design

The bioreactor, made in PMMA, consists of a bottom and one or two upper parts as shown in Figure 3. This enables change in volume, by adding or removing one of the upper parts. The bottom part is made as a negative to the platform and has a thin optically transparent layer to make sure that measurements based on optical sensing are possible (pH, DO, OD).

The top part is a cylinder with a shaft in the middle on which a magnetic stirrer is mounted. The bioreactor

can have two tubes for optional aeration (upper picture in Figure 3). Beside air sparging, there is also the possibility for exploiting surface aeration in which case aeration tubes are removed and connectors are made on the top of the microbioreactor (lower picture in Figure 3).

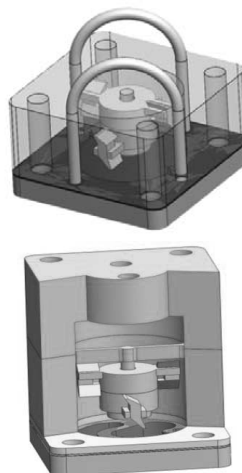


Figure 3: Two options for bioreactor design

The shaft is closed by a cap which prevents the stirrer to fall off from the shaft. The outer surface of the cap is covered with aluminum foil which serves as a mirror. Therefore, when light at 610 nm is sent into the reactor through a bundle of optical fibers, it is reflected by the aluminum foil and it reaches the detector. In this way the optical density is measured with a good linear range up to 20 g/L, which can be seen in Figure 4.

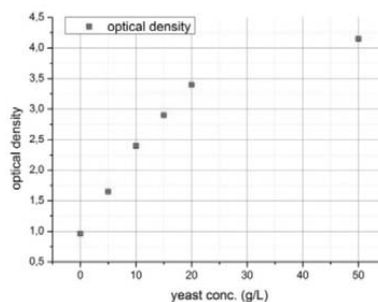


Figure 4: Measured optical density as a function of yeast concentration

The stirrer has two pairs of impeller blades placed at two levels, which can be seen in Figure 5. Each blade can be removed in order to create a different mixing behavior. A permanent magnetic ring, which is magnetized across its diameter, is placed inside the stirrer and is driven by a rotating magnetic field.

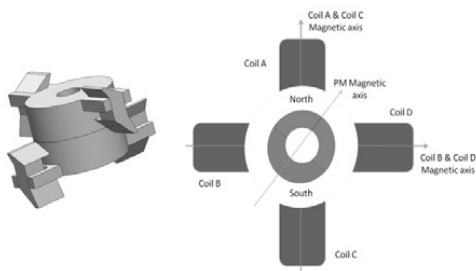


Figure 5: Stirrer design

Electromagnets were incorporated in the mixing device, in order to obtain control over the mixing by changing the speed and direction of the stirrer rotation. In this way, it is possible to prevent formation of a vortex without usage of baffles. The mixing device consists of a base fabricated by micromilling in PMMA (non-magnetic material and part of the platform), illustrated in Figure 2, on which 4 coils (electromagnets) are mounted. The coils are connected to a switch mode power supply, which is controlled by a PC running LabView software. The basic principle of the mixing control is presented in Figure 6.

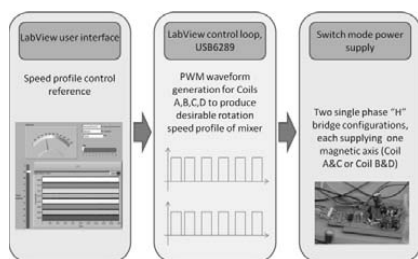


Figure 6: Mixing control principle

Results

The mixing capability of the microbio reactor was quantified by experiments where mixing time and volumetric mass transfer coefficient ($k_L a$) were evaluated against different stirrer rotational speeds.

The mixing time was determined by a colorimetric method based on acid-base reaction [2]. The change in color was filmed and the time needed to reach a homogeneous liquid phase was measured. Afterwards, the movie was analyzed frame by frame in order to determine the exact time when the color changed from pink to transparent. As expected, the mixing time in a 1 ml microbio reactor was significantly reduced with an increase of the rotational speed. Thus, 2 s mixing time at 200 rpm was reduced to 0.4 s at 1000 rpm, which can be observed in Figure 7.

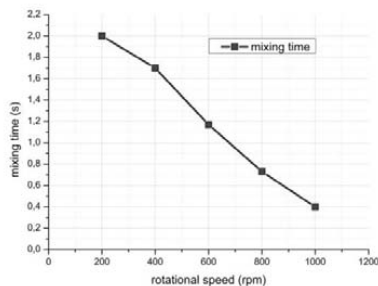


Figure 7: Mixing time at different rotational speeds

The volumetric mass transfer coefficient ($k_L a$) is one of the most critical parameters during aerobic fermentation processes. Therefore, the influence of air sparging, surface aeration, one- and bi-directional mixing on $k_L a$ value was evaluated using the gassing-out method [3,4]. First, nitrogen was continuously flushed through the medium until the oxygen concentration in the reactor dropped to zero. Subsequently, air was introduced and the change in the oxygen concentration was measured by a PreSens sensor spot at the bottom of the reactor. The response time of the DO sensor (t_1) was evaluated and it was taken into account during the development of best correlation for estimating the transfer of oxygen from air to water (t_2):

$$DO = A_1 \left(1 - (t_1 * \exp(-t/t_1) - t_2 * \exp(-t/t_2)) / (t_1 - t_2) \right); t_1 = 11.6s$$

The correlation between the volumetric mass transfer coefficient and the rotational speed during surface aeration, sparging and bidirectional mixing in a 1 ml microbio reactor is presented in Figure 8.

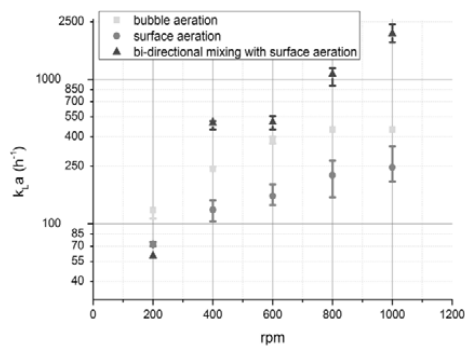


Figure 8: $k_L a$ values at different stirrer rotational speeds and aeration methods

The highest $k_L a$ values ($k_L a > 1000 \text{ h}^{-1}$) were obtained by bidirectional mixing in combination with surface aeration, where the spinning direction was changed every 2 s at different rotational speeds. In the case where air sparging with only one direction of

rotation was applied, the maximum $k_{L,a}$ value obtained was 450 h^{-1} , while with surface aeration the $k_{L,a}$ was around 300 h^{-1} . A larger difference between sparging and surface aeration was expected, but the size of the bubbles and the stirrer were not holding and dispersing bubbles sufficiently long in the liquid phase. Beside the mentioned parameters, the influence of viscosity and reactor volume on the $k_{L,a}$ was also examined and results are presented in Figure 9.

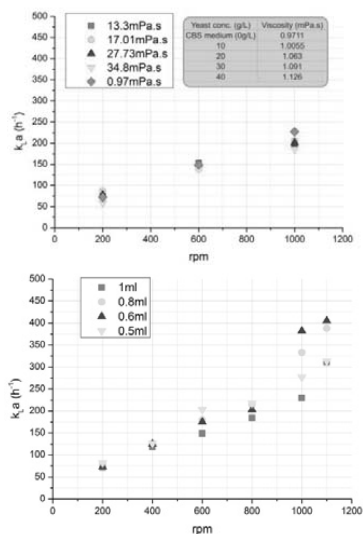


Figure 9: Influence of viscosity and reactor volume on the measured $k_{L,a}$

From the results presented in the upper graph of Figure 9, it is obvious that the influence of viscosity is negligible, especially for the cultivations with yeast. In the second graph of Figure 9, it can be seen that a decrease of the volume didn't have a major influence on the $k_{L,a}$ value, although this would be expected due to an increased surface to volume ratio. The major reason explaining this result is that the decrease of the volume in the reactor means that the stirrer is not completely submerged, and thus doesn't participate anymore in the mixing. The available surface for oxygen transfer doesn't change that much either due to the specific size and geometry of the stirrer.

After all mixing characterization and evaluation, a first series of cultivations and evaluation, a first series of cultivations were performed. An anaerobic batch cultivation with *Lactobacillus paracasei* as a model organism was performed. Comparison was made between 2 mL (batch 3 and 4) and 2L (batch CL0481-3E) scale. The end point measurements of glucose and lactic acid concentrations together with the optical density (OD) measurement are presented in Table 1.

The OD and lactic acid concentration values were significantly lower and the glucose concentration was higher after 10 and 11 hours in the 2 L fermentations

compared to the 2 mL fermentations. The same levels of OD, glucose, and lactic acid were achieved after 12 – 13 hours in the 2L fermentor. This could indicate that the lag phase of the 2 mL fermentations was shorter or that the growth in the exponential growth phase was faster.

Table 1: Cultivations at 2mL and 2L (CL0481-3E) scale [5]

Fermentation	Sample time (hours)	OD (external)	Glucose (g/L)	Lactic acid (g/L)
CL0481-3E	10	2.227	15.6	3.3
	11	3.397	14.9	5.3
	12	4.837	11.7	7.1
	13	6.577	8.70	9.9
	3	11	4.334	11.5
4	10	4.573	13.3	9.2

The first results regarding the application of the small scale reactor in fermentations with anaerobic cultivations are promising. Naturally, the next step is to test the whole system with aerobic cultivations, where evaporation can be a potential problem.

Conclusion

A flexible, disposable and cheap microbioreactor with supporting platform was developed. It has a small footprint. The system shows high level of flexibility:

- ✓ Surface or bubble aeration
- ✓ One- or bi- directional mixing
- ✓ Volume (0.5 - 2 mL)

The magnetic stirrer with adjustable geometry is low cost and maintenance free. It is a standalone mixing system, and consequently there is no need for external plate shakers and motors. Mixing can be considered almost instantaneous. Bi-directional mixing eliminates the need for baffles and drastically improves the $k_{L,a}$ value ($k_{L,a} > 1000 \text{ h}^{-1}$). The volumetric mass transfer coefficient obtained by surface aeration is sufficient for a standard fermentation.

Acknowledgements

This project is supported by the Danish Council for Strategic Research in the frame of the project "Towards robust fermentation processes by targeting population heterogeneity at microscale" (project number 09-065160).

References

1. D. Schäpper, M. N. H. Z. Alam, N. Szita, A. E. Lantz, K. V. Gernaey, Anal. Bioanal. Chem. (2009) 395:679–695
2. Paul, EL.; Atiemo-Obeng, VA.; Kresta, SM. Handbook of Industrial Mixing: Science and Practice, John Wiley & Sons, 2004
3. Suijdam JCV, Kossen NWF, Joha AC. Biotechnol Bioeng XX: (1978)1695–1709
4. Stanbury PF, Whitaker A, Hall SJ. Principles of fermentation technology: Oxford, UK: Elsevier Science Ltd. 1995, Pp 243-253
5. R.A.Prior, T.Vilby. Validation of 2 mL microbioreactors and near-infrared spectroscopy monitoring, bachelor thesis, 2012, DTU



Hande Bozkurt

Phone: +45 4525 5510
 E-mail: hboz@kt.dtu.dk

Supervisors: Gürkan Sin
 Krist V. Gernaey

PhD Study
 Started: December 2011
 To be completed: December 2014

An Optimization Based Framework for Design and Retrofit of Municipal Wastewater Treatment Plants: Case study on side-stream nitrogen removal technologies

Abstract

Wastewater treatment plant (WWTP) retrofitting problem has become a complex integrated decision making task with a number of aspects being contemplated in the early stage decision making. In this study, a superstructure optimization concept based on mathematical programming is used to manage multi-criteria WWTP retrofit problem and generate optimum network designs for domestic WWTPs. A case study, concerning a retrofitting study of an existing WWTP in Copenhagen region is formulated in order to highlight the use of the framework.

Introduction

Existing wastewater treatment plants (WWTP) need retrofitting due to several different reasons such as: change in the wastewater flow and composition, change in the influent limitations as well as changes in the wastewater treatment trends. For instance, increased nitrogen limitation in the regulations gave rise to the development of innovative nitrogen removal technologies mostly used for water stream resulting from sludge treatment. Similarly, recovery possibilities for clean water, energy and materials shifted the perception about wastewater towards being a valuable resource rather than being a waste. Therefore, process synthesis, which is the step in the design of a WWTP where the unit processes from a number of alternatives are selected and the interconnections are defined; has become a complex integrated decision making task (i.e. addition of a new task to the existing treatment line or change of one or several units as a result of emerging needs).

The Framework

The mathematical programming based optimization theory developed for chemical process synthesis [1] was modified and adapted in the context of the WWTP design/retrofitting problem. The framework is illustrated in Figure 1 and the details of the framework can be found elsewhere [2]. After defining the wastewater characterization, sink limitations and objective function in the first step, one can define a superstructure consisting of the base case of the existing WWTP (i.e.

only in the retrofitting studies), and other alternative technologies under the existing or new treatment tasks. The structure of the superstructure is then finalized by formulating the feasible connection streams between treatment tasks. Each treatment unit in the superstructure is structured using a generic model based on mass input-output, which is defined by a database containing the data to define the parameters of the model, e.g. process performances, utility consumptions, volumes and sludge production. The optimal wastewater network problem is then formulated as a mixed integer (non)linear programming (MI(N)LP) problem and solved for deterministic case and under uncertainty by defining several different scenarios.

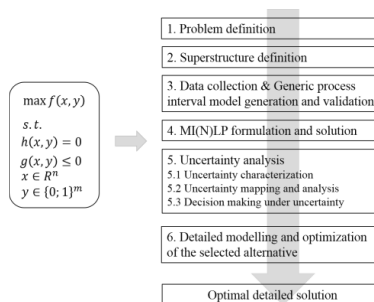


Figure 1: The superstructure based optimization methodology

Case Study

Avedøre WWTP is located west of Copenhagen, Denmark and receives wastewater from 10 suburban municipalities with a population of app. 265,000 people. The retrofitting problem is defined so that the feasibility of extending the existing treatment line of the WWTP (shown in gray highlights in Figure 2) will be analyzed by the proposed methodology by adding a new task for nitrogen removal and several alternative technologies.

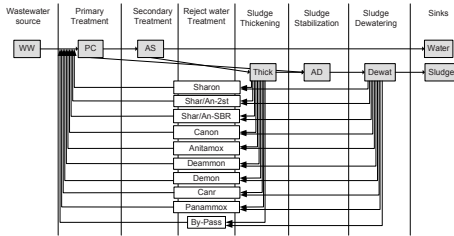
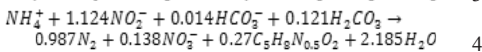
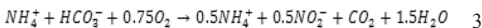
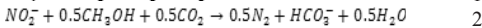
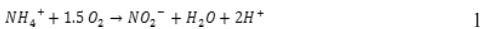


Figure 2: Avedøre WWTP superstructure

The base line is responsible for treating organics, nutrients (i.e. mainly N and P) and solids in the water line by primary clarifier (PC) and activated sludge type of treatment unit (AS); and sludge line consists of sludge stabilization and dewatering units (in the sequence of thickening, anaerobic digestion and dewatering). On the other hand, the nitrogen removal alternatives added in the reject water line, which comprises 10-20 % of the total nitrogen load into the system, works based on two mechanisms: nitrification/denitrification (Sharon) and partial nitrification/anammox (all the other alternatives). The stoichiometry of the corresponding mechanisms are given below in equations 1 and 2 for nitrification/denitrification and 3 and 4 for partial nitrification/anammox. The stoichiometry is used to define the utility consumption (i.e. aeration and methanol addition needs) as well as conversion among nitrogen components.



The different treatment alternatives are designed based on the reported performance information for different scale applications from open literature. Accordingly, the sizing of the technologies are made based on either hydraulic retention time (HRT) or volumetric loading/removal rate of nitrogen in the system. The nitrogen removal efficiency on the other hand, is calculated from the reported system performances. The details for partial nitrification anammox technologies are given in Table 1. Sharon reactor is designed by

assuming 1 day HRT and 86% and 60% efficiency for two reactions defined in Eq. 1 and 2 [3].

Table 1: Design data for partial nitrification/anammox alternatives [4]

Treatment alternative	Vol. N loading/removal rate (kg N / m ³ .d)	Efficiency - % (Total N removal)
Shar/An-2st	10	50 and 80 for 2 stages
Shar/An-SBR	0.55	90
Canon	1.5	81
Anitamox	0.8	85
Deammon	0.3-0.5	70
Demon	0.6	90
Canr	0.75	96
Panamnox	1.8 & 0.46	86

Results and Discussion

When the deterministic optimization problem is solved, 'Canon' technology is selected by the optimizer and the results comparing the base case with the selected alternative in terms of different cost items are summarized in Table 2. Accordingly, the utility cost decreased due to less oxygen consumption of the partial nitrification / anammox route as compared to the AS technology's nitrification/denitrification route. Moreover, although not very significant, the total effluent nitrogen concentration seem to decrease.

Table 2: Results of the Avedøre case study

	Utility cost (unit cost)	Landfill cost (unit cost)	Capital cost (unit cost)	OBJ (unit cost)	Eff. Total N (g N/m ³)
Base case	372.5	1898.8	-	907.9	5.99
Canon	363.3	1897.9	8.083	906.2	5.50

Conclusion

A mathematical programming concept has been introduced in this study to support the early stage decisions on WWTP network selection. By casting the problem as an optimization problem, the decision on which technology to employ is rendered on quantitative metrics which complements the experience based approach used today. Hence the tool is expected to support and facilitate generation and evaluation of ideas for identifying optimal solutions to design new or retrofit existing WWTPs.

References

1. A. Quaglia, B. Sarup, G. Sin, R. Gani, Computers & Chemical Engineering, 38 (2012) 213-223.
2. H. Bozkurt, A. Quaglia, K.V. Gernaey, G. Sin, Computer Aided Chemical engineering, 33 (2014) 37-42.
3. C. Hellings, A.A.J.C. Schellen, J.W. Mulder, M.C.M. van Loosdrecht, J.J. Heijnen, Water Science and Technology, 37 (9) (1998) 135-142.
4. Z. Hu, T. Lotti, M.C.M. van Loosdrecht, B. Kartal, Biotechnol. Lett. 35 (2013) 1145-1154.



Andreas Brændholt
Phone: +45 20823870
E-mail: andbr@kt.dtu.dk
Discipline: Ecosystem research

Supervisors: Kim Pilegaard
Andreas Ibrom
Klaus Steenberg Larsen

PhD
Started: March 2014
To be completed: February 2017

Partitioning between Heterotrophic and Autotrophic Forest Respiration by Means of Stable Isotopes

Abstract

The traditional methods used to measure CO₂ fluxes in terrestrial ecosystems do not distinguish between the two individual processes of autotrophic respiration (R_A) and heterotrophic respiration (R_H). Knowledge of these processes and their rates is however extremely important, because the exchange rates of carbon between the atmosphere and the terrestrial ecosystems are about 20 times larger than the anthropogenic emission of carbon. The PhD project aims at developing a new experimental method that will make it possible to separate R_A and R_H . The new method will be used to yield data of the two processes at a high temporal scale that will be used to develop, parameterise and validate process based models that can be used to predict future rates of CO₂ exchange and carbon sequestration in soil and biomass.

Introduction

The exchange rates of carbon between the atmosphere and the terrestrial ecosystems are about 20 times larger than the anthropogenic emission of carbon [1]. It is therefore clear that natural ecosystems play an important part in the global carbon cycling both at current and future climate [2, 3]. In order to parameterize models of the fluxes of carbon and the carbon sequestration in the biomass and soil, actual data of the fluxes and pools of carbon are needed. Currently knowledge of the two independent processes R_A and R_H are lacking. This PhD project focuses on the partitioning of these two processes in the soil of the Sorø beech forest long-term CO₂ flux observation field site [4, 5]. This site has served as the basis for continuous long-term measurements of fluxes of CO₂ by eddy covariance since June 1996 [6].

Specific Objectives

The PhD project has three main scientific objectives:

1. Collection of respiration data
2. Up-scaling of chamber fluxes and synthesis of carbon fluxes
3. Development of respiration models

1. Collection of respiration data:

In the first part of the project fluxes from leaves, stems, roots, litter, and soil will be studied by combining chamber CO₂ flux measurements with real-time isotopic C and O laser spectroscopy.

An automated multiplexed soil chamber system (Li-8150) will be set up to measure CO₂ fluxes from intact soil, root-free soil, tree stems and isolated coarse roots continuously over 1 year. To estimate the contribution of R_A to the total respiration of the intact soils, half of the plots will be trenched. This will effectively cut of the photosynthate flow to the roots, thereby suppressing R_A in the trenched plots.

The multiplexed Li-8150 chamber system will be coupled to a new quantum cascade laser (Aerodyne QCL for CO₂ isotopes). This will allow for continuous measurement of the isotope ratios of ¹³C/¹²C and ¹⁸O/¹⁶O of the CO₂ fluxes for each respiration component.

To get information on how the fluxes vary across the site and in relation to differences in the soil C stock at the site, the continuous isotope flux measurements is supplemented by measurements of soil respiration every two weeks. Data of the fluxes at the site will thereby both be collected at a high spatial and temporal scale.

In the last part of the data collection, the isotopic signature of CO₂ respired from the soil will be studied for different soil layers at the four seasons throughout a year. During each of the four seasons the ¹³C/¹²C ratios in the respired CO₂ will be measured in 15 soil plots.

Following this each soil plot will be separated into litter, roots and soil from 3 distinct soil layers. For each fraction the $^{13}\text{C}/^{12}\text{C}$ ratios in the respired CO_2 will be measured by incubation in gas sample bags. Furthermore the $^{13}\text{C}/^{12}\text{C}$ ratios of the solid sample for each fraction will be measured by mass spectrometry.

By trenching and the isotopic approach it will be possible to have a dual-constraint for partitioning R_A and R_A from the soil.

2. Up-scaling of chamber fluxes and synthesis of carbon fluxes:

The data collected in the first part will be combined with data from repeated carbon inventory, canopy photosynthesis and ecosystem scale turbulent flux measurements that has also been collected from the experimental site. This will yield carbon budget estimates from each approach.

The carbon budget yielded from the different methods will be compared and the flux-data will be used to scale up fluxes of CO_2 to ecosystem level by using biometric data together with a 3D canopy model [7, 8]. These simulations will be used to test the hypothesis that the availability of substrate plays an important role in controlling the rate of autotrophic and heterotrophic respiration. [9].

3. Development of respiration models:

In the last part of the project various respiration models will be developed. The models will incorporate photosynthetic rates from a model of photosynthesis, and their performance will be compared to more classical respiration models.

Consistency between the independent estimates of the annual carbon budget of the forest for the different approaches will be investigated, and a Monte Carlo simulation technique will be used to find the most likely value and its uncertainty.

The model will be used to investigate the climate sensitivity of the carbon processes and the annual C budget, and by incorporating climate projections for Denmark during the next 90 years, simulations of the future carbon processes in the forest will be run.

These simulations will be used to evaluate if it is likely to retain the stored pools of carbon in soil and standing biomass under climate change. Finally it will be investigated whether forests are a source or sink for CO_2 under climate change.

Acknowledgements

The PhD project is partly founded by The Danish Council for Independent Research, Natural Sciences.

References

1. IPCC: Climate Change 2007: Mitigation. Contribution of Working Group III to the Fourth Assessment Report of the Intergovernmental Panel on Climate Change. Cambridge, Cambridge University Press.

2. C. Huntingford, J. A. Lowe, B. B. Booth, C. D. Jones, G. R. Harris, L. K. Gohar, P. Meir. Contributions of carbon cycle uncertainty to future climate projection spread. *Tellus B* 61(2) (2009) 355-360.
3. A. Arneeth, S. P. Harrison, S. Zaehle, K. Tsigaridis, S. Menon, P. J. Bartlein, J. Feichter, A. Korhola, M. Kulmala, D. O'Donnell, G. Schurgers, S. Sorvari, T. Vesala. Terrestrial biogeochemical feedbacks in the climate system. *Nature Geosci* 3(8) (2010) 525-532.
4. P. Formánek, P. Ambus. Assessing the use of $\delta^{13}\text{C}$ natural abundance in separation of root and microbial respiration in a Danish beech (*Fagus sylvatica* L.) forest. *Rapid Communications in Mass Spectrometry* 18(8) (2004) 897-902.
5. P. Millard, A. J. Midwood, J. E. Hunt, M. M. Barbour, D. Whitehead. Quantifying the contribution of soil organic matter turnover to forest soil respiration, using natural abundance $\delta^{13}\text{C}$. *Soil Biology and Biochemistry* 42(6) (2010) 935-943.
6. K. Pilegaard, A. Ibrom, M. S. Courtney, P. Hummelshøj, N. O. Jensen. Increasing net CO_2 uptake by a Danish beech forest during the period from 1996 to 2009. *Agricultural and Forest Meteorology* 151 (2011) 934-946.
7. B. Medlyn, A MAESTRO retrospective.in: *Forests at the Land-Atmosphere Interface*. M (2004).
8. A. Ibrom, P. G. Jarvis, R. B. Clement, K. Morgenstern, A. Oltchev, B. Medlyn, Y. P. Wang, L. Wingate, J. Moncrieff, G. Gravenhorst. A comparative analysis of simulated and observed photosynthetic CO_2 uptake in two coniferous forest canopies. *Tree Physiology* 26(7) (2006) 845- 864.
9. K. S. Larsen, A. Ibrom, C. Beier, S. Jonasson, A. Michelsen. Ecosystem respiration depends strongly on photosynthesis in a temperate heath. *Biogeochemistry* 85(2) (2007) 201-213.



Albert Camós Noguera

Phone: +45 4525 2829

E-mail: alno@kt.dtu.dk

Supervisors: Søren Kiil
Søren Hvilsted
Stefan Olsen, Hempel A/S

Industrial PhD Study

Started: December 2013

To be completed: December 2016

Design of Hydrophilic Polymers for Activated non-Fouling Coatings

Abstract

Biofouling accumulation on ship-hulls is a key problem that results in negative consequences, both economic and environmental. The increased drag resistance due to the presence of the fouling cause increased fuel consumption and thus higher expenses and higher release of CO₂ among others. Therefore, one of the main objectives of the coatings industry is the development of protective coatings that avoid the process of fouling on ships. Traditional solutions are based on the presence of large amounts of biocides that, upon release, keep the hull free of fouling. Nevertheless, this solution has not been satisfactory due to the release of high toxicity biocides to the seawater and the consequent effects. Thus, Hempel A/S has developed recently a series of products based on a technology that reduces significantly the amount of biocide release (up to 95% compared to traditional antifouling coatings) while prolonging the fouling release properties of these coatings. These contain a modified silicone polymers, which are added to traditional silicone coatings. These polymers saturate the surface upon immersion and provide the aforementioned antifouling effect with a much lower release of biocides. It is believed that this technology has an important potential and is the focus of this study. Understanding the working mechanism and discovering ways to prolong its effects are the main objectives to be assessed.

Introduction

Accumulation of biofouling on ship-hulls has adverse effects for the ship operator and the environment. The increase in skin friction that arises from the roughness inflicted by the fouling organisms, increases fuel consumption significantly. Heavily fouled ships may need to increase shaft power with up to 86% to compensate for the speed loss inflicted by the increased drag resistance [1]. Historically, fouling has been combatted by antifouling coatings, and these have generally contained high amounts of biocides. It is estimated that 3,000 tonnes of copper are released to the marine environment every year by antifouling coatings [2]. An alternative to biocide-based antifouling coatings is the fouling release coatings, which traditionally do not contain any biocides. Generally fouling release coatings are characterised by being smooth, flexible, and having a low surface-energy [3]. Therefore, the strength of adhesion of an adhered biofouling organism is low, and flexibility of the substrate allows for the motion of seawater to peel off the organism during operation of the vessel. Presently, fouling release coatings have a market share of about 6% [4].

In 2008 Hempel A/S invented a hydrogel-based fouling release coating. To increase biofouling resistance, it

contains a hydrophilic modified silicone polymer that migrates to the surface upon immersion and creates a hydrogel layer [5]. Hydrogels offer a significant improvement to the performance of fouling release coatings. However, fouling still eventually accumulates on these coatings.

Therefore, there has been a need for prolonging and improving the deterring properties of fouling release coatings.

Biocide-release from fouling release coatings has, until recently, not been possible due to:

- Only low amounts of biocides can be used to maintain surface smoothness.
- A very rapid release of biocides from the silicone matrix.

With this new technology, however, the tightly bound water of the hydrogel layer on the surface effectively hinders biocides from diffusing through the hydrogel-layer. Thus, the biocide is temporary trapped at the surface of the coating where it meets the fouling organisms. This happens without increasing the overall release of biocide to the environment. In fact, these coatings only release around 5% of the amount of biocide release by conventional antifouling coatings. These coatings became commercial in September 2013.

Because the biocides are completely ineffective without the hydrogel, the hydrogel-generating polymers become the key to the further optimization of the biocide containing coating. Unveiling the working mechanism by finding the relation between the hydrogel chemistry and the biocide, and monitoring the fate of these two components, are the keys to improvement of the technology. Prolonging the performance of the hydrogel-based technology will be applicable in both biocide-free and biocide-containing fouling release technology. Because these coatings improve fuel efficiency, while having very little to no release of biocide, the improvement of hydrogel-polymers is considered the most efficient way of making shipping greener from a hull-coatings perspective.

Specific Objectives

The overall aim of this project is to develop new polymers that will improve and prolong the performance of fouling release coatings. In order to achieve this, the project is divided into three tasks. A first task, concerned with monitoring the fate of the modified silicone polymer responsible for the hydrogel-effect of the coatings. A second task concerned with the combinatorial design of optimal polymers. And a third task focused on the synthesis and testing of novel optimised polymers.

For the initial step of the project, advanced analytical techniques are being applied to monitor the distribution and fate of the modified polymers. This will allow for in-depth understanding of a technology that has been developed primarily by trial and error, as such the findings will be very relevant for the research community dealing, not only with marine antifouling, but also with non-fouling surfaces in all applications. The knowledge generated during this project) will allow for a greater understanding on the mechanisms involved in the current state-of-the-art of fouling release coatings. Subsequently, hydrophilic polymers will be designed based on compatibility with silicone-based binders, effect of hydrogels formed, and stability during exposure to the marine environment.

Finally, entirely new polymers or oligomers will be synthesised and tested for their impact on coating performance and stability. These results will most likely be adaptable by other research communities dealing with hydrogels as non-fouling surfaces (e.g. biomedical or conservation).

Conclusion

Avoiding accumulation of biofouling on ship-hulls in a more environmentally friendly manner has become a very relevant topic in the last few years. The reasons are diverse: while low consumption of fuel reduces the costs of transportation and CO₂ emissions, low/non toxicity of ship coatings avoid negative consequences for the marine environment.

The efforts in improving the technology that Hempel A/S developed in 2008 are the key to achieve better products, both in economic and environmental terms.

To that purpose, the objectives of this project will focus on two aspects. The first one is a deep understanding of the processes taking place in these coatings. This will make the second possible, that is, develop a product with extended and upgraded properties.

That will lead to a more eco-friendly technology that will be profitable both from an economic and environmental point of view.

References

1. M. P. Schultz, *Biofouling* 23 (5) (2007) 331-341.
2. D.M. Yebra, S. Kiil, K. Dam-Johansen, *Progress in Organic Coatings* 50 (-) (2004) 75-104.
3. D.M. Yebra, P. Catalá, *Redifining Fouling Control Technology*, Report No. Nov 2010, The Naval Architect, 2010.
4. S. V. Karunanidhi, *Strategic Analysis of the Global Market for Marine Coatings*, Report No. M861-39, Frost and Sullivan, 2012.
5. D.M. Yebra, P. Catalá, *Smooth Operator*, Report No. Jan 2011, The Naval Architect, 2011.



Gerard Capellades Méndez
Phone: +45 4525 2923
E-mail: gcap@kt.dtu.dk
Discipline: Continuous pharmaceutical production

Supervisors: Søren Kiil
Kim Dam-Johansen
Troels V. Christensen, H. Lundbeck A/S
Michael J. Mealy, H. Lundbeck A/S

PhD Study
Started: September 2014
To be completed: September 2017

Continuous Crystallization and Filtration of Active Pharmaceutical Ingredients and Intermediates for Pharmaceutical Production

Abstract

The pharmaceutical industry, which is traditionally using batch processes, has recently turned focus towards continuous production with the desire of remaining competitive in an industry with increasing challenges. As part of the development of a fully continuous process at H. Lundbeck A/S, the objective of this project is to design and optimize a versatile crystallization and filtration unit that can be integrated in several continuous processes for the isolation of a solid compound with a specified purity and particle size distribution.

Introduction

The production of Active Pharmaceutical Ingredients (APIs) is performed primarily in batch processes. This has arisen for historical reasons and is reinforced by the regulatory environment and the need to rapidly release new products to the market once they are patented. However, the regulatory and business environments are now changing. New products are becoming more expensive and time consuming to discover, develop and launch to the market, and competition from generic manufacturers is becoming increasingly intense. The life of a patent is finite and generally more than half of the patent life of a new drug is spent before the product is launched. Once the patent protection has been terminated it is typical for the original manufacturer to lose up to 90% of their market share to generic manufacturers within 12 months [1]. Hence there is an increasing research interest for cost reduction in the pharmaceutical industry.

Continuous processes enable the use of smaller and safer equipment, in-line monitoring of process conditions and real-time product release with consistent quality. In addition, the amount of waste and the energy consumption are reduced as heating/cooling and recycle streams are handled more efficiently [1–3]. Several research projects have recently been carried out between DTU Chemical Engineering and H. Lundbeck (Lumsås) with the aim of developing fully continuous manufacturing processes.

Crystallization plays an important role in the pharmaceutical industry, both in the purification of intermediates and as most of the APIs are delivered in a

crystalline form [4]. The objectives behind crystallization are usually the isolation of a compound with the desired purity and the recovery of the crystalline material with the right crystal form and Particle Size Distribution (PSD). Control of crystal size, shape and crystal form is crucial as they can influence downstream operations such as filtration, drying and milling [5]. Furthermore the dissolution rate of the API, which is directly related to its particle size, will have an influence on the bioavailability of the drug. Crystal specifications in pharmaceutical production are often very strict and demand the use of controlled crystallization and filtration steps.

In spite of the wide-spread use of crystallization, a clear understanding of its thermodynamic, kinetic and hydrodynamic aspects is not yet well established. Advances in chemical synthesis have achieved control over drug identity and purity, but control over the physical form and crystallinity remains poor [6–7].

Specific objectives

This project is conducted in cooperation with H. Lundbeck A/S. The objective is to design a versatile crystallization and filtration unit that can be used in continuous production for isolation of different APIs and intermediates.

The studied compounds will be existing pharmaceuticals that are currently isolated using batch crystallization and filtration. Ideally, the versatile unit should also be able to accomplish the recovery of other compounds, reducing the time required for process development and fastening the release of a new drug.

The upcoming research is expected to include the following steps:

- Experimental characterization of a given set of pharmaceuticals according to crystallization thermodynamics and kinetics.
- Design of a versatile crystallization unit. Crystallization objectives will be focused on particle size distribution, crystal purity and separation of a desired isomer.
- Design of an appropriate continuous filtration unit for effective separation of the crystallized pharmaceuticals.
- Integration and optimization of the crystallization and filtration steps, based on selected model compounds.

Results and discussion

Crystal purity and particle size distribution are directly related to crystallization kinetics. For a given step recovery, the obtained crystals will have different characteristics depending on whether the process conditions promote nucleation or crystal growth. Fig. 1 shows the effect of the supersaturation ratio (crystallization driving force) on nucleation and growth kinetics. Different overall crystallization kinetics as well as different PSDs in the final product are expected depending on the supersaturation in the crystallizer.

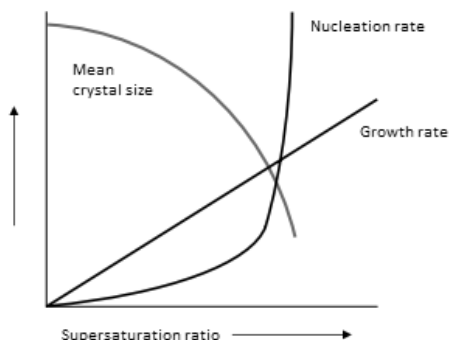


Figure 1: Qualitative effect of the supersaturation ratio on crystallization kinetics. Modified after Tung et al [8]

Other process conditions such as agitation intensity, impurities and even the size of the particles in the crystallizer have a significant effect on crystallization kinetics. A versatile crystallization unit is expected to be able to operate with a wide variety of process conditions so that the optimal parameters can be found for each given set of specifications.

Quantification of nucleation and growth kinetics at different operating conditions should give the basis for optimization of the designed unit. For each compound, process conditions will be adjusted so that crystal requirements are met.

Conclusions

Transition from batch to continuous production is currently one of the important research areas in the pharmaceutical industry. Continuous crystallization and filtration of pharmaceuticals will be investigated during this project as a necessary step for the development of a fully continuous pharmaceutical process. It is expected that a versatile crystallization unit should be able to operate under a wide variety of process conditions. From precise kinetic data on crystallization of a target compound, process conditions in the versatile unit can be optimized to meet its crystallization requirements.

Acknowledgements

The project is done in cooperation between DTU – CHEC and H. Lundbeck A/S (Lumsås). I would like to acknowledge both entities for their financial support as well as the project supervisors for their useful suggestions.

References

1. K. Plumb, *Chemical Engineering Research and Design* 83 (6) (2005) 730-738.
2. K. M. Christensen, M. J. Pedersen, K. Dam-Johansen, T. L. Holm, T. Skovby, S. Kiil, *Chemical Engineering Science* 71 (2012) 111-117.
3. S. D. Schaber, D. I. Gerogiorgis, R. Ramachandran, J. M. B. Evans, P. I. Barton, B. L. Trout, *Industrial and Engineering Chemistry Research* 50 (17) (2011) 10083-10092
4. A. J. Alvarez, A. S. Myerson, *Crystal Growth and Design* 10 (5) (2010) 2219-2228
5. J. Chen, B. Sarma, J. M. B. Evans, A. S. Myerson, *Crystal Growth and Design* 11 (2011) 887-895.
6. S. Vedantam, V. Ranade, *Sādhanā* 38 (2013) 1287-1337.
7. B. Yu. Shekunov, P. York, *Journal of Crystal Growth* 211 (1-4) (2000) 122-136
8. Hsien-Hsin Tung, Edward L. Paul, Michael Midler, James A. McCauley, *Crystallization of Organic Compounds: An Industrial Perspective*, John Wiley & Sons, inc., 2009, p. 78.



Krishna Hara Chakravarty

Phone: +45 4525 4637
E-mail: krich@kt.dtu.dk

Supervisors: Kaj Thomsen
Philip Loldrup Fosbøl

PhD Study: (Smart Water Project)

Started: September 2012

To be completed: August 2015

Microscopic simulation of wettability alteration during smart water flooding on chalk reservoirs

Abstract

Microscopic analysis of Smart water flooding has been conducted using Density Functional Theory (DFT) based molecular dynamic simulation. Herein simulations for feasible surface reactions; based on free energy profiles for different combinations of water, metal ions (Ca^{2+} , Sr^{2+} and Mg^{2+}) and hydrocarbons was conducted. The study shows both: (1) stability of the water film through adsorption of hydrated ions and (2) desorption of carboxyl compounds at higher temperature together lead to enhanced oil recovery.

Introduction

Carbonate/chalk oil reservoirs, in both the North Sea and the Middle East, have been flooded with modified seawater to attain sufficient recovery [1]. Some studies claim the sulfate in seawater acts as a reagent for desorbing carboxylic material from the carbonate surface [2], while others find the effect of sulfate to be very core specific [3]. But there is no microscopic model to explain this phenomena.

Specific Objectives

In order to address the phenomenon at microscopic scale and exploring the principles to this theory, a platform needs to be developed on a strong mathematical basis. In this work the calcite bulk properties are presented, followed by the calculated properties of energetics, structural characteristics, and kinetic reactions for cation and hydrocarbon complex adsorption on calcite surfaces.

First principle calculation represents an important and accurate tool to obtain information about the wettability process at atomistic level[4]. In this work a model for exploring calcite surface reactions has been developed using free energy contours. The interaction to water, Calcium, Strontium, Magnesium ions and hydrocarbons is calculated in the temperature range from 0°C to 100°C. The goal is to understand the adsorption and desorption mechanism of a carboxyl group on the calcite surface over varied temperatures in presence of brine.

Results and Discussion

Initially, the crystal parameters (atomic positions and cell vectors) of bulk calcite was fully relaxed. The hexagonal structure of calcite $R\bar{3}m$ space group was obtained through the geometry optimization calculation. Cell vectors of the optimized crystal lattice obtained are, $a = b = 4.997 \text{ \AA}$ and $c = 17.051 \text{ \AA}$. While the atomic distance between C-O = 1.295 \AA & Ca-O = 2.374 \AA . The obtained result was compared with the experimental values. Previous studies the cell vectors obtained from XRD are in consistency with these results. The obtained elastic constants are $C_{11}=148 \text{ GPa}$, $C_{33}=85 \text{ GPa}$, $C_{44}=34 \text{ GPa}$, $C_{66}=46 \text{ GPa}$, $C_{12}=55 \text{ GPa}$, $C_{13}=54 \text{ GPa}$ and $C_{14}=-21 \text{ GPa}$ were correlated with experimental results.

Thereafter simulations were conducted by introducing the water molecule at various heights from the calcite surface. The obtained Gibbs free energy (ΔG) was plotted in Figure 1 with the corresponding height of the central atom. As shown in Figure 1 locations of high water stability at an average height of 2.4 \AA (layer I) and 4.2 \AA (layer II) from the crystal surface were obtained. These results correlate to the previously predicted two shell water adsorption on the crystal surface.

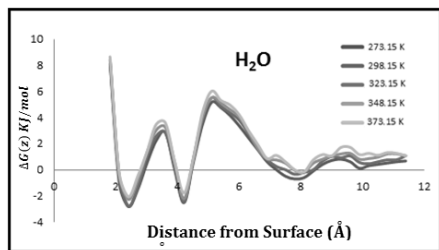


Figure 1 Free energy profile of water at different temperature, showing consistent high stability zone around 2.4 Å and 4.2Å.

On a Calcite surface Mg^{2+} ions readily get adsorbed by forming complex with 6 water molecules of hydration. This results in release of energy. The Mg^{2+} ion is significantly more stable on the calcite surface than the Ca^{2+} or Sr^{2+} ions. Thereby substitution of Ca^{2+} by Mg^{2+} is feasible on calcite surfaces. In absence of any other polar molecule the release of energy during adsorption of Mg^{2+} ions favors desorption of Ca^{2+} ions. As shown in Figure 2 the energy barrier for adsorption of $Mg^{2+}[H_2O]_6$ decreases with increase in temperature. The $Mg^{2+}[H_2O]_6$ complex remains stable at higher temperatures[5]. Thus adsorption of Mg^{2+} ions by substituting Ca^{2+} becomes more feasible at higher temperatures [2].

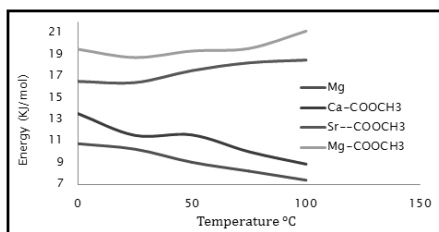


Figure 1: Energy barrier increases with temperature for Carboxyl- Sr^{2+} and Carboxyl- Mg^{2+} , while energy barrier to release carboxyl- Ca^{2+} is similar to energy released in Mg adsorption on calcite surface. Both decreases with temperature rise.

But in this experiment polar hydrocarbons were not introduced to the cores before water flooding. So these results are consistent with the simulation values, that Mg^{2+} ion has more affinity towards calcite surface than Ca^{2+} . Also, in the experiments from the same Stevns Klint cores it is reported [3] that substitution of ions on the surface was not observed. But in this experiment oil(containing polar components) was initially introduced to the cores. With increase in temperature increase in Ca^{2+} concentration, and decrease in Mg^{2+} ion concentration was observed in the effluent water only when flooding water did not contain sulfate ions[5,6].

Discussion & conclusion

Micro scale behavior of brine and hydrocarbon during water flooding on calcite surface was simulated using first principle molecular dynamics simulation. Calcite crystal structure was optimized and the elastic constant was calculated. The obtained values were in correlation with the experimental data. Primary adsorption studies for different complexes of water, carboxyl group and Ca^{2+} , Mg^{2+} and Sr^{2+} ions on the calcite surface was studied from 0°C to 100°C. Through the simulations it was observed that water molecules are more stable at two locations; at an average height of 2.4 Å and 4.2 Å from the calcite surface. It was observed that Mg^{2+} behaves significantly different from Ca^{2+} on the calcite surface. Mg^{2+} preferred to be adsorbed alone, while Ca^{2+} preferred to be adsorbed with carboxyl ion. The carboxyl ion adsorption was modeled which is briefly explained as Mg adsorption released energy. This energy helped to release carboxyl ions. The model explains the temperature effect in smart water flooding. The obtained results were in correlation with the experimental data in the literature. The controversy of whether or not at high temperature Mg^{2+} substitution of Ca^{2+} was explained. It study also puts emphasis on functional group based analysis, of the oil, for adsorption and wettability analysis.

Acknowledgement:

We acknowledge Maersk Oil and Doing energy for funding the Smart Water project. We also appreciate the comments and help provided by Alexander Shapiro and Ida L. Fabricius in smart water meetings.

References

1. RezaeiDoust, A., Puntervold, T., Strand, S., & Austad, T. Energy & fuels 23(9) (2009) 4479-4485.
2. Fathi, S. Jafar, Tor Austad, and Skule Strand. Energy & fuels 24, no. 4 (2010): 2514-2519.
3. Fernø, M. A., R. Grønnsdal, J. Åsheim, A. Nyheim, M. Berge, and A. Graue. Energy & fuels 25, no. 4 (2011): 1697-1706.
4. Mandal, Nibir, Krishna Hara Chakravarty, Kajaljyoti Borah, and S. S. Rai. Solid Earth (1978–2012) 117, no. B12 (2012).
5. Hara Chakravarty, Krishna, and Kaj ThomsanIn EGU General Assembly Conference Abstracts, vol. 15, p. 11615. 2013.
6. Chakravarty, Krishna Hara. Graduate Schools Yearbook 2012 (2013): 33.



Peam Cheali
Phone: +45 4525 2911
E-mail: pche@kt.dtu.dk

Supervisors: Gürkan Sin
Krist V. Gernaey

PhD Study
Started: May 2012
To be completed: April 2015

Synthesis and design of integrated-intensified chemical/biochemical processes

Abstract

The reduction of fossil fuel feedstock causes a serious challenge on economic growth and environmental sustainability. This motivates the development of renewable technologies to bridge the gap for fuel, chemical and materials production. This project is focusing on the development of methodologies for fast, flexible and future design of integrated-intensified chemical/biochemical processes, with particular focus on a biorefinery case study.

Introduction

The limited resources of fossil fuel as well as other important driving forces (e.g. environmental, social and sustainability concerns) are expected to shape the future development of the chemical processing industries. These challenges motivate the development of new and sustainable technologies for the production of fuel, chemicals and materials from renewable feedstock instead of fossil fuel, in particular, biorefinery. The biorefinery is defined as the set of processes converting a bio-based feedstock into products such as fuels, chemicals, materials and/or heat and power. Therefore, the design of a biorefinery process is a challenging task due to a number of alternatives: (i) several different types of biomass feedstock and many alternative conversion technologies can be selected to match a range of products; (ii) a large number of potential processing paths are available for biorefinery development. Designing a biorefinery, therefore, requires screening among a set of potential configurations, in order to identify the most convenient option for the given set of conditions.

Detailed evaluation of each process alternative requires a substantial amount of information such as conversions and efficiencies for the different steps involved. Moreover, considerable time and resources are needed to execute the analysis, and it is therefore not practically possible to consider more than a handful of candidate processing paths. Hence, the ability of performing the early stage screening is important and supportive to be processed to identifying of the optimal biorefinery processing path with respect to economics, consumption

of resources, sustainability and environmental impact prior the detailed design.

The challenge during the early stage of biorefinery planning and design is the enormous need for data, which is often not available and hence proper assumptions and simplifications need to be made to manage the complexity of the problem. This is especially complicated when one broadens the scope of biorefinery network design, that is, by simultaneously focusing on different conversion platforms. The data characterization representing each process alternative requires a substantial amount of information: parameters, variables, models of known reactions, thermodynamic properties, process efficiencies resulting in a detailed and complex model, and these require the adapted systematic optimization approach to solve the complex problem. Therefore, it is important to simplify and manage the complexity related to the vast amount of data.

In this contribution, as we focus on early state design and analysis of biorefinery systems, the scope of biorefinery synthesis is broadened by considering a combination of thermo-chemical, biochemical platforms and bioethanol upgrading processes. Moreover, uncertainties in data and models (cost estimation) are also considered to provide more information on the optimal solution resulting in the robust decision-making solutions.

In this way, the design space is extended significantly meaning that more potential platforms and design alternatives can be compared resulting in a more robust and sustainable design solution.

Framework

Step 1: Problem formulation (i.e. problem definition, superstructure definition, data collection, model selection and validation). This step includes the definition of the problem scope, the selection of suitable objective functions and optimization scenarios with respect to certain metrics (e.g.: economic/business metrics, engineering performance, or sustainability). Superstructure definition together with data collection, model selection and verification are then performed.

Step 2: Uncertainty characterization. In this step, the statistical analysis tools, i.e. Latin Hypercube Sampling with correlation control and Monte Carlo simulation, are implemented and integrated within the deterministic problem. In particular, the specific parameter needs to be: *i)* selected as uncertain input data; *ii)* characterized; *iii)* analyzed in terms of correlations; and, *iv)* sampled to generate the possible scenarios.

Step 3: Deterministic formulation and solution. The deterministic optimization problem, which is fully formulated in *Step 1*, is solved in this step. Moreover, different scenarios regarding different objective functions as defined in *Step 1* are also analyzed in this step. The result of this step is the deterministic solution of the optimal processing path, i.e. one optimized biorefinery flowsheet scenario on the basis of mean values of the input data.

Step 4a: Decision-making under under uncertainties (deterministic). In this step, the deterministic optimization problem is solved for each scenario generated by the sampling from the uncertainty domain (in *Step 2*). The results are: *i)* the probability distribution of the objective function value; and, *ii)* the frequency of selection of the optimal processing path candidates under the generated uncertain samples.

Step 4b: Decision-making under under uncertainties (stochastic). In this step, the optimization problem is modified and formulated as a stochastic programming problem by including the uncertainty domain into the parameter domain. Therefore, the objective function is reformulated as minimizing or maximizing the expected value of the objective function over the uncertain domain.

Step 4c: Decision-making under under uncertainties (optimal flexible network, multi-products and risk reduction). In this step, a network design problem is addressed to explore robust solutions under uncertainties. This solution seeks a balance between a larger capital investment and an increased flexibility of the network design to better cushion and absorb the impact of uncertainties during the operational stage once the planned biorefinery has been built and subjected to market uncertainties.

Uncertainty analysis of a superstructure-based optimization

The specified objective function is to minimize the total annualized cost. The superstructure (Figure 1) of the biorefinery processing network is to convert corn stover and wood to bioethanol developed [1]. Moreover, the

uncertainties of market prices (raw material costs and product prices) were identified as the important sources of uncertainty affecting the decision concerning the biorefinery design.

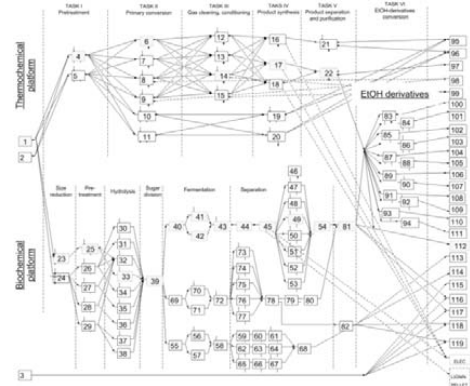


Figure 1: The combined superstructure.

Table 1: An identification of optimal solution under market prices uncertainties (max. operating profit) [1]

Solutions	Processing paths	Operating profit (MMS/a)
Optimal network (Step 3)	Wood, Entrained-flow gasifier, steam reforming, scrubber, acid gas removal using amine, alcohol synthesis, mol. sieve, distillation, diethyl ether production	247
Network under uncertainties (Step 4b), diethyl ether and 1,3-butadiene production	161
Optimal flexible network (Step 4c), diethyl ether and 1,3-butadiene production	187

Conclusion

In this study, the impact of data uncertainties on design of optimal biorefinery networks using superstructure-based approach is discussed. The combination of the deterministic problem, the deterministic problem under uncertainty and the stochastic problem was used to effectively identify the impact of uncertainty on the optimal solution. Thermochemical conversion platform of biomass with upgrading an ethanol to diethyl ether (and 1,3-butadiene) is the most promising solution respect to techno-economic criteria. These study is expected to provide useful information regarding economic and sustainability drivers for the future development of a biorefinery.

References

1. P. Cheali, J. A. Posada, K. V. Gernaey, G. Sin, Biomass & Bioenergy, submitted.



Stefano Cignitti
Phone: +45 4525 2808
E-mail: steci@kt.dtu.dk
Discipline: CAPEC-PROCESS

Supervisors: Professor Rafiqul Gani
Professor Krist V. Gernaey
Professor John M. Woodley

PhD Study
Started: September 2014
To be completed: August 2017

Computer-aided Mixture and Blend Design

Abstract

Product design of novel pure, mixed and blended products with the considerations of process and application is an emerging topic in the field chemical and biochemical engineering. Many methods, such as Computer Aided Molecular Design (CAMD), and Computer-aided Mixture and Blend Design (CAM^bD) provide the possibility of design such products. However, these product design problems can quickly become large and difficult, if not infeasible, to solve in the area of mathematical optimization. In addition, considerations of process, application, advanced products, economic feasibility, environmental and sustainable metrics that must be included in today's product design consequently makes the problem harder to mathematically define and to solve. The use of process systems engineering (PSE) methodologies and tools can make it possible to obtain the optimum designed product that is competitive with today's demands. In this research project, a computer-aided systematic methodology will be developed for the design of pure, mixed and blended products using extended CAM^bD methods. The methodology is to be implemented into a software and applied in various case studies, specifically the design of working fluids for heat pump cycles.

Introduction

One of the greatest challenges in the chemical, biochemical and pharmaceutical industry is the design of novel products. The need for tailor-made products that are more environmentally acceptable, sustainable and economically feasible require advanced methods for product design. In figure 1 the four large areas that are to be considered in product design are: Product needs and application, process needs and application and synthesis routes. The product needs and application refer to the actual design and application of the product, whereas the process refers to production and use of products in processing, synthesis routes of the product, and the economic, sustainable and environmental metrics. An optimum product should be generated through a mathematical optimization of these four domains. Several methods exist for finding the optimum product. One of these are computer-aided molecular design (CAMD) for the design of molecules [1], which has been extended to compute-aided mixture/blend design (CAM^bD) for the design of mixtures and blends [2]. Property prediction methods are the backbone of the any CAMD method. The property prediction methods ensure that product generation is not hindered by experimental data resources. Group contribution method is one of the prediction methods where by knowing the

molecular groups present in a molecule, the properties can be predicted. For mixtures and blends, the ensemble properties can as well be predicted. This enables the possibly of generating novel pure compounds, mixtures and blends alike. The synthesis routes of a product can also be found through the application of a CAMD method, which was shown in [4]. This will be one of the application areas of the methodology.

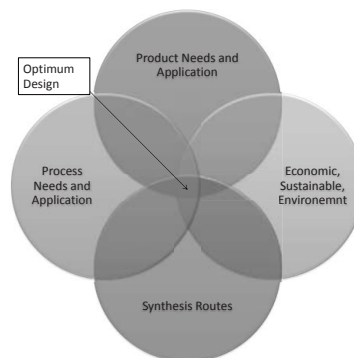


Figure 1: Four main areas that must be considered to find the optimum product design

Computer-aided Systematic Methodology

In this work, a generic systematic computer-aided methodology will be developed for the design of novel pure, mixed and blended products. Given a set of product and process needs, the feasible and optimum mixture/blend design can be found. The method will formulate the product needs into a mixed-integer non-linear programming problem, which will be solved with mathematical optimization through specialized algorithms.

The general CAMD problem can be formulated as the following Mixed Integer Non-Linear Programming (MINLP) problem. The MINLP formulation is divided into objective function and four types of constraints.

$$\min/\max f_{obj}(\mathbf{X}, \mathbf{N})$$

s.t.

$$\text{structural constraints: } g_1(\mathbf{N}, \mathbf{Y}) \leq 0$$

$$\text{pure component property constraints: } g_2(\mathbf{N}) \leq 0$$

$$\text{mixture property constraints: } g_3(\mathbf{X}, \mathbf{N}) \leq 0$$

$$\text{process model constraints: } g_4(\mathbf{X}, \mathbf{N}) = 0$$

$$\mathbf{X} \in \mathbb{R}^n, \mathbf{N} \in \mathbb{Z}_+^m, \mathbf{Y} \in \{0, 1\}^q$$

\mathbf{N} is a vector of integer variables, which are related to the numbers of the building blocks and/or molecules (1st and 2nd order groups). \mathbf{Y} is adjacency matrix which is related to the description of the molecular structure. \mathbf{X} is a vector of continuous variables, which are related to the mixture and/or process variables.

The first constraint deals with the structural stability of the generated molecules. Here, molecules that do not follow rules such as the octet rule (valency) will be rejected as infeasible molecules. The second constraint includes pure component property constraints, such as thermodynamic or environmental properties. These are, for the case of group contribution methods, often linear equations. In the third property constraint the mixture properties are investigated. Here, both mixture composition dependent properties, such as density, and independent properties, such as solvent selectivity, are considered. In the last and fourth constraint type, the process model are included, such as mole balance for a unit operation. Other models may also be included here such as phase equilibrium equations.

To solve this MINLP problem, a database is used for group contribution coefficients for the molecular groups, which will generate the molecules. In most CAM³D problems, and in general MINLP formulations as the one given, the need of using highly nonlinear property models and process models can lead to non-convex and non-smooth problems, which is difficult to solve. One of the method to solve these types of problems is by Karunanithi et al. [2] who proposed a decomposition-based algorithm to solve this MINLP problem by first solving sub-problems consisting of a set of property constraints only. The search space is reduced by using this decomposition algorithm. The

MINLP problem is converted to several Non-Linear Programming (NLP) problems corresponding to fixed values of the integer variables. The decomposition-based algorithm is shown in a bulls-eye analogy in figure 2. It has been shown that through this solution strategy it is possible to obtain a solution to the large MINLP problem.

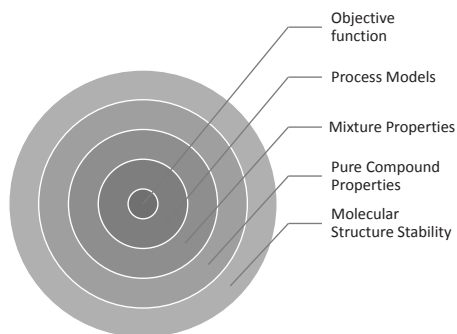


Figure 2: Decomposed Solution Strategy

Future works

The future developments of this research topic will be the full development of the methodology. Apply the methodology to working fluid design problems for heat pump cycles, and application in reaction path synthesis problems. In addition, a computer-aided software is under development that enables the possibility to automatically solve the product design problem using this methodology.

References

1. Harper, P. M., Gani, R., Kolar, P., & Ishikawa, T., 1999, Computer-aided molecular design with combined molecular modeling and group contribution. *Fluid Phase Equilibria*, 158-160, 337–347.
2. Karunanithi, A. T., Achenie, L. E., & Gani, R., 2005, A new decomposition-based computer-aided molecular/mixture design methodology for the design of optimal solvents and solvent mixtures, *Industrial & engineering chemistry research*, 44(13), 4785-4797.
3. Yunus, N. A., Gernaey, K. V., Woodley, J. M., & Gani, R., 2014, A systematic methodology for design of tailor-made blended products. *Computers & Chemical Engineering*, 66, 201–213.
4. Cignitti, S., 2014, Computer-Aided Reaction Path Synthesis, Master's Thesis, DTU Lyngby.

**Larissa Peixoto Cunico**

Phone: +45 4525 5510

E-mail: lacu@kt.dtu.dk

Supervisors: Rafiqul Gani
Roberta Ceriani, UNICAMP
Bent Sarup, Alfa Laval Copenhagen A/S**PhD Study**

Started: February 2012

To be completed: January 2015

Consistent thermodynamic properties of lipids systems

Abstract

Physical and thermodynamic properties of pure components and their mixtures are the basic requirement for process design, simulation, and optimization. In the case of lipids, our previous works [1,2] have indicated a lack of experimental data for pure components and also for their mixtures. To contribute in this area, experimental data were obtained using the Differential Scanning Calorimetry (DSC) technique for isobaric vapor-liquid equilibrium (VLE) of two binary mixtures at two different pressures (1.2 and 2.5 KPa): system 1 [monoacylglycerol (monocaprylin) + fatty acid (palmitic acid)] and system 2 [monoacylglycerol (monocaprylin) + fatty ester (methyl stearate)]. System 1 is relevant in the purification steps of the deodorizer distillates while system 2 is relevant in the purification steps of biodiesel and bioglycerin. Available thermodynamic consistency tests for TPx data were applied before performing parameter regressions for Wilson, NRTL, UNIQUAC and original UNIFAC models. The relevance of enlarging experimental database of lipids systems in order to improve the performance of predictive thermodynamic models was confirmed in this work by analyzing the calculated values of original UNIFAC model. For solid-liquid equilibrium (SLE) data, new consistency tests have been developed [2]. The SLE consistency test and data evaluation is performed in a software containing option for data analysis, model analysis and parameter regression.

Introduction

In edible oil/fat and biodiesel production, modeling, simulation and design of unit operations require knowledge of phase equilibria in vapor-liquid (VLE), liquid-liquid (LLE) as well as solid-liquid (SLE) circumstances. The use of DSC technique for measuring thermophysical properties of fatty systems is increasing due to its clear advantages i.e., it uses very small samples, 3-5 mg in comparison to ebulliometry (cost-effective) and it provides the results in a shorter operation time, avoiding thermal degradation of compounds prior to vaporization. Differences in accuracy can be found for original UNIFAC model in comparison with correlated models such as NRTL and UNIQUAC, though they are not large for some of the systems. However, for complex compounds such as acylglycerols, phospholipids, tocopherols, among others, high deviations are observed in some cases for physical and thermodynamic properties prediction. In order to improve the performance of predictive thermodynamic models for lipids data, we proposed new interaction parameters for UNIFAC model and lipids systems. A total of 358 data sets from the DECHEMA® database for solid solubility data and 70

SLE data sets in CAPEC Lipids Mixtures Database were analyzed with the thermodynamic consistency tests for SLE [2]. Application of the software for the collection of SLE data sets can establish the general idea of the quality of the available data.

Experimental work

Novel VLE data for monocaprylin plus palmitic acid and monocaprylin plus methyl stearate were measured using the DSC technique, which is considered suitable for these two binary mixtures, mainly because of the low amounts of sample used in each trial. Satisfactory results for the measured data were obtained and confirmed by the thermodynamic consistency tests applied in this work (pure component test and Van Ness test) with quality factors for the binary mixtures higher than 0.77 (in a range between 0 and 1). The regressions of parameters were obtained for Wilson, NRTL and UNIQUAC, with average relative deviations lower than 0.3 % for all cases. The phase diagram with the thermodynamic model performance for system 1 [monoacylglycerol (monocaprylin) + fatty acid (palmitic acid)] can be seen in Figure 1.

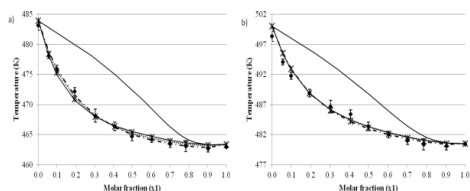


Figure 1: Vapor liquid equilibrium for the system 1 [monocaprylin(1) + palmitic acid(2)] at a) 1.2 kPa and b) 2.5 kPa. ◆ Experimental data [3]; —NRTL (with vapor phase calculated by the model); *UNIQUAC; -.- Wilson; ••Modified UNIFAC

UNIFAC model representation for lipids systems

Since the original UNIFAC model parameters may not have been regressed with data from lipid systems, a possible way to improve the original UNIFAC performance is to fine-tune group interaction parameters using the lipid data-sets. This was done by regressing the interaction parameters for the functional group with the chain group, such as COOH with the CH₃/CH₂ group for fatty acids. Since a large number of interaction parameters were necessary for the VLE calculation compared with the measured data points an objective function employing a regularization term as done by Balslev and Abildskov [4]. One example was selected to better exemplify the improvement found for some existing systems in literature and can be seen in Figure 2. The measured experimental data [3] had considerable improvement considering the new set of parameters (Mod. UNIFAC), as ARD (%) given by Table 1. In total, 48 binary interaction parameters (a_{mn}) for UNIFAC model were regressed considering a database containing around 52 VLE data sets and more than 632 data points.

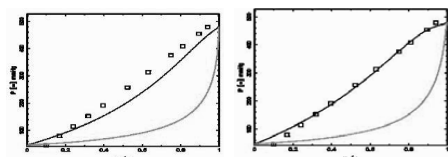


Figure 2: Acetone (1) and triolein (2) – original UNIFAC model representation a) before and b) after consider the new set of parameters. Experimental data [5]: liquid phase (x) and vapor phase (□). Original UNIFAC model prediction of liquid phase (—) and vapor phase (---).

Table 1: Average relative deviations, ARD (%), for UNIFAC calculations

System	Pressure (kPa)	Temperature range (K)	ARD (%)	
			Orig. UNIFAC	Mod. UNIFAC
Monocaprylin(1) + palmitic acid(2)	1.2	462.94 - 483.15	0.232	0.1810
	2.5	480.41 - 498.35	0.497	0.471
Monocaprylin(1) + methyl stearate(2)	1.2	462.94 - 475.97	Unstable†	0.355
	2.5	480.41 - 493.38	Unstable†	0.676

† Liquid mixture is unstable

For VLE systems, improvement in the experimental data representation was observed for non-ideal mixtures containing complex compounds with and without solvents, which include different classes of lipids, such as acylglycerols, fatty acids and fatty esters. In addition, the same parameters were utilized for SLE data without loss of performance by the model. The considered cross-validation method shows the efficiency of the proposed new parameters.

Software implementation of the proposed consistency tests for SLE systems

Though no rigorous consistency tests exist for such systems, using a reliable activity coefficient model along with comparing limits with independent pure component data allows Quality Factors (Q) to be established for complete composition range and limited range solubility SLE. It was found that the FST model is normally more accurate than both the NRTL and UNIQUAC models. One example of a data set containing a lipid as one of the compounds is seen in Figure 3. The same approach adopted here for SLE. This algorithm is an option to be used in thermophysical and thermochemical property data validation.

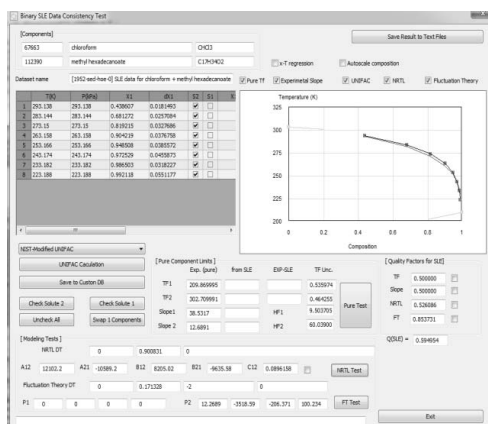


Figure 3: Screen shot from the software developed for thermodynamic consistency tests analysis. Experimental data for the binary mixture of methyl palmitate(1) + chloroform(2) ■ Experimental data [6] at pressure equal 101.325KPa using ■ Test-1 (Pure Test), —Test-2 (Slope), —Test-3 (NRTL model capability) and —Test-4 (FST).

References

- L.P. Cunico, A.S. Hukkerikar, R. Ceriani, B. Sarup, R.Gani, *Fluid Phase Equilib.*, 2013, 357, 2-18.
- L.P. Cunico, R. Ceriani, B. Sarup, J.P. O'Connell, R. Gani, *Fluid Phase Equilib.*, 2014, 362, 318-327.
- L.P. Cunico, D.S. Damasceno, R.M.M. Falleiro, B. Sarup, J. Abildskov, R. Ceriani, R. Gani, *AIChE J.* (submitted).
- K. Balsle, J. Abildskov, *Ind. Eng. Chem. Res.*, 2002, 41, 2047-2057.
- G.H. Eduljee, A.P. Boyes, *J. Food Process Eng.*, 1981, 26, 55-57.
- R.S. Sedgwick, C.W. Hoerr, H.J. Harwood, *J. Org. Chem.*, 1952, 17, 327-337

**Jakob Dragsbæk Duhn**

Phone: +45 2552 9471
E-mail: JADU@kt.dtu.dk
Discipline: Catalysis

Supervisors: Anker Degn Jensen
Stig Wedel
Claus Friis Pedersen, Haldor Topsoe A/S

Industrial PhD Study

Started: December 2013
To be completed: December 2016

Development of Highly Efficient Solid Oxide Electrolyzer Cell Systems

Abstract

With the increasing amounts of renewable and fluctuating energy in the Danish energy system, effective and high capacity storage solutions are necessary. A solution could be electrolyzers capable of utilizing electrical energy to transform H_2O and CO_2 to gas and liquid fuels. This project is about designing optimized components for such systems using experimental investigations as well as theoretical tools.

Introduction

The present Danish energy plans envision a rapid introduction of large amounts of renewable and fluctuating power sources into the Danish energy system. By 2020 it is for example planned to have 50% of the energy in the power grid produced by wind turbines [1]. In order to make efficient use of such large amounts of fluctuating electrical power sources, there will be an increasing need for high capacity storage of electrical power over days and even months [2]. Energinet.dk is working with scenarios where 5 GW [2] of electrolyzer capacity is required in 2050. Here it is also expected that electrolysis will be combined with catalytic fuel synthesis where H_2 and CO_2 are converted to fuels, such as methane (CH_4) or methanol (CH_3OH), which can be stored easily in the existing infrastructure (e.g. the natural gas grid) and can be used directly for transportation.

When using electrolysis for energy storage, power efficiency is the key performance parameter. Solid Oxide Electrolysis Cells (SOEC) have a unique potential for very efficient operation. Being a high temperature ($>700\text{ }^\circ\text{C}$) system, SOEC can utilize up to 33 % (at $800\text{ }^\circ\text{C}$) of the energy required for the electrolysis process as heat, compared to only 17 % for traditional alkaline room temperature electrolysis [3]. It also gives the opportunity to use waste heat/steam, which might be available from external processes, such as fuel synthesis processes.

Based on commercially available heat exchangers, Haldor Topsoe has developed SOEC systems, with efficiencies of around 75 %. This is better than typical alkaline electrolyzer, but there is still room for improvement by developing very efficient heating

components (e.g. heat exchangers), fully optimize the mechanical and functional integration between heat exchanger and SOEC stack, and integrate catalytic fuel synthesis in the heat exchanger. To achieve this kind of optimization, advanced mathematical models of the stack and heat exchanger are needed.

The models for H_2 and CO production in SOECs have only recently been coupled together in a 2D model [4]. However, the effect of the shift reaction ($CO + H_2O \leftrightarrow CO_2 + H_2$) and the carbon formation reaction ($CO + CO \rightarrow CO_2 + C$) are still to be fully understood and modeled. These reactions are important for the components, since e.g. C can cause metal dusting on the used materials and fouling of stacks and heat exchangers.

Few literature examples of modeling and/or experimental characterization of heat exchanger-based reactors in connections with fuel cells exist [5-9]. These studies are focused on complete reforming before entering the fuel cell (e.g. $CH_4 + H_2O \rightarrow 3H_2 + CO$). However, heat exchange-based reactors capable of transforming the produced synthesis gas to higher value fuels (e.g. $3H_2 + CO \rightarrow CH_4 + H_2O$) are desirable for SOEC systems, but have not been investigated so far.

Specific Objectives

The first scientific objective of the project is to develop computational fluid dynamics (CFD) models for SOECs. Compared to the state-of-the-art, these models are to include the critical formation of carbon, which may cause destruction of the cell and heat exchanger.

Models for compact plate heat exchangers will be developed to enable the design of counter-flow heat exchangers operating with large temperature differences. The models will be used to predict important parameters, such as pressure drop. As a second scientific objective, this model will include the effects of carbon formation and metal dusting on the heat exchangers to predict lifetimes of the heat exchangers for different operating conditions and for different materials.

A third scientific objective is to include chemical reactions into the heat exchanger model to simulate the possible integration of fuel synthesis in catalytically coated plate heat exchangers. For this modeling, new experimental data will have to be obtained for the kinetics of relevant catalysts to be coated onto the heat exchanger surfaces, and the model must be experimentally verified by preparing and testing catalytically coated plate heat exchangers

Finally, the developed models and experiments will be used to identify which parameters have the largest effect on the construction and performance of SOEC systems. This knowledge can thus be used as a starting point for further research and development.

Results and Discussion

So far a new plate heat exchanger has been designed and tested with nitrogen. The heat exchanger was also modeled with Matlab using a finite volume method and the experimental data was used to fit the model. The efficiency of the heat exchanger was calculated by:

$$\eta = \frac{T_{cold,out} - T_{cold,in}}{T_{hot,in} - T_{cold,in}}$$

Figure 1 shows the efficiency of the heat exchanger vs. inlet flow rate. Unexpected, the efficiency increases with increased flow rate. This matter is currently being investigated further.

When replacing nitrogen with the actual used gasses, the model predicts the efficiency of the heat exchanger to be 82% and 90% for the cathode and anode heat exchanger respectively. In comparison, the current commercial heat exchangers have an efficiency of 78% and 73%, respectively. However, the new developed plate heat exchangers have a significantly larger pressure drop than the current heat exchangers.

Conclusions and Further Work

The model predicts that the developed heat exchangers will have a higher efficiency, especially the anode heat exchanger. However, the higher pressure drop might be unacceptable from a system point-of-view.

The next step in the project is to validate if the measured values are correct and to test if the pressure drop can be reduced.

After that the effects of carbon formation and metal dusting on the lifetime of the heat exchanger will be investigated. Subsequently, the possibility of integrated fuel synthesis in the heat exchanger will be explored.

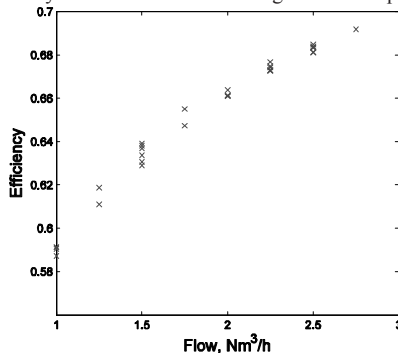


Figure 1: Calculated efficiency of the special designed plate heat exchanger versus the flow rate.

Acknowledgements

This project is a collaboration between the CHEC group at DTU Chemical Engineering and Haldor Topsoe A/S and is partially funded by the Danish Industrial Ph.D. Fellowship Programme administered by the Danish Agency for Science Technology and Innovation (no. 1355-00140)

References

1. Klima, Energi og Bygningsministeriet, "Energiaftalen i korte træk", Visited September 04, 2013 on <http://www.ens.dk/sites/ens.dk/files/politik/dansk-klima-energipolitik/politiske-aftaler-paa-energiomraadet/energiaftalen-22-marts-2012/Faktaark%201%20Energiaftalen%20kort%20fortalt.pdf>
2. Energinet.dk, "Energi 2050 – Vindsporet", Visited September 04, 2013 on <http://energinet.dk/SiteCollectionDocuments/Danske%20dokumenter/E1/Energi%202050%20Vindsporet%203.pdf>
3. T. Smolinka in: Jürgen Garche (Eds.), Water Electrolysis, In Encyclopedia of Electrochemical Power Sources, Elsevier, Amsterdam, 2009, p. 394-413.
4. Meng Ni, International Journal of Hydrogen Energy, 37 (8) (2012), 6389-6399
5. Anxionnaz, Z., et al., Chem. Eng. Process. 47 (2008) 2029-2050.
6. Ki, Jeongpill, Kim, Daejong and Honavara-Prasad, Srikanth, J. Fuel. Cell. Sci. Tech 9 (2011).
7. Huisheng Zhang, Lijin Wang, Shilie Weng, Ming Su, J. Power Sources, 183 (1) (2008) 282-294
8. M. Zanfir, A. Gavriilidis, Chem. Eng. Sci. 58 (2003) 3947-3960
9. Sigurdsson HO, Kær SK., J. Fuel Cell Sci. Technol. 9 (2) (2012)



Francesco Cristino Falco

Phone: +45 4525 2992

E-mail: frac@kt.dtu.dk

Supervisors: Krist V. Germaey
Anna Eliasson Lantz

PhD Study

Started: October 2014

To be completed: September 2017

Characterization of Microbial Consortia for Keratin Degradation Processes

Abstract

Especially in the last decade, the number of biofuels and biobased chemicals which can be obtained through microbial fermentation technologies has continuously increased. Nevertheless, a major step towards the sustainable and cost-effective production of such new biocommodities will certainly be the possibility to employ, in a larger extent, cheaper and widely available renewable feedstocks such as residual biomass and organic waste materials. This PhD project is part of a larger multi-partner research project, namely “Keratin2Protein”, where the potential of novel process technologies will be investigated in order to efficiently convert organic agro-industrial residual biomass into new alternative added-value products. Specifically, tailor-made microbial consortia, which can be cultivated in an industrial process for keratin degradation, will be employed to valorize slaughterhouse keratin-rich by-products for production of protein-enriched feed. In particular, the PhD project will focus, on the one hand, on the development and optimization of fermentation protocols to cultivate microbial consortia for efficient keratin biodegradation and, on the other hand, on the implementation of mathematical, deterministic, models describing microbial interactions within these synthetic ecological webs.

Introduction

A large part of the research efforts for the production of fuels and chemicals from renewable resources have focused on the identification and engineering of single microbial cell factories in order to utilize complex substrate mixtures. Nevertheless, microbial species living in a large variety of naturally occurring environments have, after billions of years, evolved towards the formation of highly efficient consortia in which they perform multiple tasks in a synergistic manner. In particular, at the community level, this cooperation gives rise to higher-order properties such as improved stability, optimized use of the available nutritional and energetic resources, enhanced substrate degradation rates etc. Within this context, microbial communities can be defined as complex adaptive systems [1] which dynamically adjust their structure and function in response to external stimuli – that is to changes in the environmental conditions.

One of the major challenges in developing models capable to predict the structural and dynamical behavior of a microbial consortium is the complex relationship describing the inter-specific interactions that are established both in between community members and with respect to their local environment and the resulting

physiological phenotypes expressed by each individual species.

This PhD project will focus on the development of mechanistic models which will be used as simulation platforms to obtain a more clear insight into the interplay between different consortia members. In particular, these models will be employed to design and optimize synthetic microbial consortia for the efficient degradation of keratin-rich residual biomass.

Methodology

Kinetic characterization of each possible consortium member will be performed at bench-top fermenter scale, and optimal conditions for efficient cultivation of these keratinolytic microorganisms will be determined. In particular, by means of pure culture experiments, the effect of keratin-rich substrates, medium composition and environmental conditions (i.e., temperature, pH, dissolved oxygen, agitation speed, etc.) on microbial growth and keratin degradation kinetics will be studied. In order to optimize both medium composition and cultivation parameters using a reduced number of experiments, statistical methods such as central composite design (CCD) and response surface methodology (RSM) will be employed [2].

Experimental information obtained in the fermenter for each keratinolytic strain tested will be employed to formulate and implement, in the MATLAB-Simulink programming environment, mathematical models capable to describe the effect of keratin-rich substrates, culture medium composition and selected environmental conditions on microbial growth and keratin degradation kinetics. In order to represent the biochemical transformations occurring in keratin-rich residual biomass degradation through some simplified process descriptions, mechanistic models, inspired by those typically used to represent microbial wastewater treatment processes [3], will be developed. Thereafter, kinetic models of pure cultures developed for optimal growth conditions will be adapted to suboptimal, common growth, conditions for co-cultures of interest.

To gain a better understanding about the interactions between different consortia members, the range of application of the deterministic models previously developed will be extended to the case of mixed microbial cultures. Subsequently it will be possible to apply these models in simulating keratin substrate degradation for a variety of consortia constellations in order to verify their potential as simplified tailor-made consortia that could be easily cultivated in a bioreactor. In more detail, the effect of medium formulation and environmental conditions on the behavior of the mixed population will be simulated, providing guidelines for further process design and optimization.

Cultivations in bioreactors of simplified consortia consisting of predicted optimal combinations of selected pure cultures will be established. Experimental information and model predictions will be used to evaluate dynamics between consortia members and the stability of the consortia itself. For some of the best performing co-cultures a more detailed quantitative characterization, involving enzyme profiling, analyses of substrates and microbial biomass will be performed in combination with omics profiles. Data from cultivation experiments will then iteratively be used for model validation and to improve model predictions. Finally the mathematical model will be used to support the design of the best reactor configuration: batch, fed-batch and different hybrid cultivation strategies will all be evaluated.

Importance of the Mechanistic Model

In Figure 1 all the main steps involved in defining a quantitative description of a fermentation process are summarized. In particular, deterministic models used to describe fermentation processes involving microbial communities should be able to:

- describe, in a quantitative manner, fluxes through pathways for nutrient resources and energy,
- identify and quantify the effect of interactions of consortium members with each other and with the surrounding environment on the overall community performance,
- infer on the system's higher-order properties – that is the capability of the model to predict, based on

mechanistic considerations, to which extent, for a selected microbial consortium, the biodegradation performance of the system has been improved.

Therefore, during each phase of the PhD study, the model structure will be continuously and iteratively updated. First of all, the structured model will be fitted to experimental data collected during both pure and mixed culture experiments; if the model structure will not permit an accurate description of the data after parameter estimation, the model structure will need to be updated, and parameter estimation will be repeated. Model analysis tools, such as uncertainty and sensitivity analyses, will also be used to direct experimental efforts. In particular, ranking of parameters via sensitivity analysis will allow to direct experimental efforts only towards the most significant parameters [4].

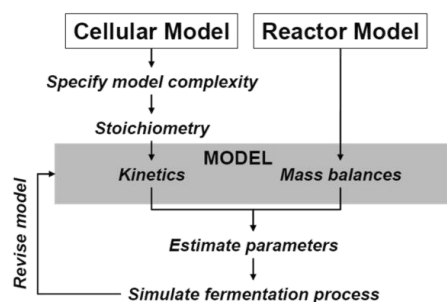


Figure 1: Main steps involved in the quantitative description of a fermentation process [5].

Acknowledgments

The research project has received founding from the Danish Council for Strategic Research (DCSR) (project Keratin2Protein: Novel approach to protein recovery from unutilized slaughterhouses waste through microbial conversion). The article represents only the author's view and DCSR is not liable for any use of the information presented here.

References

1. H.-S. Song, W.R. Cannon, A.S. Beliaev, A. Konopka, *Process* 2 (4) (2014) 711-752.
2. D.J. Daroit, A. Brandelli, *Crit. Rev. Biotechnol.* 34 (4) (2014) 372-384.
3. H. Hauduc, L. Rieger, A. Oehmen, M.C.V. Loosdrecht, Y. Comeau, A. Héduit, P.A. Vanrolleghem, S. Gillot, *Biotechnol. Bioeng.* 110 (1) (2013) 24-46.
4. K.V. Gernaey, A.E. Lantz, P. Tufvesson, J.M. Woodley, G. Sin, *Trends Biotechnol.* 28 (7) (2010) 346-354.
5. C. Ratledge, B. Kristiansen, *Basic Biotechnology*, 3rd Ed., Cambridge University Press, New York, USA, 2006, p. 156.



Marina Fedorova

Phone: +45 4525 2911
E-mail: mfad@kt.dtu.dk

Supervisors: Rafiqul Gani
Gürkan Sin

PhD Study
Started: April 2012
To be completed: March 2015

Systematic Methods and Tools for Computer Aided Modelling

Abstract

Modelling is an important enabling technology in modern chemical engineering applications. A template-based approach has been developed in this work to facilitate the construction and documentation of the models and enable their maintenance for reuse in a wider application range. This concept is implemented as a software tool, which provides a user-friendly interface for following the workflow steps and guidance through the steps providing additional information and comments on model construction, storage and future use/reuse.

Introduction

Computer-aided modelling is an important enabler in facing current and future challenges in product-process engineering. Modelling technology helps to reduce number of resource-demanding experiments and, at the same time, to deliver truly innovative solutions. Process model of reliable quality allows predicting process behaviour and based on this, to optimize the process and to improve understanding of the domain system. However, the modelling technology also requires the necessary methods and tools to perform these functions. The construction of models is mainly manual, which is still not very effective. Manually developed models usually can be applied only for the specific problem for which it was developed, such models are usually not well documented and therefore difficult to maintain.

Better application of the developed models can be achieved by reusing them through a specially developed modelling framework. This framework should increase reuse and exchange of models, provide proper documentation and support a variety of models. By using this modelling framework, the user will get a model structure, guidance and support during model development and model application and, therefore, efficiency of the modelling process will increase and the quality and reliability of the models will be improved.

Klatt and Marquardt [1] have identified prospective improvements for the present modelling tools, such as multi-scale modelling features together with documentation, maintenance and reuse of models in an efficient and economical way. The benefits of the integration of modelling tools are highlighted in the study of Zhao et al. [2], which shows the potential for

generic, non-case-specific tools. Heitzig [3] points to the importance of the systematic framework for model development and the need for implementation of templates for modelling cases and creation of the template library.

Objective

The objective of this study is to create modelling templates and combine them with other modelling tools within a modelling framework. The goal is to create a user-friendly system, which will make the model development process easier and faster and provide the way for unified and consistent model documentation.

Computer-aided Template-based Modelling

A modelling template is a generic model on which other problem-specific models are based – in this way, it is similar to a superstructure of process alternatives – that is, it includes a collection of models for the process it represents. In the template, a model is decomposed into three sets of equation types: balance equations, constitutive relations and connection and/or conditional equations. This decomposition is based on the modelling hierarchy proposed by Cameron and Gani [4]. Within each type of equations, multiple versions of model equations may be stored in the template and retrieved when necessary to generate different problem-specific models.

Model-templates are based on the knowledge representation structure (also known as ontology) as highlighted in Fig. 1. The knowledge in each model template is structured in terms of three main classes of information: upper-layer, sub-layer and block. Here, a

class is a pattern with specific parameters or characteristics, which is used for creation of the model objects. These objects are therefore the instances of the class. The collection of instances of the classes represents the total model in the template or the system.

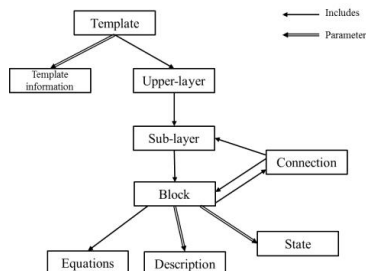


Figure 1. Structure of hierarchy in the modelling template.

Each model template includes four upper-layers, according to the structure of the decomposed model: system information, balance equations, constitutive equations and connection equations. Each upper-layer may include one or more sub-layers, which are related to the description of the system and the phenomena occurring within it. Each sub-layer may include one or more blocks, which contain the data, parameters and/or equations of the corresponding instances of the sub-layer. Each instance of a block is related to one option of the phenomena representing the connected sub-layer. Also the structure includes certain parameters and minor classes for describing template, those are equations, block description, connections and block state (see Fig. 1). Description contains information about phenomena to which the block is related. For most of the sub-layers, a block also includes one or more equations, however, some blocks, especially blocks from the upper-layer of the system information, may not include any equations, but they contain information, which effects equations of the subsequent blocks, for example, number of compounds in the reaction will change the number of balance equations. Therefore, additionally each block includes information about possible connections with blocks related to other sub-layers.

Software implementation

The template-based modelling approach is implemented as a software tool, providing easy and user-friendly interface for rapid and more efficient development and use of models. It provides an environment for creation of new templates or addition of new building blocks for existing templates and an environment for template use (see Fig. 2). It guides the user through the steps of the work-flow for template-creation or use. It allows the user to impose changes to an existing template to create new templates and/or prepare an existing model for use in a specific application. The final model equations are translated as an MoT-object and can be solved and identified through the ICAS-MoT modelling platform or

can be transferred to a text or xml-file in order to use it in external simulation environment (e.g. EXCEL, Matlab, gPROMS™). Moreover, the newly created model can be added to the model library and used as well for template creation and/or updates.

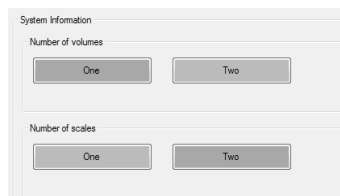


Figure 2. Upper-layer of system information including two sub-layers: number of volumes and number of scales, each of them contains two blocks, representing template options. Green (light-coloured) blocks indicate currently chosen options, blue (dark-coloured) shows the options of the template that are available.

Conclusion

The modelling template is intended to be a model repository for storing, retrieving, modifying, updating models in knowledge based systems for easy maintenance and connection to model solution and analysis software. The end goal is to make the model development process easier and more efficient. The models constructed by the template can then be exported to different simulators for various model application purposes including simulation, parameter estimation, optimization, etc. Current and future work is extending the application range for the template-based modelling including unsaturated fatty acid oxidation, as well as improving the different aspects of workflow and its software implementation

Acknowledgements

This work is performed in the framework of the project ‘Model-Based Optimization & Control for Process-Intensification in Chemical and Biopharmaceutical Systems’ (OPTICO/ G.A. No. 280813) funded by the European Commission. The contents of the publication reflect only the authors’ view.

References

1. K.-U. Klatt, W. Marquardt, 2009, Perspectives for process systems engineering - Personal views from academia and industry, *Computers and Chemical Engineering*, 33, 536-550.
2. Y. Zhao, C. Jiang, A. Yang, 2011, Towards a Generic Simulation Environment for Multiscale Modelling based on Tool Integration, *Computer Aided Chemical Engineering*, 29, 76-80.
3. Heitzig M., 2011, Computer-aided modeling for efficient and innovative product-process engineering, PhD Thesis, Technical University of Denmark, Lyngby, Denmark.
4. Cameron I., Gani R., 2011, *Product and Process Modelling. A Case Study Approach.*, Elsevier.



Ana Carolina Fernandes

Phone: +45 4525 2958
E-mail: ancafe@kt.dtu.dk
Discipline: Select from www.kt.dtu.dk

Supervisors: Associate Professor Ulrich Krühne
Professor Krist Gernaey
Project Manager Adama Marie Sesay

PhD Study
Started: July 2014
To be completed: June 2017

Micro Scale Reactor System Development with Integrated Advanced Sensor Technology

Abstract

Process development and optimization is a costly and time-consuming process involving the optimization of relevant process parameters tested at different process scales [1]. Differences between phenomena across scales often results in attaining less than optimum process parameters which will affect process productivity. These differences are usually not detected due to insufficient process control at smaller scales [2]. The development of a screening setup able to operate processes at different process conditions in parallel while providing adequate quantification and control of process parameter conditions would streamline and greatly reduce the cost of this development process and increase its reliability [3],[4],[5]. This project aims to develop such a setup through the use of microtechnology and sensor integration.

Introduction

Bioprocess optimization and development requires the study of relevant process parameters, their influence and interaction, in a reliable and scalable way. This is, often due to a high number of variables, very expensive and time-consuming [1]. High-throughput (HTP) technology, in the form of parallelized controlled reactions, allows reducing the cost and duration of industrial bioprocess development and scale-up. This is achieved by enabling the simultaneous study of several process parameters, such as temperature, pH, oxygen transfer, mixing, culture mode, media composition, type of cell or strain, available vectors, among others [3],[6]. Microtiter plates (MTP) and shaking flasks offer a simple way of increasing cultivation throughput, but without process control and limited information on process conditions [5],[6]. Furthermore, the implementation of culturing strategies as fed-batch and continuous fermentation, which are common in industrial processes, is complicated in these systems. However, since differences in the cultivation strategy between initial screening experiments and final production process may lead to a selection of suboptimal strains and/or process conditions, distinct parallelization strategies have to be applied [7],[8].

Microbioreactors (MBR) offer the potential to find a balance between process control and cultivation throughput in order to turn HTP cultivation economically and practically feasible [3]. Two

approaches are possible: bottom-up and top-down. Bottom-up approaches, represented by microchannels and shake-flasks and MTP-based setups, attempt to reproduce large scale processes but applying diverse reactor shapes and mixing or feeding strategies. Some recent MTP-based commercial approaches already integrate sensors on cultivation chambers (e.g. Biolector system from m2p labs [9]; Micro-24 MicroReactor Instrument from Pall Corporation [10]; SensorDishes® from PreSens), with fluid handling equipment for automatic small volume sampling or inocula or medium addition. Nonetheless, scale-up of the process parameters obtained with these systems can be difficult due to application of different mixing, heating or feeding strategies inherent to a bottom-up approach. Top-down approaches, on the other hand, miniaturize the entire process by mimicking large scale conditions (e.g. mixing) and reactor type, as closely as possible. Thus, the miniaturization (5 - 100 mL) and parallelization of stirred tank, batch or fed-batch reactors with respective sensor systems (e.g. ambr™ from Applicon; DASGIP Parallel Bioreactor System from Dasgip; HexaBatch System from Hexascreen Culture Technologies S.L.), allow understanding high volume processes better towards a more effective process troubleshooting. Most of MBR systems developed so far, however, lack online sensors for the most significant parameters (such as cell viability, product

concentration and quality, glucose, antibody, reaction metabolites, etc.) [11].

This PhD project, performed within the European Network for Innovative Microbioreactor Applications in Bioprocess Development (EUROMBR) project, aims to develop a HTP MBR setup with integrated sensors for relevant reaction constituents, besides sensors for the common physical parameters (Temperature, pH, DO and OD). Near Infrared (NIR)-based sensors will be considered and evaluated in terms of applicability and design integration in order to attain the best performing sensor for the target parameters. Three sensor approaches are available: NIR luminescent polymer patches [12], NIR luminescent nanoparticles [13], and miniaturization of a conventional NIR setup for MBR integration. Further, a new design for a MBR setup will be developed starting from existing platform configurations with the intention to integrate the sensors in an easily operable, reliable and scalable way.

In order to validate the applicability and operation range of both the new MBR design, as well as the developed sensors, both biocatalytic and fermentation applications will be tested. Two biocatalytic reactions, Gluconic acid production with Glucose oxidase (GOx) and (S)- α -Methylbenzylamine (α -MBA) production with an ω -Transaminase (ω -TAm) [14] were chosen as the biocatalytic specific applications. These will be compared against batch MTP-based systems. Further, a relevant fermentation process with *Sacharomyces cerevisiae* will also be tested and a comparison with bench scale reactors will be performed. Since this project's objective is the development of a parallelized HTP MBR setup with sensor and control integration, the focus will be on platform development towards a multi-process usable MBR platform.

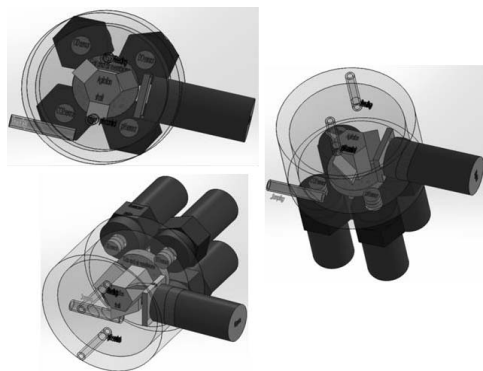


Figure 1: Schematics of MBR design with integrated sensors for continuous processing and sampling.

Specific Objectives

1. Literature investigation of relevant metabolites in bioprocesses currently not detected in HTP platforms. Identification of best sensor configuration for chosen metabolites in the literature.

2. Design of a MBR setup for integration of the chosen sensors. The new design will take into consideration the usual range of conditions for bioprocess reactions in terms of temperature, pH, mixing, DO and OD, with integration of commercially available sensors for these parameters. Pump assisted addition and sampling of fluids will be included, as well as, control for temperature, pH, mixing/DO and feeding.

3. Test and optimization of sensors and final integrated in MBR setup.

4. Determination of sensor's detection limits and sensitivity in MBR setup for all chosen process applications.

5. Final validation (proof-of-concept) of complete MBR setup and comparison with results from bench top setup for all process applications.

6.

Acknowledgements

The research leading to these results has received funding from the People Programme (Marie Curie Actions) of the European Union's Seventh Framework Programme FP7/2007-2013/ under REA grant agreement n° 608104 (EUROMBR). The article reviews only the authors' views and European Union is not liable for any use of the information presented here.

References

1. Rameez S, Mostafa SS, Miller C, Shukla AA.. *American Institute of Chemical Engineers* 30 (2014) 718-727.
2. Funke M, Buchenauer A, Schnakenberg U, *et al. Biotechnology and Bioengineering* 107(3) (2010) 497-505.
3. Long Q, Liua X, Yanga Y, *et al. Journal of Biotechnology* (2014).
4. Bareither R, Pollard D. *American Institute of Chemical Engineers*. 27 (2010) 2-14.
5. Betts JI, Baganz F. *Microbial Cell Factories* 5(21) (2006).
6. Rohe P, Venkanna D, Kleine B, Freudl R, Oldiges M. *Microbial Cell Factories* 11(114) (2012).
7. Lee H, Boccazzi P, Ram R, Sinskey *Lab on a Chip* 6 (2006) 1229-1235.
8. Szita N, Boccazzi P, Zhang Z, Boyle P, Sinskey AJ, Jensen KF. *Lab on a Chip* 5 (2005) 819-826.
9. Huber R, Roth S, Rahmen N, Büchs J. *BMC Biotechnology* 11(22) (2011).
10. Chen A, Chitta R, Chang D, Amanullah *Biotechnology and Bioengineering* 102(1) (2009) 148-160.
11. Schäpper D, Alam, Muhd Nazrul Hisham Zainal, Szita N, Lantz AE, Gernaey KV. *Anal Bioanal Chem.* 39 (2009) 679-695.
12. Ungerböck B, Charwat V, Ertl P, Mayr T. *Lab on a Chip* 13(8) (2013) 1593-1601.
13. Ungerböck B, Fellinger S, Sulzer P, Abel T, Mayr T. *Analyst* 139 (2014) 2551-2559.
14. Tufvesson P., Jensen J.S., Kroutil W., Woodley J.M. *Biotechnol Bioeng.* 109(8) (2012) 2159.



Diana Carolina Figueroa Murcia

Phone:
E-mail: difm@kt.dtu.dk
Discipline: DTU Kemiteknik

Supervisors: Kaj Thomsen
Philip Loldrup Fosbøl

PhD Study
Started: December 2013
To be completed: December 2016

Risk Associated With the Decompression of High Pressure High Temperature (HP/HT) Fluids - Study on Pure Liquid Water

Abstract

Significant changes in the final temperature after the decompression of pure liquid water are experienced when decompressed from high pressures and high temperatures (HP/HT). A temperature increase is observed for pure liquid water upon decompression, opposite to what is expected for a decompression process. This is a consequence of the inversion of the Joule Thomson Effect for liquid water at temperatures below 250°C. A prediction of the final temperature is performed based on a thermodynamic analysis of the phenomenon. The study is done on pure liquid water at initial pressures of 1500, 1000 and 500 bars and at initial temperatures between 100 and 350°C.

Introduction

The increase of temperature during decompression as a result of the inverse Joule Thomson Effect (JTE) can cause serious operational problems in different processes. For instance in a geothermal reservoir, i.e. a brine system at high pressure, the decompression process might lead to sudden evaporation of the aqueous phase. As a consequence precipitation of the salts in the brine can occur. The resulting scaling can cause problems of clogging pipes and fittings among other problems.

The inverse JTE stands for an increase of temperature during the expansion of a fluid. A decrease (JTE) or an increase in temperature (inverse JTE), are directly correlated to the inversion temperature of the fluids which depends on the physicochemical and thermodynamic properties of the fluid and the initial temperature and pressure of the process. For example in the case of Argon (Ar) and carbon dioxide (CO₂) the inversion temperatures are 449.8°C and 1226.8°C respectively at 1 bar and 25°C.

Studying the JTE and its inversion is of the utmost importance since these effects may drive adverse consequences in different processes if they are not considered due to an anomalous heat flow. Instead, the JTE and the inverse JTE can be anticipated if a rigorous study is done based on the fluid characteristics and the thermodynamic analysis of the process.

The JTE has been mostly studied for the expansion of gases as mentioned above and implemented for the liquefaction of gases and refrigeration cycles (e.g. Linde

refrigerator), but this effect is also observed in liquid and in solid phase, meaning that the gaseous behavior as it is stated in the Joule Thomson experiment is not a requirement as mentioned by Adkins [1] and by Atkins and Paula [2].

Theoretical background

The Joule Thomson effect is quantified by the Joule Thomson Coefficient (JTC), which is positive in the case of the classic definition of the JTE and negative in the case if the inverse JTE. The conventional thermodynamic definition of the JTC (μ) is shown in Eq. (1) (Vrabec, Kumar, & Hasse, 2007):

$$\mu = \left(\frac{\partial T}{\partial P} \right)_H = \frac{V}{C_p} [T\alpha - 1] \quad (1)$$

Where μ is the JTC, C_p is the isobaric heat capacity and α is the isobaric expansivity. As can be observed in Eq. (1) the Joule Thomson coefficient is a state quantity which depends on the actual pressure and temperature.

Methodology

The JTE and the inverse JTE during the decompression of pure liquid water are addressed by setting up an energy balance of the system. The decompression process is assumed to occur at adiabatic conditions with no change of phase. The decompression is thus completed before reaching the bubble point of liquid

water. The energy balance is set up for two different cases. The first case is a steady-state process that includes significant terms for kinetic and potential energy (non-isenthalpic). The energy balance expression is shown in Eq. (2) [3]

$$\Delta H + \frac{\Delta u^2}{2} + g\Delta z = Q - W_s \quad (2)$$

ΔH is the change of enthalpy in the process, Δu is the change of velocity of the flowing fluid, g is the gravitational acceleration, Δz is the change in elevation, Q is the heat transfer to the system and W_s the shaft work. The second case is a process without significant changes in potential and kinetic energy (an isenthalpic process).

Results and analysis

The results of the JTE and inverse JTE for pure liquid water are presented in this section and are shown as the difference in temperature ΔT ($T_{\text{final}} - T_{\text{initial}}$) versus pressure for a decompression process. The final temperature calculations are performed using the IAPWS 95 formulation for the Properties of Water and Steam [4]

For the calculation of the Joule Thomson Coefficient (JTC) the initial pressure and temperature of the process are set. The JTC at initial temperatures of the process between 100 – 350 °C against pressure is presented in Fig. 1. There are two types of lines shown, solid lines represent the JTC at non-isenthalpic conditions and the dashed lines represent the JTC at isenthalpic conditions.

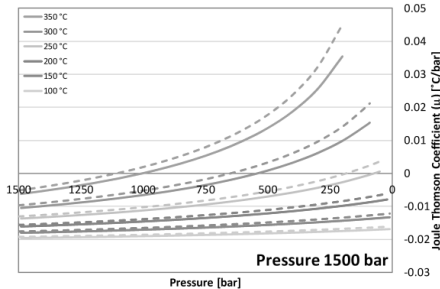


Figure 1 Joule Thomson coefficient for liquid water at initial pressure of 1500 bars [4].

Figure 1 shows that for temperatures below 250 °C the JTC for water remains negative. It means that an increase in temperature is expected upon decompression. The change in temperature ΔT for a de-compression process initially starting at 1500 bars is shown in Fig. 2. The difference between the non-isenthalpic and the isenthalpic process is expressed in the fact that the lines for the non-isenthalpic process are shifted down compared to those at isenthalpic conditions; this is due to a change in enthalpy as a result of the contribution of the potential and kinetic energy to the process. As stated by Ramberg [5] the change in potential energy “compensates for major part of the decompression” and as a consequence the final temperatures are lower than

those obtained at isenthalpic conditions. The decompression at initial temperatures between 100 and 300 °C ΔT is always positive at isenthalpic conditions, meaning that the final temperature is higher than the initial temperature, but at non-isenthalpic conditions the scenario is different. For instance, the case of initial temperature of 200 °C shows that the final temperature at non-isenthalpic conditions is lower than the final temperature obtained at isenthalpic conditions.

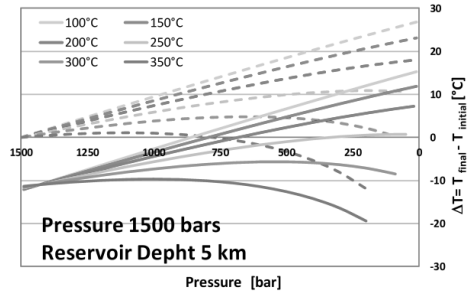


Figure 2: Decompression of liquid water at 1500 bar ΔT vs P at 5 km reservoir depth

Conclusion

The adiabatic decompression of pure liquid water does not occur at constant temperature. Changes of the final temperature compared to the initial temperature are observed. An increase in the final temperature of up to 15°C is observed. The inclusion of the terms for kinetic and potential energy into the energy balance, lower the effect over the final temperature. The behavior of pure liquid water in a decompression process is unexpected. This unusual behavior of liquid water is a consequence of an inversion of the Joule Thomson Effect. The accurate prediction of the final temperature of liquid water can benefit the operating conditions in the production of e.g. geothermal energy or understanding the behavior of other fluids confined in reservoirs at high pressure and high temperature such oil.

References

1. Adkins CJ. Equilibrium Thermodynamics. 1983.
2. Atkins PW, Paula Jd. Atkins' physical chemistry. : Oxford University Press, 2006.
3. Smith JM, Van Ness HC. Introduction to chemical engineering thermodynamics. 1987.
4. NIST/ASME. NIST/ASME Steam Properties Database 10: Version 3.0 Based upon the International Association for the Properties of Water and Steam (IAPWS) 1995 formulation. 2013.
5. Ramberg H. Temperature Changes Associated with Adiabatic Decompression in Geological Processes. Nature 1971;234:539.



Rebecca Frauzem
Phone: +45 4525 2912
E-mail: rebfra@kt.dtu.dk
Discipline: Process and Plant Design

Supervisors: Rafiqul Gani, DTU
John M. Woodley, DTU
Krist Gernaey, DTU

PhD Study
Started: October 2014
To be completed: September 2017

Sustainable Process Design with Process Intensification

Abstract

According to the regulatory groups, the effect of carbon dioxide on global warming is an issue that needs to be addressed. In order to achieve the reduction of carbon dioxide emissions, sustainable industrial practices and processes need to be implemented. In order to achieve this, a framework is being developed which provides a systematic method of developing more sustainable processes. Through the use of tools and methods, a step-by-step procedure can be followed to yield sustainable process design alternatives. This methodology will then be validated with the use of case studies.

Introduction

According to the Intergovernmental Panel on Climate Change, global warming is becoming an ever-increasing problem that needs to be addressed by social, industrial, academic, and government groups [1]. As a result of this issue, various industrial contributors to global warming are being addressed [2]. One of the main sources of global warming is the emission of greenhouse gases, including carbon dioxide. In order to accomplish the reduction of global warming, sustainable practices must be incorporated into industrial processes [1]. Chemical, petroleum and other manufacturing processes emit significant amounts of greenhouse gases and other pollutants that contribute largely to global warming [2]. Sustainability needs to be incorporated in various elements of these processes to help reduce emissions, pollution and waste. Currently, a variety of possibilities are being investigated. The primary goal of all methods is the reduction of harmful emissions and the introduction of sustainable practices.

In order to achieve the necessary sustainability in industrial processes, procedures need to be developed that allow companies to target specifics of their processes for improvement. For the reduction of carbon dioxide emissions into the atmosphere, it is possible to create a framework to accomplish this. The implementation of this framework allows for the systematic reduction of emissions and the improvement of the sustainability for various processes. This can then be verified using case studies.

Specific Objectives

By targeting carbon dioxide emissions, it is possible to improve the sustainability of a process. Finding methods of reducing the emissions is the goal of the framework that is being created. Carbon dioxide utilization is a promising addition to carbon capture and storage [3]. By using the carbon dioxide as a feedstock and converting it to valuable products, it is possible to eliminate some emissions and form other compounds that can be used. Using a systematic framework a network of carbon dioxide conversion methods will be optimized to yield the most sustainable options. The following will be achieved in this PhD project:

- 1) Generation of a framework that is a step-by-step procedure for the formulation of more sustainable processes. This framework will guide the user through steps and will be governed by rules to ensure proper implementation.
- 2) Utilization of outside data, tools and models to acquire the necessary information. Within the steps, there are various inputs that are necessary. To obtain all the information that needs to be input for each step, outside sources are useful.
- 3) Creation of a superstructure-based method for the determination of the optimal processes to target for improved sustainability [4] [5].
- 4) Implementation of process synthesis and intensification to further improve the sustainability of targeted processes [6].
- 5) Validation of the method through the study of specific cases.

Results and Discussion

Due to an increasing global population, there is increasing development. With this development comes the increasing emission of greenhouse gases, primarily carbon dioxide. While Carbon Capture and Storage is a long-term method of reducing emissions, additional solutions are needed. Carbon dioxide is also a valuable chemical compound that can be used in conversion processes to make other valuable products. With the help of data and literature, the feed and products can be defined.

Next is the implementation of process synthesis and design. This uses a superstructure-based approach, which makes it possible to develop a network linking raw materials and products. For this, carbon dioxide is a primary raw material involved in all the steps. In order to optimize this, a variety of information needs to be supplied to detail all elements of the superstructure. This includes a detailed description of the materials, information about the reactions, information about the separation and other unit operations involved, and a description of the linkage between processes. The result is a network of feasible conversion processes. In order to optimize this, more information is necessary to fully describe all process steps and the paths mathematically.

Once the network is described, it is also possible to design a base case for the individual processing paths. This base case design can then be used to provide more mathematical insight into the superstructure as well as provide the foundation for the performance of analysis and improvements. With the help of software, the detailed base case design can be analyzed. Determining the hotspots then allows for improvements through intensification, integration and optimization. Comparing the net carbon dioxide of the process (both the amounts in material streams as well as in the energy and electricity production) and ensuring that the economics are not compromised results in a non-trade-off solution. The end result is a more sustainable design for the processing path within the superstructure.

Conclusions

Sustainability is a major issue that needs to be addressed in industrial processes. Targeting carbon dioxide emissions is one element of this. With the help of a systematic framework, it is the goal to improve the sustainability with respect to carbon dioxide emissions for chemical processes. By using a superstructure-based approach it is possible to determine the optimal path or set of paths for the conversion processes. These can then be further improved to create the most sustainable design alternative.

References

1. Climate Change 2007: Mitigation of Climate Change, Fourth Assessment Report, Intergovernmental Panel on Climate Change (IPCC), 2007.
2. International Energy Outlook, U.S. Energy Information Administration (EIA), 2013.

3. M. Aresta, Carbon Dioxide as a Chemical Feedstock, Wiley-VCH Verlag GmbH, Weinheim, 2010. doi:10.1002/9783527629916
4. A. Quaglia, B. Sarup, G. Sin, R. Gani, Integrated business and engineering framework for synthesis and design of enterprise-wide processing networks. *Computer Aided Chemical Engineering* 38 (2012) 213-223. doi:10.1016/j.compchemeng.2011.12.011
5. E. Zondervan, M. Nawaz, A. B. de Haan, J. M. Woodley, R. Gani, Optimal design of a multi-product biorefinery system. *Computer Aided Chemical Engineering* 35 (2011) 1752-1766. doi:10.1016/j.compchemeng.2011.01.042
6. D. K. Babi, J. M. Woodley, R. Gani, Achieving More Sustainable Designs through a Process Synthesis-Intensification Framework. *Computer Aided Chemical Engineering* 33(2014) 31-36. doi:10.1016/B978-0-444-63456-6.50006-5

List of Publications

1. R. Frauzem, P. Kongpanna, K. Roh, J. H. Lee, V. Pavarajarn, S. Assabumrungrat, R. Gani. Sustainable Process design: Sustainable Process Networks for Carbon Dioxide Conversion, in: F. You (Ed.), *Sustainability of Products, Processes and Supply Chains*, Elsevier Ltd., New York, 2015.



Jerome Frutiger

Phone: +45 4525 2911
E-mail: jfru@kt.dtu.dk
Discipline:

Supervisors: Gürkan Sin
Jens Abildskov

PhD Study
Started: Jun 2014
To be completed: May 2017

Computer-aided molecular design and property prediction models for working fluids of thermodynamic cycles

Abstract

The aim of the PhD project is the development of novel working fluids for thermodynamic cycles such as organic Rankine cycles. Through the use of Computer-aided molecular design (CAMD) novel candidates for both pure components and mixtures will be generated and evaluated. In this scope the development of new property prediction models is an important fundamental tool for the design.

Introduction

The efficient use of heat sources is crucial in terms of resource efficiency and decreasing environmental impact of industrial application. Power cycles such as organic Rankine cycles (ORC) allow the conversion of heat into electric energy. The basic technology relies on thermodynamic cycles which consist of a compressor, an expansion valve and two heat exchangers (evaporator and condenser) (see Figure 1) [1].

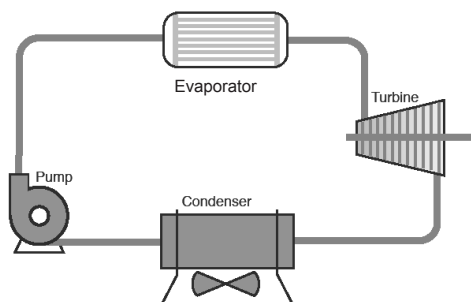


Figure 1: Scheme of an organic Rankine cycle (ORC).

Currently this technology is known to be well established for high-temperature heat sources. However, in recent years there is a large availability of low-temperature heat sources in different applications such as waste heat from marine diesel engines, industries and refrigeration plants as well as renewable energy sources such as biomass combustion, geothermal and solar heat sources. So far the low-temperature heat cannot be

utilized efficiently for heat pump operation. This means, a large amount of moderate temperature heat is simply wasted [2].

In order to optimize industrial heat pump processes for adding and removing heat from the cycle, the influence of the working fluid, the cycle designs and the operating conditions can be vital.

The objective of this project is to develop new working fluids by the use of multi-criteria database search and Computer Aided Molecular Design (CAMD) principles [3] and is carried out in collaboration with DTU Mechanical Engineering.

In order to be able to design novel working fluids it is necessary to identify and develop property prediction models for estimating pure component as well as mixtures properties. Furthermore it is necessary to integrate the optimization of the working fluid and the cycle design, because the two key features influence each other strongly.

Framework

The framework for the development of novel working fluids [4] looks as follows (see Figure 2).

1. Identification of needs of working fluids: The general requirements and desired behavior of a working fluid have to be identified and formulated in collaboration with DTU Mechanical Engineering.
2. Translation of needs into target properties: The target properties are specified from the needs. Examples of target properties are thermodynamic properties such as thermal conductivity or heat capacity, kinetic properties

such as viscosity and density, but also safety properties such as the lower flammability limit and environmental properties such as the ozone depletion potential.

- 2a) Development of pure component and mixture property models: Most of the specific properties have to be estimated and therefore novel property prediction models have to be developed.
- 2b) Database for experimentally measured properties: The estimated and experimental properties have to be stored for the use for specific thermodynamic cycle application
3. Generation candidates as working fluids: A CAMD algorithm is developed in order to generate new molecular candidates as well as mixtures as process fluids candidates. The optimization is subject to feasibility criteria and target application constraints.
4. Evaluation of candidates: The set of generated working fluids for a specific application is evaluated using a variety of assessment criteria such as heat transfer ability, safety and environmental constraints such as ozone depletion potential (ODP) and Global Warming Potential (QWP), chemical stability as well as efficiency and compatibility with compressor lubricants and equipment materials.

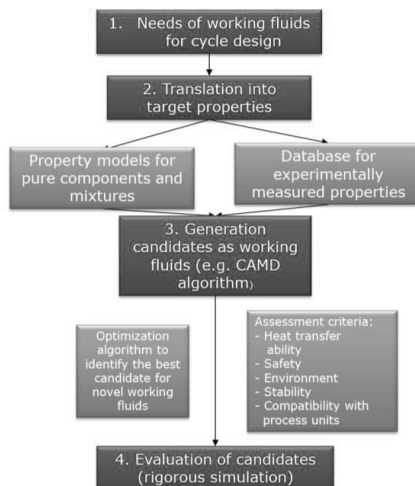


Figure 2: Framework of the project.

Current and future work

We are developing a framework for group contribution property prediction models including algorithms, methodology development and uncertainty analysis. We are applying the model for the estimation of the upper and lower flammability limit of chemicals, which is important information to quantify the risk of working fluids for fire and explosion.

References

1. C. M. Invernizzi, Closed Power Cycles, Springer-Verlag, London, UK, 2013.
2. H. Chen, D. Y. Goswami, E. K. Stefanakos, Renewable and Sustainable Energy Reviews, 14, (2010) 3059.
3. P. M. Harper, R. Gani, P. Kolar, T. Ishikawa, 1999. Fluid Phase Equilibria, 99, (1999) 158–160.
4. N. A. Yunus, K. G. Gernaey, J. M. Woodley, R. Gani, Computers and Chemical Engineering, 66, (2014), 201-213.



Rasmus Østergaard Gadsbøll
Phone: +45 6066 8815
E-mail: rgad@kt.dtu.dk
Discipline: Thermal Gasification and Pyrolysis

Supervisors: Ulrik Birk Henriksen, CHEC, DTU
Jesper Ahrenfeldt, CHEC, DTU
Lasse Røngaard Clausen, MEK, DTU
Jens Dall Bentzen, Dall Energy

PhD Study
Started: December 2014
To be completed: March 2018

Investigation of oxygen-blown biomass gasification

Abstract

This project aims to investigate oxygen-blown biomass gasification and project larger scale plants using the concept of the Viking gasifier at DTU. Tests with oxygen-blown gasification will be carried out at Risø campus on a modified Viking gasifier, where efforts especially related to process optimization and gas analysis will be made. Tests with the gasifier coupled to a SOFC will be carried out as well. Studies will be carried out to investigate upscaling the Viking gasifier to 10-50 MW_{th}, by analyzing different reactor designs, flow configurations, tar reducing measures, while still obtaining very high gas quality.

Introduction

This project is a part of the Biomass Gasification Polygeneration (BGP) project under ForskVE. The project's aim is to design and optimize a flexible biomass gasification system, that in batch-operation can either: produce power through a solid oxide fuel cell (SOFC) when demand is high or consume power through a solid oxide electrolysis cell (SOEC) to produce Bio-SNG (synthetic natural gas) when the demand is low. While power production via biomass gasification and a SOFC stack has been done recently, conversion of biomass, oxygen and hydrogen into Bio-SNG is a very limited research subject.

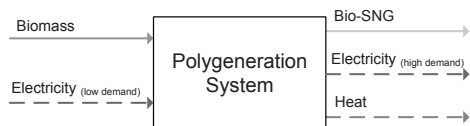


Figure 1: Flexible biomass gasification polygeneration concept. At high power demand, electricity is produced by a SOFC. At low demand, electricity is consumed in a SOEC to produce Bio-SNG.

This project is an applied research project that will research oxygen-blown biomass gasification (thermal), both experimentally and theoretically. The project will modify, test and operate the 75 kW_{th} Viking gasifier located at Risø campus with an oxygen-steam mixture (rather than its usual air-blown configuration) and

investigate large-scale versions of the system at 10-50 MW_{th}.

The Viking gasifier processes wood chips into high quality gas at high temperatures that can be utilized in combustion applications, engine operation, chemical synthesis etc. – see flow diagram of the gasifier on **Error! Reference source not found.** The gasifier is characterized by high efficiency and very good gas quality. The *product* gas consists mostly of CO, H₂, CO₂ and N₂ and has a 5.6 MJ/Nm³ lower heating value [1]. The gasifier uses partial combustion to convert the solid biomass to product gas, by injecting air into the reactor – producing a high-volume nitrogen containing gas (33 vol %).

It is desired to examine the potential for using the product gas in chemical synthesis and therefore the nitrogen content is unwanted, due to costly separation processes.

The Viking gasifier is constructed with a pyrolysis unit that features an externally heated conveyor screw and a fixed bed reactor for oxidation and char gasification. These reactors are however not easily scaled and new designs are needed to project larger plants of the gasifier.

Through extensive experimental work, this project will modify, operate and optimize oxygen-blown gasification on the Viking gasifier in order to investigate the potential for producing a nitrogen free product gas suited for chemical synthesis.

The reactors for pyrolysis and char gasification are not suited for significant upscaling, due to limited heat transfer capabilities and other aspects. The plant concept



Carina Lira Gargalo

E-mail: carlour@kt.dtu.dk
Discipline: Process Systems Engineering
Supervisors: Gürkan Sin
Rafiqul Gani

PhD Study
Started: November 2013
To be completed: November 2016

Sustainable design of Biorefinery Systems for Biorenewables

Abstract

The design assessment and design of sustainable chemical/biochemical processes is shown to be a complex multi-criteria/objective decision-making process, not only regarding the multi-level evaluation, but also due to the significant amount of uncertain input data [1]. As a guide through this process, sustainability indicators [2] have been being proposed along the years as a performance measurement tool. Furthermore, replacing oil in all applications (including plastics, chemicals and other value-added products) by biobased products could be the key to achieve this goal [3]. Therefore, the objective of this project is to develop a framework that allows the user to systematically generate competing solutions and optimal biorefinery options. The framework will be validated through several case studies on the integrated biorefinery concept, such as the production of biodiesel and value-added derivatives from vegetable oil or lignocellulosic biomass.

Introduction

One of the biorefineries biggest challenges is to develop the ability to sustainably convert different biorenewables into high value-added chemicals and fuels as efficiently as the current petrochemical industry. Moreover, it is important to note that there are significant sources of uncertainty that biorefineries are subject to. Among others, these uncertainties may include market price fluctuations, technical performance variations and environmental model predictions. Several studies have developed methods to create new designs or improve an already existing design by retrofit techniques with the objective of decreasing for instance the energy, water or raw material consumption. Among them, Uerdingen *et al.* (2003), El-halwagi (1998), Rapoport *et al.* (1994), Carvalho *et al.* (2008) and Cheali *et al.* (2013).

However, there is still a need to systematically collect and manage the overwhelming amount of data required for analysis, and to efficiently identify the sources of uncertainty and their propagation into the decision-making procedure. The objective of the present project is to propose a systematic multi-level framework under uncertainty analysis which uses superstructure optimization to obtain a base-case design subject to design constraints and a set of performance criteria. The base-case design will be evaluated through sustainability analysis in order to logically identify the

process hot spots. The obtained information is then used to set design targets for achieving a more sustainable design through retrofitting techniques.

Discipline

The research is mainly conducted within the field of process systems engineering and sustainable design.

Research Methodology & Tasks

The objective of this work is achieved by developing a systematic step-by-step methodology. The workflow is presented in Figure 1, and a brief description follows. Part 1 & Part 2: to actively and efficiently manage the data collection by a superstructure generation technique, Part 3: to perform economic analysis under deterministic and uncertainty analysis. Part 4: to perform environmental impact analysis by applying life-cycle assessment models under uncertainty and sensitivity analysis. Part 5: multi-criteria decision making.

Integrating parts 1 to 5, the user will be able to (i) comprehensively collect all the alternatives, (ii) identify the process's critical points, (iii) propose alternatives to overcome them and, (iv) to evaluate the system through a full sustainability set of metrics, under uncertainty and sensitivity analysis.

The framework will be validated by applying it to biorefinery case studies, such as, the lignocellulosic and

vegetable oil conversion to biofuels and value-added chemicals, identifying the respective optimal solutions with respect to the selected set of constraints.

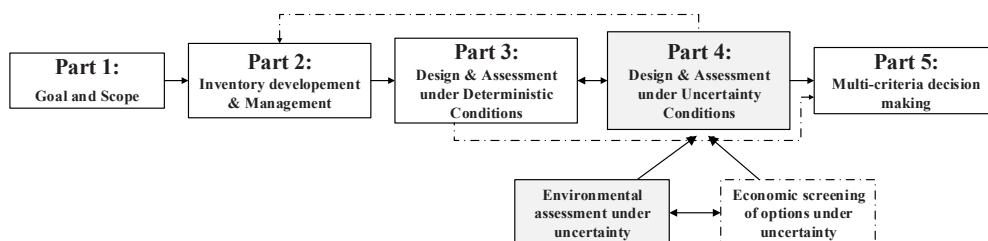


Figure 1: Workflow for sustainable process design under uncertainty. Adapted from [9].

Conclusions

The integrated use of detailed sustainability analysis and life cycle assessment models in selecting the best design has not yet been proposed. Therefore, the framework objective is to systematically generate and identify the optimal flowsheet alternative(s) with respect to the objective function subject to a set of performance criteria given by sustainability metrics involving economic and environmental indicators. The framework, it will be applied to several case studies, such as the production of biofuels and high value added chemicals from vegetable oil and lignocellulosic feedstocks.

References

1. A. E. Bjrklund, "Survey of Approaches to Improve Reliability in LCA," vol. 7, no. 2, pp. 64–72, 2002.
2. A. Azapagic, A. Howard, A. Parfitt, B. Tallis, C. Duff, and C. Hadfield, "Sustainable Development Progress Metrics," *ICHEME*, 2002.
3. I. K. K. 2009. de Jong, Ed, René van Ree, "Biorefineries: Adding Value to the Sustainable Utilisation of Biomass.," *IEA Bioenergy*, 2009. [Online]. Available: www.ieabioenergy.com/LibItem.aspx?id=6420.
4. E. Uerdingen, U. Fischer, K. Hungerbühler, and R. Gani, "Screening for Profitable Retrofit Options of Chemical Processes: A New Method," *AIChE J.*, vol. 49, no. 9, pp. 2400 – 2418, 2003.
5. M. M. El-Halwagi, "Pollution Prevention Through Process Integration: Systematic Design Tools," in *Academic Press*, CA., San Diego, 1997.
6. H. Rapoport and R. Lavie, "Retrofit Design of New Units into an Existing Plant," *Comput. Chem. Eng.*, vol. 18, pp. 743–753, 1994.
7. A. Carvalho, R. Gani, and H. Matos, "Design of sustainable chemical processes: Systematic retrofit analysis generation and evaluation of alternatives," *Process Saf. Environ. Prot.*, vol. 86, no. 5, pp. 328–346, Sep. 2008.
8. P. Cheali, K. V. Gernaey, and G. Sin, "Towards a computer-aided synthesis and design of biorefinery networks – data collection and management using a generic modeling approach," 2013.
9. C. L. Gargalo and G. Sin, "Sustainable Process Design under uncertainty analysis: targeting environmental indicators," 2015.

**Jozsef Gaspar**

Phone: +45 4525 2876
E-mail: joca@kt.dtu.dk
Discipline: DTU Kemiteknik

Supervisors: Philip Loldrup Fosbøl
Kaj Thomsen, Nicolas von Solms
John Bagterp Jørgensen

PhD Study
Started: December, 2013
To be completed: April, 2016

A Dynamic Mathematical Model for Packed Columns in Carbon Capture Plants

Abstract

In this paper we present dynamic mathematical models for the absorption and desorption column in a carbon capture plant. Carbon capture plants must be operated in synchronization with the operation of thermal power plants. Dynamic and flexible operation of the carbon capture plant is important as thermal plants must be operated very flexibly to accommodate large share of intermittent energy sources such as wind and solar in the energy system. To facilitate such operation, dynamic models for simulation, optimization and control system design are important. The dynamic model presented in this paper is suitable for gas-liquid packed columns, e.g. for CO₂ absorption and desorption modelling. The model is based on rigorous thermodynamic and conservation principles and it is set up to preserve these properties upon numerical integration in time. Furthermore, a reduced order model for CO₂ post-combustion capture modelling is presented.

Introduction

Carbon Capture and Storage (CCS) has emerged as one of the main alternatives for sustainable energy infrastructure development and it is moving towards industrial deployment. Post-combustion capture (PCC) is a mature technology that is suitable for various processes in power plants, the steel industry, cement production, petroleum refining, and the bio-chemical industry, etc. There are several industrial scale demonstration post-combustion units. Later this year, the Canadian Boundary Dam coal-fired power plant is to be the first implementation of CCS on a commercial scale. This unit will capture and pipe around 1 million tons of CO₂ annually.

The growing focus to reduce CO₂ emissions imposes the need to implement CO₂ capture technologies in fossil fuel-fired power plants. However, issues related to the large costs and high energy use of the CCS technology is still issues that need to be resolved. One possible solution is the part load operation of capture units during periods of high peak electricity prices which leads to the increase of the energy output of thermal power plants. In addition, the increasing use of renewable energy sources, e.g. wind and solar energy also impose the need for flexible operation of power plants. Power plants already operate with large and frequent load changes on a daily basis to balance the power production and the electricity demand [1]. Therefore, plant-wide dynamics of the thermal power

plant with an integrated PCC plant must be understood and controllable to maintain flexibility of the thermal power plant operation. Consequently, dynamic models for simulation and control of the units as well as the entire CCS plant during fluctuating electricity production are needed.

The purpose of the present work is to derive a dynamic model for packed columns transient simulation. The model uses rigorous heat and mass transfer models and it is based on rigorous thermodynamics. Simplifications to obtain reduced order models CO₂ absorption and desorption modelling are discussed. These discussions facilitate fast model prototyping and accelerated progress of advanced control and optimization structures. The differential equation scheme is kept compact and robust but also modular in order to maintain the flexibility of the system and to make it easy to implement. The developed model is validated against the DTU-CAPCO₂ steady-state model and experimental data respectively. Furthermore, a sensitivity analyses is performed to show the response of CO₂ absorption respectively desorption column at various design and operational conditions. This work represents a first step towards dynamic modelling and control of CCS processes using our in-house dynamic capture unit in conjunction to industrial simulators, such as Aspen Dynamics, Hysys, GPRoms, etc.

Dynamic CO₂ capture model

In this section, we provide an overview of a mechanistic first principle based model for CO₂ absorption and desorption using monoethanolamine. The mathematical model of the absorber and stripper are similar with the exception that the stripper requires a reboiler unit. Mass and energy balances for the gas and liquid phase represent the base of the model. These equations depend on heat and mass transfer fluxes between the liquid phase and the gas phase and on the rate of reaction between CO₂ and MEA. To keep the model flexible and generic, we consider that the mass transfer between the phases is bi-directional.

In addition, we assume:

- The flow fields of the column are turbulent.
- No accumulation in the gas and liquid films.
- MEA is non-volatile.
- Reaction takes place only in the liquid film.
- Heat loss to the surroundings is negligible.

Mass and energy conservation equations

The plug-flow model is a common model to describe packed columns, e.g. the CO₂ absorber and desorber. According to the plug-flow model, we divide the column in infinitely small elements, the so called control volume. The conservation of mass and energy is applied to these control volume.

Therefore, the resulting differential mass balances in the gas phase and the liquid phase are as follow:

$$\frac{\partial y_i}{\partial t} = -\frac{1}{C_g} \frac{\partial N_{i,g}}{\partial z} - \frac{a}{\varepsilon(1-h_L)} J_{i,gl} \quad (1)$$

$$\frac{\partial X_i}{\partial t} = \frac{1}{C_l} \frac{\partial N_{i,l}}{\partial z} + \frac{a}{\varepsilon h_L} J_{i,gl} \quad (2)$$

y_i is the mole fraction of component i in the gas phase; X_i is the apparent mole fraction of component i in the liquid phase. $N_{i,g}$ and $N_{i,l}$ denotes the gas and liquid flux of component i ; $J_{i,gl}$ is the mass transfer flux of component i through the gas-liquid interface [2]. Component i can be CO₂, H₂O and MEA.

To facilitate the application of the energy conservation principles, we assume that the mass and heat transfer area are equal. In addition, it is assumed that the volatile components condense at the gas-liquid interface releasing the heat to the liquid. Based on these assumptions, the conservation of energy for the gas phase and the liquid phase are:

$$\frac{\partial U_g}{\partial t} = -\frac{\partial Q_g}{\partial z} - \frac{a}{\varepsilon(1-h_L)} q_{cond} \quad (3)$$

$$\frac{\partial U_l}{\partial t} = \frac{\partial Q_l}{\partial z} + \frac{a}{\varepsilon h_L} (q_{conv} + q_{cond} + q_{gen}) \quad (4)$$

where U_g and U_l are the internal energy of the gas and liquid phase; Q_g and Q_l is the heat flux; q_{conv} refers to the heat transported through the gas-liquid interface; q_{cond} is the heat flux by conduction; and q_{gen} gives the generated heat by reaction or condensation/evaporation.

Results and discussion

The present study investigates the accuracy of the developed dynamic model for CO₂ absorption and desorption. The simulation case corresponds to a 200 t/hr CO₂ capacity post-combustion capture plant using 30 wt.% MEA solution. Fig. 1 shows the comparison of the model with the CAPCO2 steady-state results.

Fig. 1a shows the CO₂ concentration profiles, calculated with the dynamic model and CAPCO2, at three liquid to gas flow ratios (L/G) as function of the column height. This figure underlines that the results obtained by the dynamic model and the steady-state model overlap. Fig. 1b presents the performance of the implemented model for desorption simulation. This figure illustrates the liquid temperature profiles as function of the height of the desorber when the reboiler temperature is set to 121°C and 118°C. The comparison underlines the good agreement between the two models. The deviation between the dynamic model and CAPCO2 are up to 7°C

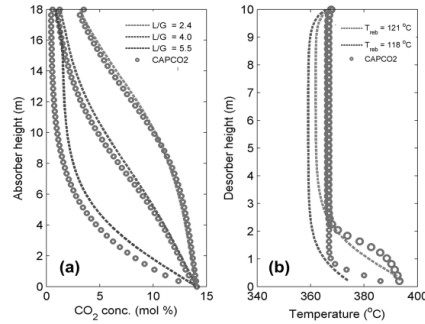


Figure 1: Comparison of the dynamic model with the steady state CAPCO2 model: (a) CO₂ profile vs. absorber's height (b) Temperature profile vs. desorber's height.

Conclusions

This work presents a dynamic mathematical model for the absorption and desorption column in a carbon capture plant. The model is aimed for robust and rigorous dynamic simulation but also for online optimization and control strategies development. For this, we intend to couple the dynamic model for CO₂ absorption and desorption with models of other sub-units (heat exchangers, sumps, pumps) to form a complete model of a post-combustion capture plant.

References

1. M. Bui, I. Gunawan, V. Verheyen, P. Feron, E. Meuleman, S. Adeloju, Dynamic modelling and optimization of flexible operation in post-combustion CO₂ capture plants - A Review, Computer and Chemical Engineering, vol. 61, pp. 245-265, 2014.
2. J. Gaspar, K. Thomsen, N. von Solms, P.L. Fosbøl. Solid formation in piperazine rate-based simulation. Energy Procedia, 2014. DOI: 10.1016/j.egypro.2014.11.115



Arne Gladis
Phone: +45 4525 2978
E-mail: arng@kt.dtu.dk
Discipline: DTU Kemiteknik

Supervisors: Von Solms, Nicolas
Woodley, John
Fosbøl, Philip

Started: March 2014
To be completed: February 2017

Enzyme enhanced carbon dioxide absorption

Abstract

Carbon dioxide capture using an amine based solvent is already a well-established process and a lot of studies on kinetics and energy requirements as well as pilot plant tests are available in literature. The chemical solvent monoethanolamine (MEA) gained the most focus over the last years, because of its fast reaction kinetics and high mass transfer of CO₂ even at low partial pressure; in a 30 % (w/w) mixture with water it can be seen as the “base case” solvent [1]. There are though few issues with MEA, besides environmental aspects, volatility, chemical degradability and corrosion problems of the solvent there are also high energy requirements in the desorption process due to the breakage of the covalent bond between solvent and the CO₂ molecule in the desorber that established in the absorption step. Gary T. Rochelle stated in Science: “Reduced capital and energy costs will come with amines other than MEA” [2]. We should therefore consider changing the solvents. Solvents that are not directly reacting with the CO₂ molecules like MEA, but are forming bicarbonates instead, show slow reaction kinetics and can make the absorption process uneconomically. To enable the use of slow but energy efficient solvents kinetic promoters are employed to enhance the kinetics and mass transfer [3]. In a biomimetic approach the possibility of using carbonic anhydrase enzymes as kinetic promoters to enhance the carbon dioxide absorption and generate an energy efficient and economical process will be investigated in lab and pilot scale experiments.

Introduction

One of the largest obstacles today’s society faces is to provide safe and reliable energy sources, while reducing carbon dioxide emissions. Post combustion carbon capture technology is capable of resolving these two issues in the near future. Until the regenerative technologies are mature enough to provide energy for the whole population, carbon dioxide emitted by fossil fuel burning power plants can be captured and stored beneath the surface.

In this process technology a liquid solvent is cycled continuously between the absorber and desorber as it can be seen in Figure 1. In the absorber CO₂ is captured from the exhaust gas at a moderate temperature and it is released in the desorber under the input of thermal energy. The driving force for this process is the difference between the partial pressure of CO₂ in the gas phase and its corresponding thermodynamic CO₂ solubility in the solvent. As the process is performed at almost ambient pressure the partial pressure of CO₂ in the exhaust gas of a power plant is rather low and places high requirements on the absorption process. For this purpose a chemical absorption process is chosen where the solvent reacts with the physically bound CO₂. The

decrease of CO₂ in the liquid bulk leads to an increased diffusion of CO₂ from the gas interface and therefore enhances the mass transfer.

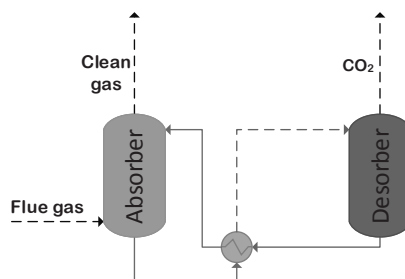
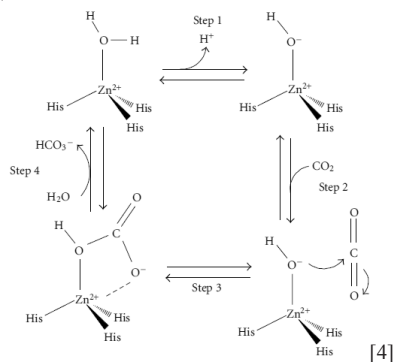
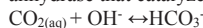


Figure 1: Basis scheme of a solvent-based post-combustion carbon dioxide capture process

The rate of chemical absorption is dependent on the reaction rate between the solvent and CO₂ and the diffusion of all the involved compounds. The fastest reaction kinetics comes from a direct reaction of the solvent with the CO₂ molecule forming a carbamate,

versus indirect base-mechanism forming bicarbonate (HCO_3^-). The downside of the carbamate formation is that the covalent bond has to be broken in the desorber again, leading to an additional energy requirement compared to the bicarbonate.

As the energy requirement of desorption is the most crucial part of the process in terms of economic viability, there is great interest in reducing the energy requirement of desorption. But the change of the solvent to a non carbamate forming species leads to lower mass transfer and increases the equipment size for the absorber. An interesting approach to overcome this shortage is the use of kinetic promoter. One interesting and very promising promoter is the enzyme carbonic anhydrase that catalyzes the following reaction:



It can be found in almost all living organisms and is involved there in multiple biological processes [3], it is also one of the fastest enzymes known; one enzyme can catalyze up to 10^6 reactions per second [5].

Specific Objective

In this PhD study the application of carbonic anhydrase (CA) as kinetic promoters will be investigated. To get a better understanding of the reaction kinetics and mechanism of CA enzymes the effect of enzyme addition on absorption will be experimentally determined for different solvents. These solvents represent a solvent group defined by their molecular structure and their different reaction mechanisms with CO_2 , like primary amines (MEA), tertiary amines (MDEA), sterically hindered amines (AMP) and buffer salt solutions (K_2CO_3). The nomenclature of the amines describes the number of substituents bonded to the nitrogen group, sterically hindered means that the α -C-atom has substituents. From these groups, just the primary amines form stable carbamates, whereas the others work as a base creating bicarbonate (HCO_3^-).

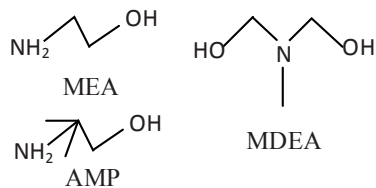


Figure 2: Different amine solvents

Absorption experiments will be carried out in a wetted wall column reactor that allows for measuring CO_2 absorption kinetics in a steady state from the known dimension of the reactor and the well-defined gas streams. By comparing experimental results from the same solvent with and without enzymes, the intensification of the absorption through the CA enzymes can be evaluated.

From these results a mathematical model for the enzyme kinetics will be developed describing the effect of enzyme addition on the absorption of carbon dioxide, where the key parameters will be the enzyme concentration and the solvent loading, i.e. the mole of dissolved and chemical reacted CO_2 per mole of solvent. This model will later be implemented in an in-house model for absorption columns. In a pilot run in an absorber column with the height of 10 m this model and in specific the enzyme contribution will be validated on pilot plant scale.

This model can then be applied in commercial process simulation software to determine the capital costs and energy requirements for this process.

Acknowledgements

This PhD project is funded by the FP7 EU project INTERACT that comprises 11 partners, including industry and universities from Europe and north America. Web-link:

<http://www.interact-co2.eu/>

References

1. M. Wang, A. Lawal, P. Stephenson, J. Sidders, C. Ramshaw, *Chem Eng Res Des* 89 (2011)
2. G.T. Rochelle, *Science* 325 (2009) P.1652-1654
3. J.K.J., Yong, G.W. Stevens, F. Caruso, S.E. Kentish, *J Chem Technol Biotechnol* 2014, doi: 10.1002/jctb.4502
4. Pierre, A C, *ISRN Chemical Engineering*, vol. 2102, 2012, P. 1-22
5. C.K Savile, Lalonde, J.L *Current Opinion in Biotechnology* 22 (2011), P. 818-823

**Helge Grosch**

Phone: +45 4677 5417
E-mail: hgch@kt.dtu.dk
Discipline: CHEC

Supervisors: Alexander Fateev
Sønnik Clausen

PhD Study

Started: December 2011
To be completed: November 2014

Optical Spectroscopy for Gas Analysis in Biomass Gasification

Abstract

The analysis of the gas composition is important in determining the quality of a product gas. In biomass gasification, aromatic compounds play an important role in regard to the quality of the gas that is a key parameter for various product gas applications. The use of optical spectroscopy for gas analysis is beneficial, because it can be applied online and in-situ. In the laboratory, the absorption cross-section of the most important aromatic compounds, phenol and naphthalene, were determined through measurements in the ultraviolet (UV) range and applied for the analysis of the product gas of the low temperature circulating fluidized bed (LT-CFB) gasifier at DTU Risø Campus. In this article, the results from in-situ and extraction measurements at the LT-CFB gasifier are compared and discussed.

Introduction

In recent years, the importance of renewable energy and a suitable waste management have increased. Biomass gasification and particularly the LT-CFB gasifier, is a technology that addresses both fields. However, the biomass gasification and product gas usage are still afflicted with certain challenges.

The most important issue is the determination of the gas quality. Notable trace gases that can reduce the conversion efficiency or are responsible for fouling of equipment and environmental damages, are H₂S, CS₂, OCS, NH₃ [1,2] but also aromatic compounds like benzene, phenol and naphthalene [2]. While the major gas species H₂, CO, CO₂ and H₂O can already be determined with sufficient accuracy by standard techniques, trace gases are still a subject of investigation.

Many different measurement techniques are currently used to tackle this problem. However, in industrial applications, direct / in-situ online measurements are favorable, because they allow the immediate results and deepen the insight of the process in research application. Especially the optical methods, such as UV and IR absorption spectroscopy, are possible techniques that can directly measure in a product gas.

By now only major gas components have been investigated by optical in-situ methods. Since in the LT-CFB, phenol and naphthalene are some of the most interesting aromatic gas species, the basic optical properties and future possibilities of their investigation

by optical absorption spectroscopy have been investigated.

To do so, the absorption cross-sections of phenol and naphthalene were measured at typical temperatures found in the product gas of the LT-CFB. These measurements have been performed in a special hot gas flow cell (HGC) suitable for the investigation of the optical characteristics of reactive and sticky gas species. Afterwards, these absorption cross-sections were used to determine the concentration of phenol and naphthalene in extraction and in-situ measurements at the LT-CFB.

Experimental techniques

The absorption cross-sections of phenol and naphthalene were determined by absorption measurements in the HGC up to 500 °C. The detailed properties of this gas cell have been published in [3]. The HGC uses the so-called flow windows principle to protect the exchangeable optical windows from possible reactions with the reactive gas and to prevent deposition of sticky gas species which might change the optical properties of the windows.

The measurements in the laboratory and at the gasifier were performed in the UV region between 195 nm and 360 nm. In all cases, a highly stable deuterium lamp was used as a light source. As spectrometer, a 50 cm Czerny-Turner spectrometer was used, equipped with a #3600 holographic grating and a CCD camera as detector. The only difference between the laboratory

experiments, the extraction measurements and the in-situ measurements was the absorption path length through the gas. Through the determination of the absorption cross-sections from the measurements in the laboratory, these differences could be accounted for.

Results and Discussion

In Fig. 1, the UV absorption cross-sections of naphthalene at room temperature, 150 °C, 300 °C and 500 °C are shown.

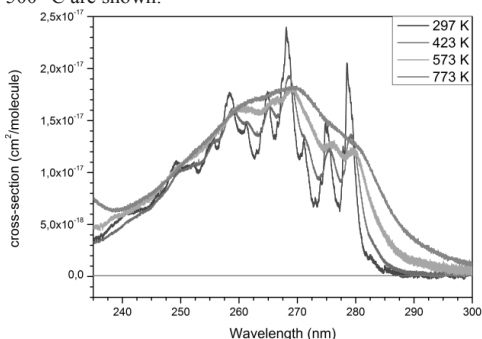


Figure 1: Absorption cross-section of naphthalene at various temperatures in the UV range between 235 nm and 300 nm (from [4]).

From these absorption cross-sections, the differential absorption spectra (DOAS) were calculated. The calculated DOAS spectra were used to fit the DOAS spectra obtained in the extraction and in-situ measurements at the LT-CFB. The results for the extraction measurements are shown in Fig. 3. In general a good agreement between the peaks can be seen, if the concentration of phenol and naphthalene is 407 ppm and 33.2 ppm, respectively. However, a few peaks cannot be explained by phenol or naphthalene. These peaks are most likely those of other aromatic components.

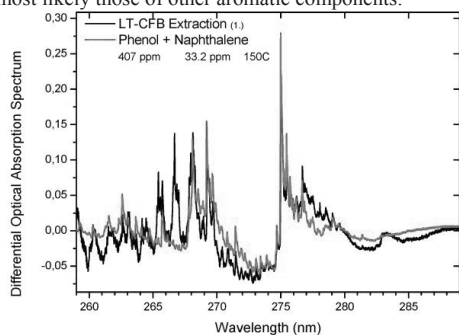


Figure 2: Comparison between extraction measurements (black) and calculations from the DOAS absorption cross-section (red) at 150 °C.

In figure 4 the same can be observed for the in-situ measurements. Especially between 268 nm and 275 nm a mismatch can be observed. In addition, the values are

significantly higher. The concentration of phenol is 7700 ppm and the one of naphthalene is 1000 ppm.

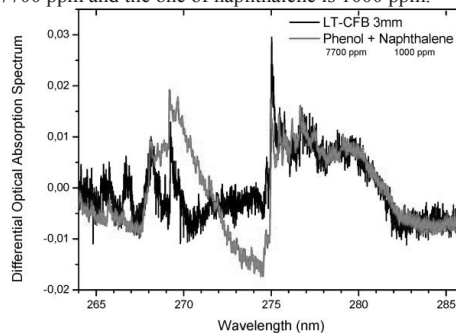


Figure 3: Comparison between in-situ measurements (black) and calculations from DOAS absorption cross-sections at 500 °C.

One possible explanation for this significant difference in the obtained values may lay in the setup used for the in-situ measurements. It cannot be excluded that during the measurements the hot product gas has partly entered the cooler gas flow that protected the optical windows and therefore caused a longer path length than expected. Based on information available at the moment those possible effects (if any) are difficult to quantify.

Conclusion and future works

Accurate absorption cross-sections of phenol and naphthalene were measured for the first time at high temperatures. This enabled the determination of the concentrations of both compounds in extraction and in-situ measurements of the real product gas of the LT-CFB. Here, significant differences between the in-situ and the extraction measurements have been found. The difference may occur as a result of a longer path length because of product gas penetration. A redesigned setup can circumvent this problem and make measurements with very short absorption path lengths possible.

The knowledge obtained in this project is the basis for the future development of UV sensors for the quantification of phenol and naphthalene, but also H₂S, CS₂ and OCS.

Acknowledgements

Project acknowledgments to Energinet.dk Project Nr. 2011-1-10622.

References

1. R. Ma, R. M. Felder, J. K. Ferrell, Ind. & Eng. Chem. Res., 28 (1) (1989) 27-33
2. P. Ståhlberg, et al., Sampling of contaminants from product gases of biomass gasifiers, Research Notes 1903, VTT Energy, 1998
3. H. Grosch, A. Fateev, K.L. Nielsen, S. Clausen, J. of Quant. Spect. & Rad. Trans. 130 (2013) 392-399.
4. H. Grosch, A. Fateev, S. Clausen, J. of Quant. Spect. & Rad. Trans. (2014) submitted.



Maria Gundersen Deslauriers

Phone: +45 4525 2926
E-mail: mgun@kt.dtu.dk

Supervisors: John M Woodley
Nicolas von Solms

PhD Study
Started: September 2013
To be completed: September 2016

Evaluating Enzymatically Assisted CO₂ Removal from Flue-Gas with Carbonic Anhydrase

Abstract

To reach the necessary carbon emissions reductions and to minimize effects on the climate, it is well established that carbon capture and storage (CCS) must be part of the solution together with renewable energies. Here we focus on an emerging technology in CCS, as a compliment to existing technologies, namely enzyme assisted CO₂ removal from flue-gas, by the enzyme Carbonic Anhydrase (CA). A technology which has shown potential but has yet to reach commercial implementation. In order to reach such a scale, economic viability must be demonstrated, in part evaluated by the first parts of this PhD study. Here CA stability under process relevant conditions for extended times were investigated with respect to pH, temperature and solvents. This study shows that the enzyme used in this study can be used for extended periods in process relevant conditions, and thus shows promise for industrial implementation as a catalyst in carbon capture. This work will lead to further studies in reaction kinetics and benchmarking studies towards commercialization.

Introduction

The leading technology for CO₂ removal from flue-gas is amine scrubbing, where amine solvents with a high capture capacity are used to remove CO₂ from a mixed gas at relatively low temperatures in an absorption unit. The highly loaded solvent is then transferred to a desorption unit, where the CO₂ is removed by heating producing a pure CO₂ gas for storage or utilization.

Biocatalysis is the use of biological materials to produce chemical products, and has been around for millennia in the form of brewing [1]. Today it offers a wide range of new catalytic options for industrial applications [2]. Enzymes are now extensively applied in many processes for single step conversions [3]. Furthermore, new opportunities are arising in enzymatic removal of toxic or harmful substances, where the exquisite selectivity and activity of enzymes at low concentrations are utilized. CO₂ removal from flue-gas is such an application.

Specific Objective

We are using the enzyme Carbonic Anhydrase (CA) (EC 4.2.1.1) which hydrates CO₂ to bicarbonate, to enhance capture rates and reduce the energy and penalty associated with carbon capture. CA is found from

various sources in nature and as several isozymes. The enzyme used in this study is provided by Novozymes. The implementation of this technology is part of a wider EC funded project (INTERACT) [4] where we will focus on evaluation and implementation of this technology in relation to other technologies (ionic liquids) developed by the project partners for removal of CO₂ from flue-gas.

Here we have evaluated the 3 parameters pH, temperature and solvents, which will vary over the course of the process (Figure 1)

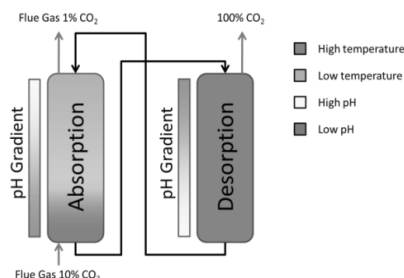


Figure 1: Schematic of variation in pH and temperatures of the solvent liquid in a post-combustion solvent based capture process.

Temperature and pH stability were tested for up to 100 hours incubation and CA was found to be temperature stable up to 60 °C (Table 1) and in the pH range from 7 to 11, with some residual activity between pH 5 and 12 (Figure 2). Furthermore, enzyme stability was tested for 7 different capture solvents for 150 days, at 1 M or 3 M solvent concentrations, 40 °C and pH between 8-9 and 10. Residual activity was found with all samples ranging from 12 to 91 % of the initial activity (Table 2).

Table 1: Residual activity after incubation at temperatures from 50 to 80 °C for up to 100 hours with 0.1M Tris-HCl buffer, pH 7.6. All results are given in % residual activity

T (°C)	Time (hours)				
	1.5	25	48	72	100
50	105	121	132	196	280
60	84	87	64	66	74
70	47	41	49	36	0
80	7	9	2	0	0

Table 2: Remaining activity after 5 and 150 days

Solvent (concentration)	pH	Residual Act.	Residual Act.
		5d (%)	150d (%)
Monoethanolamine (3M)	8.3	95	73
	10	76	33
2-Amino-2-methyl-1-propanol (3M)	9	99	42
	10	104	12
N-Methyldiethanolamine (3M)	9	92	62
	10	91	54
2-Aminoisobutyricacid (3M)	8	106	91
	10	95	35
K ₂ CO ₃ (1M)	8	116	83
	10	85	29
3-(Methylamino)propylamine (1M)/ N-Methyldiethanolamine (2M)	8.6	86	85
	10	99	69
Ammonium Chloride (3M)	8	99	71
	10	100	22

The results give an indication that the enzyme is stable under operating conditions. The results correlate well with results found with engineered CA's [5], which have been found to be stable at high temperatures. In particular Ye and colleagues have tested a Novozymes CA stability over 6 months with potassium carbonate, and found approximately 20% activity loss after 6 months at 40 °C, and an increased loss in activity at elevated temperatures (50 °C and 60 °C) [6].

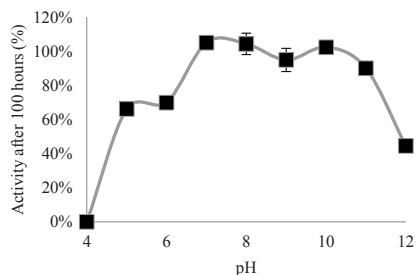


Figure 2: Residual activity after 100 hours of incubation at pH 4 to 12

These results form the basis for which we are carrying out further studies in the impact of these parameters on CO₂ capture kinetics. In the aim of this project we aim to have a better understanding on the optimal processes for implementation of enzymes in CO₂ capture applications.

Conclusions

We offer here a promising solution to an increasingly pressing problem, reduction of CO₂ emissions to the atmosphere from power plants, which are among the major contributors to atmospheric CO₂ and global warming. We believe that enzyme assisted technologies have the potential to greatly improve CO₂ removal from flue-gas, by lowering the energy penalty for solvent regeneration. Thus, it reduces both the carbon footprint and the operating cost.

Acknowledgements

The research leading to these results has received funding from the European Union Seventh Framework Programme FP7/2007-2013 under grant agreement n°608535.

References

1. F.G. Meusdoerffer, A Comprehensive History of Beer Brewing, Royal Society of Chemistry, Cornwall, UK, 2009.
2. U.T. Bornscheuer, et al. Nature 485 (2012) 185–194
3. J.M. Woodley, Trend. Biotechnol. 26 (2008) 321–327
4. <http://www.interact-co2.eu>
5. C. K. Savile, J. J. Lalonde, Curr. Opin. Biotechnol. 22 (2011) 818–823.
6. X. Ye, Y. Lu, Chem. Eng. Sci. 116 (2014) 567–575.

**Timo Hagemann**

Phone: +45 30 77 14 20
E-mail: timoh@kt.dtu.dk
Discipline: Bioprocess Technology

Supervisors: Krist Gernaey
Ulrich Krühne
Stuart Stocks (Novozymes A/S)

PhD Study (with Novozymes A/S)

Started: November 2013

To be completed: November 2016

Investigation of *Aspergillus niger* aggregation behavior and its relationship to industrial fermentation

Abstract

The existence of a company like Novozymes A/S demonstrates the added value that can be obtained by production of enzymes with *Aspergillus niger*. Deeper knowledge about the fungus' behavior is of interest though. The aim of this project is therefore to follow the development of the biomass from spores to mature biomass. With manipulations of the fungus (fermentation) environment in terms of particle (inoculum) concentration, ion strength, pH value, mechanical power input by agitation as well as aeration and back pressure, the biomass configuration will be designed towards free mycelial or pelleted growth, with the aim of finding an answer to the question of how important the morphology is for productivity in an industrial strain.

Introduction

This PhD project is done in cooperation between the DTU and Novozymes A/S. The work is a continuation of academic work that has been started at the Institute of Biochemical Engineering at the Technische Universität Braunschweig. This project will build on the findings of this previous work, with the final goal of answering the question of morphology - which is important from both an industrial and an academic point of view.

The academic strain *Aspergillus niger* AB1.13 [1] was researched during this first part of the project. Along with the common fermentation analysis, like biomass and metabolites, online laser diffraction analysis was employed to follow biomass development under specific fermentation conditions. On the basis of the different factors that were varied in the fermentations, one important result is that the biomass reaction can be predicted in order to design the amount and the state of the biomass and the respective expected particle size for future fermentations with *Aspergillus niger* AB1.13 during pelleted growth.

The latter is important in order to keep the broth's rheology in control and to keep the OTR into the liquid phase at the desired/highest possible level. With morphology control in seed tanks, the subsequent main fermenter can truly be optimized in terms of productivity.

Experiments have been conducted at Novozymes pilot plant and in Fermentation optimization close to the production site in Kalundborg to investigate the

influence of power input by particle (inoculum) concentration, ion strength, pH value, mechanical power input by agitation as well as aeration and back pressure on the morphological development and productivity of an industrial *Aspergillus niger* strain. With the particle size distributions as linking factor, a model should now be established for precise predictions of biomass behavior/productivity. This will be verified with additional fermentations in a final screening design in order to connect a chosen morphology with the productivity of an industrial strain.

Methods

The results from the previous work were mainly achieved by introducing step changes to the fermentation system. The biggest contribution to manipulating the morphology at the onset of the fermentation is supposed to be the pH of the broth: Cultivations started with non-aggregating behavior at a pH of 3 were later shifted to aggregating conditions at a pH of 5.5.

Besides the normal sampling for HPLC and biomass determination, a Malvern MasterSizer 2000 was installed in a bypass to a 2 L fermenter. Measurements were taken every five minutes over a time frame of 20 h. The resulting particle size distributions were split into the volume shares of spores and biomass aggregates (later pellets), respectively, to differentiate between particle size growth due to aggregation and biomass growth (see fig. 1).

Results and Discussion

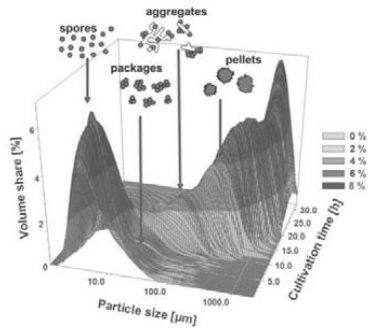


Figure 1: Display of the volume share (Y-axis) over the particle size class (X-axis) during the course of the fermentation (Z-axis): At time = 0, i.e. at the start of the fermentation, only spores can be detected with laser diffraction while at time = 8 h and with a pH of 5.5 in the broth, spore packages can be seen. Aggregates consisting of hyphae and spores are detected after growth began.

The split of volume shares of different particle classes allows tracking the spore development.

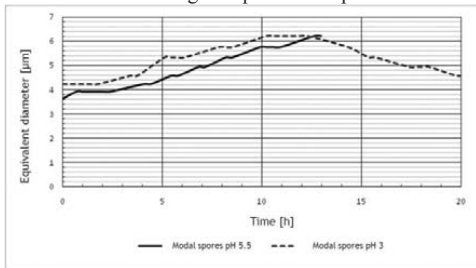


Figure 2: Particle size of mode of spores over time at different inoculation pH: At pH 5.5, the spores are smaller compared to the ones at pH 3 and after 12-13 h, they are completely aggregated towards growing biomass (hence no longer detectable).

Measurements show that *A. niger* spores desorb melanin at a pH around 5-6. Additionally, zeta-potential measurements show a minimum at pH 5.5 indicating the best potential for aggregation.

As a consequence, it should be possible to alter the aggregation by changing the pH from 3 to 5.5. Fig. 3 displays the results of different long duration pH shift experiments which each started at 8 h. Fermentations started at pH 5.5 were the first to show aggregates and the first where the aggregate mode dominates the measured particle sizes. With longer pH shift durations, the detectability of aggregates and the point in time where they dominate the particle size distribution is postponed, and the particle size of the resulting pellets is smaller.

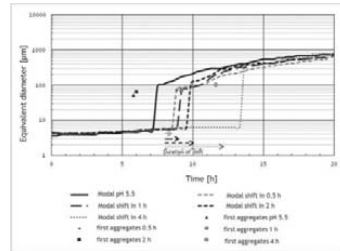


Figure 3: Display of particle sizes of the modes over time; during the first hours, spores form the majority of measured particles. The “jump” in particle size indicates the point in time when biomass aggregates form the majority of the measured particles. The single dots mark their first appearance.

Conclusions

Spore aggregation can take place at the onset of the cultivation and it is dependent on particle concentration, the power input, the ion strength and the pH of the broth [2]. With the academic strain, the pH was deemed to be the most powerful handle for controlling the morphology by postponing aggregation. The recent work with the industrial strain indicates though that these findings might be very strain dependent and generalization of the results is not as straightforward as expected.

Publications

Formenti, L. R., Nørregaard, A., Bolic, A., Quintanilla Hernandez, D. A., Hagemann, T., Larsson, H., Mears, L., Mauricio Iglesias, M., Krühne, U., Heins, A.-L., Gernaey K.V. (2014). Challenges in industrial fermentation technology research. *Biotechnology Journal*, 9(6), 727-738.

Acknowledgements

The presented results were achieved through research at the Technische Universität Braunschweig and were funded by the German Research Foundation via the “SFB578” [3].

References

1. I. E. Mattern, J.M. van Noort, P. van den Berg, D.B. Arbacher, I.N. Roberts, C.A.M.J.J. van den Hondel, Isolation and characterization of mutants of *Aspergillus niger* deficient in extracellular proteases, *Molecular Genetics and Genomics* 234 (1992) 332-336.
2. A. Wargenau, A. Kwade, Determination of adhesion between single *Aspergillus niger* spores in aqueous solutions using an atomic force microscope, *Langmuir* 26/13 (2010) 11071-11076.
3. C. Wittmann, D. Jahn, R. Krull, From gene to product - Development of biotechnological processes by integrating genetic and engineering methods, Cuvillier Verlag, Göttingen, Germany, 2012.

**Amalia Halim**

Phone: +45 4525 2892
E-mail: amah@kt.dtu.dk

Supervisors: Alexander Shapiro
Sidsel M. Nielsen
Anna E. Lantz

PhD Study

Started: February 2012
To be completed: April 2015

Microbial Enhanced Oil Recovery for North Sea Oil Reservoir

Abstract

Some microorganisms living in petroleum reservoirs produce substances like gases, surfactants, polymers and/or acids, facilitating enhanced oil recovery (EOR). Therefore, selective stimulation of certain microbial species may be an inexpensive method for additional oil recovery. In addition, microbes can selectively plug reservoir formation, thus divert the flow of the injected water into regions of the reservoir with low permeability-high oil saturations. The present study focused on core flooding experiments to see microbial plugging and its effect on oil recovery. A pressure-tapped core holder with pressure ports at 1.2 cm, 3.8 cm, and 6.3 cm from the inlet was used for this purpose. A spore-forming bacterium, *Bacillus licheniformis* 421, was used as it was shown to be a good candidate in the previous study. Bacterial spores can penetrate deeper into the chalk rock, squeezing through the pore throats. Our results show that *B. licheniformis* 421 injected after waterflooding, when injection of water cannot produce any more oil, can recover 1.4% of the residual oil (tertiary type technique). In addition, when *B. licheniformis* 421 was injected right after water breakthrough (secondary type technique), it can recover 3.3% more of the original oil in place (OOIP) as compared with the tertiary technique. The effective permeability decreased in the first two sections of the core (0-1.2 cm and 1.2-3.8 cm) during bacteria injection. Further water flooding after three days shut in period showed that permeability gradually increased in the first two sections of the core and started to decrease in the third section of the core (3.8-6.3 cm). Complete plugging was never observed in our experiments.

Introduction

It is credited to Beckman in 1926, who found that microorganisms could be used to release oil from porous media [1]. Numerous mechanisms have been proposed in the literature through which microorganisms can be used for enhanced oil recovery [1]. However, the mechanisms are poorly understood and the effectiveness of each mechanism for different reservoir parameters is also unknown [2, 3]. Recent publications on the bacteria-fluid-porous media interaction classified the mechanisms into two broad categories: 1) alteration of oil/water/rock interfacial properties and/or wettability [2-5], 2) changes in flow behaviour due to bioclogging or selective plugging [2-4, 6]. This study was conducted to see the effect of spore-forming bacteria injection to oil recovery. The plugging effect caused by bacteria was investigated by monitoring the pressure during bacteria injection.

Specific Objectives

The main goal of the project is to investigate the effect of bacteria injection on oil recovery. This study was conducted in a core flooding experiment to mimic the reservoir conditions. Three conditions were investigated: 1) injection of water flooding as tertiary oil recovery technique (control experiment), 2) injection of bacteria as tertiary oil recovery technique, 3) injection of bacteria as secondary oil recovery technique.

Experimental Work

An illustration of core flooding experiment is depicted in Fig. 1. Injection pressure, pressure along the flooded core plug and differential pressure were monitored throughout the experiment. The recorded pressure was used to calculate effective permeability using Darcy's Law. The effective permeability in different sections of the core plug can be calculated by indications of the pressure sensors as illustrated in Fig. 2. The camera at the outlet of the core holder was set to take pictures every 30 second to capture the oil production during the experiment.

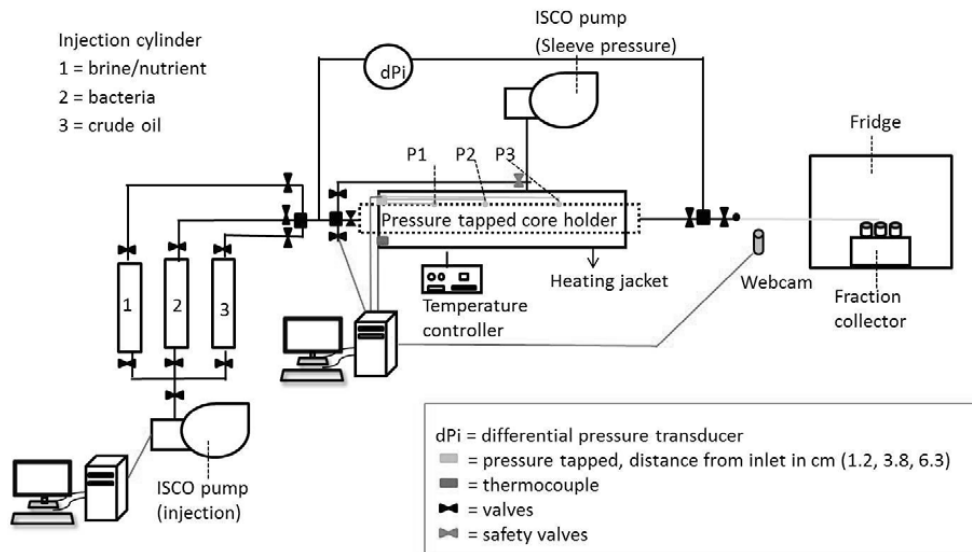


Figure 1: Core flooding experiment

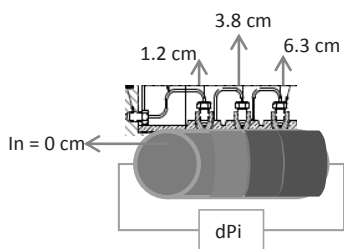


Figure 2: Illustration of effective permeability in different sections of the core plug

Core cleaning and basic properties measurement

Prior to flooding experiments, all the cores were scanned using a fourth generation Siemens SOMATOM scanner. The X-ray computer tomography (CT) scanning was conducted in lateral and longitudinal directions to ensure no fractures in the cores used for the experiments. Each individual core was then cleaned by flooding with toluene and methanol to remove any organic material inside the core. After cleaning, the core was dried in the oven at 100°C overnight. The core porosity and permeability was measured by PoroPerm 2. This protocol was repeated after each experiment because the same core was used for different proposes (control, tertiary, and secondary test).

Core saturation and initial flooding

The core was then saturated with synthetic seawater (SS) under vacuum for 24 hours followed by further saturation with SS at high pressure (100 bar) in a

stainless steel cylinder for 48 hours. The SS saturated core was then inserted in pressure tapped core holder. The core holder was heated to 50°C overnight.

The core was flooded with 3-5 pore volume (PV) of sterile SS in order to fill all the dead volume in the core holder. Then the crude oil was injected until irreducible water saturation was observed (S_{wi}), a condition where no more water can be displaced by oil.

The following steps were different depending on the purpose of the study (control, tertiary or secondary recovery).

Water flooding control experiments

The core was flooded with SS until irreducible oil saturation (S_{oi}) was observed. The shut in, or incubation, period was performed by closing both inlet and outlet valves for 3 days. The core was flooded with SS again for ca. 5 porous volumes (PV).

Tertiary oil recovery technique

The core was flooded with SS until irreducible oil saturation (S_{oi}) was observed, followed by injection of 1PV bacteria. The incubation period was performed by closing both inlet and outlet valves for 3 days. The core was then flooded with SS again until no more oil was produced.

Secondary oil recovery technique

The core was flooded with SS for 1PV, followed by injection of 1PV bacteria. The incubation period was performed by closing both inlet and outlet valves for 3 days. The core was flooded with SS again until no more oil was produced. The core was then flooded with 1PV

nutrient, followed by 7 days incubation and another SS flooding until no more oil was produced.

Effluent analysis

The effluent was collected every 6 ml using a fraction collector (BioRad). The bacteria were counted using a plate count method. The oil production was analyzed by using known prepared samples as standard. However, when oil concentration was below 1 ml, the oil concentration was measured using UV-vis method [7].

Inoculum preparation and bacteria enumeration

The bacteria inoculum was grown in the synthetic seawater nutrient media (SSN), the composition was similar to SS media with addition of 16.9 g/l molasses, 2 g/l NaNO₃, 0.1 g/l KH₂PO₄, 1% vitamin and 1% trace elements for 18 hours. The cells were then harvested by centrifugation at 10.000xg for 10 minutes. The pellet was re-suspended in 0.85% NaCl and added to the SSN media used for injection. The optical density at 600 nm (OD₆₀₀) of the bacteria solution was adjusted to the final concentration of OD₆₀₀=0.5. The resulting bacteria and SSN medium suspension was homogenized by a vortex for 3 minutes. Bacteria enumeration was conducted by serial dilution plate method using enrichment medium.

Results and Discussion

No significant change in the core properties on both porosity and permeability (Table 1). This means that the bacteria did not significantly modify the core after each experiment. It was also shown that the shut in period (incubation period) in the control experiment, without bacteria, did not give any additional oil production (Fig. 3). On the other hand, application of *B. licheniformis* 421 as tertiary oil recovery technique gives 1.4% additional oil production. This confirms that bacteria do produce more oil. Application of *B. licheniformis* 421 as a secondary technique gave even better result, 3.3% more oil, as compared to the tertiary technique (Fig.3). The video camera pictures confirmed that when the cumulative oil production showed flattening curve, no more oil was produced. In addition, the webcam also captured the moment when additional oil started being produced again after bacteria injection.

Table 1. Core plug properties

Core ID	k before (mD)	k after (mD)	φ Before (%)	φ after (%)
26 water	3.2	2.8	30.8	30.7
26 3rd m	3.2	3.1	31.1	30.7
26 2nd m	3.1	3.2	30.7	30.8

The effective permeability was calculated by using Darcy's Law (1), assuming that the amount of oil is negligible and the main liquid that flows is the SS.

$$k = \frac{Q\mu L}{A(\Delta P)} \quad (1)$$

It can be seen that during bacteria injection (Fig. 4), the permeability decreases in the first two sections of the core plug (0 cm-1.2 cm and 1.2 cm-3.8 cm)

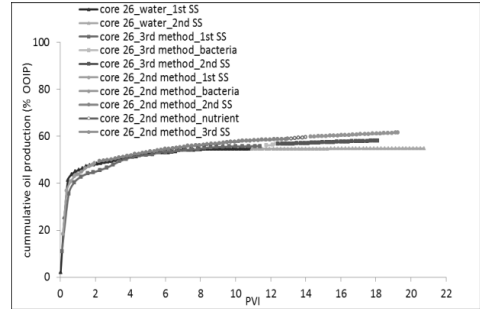


Figure 3: Cumulative oil production during core flooding experiments

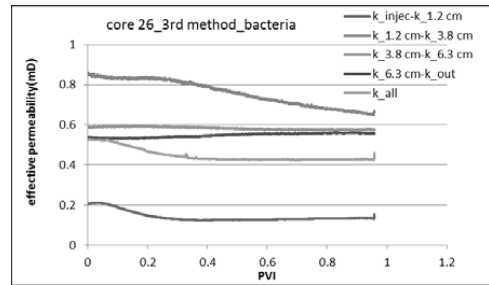


Figure 4: Permeability changes during bacteria injection

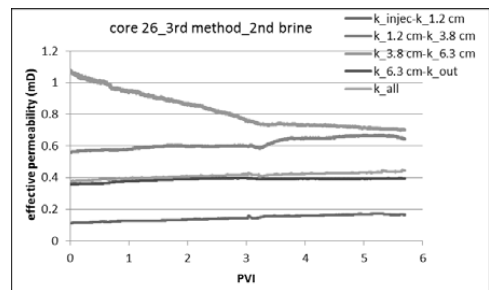


Figure 5: Permeability changes 2nd synthetic seawater (SS) injection after 3 days bacteria incubation

After 3 days incubation, permeability in the first sections of the core (0 cm-1.2 cm and 1.2 cm-3.8 cm) slightly increases and the permeability in the middle part of the core (3.8 cm -6.3 cm) rapidly decreases (Fig. 5). This indicates that the bacteria move further from the first section of the core (near inlet) to the

middle part of the core. This result is in correlation with the oil production results, as when the bacteria move further in the core section, they selectively block some high permeable channels of the core and alter the water to the low permeability-high oil saturations.

Conclusions

Spore-forming bacteria, *B. licheniformis* 421, have a potential to be applied as MEOR approach in chalk reservoirs, as more oil can be recovered when the bacteria are injected. Application of bacteria as secondary technique gives more additional oil production as compared to the tertiary technique. The pressure tapped core holder can give an overview of bacteria migration in the rock formation. During injection, bacteria accumulated near injection side of the core and further incubation period allowed bacteria to move forward/deeper into the formation. When bacteria migrate they can selectively block some high permeable channels, alter the water flowing path, and thus improve sweep efficiency. Selective plugging mechanism may be a way forward for application of MEOR in chalk reservoirs. This hypothesis should be tested in experiments with the heterogeneous core plugs.

References

1. Lazar, I., I.G. Petrisor, and T.F. Yen, (2007) *Pet. Sci. Technol.*, 25, 1353-1366.
2. Kowalewski, E., I. Rueslåtten, K.H. Steen, G. Bødtker, and O. Torsæter, (2006) *Journal of Petroleum Science and Engineering*, 52, 275-286.
3. Armstrong, R.T. and D. Wildenschild, (2012) *Transport in Porous Media*, 92 (3), 818-835.
4. Afrapoli, M.S., C. Crescente, S. Alipour, and O. Torsæter, (2009) *Journal of Petroleum Science and Engineering*, 69, 255-260.
5. Karimi, M., M. Mahmoodi, A. Niazi, Y. Al-Wahaibi, and S. Ayatollahi, (2012) *Colloids and Surfaces B: Biointerfaces*, 95, 129-136.
6. Afrapoli, M.S., S. Alipour, and O. Torsæter, (2011) *Transport in Porous Media*, 90, 949-964.
7. Evdokimov, I.N., N.Y. Eliseev, and B.R. Akhmetov, (2003) *Journal of Petroleum Science and Engineering*, 37 (3-4), 135-143.



Zainatul Bahiyah Handani

Phone: +45 4525 5590
E-mail: zbha@kt.dtu.dk

Supervisors: Rafiqul Gani
Gürkan Sin

PhD Study
Started: May 2013
To be completed: April 2016

A Simultaneous Approach for Synthesis and Design of Process and Water Networks

Abstract

A simultaneous synthesis and design of process and water networks is regarded as a complex and difficult task which involves many decision-making at the early stage of process design. Many alternatives in process and wastewater treatment technologies are available to enable the industrial practitioners to select the optimum technology network in by representing them in a superstructure. In this work, a new systematic framework for synthesis and design process and water networks using superstructure-based optimization approach is developed. In this work, a new superstructure combining both networks is developed by considering all possible options with respect to the topology of the process and water networks, leading to Mixed Integer Non Linear Programming (MINLP) problem. In addition, the simultaneous optimization approach mathematically combines the problem of process and water networks into a single step. Since the connection between the process network and the wastewater treatment network is not a straight forward connection, some converter intervals are introduced in order to convert the amount of contaminants contain in wastewater stream into wastewater characterizations. A solution strategy to solve the multi-network problem accounts explicitly the interactions between the networks by selecting suitable technologies in order to transform raw materials into products and produce clean water to be reused in the process. The interaction between two networks is visualized via selection appropriate raw materials, technologies and alternatives for process and water treatment as well as products. The applicability of the systematic approach is demonstrated using a conceptual case study to test the features of the solution approach under different scenarios depending on the design-synthesis problem.

Introduction

Water is an important substance and is used extensively in the process industries. Water can be supplied as raw material, solvent, cleaning agent or utility (steam and cooling water). Minimization of freshwater consumption and wastewater generation are being critical concerns in the process industry due to the increase scarcity in freshwater supply, the rise of freshwater and effluent treatment costs and more stringent regulations. Over the last few decades, many synthesis and design techniques have been developed to minimize water consumption and wastewater generation in process industries either using pinch analysis or mathematical programming technique. In order to reduce freshwater consumption in the process, wastewater generated from the process or utility could be reused after being treated in the wastewater treatment plant to acceptable limits by considering various treatment technologies and alternatives. In addition, different process technologies and design alternatives

are considered in the processing network to transform raw materials/feedstocks into products/byproducts while reducing freshwater consumption and wastewater generation.

The synthesis and design problem can be solved using two strategies i.e. sequential and simultaneous approach. In sequential approach, subsystems (eg. water network and heat exchanger network) are dealt and solved sequentially or separately after an optimal process flowsheet is identified [1]. As opposed to the sequential approach, the simultaneous optimization approach has advantage which all the interactions and economic trade-offs would be take into account explicitly [2-4]. However, this can lead to a very large MINLP problem. It is important to note that the simultaneous process and water network synthesis is a complex task which involves a combination of strategic decisions (selection of product portfolio, raw materials, process technology and treatment technology) and tactical decisions (considering synthesis, design and

optimization of production technology etc.). The aim of this work is to develop a systematic framework using the superstructure-based optimization approach for the optimal synthesis and design of process network that connected with water/wastewater treatment network. The strategy accounts explicitly for the interactions between both networks. The optimal raw material, product portfolio, process technology and wastewater treatment strategies as well as material flows can be achieved simultaneously by implementing the systematic approach through interaction between the process and water networks (so called as *a network within a network*). The main advantage of the integrated approach is that it enables the simultaneous synthesis and design of overall systems where water network models will be included within the process models. .

Objective

In this PhD project, a generic model-based framework will be developed for integrated analysis of process synthesis and water/wastewater treatment network synthesis problems. The integration of water consumption early at process synthesis and design stage is expected to reduce the consumption of freshwater by and considering recycled water. A systematic approach is used to manage the complexity and solving simultaneously process synthesis and water synthesis network problem with respect to economics, resources consumption and sustainability. In order to achieve this task optimally and efficiently, a new superstructure is proposed and formulated for the simultaneous synthesis of the process and water network.

Framework of Integrated Synthesis and Design of Process and Water Networks

The systematic framework consists of four main steps as shown in Figure 1. The systematic framework for processing network developed by Quaglia et al. [5] was extended and superstructure-based optimization approach is used to synthesize and design of simultaneous process and water treatment network. The framework is supplemented by a software infrastructure based on EXCEL for gathering required data. All data and information requires for problem formulation are managed and organized in a systematic way.

The methodology is based on the development and synthesizing of a generic process and water network superstructure involving all design possibilities; its modelling; determining the optimal network from the feasible set generated from the superstructure; and finally, designing and optimizing the final selected network.

The optimization problem is formulated as an MI(N)LP and solved in GAMS environment to identify optimal process and water networks under different objective function scenarios (e.g. maximize gross operating income, maximize product yield, minimize waste etc.) and constraints (e.g. effluent discharge limits, product specifications, logical constraints etc.).

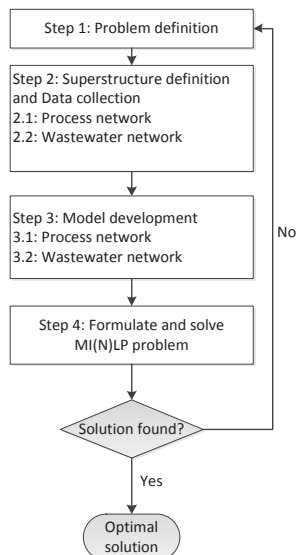


Figure 1: A systematic framework for synthesis and design process and wastewater networks.

Conclusion

A systematic approach is used to manage the complexity and solving simultaneously process synthesis and water synthesis network problem with respect to economics, resources consumption and sustainability. In order to achieve this task optimally and efficiently, a new superstructure is proposed and formulated for the simultaneous synthesis of the process and water network.

Acknowledgement

The author would like to acknowledge Universiti Malaysia Pahang and Ministry of Education of Malaysia for their financial support.

References

1. L. Čuček, Martin, M., Grossmann I.E., Kravanja, Z. *Computers & Chemical Engineering* 35 (2011) 1547-1557.
2. M.A. Duran, I.E. Grossmann, *AIChE J.*, 32 (1986) 123.
3. T. Yee, I.E. Grossmann, Z. Kravanja. *Computers & Chemical Engineering*, 14 (1990) 1151-1164.
4. L., Yang, I.E. Grossmann, *Industrial & Engineering Chemistry Research* 52(9) (2013) 3209-3224.
5. A. Quaglia, B. Sarup, G. Sin, R. Gani. *Computers and Chemical Engineering*. 38 (2012) 213-223.



Stine Broholm Hansen
Phone: +45 4525 2846
E-mail: sha@kt.dtu.dk

Supervisors: Peter Glarborg
Peter Arendt Jensen,
Flemming Frandsen
Bo Sander, DONG Energy

PhD Study
Started: January 2010
To be completed: September 2015

Deposition Build-Up in Grate and Suspension Boilers Firing Biomass

Abstract

In order to reduce the CO₂ emission from heat and power production, fossil fuels can be replaced by e.g. biomass. However, compared with fossil fuels, biomass ash has an enhanced propensity for deposition and corrosion. The objective of this project is to develop an engineering model that predicts the rate of deposit build-up and shedding during full-scale suspension firing of wood and/or straw. The model will be validated against full-scale experimental data, which have been reviewed as part of the project.

Introduction

To reduce CO₂ emissions and reduce the dependency of fossil resources, the use of biomass for power production is increased in Danish power plants. Utilization of biomass for power production do often increase the rate of formation of ash deposits, which are difficult to remove especially in the boiler chamber and on superheater coil surfaces compared to those formed during coal firing [1]. To support the development of biomass combustion equipment, deposit probe measurements have been performed in the last 20 years on many of the biomass fired power plant boilers in Denmark [2-16].

The objective of this project is to develop an engineering model that predicts the rate of deposit build-up and shedding during suspension firing of biodust. The model will initially be validated against experimental data obtained in EFR experiments and subsequently be tested against experimental data from the full-scale probe measurements of deposit build-up biodust suspension firing. The experimental data obtained in full scale suspension firing has as part of the project been reviewed and compared to the data obtained during grate-firing. This was done in order to determine similarities and differences in the deposition behaviors of the two firing technologies and to gain an idea of the influences of fuel type and boiler operation conditions on the deposition and shedding rates and the deposits chemistry. Conclusions of the review are provided here. The review can be found elsewhere [17].

Discipline

Reaction and Transport Engineering

Experiments Performed In Denmark

The experiments reviewed in this study have been conducted at several Danish CHP plants, both grate [2-8] and suspension fired [9-16]. In the investigated grate fired units, straw is the primary fuel, while in the biomass suspension-fired units, both wood and straw pellets have been utilized as fuels. The data set from the full scale measuring campaigns are obtained with deposit probes for collection and quantification of deposits and with a video camera for visual observation.

Fly Ash and Deposit Chemistry

Firing technology and fuel type had a significant impact on the fly ash chemistry. During grate-firing of straw the fly ash was enriched in K, Cl, and S compared to the fuel ash. During suspension-firing, the fly ash composition largely resembled the fuel ash composition, due to a higher degree of entrainment of ash in the combustion zone. The fly ash from suspension firing of straw was thus dominated by K and Si while wood-firing in suspension boilers leads to fly ash dominated by Ca and K.

The deposit chemical composition was influenced by firing technology, fuel choice, and flue gas temperature. At low local flue gas temperatures (<800 °C), the deposit compositions were similar to those of fly ash. Increases in local flue gas temperatures increased the content of Si and Ca in the deposits and decreased the Cl content. The influence of flue gas temperature is similar for grate and suspension-firing.

Rate of Deposit Build-Up

The rate of deposit build-up has been defined by two measures: an IDF rate, possibly including shedding events, and a DDF rate, which is the build-up rate without interference from shedding events. For grate boilers limited natural shedding is expected for flue gas temperatures <900 °C. Above this temperature, shedding by melting may influence IDF rates. Shedding has significant influence on the IDF rates in suspension boilers, and these should be regarded as uncertain estimates of the deposit accumulation. DDF rates are currently mainly available from probe measuring campaigns in suspension boilers.

The IDF rates in the two combustion systems are at similar levels; 0–100 g/m²·h. Differences in the ash flux in the different boilers are included by calculating ash deposit propensity. The ash deposit propensity is an order of magnitude larger in grate-fired boilers than in suspension boilers. This can be related to differences in fly ash chemistry.

Ash deposit propensity increases with flue gas temperatures. For all boilers and fuels examined, a steep increase in ash deposition propensity was observed at flue gas temperatures close to the temperatures where melting of the fly ash was expected based on STA analysis or ash fusion tests. The rate of deposit build-up was furthermore found to increase with K content in the fuel ash and fly ash for grate-fired boilers. For suspension-fired boilers deposition rates were low for wood firing whereas increases in deposition rates were observed with increasing straw shares.

Shedding of Deposits

During grate-firing of straw at low or intermediate flue gas temperatures (<900 °C), no natural shedding (melting, debonding or erosion) was observed. At higher flue gas temperatures (>900 °C), shedding of deposit took place by surface melting and droplet formation. For suspension firing of straw, natural shedding was observed to occur frequently primarily by debonding. Shedding by debonding was incomplete and increased deposit mass accumulated on the probe. Shedding by melting was not observed even at temperatures above 1000 °C. During wood suspension-firing, a thick layer of deposit never formed on the probe. At low flue gas temperatures, 800 °C, a small amount of deposit initially accumulated on the probe and the mass on the probe then remained constant. At high flue gas temperatures, 1300 °C, the deposition was characterized by a rapid build-up followed by complete shedding.

Soot blowing tests were conducted during grate-firing of straw and suspension-firing of straw/wood. It was found, in both cases that increased probe surface temperature and residence times lead to deposits that are more difficult to remove.

Shedding behavior was closely monitored during straw/wood firing in suspension boilers. The shedding rate [g/m²·h] and frequency [events/h] increased with increasing DDF rates, whereas the deposit mass lost per

event [g/m²] seemed to be relatively stable. The percentage of deposits removed per shedding event decreased with residence time. Up to 80% of the deposit on the probe was likely to be removed in a shedding event within the first 24 h of exposure. Contrarily, at exposure times >72 h, only up to 30% removal per shedding event could be expected. Camera observations revealed that the percentage of mass loss corresponded to a percentage of the probe length left uncovered, as the shedding occurred by debonding near the probe surface.

The net accumulation rate, calculated as the difference between the DDF rate and the shedding rate was found to increase with increasing flue gas temperature and straw share during straw/wood firing in suspension boilers.

Acknowledgement

The PhD study is part of the GREEN research center (Power Generation from Renewable Energy) funded by the Danish Strategic Research Center. The PhD study is co-funded by the MP2T Graduate School and by DONG Energy Power.

References

1. Bryers R.W. Prog. Energy Combust. Sci. 22 (1996) 29-120.
2. Jensen P.A. et al. Energy Fuels 11 (1997) 1048-55.
3. Michelsen H.P. et al. Fuel Proc. Techn. 54 (1998) 95-108.
4. Hansen L.A. et al. Fuel Proc. Techn. 64 (2000) 189-209.
5. Jensen, P.A. et al. Energy Fuels 18 (2004) 378-84.
6. Jensen P.A. et al. Final Report - Ash Deposit Formation and Removal in Biomass-fired Boilers. Fundamental Data Provided with Deposit Probes. Energinet.dk PSO-4106 (CHEC R0603) (2006).
7. Hansen J. et al. Deposit probe measurements in the Avedøre and Ensted straw fired grate boilers. CHEC Report R0705 (PSO 4792) (2007).
8. Zbogor A. et al. Energy Fuels 20 (2006) 512-19
9. Skrifvars B.-J. et al. Fuel 83 (2004) 1371-1379
10. Tobiasen L. et al. Fuel Proc. Techn. 88 (2007) 1108-17.
11. Jensen P.A et al. Measurements on the 800 MW_{th} Avedøre oil, gas and wood co-fired suspension boiler - Analysis of emission, burnout, deposit and FTIR measurements from April 2005. Energinet.dk PSO 6526 (Appendix E) (2008)
12. Bashir M.S. et al. Fuel Proc. Tech. 97 (2012) 93-106
13. Bashir M.S. et al. Energy Fuels 26 (2012) 2317-30
14. Bashir M.S. et al. Energy Fuels 26 (2012) 5241-55
15. Bashir M.S. Characterization and Quantification of Deposit Build-up and Removal in Straw Suspension-Fired Boilers. PhD Thesis, Technical University of Denmark, 2012.
16. Wu H.; et al. Fuel 113 (2013) 632–643
17. Hansen, S.B. et al. Energy Fuels 28 (2014) 3539–55



Thomas Klint Hansen

Phone: +45 4525 2952
E-mail: tkli@kt.dtu.dk
Discipline: Catalysis and Reaction Engineering

Supervisors: Anker D. Jensen
Brian B. Hansen
Ton V.W. Janssens, Haldor Topsøe A/S

PhD Study
Started: April 2013
To be completed: March 2016

Development of New Automotive Diesel Oxidation and NH₃ Slip Catalysts

Abstract

Catalytic diesel exhaust aftertreatment systems are an essential part of emission control from heavy duty diesel vehicles. These systems are under constant development in order to meet the stringent emission limits of the Euro VI and future regulations. The focus of this project is the development of a low noble metal content/low cost diesel oxidation catalyst (DOC) and a highly selective NH₃ slip catalyst (ASC). A more selective ASC will enable the use of higher NH₃ loads in the Selective Catalytic Reduction (SCR) unit and thereby ensure a higher NO_x removal. The research and development of these units will include identification and screening of new catalyst formulations, as well as kinetic studies and mathematical modeling.

Introduction

Heavy duty diesel (HDD) vehicles handle a substantial part of the world's transport and logistics. Harmful pollutants are however formed, such as nitrogen oxides (NO_x), hydrocarbons (HC), particulate matter (PM), and carbon monoxide (CO). The diesel exhaust aftertreatment (DEA) system has been developed to treat the pollutants in the exhaust gas [1].

Figure 1 illustrates the current standard DEA system consisting of a series of four catalytic units. First, the Diesel Oxidation Catalyst (DOC) oxidizes CO and HC to CO₂ and H₂O, as well as generates NO₂ from NO. Second, the Diesel Particulate Filter (DPF) is a wall-flow filter that traps PM in its monolith walls. The DPF can be regenerated actively by increasing the exhaust gas temperature by post-injection of fuel, or passively by using a catalyst. NO₂ generated by the DOC also assists regeneration. Third, NO_x is treated through Selective Catalytic Reduction (SCR) with NH₃ as the reducing agent. NH₃ is supplied to the system through urea dosing, regulated by the onboard Model Predictive Control (MPC) unit. Lastly, excess NH₃ is selectively oxidized to N₂ by the Ammonia Slip Catalyst (ASC). As a result, the treated exhaust gas exiting the DEA system meets the emissions restrictions imposed by the Euro VI regulations [1].

The DEA system is very complex, requiring efficient exhaust treatment for a wide range of operating conditions, corresponding to cold start, stop-and-start driving (inner city), and high speed driving (highways).

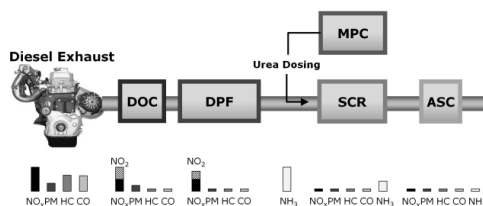


Figure 1: Example of a standard DEA system, consisting of the DOC, DPF, SCR component, urea dosing MPC unit, and the ASC.

DTU Chemical Engineering and Haldor Topsøe A/S are collaborating on the development of the next generation DEA system to meet future regulations, with funding from Innovation Fund Denmark. The underlying PhD projects concern the development of new DOC and ASC formulations (Thomas Klint Hansen, pg. 87-88), the combination of the DPF and SCR components (Kasper Linde, pg. 117-118), and the development of the MPC unit for efficient regulation of urea dosing (Andreas Åberg, pg. 215-216).

Specific Objectives

The overall objective of this PhD study is to develop new DOC and ASC formulations for the next generation of DEA systems. New catalyst formulations will be identified and screened, and the kinetics investigated using a catalyst testing unit. Mathematical modeling will be used to help prepare optimal lab scale and full

scale monolith samples based on the most promising formulations. The lab scale and full scale monoliths will be tested in a pilot setup at DTU Chemical Engineering and a full-scale engine testing unit at Haldor Topsøe A/S, respectively.

Development of the Diesel Oxidation Catalyst

The DOC is commonly a Pd-Pt based catalyst and is therefore quite expensive [1]. The next generation DOC will be developed with the goal of reducing the component price, by reducing the dependency of the catalyst on noble metals. Pt based DOC formulations promoted with, amongst others, K and Fe will be prepared, based on their potential to decrease the light-off temperature of CO oxidation for conditions similar to those in a DEA system [2,3]. A typical light-off curve for CO oxidation over the benchmark DOC (1 wt.-% Pt/Al₂O₃) is shown in Figure 2. To better understand the DOC and light-off behavior, a kinetic model will be developed.

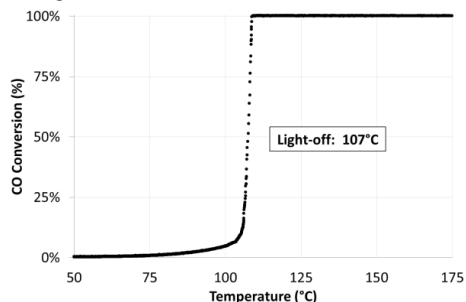


Figure 2: The light-off curve for CO oxidation over the benchmark DOC. Operating conditions: 10 mg 1 wt.-% Pt/Al₂O₃, 300 NmL/min, 250 ppm CO, 10 vol.-% O₂, and balance N₂.

Development of the Ammonia Slip Catalyst

Selective Catalytic Oxidation (SCO) of NH₃ to N₂ is the purpose of the ASC. Figure 3 illustrates the dual layer design used in the ASC. The upper layer is a SCR catalyst (Cu-beta zeolite) and the lower layer is an Ammonia Oxidation Catalyst (AMOX) (Pt/TiO₂).

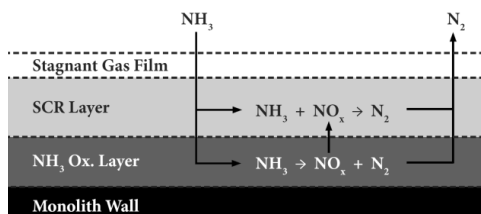


Figure 3: The dual layer design of the ASC. The lower layer oxidizes NH₃ to N₂ and NO_x. The NO_x produced in the lower layer reacts with NH₃ in the upper layer, over the SCR catalyst, increasing overall N₂ selectivity.

To further increase the N₂ selectivity, a model developed for the monolithic dual layer ASC will be used to optimize the catalyst design parameters. The

optimized design will then be the basis for catalyst preparation [4]. The kinetic models used in the dual layer ASC model are being developed through kinetic parameter studies. Figure 4 shows the light-off curve for the SCR catalyst (Cu-beta zeolite), illustrating the complexity of the reaction network involved [5]. Additionally, the significant N₂O formation (a strong greenhouse gas) indicates the importance of understanding formation mechanisms in order to increase N₂ selectivity.

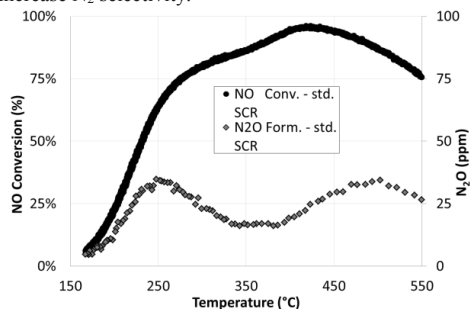


Figure 4: The light-off curve for NH₃-SCR over the Cu-beta zeolite. Operating conditions: 20 mg Cu-beta, 1000 NmL/min, 600 ppm NH₃, 500 ppm NO, 5 vol.-% H₂O, 10 vol.-% O₂, and balance N₂.

Conclusions

Improved DEA systems are needed to meet future emission regulations. Design of the next generation of DOC and ASC formulations is being performed through literature studies, mathematical modeling, and experimental investigations, including kinetic studies and activity screenings. The DOC will be improved through the reduction of the noble metal content resulting in a lower component price. The dual layer ASC design will be optimized through mathematical modelling. The next generation DOC and ASC will contribute to the overall improvement of the DEA system.

Acknowledgements

This project is a collaboration between the CHEC research center at DTU Chemical Engineering and Haldor Topsøe A/S. The financial support from Innovation Fund Denmark under Grant number 103-2012-3 is gratefully acknowledged.

References

- W. A. Majewski, M. K. Khair, Diesel Emissions and Their Control, SAE International, 2006.
- Y. Minemura, M. Kuriyama, S. Ito, Catal. Commun. 7 (9) (2006) 623-626.
- H. Einaga, N. Urahama, A. Tou, Y. Teraoka, Catal. Lett. 144 (10) (2014) 1653-1660.
- A. Scheuer, W. Hauptmann, A. Drochner, J. Gieshoff, H. Vogel, M. Votsmeier, Appl. Catal., B 111-112 (2012) 445-455.
- P.S. Metkar, M.P. Harold, V. Balakotaiah, Chem. Eng. Sci. 87 (2013) 51-66.

**Hamid Hashemi**

Phone: +45 4525 2809
E-mail: hah@kt.dtu.dk
Discipline: Reaction and Transport Engineering

Supervisors: Peter Glarborg
Jakob M. Christensen

PhD Study
Started: May 2011
To be completed: December 2014

Combustion Characterization of Bio-derived Fuels and Additives

Abstract

Characterizing the combustion of bio-derived fuels and different additives at high pressures and intermediate temperatures was the major aim of this project. To this end, experiments have been conducted in a high pressure laminar flow reactor and species conversion profiles of H_2 , CH_4 , DME, and ethanol were measured. A chemical kinetic model has been developed and evaluated against the measured data. The model predictions agreed well with the present data as well as with data from the literature.

Introduction

In recent years, fuels produced from bio-sources have generated considerable research and practical interests. Less emission of greenhouse gases and independency from limited natural sources are major causes of this emerging attention.

Natural gas (NG) will have the fastest growth among all fuels in the following decades and replace partly coal and liquid fuels in power generation for electricity and industrial processes [1]. A larger availability and less emission of pollutants from combustion are among the major reasons to replace other fossil fuels by natural gas. For an equivalent amount of heat, burning of natural gas produces around 20 and 45 percent less carbon dioxide than burning of gasoline and coal, respectively. In addition to fossil reservoirs, natural gas can be produced from the anaerobic decay of biomass, e.g., agricultural waste and sewage sludge. More restrictive regulation of the release of greenhouse gases can increase the share of natural gas in the energy market even more.

Natural gas consists mainly of methane and to a lesser extent ethane and propane. Natural gas has been used as a fuel for internal combustion engines to a limited extent around the world. Some of the challenges in using natural gas are the higher ignition temperature, longer ignition delay time, and lower burning velocity of natural gas compared to conventional petroleum-based fuels. Depending on the application, these variations can potentially have adverse consequences if appropriate measures have not been taken. As a solution, the combustion properties of methane can be improved by additives, e.g. dimethyl ether (DME).

Hydrogen has been considered as an energy carrier to be used in conventional engines. It is also a major component of syngas (H_2+CO) produced from bio-sources. Burning syngas has been an alternative way of using biofuels in conventional energy plants. Furthermore, hydrogen reactions are among the most sensitive reactions controlling the ignition of different hydrocarbon fuels, so understanding of H_2/O_2 combustion chemistry is a vital step in developing models for hydrocarbon fuels oxidation.

Ethanol can be produced from biomass through the fermentation process. In the fermentation process, different sugars are converted biologically to ethanol. Neat ethanol as well as its blends with gasoline have widely been used in spark-ignited engines. Ethanol addition to gasoline promotes the overall octane number of the fuel while it potentially reduces the emission of particulate matter and CO [2]. The relatively high energy density of ethanol makes it interesting to be used as a neat fuel too. However, widespread usage of ethanol fuel may give rise in the emission of aldehydes [2] which can cause serious health risks.

Dimethyl ether (DME) is an isomer of ethanol but with different thermodynamic and ignition properties [3]. In general, DME can be produced from different feedstocks, e.g. oil, natural gas, coal, waste products, and biomass. Bio-DME can potentially reduce the CO_2 release to the environment. Higher cetane number and lower boiling temperature of DME make it an attractive alternative to conventional diesel fuels for use in compression ignition engines. DME addition to natural gas accelerates ignition and increases the flame speed.

Combustion characteristics of the mentioned fuels and their mixtures will facilitate developing chemical models of combustion engines and other industrial applications. Even though all the discussed fuels have been studied extensively in recent years (e.g. see [4-11]), data for the high pressure and medium temperature range are scarce. Moreover, the effects of additives on methane oxidation has not well been understood.

Specific Objectives

The main aim of this work is to measure combustion characteristics of H₂, CH₄, DME and ethanol at high pressures and intermediate temperatures. In a unique high-pressure flow reactor setup at DTU Chemical Engineering, it is possible to investigate the pyrolysis and oxidation of different liquid/gaseous fuels at pressures and temperatures up to 100 bar and 900 K, respectively. A chemical kinetic model for the oxidation of the investigated fuels at high pressures and intermediate temperatures is developed and validated against the present data as well as data from literature. Finally, the model will be extrapolated to conditions relevant for industrial applications.

Results and Discussion

Figures 1-3 show the results of hydrogen experiments at four different stoichiometries. At the reducing conditions ($\Phi = 12$), oxidation started at 748–775 K while it was shifted to 798–823 K for stoichiometric and oxidizing conditions ($\Phi = 1.03$ and 0.05). At very oxidizing conditions (O₂ atmosphere, $\Phi = 0.0009$), the temperature for onset of reaction was reduced to 775–798 K. The data were interpreted in terms of a detailed chemical kinetic model. The reaction mechanism was based on recent work of Burke et al. [7], updating the rate constants for OH + OH, HO₂ + OH, and HO₂ + HO₂ based on recent determinations. As can be seen from figures 1-3, the modeling predictions were in good agreement with the measurements in the flow reactor. Further comparison and discussion can be found in [9].

Figures 4-5 represent the results of methane ignition as well as the effect of doping with DME at 100 bar pressure and under stoichiometric conditions. For neat methane, the fuel conversion was detected at 750 K and higher temperatures. Replacing 1.8% of methane by DME moved the onset of fuel conversion to 725 K and increasing the DME ratio to 3.2% triggered ignition at 700 K. The model for DME is based on work by Zhao et al. [8]. The hydrogen subset was updated according to [12] and several other reactions were modified according to new determinations. As can be seen, the predictions by the developed model agreed well with the measured values for major components. However, the consumption of DME was predicted at lower temperatures compared to the measurements. More work is required to better capture the interaction between DME and methane.

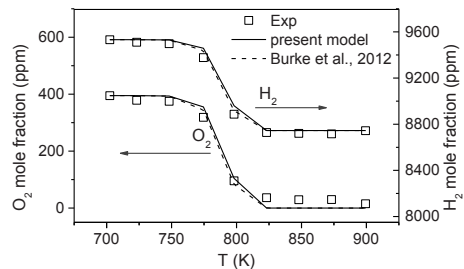


Figure 1: Results of reducing experiments on hydrogen (0.95% H₂ and 0.04% O₂ in N₂, $\Phi=11.9$) at 50 bar pressure. The residence time is given by $\tau [s] = 5661/T [K]$. Symbols mark experimental results and lines denote predictions of the present model and the model by Burke et al. [7].

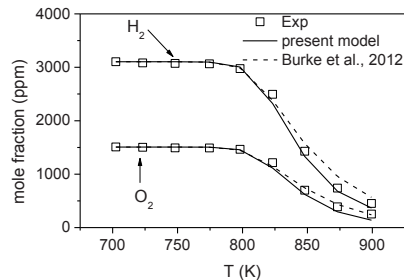


Figure 2: Results of stoichiometric experiments on hydrogen (0.31% H₂ and 0.15% O₂ in N₂, $\Phi = 1.03$) at 50 bar pressure.

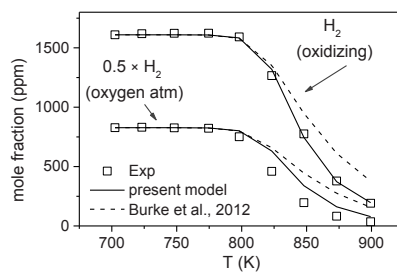


Figure 3: Results of oxidizing experiments on hydrogen (0.16% H₂ and 1.60% O₂ in N₂, $\Phi = 0.05$) and experiments in oxygen atmosphere (0.17% H₂ and 93.92% O₂ in N₂, $\Phi=0.0009$) at 50 bar pressure.

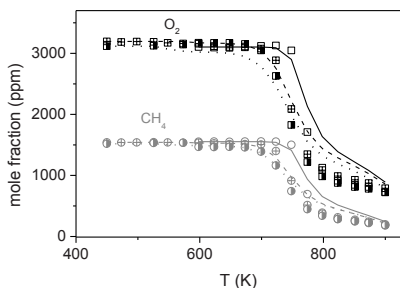


Figure 4: Results of stoichiometric experiments on neat (0.15% CH₄ and 0.32% O₂ in N₂, $\Phi=1.0$) and doped methane by DME (DME/CH₄ = 1.8, 3.2%) at 100 bar pressure. Open symbols/solid lines: the neat CH₄ experiments, Crossed symbols/ dashed lines: the doped experiment by DME (1.8%), Half-open symbols/ dotted lines: the doped experiment by DME (3.2%).

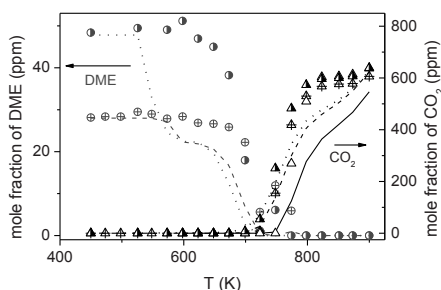


Figure 5: Results of stoichiometric experiments on neat (0.15% CH₄ and 0.32% O₂ in N₂, $\Phi=1.0$) and doped methane by DME (DME/CH₄ = 1.8, 3.2%) at 100 bar pressure. Open symbols/solid lines: the neat CH₄ experiments, Crossed symbols/ dashed lines: the doped experiment by DME (1.8%), Half-open symbols/ dotted lines: the doped experiment by DME (3.2%).

Neat DME oxidation was also studied in the flow reactor. It was found that DME conversion started at temperatures as low as 500 K. Furthermore, it seemed that the temperature for the onset of conversion is independent of stoichiometry. Negative temperature coefficient (NTC) behavior has been observed for all investigated stoichiometries whereas it was more profound at stoichiometric conditions. Generally, the developed model agreed well with the measurements.

Results from ethanol experiments in the flow reactor are shown in figures 9-11. Under reducing conditions, fuel consumption started around 675 K while it was postponed to 700 K for stoichiometric and oxidizing conditions. The model predictions for the major components were in good agreement with the measurements, but it was less accurate for some intermediate species (not shown here) such as C₂H₆.

Further work is needed to improve the accuracy of the model for such species.

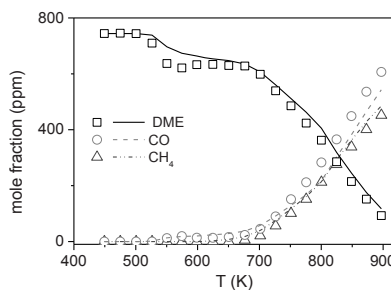


Figure 6: Results of reducing experiments on DME (0.07% DME and 0.01% O₂ in N₂, $\Phi=16.44$) at 50 bar pressure. Symbols mark experimental results and lines denote predictions of the model.

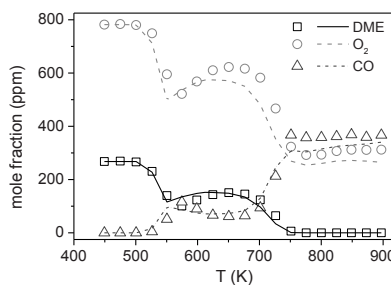


Figure 7: Results of stoichiometric experiments on DME (0.03% DME and 0.08% O₂ in N₂, $\Phi=1.03$) at 50 bar pressure. Symbols mark experimental results and lines denote predictions of the model.

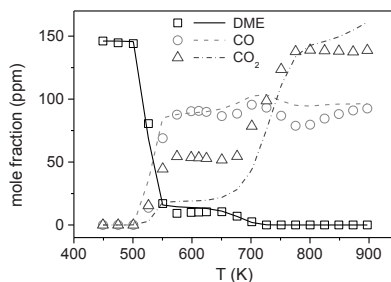


Figure 8: Results of oxidizing experiments on DME (0.01% DME and 1.08% O₂ in N₂, $\Phi=0.04$) at 50 bar pressure. Symbols mark experimental results and lines denote predictions of the model.

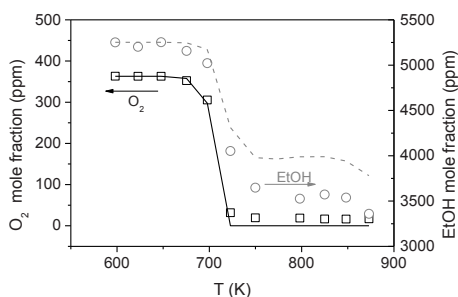


Figure 9: Results of reducing experiments on ethanol (0.53% EtOH and 0.04% O₂ in N₂, $\Phi=43.4$) at 50 bar pressure. Symbols mark experimental results and lines denote predictions of the present model.

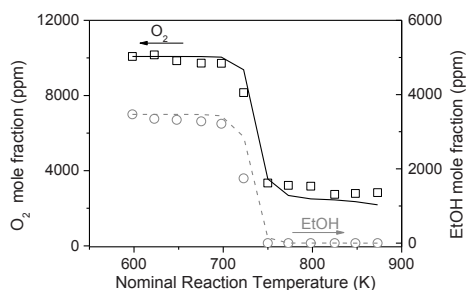


Figure 10: Results of stoichiometric experiments on ethanol (0.35% EtOH and 1.01% O₂ in N₂, $\Phi=1.03$) at 50 bar pressure. Symbols mark experimental results and lines denote predictions of the present model.

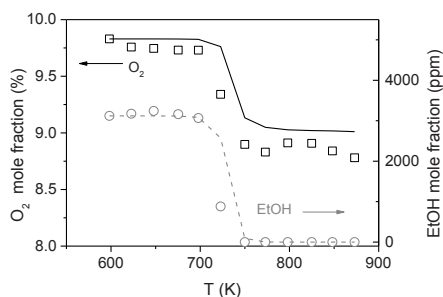


Figure 11: Results of oxidizing experiments on ethanol (0.31% EtOH and 9.83% O₂ in N₂, $\Phi=0.10$) at 50 bar pressure. Symbols mark experimental results and lines denote predictions of the present model.

Conclusion

The oxidation of hydrogen, methane, ethanol, and dimethyl ether (DME) was investigated in a laminar flow reactor at intermediate temperatures and high pressures. Results provided information about the onset

temperature for reaction and the fuel consumption rate upon initiation. A detailed chemical kinetic model has been developed and validated against the measured data as well as other available combustion characteristics. It was found that while mixture stoichiometries were changed dramatically, the onset temperatures for the conversion of different investigated fuels were affected only slightly. Furthermore, neat DME had a negative temperature dependency at intermediate temperatures and pressure of 50 bar. DME addition to methane was shown to be an effective way to promote the ignition of methane.

The developed model was able to predict the onset of conversion as well as mixture composition after ignition for a wide range of stoichiometries. However, the model prediction for some intermediate species was less than perfect and further work is needed to address such problems.

Acknowledgement

Funding from the European Graduate School as well as MAN Diesel & Turbo are gratefully acknowledged.

References

1. EIA, International Energy Outlook 2013, EIA, Washington, 2013.
2. A. K. Agarwal, Prog. Energy Combust. Sci. 33 (2007) 233–271.
3. K. Kohse-Hinghaus, P. Oswald, T. A. Cool, T. Kasper, N. Hansen, F. Qi, C. K. Westbrook, P. R. Westmoreland, Angew. Chemie Int. Ed. 49 (2010) 3572–3597.
4. C. L. Rasmussen, J. Hansen, P. Marshall, P. Glarborg, Int. J. Chem. Kinet. 40 (2008) 454–480.
5. C. L. Rasmussen, J. G. Jakobsen, P. Glarborg, Int. J. Chem. Kinet. 40 (2008) 778–807.
6. V. Aranda, J. M. Christensen, M. U. Alzueta, P. Glarborg, S. Gersen, Y. Gao, P. Marshall, Int. J. Chem. Kinet. 45 (2013) 283–294.
7. M. P. Burke, M. Chaos, Y. Ju, F. L. Dryer, S. J. Klippenstein, Int. J. Chem. Kinet. 44 (2012) 444–474.
8. Z. Zhao, M. Chaos, A. Kazakov, F.L. Dryer, Int. J. Chem. Kinet. 40 (2008) 1–18.
9. F. M. Haas, M. Chaos, F. L. Dryer, Combust. Flame 156 (2009) 2346 – 2350.
10. M. Abian, C. Esarte, A. Millera, R. Bilbao, M. U. Alzueta, Energy Fuels 22 (2008) 3814–3823.
11. T. Mendiara, P. Glarborg, Combust. Flame 156 (2009) 1937–1949.
12. H. Hashemi, J.M Christensen, S. Gersen, P. Glarborg, Proc. Combust. Inst. 35 (2014).



Suzan Sager Hassouneh

Phone: +45 4525 2971
E-mail: shas@kt.dtu.dk
Discipline: Polymers

Supervisors: Anne Ladegaard Skov
Anders Egede Daugaard

PhD Study
Started: August 2012
To be completed: January 2015

Dispersion of Carbon Nanotubes in Polydimethylsiloxane and the Influence on the Mechanical and Electrical Properties

Abstract

Dielectric elastomers (DEs) are thin elastomeric films that change shape and size when an electric field is applied. DE films can be used as actuators, sensors, and generators (i.e. transducers). To improve the performance of DE transducers, multiple DE layers are adhered together. This study focuses on dispersing carbon nanotubes into polydimethylsiloxane (PDMS) to produce a conductive elastomer to be used as adhesive between the DE layers.

Introduction

Over the last decades, the interest in smart material has increased. Smart materials are materials that exhibit a change in size and shape as respond to external stimuli, such as optical, thermal and electrical [1].

Dielectric elastomers (DEs) are a class of smart material that can be used as actuators, sensors and generators. DEs are thin elastomeric film that are sandwiched between compliant electrodes. When a voltage is applied, the elastomeric film contracts in thickness and expands in the planar direction as illustrated in Figure 1.

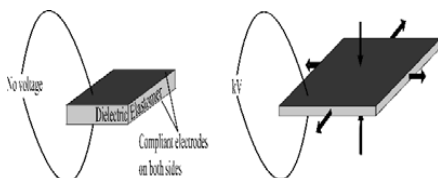


Figure 1: The working principle of DE transducers.

When the voltage is turned off, the DEs return to their original shape. The DEs produced at Danfoss Polypower A/S (DPP) are thin polydimethylsiloxane (PDMS) films that have a corrugated surface on one side and a flat side on the other. The corrugated side is coated with a thin layer of metal to yield flexible electrodes.

Specific Objectives

To enhance the performance of the transducers, multiple DE layers are added together. However, the multiple

layers are relatively independent of each other, which can cause air to be trapped between the layers and friction between the layers can reduce the lifetime of the transducer. To eliminate these issues the DE layers can be adhered together. Due to the corrugations, the films can be added in different configurations as illustrated in Figure 2.

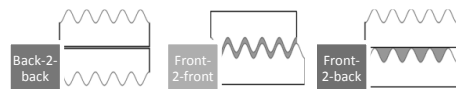


Figure 2: The different configurations for adhesion of films. The back-2-back configuration is where two flat sides are adhered together. The corrugated sides are adhered together in the front-2-front configuration and for the front-2-back configuration, a corrugated side is adhered with a flat side.

The various configurations have different requirements for the adhesive. This study focuses on the front-2-front configuration, where the adhesive should be conductive. Carbon nanotubes (CNTs) are used as fillers, due to their mechanical, electrical and thermal properties, which can be utilized to make conductive polymers [2]. The dispersion of CNTs in polymer matrices is challenging due to the very large specific surface area of CNTs, which usually leads to agglomerations [3]. Imidazolium type ionic liquids (ILs) ease the dispersion of CNTs in the matrix and improve the electrical properties of the CNT-elastomer composites [4]. The aim

of this study is to investigate different dispersion methods as well as the addition of IL to the composite and their influence on the electrical and mechanical properties.

Experimental

Commercial available PDMS, Elastosil RT625, is used as the polymer matrix. Multiwalled carbon nanotubes (MWCNTs) are used as filler material and the ionic liquid used is 1-ethyl-3-methyl imidazolium bis (trifluoromethanesulfonyl)imide ([EMIM][TFSI]). Two dispersion methods were investigated. Samples were prepared with 4 and 5 wt% CNT. For samples containing IL the CNT is grinded with the IL in a 1:1 weight ratio until gelation is observed.

In the first method (**method 1**) the CNT or CNT/IL is dispersed in heptane and ultrasonicated for 15 minutes. Afterwards, component A of the PDMS is added and the mixture is mechanically mixed for 6 hours at 900 rpm. The heptane is then evaporated using a rotary evaporator and component B of the PDMS is added to the mixture. The sample is speedmixed for 5 minutes at 2750 rpm and the sample is cast on a glass plate.

In the second method (**method 2**), the CNT or CNT/IL is speedmixed (5 minutes at 2750 rpm) with both components of PDMS as well as a 1 wt% inhibitor to slow down the curing process. The composites are then dispersed in a roll mill. The roll mill consists of three rolls and the gap between the first and the second roll was set to 30 μm while the gap between the second and the third roll was set to 15 μm . The sample was rolled six times until the CNTs were evaluated to be homogeneously dispersed.

Results and Discussion

The conductivity of the prepared samples not containing IL is investigated for both dispersion methods and compared to the commercially available conductive elastomer LR3162. The obtained conductivities are shown in Figure 3.

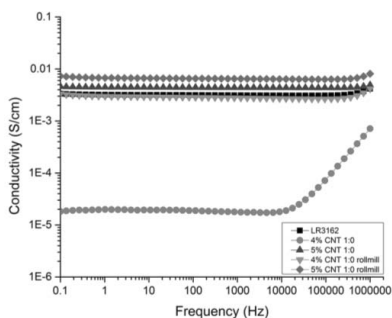


Figure 3: The conductivity of the samples with no IL for both dispersion methods.

The figure shows that the conductivity of the samples increases with increasing concentration of CNT for both dispersion methods. The samples prepared using **method 2** are frequency independent in the measured frequency interval, which show a good dispersion of the CNTs in

the matrix. For the sample containing 4 wt% CNT prepared by **method 1**, the sample is frequency dependent at higher frequencies, which indicates that the sample is not well-dispersed.

The conductivities of the samples containing IL are depicted in Figure 4.

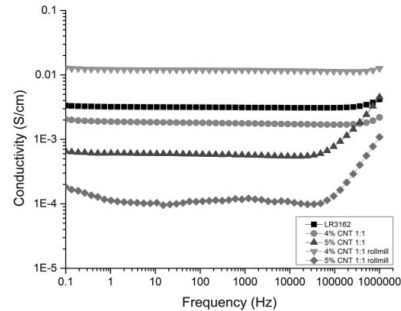


Figure 4: The conductivity of the samples containing IL for both dispersion methods.

It is clear that the conductivities of the samples decrease with increasing concentrations of CNT/IL for both methods. This indicates that the CNT/IL fillers form agglomerates and the limit for loading CNT/IL into the matrix is reached.

For the samples loaded with 4 wt% CNT/IL, **method 2** (roll mill) show the highest conductivity, which indicates a better dispersion.

Conclusions

CNTs are conductive fillers that can be used to prepare conductive elastomers. The dispersion of CNTs into a polymer matrix is challenging. Therefore, two different dispersion methods and their influence on the electrical properties were investigated. Moreover, the influence of IL on the dispersion as well as on the electrical and mechanical properties was investigated. The first method was using ultra sonication, and the second method was dispersing using a roll mill. The study showed that the conductivities decreased with the increasing concentrations of CNT for the samples containing IL. Furthermore, the conductivities obtained by dispersion **method 2** were higher than **method 1**, which indicates a better dispersion of the CNTs in the matrix.

Acknowledgements

The author would like to thank Innovationsfonden for the financial support.

References

1. X. Zhang, C. Löwe, M. Wissler, B. Jähne, G. Kovacs, *Advanced Engineering Materials* (2005) 7, 5, 361-367
2. Seo, D.K., Kang, T.J., Dae, W.K., Yong, H.K.; *Nanotechnology* (2012) 23, 075501
3. Fritzsche, J., Lorenz, H., Klüppel, M.; *Macromol. Mater. Eng.* (2009) 294, 551-560
4. Steinhauser, D., Subramaniam, K., Das, A., Heinrich, G., Klüppel, M.; *eXPRESS Polymer letters* (2012) 6, 11, 927-936



Søren Heintz

Phone: +45 4525 2949

E-mail: shein@kt.dtu.dk

Supervisors: Krist V. Gernaey

John M. Woodley

Ulrich Krühne

PhD Study

Started: September 2012

To be completed: August 2015

A miniaturized experimental platform for development of recovery processes

Abstract

The scope of this project is the use of automated microsystems as novel tools to accelerate the development of biocatalytic processes. The intention is for the microsystems to serve multiple purposes enabling full process characterization in a fast, easy and cheap manner. For example, the systems are intended for characterization of different promising biocatalysts, characterization of different process options, process optimization and testing of multiple microsystems in combination. The main focus of this PhD study is on the application of these microsystems to test, optimize and identify economically feasible product recovery options, e.g. different downstream processing scenarios and *in-situ* (co-)product removal strategies. As case studies, for the evaluation of the potential of such microsystem as process development tools, three ω -transaminase catalyzed model reactions are used. These three case studies impose different challenges to both the biocatalytic reaction performance as well as to the following product recovery. The challenges cover unfavorable thermodynamic equilibrium, product inhibition, low aqueous solubility and similar physicochemical properties of the reaction species. Addressing these challenges will ensure that the microsystems are really put to a test.

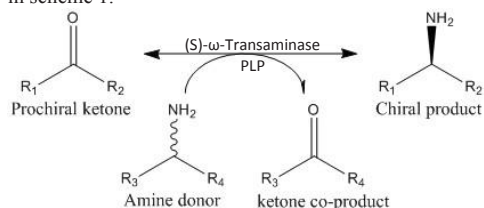
Introduction

Chiral amines are important building blocks for many pharmaceuticals and precursors [1]. As a consequence of their role in such applications it is, in most cases, required to ensure production of enantiomerically pure compounds for patient safety reasons, as defined by regulatory authorities [2]. However, the production of enantiomerically pure chiral amines, i.e. achieving a high enantiomeric excess (*e.e.* > 99%), can be quite a challenging task.

An alternative to conventional chemical synthesis methods is synthesis using biocatalysis. Biocatalysis is organic synthesis mediated by an isolated enzyme, immobilized enzyme, mixtures of isolated and/or immobilized enzymes or alternatively a whole-cell catalyst containing one or more enzymes. Biocatalysts have the advantage of enabling high selectivity (high *e.e.* values); they can potentially use a range of substrates while forming relatively few by-products, and potentially allow the establishment of simplified process routes [3]. Other drivers for industrial implementation of biocatalytic processes are the potential of improved process economy and a better environmental profile than conventional chemical processes [3-7]. All these

factors make biocatalysis attractive for the production of chiral amines.

There are multiple types of biocatalysts enabling the synthesis of chiral amines, where one is the asymmetric synthesis using ω -transaminases [8]. ω -transaminases (E.C.2.6.1.1) are quite attractive as they potentially enable asymmetric synthesis of pure chiral amines with *e.e.* > 99%, under mild reaction conditions [9]. ω -transaminases facilitate the transfer of an amino group from a primary amine to a carbonyl compound mediated by pyridoxal-5'-phosphate (PLP) [10]. The general reaction scheme of ω -transaminase reactions is shown in scheme 1.



Scheme 1: General reaction scheme for the asymmetric synthesis of chiral amines using ω -transaminases.

Despite all the benefits related to applying ω -transaminases for the synthesis of chiral amines, the application of such biocatalytic processes is not very common. This is a consequence of the many challenges related to operating these biocatalytic processes, making it difficult to achieve economically feasible processes. The challenges related to ω -transaminase applications are in many cases related to unfavorable thermodynamic reaction equilibrium, low solubility of reaction species and different inhibition effects, to name a few [11].

The effect of such process limiting challenges can be reduced in different ways during the development of a biocatalytic process, such as biocatalyst and process engineering. Well-known examples are the modification of the biocatalyst to improve process compatibility and/or exploiting different *in-situ* co-product (IScPR) and/or product removal (ISPR) options [9]. The general principles of the development of biocatalytic processes are illustrated in the development cycle in figure 1. The development cycle identifies the major areas of development and the key decisions which have to be taken during the development and optimization phase of a process [4].

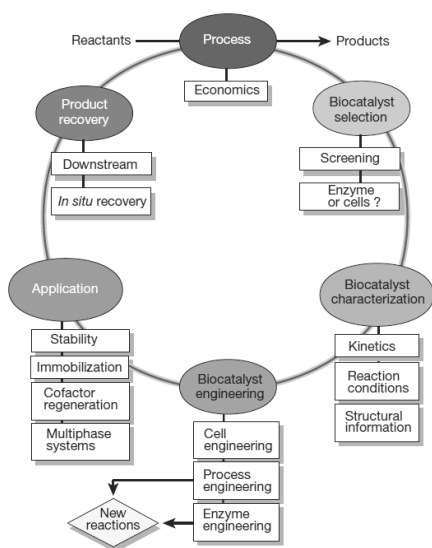


Figure 1: Development cycle of biocatalytic processes [4].

Currently, it is quite time demanding to develop new biocatalytic processes, imposing a need for better and faster technologies to ensure faster process development. The EU FP7 financed project BIOINTENSE (grant agreement n°. 312148) intends to provide such technologies with the aim of ensuring accelerated process development, in the form of automated microsystems. Such automated microsystems should provide tools to achieve fast screening, characterization and optimization of new processes,

with a low consumption of expensive and scarce resources.

This PhD project will mainly concern the development and testing of different process options for product recovery using microsystems, i.e. characterization and evaluation of different downstream processing (DSP), IScPR and ISPR methods in combination with reactor modes.

Aspects of product recovery

In addition to the importance of improving the performance of the biocatalytic reaction it is equally important to consider the following downstream recovery. Downstream recovery of products from biocatalytic reactions can be quite challenging, due to the complexity of the reaction mixtures. Also, the recovery procedures vary dependent on the biocatalytic reaction. For ω -transaminase reactions the recovery can be quite problematic as a consequence of the very similar physicochemical nature of substrates and products making selective and efficient separation challenging. The latter is especially due to the fact that many separation techniques exploit differences in physicochemical properties of the species to be separated.

The function of the microsystems in this relation is to aid in fast identification of the most feasible separation method, i.e. the method enabling the highest economical profit. Shown in figure 2 is an example on one way to test liquid-liquid extraction in a microsystem.

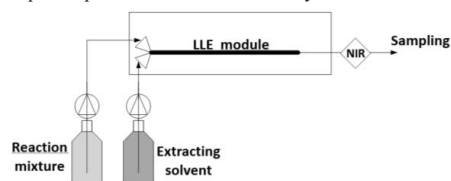


Figure 2: Conceptual microsystem for screening and characterizing liquid-liquid extraction (LLE) operations.

In some cases it will be required to exploit the separation methods to improve the biocatalytic reaction performance, i.e. by combining the separation and reaction referred to as *in-situ* removal (IScPR and ISPR). Implementation of IScPR and/or ISPR will aid in reducing effects such as product degradation, inhibition and unfavorable thermodynamic equilibrium [4]. IScPR and ISPR methods will always have a positive influence on such process limiting effects and can potentially simplify the following product purification.

However, the implementation of different *in-situ* removal methods is not straightforward. There is the issue of achieving selective and efficient removal as with conventional downstream processing options, but there are also issues such as the compatibility of the removal method with the biocatalyst and vice versa. An overview of some general aspects which influence the ISPR and IScPR options applicable for any given biocatalytic process is given in figure 3 [3].

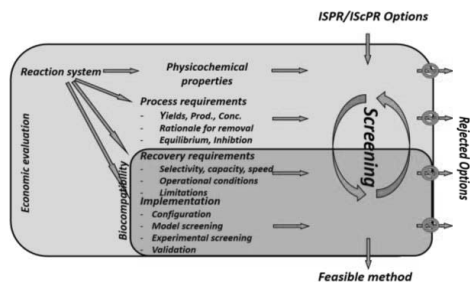


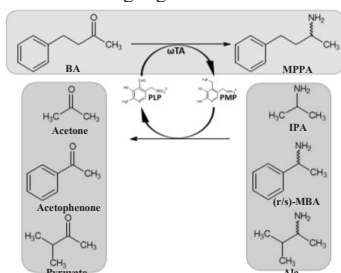
Figure 3: Overview of some general aspects of ISPR/IScPR development for biocatalytic processes [3].

A good example of the complexity of applying *in-situ* removal options is the implementation strategy. The implementation strategy is highly dependent on the compatibility of the biocatalyst and the selected *in-situ* removal option. For example, dependent on their compatibility with one another it will either be necessary to have them in direct contact or in indirect contact with one another. Also, there is the possibility to implement the removal option internal or external of the reactor, dependent on the specific requirements, e.g. operating conditions, cost of implementation and configuration limitations.

Flexible microsystems will make it possible to test the influence of different separation options on the biocatalyst, enabling fast identification of potentially feasible *in-situ* removal options.

Case studies

During this PhD project the main focus will be kept to three specific reaction systems using ω -transaminase ATA-50. These three case studies will be used to validate the use of microsystems for process development. The overall reaction scheme which is in focus is the formation of 1-methyl-3-propylphenylamine (MPPA) from benzylacetone (BA) using three different amine donors: Methylbenzylamine (MBA), isopropylamine (IPA) and alanine (ALA), i.e. the three case studies. The general reaction schemes of these model reactions are highlighted in scheme 2.



Scheme 2: General reaction scheme for the asymmetric synthesis of 1-methyl-3-propylamine from benzylacetone using ω -transaminases and three different amine donors: methylbenzylamine, isopropylamine and alanine.

These case studies impose different challenges, which have to be addressed in order to improve the reaction performance. These challenges are also the motivation for the selection of precisely these case studies as they will put the application of microsystems for process development to the test. The challenges related to the case studies cover different equilibrium scenarios, i.e. favourable and unfavourable scenarios, potential inhibiting effects, low solubility of certain reaction species and separation of reaction species with very similar physicochemical properties. The relative thermodynamic equilibria of each of the reactions are roughly: ~30:1 (MBA-donor), ~1:1 (IPA-donor) and ~1:1000 (ALA-donor) [13].

Analytics

An important factor for the successful application of microsystems is the implementation of analytics enabling on-line measurements. Working in such small scales, manual sampling gives large uncertainties as a consequence of handling difficulties. Having flexible microsystems where it is possible to implement different standard analytical methods (e.g. NIR, UV, HPLC, GC) and/or novel sensor technologies is of utmost importance for the microsystems to reach their full potential. It should be aimed at having on-line monitoring in the systems not only to avoid the uncertainties resulting from manual sampling, but also to overcome some of the current analytical bottlenecks and thereby enabling high throughput characterization systems. The focus will mainly be kept on the implementation of optical sensors, so the impact of the sensors on the process is avoided as much as possible.

Influence of scale

An important cornerstone of this PhD project is the transfer of the knowledge obtained from process characterization in microsystems across scales. The different dominant phenomena across scales make this knowledge transfer difficult. It is the hypothesis that fundamental process knowledge, e.g. kinetic parameters, is transferable across scales as long as the influence of the scale, e.g. mass transfer limitations, is taken into account. The intention of this work is also to investigate this hypothesis based on a combination of experiments at various scales in combination with modelling, e.g. computational fluid dynamics (CFD) simulation, to obtain more detailed process knowledge.

Specific objectives

The main objectives, which will be covered in this PhD project are:

- Propose general protocols for the evaluation of various standard separation options using microsystems in combination with biocatalytic processes. Focus both on traditional downstream and *in-situ* development applications.

- Provide standard automated microsystems with integrated on-line monitoring using standard analytical methods.
- Combine modelling tools with experimental investigations to improve the basis for obtaining process knowledge.
- Propose procedures for transferring knowledge obtained in microsystems across scales.
- Evaluate and validate the proposed procedures.
- Establish a microfluidic demonstration system where a reactor module is combined with separation modules.

Conclusion

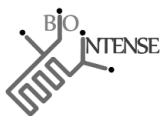
Currently, development and optimization of industrially relevant biocatalytic processes is quite time consuming, and in some cases the available quantities of substrates and/or catalyst are quite sparse and expensive. It is therefore evident to develop new technologies which can aid in accelerating the process development and at the same time ensure better use of available resources. The application of automated microsystems is in this context recognized as a potential technological solution to these requirements.

In order to exploit the full potential of automated microsystems it is required to successfully implement on-line analysis methods to ensure high throughput along with reduced experimental uncertainty. Another important factor for the success of such micro-scale technologies is successful demonstration that it is possible to transfer the obtained process knowledge in microsystems across scales.

The technology and procedures developed during this project will entirely be based upon ω -transaminase applications, but the intention is that the technologies, methods and procedures should be generally applicable.

Acknowledgements

This Ph.D.-project is financially supported by the European Union 7th Framework Program: BIOINTENSE (grant agreement n°. 312148).



References

1. S. Panke, M. Held, M. Wubbolts, *Current Opinion in Biotechnology* 15 (2004) 272-279.
2. U.S. Food and Drug Administration (FDA), *Development of new Stereoisomeric Drugs*,

<http://www.fda.gov/drugs/guidancecompliance/regulatoryinformation/guidances/ucm122883.htm>.

3. J.M. Woodley, *Synthetic Methods for Biologically Active Molecules*, Wiley-VCH (2013) 263-284. ISBN:978-3-527-33387-5
4. A. Schmid, J.S. Dordick, B. Hauer, A. Kiener, M. Wubbolts, B. Witholt, *Nature* 409 (2001) 258-268.
5. J.M. Woodley, *Trends in Biotechnology* 26 (2008) 321-327.
6. U.T. Bornscheuer, G.W. Huisman, R.J. Kazlauskas, S. Lutz, J.C. Moore, K. Robins, *Nature* 485 (2012) 185-194.
7. J.M. Woodley, *Current Opinion in Chemical Biology* 17 (2013) 310-316.
8. M. Höhne, U.T. Bornscheuer, *ChemCatChem* 1 (2009), 42-51.
9. P. Tufvesson, J. Lima-Ramos, J.S. Jensen, N. Al-Haque, W. Neto, J.M. Woodley, *Biotechnology and Bioengineering* 108 (2011) 1479-1493.
10. M.S. Malik, E.-S. Park, J.-S. Shin, *Applied Microbial Biotechnology* 94 (2012) 1163-1171.
11. S. Mathew, H. Yun, *ACS Catalysis* 17 (1999) 395-402
12. J.M. Woodley, M. Bisschops, A.J.J. Straathof, M. Ottens, *Journal of Chemical Technology and Biotechnology* 83 (2008) 121-123
13. P. Tufvesson, J. S. Jensen, W. Kroutil, J. M. Woodley, *Biotechnology and Bioengineering* 109 (2012) 2159-2162

List of publications

- A. Mitic, S. Heintz, R.H. Ringborg, V. Bodla, J.M. Woodley, K.V. Gernaey, *Chimica Oggi – Chemistry today* 31 (2013) 4-8
- B. U. Krühne, S. Heintz, R.H. Ringborg, I.P. Rosinha, P. Tufvesson, K.V. Gernaey, J.M. Woodley, *Green Processing and Synthesis* 1 (3) (2013) 23-31
- C. U. Krühne, H. Larsson, S. Heintz, R.H. Ringborg, I.P. Rosinha, V.K. Bodla, P. A. Santacoloma, P. Tufvesson, J.M. Woodley, K.V. Gernaey, *Chemical and Biochemical Engineering Quarterly* 2 (28) (2014) 203-214
- D. U. Krühne, S. Heintz, I.P. Rosinha, R.H. Ringborg, P. Tufvesson, K.V. Gernaey, J.M. Woodley, *Dansk kemi* 94 (11) (2013) 18-22
- E. A. Poulsen, S. Heintz, R.H. Ringborg, J.M. Woodley, K.V. Gernaey, U. Krühne, *Dansk kemi* 94 (10) (2013) 32-34



Hengeller Ludovica

Phone: +45256813

E-mail: luhe@kt.dtu.dk

Supervisors: Professor Ole Hassager
Associate Professor Anne Skov Ladegaard
Professor Kristoffer Almdal

PhD Study

Started: April 2013

To be completed: March 2016

Relaxation Mechanism Study of Polymer Blends by Rheological Experiments

Abstract

Industrial polymers are largely poly-disperse systems. One step towards understanding poly-disperse polymers is the characterization of bi-disperse blends. Even though linear viscoelastic properties of bi-disperse polystyrene blends have been investigated thoroughly both theoretically and experimentally in recent years [1], both nonlinear shear and extensional flow properties are lacking. In a recent study on solvent effects in mono-disperse concentrated polymer solutions, Huang et al. (2013) [2] introduced a hypothesis that there exists nematic interactions between solvent-polymer and polymer-polymer molecules. However, this hypothesis needs further testing and is still an open question. The purpose of the present study is to investigate the existence of nematic interactions, namely polymer-polymer, in strong elongational flow using a bi-disperse polystyrene blend of 95 K and 545 K Mw with 50% weight ratio. We present both shear and stress relaxation experiments to determine if orientation and extension of long PS chains induce orientation and extension in shorter chains (whose orientation should be unaffected by the flow).

Introduction

Liquid bridges arise in a variety of situations in nature. Yet our understanding of the dynamics and stability of liquid bridges is limited. We simply do not have sufficient generic knowledge about the process in which macromolecular fluid filaments are extended and stretched and how the extensional properties are related to the molecular constitution. That is, we have a lack of knowledge about extensional rheology.

The purpose of the present work is to make well-defined experiments to evaluate the influence on the rheological properties of bi-disperse entangled polymer melts due to the interaction between long and short polymer molecules.

Two nearly mono-disperse polystyrenes of molecular weight of 95 kg/mol and 545 kg/mol have been used to prepare a binary blend, with 50% weight of each component. The melt are measured in shear flow and extensional flow. In the latter and more interesting case the hypothesis is that the stretching of the long chains in fast extensional flows can induce the alignment of the short ones even if the extensional rate is not enough high to influence the orientation of the lower molecular weight chains.

Synthesis and Chromatography

The two polystyrenes PS-95k and PS-545k with narrow molecular weight distributions have been synthesized by

living anionic polymerization according to the standard procedure. Size exclusion chromatography (SEC) was employed for sample characterization.

Stabilized tetrahydrofuran (THF) was used as the eluent. Table 1 summarizes the weight-average molecular weight Mw and the glass transition temperature Tg of the synthesized polystyrenes.

Table 1: Molecular Weight and Glass Transition Temperature of the mono-disperse Polystyrenes.

Sample name	Mw[g/mol]	T _g [°C]
PS-545k	545000	106.5
PS-95k	95000	109

Preparation of Blend

Two polystyrene blends were made using PS-95k and PS-545k and were prepared by dissolving both the polystyrenes in THF (overlap concentration around 10~15mg/ml) and stirring at room temperature overnight. When the components were well dissolved and mixed, the THF solution was carefully put into methanol drop by drop and the blends were recovered by precipitation and filtration. Finally the blends were dried under vacuum at 70 °C for 2 weeks. The concentrations of all the polystyrene blends were determined by the peak areas of the bimodal curve in

SEC. For each sample, two randomly picked parts were checked in SEC in order to ensure the concentration is homogeneous throughout the sample. Table 2 summarizes the components and the weight fraction ϕ in % of the bi-disperse blends.

Table 2: Compositions of the polystyrene blend.

Sample name	95000 [g/mol]	545000 [g/mol]
Blend	50%	50%

Results: Linear Viscoelasticity

The linear viscoelastic properties of the polystyrene blend were obtained from small amplitude oscillatory shear flow measurements. An 8 mm plate-plate geometry was used on an ARES-G2 rheometer from TA Instruments. The measurements for the blend were performed at temperatures between 130 and 170 °C under nitrogen, afterwards the data were shifted to a single master curve at 130 °C using the time-temperature superposition procedure.

The shift factor a_T is reported in Table 3 for different temperatures.

Table 3: Temperature Shift Factor a_T for the blend.

Sample name	150 to 130 °C	170 to 130 °C
Blend 2	0.020124	0.001242

We analyze the LVE data by fitting the loss modulus G'' and the storage modulus G' vs. frequency to a Multimode Maxwell relaxation spectrum as illustrated in Fig. 1.

The relaxation behavior of the moduli in the high frequency region is essentially the same as the pure melts. That is in agreement with the theory since the Rouse time (which express the shortest mechanism of relaxation of a polymer chain) is an essentially constant material parameter that is unaffected by the distribution and the polydispersity of the polymer.

On the other hand, both the moduli show a dependence on the molecular weight distribution in the so called terminal region, at low frequencies.

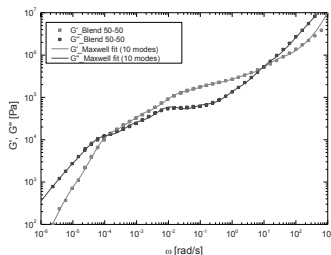


Figure 1: LVE data fitted with the Multimode Maxwell spectrum for the blend 50% PS-545k and 50% PS-95k at 130 °C.

Results: Stress Relaxation after Elongational flow

The experiments of stress relaxation were performed at 130 °C following start-up of uniaxial elongation. The flow was stopped at Hencky strain 3 for each stretch rate, and the stress was followed during the relaxation phase. Fig. 2

In the plot there is agreement between measurements and LVE predictions up to a certain level of strain.

We also analyzed the stress decay by fitting the data with a sum of exponentially decaying modes in order to understand if the short molecules in the strong elongational flows are induced to be aligned by the long ones.

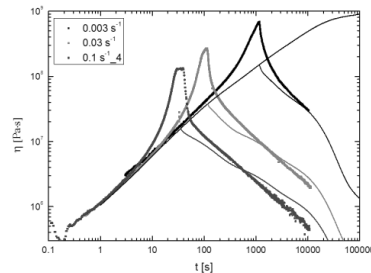


Figure 2: The measured corrected transient elongational viscosity, $\bar{\eta}^+(t)$ followed by the viscosity $\bar{\eta}^-(t)$ during the stress relaxation performed at Strain rates: 0.1, 0.03, 0.003 s⁻¹ at 130 °C. In all cases the flow is stopped at an extension of hencky strain 3 and allowed to relax for 3 h. The solid lines are the predictions from LVE of the transient elongational viscosity and the stress relaxation.

Conclusions

In summary, the molecular weight and polydispersity of linear polymers are strongly reflected in the linear viscoelastic response. It is clear that the low frequency response is sensitive to a small high molecular weight tail of the distribution due to the very strong molecular weight scaling of relaxation times.

The non-linear response and the analysis of the stress relaxation spectrum have shown that the nematic interactions between polymer-polymer are not present in the system analyzed.

Acknowledgements

I would like to express my sincere gratitude to my main supervisor Prof. Ole Hassager for his support and encouragement throughout this project. I am grateful to Dr. Qian Huang for her guidance.

References

1. J. K. Nielsen., H. K. Rasmussen, O. Hassager, and G. H. McKinley, *J. Rheol.* 2006, 50, 453–476.
2. Q. Huang, N. J. Alvarez, Y. Matsumiya, H. K. Rasmussen, H. Watanabe and O. Hassager *ACS Macro Lett.* 2013, 2, 741–744.



Christian Hoffmann

Phone: +45 4525 6195
E-mail: chhof@kt.dtu.dk

Supervisors: Anders Egede Daugaard
John Woodley
Manuel Pinelo

PhD Study
Started: August 2014
To be completed: July 2017

Modification of polymer surfaces to enhance enzyme activity and stability

Abstract

The immobilization of enzymes for biocatalytic reactions is an expanding area both in terms of research as well as industrial applications. The essential challenges are to develop catalytic systems with high temperature stability, tolerance to a larger pH range, improved long-term stability and higher activity. For this purpose, the understanding of the interfacial behavior between enzyme carrier surfaces and enzymes is extremely important. Therefore, this project deals with the modification of polymer surfaces to prepare platforms for immobilization of enzymes with increased enzymatic stability and improved activity.

Introduction

Enzyme catalyzed processes have been highly studied during the past few decades and are becoming more valuable due to several advantages over convenient metallic organic catalysis, such as mild reaction conditions, energy efficiency, environmentally friendliness and their substrate specificity and selectivity [1,2]. Nevertheless, one of the main challenges is the retention of enzymatic activity of immobilized enzymes. Immobilization is used to provide the necessary stability and tolerance to solvents and pH, however it generally results in a reduction in the activity of the enzyme. Several studies have been performed during recent years, focusing on recent developments and novelties of enzyme immobilization in general [2,3], the activity and selectivity of immobilized enzymes [4], the industrial potential of immobilized enzymes [5] and the interaction between enzyme and material surfaces [6].

Objectives

The overall goal of this project is the investigation of interfacial behavior between polymeric surfaces and enzymes in order to determine influencing parameters for the enzymatic activity and stability of immobilized enzymes. For this purpose, polymeric surfaces will be chemically modified, to prepare materials with specific surface properties, such as a given hydrophilicity or hydrophobicity as well as more advanced properties such as pH or temperature responsiveness. In a subsequent step, enzymes will be immobilized and an enzymatic reaction of the immobilized enzyme will

provide data, from which various impact factors for the stability and activity of the enzyme will be determined.

Enzyme Immobilization

Several different approaches to immobilize enzymes have been developed, which can be divided into a subset of methods. Cross-linking of enzymes is a method requiring no carrier (Figure 1, a), whereas the entrapment of enzymes into a carrier matrix and the binding on a carrier make use of a support material (Figure 1, b and c). For the latter, the immobilization through physical or chemical binding on a support material has gained high importance.

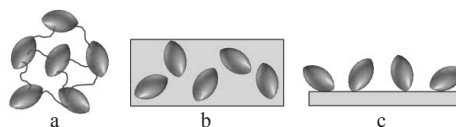


Figure 1: Examples of immobilization approaches: a) Cross-linking of enzymes without a carrier; b) entrapment of enzymes in a surface layer and c) direct bonding to a carrier through physical or chemical interaction.

Both methods offer advantages and disadvantages. Physically adsorbed enzymes show higher activity retention compared to chemically bound enzymes, but tend to be more prone to leach out from the support. Covalent bonds between the support and an immobilized enzyme generally lead to a strong binding and a reduced risk of enzyme leaching. However, due to

the fixed conformation of the enzyme, a loss of activity is often observed. In order to identify novel highly efficient immobilization strategies it is necessary to obtain a fundamental understanding of the individual properties of enzyme and support materials as well as the interfacial interaction between both.

Surface modification for enzyme immobilization

The surface properties of the support or carrier material can be controlled through introduction of new polymer layers on the surface. Such modifications are generally performed through either “grafting to” or “grafting from” reactions, resulting in the formation of polymer brushes with a specific distribution, density and chemistry [7]. Specifically, it has been found that hydrophobic surfaces and their interaction with enzymes reduce their activity, with lipases being the only exception, which seem to increase their activity when immobilized on hydrophobic surfaces [8,9].

Covalent Enzyme immobilization

The immobilization of biomolecules within this new surface layer of polymer brushes can be done by physical interaction or covalent bond formation. For the latter, functional groups from the polymers can be used directly (e.g. epoxide groups, Figure 2, a) or after modification, e.g. the activation of esters with glutaraldehyde or hydroxyl succinimide, maleimide or dithiol pyridyl groups (see Figure 2, b-e, R represents the support structure to react with different functionalities within the enzymatic structure).

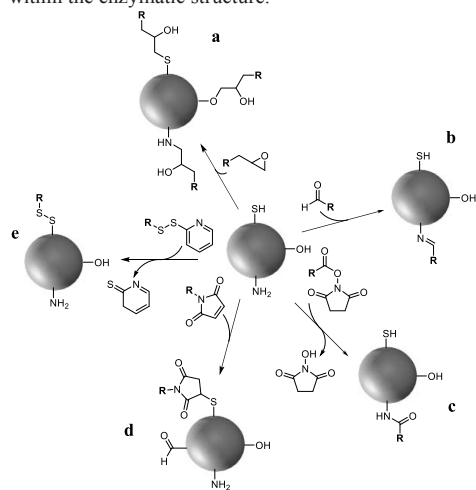


Figure 2: Covalent reactions of enzymes suitable for immobilization: a) epoxide groups, b) aldehyde groups (potentially from glutaraldehyde), c) with hydroxyl succinimide, d) with maleimide or e) dithiol pyridyl groups

These are usually residual amino or thiol groups originating from lysine or cysteine in the protein. Site

specific binding, such as affinity conjugation can be used for the immobilization of biomolecules in order to immobilize well defined and highly active enzymes. This includes methods such as interaction between polyhistidine (poly-his) and bivalent metal ions [10-14] and the interaction between avidin (or streptavidin) and biotin.

Conclusion

For development of novel immobilization strategies of enzymes on surfaces, it is crucial to obtain a broader knowledge of the interfacial interaction between surface and biomolecule. The aim of this project is the investigation of different polymer surface characteristics with regards to enzymatic stability and activity. Ultimately, these findings will be used to prepare a number of novel immobilized enzymes, which will be tested in enzymatic reactor systems.

Acknowledgements

The author wants to thank Aage Louis-Hansens Legat for Teknisk Forskning for financial support.

References

1. Bornscheuer, U. T.; Huisman, G. W.; Kazlauskas, R. J.; Lutz, S.; Moore, J. C.; Robins, K. *Nature* 2012, 485, 185.
2. Sheldon, R. A.; van Pelt, S. *Chem. Soc. Rev.* 2013, 42, 6223.
3. Cantone, S.; Ferrario, V.; Corici, L.; Ebert, C.; Fattor, D.; Spizzo, P.; Gardossi, L. *Chem. Soc. Rev.* 2013, 42, 6262.
4. Rodrigues, R. C.; Ortiz, C.; Berenguer-Murcia, Á.; Torres, R.; Fernández-Lafuente, R. *Chem. Soc. Rev.* 2013, 42, 6290.
5. DiCosimo, R.; McAuliffe, J.; Poulouse, A. J.; Bohlmann, G. *Chem. Soc. Rev.* 2013, 42, 6437.
6. Talbert, J. N.; Goddard, J. M. *Colloids Surf. B. Biointerfaces* 2012, 93, 8.
7. Jiang, H.; Xu, F.-J. *Chem. Soc. Rev.* 2013, 42, 3394.
8. Shah, S.; Solanki, K.; Gupta, M. N. *Chem. Cent. J.* 2007, 1, 30.
9. Petkar, M.; Lali, A.; Caimi, P.; Daminati, M. J. *Mol. Catal. B Enzym.* 2006, 39, 83.
10. Kim, Y.-R.; Paik, H.-J.; Ober, C. K.; Coates, G. W.; Batt, C. a. *Biomacromolecules* 2004, 5, 889.
11. Balland, V.; Hureau, C.; Cusano, A. M.; Liu, Y.; Tron, T.; Limoges, B. *Chemistry* 2008, 14, 7186.
12. Sosna, M.; Boer, H.; Bartlett, P. N. *Chemphyschem* 2013, 14, 2225.
13. Cullen, S. P.; Liu, X.; Mandel, I. C.; Himpfel, F. J.; Gopalan, P. *Langmuir* 2008, 24, 913.
14. Xu, F.; Geiger, J. H.; Baker, G. L.; Bruening, M. L. *Langmuir* 2011, 27, 3106.

**Joakim M. Johansen**

Phone: +45 4525 2830
E-mail: jjoha@kt.dtu.dk
Discipline: Reaction and transport engineering

Supervisors: Peter Glarborg, professor
Peter A. Jensen, associate professor

PhD Study
Started: September 2011
To be completed: February 2015

Biomass Burners for Biodust Combustion

Abstract

In the strive for at CO₂-neutral energy profile the exploitation of biomass in central and decentral heat and power plants has continuously increased in recent decades. This PhD-project aims to establish a scientific basis for the development of a new generation of biodust burners for utility boilers. The project focuses on particle ignition and flame stabilization through parametric studies both in full-scale measurements and from a CFD (Computational Fluid Dynamics) point of view. This article will introduce the reader to work flow established to fulfill this goal.

Introduction

In recent decades, central power and heat production through thermal conversion of biomass has gained ground concurrently with the political agenda both on a national and an international level. The development of high efficiency biomass plants are required in order to balance the fluctuating power production from wind mills and other alternative energy sources, while still striving towards a CO₂-neutral energy profile. In addition, thermal plants are a necessary need in the provision of district heating.

Development and implementation of high efficiency biomass combustion technology is arguably the best near-term solution to provide stable and CO₂-neutral centralized power and district heating to larger cities and industrial areas.

Biomass differs from conventional solid fossil fuels (traditionally coal) in a number of essential area including both chemical composition and physical structure and appearance. Thus, direct utilization of existing high efficiency pulverized power or combined heat and power facilities is not an option when considering biodust as an energy source.

The fibrous nature of the biomass complicates particle pretreatment implying larger and oddly shaped fuel particles; changing the aerodynamics and particle size distributions. In addition, the larger fraction of volatile matter changes the conditions at which a stable flame is achieved. A turbulent development of the technology aiming to convert existing high efficiency burner installations has been conducted in Denmark throughout the past couple of decades. However, technical difficulties lower the efficiency and limit the

operation flexibility both with regards to biomass type and quantity.

Objectives

This work aims to establish a scientific basis for the development of a new generation of biomass burners designed to facilitate simultaneous high power efficiency and fuel flexibility combined with good particle burn-out and stable flame capabilities of dedicated biodust fueled plants. The project will link fuel properties to flame properties, considering both fluid dynamic effects due to the differences in particle characters and chemical effects due to changes in the chemical composition and kinetics.

Content

The project will include full scale combustion measurements from relevant plants operated by the industrial partners: Dong Energy Power and Vattenfall. This will include advanced in-situ high speed thermal imaging, optical and extractive probe measurements of the flame, ear burner area, and fuel conveying system. Close coordination with other work-packages will ensure thorough fuel characterization of a range of different biomass fuels. Flame detection by state of the art diagnostic techniques will be evaluated for optimized operational control.

Fundamental research will be conducted in lab and pilot-scale forming the basis for the modeling work applicable to computational fluid dynamics calculations taking both chemical kinetics and aerodynamic differences between fossil fuels and biodust into account, for the development of novel burner designs.

Devolatilization Kinetics at High Heating Rates

Devolatilization experiments at high heating rates aim to mimic the conditions seen by particles entraining e.g. a pulverized fuel flame. This is typically described by heating rates in the order of 10^5 - 10^6 K/s which can be achieved in entrained flow reactors. Figure 1 shows the conversion degree as function of residence time when rapidly heating a woody and an energy crop at high heating rates and reducing conditions.

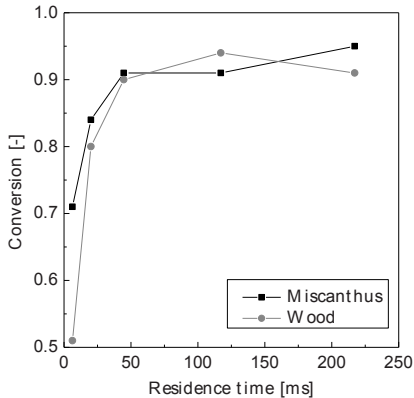


Figure 1: Devolatilization progression as function of residence time for two different fuels heated in a laminar entrained flow reactor in reducing conditions.

From such data the devolatilization kinetics can be extracted and used in CFD modeling.

Evaluation of the kinetic data

Kinetic data is evaluated in pilot scale facilities employing a 15 kW drop tube furnace allowing for in-situ temperature and gas concentration measurements as well as particle extraction. The validity of the determined devolatilization kinetics may then be evaluated by comparing the observed flame characteristics with corresponding CFD simulations.

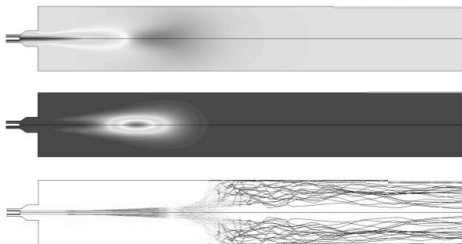


Figure 2: CFD calculations of (top) temperature, (middle) CO mass fraction, and (bottom) particle trajectories and mass loss of wood particles burning in a 15 kW entrained flow reactor.

Extrapolating Numerical Models

Because the issue of scaling is a broadly accepted phenomenon, creating guidelines for novel technology development based on either numerical simulations or experimental studies the final result will benefit from the study being carried out at the scale intended.

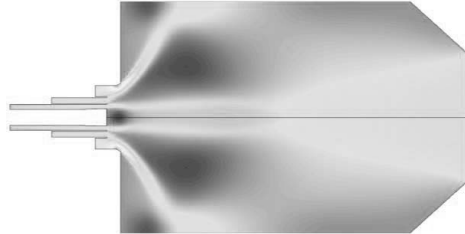


Figure 3: Axial velocity predictions of 2D-axisymmetric full-scale burner modeling firing 30MW of wood dust.

Figure 3 shows a velocity prediction of a scaled up numerical simulation of a full-size biodust burner. These models, with sub-routines developed on the basis of the lab-scale data, can be used to simulate a broad range of scenarios of operating conditions leading to the development of guidelines for burner construction.

Full-Scale Measurements

Because scaling issues are not specific to experimental setups but also applies to numerical simulations. The full-scale CFD models are validated against in-situ power plant measurements, e.g. temperature profiles as presented in Figure 4.

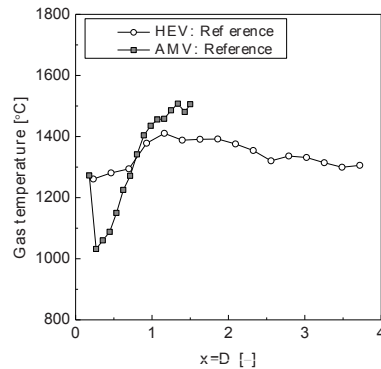


Figure 4: Gas phase temperature profiles along the flame center axis for HEV: Herningværket and AMV: Amagerværket.

Acknowledgements

This PhD project is part of the GREEN Research Center (Center for Power Generation from Renewable Energy) financed by the Danish Strategic Research Council.

**Sawitree Kalakul**

Phone: +45 52799890
E-mail: sawit@kt.dtu.dk

Supervisors: Rafiqul Gani
Georgios Kontogeorgis
Sponsors QNRF-Qatar, Alfa Laval Copenhagen,

PhD Study
Started: 1 June 2013
To be completed: 30 May 2016

VPPD Lab – A Computer Aided Tool for Product-Process Design

Abstract

In chemical product design, it is not only important to find the chemical product that exhibits certain desirable properties but increasing the product performance and making products more versatile have become growing concerns in recent times. Rather than design chemicals based products through an experimental-based trial and error approach, the model-based approach can speed-up the design and reduce some experiments. In order to solve a large range of chemical product design problems, this work present a systematic framework for product design and the implementation in a new computer aided tool, VPPD Lab (The Virtual Product-Process Design Laboratory). The application of the systematic computer-aided framework is highlighted through a case study of a tailor-made blend design of jet-fuels.

Introduction

Chemical product design involves the design of the candidate chemicals that exhibit a certain desirable or targeted properties (functions) then try to find the process that can manufacture them with the specified qualities [1]. In general, the design of chemical product relies on experiment-based trial and error approach. Since, chemical industries is moving beyond the production of commodity chemicals towards higher value added chemicals, model-based computer-aided tools have been used to replace some experimental steps to reduce design cost and reach the market earlier. Various model-based methodologies have been developed [2, 3]. Such approaches require predictive mathematical models that adequately describe the relationship between the product performances, data acquisition, data testing, model development and model-based design method development, etc., that needs to be integrated in a computer-aided framework so that chemicals based products can be design, analyzed and verified in a fast, efficient and systematic manner. In order to address these issues, this work presents the development of a systematic model-based framework for product design and implementation in the product design software called VPPD-Lab. The systematic framework for product design employs its in-house knowledge-based system to (1) identify target properties of a desired product; (2) provide suitable property

models to calculate the necessary properties classified as primary, secondary, functional, and mixture properties; (3) formulate and solve the design-analysis problems in a fast, robust and systematic manner; and (4) guide the user to the final experimental verification tasks.

Objectives of the project

- (i) Develop systematic framework for chemical product design and implement the framework in VPPD-Lab
- (ii) Apply the software for the design of various types of products.

Framework of VPPD-Lab

The framework and its implementation as VPPD-lab are based on a generic workflow (as shown in Fig. 1) that allows different problem specific design templates to be used for different product design scenarios such as blends, and formulations. 6 Tasks are highlighted through the case study of blend design of jet-fuels.

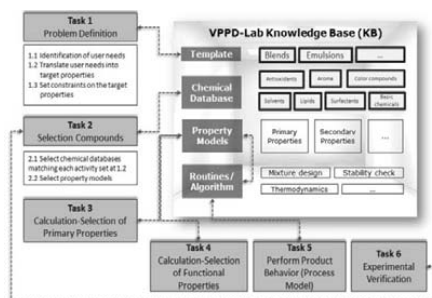


Figure 1: Systematic framework for product design in VPPD Lab

Case Study: Blend design of jet-fuels

Task 1: Problem definition

The sets of product needs for jet-fuels are retrieved from the knowledge-base. Table 1 lists the sets of product needs for jet-fuels respectively. The knowledge base translates needs into target properties and also helps to define the property target values.

Table 1: Product needs and translated target properties

Need	Target Property	Target Value
Ability to be burned	Reid vapor pressure (RVP)	$RVP > 1$ kPa at 310.95 K
Engine efficiency	Higher heating value (HHV)	$HHV > 6125$ kJ/mol
Consistency of fuel flow	Dynamic viscosity (η)	$\eta < 6.8$ cP at 253.15 K
	Melting point (T_m)	$775 < \rho < 840$ kg/m ³ at 288.15
Flammability	Flash point (T_f)	$T_f > 310.95$ K
Stability	Gibbs energy of mixing (ΔG^{mix})	$\Delta G^{mix} < 0$
Environmental impacts	Toxicity (LC_{50})	$-\log LC_{50} (mol/L)$
	Carbon footprint (CF)	$CF < 3.6$ < 1.8 CO ₂ eq.

Task 2: Selection of compounds

Conventional jet-fuels (Jet-A1) is the main ingredient and 221 chemicals from different groups are additive to be mixed with the conventional jet-fuels.

Task 3: Calculation-selection of primary properties

Molecular weight (M_w), critical temperature (T_c), critical pressure (P_c), acentric factor (ω), constant of the Modified Rackett equation (Z_{RA}), LC_{50} , heat of combustion (ΔH_c), RON , and Wt_{O_2} which are primary properties related to the calculation of target properties are retrieved from the chemical databases in the knowledge base to be used for calculations in task 4 and task 5.

Task 4: Calculation-selection of functional properties

ρ , Dynamic viscosity (μ), and vapor pressure (P_{vap}) are calculated.

Task 5: Perform product behavior

The tailor-made blend design problems of jet fuels are formulated as MINLP problem. The objective is to minimize fuel consumption subject to product stability and target properties. The results are the formulation of blended jet-fuels and calculated target properties as shown in Figure 2.

Chemicals	Composition, vol (%)
n-dodecane	20.4
n-tetradecane	13.6
isooctane	6.8
Methylcyclohexane	13.6
tetralin	3.4
p-Xylene	10.2
Decane	0.32

HHV	Tm	Properties					
		ρ	η	log(LCS ₀)	RVP	If	CF
6395.4	210.7	0.775	2.0	2.9	1.87	325.5	1.49
6128.2	224.5	0.802	2.1	4.0	1.48	326.8	1.57
6127.7	224.1	0.801	2.1	4.0	1.44	347.1	1.66

Figure 2: Results for jet-fuels blend problem from VPPD Lab

Task 6: Experimental verification

The final jet-fuels blends will be validated with experimental tests to issue η , T_m , T_f , ρ , LHV , RVP . Furthermore, distillation profiles and JFTOT ΔP at 260 °C will be tested in order to ensure that the final blends meet the aviation fuel standard.

Conclusions

A computer-aided framework for design of chemical products has been developed and implemented into the Virtual Process-Product Design Laboratory software. New templates that are employed through a generic workflow have been added to the software, making it more flexible and capable of solving a wide range of product design problems. The use of the framework has been highlighted through two representative case studies involving an emulsion-based detergent and a tailor-made gasoline and jet-fuels blends. VPPD Lab as the new product simulator that works in the same way as a typical process simulator, it can guide a user to design product, study product behaviors, systematically formulate and robustly solve various type product design problems. Future work is to integrate the software with the process design software in order to systematically solve product-process design problems.

References

1. R. Gani, "Chemical product design: challenges and opportunities," Computers and Chemical Engineering., no. 28, pp. 2441-2457, 2004.
2. E. Conte, and R. Gani, "Chemical-Based Formulation Design: Virtual Experimentations," Computer Aided Chemical Engineering, vol. 29, pp. 1588-1592, 2011.
3. N. A. Yunus, K. V. Gernaey, J. M. Woodley, and R. Gani, "A systematic methodology for design of tailor-made blended products," Computer and Chemical Engineering, vol. 66, pp. 201-213, 2014.



Andreas Kamp

Phone: +45 2133 05 17
E-mail: ankam@kt.dtu.dk

Supervisors: Hanne Østergård
Simon Bolwig

PhD Study
Started: August 2011
To be completed: April 2016

Sustainability Assessment of Integrated Food & Bioenergy Systems in Ghana

Abstract

Two Ghanaian food and bioenergy systems were assessed using the Emergy Analysis (EmA) methodology. The aim of the study was to evaluate whether an integrated system built around maize-beans cultivation and biogas from crop residues including nutrient recycling improves resource use efficiency compared to food and wood fuel production in parallel. This is not the case under the considered circumstances: Reduced dependence on material inputs (wood and synthetic fertiliser) was achieved but were cancelled out by increased labour inputs. Labour constitutes the single-largest input and thus, the result is sensitive to the way labour inputs are calculated. The study led to suggestions on improving the calculation approach for labour inputs in EmA.

Introduction

Ghana has a growing economy and energy demand usually increases with economic growth. New bioenergy technologies using hitherto unused biomass from agriculture and agro-industry provides Ghana with the opportunity to meet the growth in energy demand and increase energy security by being less dependent on imports. Basing energy production on biomass resources must however, take into consideration competing uses and availability of the feedstock, the requirement of inputs to biomass production and conversion including their origin, and the substitutability of bio-based energy carriers with the carriers they aim to substitute for.

In this project, systems analysis with a multi-disciplinary approach is undertaken to evaluate the environmental and socio-economic consequences of residue-based bioenergy production in Ghana. Two integrated food and bioenergy case systems are assessed with the aim of suggesting possible alternatives to the present reliance on imported fertiliser and energy for food processing. Additionally, the project identifies methodological aspects that supports the systems scope.

The cases are assessed in a systems perspective meaning that the system boundary encompasses biomass production as well as bioenergy production (Figs. 1 and 2). The reason for this is that optimisation of an integrated system may be hindered by attempting to optimise just a subsystem.

The project roadmap includes publication of methodological aspects concerning: co-production [1,2]

and labour [3,4], and empirical studies of: Ghanaian bioenergy potentials [5,6], production of food and cooking energy in a rural farming village [7], and biogas production from fruit residues for process energy [8].

Specific Objectives

In this text, the particular objective of how to account for labour inputs in environmental sustainability assessment using Emergy Analysis (EmA) is in focus. The study is based on a case example of a small-scale, semi-mechanised farming system coupled with household-scale biogas production for cooking, based on crop residues. The case results are also shown.

Materials and methods

EmA is an upstream method that assesses the accumulated, direct and indirect exergy use in provision of a product or service, converted to solar equivalent Joules (seJ). It includes work by natural and human systems alike. The Unit Emergy Value (UEV) indicates the efficiency of a process in converting (scattered) solar energy to (concentrated) available energy and is considered a measure of energy quality [9,10].

EmA is particularly useful in the study of co-production systems because of its intrinsic emphasis on systems perspective vis-a-vis product perspective. This is important in studies of bioenergy systems where outputs in one subsystem, farming, is considered 'waste' but are then considered valuable resources in another subsystem, bioenergy production.

The UEV for labour indicates the resource requirements of a specified unit of labour input and is thus used to assess the dependence of a given process on the labour market. Including labour inputs is argued to give a more accurate picture of the environmental effect of a given process. Labour is distinguished as being ‘direct labour’ – occurring in the foreground of the studied system or ‘indirect labour’ – representing labour that has taken place upstream in the value chain and accompanying products and services that are purchased.

The usual labour UEV calculation approach is to apply a national average, based on the total national energy budget of the relevant country divided with e.g. the amount of hours worked (for direct labour) or the sum of monetary value generated (the GDP) (for indirect labour) over the course of a time period, usually a year.

Results and Discussion

Two systems for provision of food and cooking energy

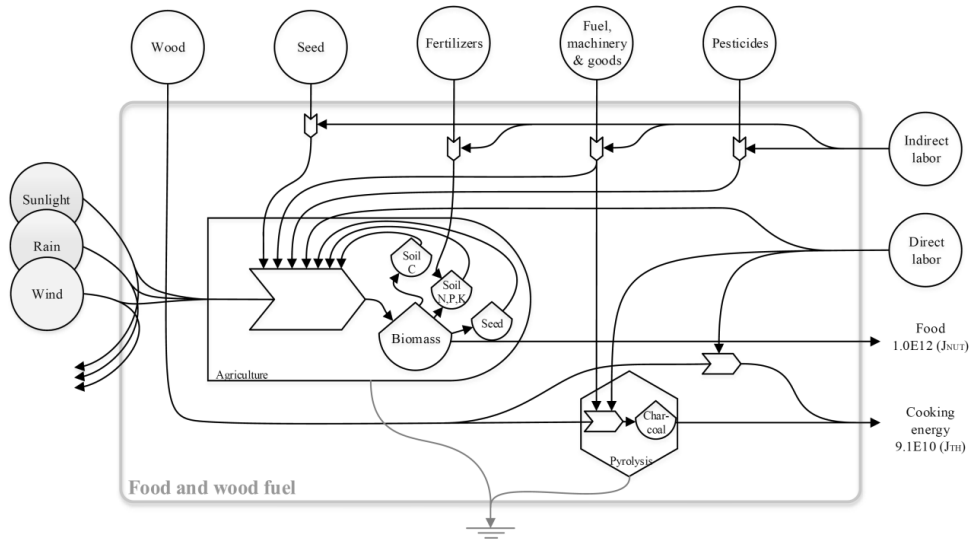


Figure 1: Present system: Food and wood fuel are produced separately contributing to net deforestation and resulting in dependence on synthetic fertiliser.

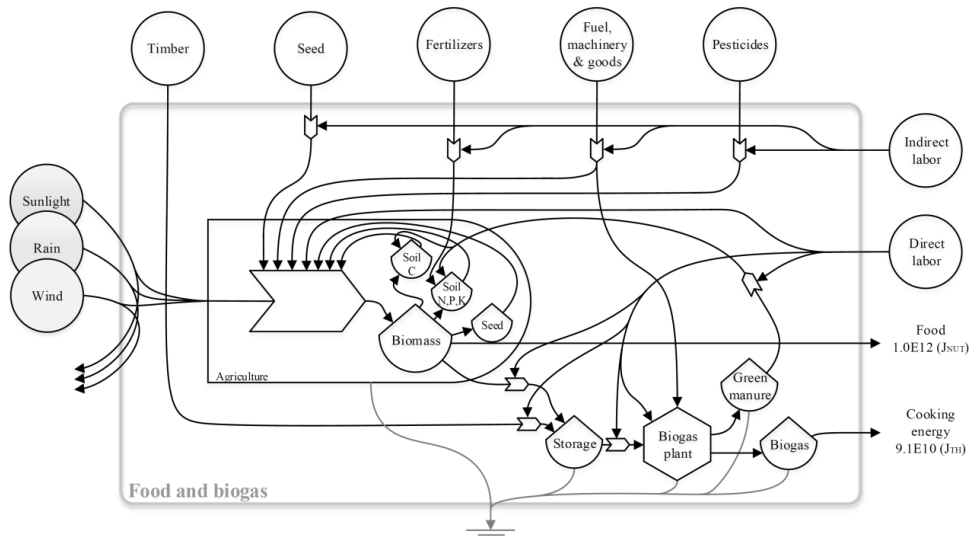


Figure 2: Modelled system: Food and bioenergy production are integrated by using crop residues for biogas and by returning the biogas effluent to fields.

were compared. At present (Fig. 1), food comes from a maize-beans farming system, synthetically fertilised, and cooking fuel from wood or charcoal, harvested beyond the natural replenishment rate. The suggested system (Fig. 2) couples the maize-beans farming system with biogas from crop residues and attempts to reduce the dependence on wood fuel by using biogas for cooking and on synthetic fertiliser by returning biogas effluent to the fields.

The case study results are summarised in Table 1. There are no significant resource use efficiency gains from integrated production ($4.9\text{E}+05$ seJ/J versus $5.1\text{E}+05$ seJ/J). The most significant inputs were direct and indirect labour, followed by rain. This led us to scrutinise the approach to calculation of the labour UEVs. The approach was refined by differentiating between different income groups, leading to direct labour UEVs for labourers considered poor, middle-income, or high-income, respectively. Since direct labour inputs in the studied system are mainly from poor labourers, this novel approach alters the results (Table 1, right). The indirect labour UEV was adjusted to reflect that most indirect labour takes place abroad.

Instead of using a national, indirect labour UEV, we used the global, indirect labour UEV. This resulted in reduced resource use associated also with indirect labour. This change in calculation approach leads to no significant change in the conclusion. It does suggest however, a tendency for favouring the integrated system as slightly less resource intensive.

The emery profiles of the two systems show the relative importance of various inputs (Fig. 3). The relative importance of labour diminishes when applying the differentiated labour UEV approach. This has the effect of increasing the relative importance of local, renewable flows.

Conclusions

Under the considered circumstances, integrated food and biogas production does not provide a significant reduction in resource use. Recycling of effluent has a minor effect on the dependence on synthetic fertiliser.

When the labour UEV was adjusted to more correctly reflect the type and origin of labour inputs, the comparison of the two systems is slightly more positive toward the integrated system.

Table 1: Summary table of two food and bioenergy systems, *Food and wood fuel* and *Food and biogas*. See text for system descriptions. The joint UEV calculated in the three bottom lines considers the totality of inputs in solar equivalent Joules (seJ) divided with the sum of outputs in Joules (J). Three UEVs are given, one excluding labour inputs, and two including labour inputs, but with different labour UEVs. alt. = alternative.

Item (unit)	Food & wood fuel Flow (unit/45 ha/year)	Food & biogas Flow (unit/45 ha/year)	UEV (seJ/unit)	Ref. for UEV	Food & wood fuel Empower (seJ/year)	Food & biogas Empower (seJ/year)
Local, renewable flow of rain (J)	$3.6\text{E}+12$	$3.6\text{E}+12$	$3.1\text{E}+04$	a	$1.1\text{E}+17$	$1.1\text{E}+17$
Soil loss (kg Corg)	$2.5\text{E}+04$	$2.2\text{E}+04$	$1.6\text{E}+12$	b	$4.0\text{E}+16$	$3.5\text{E}+16$
Mineral fertilizer (kg)	$3.2\text{E}+03$	$2.9\text{E}+03$	$3.3\text{E}+12$	c	$1.1\text{E}+16$	$9.8\text{E}+15$
Other (mix)	mix	mix	mix	various	$3.0\text{E}+16$	$1.6\text{E}+16$
Direct labor (man-hours)	$1.8\text{E}+04$	$2.1\text{E}+04$	$1.1\text{E}+13$	d	$2.1\text{E}+17$	$2.4\text{E}+17$
Indirect labor (USD)	$4.8\text{E}+03$	$5.5\text{E}+03$	$3.1\text{E}+13$	e	$1.5\text{E}+17$	$1.7\text{E}+17$
Total emery					$5.5\text{E}+17$	$5.8\text{E}+17$
UEV, joint, for basket of food and energy outputs (seJ/J)	$1.7\text{E}+05$	$1.5\text{E}+05$				
UEV, with labor (seJ/J)	$4.9\text{E}+05$	$5.1\text{E}+05$				
UEV, with alt. labor UEVs (seJ/J)	$2.3\text{E}+05$	$2.2\text{E}+05$				

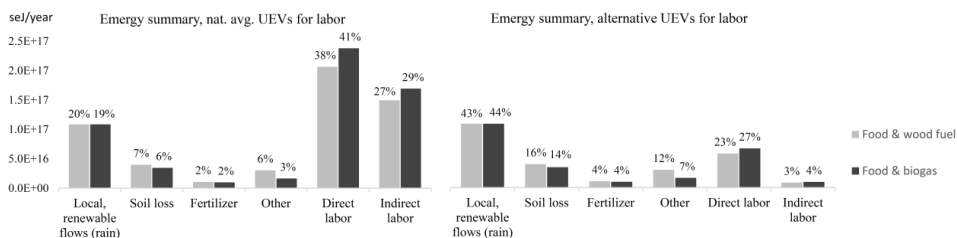


Figure 3: Emery profiles of two food and bioenergy systems. On the left, the comparison is based on the usual approach to calculating labour UEVs, using the national average. On the right, labour UEVs are calculated using the novel approach developed in this study. Regardless of calculation approach, reductions in material inputs that are made possible by integrating the production, comes at the expense of increased labour inputs.

Acknowledgements

The work is made possible through the support of 'Biofuel production from lignocellulosic materials – 2GBIONRG' DFC no. 10-018RISØ.

List of Publications

1. A. Kamp, H. Østergård. *Emergy Synthesis 7: Theory and Applications of the Emergy Methodology* (2012). University of Florida, Gainesville, USA, 2013, p. 503-511.
2. A. Kamp, H. Østergård, *Ecological Modelling* 253 (2013) 70-78.
3. A. Kamp, H. Østergård. *Emergy Synthesis 8: Theory and Applications of the Emergy Methodology* (2014). University of Florida, Gainesville, USA, in preparation.
4. A. Kamp, F. Morandi, C. Wright, H. Østergård, in preparation.
5. F. Kemausuor, A. Kamp, S.T. Thomsen, E.C. Bensah, H. Østergård, *Conservation and Recycling* 86 (2014) 28-37.
6. F. Kemausuor, E. Yakah, A. Kamp, in C. Roscoe (Ed.), *Ghana: Social, Economic and Political Issues*, Nova Science Publishers, Incorporated, 2014, p. 147-174.
7. A. Kamp, H. Østergård, S. Bolwig, in preparation.
8. A. Kamp, H. Østergård, in preparation.

References

9. H.T. Odum, *Environmental Accounting: Emergy and Environmental Decision Making*. John Wiley and Sons, New York, 1996.
10. R. Ridolfi, F.M. Pulselli, F. Morandi, S. Bastianoni, "Emergy", Reference Module in Earth Systems and Environmental Sciences, Elsevier, 2013.



Malgorzata Kostrzewska

Phone: +45 4525 6195
E-mail: malko@kt.dtu.dk

Supervisors: Anne Ladegaard Skov
Søren Hvilsted

PhD Study
Started: September 2013
To be completed: September 2016

Controlled Release from PMMA Microcapsules Triggered by Gamma Irradiation

Abstract

This study investigated the use of gamma irradiation as a triggering stimulus to activate poly(methyl methacrylate) PMMA microcapsules. PMMA and fluorinated derivatives were exposed to varying doses of irradiation and analyzed by DSC, SEC and NMR. The glass transition temperature (T_g) of polymers was found to decrease at low doses of irradiation. Therefore, irradiated PMMA microcapsules, which were previously impermeable, release encapsulated PDMS cross-linkers. This method enables the remotely controlled formation of silicone elastomers in traditionally unavailable places, and therefore has significant implications for industrial application.

Introduction

Microencapsulation attracts attention mainly due to a controlled release [1]. The technique allows for preparation of innovative materials, which appear more frequently in commercial products. For example, medicines with programmable release of active substances reduce harmful side effects and frequency of use. Moreover, controlling the chemical reaction is possible through encapsulation of compounds.

Polydimethylsiloxane (PDMS) networks usually forms at room temperature from a cross-linker and long-chain functional silicones. Encapsulation of the cross-linker within PMMA shell prevents the reaction occurring at temperatures lower than the T_g of PMMA. Heating of microcapsules above the T_g of PMMA leads to a melting of the shell and thus acts as a triggering stimulus. Additionally, the T_g may be adjusted upon other external stimulus in order to increase the response of the system.

In this study, gamma irradiation was investigated as a triggering stimulus. PMMA generally undergoes chain degradation at low doses of irradiation, however cross-linking takes place at higher doses [2]. This results in decrease or increase of T_g , respectively. Furthermore, glass transition temperature of short chain polymers is known to strongly depend on their molecular weight [3]. Hence, PMMAs with low M_w were examined. Additionally, chemical modification of PMMA through introduction of fluorine atoms was tested with the aim of promoting chain scission.

Specific objectives

The aim of this work is to design a method that enables the controlled formation of PDMS networks. It can be done through encapsulation of PDMS cross-linker. Microcapsules should be stable at 50°C and release encapsulated cross-linker in a controlled manner. The release should occur in response to an external stimulus, which can be remotely applied. This approach allows for application of silicone elastomers in traditionally unreachable places.

Results and discussion

Irradiation of PMMA and fluorinated derivatives

Two groups of polymers were examined: non-fluorinated (PMMA_1 and PMMA_2) and fluorinated (3F-PMMA_3 and 3F-PMMA_4). Polymers with two chains lengths represented each group and all samples were exposed to different irradiation doses.

Table 1 presents T_g and molecular weights of studied polymers. Apart from sample 3F-PMMA_4, all polymers had lower glass transition temperatures after irradiation due to chain scission. The scission is a two-stage process initiated at unsaturated chain ends, and followed by random scissions of the backbone [4]. Therefore, in the first stadium molecular weight does not change significantly, since the cleavage of pendant and end groups takes place. It is the scission of the main backbone, which causes observable changes in the chain length. As molecular weight of irradiated samples did not change significantly, it was assumed that mainly end-chain degradation took place. In addition, from an analysis of ^1H NMR data of irradiated samples, it was concluded that no new bonds formed. This confirmed

our assumptions, that slight change in chain length was sufficient to influence polymer properties.

On the other hand, at the highest doses of irradiation T_g started to increase due to cross-linking. When the concentration of degradation products increases, the possibility that macro-radicals recombine with each other increases as well. As a result, the glass transition temperature increased.

The presence of fluorine atoms in polymer structure enhances chain scission during irradiation. The lowest T_g for short chain sample 3F-PMMA_3 was observed at a dose of 10 kGy. It indicates that chain scission dominated over cross-linking even at higher doses, thus the glass transition temperature kept decreasing with the irradiation dose; however, sample 3F-PMMA_4 behaved similar to non-fluorinated polymers. It follows that the effect of fluorination was stronger for polymers with short chains.

Activation of PMMA microcapsules

Microcapsules with PMMA_1 shell were exposed to 1.6 kGy dose and their reactivity with vinyl-terminated DMS-V35 was examined by a controlled strain rheometer. Dynamic moduli of the mixture were measured at different temperatures and results are presented in Figure 1. Non-irradiated microcapsules reacted with DMS-V35 at 100°C, as the significant increase in storage modulus was observed. PMMA passes through phase change transition at 95°C and microcapsules become permeable. Below 100°C, microcapsules were relatively stable, since only minor changes in G' were observed. These small changes could be attributed to the presence of cross-linker on the surface of the shell. Although G' also increased below T_g of PMMA, it is evident that the cross-linking reaction took place mainly at 100°C. On the other hand, the dramatic increase in G' was observed at 30°C for irradiated microcapsules, despite the fact T_g of irradiated PMMA was around 80°C. It means that not only T_g of polymer changes during irradiation, but the local heating effects can affect the local structure of PMMA shell.

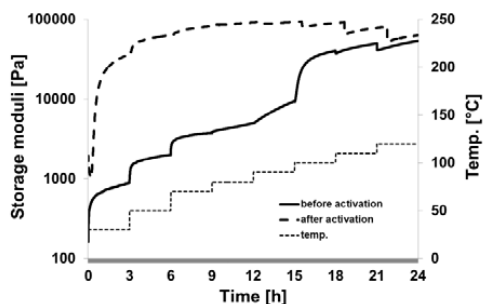


Figure 1: The reactivity of PMMA microcapsules with DMS-V35 before and after irradiation. The mass ratio between compounds was 1:10, respectively.

Conclusions

Gamma irradiation has been identified as a suitable triggering stimulus for PMMA microcapsules. Due to chain scission appearing in PMMA structure at low doses of irradiation, T_g of polymeric shell is decreased. Activated microcapsules become therefore impermeable at lower temperatures and release encapsulated cross-linker allowing for the cross-linking reaction to occur.

Acknowledgments

This project is financially supported from the Mærsk Oil & Gas Research, Qatar. I would also like to thank Arne Miller from Center for Nuclear Technologies in Risø for helping with irradiation experiments.

References

1. A. Abbaspourrad, S. S. Datta, D. A. Weitz, Langmuir, 2013, 29, 12697-12702
2. I. Y. Al-Qaradawi, D. A. Abdulmalik, N. K. Madi, M. Almaadeed, Phys. Stat. Sol., 2007, 4, 3727 – 3730
3. X. Lu, B. Jiang, Polymer, 1991 32, 471-478
4. M. A. Rauf, I. C. McNeill, Polym. Degrad. Stabil., 1993, 40, 263-266

Table 1: Glass transition temperature and M_w of non-irradiated and irradiated PMMA.

Irradiation dose [kGy]	PMMA_1			PMMA_2			3F-PMMA_3			3F-PMMA_4		
	T_g [°C]	M_w [g/mol]	PDI									
0	95	15000		58			62			71		
0.3	92	14500		53			-			-		
0.5	90	15000	2.3	54	2000*	1.6	-	1000*	2.5	-	22000*	2.1
0.8	86	15000		47			62			63		
1.6	83	13500		46			49			74		
10	89	13500		53			47			74		

*SEC calibration was made for standard PMMA molecular weights. However, calibration curves do not apply for sample PMMA_2 and fluorinated polymers.



Hilde Larsson

Phone: + 45 4525 2993
E-mail: hila@kt.dtu.dk

Supervisors: Ulrich Krühne
Krist Gernaey
Anne Ladegaard Skov

PhD Study
Started: December 2012
To be completed: November 2015

Modeling Mass Transfer in Small Scale Reactors using Computational Fluid Dynamics

Abstract

The aim of this PhD project is to use computational fluid dynamics (CFD) to increase the understanding of mass transfer processes in small scale chemical and biochemical reactors. The case study presented here describes the CFD modeling of oxygen transfer and mixing times in a 1 ml microbioreactor, and the simulated data is compared to experimental results.

Introduction

The most common way to describe oxygen transfer in bioreactors is via the oxygen transfer coefficient, $k_L a$, which describes the dynamic relationship between the oxygen concentration (C) and the oxygen saturation concentration (C_{sat}) assuming a perfectly mixed liquid according to the following:

$$\frac{dC}{dt} = k_L a (C_{sat} - C) \quad [1]$$

In CFD simulations ' $k_L a$ ' is often separated into the mass transfer coefficient ' k_L ' and the specific interfacial area ' a '. A common way to evaluate k_L is then using the correlation

$$k_L \propto \sqrt{\frac{D_L}{\nu}} (\varepsilon \nu)^{0.25} \quad [2]$$

which relates it to the diffusion coefficient (D_L) of oxygen, the kinematic viscosity (ν) and the energy dissipation rate (ε) in the fluid, which can be modeled using specific turbulence models.

For simulating mixing processes transient simulations are often performed where the spread of a scalar quantity φ in a velocity field \mathbf{U} is modeled according to

$$\frac{\partial(\rho\varphi)}{\partial t} + \nabla \cdot (\rho \mathbf{U} \varphi) = \nabla \cdot \left(\left(\rho D_\varphi + \frac{\mu_t}{Sc_t} \right) \nabla \varphi \right) \quad [3]$$

where ρ is the fluids density, D_φ the scalar kinematic diffusivity, Sc_t the turbulent Schmidt number, and μ_t the eddy viscosity which is a function of the amount of turbulence.

Specific objectives

The specific objective of this PhD project is to explore mass transfer phenomena in small scale reactor systems using CFD. The case study presented here describes the simulation of oxygen transfer and mixing in a 1 ml microbioreactor developed for fermentation purposes previously presented at [1].

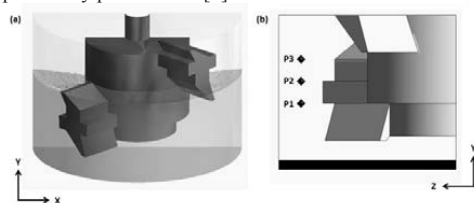


Figure 1. (a) Half of the microbioreactor studied (b) The geometry used for the simulations with the initial distribution of scalar (black) and the position of the monitoring points (P₁-P₃).

Method

The CFD software ANSYS CFX 15.0 was used to simulate the water phase of the microbioreactor shown in Figure 1 using the k- ε turbulence model. The velocity fields and turbulence scalars were calculated in steady state for five different rotational speeds, here given at rotations per minute (rpm).

In the mixing simulations were a scalar placed in the bottom of the reactors and its quantities in the monitoring points P1, P2 and P3 were recorded over time. Mixing time was defined as when the scalar had reached within $\pm 5, 10$ or 15% of its final value in these points. The position of the monitoring points as well as the initial distribution of the scalar can be seen in Figure 1b.

Mixing experiments were performed both using the original distributions of the eddy viscosity μ_t and with manipulated homogenous values, where the eddy viscosities were replaced with the averaged values from either the 200 or 1000 rpm simulations.

Results and Discussion

The experimental $k_{1,a}$ values are plotted with the simulated energy dissipation rates in Figure 2. They correlate very well, but it must be noted that they do not share the same y-axis, that the interfacial area is assumed to be constant and that the method is very dependent on the chosen turbulence model.

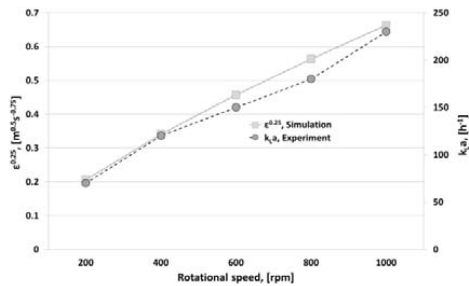


Figure 2. The experimental $k_{1,a}$ values from [1] correlated to the fourth root of the average energy dissipation rates in the liquid.

The mixing times are shown in Figure 3 and it can be seen that the experiments and simulations correlate, but also that especially the mixing time definition has a large effect on the simulation result.

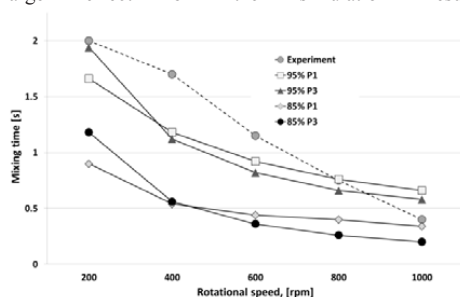


Figure 3. The experimental mixing times from [1] correlated to the simulated once for monitoring point 1 and 3 for $\pm 5\%$ and $\pm 15\%$.

Figure 4 shows the distribution of μ_t in the 200 and 1000 rpm simulations as well as their averaged values.

It can be seen that the average for 1000 rpm is considerably higher than for 200 rpm and that it also has a larger variance. Figure 5 presents the impact of the different distributions of μ_t on the mixing times.

As Figure 5 reveals, changing the eddy viscosity for the 200 rpm solution had as expected the largest effect once it was replaced with the 1000 rpm averaged value. The effects were less evident for 1000 rpm, which can be explained with the higher impact of advection at higher rotational speeds.

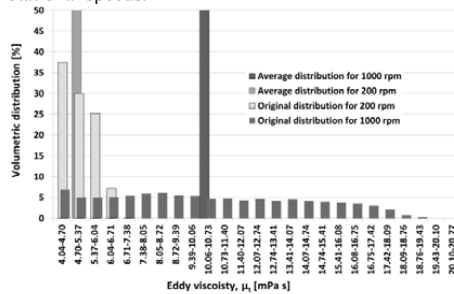


Figure 4. The distributions of eddy viscosities in the 200 and 1000 rpm simulations cases and their averaged values.

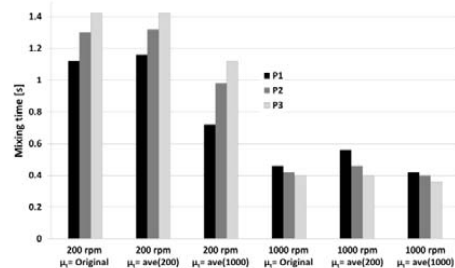


Figure 5. The mixing times for $\pm 10\%$ in all monitoring points with and without manipulated values for μ_t .

Conclusions

Oxygen transfer and mixing can be simulated using CFD, but both models are highly dependent on the turbulence model used. Mixing simulations are however preferred for quantifying bioreactor performance, since the theory and assumptions behind Eq. 3 is more well established and those for Eq. 2. Eq. 3 is also taking advection into consideration and has got the adjustable constant Sc_i in it.

Acknowledgements

This PhD project is funded by Novo Nordisk Foundation

References

- Bolić, A., Krühne, U., Prior, R. A., Vilby, T., Hugelier, S., Lantz, A. E., Gernacy, K. V., 2012. One-Millilitre Microbioreactor with Impeller for Improved Mixing, Poster presented at IMRET12.



Duy Michael Le

Phone: +45 4525 2979
 E-mail: dumi@kt.dtu.dk
 Discipline: Enzyme Technology

Supervisors: Anne S. Meyer
 Hanne R. Sørensen, DONG Energy
 Niels O. Knudsen, DONG Energy

Industrial PhD Study

Started: December 2012
 To be completed: December 2015

Biorefining of Wheat Straw: Distribution of mineral element deposits in pretreated biomass

Abstract

Mineral elements present in lignocellulosic biomass feedstocks may accumulate in biorefinery process streams and cause technological problems. Si is of particular interest due to its high abundance in lignocellulosic plant biomass. A better understanding of the distribution of mineral elements in biomass in response to pretreatment parameters is therefore important in relation to development of new biorefinery processes. This study showed that for some mineral elements, the amount ending up in the solid fraction could be controlled by varying pretreatment parameters. Other mineral elements, such as Si, are an integral part of the biomass, which will always remain in the solid insoluble fraction.

Introduction

In second generation bioethanol production, lignocellulosic agricultural waste streams are utilized as carbohydrate feed stocks instead of sucrose and starch, hence the ethical issues of turning food into fuel is avoided. A generalized linear process for producing second generation bioethanol involves pretreatment for opening up the biomass structure, enzymatic hydrolysis of the cellulose and hemicellulose to glucose and xylose, and fermentation of glucose and xylose into ethanol [1]. However, increasing interest has been on expanding the concept from production of bioethanol to biorefineries, where the co-processing streams are used for production of various chemicals, building blocks, or functional products and/or other energy carriers [2]. Biomasses containing high amounts of mineral elements (especially Si) are being increasingly used in the field of biorefinery, where agricultural waste products, such as wheat straw, corn stover and rice straw, are converted into valuable products [3]. Mineral elements therefore end up contaminating solid and liquid products, and it is important to learn how varying parameters in biorefineries affect distribution of mineral elements in the liquid and solid product.

Specific objectives

The objective of the current study was to examine mineral elements deposits in pretreated wheat straw and how they behave in response to a systematic pretreatment campaign.

Results and discussion

Wheat straw was hydrothermally pretreated at 1 kg-scale on the Mini-IBUS located at Risø campus. pH, temperature and holding time were varied to produce the samples presented in Figure 1.

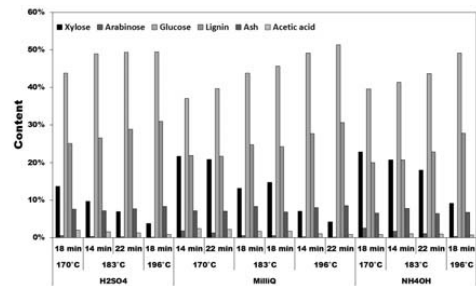


Figure 1: Composition of wheat straw solid fraction after pretreatment on Mini-IBUS (Risø campus)

The mineral composition in the solid fraction of the biomass after hydrothermal pretreatment was modelled using an empirical factor, denoted c_{pH} , in an extended severity equation, Eq. 1. c_{pH} was optimised in the interval 0 to 1 for obtaining the best linear or exponential fit to the data.

$$\log(R_p) = \text{Log} \left(t \cdot e^{\frac{T-200}{24.78}} \right) - c_{pH} \cdot \text{pH}_{\text{initial}} \quad (1)$$

where R_p is the pretreatment severity, t is the holding time in minutes, T is the temperature in K, and $\text{pH}_{\text{initial}}$ is the initial presoaking pH.

The contents of some mineral elements in the solid fraction followed this relation with the empirical factor c_{pH} describing the pH sensitivity of the given mineral elements (Figure 2). In all these cases, increasing pretreatment severity (higher temperature, longer holding times, and higher pH) resulted in less mineral elements in the solid product. Others (Si, Al, Fe, Cu) did not show any dependency with the pretreatment parameters and therefore did not follow Eq. 1.

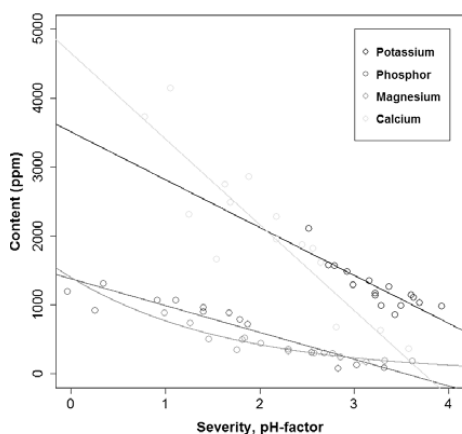


Figure 2: Content of some mineral elements vs. pretreatment severity calculated by the extended severity equation.

Of the mineral elements not depending on pretreatment parameters, Si is of particular interest, since it is present in high concentrations in many biomasses, where it is deposited either as SiO_2 incrustations of cell walls, as infillings of the interior of cells, or in intercellular spaces [4]. In wheat straw, Si deposits are located all over the straw, but are especially present in high concentrations in the outer cell layers of the straw (Figure 3). These deposits alleviate plants from abiotic (e.g. heavy metal toxicity and salinity) and biotic (e.g. fungi and insects) stresses [5]. Silica acts as a physical barrier protecting the plant from enzymatic degradation during fungal attacks. It is therefore an integral part of the biomass that cannot readily be separated from it.

Conclusions

The pretreatment conditions, especially pH, significantly influenced the levels of P, Mg, K, Mn, Zn, and Ca in the resulting solid fractions. A new expanded severity equation was proposed to model and predict mineral composition in pretreated wheat straw biomass. The level of Si in the solid fraction did however not

depend on pretreatment conditions. This is because it is a highly abundant, integral part of the biomass and very insoluble in water.

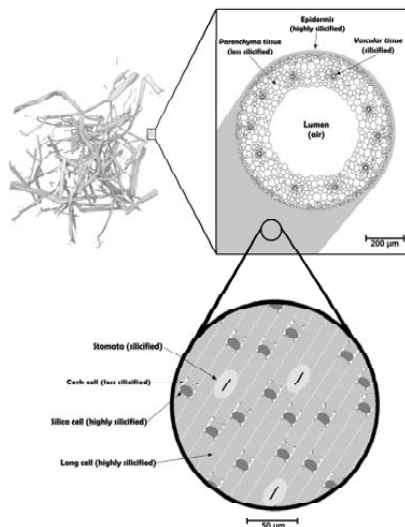


Figure 3: Structure of wheat straw and location of silica deposition are based on microscopy images from literature [6,7,8].

References

1. M.M. Demeke, H. Dietz, Y. Li, M.R. Foulquié-Moreno, S. Muttur, S. Deprez, T. Den Abt, B.M. Bonini, G. Liden, F. Dumortier, A. Verplaetse, E. Boles, J.M. Thevelein, *Biotechnol Biofuels* 6 (2013) 89.
2. J. Larsen, M.Ø. Haven, L. Thirup, *Biomass Bioenergy* 46 (2012) 36-45.
3. A.G. Vishtal, A. Kraslawski, *BioResources* 6 (2011) 3547-3568.
4. D.R. Piperno, *Phytolith analysis: an archaeological and geological perspective*, Academic Press, San Diego, 1988.
5. J.F. Ma, *Soil Sci Plant Nutr* 50 (2004) 11-18.
6. P.T. Atkey, D.A. Wood, *J Appl Microbiol* 55 (1983) 293-304.
7. R. Liu, H. Yu, Y. Huang, *Cellulose* 12 (2005) 25-34.
8. H. Chen, F. Wang, C. Zhang, Y. Shi, G. Jin, S. Yuan, *J Non-Cryst Solids* 356 (2010) 2781-2785.

List of Publications

1. D.M. Le, H.R. Sørensen, N.O. Knudsen, J.K. Schjoerring, A.S. Meyer, *Biotech biofuels* 7 (2014) 141.
2. D.M. Le, H.R. Sørensen, N.O. Knudsen, A.S. Meyer *Biofuels*, *Bioprod. Biorefin.* 2014 DOI: 10.1002/bbb.1511 (in press)



Kasper Linde

Phone: +45 2249 6663
E-mail: kaspli@kt.dtu.dk
Discipline: Catalysis and Reaction Engineering

Supervisors: Anker D. Jensen
Brian B. Hansen
Peter A. Jensen
Pär L.T. Gabrielsson, Haldor Topsøe A/S

Industrial PhD Study

Started: July 2013
To be completed: June 2016

Catalytic Materials for Combined Particulate and NO_x Removal from Diesel Vehicles

Abstract

A combined particulate filter and selective catalytic reduction unit for NO_x removal holds a great potential with respect to reducing the overall size and cost of the diesel exhaust aftertreatment system. This project will identify catalytic formulations with the required combination of soot oxidation and selective catalytic reduction properties without unwanted side reactions such as NH₃ oxidation. Recent work has focused on soot oxidation by the V₂O₅/WO₃-TiO₂ system, including extraction of kinetic parameters (A and E_a).

Introduction

Heavy duty diesel (HDD) vehicles handle a substantial part of the global transport and logistics. Harmful pollutants, such as nitrogen oxides (NO_x), hydrocarbons (HC), particulate matter (PM), and carbon monoxide (CO), are however formed. The diesel exhaust aftertreatment (DEA) system has been developed to treat the pollutants in the exhaust gas.

Figure 1 illustrates the current standard DEA system consisting of a series of catalytic units. The Diesel Oxidation Catalyst (DOC) oxidizes CO and HC to CO₂ and H₂O, as well as generates NO₂ from NO. The Diesel Particulate Filter (DPF) is a wall-flow filter, entraining PM in its monolith walls. The DPF can be regenerated actively by increasing the exhaust gas temperature using post-injection of fuel, or passively using a catalyst. NO₂ generated by the DOC also assists regeneration. NO_x is targeted through Selective Catalytic Reduction (SCR) using NH₃ as the reducing agent. NH₃ is supplied to the system through urea dosing, regulated by the onboard Model Predictive Control (MPC) unit. Excess NH₃ is controlled with the Ammonia Slip Catalyst (ASC). Upon exiting the DEA system, the emissions should meet the restrictions imposed by the Euro VI regulations.

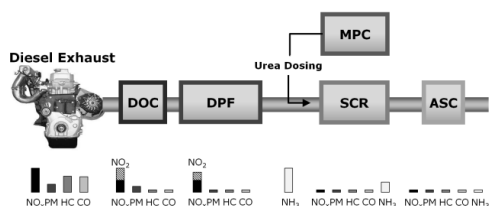


Figure 1: Example of a standard design of the DEA system, consisting of the DOC, DPF, SCR component, urea dosing MPC unit, and the ASC.

The DEA system is very complex, requiring efficient exhaust treatment for a wide range of operating conditions, corresponding to cold start, stop-and-start driving (inner city), and high speed driving (highways). As a result, DTU Chemical Engineering and Haldor Topsøe A/S are collaborating on the development of the next generation DEA system, with funding from The National Danish Advanced Technology Foundation. The underlying PhD projects concerns the development of new DOC and ASC formulations (Thomas Klint Hansen at CHEC, pg. 87-88), the combination of the DPF and SCR components (present project), and model development of the control unit for efficient urea dosing system (Andreas Åberg at CAPEC, pg. 215-216).

Specific Objectives

The two largest components of the DEA system are the DPF and the SCR. A combination of these could

therefore result in a considerable reduction in both cost and size of the overall system. In order to achieve this, the present project will develop catalytic materials for combined particulate and NO_x removal. This will be done by applying catalyst synthesis, characterization, kinetic lab-scale studies and pilot scale tests.

In order to develop such a unit with catalytic activities for combined soot and NO_x removal, two overall approaches may be used: Zone coating of the filter, allowing deposition of different catalytic formulations in different zones of the filter (e.g. entrance or exit); or a multi-function catalyst, which have activities for both reactions simultaneously. Both approaches have advantages and disadvantages, but a major benefit of the one step multi-function coating is a much simpler production.

Through a literature survey, potential catalytic materials were identified and synthesized. These were tested for activity for soot oxidation by O₂ using a Netzsch F409 STA. The resulting thermogravimetric data were used to identify the temperature at which the maximum reaction rate occurs, T_{max}, and extracting the pre-exponential factor (A) and the activation energy (E_a) using a simple rate expression ($k=1/m\cdot dm/dt=A\cdot\exp(-E_a/RT)[O_2]$), as described by Kalogirou et al. [1].

Among the tested catalysts, 2wt.% V₂O₅/10% WO₃-TiO₂ (WTi) was found to have a significant effect, i.e. the temperature of maximum reaction rate (T_{max}) decreased by 140°C. For this reason, further kinetic studies were performed on the V₂O₅/WTi system.

Results and Discussion

Table 1 shows T_{max} and the kinetic parameters for selected samples in tight contact, illustrating an increasing activity as a function of V₂O₅ content; from 0 wt% (only WTi carrier) to 100 wt% (only V₂O₅).

Based on the comparable activation energies observed for 1-6 wt% V₂O₅ the data were fitted to the model using an average activation energy, E_a=144.5 kJ/mol, and varying only the pre-exponential factors. The results can be seen in Figure 1, illustrating a good fit between the model and experimental data.

Table 1: Kinetic results for soot oxidation in 5 vol%O₂/N₂ in tight soot-catalyst contact.

	T _{max} [°C]	A [s ⁻¹]	E _a [kJ/mol]
Soot	702	2.88E+8	200.3
WTi	596	1.65E+9	177.7
2 wt%V ₂ O ₅	562	1.45E+8	152.5
4 wt%V ₂ O ₅	520	4.93E+8	152.1
6 wt%V ₂ O ₅	476	3.59E+8	141.3
V ₂ O ₅	418	1.86E+7	113.5

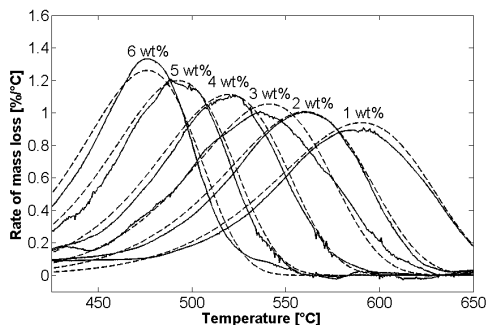


Figure 1: Soot oxidation rates of V₂O₅-WTi with varying V₂O₅-content as indicated. Raw data (-) and models fitted (--) using an average value of E_a=144.5 kJ/mol and varying A are shown. Obtained A-values (10⁸, [s⁻¹]): 6 wt%: 5.78; 5 wt%: 3.35; 4 wt%: 1.45; 3 wt%: 0.77; 2 wt%: 0.45; 1 wt%: 0.20.

For NH₃-SCR, 1.9 wt% V₂O₅-WTi reaches >90% NO_x conversion at 300-500°C [2], while Figure 1 shows soot oxidation by 2 wt% V₂O₅-WTi occurring at higher temperatures. It should furthermore be mentioned that the operating temperature should not exceed about 550°C to avoid vaporization of vanadium. The results indicate that for catalysts with V₂O₅>2wt% this may be possible. Furthermore, the soot oxidation activities may increase under more realistic conditions, in the presence of NO₂ and H₂O.

Conclusions

The development of a combined filter and SCR unit holds a great potential for reducing the overall cost and size of the diesel exhaust aftertreatment system. This work has identified promising catalytic materials with activities for both soot oxidation and NH₃-SCR for further studies, and kinetic parameters for these materials have been identified.

Acknowledgements

This project is carried out in cooperation between Haldor Topsøe A/S, the CHEC group at DTU Chemical Engineering and Innovation Fund Denmark. The financial support from Innovation Fund Denmark under Grant number 103-2012-3 is gratefully acknowledged.

References

1. M. Kalogirou, Z. Samaras, J. Therm. Anal. Calorim. 98 (2009) 215-224.
2. O. Kröcher, Stud. Surf. Sci. Catal. 171 (2007) 261-289.

**Asger Lindholdt**

Phone: +45 4525 2837
E-mail: Asli@kt.dtu.dk

Supervisors: Søren Kiil, DTU
Kim-Dam Johansen, DTU
Stefan M. Olsen, Hempel A/S
Diego M. Yebra, Hempel A/S

PhD Study

Started: December 2011
To be completed: December 2014

Fuel Efficiency and Fouling Control Coatings in Maritime Transport

Abstract

The skin friction of antifouling coatings change over time and the initial friction for clean coatings are therefore not sufficient to accurately estimate the fuel efficiency of an antifouling coating over a typical dry-docking period. Furthermore, it is found that the skin friction increases significantly faster during static immersion compared to dynamic immersion. The immersion conditions are therefore of importance when determining the most fuel efficient antifouling coatings. The need for better prediction tools of the fuel efficiency is desired because the often applied route via surface friction measurements of antifouling coatings in clean condition and after static immersion are inadequate. An experimental method has therefore been developed to measure surface friction of antifouling coatings over a desired time period under conditions which can mimic the vast majority of ship profiles (speed and activity) in today's market. The experimental method consists of two parts, i.e. an aging setup and a laboratory scale rotor capable of measuring surface on coated cylinders. It was found that the surface friction was significantly lower for a hydrogel fouling release coating compared to a fluorinated fouling release coating.

Introduction

The maritime transport sector is responsible for transporting huge amounts of goods all around the world which unfortunately has two primary negative side effects. Firstly, a vast amount of fuel is being consumed causing harmful emission of e.g. CO₂, NO_x and SO_x particles. Secondly, toxic components are released from antifouling coatings to the surrounding seawater. Surface friction constitutes a large part of a ship's total resistance which, however, depends on several factors such as e.g. the condition of the antifouling coating and the ship's speed. Marine biological fouling is known to have an undesirable impact causing a ship's drag to increase. The drag performance (fuel efficiency) of antifouling coatings are today often being evaluated based on static immersion of coated objects followed by hydrodynamic drag measurements in e.g. a towing tank. Larger ships are only rarely static, e.g. in ports, and a static test is therefore only a mediocre method when evaluating antifouling coatings drag performance. Static exposure followed by hydrodynamic exposure has been applied and it is an improved test method compared to only static exposure because this test method more closely resembles the conditions a ship is exposed to during a typical voyage. However, further improvements are desirable in order to evaluate the long-term drag

performance of antifouling coatings in conditions which mimic those antifouling coatings experience during voyages.

Specific Objectives

The purpose of this project is to improve drag test methods for antifouling coatings applicable to a typical dry-docking period, e.g. 5 years. The focus is therefore primarily on long term drag performance determination of antifouling coatings. Furthermore, the specific objectives are to develop an experimental method capable of mimicking the aging process of antifouling coatings closely and measure the drag performance over a long time. During the aging process it is desired to continuously or frequently measure the drag performance via the determination of the surface friction coefficient for a number of antifouling coatings and their development over time.

The laboratory cylindrical rotor setup, which is seen in Fig. 1, is used to measure surface friction. The system consists of a large tank where the rotating cylinder is placed. A static cylinder is placed outside the inner rotating cylinder to obtain a controlled flow, i.e. Couette type flow. The torque sensor is used to measure the torque due to rotation of the system, i.e. bearings, shaft and cylinder. The surface friction of the coating can be determined by measuring the effects due to friction from

the top and bottom of the cylinder, friction of the shaft and the bearings.

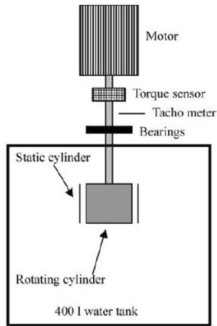


Figure 1: Laboratory cylindrical rotor setup

The seawater setup is seen in Fig. 2 where the antifouling coatings are aged in conditions mimicking those ship hulls experience during voyage. Flow conditions similar to that a ship hull experiences arises due to the rotational speed of the shaft where the coated cylinders are attached. Furthermore, the biological conditions are similar to that a ship hull experience due to the seawater immersion.



Figure 2: Cylindrical seawater test setup.

The advantage of the seawater setup compared to other setups used in the field of antifouling coating drag performance prediction is that the coating's aging process resembles the one a ship experiences due to the hydrodynamic immersion in the sea. Furthermore, the drag measurements are recorded with short time intervals, i.e. every 2 to 3 weeks, resulting in a large amount of drag measurements over time capable of making a drag performance over a long time interval.

Results and Discussion

The skin friction coefficient determined in the laboratory rotor setup due to the aging in the seawater test setup has shown that changes over time can be determined, see Fig. 3. In Fig. 3 the skin friction coefficients for four antifouling coating technologies over a period of 53 weeks at an average of 9.5, 12.6 15.8 knots is seen. Week zero (designated by round dots) is the skin friction prior to immersion. The triangles designate that prior to skin friction measurement a period of two weeks static immersion

had taken place. The squares designate that prior to skin friction measurements the coatings had been dynamically immersed at approximately 10 knots for 3 weeks. The flat lines at week 26 and 54 designate that prior to skin friction measurements mechanical cleaning of the coatings had taken place.

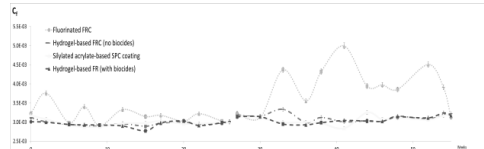


Figure 3: Skin friction coefficient over 53 weeks for fluorinated FRC, hydrogel-based FRC with biocides, SPC coating and hydrogel-based FRC without biocides. Round dots represent the coating condition prior to immersion, triangles represent static immersion for two weeks, squares represent 3 weeks of dynamic immersion at 10 knots and the flat lines at week 26 represent that the coatings had been mechanically cleaned.

The measurements show significant differences in the skin friction over time. Furthermore, it is seen that static immersion increase friction more than dynamic immersion, especially for the fluorinated fouling release coating. It was found that mechanical cleaning brought the coatings back to a skin friction coefficient value similar to the initial one. The reason for a decrease in the skin friction coefficient after immersion at week zero might be explained by the uptake of water in the coatings (swelling).

Conclusions

The developed test setup has proven capable of measuring significant surface friction differences between antifouling coating systems which is valuable when determining the optimal choice of coating with respect to fuel efficiency. It was found that the surface friction was significantly lower for a hydrogel fouling release coating compared to a fluorinated fouling release coating, especially after the periods with static immersion. The decrease in surface friction compared to condition prior to immersion shall be investigated further. It was found that the skin friction decreased in the following order: fluorinated FRC (highest skin friction), hydrogel-based FRC without biocides, SPC coating and hydrogel-based FRC with biocides.

Acknowledgements

This PhD project is supported both financially and knowledge wise from Hempel A/S which is greatly appreciated.

References

1. C.E. Weinell, K.N. Olsen, M.W. Christoffersen, S. Kiil, *Biofouling* 19 (Supplement) (2003) 45–51.
2. M.P. Schultz, G.W. Swain, *Biofouling* 23, 3 (2007) 164-170.
3. K.A. Zargiel, G.W. Swain, *Biofouling*, (2013)

**Ming Liu**

Phone: +45 4525 2861
E-mail: miliu@kt.dtu.dk
Discipline: Bioprocess Enzyme Technology

Supervisors: Anne S. Meyer
Anders Thygesen

PhD Study

Started: September 2013
To be completed: September 2016

Hemp Fibers: Enzymatic Effect of Microbial Processing on Fiber Bundle Structure

Abstract

The effects of microbial pretreatment on hemp fibers were evaluated after microbial retting using the white rot fungi *Ceriporiopsis subvermispora* and *Phlebia radiata* Cel 26 and water retting. Based on chemical composition, *P. radiata* Cel 26 showed the highest selectivity for pectin and lignin degradation and lowest cellulose loss (14%) resulting in the highest cellulose content (78.4%) for the treated hemp fibers. The pectin and lignin removal after treatment with *P. radiata* Cel 26 were of the order 82% and 50%, respectively. Aligned epoxy-matrix composites were made from hemp fibers defibrated with the microbial retting to evaluate the effects on their ultrastructure. SEM microscopy of the composites showed low porosity on the fiber surfaces after defibration with *P. radiata* Cel 26 and *C. subvermispora* indicating good epoxy polymer impregnation. In contrast, fibers treated by water retting and the raw hemp fibers were badly impregnated due to poor porosity impregnation caused by surface impurities such as epidermis and other pectin rich plant cells. The pectin and lignin mainly located in the outer part of the fibers were assumed to be extracted and degraded by pectinase and peroxidase enzymes produced by the fungi.

Introduction

Hemp fibers can be used as reinforcement agents in biocomposites due to their good mechanical properties including low density and high stiffness [1]. The principal constituent of hemp fibers is cellulose, which has a high theoretical strength (8 GPa) and functions as the reinforcing component in the fibers. Currently, the largest demand for cellulosic fibers is for the production of string, twine, cord and ropes [2]. These applications require primary processing of raw materials into yarn with a series of steps including retting, scutching, carding, cottonization and spinning. Retting is the term used for the removal of non-cellulosic components from natural fibers and separation of the fibers from the plant stem structure, to obtain cellulose-rich fibers. It is performed by microbiological methods. Retting precedes mechanical separation (scutching) of the fiber from the stem and is essential for reduction of fiber breakage [3]. However, recent data suggest that the gentle microbial retting process can enzymatically create defects in the fiber structure during the processing of hemp stems into single fibers [4-5].

Parenchyma cells rich in pectin and hemicellulose, which bind the hemp bast onto the stem surface, are located between the fiber bundles [3, 6]. This binding must be degraded to obtain useful fibers for strong

composites. As explained in more detail below, hemp fibers are classically separated from the plant stems by “water retting”, which in essence is a microbial process. In this process, indigenous bacteria and notably fungi present on the plant stems degrade pectin between the fibers and the stem surface at temperatures of around 15 °C to 30°C within six to ten days [1, 3]. It has been shown that bacterial species of *Achromobacter*, *Clostridium* and *Pseudomonas* dominate [7]. Despite its long use, the process is still largely empirical, and obviously depends on the microbial flora present on the fibers. In order for the process to be successful, it is of crucial importance that the cellulose is not degraded. Knowledge about changes in hemp fiber ultrastructure and chemical composition during processing is of great importance to produce high-quality fibers.

In this study, the basidiomycete white-rot fungi *Ceriporiopsis subvermispora* [8] and mutant strain (cellulase less) *Phlebia radiata* Cel 26 [9], which have a limited ability to degrade cellulose were used to treat hemp stems and investigate their effect on the fiber microstructure and chemical composition compared with traditional water retting. These fungi have been used for microbial separation of woody fibers. Results were analyzed based on knowledge of the cell wall active enzymes produced by the two fungi.

Specific Objectives

The primary objective of this study is to compare the effect of different pretreatments on the chemical composition and structure of the hemp fiber and also provide

Results and Discussions

The overview of the investigated hemp fibers in this study was shown in Table 1. The weight loss of each component after different treatment was shown in Table 2, and the effects of biological treatments on the chemical composition of the investigated hemp fibers were shown in Table 3.

The pectin loss in hemp fibers caused by fungal treatment with *C. subvermispora*, *P. radiata* Cel 26 or by water retting was 57%, 82% and 77%, respectively. The weight loss of hemicellulose in samples treated with water retting (44%) and *P. radiata* Cel 26 (36%) were not significantly different. *C. subvermispora* caused the lowest hemicellulose degradation (25%), while water retting caused a significant loss in cellulose with 22%. However, *P. radiata* Cel 26 and *C. subvermispora* treatment caused only 14% and 12% weight loss in cellulose respectively.

The results showed that *P. radiata* Cel 26 had the highest selectivity for pectin degradation. The

selectivity value is defined as the ratio of pectin degradation to cellulose degradation and is used to describe the depectinization efficiency. According to the definition, a higher selectivity value reflects improved preferential depectinization. On the contrary, a lower selectivity value means relatively high amount of cellulose degradation during the biological treatment resulting in a loss. As shown in Table 2, *P. radiata* Cel 26 demonstrated higher selectivity (6.0) than water retting (3.5) and *C. subvermispora* (4.6). Additionally, besides best depectinization, *P. radiata* Cel 26 also caused the highest lignin (50%) and hemicellulose degradation (36%) confirming its limited cellulase activity and that the strain can produce pectinase and hemicellulase enzymes [9]. The highest (50%) weight loss in lignin resulting from the fungal treatment with *P. radiata* Cel 26 on the stem indicates the highest activity of Pyranose oxidase (POD) and Mn-dependent peroxidases (MnP). This was suggested due to the presence of much higher concentration of H₂O₂ (1-5 mg/L) in the fungal treatment broth, since H₂O₂ produced by POD has a crucial role in the ligninolytic systems and is necessary for the ligninolytic peroxidases [10-11].

Table 1: Overview of the investigated hemp fibers

Fiber type	Code	Treatment	Fiber yield	
			(g/100 g stem)	(g/100 g raw fibers)
Loose hemp fiber bundle	H0	Untreated	38±1	100
	H1	Water retting	27±1	68
	H2	<i>C. subvermispora</i>	29±1	75±4
	H3	<i>P. radiata</i> Cel 26	28±1	70±1

Table 2: Process results obtained by fungal defibration and water retting of hemp

Fiber code	H ₂ O ₂ (mg/L)	Selectivity value*	Weight loss (%)			
			Cellulose	Hemicellulose	Lignin	Pectin
H1	n.a.	3.5	22	44	0	77
H2	0-1	4.6±2	12±5	25±5	-12±12	57±5
H3	1-5	6.0±1	14±2	36±1	50±22	82±2

* Selectivity value = Pectin loss / Cellulose loss.

Table 3: Chemical Composition and structural properties of the investigated hemp fibers

Fiber code	Chemical Composition					Structure
	Cellulose (% w/w)	Hemicellulose (% w/w)	Lignin (% w/w)	Pectin (% w/w)	Residuals (% w/w)	Transverse section (µm ²)
H0	64.4±0.8	14.4±0.1	3.4±0.2	7.3±0.5	10.5	160000
H1	73.8	11.8	5.0	2.5	6.9	10000
H2	72.4±1.4	13.8±0.8	4.9±0.4	4.0±0.6	4.9±0.2	50000
H3	78.4±1.0	13.0±0.1	2.4±1.0	1.9±0.3	4.3±0.2	3000

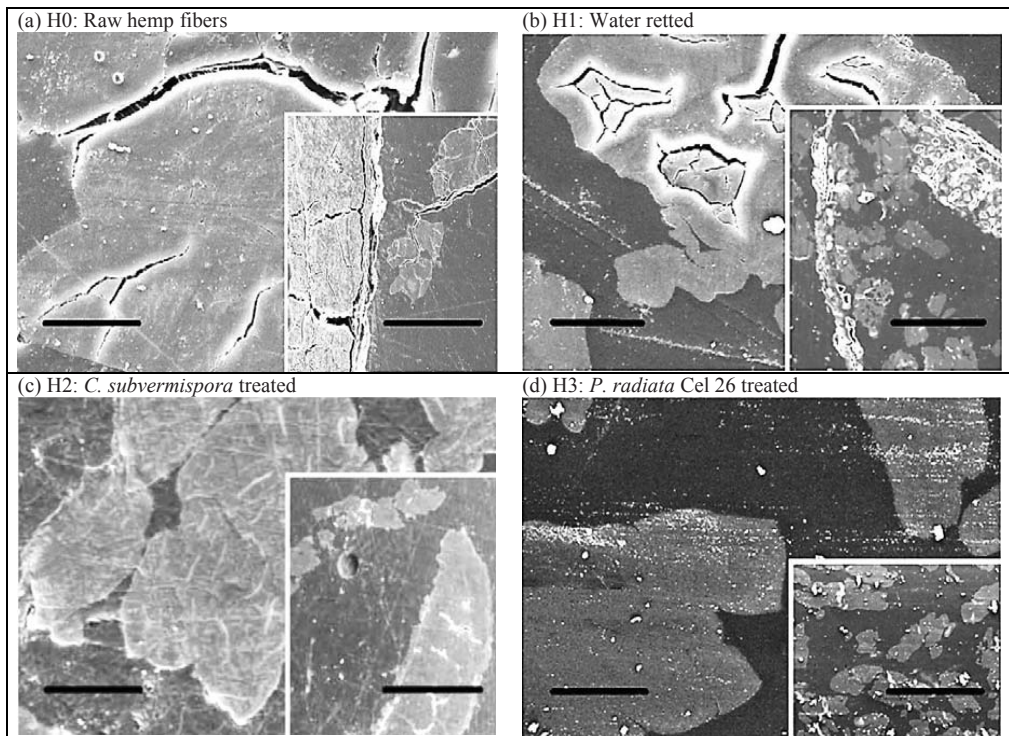


Figure 1: SEM images of transverse composite sections recorded at low and high magnification with the investigated hemp fibers. Inset images have scale bars of 200 μm and the background images 20 μm .

The microstructure was observed in transverse cross sections using SEM (Figure 1). The figure shows the fibers (light grey areas), the matrix (dark grey areas) and the air filled voids described as porosity areas (black areas). Increased porosities and cracks appeared inside the epidermis on the fiber bundle surfaces of raw hemp fibers (H0) and water retted (H1) hemp fibers (Figure 1). This resulted in incomplete impregnation of the fiber bundles resulting in gaps between the matrix and the fibers. This increase in porosity appeared to the highest extent in composites reinforced with raw hemp bast and water-retted hemp fibers due to surface impurities such as epidermis and other pectin rich plant cells. In contrast, hemp fibers defibrated by cultivation of *C. subvermispora* (H2) and *P. radiata* Cel 26 (H3) were well impregnated in epoxy since no porosity was observed on the surfaces of the fibers (Figure 1). Compared with raw (H0) and water retted fibers (H1), fewer impurities appeared on the surface of *C. subvermispora* (H2) and *P. radiata* Cel 26 treated fibers (H3). It was in accordance with the chemical composition analysis in Table 3 showing that residuals were higher in the raw fibers (10.5%) and water retted fibers (6.9%) as compared to the fibers retted with *P. radiata* Cel 26 (4.9%) and *C. subvermispora* (4.3%).

Pectin was stained using ruthenium red by reaction

with carboxylic acid side groups and shown as a red colour in Figure 2. Pectin is commonly regarded as intercellular glue having important functions in cell growth and differentiation. However, in order to separate fibers from a hemp stem, it is essential to remove pectic contents by selective attack by bacteria and/or fungi. As shown in Figure 2, compared to the raw hemp fibers (Figure 2a), significant amounts of pectin were degraded by water retting (Figure 2b) as well as by cultivation of *C. subvermispora* (Figure 2c) and *P. radiata* Cel 26 (Figure 2d). To be more specific, large amounts of dark red staining materials surrounding white areas are shown in Figure 2a. This indicated that a lot of pectin existed in the raw hemp fibers. A large amount of the same dark red area outside the cell wall existed in Figure 2c, but the vast majority of the dark red area between fibers has been removed compared to Figure 2a. This indicated that a large amount of pectin was degraded by cultivation of *C. subvermispora*.

In Figure 2b, there was also a small area of dark red on the fiber surface. However, there were almost no dark areas remaining around individual fibers while small dark areas appeared on the surface of the fibers (Figure 2d). This result suggests that most pectin was degraded by treatment with *P. radiata* Cel 26, which corresponds to the results discussed above.

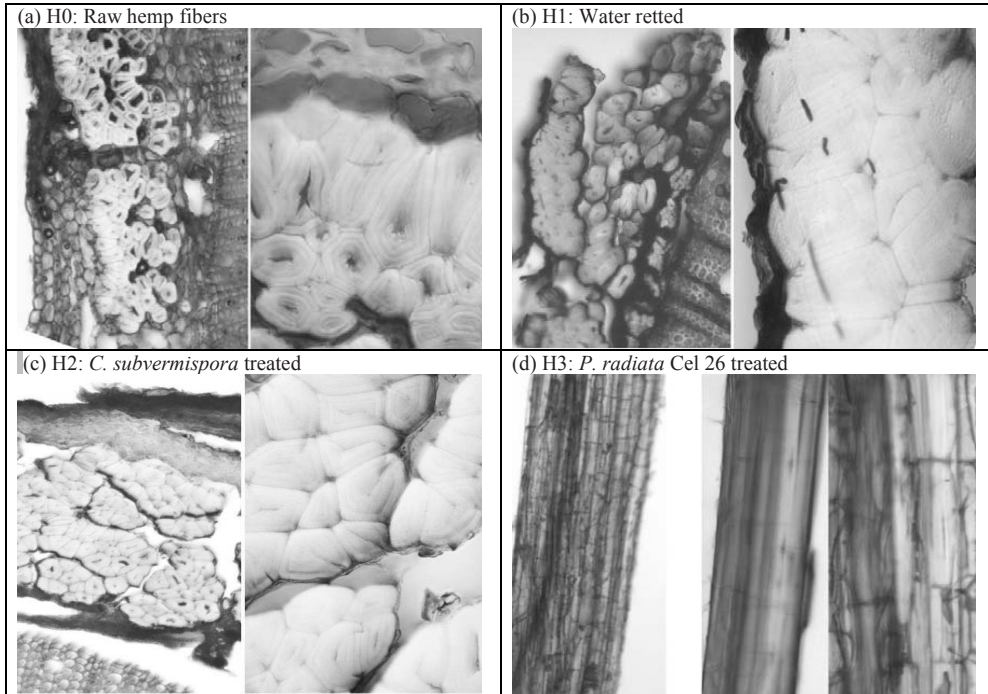


Figure 2: Pectin stained in hemp transverse sections and hemp fiber surfaces using ruthenium red.

Conclusions

1. Compared to water retting and cultivation with *C. subvermispora*, cultivation with *P. radiata* Cel 26 was the most preferable pretreatment with highest selectivity for pectin degradation resulting in 36% hemicellulose, 50% lignin and 82% pectin degradation and a minimal loss of cellulose (14%).
2. SEM microscopy of hemp fiber reinforced composites showed good epoxy polymer impregnation after treatment with *P. radiata* Cel 26 and *C. subvermispora*. In contrast, hemp samples treated by water retting and the raw hemp fibers were badly impregnated due to porosity caused by surface impurities. And the surface impurities were in accord with the chemical composition analyses showing that residuals were higher in the raw and water retted fibers as compared to the fibers retted in a controlled fashion with *P. radiata* Cel 26 or *C. subvermispora*.

Acknowledgements

The Danish Council for Independent Research is acknowledged for supporting the CelFiMat project (IP No. 12-127446: "High quality cellulosic fibers for strong biocomposite materials").

References

1. Thygesen, A., Thomsen, A.B., Daniel, G., Lilholt, H. Ind. Crops Prod. 25(2007), 147-159.
2. Sankari, H.S. Ind. Crops Prod. 11(2000), 73-84.

3. Franck, R.R., Bast and other plant fibers, CRC Press, New York, 2005, p.185-186.
4. Thygesen, A., Daniel, G., Lilholt, H., Thomsen, A.B. J. Nat. Fibers 2-4(2005), 19-37.
5. Thygesen A, Madsen B, Thomsen AB, Lilholt H. J. Nat. Fibers, 8(2011), 161-175.
6. Garcia-Jaldon, C., Dupeyre, D., Vignon, M.R. Biomass Bioenerg. 14(1998), 251-260.
7. Rosember, J.A. Appl. Microbiol. 13(1965), 991-992.
8. Akhtar, M., Attridge, M.C., Blanchette, R.A., et al. In: Kuwahara, M., Shimada, M. (Ed.), Biotechnology in pulp and paper industry, Uni Publishers CO., Tokyo, Japan. 1992, pp 3-8.
9. Nyhlen, L., Nilsson, T, Combined T.E.M. and UV-microscopy on delignification of pine wood by *Phlebia radiata* and four other white fungi rotters. In: Odier, E. (Ed.), Product of lignin enzymic and microbial degradation symposium, INRA Publications, 1987, pp. 277-282.
10. Daniel, G., Volc, J., Niku-Paavola, M.L. C. R. Biol. 9-10(2004), 861-871.
11. Kantelinen, A., Hatakka, A., Viikari, L. Microbiol. Biotechnol. 31(1989), 234-239.



Marie Lundemo

Phone: +45 4525 2958
E-mail: mande@kt.dtu.dk

Supervisors: John M. Woodley
Ulrich Krühne

PhD Study
Started: February 2012
To be completed: January 2015

Bioprocess Engineering for the Application of P450s

Abstract

The specific hydroxylation performed by P450 monooxygenases is highly interesting chemistry and hard to achieve via chemical routes. However, this class of enzymes has only been implemented in industrial processes in a few cases where growing cells have been the selected mode of operation. This can be explained by the many challenges associated with the enzyme that needs to be overcome in order to reach the typical targets characterizing a successful biocatalytic process. Typical challenges are the requirement of a cofactor, electron transporting redox partner and hydrophobic substrates and products, which all set some constraints on the process. To enable focused and directed development the bottlenecks needs to be identified for relevant systems. Theoretical identified bottlenecks have been the basis for a hypothesis driven experimental approach with the aim to identify the limitations of different model systems. These model systems have been evaluated based on reaction yield, biocatalyst yield, final product concentration and space time yield. Realistically it can be seen that there are still improvements necessary before P450 based processes in general fulfill requirements on economic viable processes.

Introduction

Biocatalysis in general is a tempting alternative to chemical catalysis especially due to the excellent selectivity of reactions where conventional chemistry requires several steps including protecting and deprotecting. The specific hydroxylation of unactivated hydrocarbons performed by P450 monooxygenases (CYP) is a good example of this and furthermore, the chemistry is difficult to perform using conventional routes. P450 monooxygenases can be found in all kingdoms and are besides the use in synthetic production also interesting in pharmaceutical research since P450s in the human liver are responsible for drug metabolism. There are however some challenges associated with the nature of the enzymes: cofactor dependence (NADPH or NADH) and the requirement of a redox partner transporting electrons from the cofactor to the active site. These requirements make a whole cell system a suitable biocatalyst form. Furthermore to utilize the cofactor regeneration of the whole cell, and avoid the addition of expensive cofactor, the cell needs to be metabolically active, i.e. the catalyst needs to be used in close connection to the fermentation. Despite the excellent chemistry performed, the potential processes need to be economically feasible and based on threshold values for metrics such as space-time yield, biocatalyst yield and final product concentration need to

be reached. Three model systems, illustrated in Figure 1, have been evaluated in this PhD project, provided by project partners in the EC funded Marie Curie project P4FIFTY.

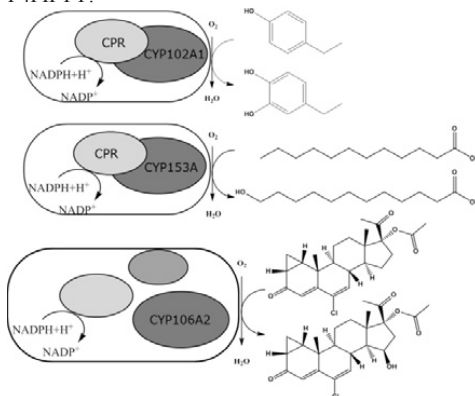


Figure 1: Model systems applied in the PhD studies: top, CYP102A1 expressed in *E. coli* hydroxylating 4-ethylphenol [1]; middle, CYP153A expressed in *E. coli* performing ω -hydroxylation of lauric acid [2]; bottom, CYP106A2 expressed in *B. megaterium* performing 15 β -hydroxylation of cyproterone acetate [3].

Specific objectives

The objectives of the project are to:

- define the requirements and bottlenecks for an industrial relevant process involving P450 monooxygenase
- evaluate different mode of operation (growing or resting cells)
- evaluate 2-phase systems involving water immiscible organic solvents
- explore oxygen supply strategies
- perform environmental and economic evaluation of a selected process

Results and Discussion

Fermentation processes have been set up for both *E. coli* and *B. megaterium* based whole cell catalysts. The individual model systems have subsequently been evaluated in terms of what biological parameter is limiting the biocatalytic process from reaching the defined metric targets defined in Table 1.

Table 1: Target metrics values for high value chemicals and pharmaceuticals.

Metric	Growing cells	Resting cells
Final product concentration	20 g/L	20 g/L
Space-time yield	2 g/L/h	
Biocatalyst yield		10 g/g cdw

The focus of the study has been the biological parameters presented in **Table 2**. Another challenge associated with P450 catalyzed reactions is the low solubility of substrate. However, this is expected to be overcome by means of immiscible or miscible solvents or application of other solubilizing agents. Substrate and product inhibition in combination with poor stability of the P450 enzyme has been identified as common challenges for all model systems. The poor stability of the enzyme confirms that a whole cell system is an appropriate form of the catalyst, since a protected environment is offered. Substrate inhibition can be overcome by e.g. substrate feeding, successfully applied in the case of lauric acid hydroxylation. *In situ* product removal is more challenging in these systems since the difference in chemical properties are very small between the substrate and product. Overexpression in a natural P450 expressing host such as *B. megaterium* showed no indications of cofactor shortage whereas the reaction catalyzed by resting cells with heterologous expression in *E. coli* could be improved by external addition of cofactor.

Table 2: Summarized limitations for model systems studied.

Potential limitation	CYP102A1 expressed in <i>E. coli</i> HMS174	CYP153A expressed in <i>E. coli</i> HMS174	CYP106A2 expressed in <i>B. Megaterium</i> MS941
Substrate inhibition?		X	
Product inhibition?	X		X
Cofactor limitation?		X	
Transport limitation?			
Stability issues of P450?	X	X	X

Conclusions

P450s catalyze very interesting reactions, with high selectivity, difficult to achieve with conventional chemistry. However, challenges associated with their use in synthetic processes make them suitable only for high value products. Furthermore, the full potential of the host cell needs to be utilized and optimized in terms of protein expression, cofactor usage and coupling efficiency to minimize formation of reactive oxygen species and unproductive consumption of cofactor and oxygen.

Acknowledgements

The author thanks Prof Bernhard Hauer and Sandra Notonier, University of Stuttgart, Prof Rita Bernhard and Flóra Márta Kiss, University of Saarland and Jürgen Riegler and Michael Ringle, Lonza for fruitful collaborations.

The research leading to these results has received funding from the People Programme (Marie Curie Actions) of the European Union's 7th Framework Programme (FP7/2007-2013) under REA Grant Agreement 289217.

References

1. Lewis, J. C., Arnold, F. H., CHIMIA International Journal for Chemistry 63 (6) (2009) 309-312.
2. Scheps, D., Honda Malca, S., Richter, S. M., Marisch, K. Bettina M; Hauer, B., Microbial biotechnology 6 (6) (2013) 694-707.
3. Bleif, S., Hannemann, F., Zapp, J., Hartmann, D. Jauch, J., Bernhardt, R., Appl. Microbiol. Biotechnol. 93 (3) (2012) 1135-1146.

**Seyed Soheil Mansouri**

Phone: +45 4525 2907

E-mail: seso@kt.dtu.dk

Supervisors: Rafiqul Gani
John M. Woodley
Jakob Kjøbsted Huusom**PhD Study**

Started: September 2013

To be completed: August 2016

Design, Control and Analysis of Intensified Processes

Abstract

Integrated process design and control of an intensified process (reactive distillation) is presented. Simple graphical design methods that are similar in concept to non-reactive distillation processes are used, such as reactive McCabe-Thiele method and driving force approach. The methods are based on the element concept, which is used to translate a system of compounds into elements. The operation of the reactive distillation column at the highest driving force and other candidate points is analyzed through analytical solution as well as rigorous open-loop and closed-loop simulations. By application of this approach, it is shown that designing the reactive distillation process at the maximum driving force results in an optimal design in terms of controllability and operability. It is verified that the reactive distillation design option is less sensitive to the disturbances in the feed at the highest driving force and has the inherent ability to reject disturbances.

Introduction

Traditionally, process design and process control are considered as independent problems, that is, a sequential approach is used where the process is designed first, followed by the control design. The limitations with the sequential approach are related to dynamic constraint violations, for example, infeasible operating points, process overdesign or under performance. Therefore, this approach does not guarantee robust performance [1]. Furthermore, process design decisions can influence process control and operation. To overcome the limitations associated with the sequential approach, operability and controllability are considered simultaneously with process design, in order to assure that design decisions give the optimum operational and economic performance. In control design, operability addresses stability and reliability of the process using a priori operational conditions and controllability addresses maintaining desired operating points of the process subject to disturbances.

A number of methodologies and tools have been proposed for addressing the interactions between process design and control, and they range from optimization-based approaches to model-based methods [2]. In this work, integrated design and control of reactive distillation processes as an intensified process is considered, since process design decisions will influence process operability and controllability. Numerous design algorithms for multi-component

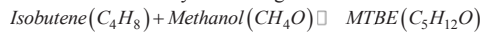
separation systems with reactions have accompanied the increasing interest in reactive distillation processes. In design, the input and (selected) output variables are specified and the task is to determine the optimal reactive distillation process configuration (for example, minimum number of stages), and the optimal design parameters (for example, optimum reflux ratio, optimal feed location) that achieve the given product specification. It is intended to achieve the optimal design in such way that it is also an operable process at pre-defined conditions under presence of disturbances.

Pérez-Cisneros et al. [3] have proposed an element mass balance approach to design the reactive distillation processes, which employs the traditional graphical tools similar in concept to design of non-reactive distillation columns, such as McCabe-Thiele method and driving force approach of Bek-Pedersen and Gani [4]. Moreover, Hamid et al. [5] have proposed an integrated process design and controller design methodology. However, their methodology covers the aspects related to design and control of non-reactive binary distillation processes. In this work, the method of Hamid et al. [5] is extended to also cover a ternary compound reactive distillation process (using element-based approach) and criteria of selecting the optimal design and the controller structure selection will be presented. In order to demonstrate the application of the aforementioned approach, production of methyl-tert-butyl-ether

(MTBE) from methanol and isobutene using a reactive distillation column is considered.

Reactive Distillation Column Design

The computation of simultaneous chemical and physical equilibrium plays an important role in the prediction of the limits for conversion and separation of a specific reactive separation process, particularly for the reactive distillation systems. Using the Gibbs free energy minimization approach, Pérez-Cisneros *et al.* [3] proposed solution procedures where the multicomponent chemical and physical equilibrium is posed as an “element phase” equilibrium problem. This transformation is based on the concept of chemical model as proposed by Michelsen [6]. This concept is derived from chemical model theory, where, the equations of chemical equilibrium together with any appropriate physical model yielding the chemical potentials are incorporated into an element-based model (called the chemical model). The main difference between the chemical model algorithm and those developed earlier, is the use of the chemical models in a way that renders the chemical and physical equilibrium problem formally identical to the physical equilibrium problem for a mixture of element (representing the system). Further details can be found in [7, 8] The reaction for MTBE synthesis is given as follows:



It is evident that the selection of the elements has an important role in the present formulation. They are traditionally chosen as the “natural” chemical elements present in the reaction mixture, but, indeed, one is free to select any reaction invariant fragment of the reactants. The element matrix is constructed based on the rules provided by Pérez-Cisneros *et al.* [3] and it is as follows:

Element	Component		
	C_4H_8 (1)	CH_4O (2)	$C_5H_{12}O$ (3)
A	1	0	1
B	0	1	1

Therefore, the ternary system of compounds can be reduced into a binary system of elements A and B and the reaction can be rewritten as: $A + B \rightleftharpoons AB$. The first component (element A) and the second component (element B) form the third component (element AB). Having the ternary system of compounds represented in form of a binary element system, similar graphical design methods, that are applied to non-reactive binary distillation column design, such as McCabe-Thiele method can be used. However, in order to use the McCabe-Thiele method, a reactive equilibrium curve is required. The reactive equilibrium curve is constructed through sequential computation of reactive bubble points [3]. In order to generate the reactive data-set, Wilson thermodynamic model for prediction of the liquid phase behavior and SRK equation of state for prediction of vapor phase behavior were used. Note that the calculation of reactive vapor-liquid equilibrium

(VLE) data set is in terms of compounds. Therefore, a ternary compound data set is obtained. To convert this data set to be represented in form of a binary element system the following expressions are used where mole fractions of elements A and B are calculated in the liquid phase:

$$W_A^l = \frac{x_1 + x_3}{x_1 + x_2 + 2 \cdot x_3} \quad (1)$$

$$W_B^l = \frac{x_2 + x_3}{x_1 + x_2 + 2 \cdot x_3} \quad (2)$$

In the above equations W_A^l and W_B^l are the liquid mole fractions of elements A and B , respectively. For calculation of the element mole fractions in vapor phase (W_A^y and W_B^y), the equations used are the same as (1) and (2) where instead of liquid molar fraction (x_i), the vapor molar fraction (y_i) is used.

The design task is to separate a binary element mixture that is 70 mole percent element A ($Z_{W_A} = 0.7$, $Z_{W_B} = 0.3$) into 50 element mole percent bottoms product ($W_{AB}^l = 0.50$) and 99 element mole percent distillate ($W_{A,d}^l = 0.99$) product. Note that based on the binary element reaction matrix, element A and B correspond to isobutene and methanol, respectively. The element feed flow rate is 100 Kg-mole element/hr at 300K and 1 atm. The operating pressure of the reactive distillation column is 1 atm and pressure drop across the column is assumed to be negligible. The reflux element ratio (RR) is 2. The physical and chemical equilibrium curve is constructed using the data set presented in Fig. 1. Theoretical reactive stages are calculated from the reactive McCabe-Thiele method. A partial reboiler, total condenser and chemically saturated liquid reflux are set for the column. In order to design the described reactive distillation column for MTBE synthesis, McCabe-Thiele method is used. Fig. 1 depicts the reactive distillation column design using reactive McCabe-Thiele method. As it is shown in Fig. 1, the reactive distillation column has five reactive stages.

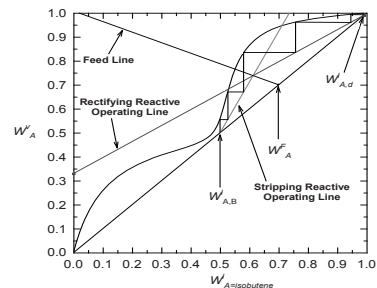


Figure 1: Reactive distillation column design. Reactive McCabe-Thiele method for the MTBE reactive system.

In this work, the optimal feed location of the reactive distillation column is determined using the driving force diagram. Reactive McCabe-Thiele method has been only used to determine the number of stages.

The feed and product specifications are already known since they were used in the reactive McCabe-Thiele method. The optimal feed location at the maximum driving force can be found using (3).

$$N_F = N(1 - D_x) \quad (3)$$

In (3), N is the number of stages which was obtained from the reactive McCabe-Thiele method (was found to be 5); D_x is the value corresponding to the maximum driving force on the x -axis ($D_x = 0.61$). The optimal feed location is identified using the additional rules for driving force [4] and therefore it is stage 1 from the top of the column.

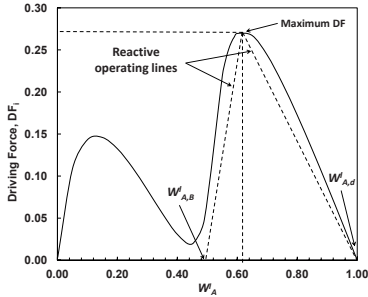


Figure 2: Reactive driving force diagram for MTBE reactive system).

Optimal Design-Control Solutions

For each reactive distillation column design problem, the driving force diagram is drawn and the design target is selected at the highest driving force (see Figure 3). From a process design point of view, at these targets, the optimal design objectives can be obtained. From a controller design point of view, at these design targets the controllability and operability of the process is best satisfied. The value of the derivative of controlled variables y with respect to disturbances in the feed, d , dy/dd and manipulated variables, u , dy/du will determine the process sensitivity and influence the controller structure selection. Accordingly, dy/dd and dy/du are defined as [9]:

$$\frac{dy}{dd} = \left(\frac{dy}{d\theta} \right) \left(\frac{d\theta}{dx} \right) \left(\frac{dx}{dd} \right) \quad (4)$$

$$\frac{dy}{du} = \left(\frac{dy}{d\theta} \right) \left(\frac{d\theta}{dx} \right) \left(\frac{dx}{du} \right) \quad (5)$$

The values for $d\theta/dx$ can be obtained from the process (dynamic and/or steady state) constraints:

$$\frac{dx}{dt} = f(x, y, u, d, \theta, Y, t) \quad (6)$$

and values for $dy/d\theta$, dx/dd and dx/du can be obtained from constitutive (thermodynamic) constraints:

$$0 = g(u, x, y) - \theta \quad (7)$$

The primary controlled variable is $D_{x,max}$, which is the x -axis value corresponding to the maximum driving force (DF_i). This resembles the purity of element A at the maximum driving force. The secondary controlled

variables are the product purities, which are the desired product composition at the top and bottom of the column, W_A^d and W_A^b . The reason behind this selection is that by controlling W_A^d and W_A^b at the maximum point of the driving force will require less control effort in terms of reflux ratio (RR), and reboil ratio (RB) in the presence of disturbances in the feed compared to any other candidate point.

There are several key concepts in analyzing the sensitivity of controlled variables to the disturbances in the feed which are outlined as follows:

- The desired element product at the top and the bottom is W_A^d (product element composition at the top, distillate product) and W_A^b (element composition at the bottom, bottom product).
- At the maximum point of the driving force diagram, W_A^d and W_A^b (controlled variables) are the least sensitive to the imposed disturbances in the feed.
- The design variables vector is $y = [W_A^d \ W_A^b]$, $x = DF_i$, is selected on the y -axis of the driving force diagram.
- The disturbances vector is, $d = [F_f \ z_{W_A^f}]$ (feed flowrate and feed composition of element A).

Using the above key concepts, the sensitivity of variable y with respect to variable d , can be expressed as follows:

$$\frac{dy}{dd} = \begin{bmatrix} \frac{dW_A^d}{dF_f} & \frac{dW_A^d}{dz_{W_A^f}} \\ \frac{dW_A^b}{dF_f} & \frac{dW_A^b}{dz_{W_A^f}} \end{bmatrix} = \begin{bmatrix} \left(\frac{dW_A^d}{dDF_i} \right) \left(\frac{dDF_i}{dW_A^d} \right) \left(\frac{dW_A^d}{dF_f} \right) & \left(\frac{dW_A^d}{dDF_i} \right) \left(\frac{dDF_i}{dW_A^d} \right) \left(\frac{dW_A^d}{dz_{W_A^f}} \right) \\ \left(\frac{dW_A^b}{dDF_i} \right) \left(\frac{dDF_i}{dW_A^b} \right) \left(\frac{dW_A^b}{dF_f} \right) & \left(\frac{dW_A^b}{dDF_i} \right) \left(\frac{dDF_i}{dW_A^b} \right) \left(\frac{dW_A^b}{dz_{W_A^f}} \right) \end{bmatrix} \quad (8)$$

Values of dDF_i/dW_A^d are calculated and shown in Fig. 4. Note that in Fig. 4, two other points (points II and III) which are not at the maximum are identified as candidate alternative designs for a distillation column, which will be used for verification purposes.

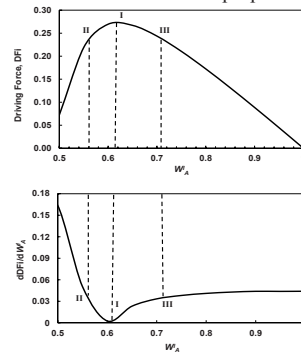


Figure 3: Driving force diagram for W_A - W_B separation (reactive zone only – top figure) and its corresponding derivative of DF_i with respect to W_A^d (bottom figure).

Furthermore, at point (I) the value of $dFDI/dW_A^I$ is equal to zero. Therefore,

$$\frac{dy}{dd} = \begin{bmatrix} \frac{dW_A^d}{dF_f} & \frac{dW_A^B}{dF_f} \\ \frac{dW_A^d}{dz_{W_{sf}}} & \frac{dW_A^B}{dz_{W_{sf}}} \end{bmatrix} \approx \begin{bmatrix} 0 & 0 \\ 0 & 0 \end{bmatrix} \quad (9)$$

The controlled variables are defined as top and bottom element A composition W_A^d and W_A^B . In this case, the potential manipulated variables are reflux ratio (RR) and reboil ratio (RB). (12) and (13) give the top and bottom product compositions with respect to the driving force. Hence, they are differentiated with respect to RR and RB . The best controller structure can easily be determined by looking at the value of dy/du . It can be noted from (10) that since the values of dW_A^d/dRR and dW_A^B/dRB are bigger, controlling W_A^d by manipulating RR and controlling W_A^B by manipulating RB will require less control action.

$$\frac{dy}{du} = \begin{bmatrix} \frac{dW_A^d}{dRR} & \frac{dW_A^d}{dRB} \\ \frac{dW_A^B}{dRR} & \frac{dW_A^B}{dRB} \end{bmatrix} = \begin{bmatrix} DF_i & 0 \\ 0 & -DF_i \end{bmatrix} \quad (10)$$

This is because only small changes in RR and RB are required to move W_A^d and W_A^B in a bigger direction. Note that most of the modelling of dynamic reactive distillation operations has been done by introducing a rate of reaction expression in the component mass balances. However, when the chemical reactions occurring are fast enough to reach the equilibrium (for example, MTBE reactive system) chemical equilibrium condition is implicitly incorporated into the element mass balances through the functionality of the phase compositions on the element chemical potentials [3].

The open-loop and closed-loop performance of the system has been tested with the Proportional-Integral (PI) controller in a discrete-time manner. The rigorous dynamic reactive distillation model [3] was used.

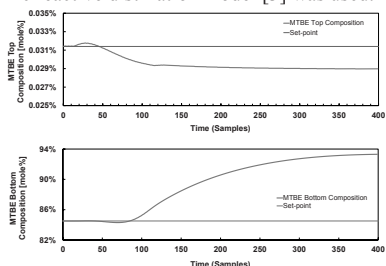


Figure 4: Open-loop performance of Design (I) to a disturbance in the feed.

Figure 4 and Figure 5 show the open-loop and closed-loop performance of the system at maximum driving force (Design (I)), respectively. The disturbance scenario is that after 15 samples, the feed flowrate of element A (isobutene) is increased from 70 kg-mole to 85 kg-mole (~12% step change in composition of

isobutene). This disturbance results in a change in total feed flowrate by +15% and also a change in the feed composition.

It can be seen in Fig. 7 that disturbance has been rejected with least interaction between the loops and both top and bottom compositions are well controlled using the selected pairing obtained from the driving force. Note that the control of the MTBE top composition is achieved with very small changes in RR .

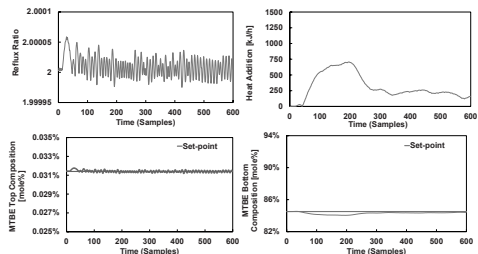


Figure 5: Closed-loop performance of the control structure for Design (I) to a disturbance in the feed.

Conclusions

Integrated process design and control of a ternary compound reactive distillation process was investigated in this work. The optimal design-control solutions were obtained analytically and verified through rigorous dynamic simulations. It is verified that the reactive distillation design option is less sensitive to the disturbances in the feed at the highest driving force and has the inherent ability to reject disturbances.

References

- Seferlis, P., Georgiadis, M. C. (2004). The integration of process design and control, Elsevier B. V., Amsterdam.
- N.M. Nikacevica, A.E.M. Huesman, P.M.J. Van den Hof, A.I. Stankiewicz, Chem. Eng. Process. 52 (2012) 1-15.
- E.S. Pérez Cisneros, Modelling, design and analysis of reactive separation processes, Ph.D. Thesis, Technical University of Denmark, Lyngby (1997).
- E. Bek-Pedersen, R. Gani, Chem. Eng. Process. 43 (2004) 251–262.
- M. K. A. Hamid, G. Sin, R. Gani, Comput. Chem. Eng. 34 (2010) 683-699.
- M.L. Michelsen, Fluid Phase Equilib. 53 (1989) 73-80. O.S. Daza, E.S. Pérez Cisneros, R. Gani, *AIChE J.* 49 (2003) 2822-2841.
- E.S. Pérez Cisneros, R. Gani, M.L. Michelsen, Chem. Eng. Sci. 52 (1997) 527–543.
- B. M. Russel, J. P. Henriksen, S. B. Jørgensen, R. Gani, Comput. Chem. Eng. 26 (2002) 213-225.



Fauziah Marpani

Phone: +45 4525 2966
 E-mail: fama@kt.dtu.dk
 Discipline: Reactive Separation Technology

Supervisors: Anne S. Meyer
 Manuel Pinelo

PhD Study
 Started: Nov 2012
 To be completed: Oct 2015

Reactive Separation Technology: Biomimetic Enzyme Immobilization on Polymeric Membrane

Abstract

Re-usability and stabilization of enzymes are important advantages of enzyme immobilization. Integration of enzyme immobilization with membrane technology enables continuous operations, facile product purification, and may prevent product inhibition. Despite these advantages, less than 20% of industrial catalytic processes currently rely on immobilized enzymes, and less than 1% employs membranes for immobilization. This is due to the inadequacy of the current enzyme immobilization techniques, which induce dramatic losses of enzyme activity. Nature has exceeded such constraints by using anchoring methods that provide the structural flexibility needed for efficient catalysis.

Introduction

Enzymes are now widely used industrially in new green chemistry processes. Many cellular reactions within metabolic pathways are not catalysed by 'soluble' enzymes, but rather via one or more membrane-associated multienzyme complexes. This has important implications for the overall efficiency, specificity, and regulation of metabolic pathways [1]. The core aim of the PhD project is to examine and reproduce selected methods of multienzyme immobilization that nature uses in metabolic pathways to make biosynthetic process more efficient and feasible. Immobilization of enzymes on membranes permits the efficient reuse of

enzymes, provides facile separation enzyme-product and enhances enzyme stability [2]. Current techniques of immobilization are often based on rigid covalent bonds enzyme-membrane which often results in significant reductions of flux across the membrane and dramatic losses in the level of enzyme activity.

Specific Objective

A part of the whole project objective is to utilize membrane systems for enzyme entrapment. Can the immobilization be done in a smart way for enhanced enzyme activity?

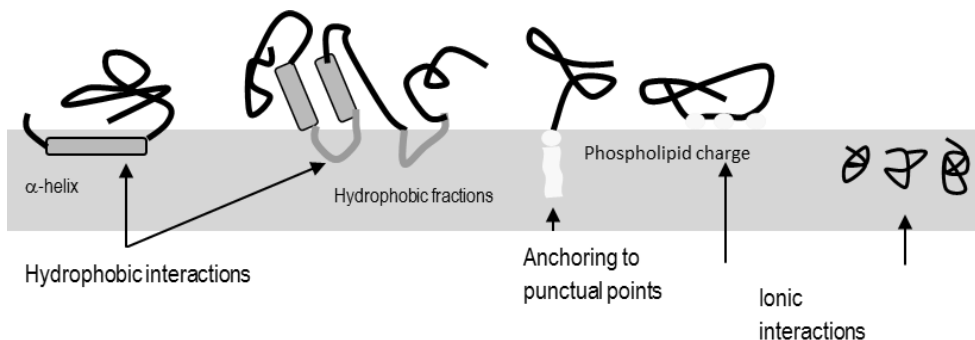


Figure 1: Strategies used by nature to maintain enzyme mobility and flexibility in/on membranes.

Fouling induced enzyme immobilization on polymeric membrane

Reactive separation technology refers to the coupling of selective biocatalytic conversion and product recovery via filtration simultaneously. Membrane separation is gaining its momentum due to limited amount of energy required to perform the separation, besides being inexpensive, and easy to operate and scale up [3]. In addition, the porous structure of the membrane which can function as a selective barrier as well as a support for enzyme immobilization enables continuous operation, facile product purification and prevents product inhibition [4]. Enzyme immobilization can furthermore enhance the overall productivity and robustness by improving reusability and stability of the enzyme and allow better control of catalysis process. In an enzymatic membrane reactor (EMR), enzymes can be either free in solution or immobilized in/on porous structure of the membrane. Either free or immobilized, the occurrence of enzymes makes membrane separation in EMR prone to fouling. Even though fouling is always

seen as an undesirable effect in membrane technology, previous studies have shown that fouling can be exploited in a positive manner when it comes to enzyme immobilization. Indeed, previous works by Luo et al. [5] have shown that membrane fouling can be used as a strategy for efficient enzyme immobilization, given the similarities between the mechanisms promoting enzyme immobilization and membrane fouling (Table 1). Alcohol dehydrogenase (ADH) has been immobilized in the support layer of a polysulfone membrane following such technique, resulting in a significant increased amount of enzyme loading per unit area of the membrane [5]. However, the hydrophobicity of the support layer was found to be unsuitable for the enzyme microenvironment. ADH has been also selected for this study, as it is known to be highly active but easily prone to lose its activity under different conditions [6]. Several attempts have been made to immobilize ADH, and in all cases it was found a trade-off between activity and stability of the enzyme [6].

Table 1: Similarities between membrane fouling and enzyme immobilization mechanisms [5].

Fouling types	Behavior description	Immobilization mechanisms
Adsorption fouling	Particles are adsorbed in/on membrane by hydrophobic and electrostatic interactions	Adsorption
Pore blocking	Particles are entrapped or embed in membrane pores	Entrapment
Membrane surface modification by foulants	Particles are combined with membrane by chemical binding between their functional groups	Covalent coupling
Combined fouling or inorganic-organic fouling or "cake" layer	Particles are combined with membrane by chemical cross-linker (acting as "bridge" between particles and membrane or among particles)	Cross-linking
Biofouling	Microorganisms or bioactive particles grow or adhere on membrane	Affinity

Current work

The current work is basically to address the main problems when entrapping enzyme on the surface of the membrane where low enzyme loading and severe enzyme leakage were observed. For this purpose, alginate is selected as the agent for enzyme entrapment as it gives natural microenvironment to the enzyme, biocompatible and ease of gelation. A stable alginate gel layer was induced and attached on the surface of polysulfone membrane using dopamine. It is worth mentioning that the induction of the gel layer was simultaneously with the immobilization of enzyme, in this case Alcohol dehydrogenase (ADH). EMR was then applied in the conversion of formaldehyde to methanol which requires cofactor of β -nicotinamide adenine dinucleotide (NADH). The model reaction is the final part of a three steps biocatalytic reaction to convert carbon dioxide to methanol.

Acknowledgement

The author would like to thank Ministry of Education and Universiti Teknologi MARA, Malaysia for the financial support.

References

1. R.J. Conrado, J.D. Varner, M.P. DeLisa, Engineering the spatial organization of metabolic enzymes: mimicking nature's synergy, *Current Opinion in Biotechnology* 19 (2008) 492-499.
2. D. Brady, J. Jordaan, Advances in enzyme immobilisation, *Biotechnology Letters* 31 (2009) 1639-1650.
3. P. Pal, J. Sikder, S. Roy, L. Giorno, Process intensification in lactic acid production: A review of membrane based processes, *Chem. Eng. Process. Process Intensif.* 48 (2009) 1549-1559.
4. J. Luo, A.S. Meyer, G. Jonsson, M. Pinelo, Enzyme immobilization by fouling in ultrafiltration membranes: Impact of membrane configuration and type on flux behavior and biocatalytic conversion efficacy, *Biochem. Eng. J.* 83 (2014) 79-89.
5. J. Luo, A.S. Meyer, G. Jonsson, M. Pinelo, Fouling-induced enzyme immobilization for membrane reactors, *Bioresource Technology* 147 (2013) 260-268.
6. J.M. Bolivar, J. Rocha-Martín, C. Mateo, J.M. Guisan, Stabilization of a highly active but unstable alcohol dehydrogenase from yeast using immobilization and post-immobilization techniques, *Process Biochem.* 47 (2012) 679-686.



Piotr Mazurek

Phone: +45 4525 6196
E-mail: pioma@kt.dtu.dk

Supervisors: Anne Ladegaard Skov
Søren Hvilsted

PhD Study
Started: January 2013
To be completed: January 2016

Novel encapsulation technique for incorporation of high permittivity fillers into silicone elastomers

Abstract

The approach investigated here is a new type of encapsulation based on a recently developed flow-focusing microfluidic technique. A versatile and robust microfluidic device has been designed and fabricated, which allows for preparation of core-shell microspheres of extremely narrow size distribution. This encapsulation method allows to uniformly distribute high dielectric permittivity polar liquids within hydrophobic poly(dimethyl siloxane) films. The study reveals a potential of PDMS/water composites as a promising dielectric electroactive material.

Introduction

There is no unequivocal answer to the question of what increases actuation performance of dielectric electroactive polymers most efficiently. The actuation performance of a DEAP, which in other words can be described as strain produced on elastomer when applying electric field and can be defined as $S = \epsilon_0 \epsilon_r Y^{-1} V^2 d^{-2}$ (1), where ϵ_0 and ϵ_r are vacuum permittivity and relative permittivity, respectively. Y is the Young's modulus of material, V is applied voltage and d thickness of investigated elastomer. According to equation (1) there are four parameters that can be altered in order to increase the actuation performance. These are ϵ_r , Y , d and the maximal value of quotient V/d which is defined as the breakdown strength of the polymer composition. Goswami *et al.* discussed merits of varying these parameters and concluded that modification of relative permittivity of material gives most prominent results and leaves most room for improvements [1].

Different approaches have been performed in order to increase relative permittivity of dielectric elastomers. One of the most frequently reported methods is based on mixing elastomers with high permittivity fillers like carbon nanotubes, carbon black, titanium dioxide etc. [2,3]. Composites containing different amounts of fillers can potentially improve not only the actuation performance but also mechanical properties of final material. Increasing attention is also attracted towards grafting of polar molecules onto the silicone polymer backbone, which significantly improves the dielectric permittivity without compromising its high inherent

breakdown strength and increasing dielectric loss [4]. As alternative to methods described above, Opris *et al.* [5] presented a novel way of incorporation of conductive fillers encapsulated within an insulating shell into elastomer networks. In their approach poly(aniline) (PANI) was encapsulated in poly(divinyl benzene) (PDVB) forming capsules smaller than 1 μm , which were later dispersed in poly(dimethylsiloxane) (PDMS) films. In this way the filler particles were efficiently separated from each other by non-conductive layers preventing formation of conductive paths throughout the material. By applying this technique they successfully improved the relative permittivity of PDMS based composites keeping breakdown strengths at acceptable levels.

In this work we focus on preparation of liquid-core microcapsules of extremely narrow size distribution and incorporating them into PDMS matrix. We show how different amounts of encapsulated filler influence mechanical and electrical properties of the formed composites.

Experimental

Thiol-ene-epoxy tailored flow-focusing microfluidic device was used in order to prepare water containing PDMS microcapsules, which were subsequently incorporated into PDMS films (Sylgard 184 mixed in ratio 13:1). 10, 20, 30 wt.% of microcapsules were introduced to composites, which corresponded to 1.5, 3 and 4.5 wt.% of incorporated water, respectively. All PDMS formulations were studied in terms of mechanical and electrical properties. Frequency sweep

tests performed on Ares G2 TA Instruments rheometer were conducted in order to determine both storage and loss moduli of investigated compositions. 25 mm of diameter and 1 mm thick disc samples were tested in the frequency range between 100 Hz and 0.001 Hz and under controlled strain mode (2% strain) at room temperature. Novocontrol broadband dielectric spectrometer was used to investigate dielectric permittivity, dielectric losses and conductivity of samples. 20 mm of diameter and 1 mm thick disc specimens were tested in the frequency range between 10^6 Hz and 10^{-1} Hz.

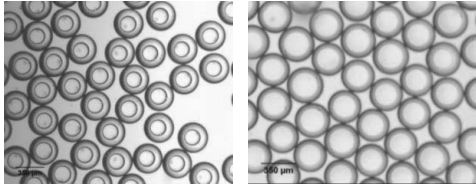


Figure 1: Microscope images of the microcapsules obtained from flow-focusing microfluidic device.

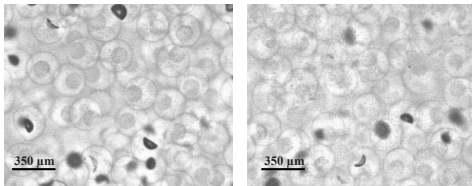


Figure 2: Microscope images of crosslinked PDMS films with incorporated core-shell microspheres.

Results and discussion

The prepared films are stable and free-standing at the current film thicknesses and have considerable strength when handling them. Rheology measurements were carried out on four different specimens and results summarizing changes of storage modulus as function of frequency were plotted in Figure 3.

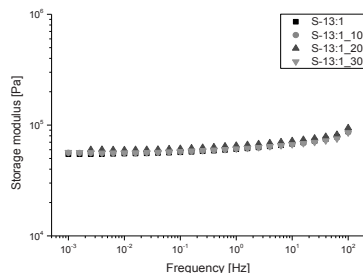


Figure 3: Storage modulus of unfilled elastomer and different PDMS-microcapsules.

It can be seen clearly that curves representing storage moduli of all tested compositions indicate nearly identical elastic behavior when applying small stresses.

In all cases the elastic modulus at plateau region (from 10^{-1} – 10^{-3} Hz) varies from 55 kPa to 60 kPa. These small differences are within the range of measurement error and therefore it can be assumed that incorporation of core-shell microspheres of the structure described in our study does not influence significantly the viscoelastic behavior of tested PDMS compositions.

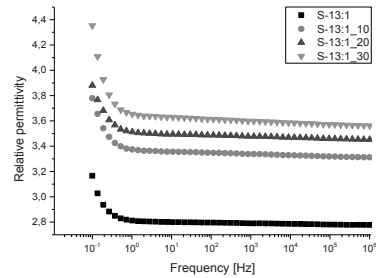


Figure 4: Relative permittivity of elastomer reference and different PDMS-microcapsules composites.

As described previously, the main reason for introducing microcapsules into PDMS films is to enhance the relative permittivity of final product without compromising other dielectric and mechanical properties. As can be seen in Figure 4 the dielectric constant of Sylgard 184 was successfully increased by incorporation of water-core microcapsules. The values of ϵ_r measured at frequency of 10^3 Hz indicate an increase from 2.8 for unfilled network to 3.6 for composite containing 30 wt.% of microcapsules (4.5 wt.% of water). Conductivity was proved to remain at nearly same level for all tested compositions. This implies that each portion of water in investigated systems was hermetically encapsulated within PDMS insulating shell and therefore conductive pathways throughout the material were unlikely to appear and wherefore the overall conductivity remained almost unaffected.

Conclusions

In this pioneer approach we present results of incorporation of high dielectric constant polar liquids into hydrophobic PDMS elastomer. Encapsulated water significantly increased the relative permittivity of PDMS without compromising its mechanical properties and resistivity.

References:

1. K. Goswami, *et al.*, Smart Mater. and Struct 22 (2013) 115011
2. A.L. Skov, *et al.*, Proc. of SPIE, 8687 (2013) 868711-1
3. F. Galantini, *et al.*, Smart Mater. and Struct., 22 (2013) 5
4. C. Racles, *et al.*, Smart Mater. and Struct., 22 (2013) 104004
5. M. Olberg, D.M. Opris, *et al.*, Adv. Funct. Mater., 20 (19) (2010) 3280-3291



Lisa Mears

Phone: +45 42 26 06 15
E-mail: lmea@kt.dtu.dk

Supervisors: Prof. Krist V. Gernaey, DTU
Ass. Prof. Gürkan Sin, DTU
Dr. Stuart M. Stocks, Novozymes

PhD Study
Started: December 2013
To be completed: December 2016

Novel Strategies for Control of Fermentation Processes

Abstract

Industrial fermentation processes are typically operated in fed batch mode, which poses specific challenges for process modelling, monitoring and control. This is due to many reasons including non-linear behaviour, and a relatively poor understanding of the system dynamics. It is therefore challenging for the process engineer to optimise the operation conditions, due to a lack of available process models, and complex interactions between variables which are not easy to define, especially across scales and equipment. The aim of this work is to develop a control strategy which is applicable to industrial scale fermentation processes. The scope of this project is to consider modelling approaches in order to characterise fermentation batches, including both mechanistic and data driven strategies. Utilising the model as a tool for process monitoring, can then aid control strategy development. This work is completed in collaboration with Novozymes A/S and considers an industrially relevant fermentation process.

Introduction

Bioprocesses are inherently sensitive to fluctuations in processing conditions and must be tightly regulated to maintain cellular productivity. Industrial fermentations are often difficult to replicate across production sites or between facilities as the small operating differences in the equipment affect the way the batches should be optimally run. In addition, batches run in the same facility can also be affected by batch variations in the growth characteristics of a specific cultivation. For these reasons it is important to have optimal control of the process to achieve the desired product quality and yields. It is especially important to regulate feed rates and achieve the highest productivity without over feeding the system.

Over feeding increases production cost, due to expensive raw materials [1], and also produces unwanted metabolites. There is demand therefore to research strategies to continually monitor the performance of a fermentation which is universal across equipment, and to design control systems which quickly and accurately respond to maintain the process within tightly controlled conditions.

Discipline

This research project focusses on the discipline of Industrial fermentation technology and is conducted in collaboration with Novozymes A/S.

Specific Objectives

The overall objective for this work is to develop a control strategy which is applicable to an industrial scale fermentation process. In order to achieve this goal, the following objectives are described:

- Literature review of control strategies applied to fermentation systems to assess the state of the art. This is focused on feed strategy development.
- A study of fermentation modelling to include both black box modelling and mechanistic modelling approaches.
- Development of a process model which characterises the process of interest operating at Novozymes A/S.
- Development of a control strategy which utilizes the model developed in the previous stage of the work to control the feed rate in the fed batch operation.

Modelling approaches

Models for fermentation processes are typically combinations of mechanistic models with empirical relations [2]. One challenge of mechanistic modelling is a lack of measurements for important variables such as biomass concentration, product concentration or substrate concentration [2]. There are however

successful applications of mechanistic models applied to fermentation processes, including work from Novozymes A/S [1][3] involving the modelling of filamentous fungal fermentations.

There is also a vast amount of data generated from each processing batch which can be investigated using data driven modelling methods. With a lack of detailed knowledge of the process this can be a powerful tool to determine trends in the data. A useful method, which has been applied in this project is multivariate analysis applied to batch process data [4]. Future work is continuing with this approach as part of this study.

Modelling approaches should combine process understanding whilst utilizing available data. Given a robust process model it may be possible to apply optimization algorithms [2] in order to guide process optimization, and control strategy development.

Control strategy approaches

Control strategy development must consider the cost of implementation balanced with the benefits brought through process optimisation [5]. Due in part to the resources and time associated with modelling, it is common to use a simple monitoring approach to feed

Table 1: Comparison of 8 advanced control strategies to assess the benefits and disadvantages for application to fermentation processes

	Open loop	Gain schedule	Adaptive control	MPC	ANN	Fuzzy control	SPC	Probing
non-linear dynamics	✓	✓	✓	✓	✓	✓	✓	✓
unpredictable dynamics		✓	✓	✓	✓	✓	✓	✓
Provides process insight						✓	✓	
Requires past data set				x	x	x		
Requires model		x	x					
Requires user experience	x	x				x		

control. This is typically single input, single output, whereby the feed rate is regulated based on a measured variable, for example the dissolved oxygen. There are many more advanced control strategies developed in the literature which show promise for more optimal control, however the application in industry is limited. A literature review of advanced control strategies applied to fermentation systems has been completed, providing an overview of the current state of the field. Table 1 shows some considerations for each strategy which has

been reviewed, showing the benefits balanced with the requirements for development.

The control strategy employed will depend on the results of the modelling stage of this project, as well as discussions with the collaborating company.

Conclusions

By combining data driven methods and mechanistic modelling techniques it is possible to characterise the industrial fermentation system. The model developed will then be used for process optimization studies, and finally provide a focus for control strategy development.

Acknowledgements

The author would like to thank the Technical University of Denmark and Novozymes A/S for the financing of this PhD study.

References

1. M. O. Albaek, K. V Gernaey, M. S. Hansen, and S. M. Stocks, "Evaluation of the energy efficiency of enzyme fermentation by mechanistic modeling," *Biotechnol. Bioeng.*, vol. 109, no. 4, pp. 950–61, Apr. 2012.
2. L. R. Formenti, A. Nørregaard, A. Bolic, D. Q. Hernandez, T. Hagemann, A.-L. Heins, H. Larsson, L. Mears, M. Mauricio-Iglesias, U. Krühne, and K. V Gernaey, "Challenges in industrial fermentation technology research.," *Biotechnol. J.*, vol. 9, no. 6, pp. 727–38, Jun. 2014.
3. M. O. Albaek, K. V Gernaey, M. S. Hansen, and S. M. Stocks, "Modeling enzyme production with *Aspergillus oryzae* in pilot scale vessels with different agitation, aeration, and agitator types.," *Biotechnol. Bioeng.*, vol. 108, no. 8, pp. 1828–40, Aug. 2011.
4. P. Nomikos and J. F. MacGregor, "Multi-way partial least squares in monitoring batch processes," *Chemom. Intell. Lab. Syst.*, vol. 30, no. 1, pp. 97–108, Nov. 1995.
5. A. Lübbert and S. Bay Jørgensen, "Bioreactor performance: a more scientific approach for practice.," *J. Biotechnol.*, vol. 85, no. 2, pp. 187–212, Feb. 2001.

**Mohd Shafiq Mohd Sueb**

Phone: +45 4525 2705
E-mail: mosh@kt.dtu.dk
Discipline: Reaction Separation Technology

Supervisors: Manuel Pinelo
Anne S. Meyer

PhD Study

Started: December 2013
To be completed: December 2016

Enzymatic Hydrolysis of Xylan Integrated With Membrane Technology: Free Enzyme System

Abstract

The needs to find alternative source of energy has led to the discovery of new environmentally materials especially hemicellulose. Xylan is one of the major components that comprises in hemicellulose has becoming the main focus in hydrolyzing it to monosaccharides so that it could be used further for the production of biofuel. In this study, a commercial xylan from beechwood was used to depolymerize it into xylose. Nanofiltration membrane with molecular weight cut off (MWCO) 1kDa was employed in the dead-end filtration system and the enzymatic hydrolysis was done in a free enzyme system.

Introduction

The recent interests of exploring new materials for producing renewable fuel have led to many studies in this area. Despite of that, these alternative materials would be appreciated if they are being recycled or abundant, hence giving the added value to the products. One of the most become concerns by researchers nowadays due to its value is lignocellulosic material. According to Saha, (2003), one of the most abundant components that comprises of hemicellulose is xylan; a heterogenous polysaccharides consisting of backbone of β -1,4-linked xylopyranosyl units, half of which are linked to acetyl, α -methylglucuronyl, or L-arabinofuranosyl residues [1]. They are most commonly found in hardwood hemicellulose [2] mainly in the secondary cell wall and is considered to be forming an interphase between lignin and other polysaccharides [3].

Degradation of xylan has said to be a resource for energy in future [4]. Due to its great abundance in nature, xylan offers a potential to be consumed once it is converted into xylo-oligosaccharides and xylose [5]. Therefore, a mixture of significant enzymes that involves in the enzymatic hydrolysis of xylan is required to deconstruct xylan into a simple monosaccharide prior to biofuel production. The enzymatic hydrolysis includes endo- β -1,4-xylanase, β -D-xylosidase, α -L-arabinofuranosidase, α -glucuronidase, acetyl xylan esterase and ferulic esterase [6].

Although the total breakdown of xylan requires the cooperative action of many enzymes (endo- β -1,4-xylanase, β -xylopyranosidase, α -L-arabinofuranosidase, acetylxylan esterases, α -D-glucuronidase), the key enzyme is the endo- β -1,4-xylanase because it cleaves the internal glycosidic bond of the polysaccharide [7]. This is also in agreed with Dodd and Cann (2009), saying that endo-1,4- β -xylanase is one of the critically vital enzymatic activities for the depolymerization of xylan for which it cleaves the β -1,4 glycosidic linkage between xylose residues in the backbone of xylan.

Specific Objectives

The main purpose of this project is to combine enzyme reactions and membrane separation, in an integrated manner, in order to increase the conversion and productivity of such reactions. The use of membranes for simultaneous removal of products from the enzyme reaction reduces possible product inhibition, and allows to reuse enzymes and to obtain the product in the range of sizes that we are interested in.

In addition, there are two main objectives were required to be accomplished for this particular study:

1. Evaluation on the filtration behaviour of endoxylanases and xylosidases on a beechwood xylan solution in a free enzyme reactor system.
2. Designing different configuration of enzymatic hydrolysis for maximizing the yield

Results and Discussion

In this research works, a dead-end filtration system was employed and hence the batch mode was applied. Consequently, the mass of the filter cake build up until all the cells are deposited whereby the filtration process will no further proceed [8]. The particles are gradually deposited on the surface of the membrane after equilibrium is established between the convection and diffusion processes. In the membrane separation process, polarization concentration cannot be avoided, and one consequence is an important reduction of permeate flux [9].

The linear graph of reciprocal flux with respect to the permeate volume was said to follow the cake-filtration model and the reduction of permeate flux was mainly caused by the internal pore blocking and the gel layer formation on the membrane surface as shown in Figure 2, corresponded to a longer filtration time.

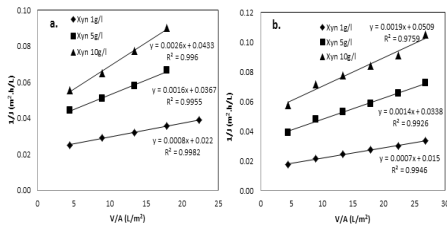


Figure 1: Reciprocal flux as a function of the permeate volume with a. 1% [E/S] xylanase b. 1% [E/S] xylosidase.



Figure 2: Formation of gel layer on the membrane surface reduces the permeate flux

Table 1: Xylan hydrolysis (%) for different configurations of enzymatic hydrolysis with xylan 5 g/l

Design configuration	Xylan hydrolysis (%)
Xylanase +xylosidase (reaction & filtration)	18.16 ± 0.58
Xylanase + xylosidase (reaction)	30.19 ± 1.46
Xylanase (reaction & filtration) + Xylosidase (reaction) – cascade	20.95 ± 0.76
Xylanase + xylosidase (reaction) then filtration	28.01 ± 1.47

Combination of both enzymes in the hydrolysis of xylan was expected to give a better hydrolysis as

compared to a single working enzyme. There were 4 different configurations designed in order to maximize the yield of hydrolysis. In Table 1, it was found that the experiment without simultaneous filtration had given the maximum yield. In contrast, the least yield was recorded by the configuration with both simultaneous filtration and reaction. Less interaction time between xylooligomers and xylose before it passed through the membrane might be a factor to have fewer yield in permeate.

Conclusion

In conclusion, the combination of xylanase and xylosidase without simultaneous filtration for xylan hydrolysis had shown significant improvement as compared to the individual hydrolytic enzyme as well the other configurations. The internal pore blocking was found to be the main fouling mechanism that substantially reduced the permeate flux especially for the hydrolysis with xylanase.

References

- P. Biely, "Microbial xylanolytic systems," *Trends Biotechnol.*, vol. 3, no. 11, pp. 286–290, Nov. 1985.
- B. C. Saha, "Hemicellulose bioconversion.," *J. Ind. Microbiol. Biotechnol.*, vol. 30, no. 5, pp. 279–91, May 2003.
- R. D. Kamble and A. R. Jadhav, "Isolation, purification, and characterization of xylanase produced by a new species of bacillus in solid state fermentation.," *Int. J. Microbiol.*, vol. 2012, p. 683193, Jan. 2012.
- Z. Minic, C. Rihouey, C. T. Do, P. Lerouge, and L. Jouanin, "Purification and Characterization of Enzymes Exhibiting b - D -Xylosidase Activities in Stem Tissues of Arabidopsis 1," *Plant Physiol.*, vol. 135, no. June, pp. 867–878, 2004.
- G. Delcheva, G. Dobrev, and I. Pishtiyski, "Performance of *Aspergillus niger* B 03 β -xylosidase immobilized on polyamide membrane support," *J. Mol. Catal. B Enzym.*, vol. 54, no. 3–4, pp. 109–115, Aug. 2008.
- I. O. Dodd, D. and Cann, "Enzymatic deconstruction of xylan for biofuel production," *GCB Bioenergy*, vol. 1, no. 1, pp. 2–17, 2010.
- R. Cannio, N. Di Prizito, M. Rossi, and A. Morana, "A xylan-degrading strain of *Sulfolobus solfataricus*: isolation and characterization of the xylanase activity.," *Extremophiles*, vol. 8, no. 2, pp. 117–24, Apr. 2004.
- G. Foley, "A review of factors affecting filter cake properties in dead-end microfiltration of microbial suspensions.," *J. Memb. Sci.*, vol. 274, no. 1–2, pp. 38–46, Apr. 2006.
- J. Shin, K. Kim, J. Kim, and S. Lee, "Development of a numerical model for cake layer formation on a membrane," *Desalination*, vol. 309, pp. 213–221, Jan. 2013.

**Victor Buhl Møller**

Phone: +45 4525 2923
E-mail: Vibum@kt.dtu.dk
Discipline: Coating and polymer technology

Supervisors: Søren Kiil
Kim Dam-Johansen
Sarah Maria Frankær, Hempel

PhD Study

Started: August 2014
To be completed: August 2017

Acid and Abrasive Resistant Coatings for the Heavy Duty Industry

Abstract

Acid and abrasive resistant organic coatings have found their uses as cheap alternatives to ceramics and metal alloys as protective measures in the heavy duty industry. Despite the use of these coatings, there are still knowledge gaps when it comes to chemical interactions in the polymer matrix with aggressive species, as well as the combined erosion/corrosion mechanism that occurs when acidic chemicals are combined with abrasive particles. Development and research in this area has commenced, leading towards the construction of test equipment capable of exposing chosen coatings to simultaneous abrasive and corrosive environments, investigating effects of process and formulation variables and possible synergistic degradation mechanisms effects.

Introduction

The heavy duty industry displays a large variety of corrosive and environmentally damaging compounds in need of proper containment. With the added effects of hostile environments such as elevated temperatures and abrasive particles, structural material is put to the test. The use of protective coating technology provides a chemical barrier between the process solutions and the structural substrate, thus giving a desired chemical inertness while retaining the physical properties.

Organic coatings are polymeric materials similar to plastics, commonly seen as decorative paints. They are capable of adhering to a surface or a substrate to create a continuous thin film, and thermoset coatings are capable of hardening on the substrate with the addition of a curing agent.

Protective coating technology has found its uses in flue gas desulphurization plants, rail car tanks and copper mineral leaching, among others. The coatings are based on the chemical resistant epoxy technology, with the front runner being a styrene-cured epoxy vinyl ester, see Fig. 1, often reinforced with glass mats. Organic coatings are cheap alternatives to installing ceramic linings or using high grade acid resistant alloys, though they are considered more risky and are not as durable when it comes to wear resistance [1][2].

Never the less, the cost factor is enough for certain end-users to choose organic coating protection. They are often end-users who do not have much capital funding, or those whose goal is more short-sighted, such as being bought by larger companies after generating a net profit.

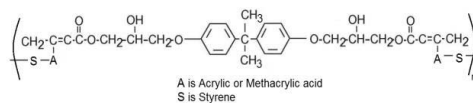


Figure 1: Structure of a repeating unit of bisphenol A epoxy vinyl ester cured with styrene.

Objectives

While currently in the initial steps of the project, efforts have been made to unearth all previously published work on the subject of acid and wear resistant organic coatings, and protective measures in acidic and/or abrasive environments.

The project will have emphasis on practical application as well as developing the research field academically, focus points include:

- Investigating physical and chemical degradation mechanisms and establishing predictive models
- Studying the effects of process and coating formulation variables
- Developing and constructing tests equipment capable of simulating abrasive slurry or/and combined acidic exposure
- Proving concept by on-site testing chosen coating candidates

Results and Discussion

When exposing organic coatings to acidic and abrasive environments they are physically worn down while

acidic chemicals slowly diffuse through the coating film and interact, if possible, with the cured resin. The resin types capable of resisting acid exposure have been identified and, as mentioned in the introduction, include epoxy technology such as epoxy vinyl ester but also bisphenol A, F and novolac type epoxies are relevant. Despite showing excellent chemical stability, both vinyl ester and amine cured epoxy matrices are not completely inert in acidic solutions, as shown in Fig. 2. The amine and ester linkages are susceptible to acids, where long term exposure can cause cracks and stress in a coating film, increasing diffusivity through the coating and thus decreasing its effective protection.

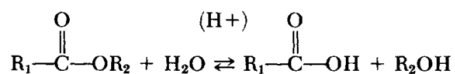
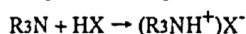


Figure 2: Chemical degradation of amine cured epoxy (top) and epoxy vinyl ester (bottom) in acidic solution [3][4].

Other important factors like curing agents, curing conditions and pigmentation have also been considered. They can have great effect on the chemical stability of the polymer matrix and diffusion rates of aggressive species through the coating film as well as the effective abrasive resistance [5][6].

The effects of sulfuric acid exposure on amine cured epoxies, is subject of little research though postulates such as those seen in Fig. 2 exist. Furthermore, acid exposure with abrasives present has not been thoroughly investigated. Are they synergistic? Which is dominant? What are the most effective methods to improve protection and lifetime? Both acid exposure and abrasive wear are important to understand if one is to develop or improve the protection of organic coatings. Therefore test equipment capable of simulating the effects of either or both simultaneously is being developed to further the understanding of protective coating applications. The test equipment will be able to vary key process conditions such as temperature, flow rates, pigmentation + acid type and concentration as well as coating formulation variables such as hardener content and binder type. All of which have profound impact on the coating's effective lifetime and performance [7][8].

Conclusion

Organic coatings have proved to be useful in providing cheap protection of vulnerable substrates in highly acidic and abrasive environments. Yet some of the underlying details of chemical interaction as well as the combined acid/abrasive exposure have only lightly been covered. It is essential to further the understanding of these topics to improve the products made for the industry. Having outlined the main areas of acid protective coating use as well as collected knowhow of coating chemistry and application, it is now possible to

commence design of test equipment to better understand and analyze the underlying causes for failure and success.

Acknowledgements

The project is funded by the Innovation Fund Denmark, co-sponsored by Hempel A/S and DTU.

References

1. P. Hag, N. Harrison, *Anti-Corrosion Methods and Materials*, 43 (2) (1996) 15-19.
2. C. Compère, J. Hechler, and K. Cole, *Progress in Organic Coatings*, 20 (2) (1992) 187-198.
3. R. C. Allen, *Polymer Engineering and Science*, 19 (5) (1979) 329-336
4. S. Ono, K. Tsuda, M. Kubouchi, H. Hojo, and T. Nishiyama, *Proceedings of ICCM-10*, 4 (1995) 215-222
5. H. Sembokuya, N. Y. Tsuda, and M. Kubouchi, *Materials Science Research International*, 9 (3) (2003) 230-234.
6. K. Tsuda, *Journal of the Japan Petroleum Institute*, 50 (5) (2007) 240-248.
7. H. Hojo, K. Tsuda, M. Kubouchi, and D. Kim, *Metals and Materials*, 4 (6) (1998) 1191-1197.
8. P. Kalenda, *Applied Polymer Science*, 45 (1992) 2235-2238.



Vikas Narayan

Phone: +45 50361335
E-mail: vina@kt.dtu.dk
Discipline: CHEC

Supervisors: Peter Glarborg
Peter Arendt Jensen
Ulrik Birk Henriksen

PhD Study
Started: July 2011
To be completed: November 2014

Ash Chemistry in Circulating Fluidized Bed

Abstract

A Low Temperature Circulating Fluidized Bed System gasifier allows pyrolysis and gasification to occur at low temperatures thereby improving the retention of alkali and other elemental species within the system. The aim of the PhD project is to study the behavior of alkali metals and biomass ash in a Low Temperature Circulating Fluidized Bed System. The focus of the study is ash transformation in the reactor system and bed de-fluidization.

Introduction

Gasification of herbaceous based fuels poses a large potential for power generation. Herbaceous fuels however, contain high amounts of alkali metals which get volatilized at high temperatures and form salts of low melting points and thus condense on pipelines, reactor surfaces and cause de-fluidization. The low Temperature Circulating Fluidized Bed Gasifier [1-2], functions without in-situ ash sintering and deposit problems and most potassium and chlorine are simply retained in a separate biomass ash stream. In this way a fuel-gas with low alkali content and a relatively high calorific value is produced that can be used for power production by use of a boiler.

Low Temperature Circulating Fluidized Bed System

As shown in Figure 1, the LT-CFB process consists of two reactors. The biomass fuel enters the first reactor which is the pyrolysis chamber. The fuel is pyrolysed at around 650°C due to good thermal contact with mainly re-circulated sand and ash particles from the char reactor. The heat for the pyrolysis reaction is thus provided by the sand bed particles and hot re-circulated char and ash particles. The residual char, pyrolysis gases and inert particles are led to the primary cyclone, which separates char and inert particles to a bubbling bed char reactor. In this reactor, the char is exposed to air to undergo gasification, at temperatures typically around 730°C. Some steam or water may also be added in order to improve the conversion of char and limit the reactor temperature.

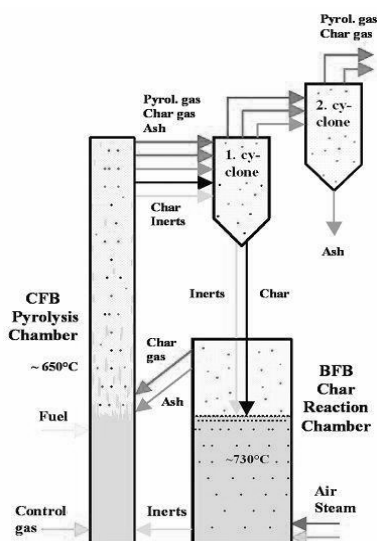


Figure 1: LT-CFB flow diagram [1-2]

The exit stream out of the pyrolysis chamber has a lower temperature compared to the temperature in the char reactor. Consequently, only small amounts of alkali species and ash components get carried off with the product gas and can therefore be separated efficiently in the cyclones. Moreover, the relatively low temperatures in the process limit the tendencies of de-fluidization in the system.

Objectives of the PhD Study

The aim of the PhD project is to study the behavior of alkali metals, Cl, S and biomass ash in a Low Temperature Circulating Fluidized Bed System. The focus of the study is on release of ash species with exit gas from the reactor system, ash transformation and bed de-fluidization.

Study of ash chemistry in the LTCFB Gasifier

To understand the behavior of alkali and ash in LTCFB reactors, exit gas measurements were made on a 100 kW LTCFB gasifier at Risø and on a 6MW LTCFB gasifier at Kalundborg. In addition to dust particle measurements, secondary cyclone ash bottoms and bed material samples from the gasifier were collected and analyzed with respect to their inorganic elemental composition. Also SEM and TGA analyses were performed on collected samples. The fuel used for all the plant runs was Danish Wheat Straw.

Observation and Results from the measurements in the LTCFB Gasifier

The dust loading in the product gas leaving the LTCFB gasifier for the 100 kW plant at Risø was measured to be 8-11 g/Nm³. In the 6 MW plant at Kalundborg, the particle concentrations were found to lie within the range of 20-30 g/Nm³. The ash content of the collected samples were also analyzed using TGA. The TGA analysis of the cyclone ash collected from the secondary cyclone bottoms and the dust samples in the exit gas showed that the samples were reasonably similar. Both the samples were found to contain about 35-40% char and 45-50% ash, rest being volatile (5-6%).

An overall ash balance on the LTCFB system was done. About 8-10% of the total ash in the fuel was found as dust in the product gas and 40-80% retained in the cyclone bottoms. The unaccounted fractions included the fractions retained within the system leading to accumulation of ash within the gasifier system. The release of the inorganic elements in the system was investigated from the inorganic elemental analysis obtained from the samples collected during the various plant runs at the 100 kW and 6 MW LTCFB gasifiers.

Table 1: Results of mass balance from measurements in 100 kW LTCFB gasifier

Secondary Cyclone Ash (%)				Dust (%)					Unaccounted (%)				
K	Si	Ca	Cl	K	Si	Ca	Cl	S	K	Si	Ca	Cl	S
49	47	33	22	13	9	11	10	3	38	44	56	68	89

Table 1 shows the fractions of K, Ca, Cl, Si and S in the fuel that were retained in the secondary cyclone ash or released with the dust in the product gas. Table 1 also shows the unaccounted mass fractions of the elements obtained by closing the mass balances. That an element is unaccounted for could mean that it is accumulated in the bed material or that it is released as gas phase species with the product gas. In the cases of Cl and S, gas phase species (CH₃Cl, HCl, H₂S, COS) probably

account for a large part of the unaccounted fraction, while in the case of K, Si and Ca, a large unaccounted fraction indicates that the K, Si and Ca from the fuel accumulate in the bed material. It can be seen from Table 1 that about 50% of K and 30% of Ca in the fuel was retained in the secondary cyclone ash. About 20% of the chlorine from the fuel was retained in the cyclone ash in the range of along with K and Ca indicating the presence of chlorides in the cyclone ash. About 40-60% of K and Ca were unaccounted for, indicating accumulation in the bed material. Si was found to be removed in substantial amounts with the cyclone ash (in the range of 50%). S was found to be removed by the cyclone in lower amounts in the range of 8-20%. Similar trends were observed in the dust particles in the exit gas (Table 1), even though the values for the retention of the inorganic elements in the dust were low compared to cyclone ash. K (13%) and Ca (11%) were seen in pre-dominant amounts in the dust along with Si (9%) and Cl (10%), probably present as silicates and chlorides. S was found to be in low amounts in the dust in exit gas (3%). The high fractions of Cl and S (70-90%) unaccounted for in the mass balance are attributed to release of S and Cl in gaseous form. The composition of cyclone ash and dust samples collected during the various plant runs is shown in Table 2.

Table 2: Composition of the inorganic elemental species in secondary cyclone ash and dust samples in exit gas collected during plant runs in 100 kW LTCFB gasifier [3].

% wt.	K	Si	Ca	Cl	S
Secondary Cyclone Ash	7.3	16	2.50	0.96	0.15
Dust	6.7	10.5	2.9	1.5	0.19

The remaining fractions in the cyclone ash and dust (not shown in the Tables) included char (as evident from the TGA analyses) and traces of other inorganic elements present in small amounts. The cyclone ash was found to be dominated by Si, K and Ca. The dust particles in the product gas showed similar trends, although with lower fractions of Si, K and Ca as compared to the cyclone ash. The amount of Cl in the cyclone ash and dust particles was about 1-1.5%, while S was found to be present in low amounts (0.15-0.2%). This shows that the cyclone ash and dust particles are dominated by silicates.

The molar ratios of K to Cl in the secondary cyclone ash and in the exit gas dust particles were found to be high (3-7), showing that K was present in substantial amounts in other forms than KCl. The tar in the exit gas collected in the Petersen Column during the plant run in the 100 kW LTCFB gasifier was analyzed. The tar present in the product gas showed very low amounts (< 0.004%) of the inorganic elements, corresponding to less than 0.002% of the respective elements in the fuel.

These results indicate low probabilities of release of the major inorganic elements with tar in the gasifier. Finally, the exit gas during the plant run in the 100 kW LTCFB gasifier was analyzed for the presence of methyl chlorides, to investigate the presence of Cl in gaseous form. The measurements showed 90-100 ppm of methyl chlorides in the exit gas [4], corresponding to about 15% of the Cl present in the fuel. As mentioned earlier, Cl could also be released in the gaseous form as HCl.

A cyclone model was developed to study the role of the cyclones in ash release and retention in the LTCFB system. Modeling predictions for the fraction of ash retained in the cyclone bottoms and that entrained with the exit gas, respectively, were close to the measured values for the 100 kW LTCFB gasifier and the 6 MW gasifier. This confirms that the cyclone design plays a crucial role in determining the release and retention of solid ash particles from the LTCFB system.

De-Fluidization of ash (bed material) samples from Pyroneer Gasifier

A major problem often encountered in fluidized beds is bed agglomeration, which may result in total de-fluidization, leading to unscheduled downtime and additional costs. The above problems are found to be critical in fluidized bed combustion and gasification of biomass fuels which have high ash and alkali contents.

The main aim of this study was to understand the agglomeration and de-fluidization behavior of alkali rich ash (bed- material) samples obtained from the 6 MW Pyroneer Gasifier, under non-oxidizing conditions. To begin with, experiments were first performed with Sand-K mixtures with varying K concentrations.

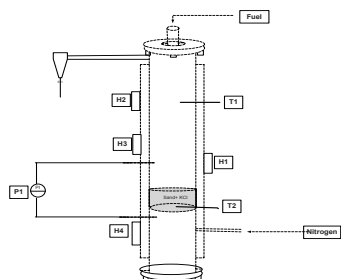


Figure 2: Fluidized Bed Set up for De-fluidization studies, T1,T2, thermocouples; P1, Pressure Indicator; H1-H4, Heating elements.

The experiments were performed in a pilot scale fluidized bed set up as shown in Figure 2. The feed samples were fed to the reactor from the top before the start of the experiment. The particles inside the reactor were fluidized using nitrogen gas as shown in the Figure 2. The exit gas leaving the reactor was cleaned of any entrained particles in a cyclone, before being released through ventilation. The pressure drop over the bed was monitored by two pressure transducers at the top and at the bottom of the bed as shown in Figure 2. The reactor was electrically heated by three independently

controlled heating elements and the temperatures increased at a constant rate during experiments. Temperatures were measured through thermocouples inserted just above the distributor plate and in the freeboard. The operating velocity of the fluidizing gas (U) was maintained at twice the minimum fluidization velocity (U_{mf}). De-fluidization in the system was observed by a sudden drop in the pressure and the temperature at which it occurred was defined as the de-fluidization temperature.

Observations and Results from the De-fluidization experiments

Table 3: De-fluidization temperatures of Sand+ KCl and Sand+ K_2CO_3 mixtures

Sand + KCl		Sand+ K_2CO_3	
Potassium content%	De-fluidization temperature, $^{\circ}C$	Potassium content %	De- fluidization temperature, $^{\circ}C$
2	766	1.5	737
4,5	762	4.5	732
6.5	756	6.5	728

The de-fluidization temperatures obtained for sand + KCl and sand + K_2CO_3 mixtures are shown in Table 3. Sand + KCl mixtures and sand + K_2CO_3 mixtures were de-fluidized at about $760^{\circ}C$ and $730^{\circ}C$, respectively. The de-fluidization temperatures decreased slightly ($4-6^{\circ}C$) with increase in K concentration. The SEM images of Sand+ KCl mixtures showed pure KCl in between sand particles. This shows that there was limited reaction between KCl and the sand particles. The SEM images of sand + K_2CO_3 mixtures showed two distinct phases. The inner phase is rich in Si, which is surrounded by a coating layer rich in K and Si. The coating layer around the particles could be due to the formation of an eutectic melt of K-silicates, formed from the reaction of K_2CO_3 with silica in sand. These observations indicate that agglomeration in sand and K_2CO_3 mixtures are coating-induced agglomeration. The de-fluidization experiments were then performed on ash (bed material samples) obtained from the Pyroneer Gasifier. The results of the above experiments are shown in Table 4.

Table 4: De-fluidization temperatures of bed material samples from Pyroneer Gasifier

% K	Defluidization temperature, $^{\circ}C$
4.7	780
4.3	785

As can be seen from the Table, the Defluidization temperatures of 4.2% ash was about $785^{\circ}C$ and for 4.7% ash was $780^{\circ}C$. Similar to the sand + K_2CO_3 mixtures, SEM images of the ash samples showed two distinct phases; the inner ash layer (spectrum 2,

dominant in Si) is surrounded by a coating layer (spectrum 1) rich in K, Ca, Mg and Si. This shows that the elements K, Ca and Mg have reacted with Si forming a coating layer of eutectic melts of silicates around the bed particles. Thus, as for the sand + K₂CO₃ mixtures, the probable mechanism of agglomeration in this case is also coating-induced agglomeration.

It can be seen that de-fluidization takes place at higher temperatures in the case of ash particles (about 780°C) as compared to the sand + K₂CO₃ mixtures (about 730°C), although in both cases, the mechanism of agglomeration is the same (coating-induced agglomeration). One reason could be the presence of Ca and Mg in the ash particles (which were not present in sand + K₂CO₃ mixtures) which if present beyond certain concentrations could shift the formation of the eutectic melts to higher temperatures

A mathematical model for de-fluidization of alkali rich bed material was developed based on the bench-scale experiments and data from literature. In the model, the adhesive forces between the particles caused by coatings were compared with the fluidization induced breakage forces to determine de-fluidization conditions. The model was used to predict the de-fluidization temperatures as a function of parameters such as initial alkali concentrations within the bed particle diameters and the fraction of K entrained from the system. The model was applied to study the de-fluidization behavior of alkali-rich samples in a large scale LTCFB gasifier. It could predict the variations in de-fluidization time with respect to parameters such as alkali concentrations within the bed and bed particle diameters.

Conclusions

A Low-Temperature Circulating Fluidized Bed System (LTCFB) gasifier allows pyrolysis and gasification to occur at low temperatures thereby improving the retention of alkali and other ash species within the system and minimizing the amount of ash species in the product gas. In addition, the low reactor temperature ensures that high-alkali biomass fuels can be used without risks of bed de-fluidization. This paper aims to understand the behavior of alkali metals and ash in low-temperature gasifiers. Measurements on bed material and product gas dust samples were made on a 100kW and a 6 MW LTCFB gasifier. Of the total fuel ash entering the system, a dominant fraction (40-50%) of the ash was retained in the secondary cyclone bottoms and a lower amount (8-10%) was released as dust in the exit gas. A dominant fraction of alkali and alkaline earth metals were retained in solid ash along with Si and some Cl, while most Cl and S were released in gaseous form. Measurements on the product gas from the 100 kW LTCFB gasifier showed the presence of Cl in the form of gaseous methyl chlorides (90-100 ppm). Release of K and other inorganic species in tar in the product gas from the LTCFB gasifier were found to be low. The release and retention of the condensed ash species from the system was seen to be controlled by the particle size and the cut size of the primary and

secondary cyclones. A model accounting for the ash collection by the plant cyclones was developed and shown to predict the product gas ash particle release reasonably well.

A major concern in thermal conversion of biomass encountered in fluidized beds is bed agglomeration, which may result in de-fluidization, leading to unscheduled downtime and additional costs. Biomass fuels, especially herbaceous plants, often contain dominant amounts of silicon, potassium and calcium, which may form viscous melts that adhere on the surface of the colliding bed particles and bind them to form agglomerates. In this paper, studies were made to understand the behavior of inorganic elements (mainly K, Si and Ca) on agglomeration and de-fluidization of alkali rich bed-material samples under non-oxidizing conditions in a bench-scale fluidized bed reactor set up. The de-fluidization studies involved measurements with sand and pure potassium salts (KCl and K₂CO₃) as well as with bed material samples obtained from a 6 MW Low Temperature Circulating Fluidized Bed (LT-CFB) gasifier using straw as a fuel. It was seen that in sand + KCl agglomerates, the sand particles were bound by KCl melts. There was no chemical reaction observed between KCl and the sand particles and no presence of silicate melts in the agglomerates. In sand + K₂CO₃ mixtures and the LT-CFB bed material samples, the agglomeration was seen to occur due to the viscous silicate melts formed from reaction of inorganic alkaline and alkali earth species with silica from the bed particles. A mathematical model that addresses the de-fluidization behavior of the alkali rich samples was developed based on the experiments performed in the bench-scale fluidized bed reactor as well as on results from literature. The model studies were then extended to predict the de-fluidization behavior of alkali rich bed material in a large-scale LTCFB gasifier.

References

1. P. Stoholm, R. G. Nielsen, The Low Temperature CFB Gasifier-Latest 50 kW Test Results and New 500kW Plant, Proceedings of World Conference and Technology Exhibition on Biomass for Energy and Industry (ISBN), ETA-Florence & WIP-Munich, Rome, 2004.
2. P. Stoholm, J. Cramer, J. Krogh, R. G. Nielsen, B. Sander, J. Ahrenfeldt, U. Henriksen, The Low Temperature CFB Gasifier-100 kW_{th} Tests on Straw and new 6 MW_{th} Demonstration Plant, International Biomass Conference, Lyon, 2010.
3. Analysis Report on the inorganic elemental composition from Enstedværket Laboratory, Dong Energy
4. Analysis Report on methyl chloride concentration in tar, Zsuzsa Sárosy, Jesper Ahrenfeldt.



Phone: +45 9175 1192
E-mail: hing@kt.dtu.dk

Supervisors: David Löf, PPG Industries
Søren Hvilsted
Anders Egede Daugaard

PhD Study
Started: August 2012
To be completed: July 2015

Synthesis of novel biobased binders for alkyd paint systems

Abstract

Totally renewable alkyds with various structures are successfully synthesized from a one-pot enzymatic process at much lower temperature compared to that of conventional methods. The method allows for high control of the alkyd structure as well as the properties of the prepared alkyds such as e.g. increased hydrophobicity. Structural and physical characteristics of the alkyds are determined mainly by NMR as well as DSC and water contact angle measurements.

Introduction

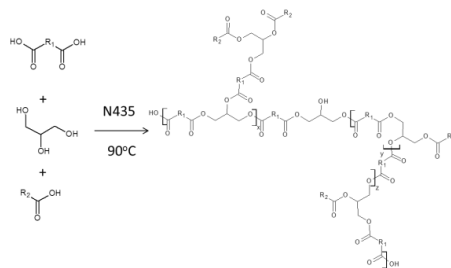
Wooden structures are used in many different outdoor applications, and alkyd coatings are one of the most popular methods of protection of these structures. Currently, the annual global production of alkyds is around one million tons [1]. The alkyd binder is the base of alkyd coatings, and its primary purpose is forming a tough and continuous film that is able to expand and contract due to fluctuations in the outside temperature to avoid cracks and protect the wood surface. An alkyd can be considered as a polyester grafted with drying fatty acids, which accounts for its film forming properties. The major challenge of recent alkyds is that the petrochemical part accounts for 50wt% of the alkyd composition and the objective of this project is therefore synthesis of new highly durable alkyds from renewable materials.

In the present project enzymes are used to provide an alternative way for alkyd synthesis. Specifically, Novozyme 435 (N435), a heterogeneous biocatalyst that consists of *Candida antarctica* lipase B (CALB) physically immobilized within a macroporous resin of poly (methyl methacrylate), is used for the polymerizations. This enzyme catalyst is able to catalyze polycondensations at temperature below 100°C with high regioselectivity for primary hydroxyl groups [2]. Since the enzymatic reaction is carried out at temperature below 100°C, this allows for a larger range of possible feed components and reduces the amount of energy used for the polymerizations. In this investigation, N435 was used to produce alkyds with

various structures from glycerol, Tall oil fatty acid (TOFA), and a biobased diacid.

Results and discussion

The enzymatically produced alkyds are synthesized in one-step procedures as illustrated in Scheme 1.



Scheme 1: Synthesis of a biobased alkyd obtained from a one-pot enzymatic process from biobased dicarboxylic acid $R_1(\text{COOH})_2$, TOFA ($R_2\text{COOH}$) and glycerol

The process directly affords a range of alkyds, where the feed composition and reaction time can be used to control both the molecular weight and the branching of the alkyd. As glycerol is the only alcohol in the feed composition, five possible glyceride units can be obtained within the alkyd structure, including the monoglycerides of 1-glyceride and 2-glyceride, the diglycerides of 1,2-glyceride and 1,3-glyceride as well

as the triglyceride as shown in Figure 1. The content of these units can provide information on both extent of reaction as well as the degree of branching in the alkyd.

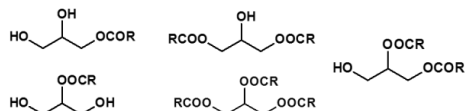


Figure 1: The five different glycerides that could be formed during the alkyd synthesis.

NMR spectroscopy was used to investigate the extent of reaction as well as the branching in the alkyd. Especially, ^{13}C -NMR was found very useful for identification of the different types of branching units [3-5], as shown in Figure 2.



Figure 2: Quantified ^{13}C -NMR spectrum of the biobased one-pot enzymatic alkyd

The developed enzymatic process was used to prepare a range of alkyds varying both the feed composition as well as the reaction time. Thereby, both alkyds with varying molecular weight characteristics, as well as a range of physical properties could be prepared. For a comparison with classical alkyds the glass transition temperature of the neat sample and the surface properties of the cured alkyd were determined, as shown in Table 1.

Table 1: Glass transition temperature and water contact angle measurements of a glycerol, TOFA, biobased acid alkyd prepared enzymatically as well as by the classical process.

	T_g ($^{\circ}\text{C}$)	Water Contact Angle ($^{\circ}$)
Enzymatic alkyd	-54	86
Classical alkyd	-46	70

It is clear from the table that the procedures have afforded two quite different alkyds. Here it is particularly interesting to see the changes in the water contact angle, where the enzymatic alkyd was found to be much more hydrophobic with a water contact angle of 88° . This illustrates how the chemical structure of the alkyd can be exploited to provide more hydrophobic coatings, which is very important when the application on wood substrates are taken into consideration. It is a

well-known challenge in wood coatings to be able to control the moisture uptake as well as the growth media for fungus in the surface and thereby reduce the degradation of the wood.

Investigating this relationship between the degree of branching as well as the composition of the coating led to a more branched alkyd. By increasing the reaction time distribution between branching elements and terminal side chains from the TOFA side groups were changed. Measurements of the relative intensity of the glyceride CH groups in the NMR spectra showed that both 1-glyceride and 1,3 diglycerides participated in further esterification to yield more triglyceride units, which in turn increased the molecular weight of the alkyd 22% to 10,500 g/mol. In a similar way, by increasing the acid content an additional increase in hydrophobicity was observed as shown in Figure 3.

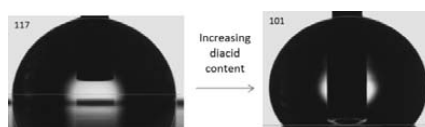


Figure 3: Sessile drops of water on the surface of the two coatings prepared from the enzymatically produced alkyds with an increasing diacid content.

The increase in hydrophobicity resulted in an increase in the water contact angle from 86 to 128° .

Conclusion

In conclusion, biobased alkyds with varying structures were successfully synthesized by a one-pot enzymatic process. All alkyds have good working ranges and it was shown that structural control could lead to formation of coatings with increased hydrophobicity compared to the corresponding classical alkyd. Further testing should be carried out on selected candidates for identification of the final products.

Acknowledgement

The authors acknowledge the financial support from the Danish National Advanced Technology Foundation (DNATF).

References

1. R.V. Gorkum, E. Bouwman, Coordination Chemistry Reviews 249 (2005) 1709–1728.
2. B.J. Kline, E.J. Beckman, A.J. Russell, Journal of the American Chemical Society 120 (1998) 9475–9480.
3. C. Rabiller, F. Maze, Magnetic Resonance in Chemistry 27 (1989) 582–584.
4. S. D. Stamatov, J. Stawinski, Tetrahedron 61 (2005) 3659–3669
5. E. Hatzakis, Agiomirgianaki, S. Kostidis, Ph. Dais, J. Am. Oil Chem. Soc. 88 (2011) 1695–1708



Anne Veller Friis Nielsen
Phone: +45 4525 6892
E-mail: avfn@kt.dtu.dk
Discipline: Enzyme technology

Supervisors: Anne S. Meyer

PhD Study
Started: September 2012
To be completed: September 2015

Robustness of Phytase Catalysis for Improved Iron Bioavailability

Abstract

Microbial phytases (EC 3.1.3.8) catalyse dephosphorylation of phytic acid, which in turn releases iron chelated to the phosphate groups and thus improve iron bioavailability in humans. For this catalysis to take place *in vivo* after ingestion of food, phytases need to be stable towards pepsin and low pH in the gastric ventricle. The recent work of this PhD study identified large differences between different commercially available phytases with regard to stability towards these factors and a correlation between loss of activity and loss of secondary structure was confirmed using circular dichroism. Finally, it was shown that phytases were able to dephosphorylate soluble phytic acid to a sufficient extent under simulated gastric conditions *in vitro*.

Introduction

Iron deficiency anaemia is the most common nutritional deficiency disorder globally. Grains, different varieties of which constitute global staple foods, often contain significant amounts of iron (e.g. 3.9 mg/100 g for oatmeal [1]), but this iron has been shown to be poorly bioavailable, meaning that an absorption efficiency of 2-3 % is common, whereas for meat, the absorption of iron ranges from 15-35 % [2]. This low bioavailability has been attributed to the presence of high amounts of phytate (*myo*-inositol (1,2,3,4,5,6)-hexakisphosphate), which can chelate iron (Fe^{3+}) and other minerals via interaction with the six phosphate groups that are negatively charged at physiologically relevant pH values (Figure 1).

It has been shown that supplementation of the diet with phytase enzyme (EC 3.1.3.8) from the mold *Aspergillus niger* can significantly increase iron absorption by dephosphorylation of the phytic acid, particularly when three or more phosphate groups are cleaved off the inositol ring [2,3]. Also, the *A. niger* phytase has recently been approved for use in food [4]. For application of a phytase such as the *A. niger* phytase for nutritional purposes, the enzyme must be able to withstand high temperatures in food processing and be robust to low pH and pepsin-catalysed proteolysis in the gastric ventricle. For phytate degradation, the gastric ventricle is favoured over other places along the alimentary tract due to the higher solubility of most phytate complexes in the lower pH range found here [5]

as well as the fact that iron is absorbed in the proximal part of the duodenum, thus not leaving much time for hydrolysis after exit from the gastric ventricle.

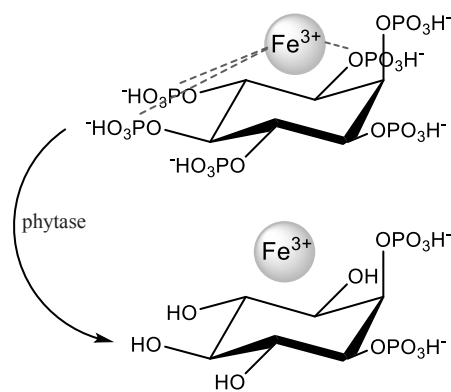


Figure 1: Chemical structure of a phytate- Fe^{3+} complex and the phytase-mediated release of Fe^{3+} .

Specific Objectives

The specific objectives of this work was to evaluate the robustness of five different microbial phytases with regard to factors relevant for use of phytase to improve iron absorption in human nutrition: Heat, protease and low pH.

Table 1: Activity retention [%] against incubation time at pH 2 of different phytases with and without pepsin (5000 U/mL). All activities are relative to activities of each enzyme prior to incubation.

Phytase	Without pepsin		With pepsin	
	60 min	120 min	60 min	120 min
<i>Escherichia coli</i>	97 ± 3	97 ± 2	112 ± 4	112 ± 0
<i>Citrobacter braakii</i>	74 ± 2	64 ± 4	60 ± 5	35 ± 4
<i>Aspergillus niger</i> (<i>P. pastoris</i>)	111 ± 5	103 ± 5	98 ± 7	95 ± 8
<i>Peniophora lycii</i>	15 ± 4	13 ± 1	16 ± 2	6 ± 0
<i>Aspergillus niger</i> (<i>A. niger</i>)	88 ± 4	86 ± 1	110 ± 8	108 ± 11

Results and Discussion

The five phytases (*Escherichia coli* phytase expressed in *Pichia pastoris* (Challenge Group, China); *Aspergillus niger* phytase expressed in *Aspergillus niger* (Sukahon Biotechnology Group, China); *Citrobacter braakii* phytase expressed in *Aspergillus oryzae* (DSM, The Netherlands); *Peniophora lycii* phytase expressed in *Aspergillus oryzae* (Novozymes, Denmark) and *Aspergillus niger* phytase expressed in house in *Pichia pastoris*) showed different stabilities both with respect to proteolysis by pepsin (Table 1), low pH (Table 1) and heat (not shown). The stability of the enzymes toward heat and low pH/pepsin did not correlate. Notably, the *Peniophora lycii* phytase showed a very high thermal stability, whereas this phytase had the lowest stability in the presence of pepsin and at low pH (Table 1). On the other hand, the *E. coli* and *A. niger* phytases showed very high stabilities towards low pH and pepsin and low thermal stability and the *Citrobacter braakii* phytase displayed intermediate stability to all three factors. Furthermore, for the *E. coli* phytase, a slight activation was observed initially when incubating with pepsin.

In the search for explanations to the differences in observed stabilities, circular dichroism spectra in the far-UV range were recorded for all five phytases at pH 2 and pH 5. For the *Peniophora lycii* and *Citrobacter braakii* phytases, a clear difference in the spectra at pH 2 and 5 was observed, whereas the spectra for the *E. coli* and *A. niger* phytase spectra at pH 2 and 5 looked very similar. This indicated a change in secondary structure for the R and H phytases caused by the change in pH. A single value accounting for 98.4 % of the variation in spectra between pH 2 and 5 were extracted using principal components analysis. This value seemed to correlate with the loss of enzymatic activity between pH 5 and 2, corroborating that this loss was caused by denaturation of the enzyme protein at low pH. It was further hypothesized that this denaturation increases the susceptibility of the phytases to proteolytic cleavage catalysed by the pepsin protease.

With regard to the application of phytic acid dephosphorylation *in vivo*, a study of soluble phytic acid degradation in a simulated gastric environment showed that three of the five tested phytases (namely, *E. coli*, *A. niger* (*A. niger*) and *C. braakii*) were able to degrade virtually all the tri- to hexa-phosphorylated inositol phosphates to lower inositol phosphates and free

phosphate (Table 2), thus theoretically leaving only inositol phosphates with insignificant ability to chelate iron.

Table 2: Inositol tri- to hexaphosphates degraded under simulated gastric conditions (% of initial amount).

Phytase	30 min	60 min	120 min
<i>Escherichia coli</i>	99 ± 0	99 ± 0	99 ± 0
<i>Citrobacter braakii</i>	100 ± 1	100 ± 0	100 ± 1
<i>Aspergillus niger</i> (<i>P. pastoris</i>)	-5 ± 11	2 ± 10	5 ± 12
<i>Peniophora lycii</i>	6 ± 9	8 ± 10	6 ± 13
<i>Aspergillus niger</i> (<i>A. niger</i>)	91 ± 11	99 ± 0	99 ± 0

Conclusions

The five tested microbial phytases have been shown to exert very different stabilities toward heat, low pH and pepsin proteolysis. Three of these have shown sufficient dephosphorylation of soluble phytic acid in a simulated gastric environment *in vitro*.

Acknowledgements

This project is supported by the Danish Council for Strategic Research under the FENAMI project.

References

1. Danish Food Composition Databank, version 7.0, 2008. Website: <http://www.foodcomp.dk/>
2. A.V.F. Nielsen, I. Tetens, A.S. Meyer, *Nutrients* 5 (2013) 3074-3098.
3. A.-S. Sandberg, L. R. Hulthén, M. Türk, *J. Nutr.* 126 (1996) 476-480.
4. World Health Organization. Safety Evaluation of Certain Food Additives. In WHO Food Additives Series: 67; WHO Press: Geneva, Switzerland, 2012.
5. K. Pontoppidan, D. Pettersson, A.-S. Sandberg, *J. Sci. Food Agric.* 87 (2007) 1886-1892.

List of Publications

1. A.V.F. Nielsen, I. Tetens, A.S. Meyer, *Nutrients* 5 (2013) 3074-3098.



Joachim Bachmann Nielsen
Phone: +45 4525 2922
E-mail: jobni@kt.dtu.dk

Supervisors: Prof. Anker Degn Jensen
Prof. John Nielsen, KU
Niels Ole Knudsen, DONG Energy

PhD Study
Started: September 2012
To be completed: September 2015

Liquid Fuel Production from Lignin Solvolysis by 2-Propanol

Abstract

Processes for solvolytic depolymerization of an enzymatic hydrolysis lignin have been investigated at the CHEC research group at DTU-Chemical Engineering. A simple one-pot process without the need for catalyst or hydrogen addition is desired. Experiments conducted in a high pressure batch autoclave with supercritical 2-propanol have shown an optimum liquid yield of 35wt% after 4 hour treatment at 430°C. The oxygen content of the obtained oil was lowered to 10wt% after treatment at 430°C relative to 34 wt% for the untreated dry lignin. A significant degree of solvent gasification was observed with more than 50% solvent loss after treatment at 430°C. Adding Raney Nickel® catalyst and pressurization with hydrogen yielded an increase in up to 40wt% oil yield recovered for treatment at a lower temperature of 300°C but only 5% of the 2-propanol added was present after reaction.

Introduction

There is an increasing pressure on the transport sector to blend fossil fuels with biofuels and recently there has been an increased focus on liquid fuel production from lignin. Lignin is of particular interest as it is found in quantities up to 30wt% in lignocellulosic biomass and the majority is burned as a low value fuel [1]. In order to transform solid lignin to a liquid fuel the lignin polymer needs to be depolymerized and the oxygen content must be lowered. Depolymerization can be obtained by direct liquefaction where lignin is dissolved in a solvent at elevated temperatures and a significant altering of the lignin structure at these conditions may effectively allow for a lowering of the oxygen content.

At the CHEC research center at DTU-Chemical Engineering experiments on lignin depolymerization in 2-propanol have been carried out in batch autoclaves. The lignin used is a hydrothermally extracted lignin from a 2G bioethanol plant (Inbicon, DONG Energy).

Specific Objectives

It is desired to transform solid lignin from a low value fuel to a higher value liquid transport fuel. It will be satisfactory to obtain a product that can satisfy a 10vol% blend with a marine diesel. This requires a depolymerization of the lignin polymer and lowering of the oxygen content from about 30wt% to a level where blending with a nonpolar diesel is possible. Furthermore it is important to ensure a very low ash content of the

obtained liquid product as ash particles can cause excessive wear to internal combustion engines.

Experimental Setup

A 500ml stirred HT 4575 Parr batch autoclave capable of handling temperatures up to 500°C and pressures up to 345bar has been used for lignin solvolysis experiments. The lignin used is a hydrothermally extracted lignin from a 2G bioethanol plant. Experiments have been carried out by mixing a weighed amount lignin with 2-propanol. The catalyst used in some of the experiments was 3g of Raney®-Nickel 4200. Rapid cooling of the vessel in an ice bath was conducted after each experiment. The product mixture was filtered prior to removal of solvent by rotary evaporation (45°C, 5mbar and 30 min). The heavy fraction indicated the yield of isolated oil.

Results and Discussion

I. Yields and Oxygen Content

Figure 1 shows yields of oil and residual solids and the oxygen content of the obtained oils. Addition of Raney Nickel to the reaction vessel pressurized with hydrogen at 300°C yielded an increase in oil yield up to 40wt% relative to 26wt% with no catalyst added. The oxygen content of the oil from the catalyzed reaction was however, higher than for the non-catalyzed reaction indicating a tradeoff between yield and oil quality.

For treatment of 10g lignin at non-catalytic conditions with no hydrogen pressurization prior to heat-up a maximum oil yield of 35wt% for treatment at 430°C was observed relative to 32wt% at 380°C. The oxygen content of the obtained oil was however lowered considerably to 10wt% after treatment at 430°C relative to 18wt% at 380°C.

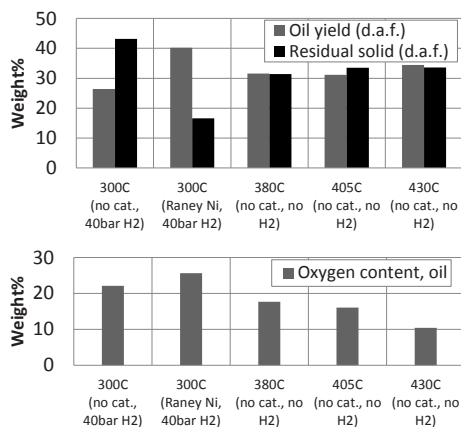


Figure 1 Oil yields and residual solids obtained (top) and oxygen content of the obtained oils (bottom) after treatment of 10g lignin for 4 hours in 100ml 2-propanol with autogenous pressure at different temperatures.

II. Solvent Consumption

Figure 2 below shows the composition of the contents of the batch autoclave on a mass basis for both the experiments without pressurization prior to heat up and the experiments with pressurization with hydrogen respectively.

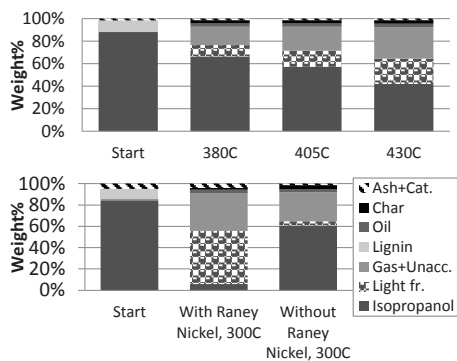


Figure 2 Composition of the contents of the autoclave on a mass basis as a function of the reaction temperature for 4 hour experiments with 10g lignin in 100ml 2-propanol. Top: Non-pressurized vessel with an inert N₂ atmosphere prior to heat up. Bottom: pressurized vessel a 40bar H₂ atmosphere prior to heat up.

An increase in reaction temperature from 380°C to 430°C shows an increase in 2-propanol consumption from 25wt% to 53wt%. Addition of Raney Nickel® yielded a 95wt% consumption of 2-propanol at 300°C. 2-Propanol is both gasified and transformed into a light organic liquid fraction.

III. Elemental Composition and HHV

The elemental composition of the lignin feedstock as well as the oil obtained with the lowest oxygen content from treatment in 2-propanol at 430°C can be seen in Table 1. Treatment of lignin in 2-propanol at 430°C yielded a higher heating value of 37.8 MJ/kg of the isolated oil yield which is twice the value of the feedstock. This value is not far from the higher heating value of 45 MJ/kg for commercial diesel fuels.

Table 1 Elemental composition (wt%) of lignin and oil obtained by treating 10g of lignin in 100ml 2-propanol for 4 hours at 430°C in an inert N₂ atmosphere at autogenous pressure. Oxygen content is determined by difference. Higher heating value is calculated.

Sample	C	H	N	S	O	Ash	HHV
Lignin (dry)	47	4.9	1.5	-	34	13	18.5
							MJ/kg
Lignin (d.a.f.)	54	5.6	1.7	-	39	-	-
Oil	78	10	1.4	-	10	<1	37.8
(<i>i</i> -PrOH,430°C)							MJ/kg

Conclusions

Experiments with supercritical 2-propanol have indicated a minor increase in isolated liquid yield of 35wt% after 4 hour treatment at 430°C relative to 32wt% at 380°C. The oxygen content of the obtained oil was however lowered to 10wt% after treatment at 430°C relative to 18wt% at 380°C.

A significant degree of solvent gasification was observed with more than 50% solvent loss after treatment at 430°C. Adding Raney Nickel® catalyst and pressurization with hydrogen yielded an increase in up to 40wt% oil yield recovered for treatment at 300°C but only 5% of the 2-propanol added was present after reaction.

The oil obtained from treatment of 10g lignin in 100ml 2-propanol for 4hrs in an inert atmosphere yielded the highest higher heating value of 37.8 MJ/kg which is twice the value of the lignin feedstock.

References

- Zakzeski, J., Bruijninx, P.C.A., Jongerius, A.L. and Weckhuysen, B.M., *Chem. Rev.*110 (2010) 3552-3599.



Mads Willemoes Nordby

Phone: +45 4525 2809
E-mail: mwnor@kt.dtu.dk

Supervisors: Kim Dam-Johansen
Weigang Lin

PhD Study
Started: December 2012
To be completed: February 2016

Agglomeration in Dual-Fluidized Bed Gasification

Abstract

Biofuels high in potassium and silica content, such as wheat straw, are problematic when used for combustion or gasification in fluidized bed reactors as there is a high risk of bed agglomeration. The fundamental mechanisms for agglomeration are still not fully understood, and this is especially true for gasification conditions. Therefore the purposes of this project are to gain a better understanding of alkali release and the ash chemistry observed during biomass gasification and how this might affect agglomeration tendencies.

Introduction

The utilization of biomass with high alkali metal content in fluidized bed combustors has proven to be problematic due to agglomeration. The agglomeration occurs due to the presence of melt-phases containing mixtures of reacting silica and potassium. However, the mechanisms at gasification conditions are not completely revealed. It is therefore important to know the behaviour of these problematic species during gasification. The release of elements during gasification can be separated into two steps: Release during pyrolysis and release during char gasification.

The release characteristics of alkali metals during pyrolysis and subsequent char gasification have shown that 53-76 % of the alkali metals were volatilized during the pyrolysis step, while during the char gasification it was 12-34 %. Expanding upon these results showed that during pyrolysis the evaporation was partly with the decomposition of lignin, hemicellulose and cellulose, and partly due to char-volatile interactions [1].

Research has also shown that during gasification the majority of the released alkaline species are combined with tar, primarily in the water-soluble fraction. At a temperature of 873 K 65 % of sodium and 63 % of potassium were released and present in the tar. Increasing the gasification temperature lead to secondary decomposition of the water-soluble tar, where the resulting released alkali species, could not be captured by quartz glass filter, which indicated that the alkaline species were released as very fine particles during secondary decomposition of the water-soluble

tar. The yield of condensed alkaline species also increased significantly along with increasing gasification temperature [2].

Char reactivity has also been seen to drastically reduce during contact with steam. This was due to changes in the char structure, and was found to have no connection to the volatilization of the catalytically active alkali metals [3].

Increasing the amount of phosphor present in biomass, either by additives or by co-combustion with fuels high in phosphor such as sewage sludge, could potentially be used as a means of reducing agglomeration tendency, as during combustion phosphor has been shown to react with potassium, reducing the amount available to volatilize or react with the bed material. However some of the phosphate rich ash particles were found to form low-temperature – melting alkali-rich phosphates promoting agglomeration behaviour. A general observation is that phosphor plays a controlling role in ash transformation reactions during biomass combustion, due to the high stability of phosphate compounds [4, 5].

Specific Objectives

As the effects of gasification conditions on alkali release and ash chemistry in biomass are not currently well understood, this PhD project aims to investigate some of the release characteristics in differing atmospheres, and how it might affect the ash chemistry and agglomeration behaviour. The goals are:

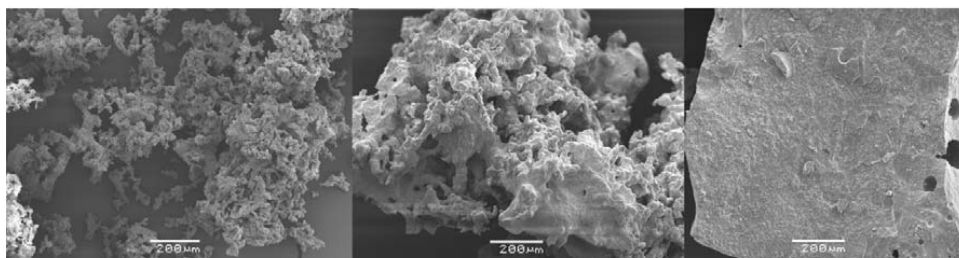


Figure 1: SEM images of ash particles from CO₂ gasification of wheat straw. (left) Gasified at 750°C. (middle) Gasified at 900°C (right) Gasified at 1000°C.

- Investigate how the transformation of alkali metals is affected under gasification conditions.
- Determine the effects of various operating conditions such as temperature, gas flow, fuel composition, etc., have on the agglomeration tendency as well as the effect on the physical properties of ash.
- Study what role phosphor plays in the ash chemistry in gasification conditions.

Table 1: Ash composition of wheat straw gasified by steam predicted by EDS. Results is in atomic% and is only indicative of actual composition.

Temp	O	K	Si	Ca	P
650°C	69	15	3	3	2
750°C	56	22	3	5	3
900°C	63	25	2	5	2
1000°C	69	18	1	6	2

Results and Discussion

Wheat straw samples have been combusted or gasified using 50% CO₂ or steam in a fixed bed reactor at temperatures ranging from 550 to 1000 °C.

A slight decline in ash content as temperature increases has been observed in experiments, although not much difference is seen when distinguishing between the different atmospheres used as the ash content generally appear similar to each other at the same temperature.

The ash samples have also been analysed using SEM/EDS. Based on the general morphology and pore size changes observed, the SEM results indicated increasing sintering/melting of the ash with increasing temperature as seen in Figure 1. This is expected behaviour as the biomass ash containing high amount of potassium and silica would gradually begin melting at temperatures above around 750°C. In Table 1 EDS results from the samples indicates that at across the entire temperature range, main components of the ash are O and K and to a lesser extent Si, Ca and P, which is also generally what would be expected. Additionally the presence of Cl was detected from 550-800 C, but not at 900 and 1000 C, meaning that almost all of the Cl will have devolatilized between 800 and 900 C. Char samples collected at the same temperatures still showed

a significant presence of Cl, meaning that some of the Cl is bound in or captured by the char matrix.

Conclusion

Initial results indicate that wheat straw ash across the entire temperature interval and in all atmospheres is comprised mainly of K₂O, which is the main constituent causing agglomeration.

Future Work

Further analysis of the ash samples in order to determine the exact chemical composition of the ash samples is needed in order to determine the exact alkali release and retention in the ash.

Additional experiments will determine the physical properties of ash at different temperatures and atmospheres by using Thermo Mechanical Analysis on biomass and synthetic ash.

Furthermore the effects of phosphor additives or high phosphor biomass on the ash chemistry as well as the physical properties will also be investigated.

Using the results from these experiments, a release mechanism for the alkali metals and a reaction mechanism for phosphor under gasifying conditions are to be proposed.

Acknowledgements

This project is part of DANENGAS and is funded by the Innovation Fund Denmark and the Sino-Danish Center for Education and Research, and I would like to thank the Chinese Academy of Sciences for their hospitality and support.

References

1. L. Jiang, S. Hu, J. Xiang, S. Su, L.-S. Sun, K. Xu, Y. Yao, *Bioresour. Technol.* 116 (2012) 278-284.
2. O. Hirohata, T. Wakabayashi, K. Tasaka, C. Fushimi, T. Furusawa, P. Kuchonthara, A. Tsutsumi, *Energy Fuels* 22 (6) (2008) 4235-4239.
3. D. M. Keown, J.-I. Hayashi, C.-Z. Li, *Fuel* 87 (2008) 1127-1132.
4. A. Grimm, N. Skoglund, D. Boström, M. Öhman, *Energy Fuels* 25 (2011) 937-947.
5. A. Grimm, N. Skoglund, D. Boström, C. Boman, M. Öhman, *Energy Fuels* 26 (2012) 3012-3023.

**Anders Nørregaard**

Phone: +45 4525 2990
E-mail: andno@kt.dtu.dk

Supervisors: Krist V. Gernaey
Brian Madsen, Novo Nordisk
Stuart M. Stocks, Novozymes
John M. Woodley

PhD Study
Started: January 2013
To be completed: January 2016

Mixing and oxygen transfer processes in bioreactors

Abstract

Biotechnological production in stirred tank reactors suffers from limited available knowledge about the oxygen mass transfer properties and flow patterns in the fermentation broth. This knowledge could be valuable in order to design and optimize the fermentation processes that account for production of a large variety of products. This project investigates the concentration gradients that emerge in the fermentors, and more specifically the focus will be on characterizing the oxygen concentration in the broth. New experimental techniques with minimal impact on the process together with mathematical modeling are necessary in order to investigate this problem in more detail. Experiments will be performed in industrial scale fermentors.

Introduction

Biochemical production by suspended aerobic fermentation processes is nowadays used to produce most industrial enzymes, many pharmaceuticals and chemical precursors. The processes are based on the conversion of a carbon substrate by a microorganism, in the presence of oxygen, to form biomass, products and carbon dioxide. During production, mass transfer of oxygen to the fermentation broth is the rate-limiting factor which has large importance for the process. Due to the large size of the industrial-scale fermentation vessels, concentration gradients inside the reactor will occur, and thereby the often made assumption of perfect mixing in the reactor - usually applied in process models - does not apply. Differences in pressure, agitation intensity and viscosity together with organism growth differentiation make this heterogeneity difficult to predict. The purpose of this project is therefore to investigate the properties of mixing and oxygen transfer in large scale bioreactors in order to better understand the processes and phenomena that take place in these vessels.

Modelling large-scale bioreactor systems is challenging because only a limited experimental basis exists in large scale vessels, and significant differences between laboratory scale and production scale are often observed. Since the processes take place inside a sealed steel vessel, sampling from the vessel is limited to probes that can tolerate the high temperature of the initial heat sterilization of the vessel together with

surface growth of the production organism. A limited number of ports are available for inserting these kinds of probes, often limited to ports in one location in the bottom of the fermentor. The fermentation broth is also opaque which limits the applicability of many optical methods.

Getting access to large scale bioreactors is difficult, since the industries operating such bioreactors usually do not reveal any details related to the dimensions of the reactors. Furthermore, they are normally part of existing industrial processes which means that they cannot be modified for academic reasons due to the risk of disturbing the production.

The time scale of oxygen consumption in a bioreactor is measured in seconds. That is, if the oxygen supply to the fermentor is shut off it will be starved for oxygen within seconds. That makes oxygen a good process parameter for the bioprocess, but it also requires equipment that can detect this parameter fast enough in order to detect the changes. This is not the case for the existing oxygen probes that are build more rugged for the reasons mentioned above.

The volumetric mass transfer coefficient ($k_L a$) is dependent on many of the physical factors of the process and is described by eq. 1, an empirically derived correlation proposed by Cooke et al. [1]

$$k_L a = C * \left(\frac{P}{V}\right)^\alpha * v_s^\beta * \mu_{app}^\gamma \quad \text{Eq. 1}$$

Here P/V is the volumetric power input from agitation (W/m^3), v_g is the superficial gas flow rate if plug flow is assumed (m/s), and μ_{app} is the apparent viscosity of the broth ($Pa \cdot s$). C , α , β and γ are empirically derived constants that are dependent on the fermentor design, production organism and process conditions.

Figure 1 describes the typical flow patterns depending on different impeller configurations. Each set of empirically derived constants for eq. 1 is therefore specific for a given process.

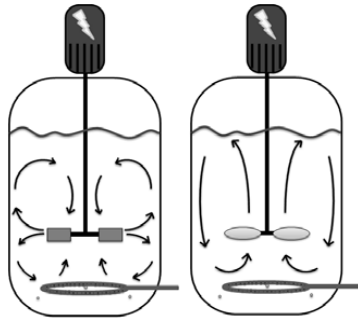


Figure 1: Typical flow patterns inside the fermentor depending on radial (left) and axial (right) pumping impellers.

Specific Objectives

The first part of the project is focused on finding a proper way to establish informative measurements in the bioreactor with the lowest degree of disruption of the fermentation process in the reactor. The first processes to be investigated are the production of cellulase enzyme from cultivation of the filamentous fungus *Trichoderma reesei*, and insulin production with the yeast *Saccharomyces cerevisiae*. These production methods both utilize pure cultures of fungi to produce a secreted protein, but differ significantly in the morphology of the production strain together with the product purity requirements and value.

Knowledge about the spatial heterogeneity in the bioreactor can be put into a compartmentalized model that is described in principle in figure 2 for a 5 compartment model.

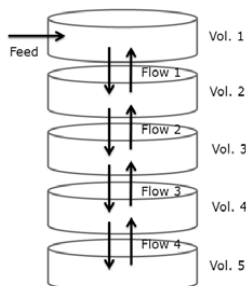


Figure 2: Compartment model with 5 separated well mixed compartments. Flow 1 through 5 represent the transfer rate between the compartments, Vol. 1 through 5 represent the volume of each compartment.

A growth model for the bioprocess e.g. the one presented by Albæk et al. [2], can be applied for each compartment with a different $k_{l,a}$. This could improve the model accuracy and could also be represented in downscaled experiments that utilize several small fermentors in series each with appropriate oxygen mass transfer to mimic the spatial heterogeneity of the larger fermentors. This method can not only be applied to improve existing models, but also facilitates design of new processes and screening of new production strains. It can also be used to rethink some of the more practical aspects of the equipment design, such as where to add substrate and pH control in order to reduce the concentration gradients.

Results and Discussion

An experimental method for oxygen measurement has been proposed; equipment has been acquired and tested in lab scale. Some adaption is necessary before the setup is tested in large pilot scale on a real fermentation.

Conclusions

The issue concerning characterization of the spatial heterogeneity in fermentors has long been known and several studies to investigate the problem by means of mathematic modeling supported with pilot scale experiments have been carried out. These experiments often suffer from the highly dynamic and complex issue of scalability of the processes. Characterization of the spatial heterogeneity in a production scale fermentor has still not been carried out, and the potential benefits of such a characterization cover all aspects of cultivation of suspension cultures in large vessels, including design of production equipment, production organisms and process conditions.

Acknowledgements

The project is carried out in collaboration with Novo Nordisk A/S and Novozymes A/S. The project is financed by the BIOPRO project, and by the Technical University of Denmark

References

1. M. Cooke, J.C. Middleton, J.R. Bush. Mixing and mass transfer in filamentous fermentations. 2nd International Conference on Bioreactors. Cambridge, UK 1988.
2. M.O. Albæk, K.V. Gernaey, M.S. Hansen, S.M. Stocks. Modeling enzyme production with *Aspergillus oryzae* in pilot scale vessels with different agitation, aeration, and agitator types, *Biotechnol. Bioeng.* 108 (2011) 1828-1840.

List of Publications

A. Nørregaard, S.M. Stocks, K.V. Gernaey, J. Woodley, Filamentous fungi fermentation. In: Meyer, H.P. & Schmidhalter, D. (eds.) *Industrial scale suspension culture of living cells*, Wiley-VCH, 2014.
L.R. Formenti, A. Nørregaard, A. Bolic, D. Q. Hernandez et al. (2014) Challenges in industrial fermentation technology research. *Biotechn. J.* 9, 727-738.



Brian Kjærgaard Olsen

Phone: +45 4525 2830

E-mail: bria@kt.dtu.dk

Supervisors: Anker Degn Jensen
Francesco Castellino, Haldor Topsøe A/S

PhD Study
Started: June 2011
To be completed: March 2015

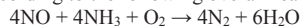
Deactivation of Selective Catalytic Reduction Catalysts in Biomass Fired Power Plants

Abstract

In order to study the alkali poisoning of vanadia based catalysts for selective catalytic reduction of nitrogen oxide, catalyst samples have been exposed to potassium rich aerosols in a bench scale setup. Activity measurements of exposed catalysts indicate that tungsten oxide promoted samples deactivate faster. This is speculated to be due to a higher Brønsted acidity which facilitates the transport of potassium. A newly developed experimental protocol involving three-layer pellets indicate that an alkaline barrier material can hinder the potassium transport.

Introduction

Selective catalytic reduction (SCR) of nitrogen oxides (NO_x) with ammonia (NH_3) is a well established method for controlling the NO_x emissions from stationary sources such as coal fired heat and power plants [1,2]. In the presence of oxygen (O_2), nitrogen oxide (NO) is catalytically converted into molecular nitrogen (N_2) according to the following overall reaction [1]:



The most widely used catalysts for such applications consist of titania (TiO_2) supported vanadia (V_2O_5), promoted with either tungsten oxide (WO_3) or molybdenum oxide (MoO_3), in the shape of honeycomb monoliths [2].

Topsøe and co-workers [3,4] proposed a mechanism for the SCR reaction over V_2O_5 based catalysts consisting of two catalytic cycles involving Brønsted acid sites ($\text{V}^{5+}\text{-OH}$) and the redox sites ($\text{V}^{5+}=\text{O}$).

In a time with great focus on decreasing the release of carbon dioxide (CO_2) to the atmosphere, firing (or co-firing) of biomass (straw, wood chips, etc.) is being applied in order to reduce the net CO_2 emissions. Unfortunately, alkali and alkaline earth metals, which can be present in biomass in high concentrations, may act as poisons to the industrially applied SCR catalysts and can reduce their life-time dramatically [5]. Potassium, released e.g. during firing of straw, may form submicron aerosols of potassium chloride (KCl) and/or potassium sulfate (K_2SO_4) which can deposit on the catalyst surface. Most likely through a surface diffusion mechanism, potassium subsequently diffuses into the catalyst wall [6]. It is believed that potassium,

due to its alkaline nature, poisons the SCR catalyst by reacting with the acidic $\text{V}^{5+}\text{-OH}$ sites [6,7]. Research has furthermore shown that the reducibility of $\text{V}^{5+}=\text{O}$ species is inhibited upon alkali poisoning [8].

While the effect of potassium on commercial SCR catalysts is generally well understood, a more systematic study of the deactivation mechanism will provide useful information for development of new alkali resistant catalysts and/or improved means of operation.

Specific Objectives

The main objective of this PhD study is to investigate the influence of catalyst composition and operating conditions on the rate of deactivation during alkali poisoning. It is particularly of interest to study the relationship between surface -OH sites and the rate of alkali penetration.

Experimental

Plate shaped catalysts have been exposed to potassium rich aerosols in a bench scale reactor described in detail in [6]. The catalysts, obtained from Haldor Topsøe A/S, consisted of samples of varying composition with respect to V_2O_5 and WO_3 . Parameters such as exposure time, operating temperature and aerosol particle size distribution have been varied between each exposure experiment. Catalytic activities were measured in a fixed bed reactor at temperatures between 250 and 400 °C using a total gas flow of 2800 NmL/min composed of 500 ppmv NO , 600 ppmv NH_3 , 5 vol.% O_2 , about 1.4 vol% H_2O and balance N_2 .

A new method to study the transport of potassium in SCR catalysts has been developed. Here, multi-layer pellets of crushed plate catalyst, consisting of one layer of fresh SCR catalyst and one layer of the same catalyst impregnated with about 0.8 wt.% potassium, have been made. Pellets with a central layer of MgO, which may ultimately be used as an alkali resistant coating [9], were produced as well. The pellets were exposed at 350 °C in a flow of 6 vol.% O₂, 3 vol.% H₂O and balance N₂. The potassium profiles through the three layers were recorded by SEM-EDS.

Results and Discussion

The relative activities measured at 350 °C of the exposed catalysts are given in Table 1 together with the conditions at which the samples were exposed. While the absolute activity of a WO₃ promoted catalyst generally is higher than that of an un-promoted one, the relative activity drop upon exposure to a potassium rich aerosol is, in most cases, larger for promoted samples. This indicates that the increased Brønsted acidity provided by the WO₃ facilitates the transport of potassium in the catalysts, accelerating the poisoning. Furthermore, it is apparent that the catalysts deactivate slower at lower exposure temperatures.

Table 1: Exposure conditions and relative activities of V₂O₅-(WO₃)/TiO₂ catalysts.

V ₂ O ₅ content (wt. %)	K source	Temperature (°C)	Time (h)	Relative activity at 350 °C (%)	
				0 % WO ₃	7 % WO ₃
1	KCl	350	600	24	11
3	KCl	350	600	19	2
6	KCl	350	600	1	4
1	KCl	150	300	77	29
3	KCl	150	300	32	52
6	KCl	150	300	47	34
1	KCl	350	300	0	6
3	KCl	350	300	14	1
6	KCl	350	300	2	3
3	K ₂ SO ₄	150	240	77	64
3	K ₂ SO ₄	300	240	37	50

Figure 1 shows the potassium profiles in two-layer pellets exposed for 8 hours.

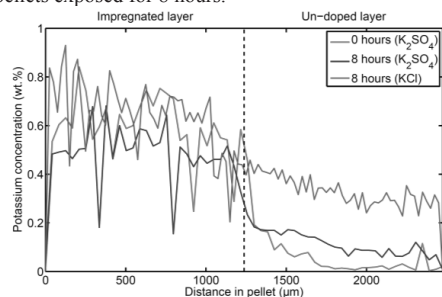


Figure 1: Potassium profiles through two-layer pellets.

In the figure, a significantly higher potassium level can be observed in the un-doped side of a pellet with a KCl impregnated layer, compared to one impregnated with K₂SO₄. This indicates that potassium bound in KCl can more easily leave its counter-ion compared to that bound in K₂SO₄. This may partly explain the lower deactivating effect of K₂SO₄ seen in Table 1.

Figure 2 shows the potassium concentration through a pair of three-layer pellets which have been heat treated for 32 hours. While potassium has diffused into the un-doped 3%V₂O₅-7%WO₃/TiO₂ layers in one pellet, the alkaline MgO layer has prevented the transport of potassium in the other, indicating that potassium is more readily transported over acid sites, while the basic MgO provides an efficient barrier for potassium.

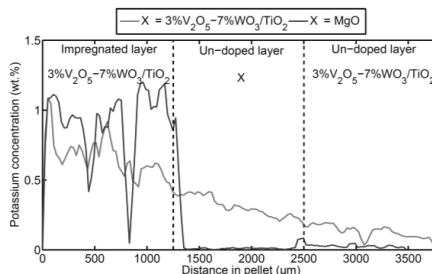


Figure 2: Potassium concentration profiles through three-layer pellets.

Conclusion

Both the activity of potassium aerosol exposed SCR catalysts of varying composition as well as potassium concentration profiles through three layer pellets indicate that the potassium transport in V₂O₅ based catalysts is facilitated by acid sites.

Acknowledgements

This PhD project is a part of the GREEN Research Center (Center for Power Generation from Renewable Energy) financed by the Danish Council for Strategic Research (DSF-10-093956).

References

- H. Bosch, F. Janssen, *Catal. Today* 2 (1988), 369-532.
- P. Forzatti, *Appl. Catal. A* 222 (2001), 221-236.
- N.-Y. Topsøe, *Science* 256 (1994), 1217-1219.
- J.A. Dumesic, N.-Y. Topsøe, H. Topsøe, Y. Chen, T. Slabiak, *J. Catal.* 163 (1996), 409-417.
- Y. Zheng, A.D. Jensen, J.E. Johnsson, *Ind. Eng. Chem. Res.* 43 (2004), 941-947.
- Y. Zheng, A.D. Jensen, J.E. Johnsson, J.R. Thøgersen, *Appl. Catal. B* 83 (2008), 186-194.
- J.P. Chen, R.T. Yang, *J. Catal.* 125 (1990), 411-420.
- L. Chen, J. Li, M. Ge, *Chem. Eng. J.* 170 (2011), 531-537.
- A.D. Jensen, F. Castellino, P.D. Rams, J.B. Pedersen, S.S.R. Putluru, *European Patent Application EP 2338591* (2011).

**Emmanouil Papadakis**

Phone: +45 4525 2808
E-mail: empap@kt.dtu.dk
Discipline: CAPEC-PROCESS

Supervisors: Professor Rafiqul Gani
Professor Krist V. Gernaey
Associate Prof. Gürkan Sin

PhD Study
Started: October 2013
To be completed: September 2016

Modeling and Synthesis of Pharmaceutical Processes: Moving from batch to continuous manufacturing

Abstract

A survey in pharmaceutical industry has shown a majority of the production systems involve batch processes which offers the equipment flexibility and the product quality control. However, the batch processes are not very good for the product quality assurances and have some drawbacks such as low productivity, high operational cost and big amounts of generated waste. Therefore, the objective of this study is to develop a method to tackle key research areas to improve pharmaceutical processes and to evaluate different alternatives to lead in more sustainable design by using systematic model based methods. The developed method has been applied in two case studies (1) BHC ibuprofen synthesis and (2) glucose isomerization.

Introduction

The delay with the introduction of innovative systems into pharmaceutical manufacturing can be attributed to the regulatory uncertainty. Generally, the batch processes are not good for product quality assurance and possess a number of drawbacks such as poor process understanding, low productivity, high energy consumption, high capital cost, low product purity, scalability and waste production [1].

However, over the last decade the regulatory bodies (FDA in USA, EMA in Europe etc.) require the pharmaceutical companies to demonstrate more process understanding. Moreover, the pharmaceutical companies need to meet their profit expectations due to increasing R&D costs and market competition [2, 3]. Consequently, pharmaceutical industry is expected to look for opportunities to rapidly evaluate the different alternatives for process improvement.

Process Systems Engineering (PSE) methods and tools can have important roles to play, for example: (a) apply computer aided-methods and tools that are mature for other industries (such as chemical and petrochemical) also in solving problems in pharmaceutical industries, (b) in the evaluation and implementation of alternative solutions and/or design and (c) to evaluate opportunities for continuous manufacturing [4, 5, 6].

It has been recently published a list with ten key research areas to achieve sustainable pharmaceutical process development [2]. One of this research areas is the development and the implementation of continuous

manufacturing (CPM) which naturally eliminates some of the batch process drawbacks and enhances the process understanding. CPM involves smaller equipment which leads to lower capital cost, reduced energy and solvent demands and reduced plant footprint. Bioprocesses and bio-catalysis can improve the sustainability of the pharmaceutical process due to the high selectivity to the desired product which reduces the number of the synthesis steps and consequently the generated waste. Also, the typical synthesis of APIs requires the use of sequences of reaction and separation tasks which are energy and mass intensive processes. Optimization and introduction of novel unit operations and intensified equipment are necessary in order to improve the reaction and the separation efficiency. Solvents are used for the synthesis, separation and washing in the pharmaceutical industry, proper solvent selection can lead to the reduction of number of solvents and optimize the use. Life cycle assessment (LCA) analysis help to identify the process hotspots from the extraction of the raw materials to the product end. Finally, mass and heat integration can reduce the use of the energy and solvents.

The objective of this project is to develop a systematic integrated methodology which its objective is to improve pharmaceutical process operation/design and to evaluate opportunities for continuous manufacturing through better understanding of pharmaceutical processes. The integrated systematic framework needs to be applicable in the multipurpose pharmaceutical industry in order to

achieve greener and safer processes with higher product quality by using systematic model-based methods [2].

Integrated Systematic Methodology

The systematic integrated framework (Figure 1) is developed with the specific aim of assisting the multi-purpose pharma/biochemical industry to systematically solve the multiple complex problems that are faced when seeking to develop an enhanced process understanding and exploiting potential improvements of the pharma/biochemical processes. The framework starts with the problem definition where the objectives of the study are defined. The subsequent reaction pathway identification section (Section A) aims at identifying the number and the type of necessary reaction steps to produce a pharma/bio-product of interest. Section B is the reaction analysis, and aims at collecting data for each reaction, to perform kinetic analysis, to identify reaction limitations, to evaluate the reaction variables, and to make a decision on whether the reaction can be operated in continuous or batch mode, to design the reactor, and finally to define the objectives of the separation if needed [6]. Section C (Separation Synthesis and Design) is performed in case separation of a specific compound is needed. Section C starts with the mixture analysis to identify separation limitations, and generates the binary ratio mixtures in order to identify the most feasible separation task. Based on the driving force principles, the separation alternatives can be generated and evaluated in order to select the most feasible ones. Once a flowsheet has been obtained, a process simulation (Section D) needs to be performed in order to evaluate the process and identify the process hotspots. Based on the process evaluation, process optimization and process operation can be performed.

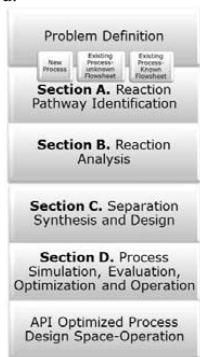


Figure 1. Integrated Systematic Framework.

Methods and Tools

In order to collect the information for each section of the framework, the use of model-based methods and tools are necessary. Such methods and tools are knowledge databases, model libraries, solvent selection tools, mathematical solvents and evaluation tools. Knowledge databases need to provide information for the reactions (APIs Synthesis database), for the unit operations (Unit Operation database), pure compound property database

(CAPEC database) and monitoring-control (ICAS-PAT) database. Model libraries need to provide information for different unit operation models, property prediction models, and reaction kinetics models. Solvent selection tools for proper solvent selection, and finally evaluation tools for economics, sustainability and LCA analysis.

Case Study 1-BHC ibuprofen Synthesis

The objective of this case study is to apply and verify the developed framework in order to generate the batch process to produce high purity ibuprofen crystals. Also, process alternatives need to be generated to achieve the objectives and finally, to identify possible process hotspots to improve the process such as possibilities of CPM, solvent selection and optimization, reaction improvement and separation improvement.

Case Study 2-Glucose Isomerization

In this study, the use of model-based methods within the systematic framework is illustrated through a glucose isomerization (GI) reactor case study. The objective of this study is the use of a multi-scale reactor model which includes the reaction kinetics and the enzyme activity decay as a function of temperature with and without the diffusion term, to simulate the reactor and to investigate opportunities for improving the productivity of the reactor.

Conclusions-Future work

A systematic integrated framework to enhanced process understanding and exploiting potential improvements of the pharma/biochemical processes and applied to two different cases studies. The framework needs to be applied in other cases studies, to be extended and include bioprocesses, to be integrated with reaction synthesis pathways and to extend the knowledge databases (APIs database and Unit Operation database) and the model libraries.

References

1. K. Plumb, Chem. Eng. Res. Des., 83 (6), (2005), 730-738.
2. C. Jiménez-González, P. Poehlauer, Q. B. Broxterman, B.-S. Yang, D. am Ende, J. Baird, C. Bertsch, R. E. Hannah, P. Dell'Orco, H. Noorman, S. Yee, R. Reintjens, A. Wells, V. Massonneau, and J. Manley, Org. Procces Res. Dev. 15(4), (2011), 900-911.
3. S.D. Schaber, D.I. Gerogiorgis, R. Ramachabdran, J.M. Evans, P.I. Barton, B. L. Trout., Ind. Eng. Chem. Res. 50 (17), (2010), 10083-10092
4. K.V. Gernay, A. E. Cervera- Pardell, J. M. Woodley, Comput. Chem. Eng., 42, (2012) 30-47
5. A. Rogers, A. Hashemi, M. Ierapetritou, I, (2013), 67-127
6. A. E. Cervera- Pardell, T. Skovby, S. Kiil, R. Gani, K.V. Gernay, Eur. J. Pharm. Biopharm., 82 (2), (2012), 437-456



Christine Malmos Perfeldt

Phone: +45 4525 2892
E-mail: mmos@kt.dtu.dk
Discipline: Enhanced oil Recovery

Supervisors: Nicolas von Solms
John M. Woodley

PhD Study
Started: August 2011
To be completed: May 2015

Inhibition of Gas Hydrate Formation by Antifreeze Proteins

Abstract

Antifreeze proteins (AFPs) have shown in the literature to be promising green and environmentally benign inhibitors for gas hydrate formation. Especially insect AFPs express high antifreeze activities which is their ability to prevent ice from freezing. In this study we showed that RmAFP1 from the long horn Danish bark beetle, *Ragium mordax*, can perform as an effective kinetic hydrate inhibitor (KHI) on the same level as the commercial synthetic inhibitor polyvinylpyrrolidone (PVP).

Introduction

Gas hydrates are crystalline solid compounds of gas molecules and water which forms at low temperature and high pressure. In the oil and gas industry gas hydrates block flow lines and pipelines in during production causing huge production losses and safety problems.

Hydrate formation is a stochastic time-dependent process consisting of the steps of nucleation and growth. Several theories and hypothesis are suggested in order to describe the nucleation mechanism of hydrates. Sloan et al. 2007 proposed the 'labile cluster nucleation' hypothesis. A labile cluster is an unstable entity (cavity occupied by a guest molecule) that readily undergoes changes. First pressure and temperature are at hydrate forming conditions but no gas is dissolved. Then gas dissolve into the water and labile clusters form. These clusters undergo agglomeration and finally hydrate growth begins when the size of clusters reaches a critical value.[1] Pictures corresponding to the steps were taken during a hydrate formation experiment with natural gas and water (Figure 1).

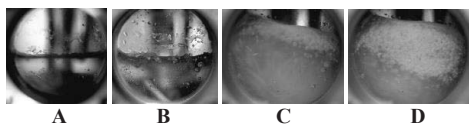


Figure 1: Photographs of hydrate formation.

To provide flow assurance the industry use thermodynamic inhibitors as methanol, which are uneconomical and not environmentally friendly as large

amounts are needed. Low dosage hydrate inhibitors are developed as an alternative which can be applied in much lower concentrations. Most of these suffer from low biodegradability which means that they cannot be applied in the North Sea.

Recent studies have shown that antifreeze proteins may hold a promising potential to work as a low-dosage hydrate inhibitors in both natural gas [2,3] and methane gas [4] systems while at the same time being environmentally benign. AFPs protect organisms from deep freezing temperatures by preventing ice from growing upon cooling below the melting point. Especially AFPs from insects show considerable higher antifreeze activities than AFPs from other organisms. The long horn Danish bark beetle *Ragium mordax* (RmAFP1) can express antifreeze activity in excess of 8°C which is more than other insect proteins.[5]

Specific Objectives

The objective of this PhD project is to investigate if AFPs can be applied in field conditions to control the formation of gas hydrates.

The focus is therefore to setup laboratory scale experiments to simulate realistic hydrate formation scenarios using three different experimental apparatus: high pressure micro-Differential Scanning Calorimeter (HP- μ DSC), Rocking Cells, and a pressurized stirred autoclave. Using these high pressure equipments, different types of water soluble polymeric commercial low-dosage hydrate inhibitors will be evaluated and the performance will be compared to AFPs. Synergy effects between inhibitors and other production chemicals will be studied and an evaluation of health, safety and

environmental matters related to AFPs will be carried out. Finally a feasibility study will be carried out to investigate if AFPs can be implemented in field applications.

Measurements of the onset hydrate nucleation temperatures by constant cooling experiments were studied in Rocking Cells produced by PSL Systemtechnik (Figure 2). The methodology applied is based on the precursor (memory effect) method described by Duchateau et al. [6] The apparatus consists of 5 test cells placed on a cell drive in the cooling bath.



Figure 2: Rocking Cells.

The measuring principle is based on a uniform rocking movement of the test cells. When the cell is rocked the ball inside the cell is rolling along the length of the cell and thereby blends the test mixture. Through movement of the ball shear forces and turbulence are created in the cell, thereby reproducing the conditions in the pipelines.

Results and Discussion

Previous studies showed that AFPs do inhibit hydrate nucleation [2,4]. In Figure 3 the onset hydrate nucleation temperatures for fresh and memory solutions are shown. The amino acids L-valine and L-threonine do not exhibit any KHI effect in the form of pure amino acids as they do not delay hydrate nucleation compared to the non-inhibitor system. RmAFP1 shows a very promising result as a KHI compared to PVP.

The ranking of the KHI performance in both fresh and memory constant cooling tests, using the onset hydrate temperatures was clearly:

RmAFP1 = PVP10 > BSA > L-threonine = L-valine = 50mM NaCl in MilliQ water

Daraboina et al. 2011 observed a similar result for PVP and AFP for inhibition of natural gas hydrates. Using an isothermal nucleation procedure to obtain the nucleation time (time delay of hydrate formation) it was shown that PVP and AFP obtained very similar nucleation times using both a stirred tank and the HP μ DSC. [2] This indicates that the AFPs are performing similar for both methane systems (SI hydrates) and natural gas systems (SII hydrates).

For antifreeze proteins at equimolar concentrations an increase in size of protein decreases the solubility of the protein in the water phase which will lead to increased antifreeze activity [8]. We speculate that the observed KHI effect of BSA could be due to decreased solubility

as the molecular weight of BSA (67 kDa) is significantly higher compared to RmAFP1 (14 kDa).

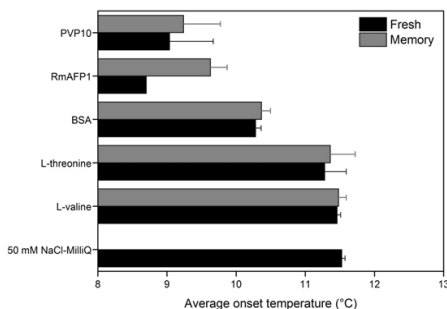


Figure 3: Onset hydrate nucleation temperatures using KHIs at a concentration of 2770 ppm.[7]

Conclusions

Hydrate nucleation tests showed that the RmAFP1 from the long horn Danish bark beetle, *Ragium mordax*, perform as an effective hydrate nucleation inhibitor as the synthetic inhibitor PVP.

Further tests are needed to verify the performance of the RmAFP1. To simulate realistic scenarios moreover, experiments are planned to be carried out in different salinity levels in order to simulate the variations observed in the fields. The biodegradability of RmAFP1 compared to synthetic inhibitors will be studied as it is of great importance for selection of future KHIs.

Acknowledgements

The project is a part of the advanced technology project 'Biotechnology in Oil Recovery', funded by the Danish National Advanced Technology Foundation, the Technical University of Denmark, Maersk Oil A/S, Dong Energy A/S, Novozymes A/S, Danish Technological Institute and Roskilde University.

References

1. R.L. Christiansen, Jr ED. Sloan, Annals of the New York Academy of Sciences 715 (1994) 283-305.
2. N. Daraboina, P. Linga, J. Ripmeester, V.K. Walker, P. Englezos, Energy Fuels 25 (2011) 4384-4391.
3. L. Jensen, K. Thomsen, N. von Solms, Energy Fuels 25 (2011) 17-23.
4. L. Jensen, H. Ramløv, K. Thomsen, N. von Solms Ind. Eng. Chem. Res. 49 (2010) 1486-1492.
5. E. Kristiansen, C. Wilkens, B. Vincents, D. Friis, A.B. Lorentzen, H. Jenssen, A. Løbner-Olesen, H. Ramløv, J. Insect Physiol. 58 (2012) 1502-1510.
6. C. Duchateau, J. Peytavy, P. Glénat, T. Pou, M. Hidalgo, C. Dicharry, Energy Fuels 23 (2009) 962-966.
7. C.M. Perfeldt, P.C. Chua, N. Daraboina, D.S. Friis, E. Kristiansen, H. Ramløv, J. Woodley, M.A. Kelland, N. von Solms, Energy Fuels 28 (2014) 3666-3672.
8. E. Kristiansen, K.E. Zachariassen, Cryobiology 51 (2005) 262-280.

**Thomas Petersen**

Phone: +45 4174 8010
E-mail: tpet@kt.dtu.dk
Discipline: Transform Phenomena

Supervisors: Ole Hassager
Thorvald Ullum,
GEA Process Engineering A/S
Jakob Sloth, GEA Process Engineering A/S

Industrial PhD Study

Started: September 2012
To be completed: August 2015

Model of Stickiness in Spray Drying

Abstract

Wall deposits are a major concern in the design of spray drying equipment and the most troublesome type is a result of a property referred to as 'stickiness'. The cause for stickiness is currently not determined conclusively and no accurate models exist for predicting stickiness in spray drying quantitatively. It is the purpose of this study to understand the phenomena causing stickiness in spray drying, using experimental as well as modelling techniques. In this endeavour a novel measurement setup has been designed.

Introduction

Spray drying is a well described method for obtaining dry particles from a liquid feed, used in many industries, ranging from food and dairy, through chemicals to pharmaceuticals. Amongst other things it has the advantage of relatively low drying temperatures and well-controlled, uniform particle size distribution. In spite of this some challenges remain with the method, one of the most dominant of which is wall deposits [1]. Deposits can occur for various reasons depending on the condition of the impacting droplet or particle and various techniques are already in use in order to avoid it. Wet particle-wall impact is avoided by use of controlled flow conditions and dry particles that are deposited because of attractive contributions from Van der Waals and electrostatic forces can be removed by application of pneumatic hammers or air brushes. However one type of wall deposits remains a problem, namely those caused by what is known as stickiness in the industry. The term stickiness refers to the condition when a material is very close to dry and yet still adheres. Several studies of sticky materials have shown that stickiness of a substance occurs at a temperature close to and above its glass transition temperature T_g – a point at which a substance changes from a glassy (below) to a rubbery (above) state – some of which are reviewed in [2]. However the range of temperatures (even within the same study) varies between 5-40 °C with no conclusive explanation given. Furthermore most of these measuring techniques fail to match the conditions seen during spray drying. As such the phenomena determining stickiness in spray drying

remain unidentified and an accurate measuring technique has yet to be published.

Specific Objectives

The purpose of this study is to identify the phenomena determining stickiness. This will be done through both experimental work and mathematical modelling.

The experimental contribution will consist of a novel technique for measuring stickiness with relevance to spray drying (this is elaborated below). The primary purpose of modelling will be to understand the results of these measurements as well as determining parameters of importance to scaling.

The modelling work will consist of simulating the drying of a droplet and the impact between a partially dried droplet and a wall. Numerical tools will be used to obtain a mathematical model for the drying in order to describe the conditions (temperature and humidity distribution) in the wet particle upon impact and how this depends upon drying conditions and droplet size. The Finite Element Method combined with the Level Set Method will be used to understand how the impact of a wet droplet covered by a highly viscous skin may lead to either adhesion (in the case of a sticky particle) or not (in the case of a non-sticky particle) and how this behaviour scales with droplet size and impact velocity.

New Setup

The description of the new experimental setup will be separated into two parts. The first is the description of the droplet levitator that allows for controlled drying of a single droplet. The second is the component which

allows for impact between a wall and the partially dried droplet.

Droplet Levitator

The droplet levitator is based on an experimental setup used to study drying kinetics and particle morphology during spray drying [3]. The levitator setup is also referred to under the trademark DRYING KINETICS ANALYZER™. The levitator setup consists of 4 separate parts shown in figure 1: 1) an ultrasonic horn and a concave reflector, 2) an optical system of a diffuse light source and a CCD camera and lens, 3) a gas conditioning system used to control the gas temperature and humidity of the drying environment as well as the slip velocity and 4) a droplet injection system consisting of a syringe with a microtip and a mechanical actuator.



Figure 1: Illustration of the levitator setup. The horn and reflector are enclosed in a chamber which is not shown in the figure.

Particle Impactor

The particle impactor is the new addition to the levitator setup to allow for a stickiness measurement. The particle impactor is a linear DC-servomotor attached in such a way that upon activation a piston will move forward and strike the particle from the side as recorded by the CCD-camera seen in figure 1. The velocity of this piston upon impact may be controlled up to 2 m/s. Depending on the time a droplet has dried, different results are seen. Examples of these are shown in figure 2. Figure 2a shows a levitating droplet while it is drying. If a droplet is dried only for a short time, a result similar to that shown in figure 2b is obtained where the droplet is still wet and thus spreads like a droplet of water on stainless steel.

Once a droplet has dried longer a highly viscous skin or solid crust (depending on product and drying time) is formed on the surface (the droplet thus becomes a “wet particle”). If impact occurs in this region a result as seen in figure 2c may be obtained. Notice that the particle does not spread upon the piston, but adheres nonetheless. If drying extends even further, the piston may impact the particle, with no adhesion occurring, thus showing a non-sticky particle.

Drying multiple droplets for different durations of time allows for the determination of a critical drying time at which a sticky, wet particle becomes a non-sticky particle. Doing this for various products, with differing drying conditions, impact velocity or yet other

parameters, the dependence of stickiness upon these may be investigated.

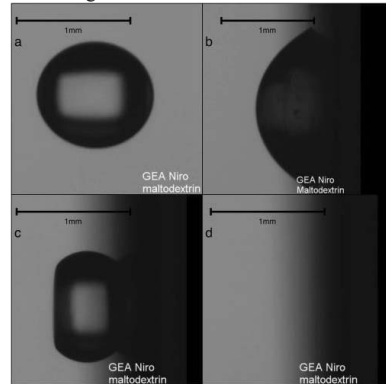


Figure 2: Snapshots of droplets during drying (a) and after impact (b,c,d). a) Before impact. b) Wet droplet, post-impact. c) Sticky particle, post-impact. d) No particle, post-impact.

Conclusion and Outlook

An accurate model would allow improved equipment design for avoiding stickiness in spray drying during operation. Such a model would require knowledge of the phenomena which determine stickiness; however this is not currently available.

In order to further this understanding a novel measurement technique has been designed based on a droplet levitator (allowing for controlled drying under conditions comparable to those expected in a spray dryer) and a particle impactor (allowing the mimicking of the wet particle impacting a wall). This tool may be applied to map stickiness for a given material, with different drying and impact conditions.

Drying and impact models are being developed so that the results of this setup may be fully understood and scaling may be possible in the future, thus minimizing the necessary measurements on a new feed to be spray dried.

Acknowledgements

This project is carried out in cooperation between GEA Process Engineering A/S and the DPC group at DTU Chemical Engineering. Furthermore it is partially funded by the Danish Industrial Ph.D. Fellowship Programme administered by the Danish Agency for Science Technology and Innovation.

References

1. K. Masters, Deposit-Free Spray Drying: Dream or Reality? Proc. Tenth International Drying Symposium IDS '96; Vol. A, 52-60; Krakow, Poland, 1996
2. B. Adhikari, T. Howes, B.R. Bhandari. V. Truong, International Journal of Food Properties, 4 (1) (2001) 1-33
3. A. Brask, T. Ullum, P. Thybo, S.K. Andersen, In 6th International Conference on Multiphase Flow, Leizig, Germany, July, 2007, paper no. 789.



Daniela Quintanilla
Phone: +45 4525 2990
E-mail: danaquh@kt.dtu.dk

Supervisors: Krist V. Gernaey
Ole Hassager
Kim Hansen, Novozymes

PhD Study
Started: November 2013
To be completed: October 2016

Morphology, Rheology and Mass Transfer in Fermentation Processes

Abstract

It is believed that the morphology of filamentous fungi is closely associated with productivity in fermentation processes. However, until now there is no clear evidence of this relation and there is an ongoing discussion around the topic, due to the poor understanding of fungal morphogenesis. Therefore as well, fungal morphology is usually a bottleneck for productivity in industrial production, and will be extensively studied in this work. This will allow us to determine whether a certain microorganism's phenotype has an influence on process performance, and how this performance can be influenced actively by manipulating different process variables or by genetic engineering, as a means of improving the design and operation of filamentous fungi fermentations.

Introduction

Fermentation processes for the production of industrial enzymes are under continuous optimization so that the enzymes can be produced with a lower cost. Manipulation of media, strain improvements and various parameter optimizations (pH, temperature, etc.) are among the most relevant strategies for promoting the overproduction of bulk enzymes to meet the global demand [1]. However, further improvements are needed if enzyme cost has to be reduced to make some processes economically feasible - one example of such a process is the production of second generation bioethanol from renewable feedstock; where the enzymes represent one of the major expenses related with the utilization of cellulosic biomass [2]-. Some of these improvements have to do with process understanding and the comprehension of the interaction of all the variables involved on it.

Production of industrial enzymes is usually carried out as submerged aerobic fermentation, a process that is performed with a substrate, which is either dissolved or remains suspended in an aqueous medium in a closed fermentation vessel where the production microorganism is grown. Filamentous microorganisms are widely used as hosts in these processes due to their ability of secreting large amounts of proteins, post-transcriptional modifications machinery and the fact that a large number of species are generally recognized as safe (GRAS). Nevertheless, they also present major disadvantages, due to the unavoidable oxygen transfer limitations as a consequence of the high viscosity of the

medium that they develop, which is believed to be related to the biomass concentration, growth rate and morphology [3]. This last variable is one of the most outstanding characteristics of the filamentous fungus due to its great complexity [4], and will be fully studied in this project.

Further Background

In submerged cultivations one can recognize different types of morphology, which are usually classified as dispersed and pelletized, as shown in Figure 1. According to this first classification the biomass can be found in the form of freely dispersed hyphae or mycelial clumps. Pellets are highly entangled and dense spherical agglomerates of hyphae which can have diameters varying between several hundred micrometers up to several millimeters [5]. Depending on the desired product, the optimal morphology for a given bioprocess varies and cannot be generalized; in some cases both types of morphology are even combined in one process [6], as illustrated in Figure 2.

A pellet type morphology is preferred since it allows for simplified downstream processing and yields a Newtonian fluid behavior of the medium, which results in low agitation power input. However, the pelleted morphology results in nutrient concentration gradients within the pellet. This situation is obviously not observed in freely dispersed mycelia allowing for enhanced growth and production, which has been attributed to the fact that at the microscopic level the morphology has an influence on the production kinetics,

e.g. on the secretion of enzymes [7]. Therefore, dispersed morphology is the preferred morphology for industrial enzyme production, even though on the macroscopic level this type of morphology greatly affects the rheology of the fermentation broth, and therefore the transport process in the bioreactor increasing the power inputs [7][8].

Specific Objectives

This project aims to improve fermentation processes by understanding and possibly controlling strain morphology. Therefore, the relationships between morphology and productivity will be extensively investigated in this project at the microscopic and macroscopic level, as a means of improving the design and operation of filamentous fungus fermentations. The specific project objectives are:

- In lab scale fermentations, conduct morphological characterization of a filamentous fungus strain at the microscopic and macroscopic level together with the determination of the rheological properties of the fermentation broth.
- Determination of the main process variables influencing the strain morphology and association of specific microscopic morphology with productivity.
- Linking morphology and rheology, and furthermore prove the applicability of the developed model in pilot scale and full scale fermentations.
- Investigate whether rheology can be influenced actively, by modifying strain morphology genetically or by changing process operating mode.

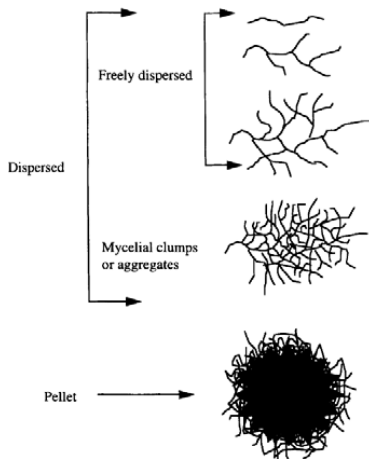


Figure 1: Forms of morphology found in typical submerged cultures of filamentous fungi. Adapted from [5].

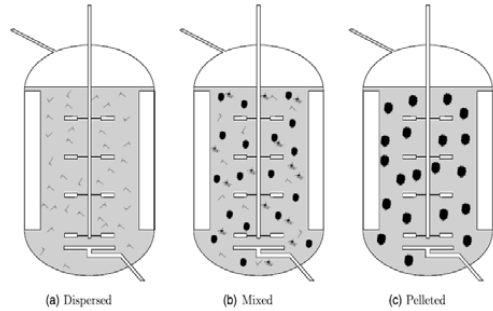


Figure 2: The morphology of filamentous microbes cultivated in bioreactors can range from dispersed hyphal elements to distinct pellets.. Adapted from [6].

Strain

The studies will be conducted on the filamentous fungus *Trichoderma reesei*, specifically on the widely used strain RUT-C30 (ATCC 56765). This microorganism is the host for the production of cellulases, enzymes which are widely used in the production of second generation bioethanol [9].

Acknowledgements

The project is funded by the Novo Nordisk Foundation, Novozymes A/S and the Technical University of Denmark.

References

1. S. Sivaramakrishnan, D. Gandadharan, K. M. Nampoothiri, C. R. Soccol & A. Pandey. Food Technol. Biotechnol., 44 (2006) 173-184.
2. N. Patel, V. Choy, P. Malouf & J. Thibault. Process Biochemistry 44 (2009) 1164-1171.
3. J. J. Smith, M. D. Lilly & R. I. Fox. Biotechnol. Bioeng. 35 (1990) 1011-1023.
4. T. Wucherpfenig, T. Hestler and R. Krull. Microbial Cell Factories 10 (2011) 58.
5. P. W. Cox, C. G. Paul & C. R. Thomas. Microbiology. 144 (1998) 817-827
6. D. J. Barry & G. A. Williams. Journal of Microscopy 244 (2011) 1-20
7. A. Spohr, C. Dam-Mikkelsen, M. Carlsen, J. Nielsen & J. Villadsen. Biotechnol. Bioeng. 58 (5) (1998) 542-553.
8. T. Wucherpfenig, K. A. Kiep, H. Driouch, C. Wirmann & R. Krull. Advances in Applied Microbiology. Elsevier Inc. Oxford U.K, 2010 p. 92.
9. R. Peterson & H. Nevalainen. Microbiology 158 (2012) 58-68.

**Dominik Bjørn Rasmussen**

Phone: +45 4525 2922
E-mail: dbjra@kt.dtu.dk
Discipline: Catalysis

Supervisors: Anker Degn Jensen
Jakob Munkholt Christensen
Anders Riisager, DTU Chemistry
Jan Rossmeisl, DTU Physics
Burçin Temel, Haldor Topsøe A/S
Poul Georg Moses, Haldor Topsøe A/S

PhD Study

Started: December 2011
To be completed: May 2014

Selective and Efficient Synthesis of Ethanol from Dimethyl Ether and Syngas

Abstract

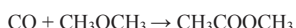
In the present work, carbonylation of dimethyl ether (DME) to methyl acetate (MA) over Mordenite is studied at atomic level with density functional theory (DFT) and experimentally in a high-pressure fixed-bed reactor. The DFT calculations show that MA is primarily formed in the side pockets of Mordenite due to a lower energy barrier for the rate limiting reaction step at this site. Additionally, it is shown experimentally that ketene is a reaction intermediate, in agreement with the DFT calculations. Finally, MA is shown to strongly inhibit the reaction.

Introduction

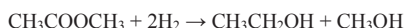
Currently, most transportation fuel is of fossil origin and its continuous use is thus not sustainable. The steadily increasing prices of fossil fuels and the vulnerability of the global economy to disruption of oil supplies are other factors, which make it evident that the demand for alternative fuels will continue to increase. Ethanol (EtOH) can play an important role in this context as gasoline additive or substitute. Catalytic conversion of syngas to ethanol is an interesting option due to its flexibility considering the feedstock and energy efficiency. Syngas can be produced from biomass, making the entire process environmentally friendly.

Catalysts based on Co-MoS₂, converting syngas directly to EtOH, have been developed [1], but their activity as well as selectivity to ethanol is fairly low. In addition, they suffer from the undesirable property of incorporating sulfur compounds into the product, making their industrial use unlikely.

Recently, an alternative, two-step process has been demonstrated [2], where DME, formed from syngas, and CO first react to MA:



MA in turn is hydrogenated to EtOH and methanol (MeOH):



MeOH can afterwards be easily converted to DME, using well-established processes. The main benefit of this method is its unprecedented selectivity towards ethanol, while MeOH, the primary by-product, and the unreacted syngas are easily recycled.

The principal challenges that need to be solved before this method can find industrial application are an increase of the activity and stability of the catalyst for MA synthesis. The subsequent hydrogenation of MA to MeOH and EtOH is facile.

A number of acidic zeolites such as H-MOR, H-ZSM-35 and H-FER may act as selective (> 99 mol %) catalysts for synthesis of MA [3-6]. Mordenite has been identified to have the highest initial activity but there is evidence that H-ZSM-35 may have higher long-term stability [6].

The framework of Mordenite contains three types of cavities (Figure1): 1) the main channel, circumscribed by 12 Si atoms (12 membered ring = 12-MR), 2) 8-MR parallel to the main channel and 8-MR side pockets (SP), which do not interconnect the 12-MR.

A previous experimental [5] study indicates that SP are the active sites for MA synthesis. The main reaction products in 12-MR are large aromatic compounds, which block the channels and are coke precursors. It has been shown that the resistance of Mordenite towards deactivation is significantly increased if the acidic sites in 12-MR are blocked [7] or

removed [8]. Such a treatment does not affect the activity towards MA. To investigate the effects of the channels, all relevant species and reactions, considered in this work, are studied both in 12-MR and SP. Up to the pressure of 10 bar, MA synthesis has been proposed to be zero- and first-order with respect to the partial pressure of DME and CO, respectively [3].

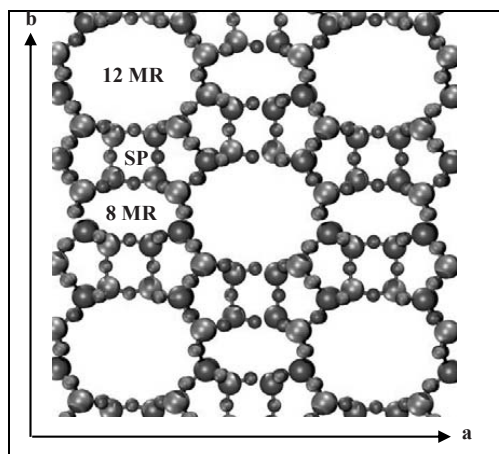


Figure 1: View of the main channel of Mordenite along the c-axis. Oxygen-red (small circles), Silicon-blue (big circles).

Specific Objective

The objective of this work is to improve the understanding of DME carbonylation on Mordenite in a dual experimental/theoretical study. The reaction is examined at the atomic level with density functional theory (DFT) and a microkinetic model will be developed using the data. Additionally, the activity and stability of Mordenite is tested in a high-pressure fixed-bed reactor to verify the theoretical predictions.

Methods

All DFT calculations are performed using the GPAW DFT program [9] and the structure optimizations are done with the ASE [10] program package. For all systems, except molecules in vacuum, periodic boundary conditions are applied with a (1,1,2) k-point mesh of the Monkhorst-Pack type and the electronic temperature of 0.1 eV. The real-space grid spacing for all calculations is 0.18 Å. The BEEF-vdW [11] exchange-correlation (XC) functional is employed for calculations on a pure DFT level (without dispersion forces) and DFT-D, including the dispersion forces, respectively. All geometry optimizations are done until the residual force component is below 0.03 eV/Å. In carbonylation reactions the formation energies of the initial/final state (E_i) are calculated relative to the system with a methyl group, adsorbed at the same site (SP or 12MR), and a CO molecule in vacuum. For reactions involving DME, the reference system is extended by a DME molecule in vacuum.

In the experimental work the Mordenite ($\text{SiO}_2/\text{Al}_2\text{O}_3=20$) obtained from Zeolyst (CBV21A) is used. The initial ammonium form is converted to the acidic form, H-MOR, by heating it at 773 K (heating rate 1K/min) overnight in a flow of air. Before the experiments the catalysts are calcined at 773 K in 10% O_2 in N_2 for 3h (heating rate 1K/min). The experiments are performed in a high-pressure fixed-bed reactor setup (Figure 2) at a temperature of 438 K and at pressures 10-100 bar. The flow of the reactants (2% DME in CO) in all experiments is 300 Nml/min and the amount of catalyst is 1.500g (particle size 125-250 μm). The product characterization downstream from the reactor is conducted using an online GC/MS system.

Results and Discussion

Figure 3 (all energies calculated using BEEF-vdW) shows that formation of methyl acetate mainly occurs in the side pockets because the energy barrier for the rate limiting step is 0.06 eV lower in SP than in 12-MR (the 0.06 eV difference in barriers translates into a factor of

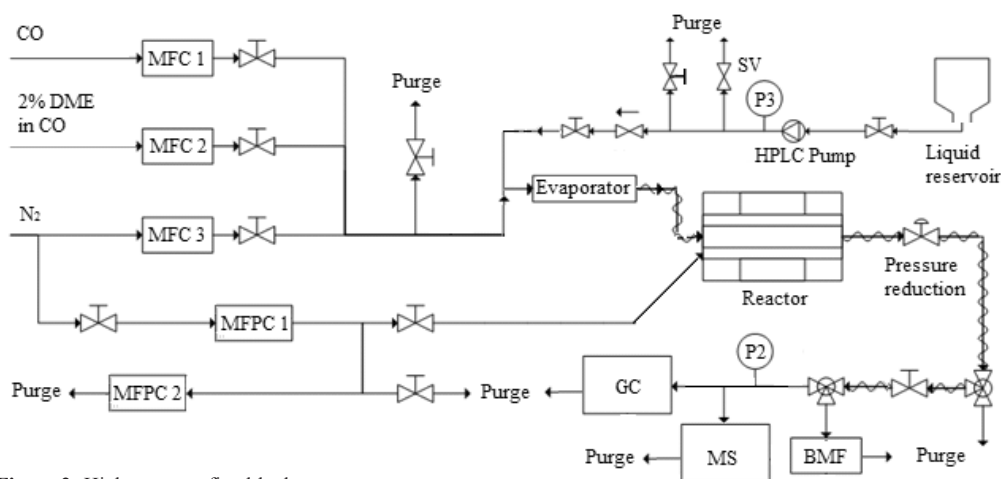


Figure 2: High-pressure fixed-bed reactor.

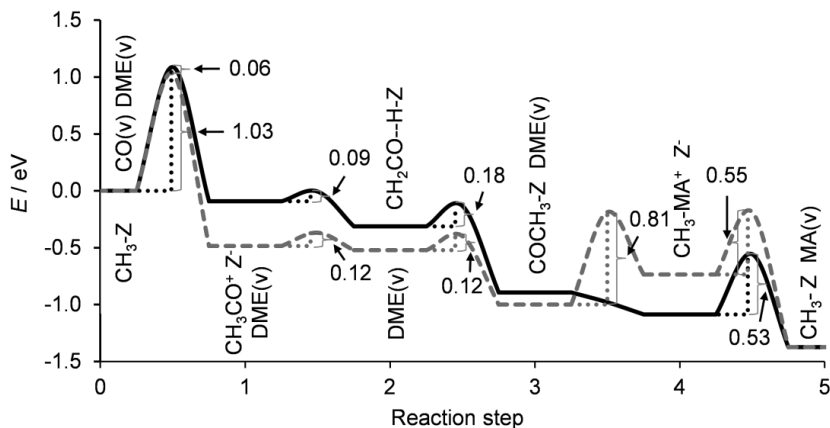


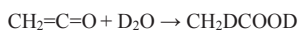
Figure 3: Reaction paths for formation of methyl acetate within the 12-MR and SP of Mordenite. Reaction steps: 0 CO and DME in vacuum, methyl group on the zeolite; 1 Acetyl carbocation and negatively charged zeolite; 2 Ketene physisorbed on a Bronsted acid site; 3 Acetyl group on zeolite; 4 Methylated methyl acetate cation and negatively charged zeolite; 5 Methyl acetate in vacuum and methyl group on the zeolite. Full-drawn line: reaction steps in the main channel (12-MR); Dashed line: reaction steps in the side pocket (SP).

about 5 on the rates at 438 K). The calculations also show that ketene is a reaction intermediate in both the 12-MR and the SP.

These findings are in agreement with the literature and in a recent study of Li et al. [12] it has been observed, using in-Situ Solid-State NMR spectroscopy, that acetyl is only formed in the side pockets during DME carbonylation on Mordenite. Very small amounts of methyl acetate were detected in the main channel, which could mean that some of the methyl groups are carbonylated, and then, as Figure 3 shows, the subsequent reactions are swift. Mordenite is known to undergo a fast deactivation, which is attributed to coke formation in the main channel, whereas zeolites with smaller channels are more stable [6]. Deactivation of Mordenite may be related to the oligomerization of ketene, which is relatively weakly bound and probably has some mobility. Bonati et al. [13] has studied aromatic acylation on zeolites, in which ketene is the acylating agent, and proposed that oligomerization of ketene in zeolite pores plays an important role in the deactivation of the H-Beta zeolite.

To verify the theoretical result that ketene is a reaction intermediate, an experiment with deuterated water (D_2O) was performed. In the experiment, a DME carbonylation reaction was performed and at the time of maximum MA synthesis rate, deuterated water was introduced to the reactant stream.

If D_2O reacts with gas phase ketene ($CH_2=C=O$), acetic acid with 2 deuterium atoms and mass 62u is formed:



All other reaction intermediates, which potentially can form acetic acid upon reaction with deuterated water, create the isotope with mass 61u (CH_3COOD). During

the first 5.7 h of the experiment (Figure 4) the rate of MA synthesis gradually increased, whereas the rate of methanol synthesis concurrently decreased. Then, D_2O was introduced into the CO/DME feed. Upon the introduction of deuterated water the carbonylation reaction was terminated by removal of the methyl groups as CH_3OD , and the MA production stopped. Figure 5 shows the mass ratio between $m/z = 62$ (CH_2D_2COOD) and $m/z = 61$ (CH_3COOD) as a function of time on stream during the experiment. Before the addition of D_2O into the system, the ratio between the signals from doubly and singly deuterated acetic acid isotopes was a noise signal, but as D_2O was introduced, a well-defined peak emerged. The peak in the mass ratio can be rationalized in terms of our theoretical model. Ketene is an intermediate in the carbonylation of DME to MA. Immediately upon the introduction of D_2O the carbonylation reaction was still running, and ketene intermediates were available for conversion to CH_2D_2COOD , whereby the $m/z = 62$ signal became prominent. However, as shown in Figure 4, deuterated water also suppressed the carbonylation reaction by removing the essential methyl groups on the zeolite, and when the carbonylation reaction thus stopped and no more ketene intermediate was formed the $m/z = 62$ signal from CH_2D_2COOD dropped towards the noise level.

Figure 6 shows the dependence of the reaction rate of MA synthesis on the total pressure (gas mixture 2 vol% of DME in CO). The measured reaction rates deviate from the straight line and the deviation increases for increasing reaction pressure. The divergence from the straight line can be viewed as “missing activity” and Figure 7 shows that the “missing activity” is proportional to the average pressure of MA in the

catalyst bed, showing that MA is most likely inhibiting the reaction.

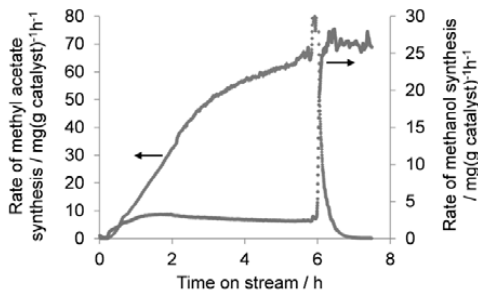


Figure 4: The rate of methyl acetate and methanol formation on H-MOR. Conditions: 9.8 bar CO, 0.2 bar DME, 300 Nml/min, 3.0 g catalyst, 438 K

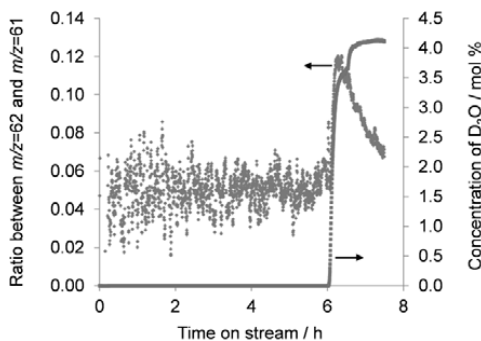


Figure 5: The ratio between the MS signal at $m/z=62$ (doubly deuterated acetic acid) and $m/z=61$ (singly deuterated acetic acid). Conditions: 9.8 bar CO, 0.2 bar DME, 300 Nml/min, 3.0 g catalyst, 438 K.

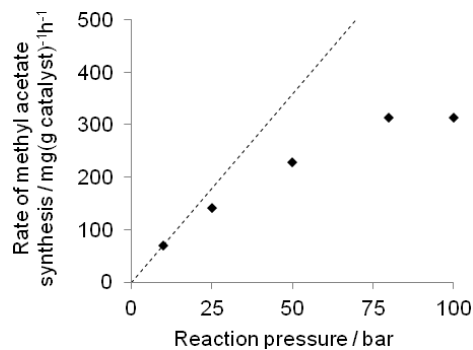


Figure 6: Pressure dependence of MA synthesis.

Conclusion

The present work shows that DME carbonylation on Mordenite primarily takes place in the side pockets. Additionally, it has been shown experimentally that ketene is a reaction intermediate, in agreement with the

DFT calculations. Finally, MA, the reaction product, has a profound inhibiting effect on the reaction.

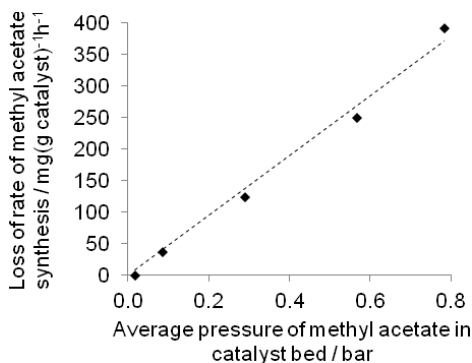


Figure 7: MA inhibition of the reaction rate.

Acknowledgments

The project is financed by DTU and the Catalysis for Sustainable Energy research initiative (CASE), funded by the Danish Ministry of Science, Technology and Innovation.

References

1. J.M. Christensen, P.M. Mortensen, R. Trane, P.A. Jensen, A.D. Jensen, *Applied Catalysis, A: General* 366 (2009) 29-43.
2. X. San, Y. Zhang, W. Shen, N. Tsubaki, *Energy & Fuels* 23 (2009) 2843-2844.
3. P. Cheung, A. Bhan, G.J. Sunley, E. Iglesia, *Angewandte Chemie, International Edition* 45 (2006) 1617-1620.
4. A. Bhan, A.D. Allian, G.J. Sunley, D.J. Law, E. Iglesia, *Journal of the American Chemical Society* 129 (2007) 4919-4924.
5. P. Cheung, A. Bhan, G.J. Sunley, D.J. Law, E. Iglesia, *Journal of Catalysis* 245 (2007) 110-123.
6. J. Liu, H. Xue, X. Huang, Y. Li, W. Shen, *Catalysis Letters* 139 (2010) 33-37.
7. J.L. Liu, H.F. Xue, X.M. Huang, P.H. Wu, S.J. Huang, S.B. Liu, W.J. Shen, *Chinese Journal of Catalysis* 31 (2010) 729-738.
8. H.F. Xue, X.M. Huang, E.S. Zhan, M. Ma, W.J. Shen, *Catalysis Communications* 37 (2013) 75-79.
9. J.J. Mortensen, L.B. Hansen, K.W. Jacobsen, *Physical Review B* 71 (2005)
10. S.R. Bahn, K.W. Jacobsen, *Computing in Science & Engineering* 4 (2002) 56.
11. J. Wellendorff, K.T. Lundgaard, A. Mogelhoff, V. Petzold, D.D. Landis, J.K. Nørskov, T. Bligaard, K.W. Jacobsen, *Physical Review B* 85 (2012)
12. B.J. Li, J. Xu, B. Han, X.M. Wang, G.D. Qi, Z.F. Zhang, C. Wang, F. Deng, *Journal of Physical Chemistry C* 117 (2013) 5840-5847.
13. M.L.M. Bonati, R.W. Joyner, M. Stockenhuber, *Microporous and Mesoporous Materials* 104 (2007) 217-224.

therefore envisaged to be very cost effective for biocatalyst evaluation.

Batch experiments are traditionally seen as better suited for generating kinetic data because of the ability to collect data from many time points in a single experiment [7]. Traditionally, using flow reactors for obtaining kinetic data requires the condition of steady-state. This condition can though be avoided by operating the flow reactor as an ideal plug flow reactor (PFR). However, the PFR requires turbulent flow to be close to ideal, but obtaining this at μ -scale is quite difficult due to the large surface tension. It is though possible to operate the reactor where the radial diffusion across the channel is much faster than convective mass transfer down the channel, this is termed low-dispersed flow. At this condition, the flow profile will be similar to that of a PFR and the steady-state condition can therefore be evaded [8,9]. Operating the reactor in this window will be a cornerstone of this project. **Figure 3** displays the current experimental setup and the dynamics of it. The flow to the reactor is kept constant until a steady-state flow profile has developed, imagine the whole channel as dark green. Hereafter the flow rate is ramped down, and this is what the gradient of the figure shows. The first fluid elements exiting the reactor will have a small (green) residence time, which is gradually increased by ramping down the flow (gradient towards red). The fluid elements will therefore exit the reactor with longer and longer residence times. The measurement on the outlet will show the same dynamics as if you could probe directly in an ideal batch reactor. This analysis is only possible because a batch reactor and a plug-flow reactor have the same kinetics equation, they will have the exact same conversion as a function of conditions and time for any reaction, as time in the batch reactor corresponds to residence time in the plug-flow reactor [10].

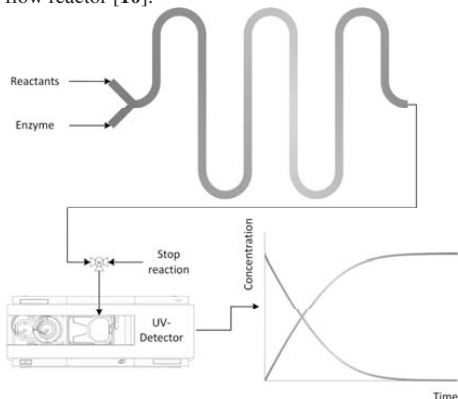


Figure 3: schematic of experimental set-up

A UV-detector has been chosen as it has high sensitivity, can detect aqueous mixtures and collect full spectra (190 to 900 nm) at rates of up to 20Hz. This type of detector is often used in connection with a HPLC system and is hence built for handling of small

volumes. The communication for this unusual use is not commercially supported and a custom control has therefore been built with LabVIEW.

Specific Objectives

- Create protocols for experiments and kinetic data collection
- Test and develop ω -TA kinetic modelling
- Guidelines for application of kinetic enzymatic modelling in practice

Conclusion

The development of online analytical methods for aqueous systems is essential for the progress of enzymatic processes as these often start as aqueous catalysts. Herein is presented one such methods by UV-VIS spectrophotometry coupled with chemometric data analysis. Applying chemical engineering to μ -technology furthermore enables the collection of kinetic data from microfluidic flow reactors reducing the consumption of both substrate and enzyme. The collected data will be used to characterize the performance of the desired enzyme and form a better basis for selection.

Acknowledgements

Many thanks to the European Union for funding this project. All projects have received funding from the European Union Seventh Framework Programme (FP7/2007-2013) BIOINTENSE is under grant agreement n°312148

References

1. D. Koszelewski, K. Tauber, K. Faber and W. Kroutil, *Trends in Biotechnology* 28 (2010) 324-332.
2. J. M. Woodley, *Trends in Biotechnology*, 26 (6) (2008) 321-327
3. P. Tufvesson, J. Lima-Ramos, J. S. Jensen, N. Al-Haque, W. Neto, J. M. Woodley, *Biotechnology and Bioengineering*, 108 (2011) 1479-1493.
4. K. Drauz, H. Gröger, O. May, *Enzyme Catalysis in Organic Synthesis*, third ed., Wiley, 2012
5. U. Krühne, S. Heintz, R. Ringborg, I. P. Rosinha, P. Tufvesson, K. V. Gernaey and J. M. Woodley, *Green Process Synth* 3 (2014) 23-31.
6. N. Al-haque, P. A. Santacoloma, W. Neto, P. Tufvesson, R. Gani and J. M. Woodley, *Biotechnology Progress* 28 (5) (2012) 1186-1196
7. F. E. Valera, M. Quaranta, A. Moran, J. Blacker, A. Armstrong, J. T. Cabral and D. G. Blackmond, *Angewandte Chemie International Edition* 49 (2010) 2478-2485.
8. J. S. Moore and K. F. Jensen, *Angewandte Chemie International Edition* 53 (2014) 470-473.
9. K. D. Nagy, B. Shen, T. F. Jamison and K. F. Jensen, *Organic Process Research and Development* 16 (2012) 976-981.
10. O. Levenspiel, *Chemical Reaction Engineering*, 3rd ed., Wiley, New York, 1999



Inês Pereira Rosinha

Phone: +45 4525 2993
E-mail: inros@kt.dtu.dk
Discipline: Process modelling, microfluidics

Supervisors: Ulrich Krühne
John M. Woodley
Krist V. Germaey
Anders Daugaard

PhD Study

Started: November 2012
To be completed: October 2015

Shape optimization of a microreactor for biocatalytic synthesis of optically pure chiral amines

Abstract

In early stage development of processes, it is important to understand what challenges of a reaction system are present and to figure out strategies which could overcome them and possibly be applied in industrial processes. The biocatalytic synthesis of optically pure chiral amines by ω -transaminase occurs under conditions of unfavourable equilibrium and both substrate and product are inhibitory substances of the enzyme. In this study, it is also taken into account that one of the substrates and the enzyme are both slow diffusing compounds.

This study consists of a development of an evolutionary shape optimisation procedure for a microreactor using an interface between MATLAB[®] and ANSYS CFX[®]. From the results, it was possible to evaluate the influence of the microreactor shape on mixing and yield of the investigated enzymatic reaction.

Introduction

During the early stage of development of biocatalytic processes the enzyme costs are high and only low amounts are commonly available. This is often making the process screening at bench-scale impossible.

Therefore, microsystems are a good alternative due to their high throughput or high content screening of process parameters, reaction kinetics or solvents. Additionally, microsystems have as well advantages related to very large surface-area-to-volume-ratio, very effective heat and mass transfer, easier control of process parameters and versatility of fabrication. Furthermore, these systems have the potential of introducing new synthesis concepts by numbering up, instead of scale-up in order to increase the production capacity.^[1,2] From all the advantages mentioned above, the following questions arise: How does the shape of a microreactor play a role on production yield? What about the spatial distribution of biocatalyst inside of a microreactor? Where is it more important to deposit the biocatalyst considering different mixing zones inside of the microreactor?

To answer these questions topology and shape optimisation methods often used in mechanical and structural engineering might be very efficient tools. This PhD project investigates the application of topology and shape optimisation to enzymatic reaction systems in microreactors and collects information

which can be further investigated and used for strategies on industrial processes. In this way, it is possible to configure beforehand an optimal reactor design and test it in laboratory. Hence, it will also cut down the fabrication costs of the miniaturized reactor system while demonstrating the validity of the mathematical optimisation procedure.

Reaction system

This computational fluid dynamics (CFD) study investigates a microreactor for the production of optically pure chiral amines. The chosen model reaction consists of the synthesis of the chiral product (*S*)-1-phenylethylamine from acetophenone by using ω -transaminase (ω -TAm) as biocatalyst.

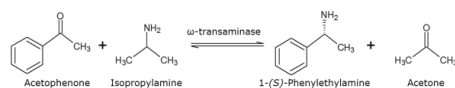


Figure 1: Reaction system for microreactor optimisation

Isopropylamine is the amino donor which is converted into acetone by the same reaction. ω -TAm is known for following the Ping Pong Bi Bi kinetic mechanism. The kinetic parameters specific for this reaction system

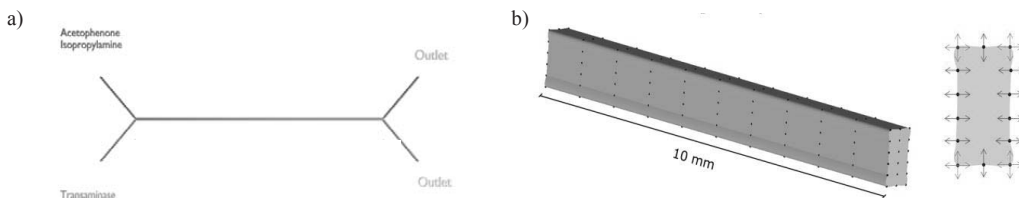


Figure 2: a) YY-microreactor configuration; b) Structure to be optimized with all surface points represented and the directions for modification of the points.

were determined and fit to the enzymatic mechanism by Al-Haque *et al.* (2012). At the inlet, the concentrations are the following: 10 mM of Acetophenone, 0.5 M of Isopropylamine and 0.0759 M of ω -TAM.

In microfluidics, mixing by diffusion plays an important role. In this case, two compounds are considered as slow diffusing compounds: Acetophenone ($1 \cdot 10^{-13} \text{ m}^2 \text{ s}^{-1}$)^[4] and ω -TAM ($1 \cdot 10^{-12} \text{ m}^2 \text{ s}^{-1}$). All the other compounds involved in this reaction system were considered to have the same diffusion coefficient, $1 \cdot 10^{-9} \text{ m}^2 \text{ s}^{-1}$.

Initial reactor shape

The initial shape of the studied microreactor consisted of a YY-microchannel with a rectangular cross-section

where the inlet and the outlet are located at the respective ends of the reactor.

Both inlet and outlet consisted of a Y shape where two streams meet at the entrance of the flow chamber and are split into two streams at the exit of the chamber. The flow chamber consists of a channel without divisions. The initial configuration has the following dimensions: 0.25 mm of width for each inlet and outlet, 1 mm of height and 100 mm of length. In one inlet, enters a solution with ω -TAM and in the inlet enters a solution of acetophenone and isopropylamine.

The residence time inside of the microreactor is 30 minutes for all simulations. Since the volume of the microreactor varies from simulation to simulation, the flow rate has to be adjusted in order to maintain the residence time.

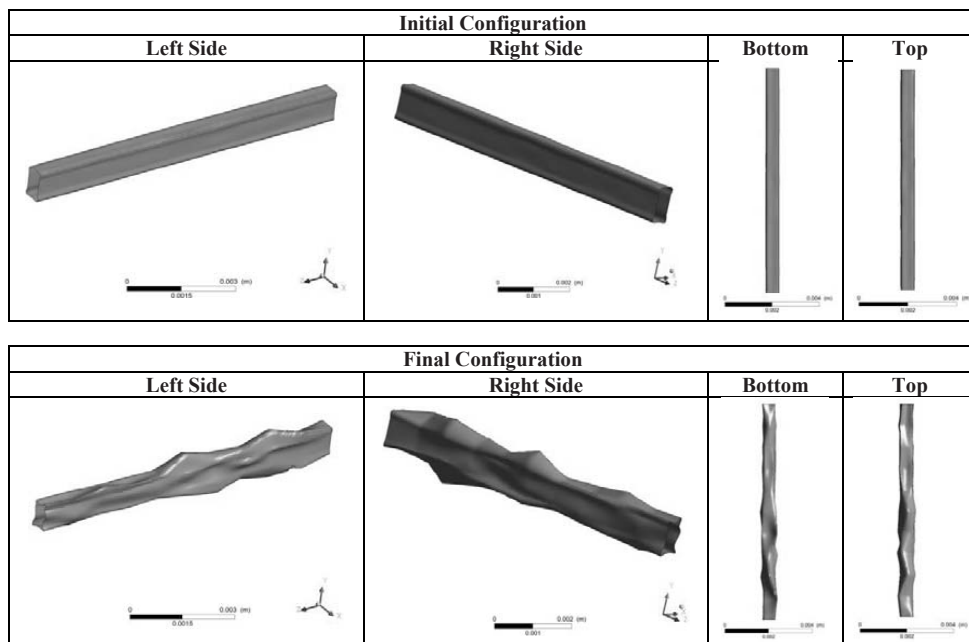


Figure 3: Views from the four directions of the Initial and final configurations

Shape optimization routine

The optimisation routine focuses on the modification of the surface of the main channel of the reactor. The surface optimized consists of the first 10 mm of the main channel and selected points dispersed on the surface are modified according to an evolutionary optimisation procedure.

The 140 points are divided in ten groups of points, each group of points forms a ring on the shape and these rings are connected and form the surface of the channel. These rings are modified due to the alteration of disposition of the points and consequently the shape of the channel is also modified. The points which are on the lateral parts of the channel can be moved horizontally, the points on the top and bottom of the channel can be moved vertically and the corner points can be moved in both vertical and horizontal directions. For an optimisation, it is necessary to define the objective function and restrictions. In this study, the objective function is the concentration of substrate at the outlet of the microreactor must be minimized (or maximize product concentration). The optimisation routine consists of a finite element analysis performed by a CFD software (ANSYS CFX®) coupled with a

MATLAB® routine which performs the optimisation. The CFD software solves the fluidic problem with the reaction system integrated and MATLAB® makes the changes to the geometry of the reactor to the CFD script according a random search procedure and starts the CFD simulation. The random search algorithm^[5,6] has the goal to minimize cost function f by changing the surface points' positions. The random search algorithm is described as the following:

- Initialize the random search with initial vector $x = \{x_1, x_2, \dots, x_n\}$ which gives the shape presented in Figure 2.
- Until either the concentration of substrate is ten times lower or the number of iterations between local optima is more than 1500, run the following cycle:
 - Considering a vector $y = \{y_1, y_2, \dots, y_n\}$, for $j=1 \dots n$:
 - Sample a new position y_j from the 0-sphere in the segment given by the pair of points $\{x_j - 0.03x_j, x_j + 0.03x_j\}$

If $f(y) < f(x)$ then set vector $x=y$ and a new local optimum set of points has been found.

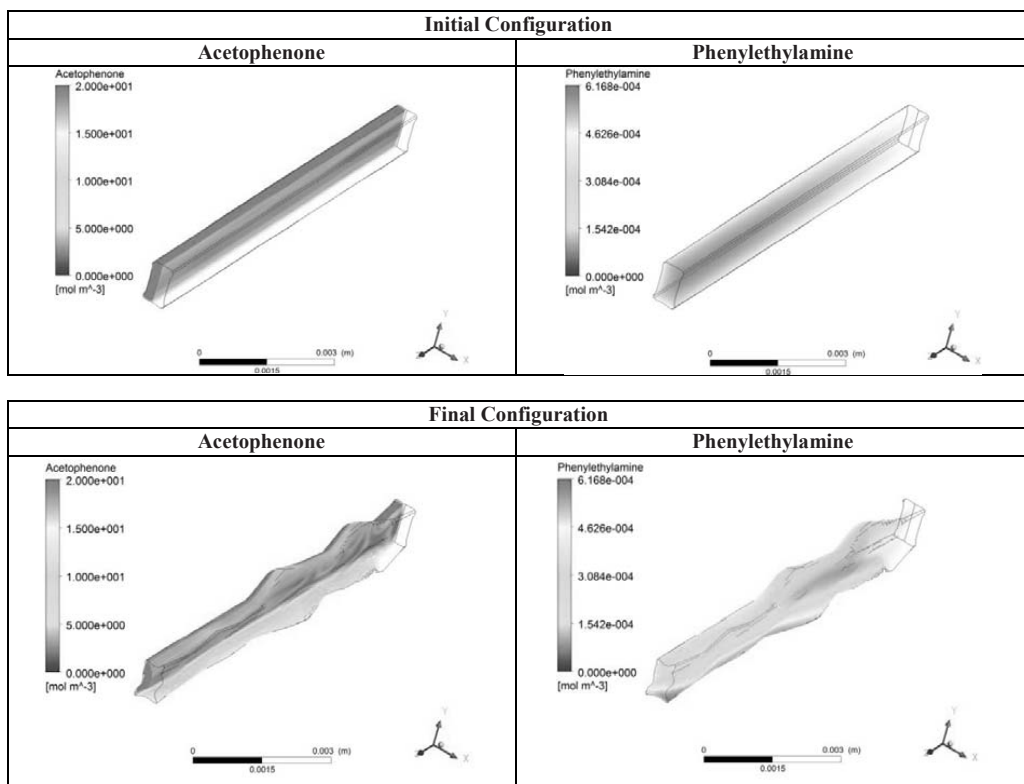


Figure 4: Concentration of acetophenone and phenylethylamine along the channel for initial and final configurations.

Results

This optimisation study included in total 9296 simulations and the best shape achieved has the aspect of a wavy structure on all four walls of the channel. On one hand, $4.4 \cdot 10^{-5}$ mM of substrate were converted with the initial configuration, on the other hand, $37.1 \cdot 10^{-5}$ mM of substrate were converted with the final shape. In the end, the shape optimization resulted on an improvement of 8.4 times higher conversion of the substrate when compared to the initial shape which was very close to the goal for improvement (10 times higher conversion of the initial shape). However, the amount of iterations to find the next local optimum was increasing exponentially which made the optimisation procedure very expensive from a simulation point of view.

Therefore, the restriction of maximum 1500 iterations between local optima was implemented.

The channel expansions and restrictions have an important impact on the mixing of the two streams. However the displacement of the points of the top and the bottom seem to have a higher importance. From the bottom view, it is possible to see that a deep and narrow expansion contributes a lot for the mixing of the two streams and consequently for the substrate conversion as it can be verified in the bottom of the reactor. The narrowing of the channel contributes to the short diffusion distances of the compounds and therefore it contributes to the mixing. From the top view, it is possible to see that the channel takes an S-shape resembling a meander channel. Meander channels are very well known in microfluidics and their arcs contribute for the mixing of parallel streams.

Conclusions

From this optimisation study, it was possible to gain understanding regarding the impact of the microreactor shape on the mixing of two streams with low diffusing compounds. The mixing plays as expected a crucial role for the improvement of the yield of an enzymatic reaction.

The understanding from this optimisation study is very useful for the experimental work since the shape optimisation also allows finding new strategies to construct reactors for application in laboratory. Furthermore, it allows avoiding unnecessary experimental studies which can otherwise result in waste of materials. In this way it is possible to design the reactor in a new approach. Instead of adapting the reaction system to an existing microreactor shape it is possible to adapt the microreactor to the reaction system.

Future Work

The shape optimisation is not the only type of optimisation that can improve the yield of a reaction. The topology optimisation can also influence the improvement of a reaction. The next stage of this

project will be the topology optimisation of enzyme inside a microreactor. The topology optimisation will include the spatial distribution of the enzymes inside of a miniaturized packed bed reactor. The idea is to immobilize the enzyme on the surface of particles which form the packed bed and to change the distribution of the biocatalyst inside the packed bed reactor. This study will allow the identification of crucial areas that influence more considerably the conversion of substrate. This study will be carried out by using ANSYS CFX® 14.5 for finite volume analysis and the topology optimisation procedure consists of an adaptation of the Evolutionary Structural Optimization commonly used for topology optimization of structures in mechanical and civil engineering.

Acknowledgment

The research leading to these results has received funding from the European Union FP7 (FP7/2007-2013) Project BIOINTENSE – Mastering Bioprocess integration and intensification across scales (Grant Agreement number 312148).

References

1. K. F. Jensen, B. J. Reizman, S.G. Newman, *JALA*, 14(17) (2014), 3206-3212
2. D. Schäpper, M. N. H. Zainal Alam, N. Szita, A. E. Lantz, K.V. Gernaey, *Anal. Bioanal. Chem.*, 395(3) (2009) 679-695
3. N. Al-Haque, P.A. Santacoloma, W. Neto, P. Tufvesson, R. Gani, J.M. Woodley, *Biotechnol. Prog.*, 28 (5) (2012), 1186-1196
- 4.
5. V. K. Bodla, R. Seerup, U. Krühne, J. M. Woodley, K. V. Gernaey, *Chem. Eng. & Tech.*, 36 (6) (2013) 1017-1026
6. L.A. Rastrigin, *Autom. Remote Control* 24 (10) (1963) 1337-1342
7. F. J. Solis, R. J-B. Wets, *Math. Oper. Res.* 6 (1) (1981), 19-30



Koldo Saez de Bikuña Salinas

Phone: +45 24648965

E-mail: ksde@kt.dtu.dk

Supervisors: Andreas Ibrom
 Michael Zwicky Hauschild
 Kim Pilegaard
 Ulrik Birk Henriksen
 Gürkan Sin

PhD Study
 Started: December 2012
 To be completed: May 2016

Biochar Fraction Needed on Willow Gasification to Be a Carbon Neutral Bioenergy: Offsetting Direct and Indirect Land Use Changes

Abstract

Direct and indirect land use changes (dLUC and iLUC) have been widely recognized to play an important role in bioenergy's carbon footprint and should be considered in biofuel's greenhouse (GHG) accountings. DLUC represent the soil organic carbon (SOC) losses or gains inflicted by a specific land use type and management, while iLUC emerge whenever an energy crop is planted in arable land, displacing food crop production elsewhere. A life cycle assessment (LCA) of a short rotation coppice (SRC) willow case combined with a medium-scale gasification plant has been performed, which includes iLUC and dLUC. Results show that willow on marginal land remains carbon negative, regardless of substituted energy type or time scope, while arable land willow displacing natural gas would require a biochar fraction (biomass C based) of 6,8% to 48,9% (0,366 – 2,6 Mg C ha⁻¹ yr⁻¹) to remain carbon neutral.

Introduction

Due to their overarching role of land use changes (dLUC and iLUC) in bioenergy systems from a life-cycle perspective, they have been repeatedly recommended to be included in bioenergy's greenhouse gas (GHG) accountings, despite their challenging quantification and inherent uncertainties [1]–[3]. Large extensions of marginal or abandoned lands have been often quoted as the solution for dedicated energy crops to avoid these undesired effects [4], [5]. However, land abandonment and marginalization is to a large extent a socio-economic process, and thus heavily depends on specific, constantly changing economic circumstances and socio-political context in place [6]–[8]. That is, if policy-makers create a bioenergy-friendly agricultural framework that promotes the use of marginal lands through economic support and incentives, these lands will be no more marginal. The question is then: will it be iLUC from dedicated energy crops? Finding a solution to this dilemma is the motivation of this project.

Materials and methods

A consequential LCA on willow bioenergy has been performed, distinguishing between marginal and arable land scenarios. Specific soil types and their estimated SOC changes have been considered [9], as well as iLUC

emissions for the arable case [10]. Due to the iLUC factor being limited to GHG emissions, and missing characterization factors (CF) for biochar effects on soil quality, only the Global Warming Potential (GWP) impact has been considered.

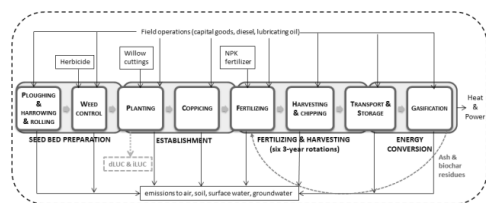


Figure 1: System boundaries of the willow-gasification bioenergy system.

Taking the study case of a short rotation coppice (SRC) willow plantation combined with a medium-scale gasification plant in Denmark (Figure 1), we illustrate the biochar needed from the process in order to remain truly carbon neutral. After 2050 it is assumed that Denmark will be fossil free as targeted by the Danish government. Two time scopes, 20 and 100 years, have been therefore assessed, which take into account the different soil carbon dynamics in the long and the short term. For the long time assessment, no crediting from

fossil fuel displacement has been considered from 2050. Natural gas substitution was assumed for the reference case (marginal decentralized Danish plant), and tested against the average grid (coal) case.

Results and Discussion

The results show that regardless the biochar fraction from the gasification process and the time scope of the assessment, all marginal land scenarios remained carbon negative, while only the arable land scenario displacing coal was carbon negative. If arable land is undertaken in the short term for growing SRC willow, intended to substitute natural gas from a medium-scale, decentralized cogeneration plant in Denmark (a highly likely scenario), a 6.86% biochar fraction (biomass carbon based), or 366 kg C ha⁻¹ yr⁻¹ are deemed necessary for this bioenergy type to remain carbon neutral (iLUC included). For a 100 year time scope, during which only 40 years fossil fuel is substituted, the willow grown in arable land would need to convert, under modelled assumptions, 48.9% of the harvested biomass C (2.6 Mg C ha⁻¹ yr⁻¹) into highly stable biochar in order to compensate for the induced iLUC, SOC losses and other agricultural emissions (N₂O, fertilizer production, etc.). When such high biochar fractions are needed (> 10%), the process is not anymore gasification but pyrolysis. Stability of pyrolyzed biochar is generally lower than high-temperature biochar, which can put at risk, and therefore into question, the claimed GWP reduction benefits.

Conclusions

Our results show the sensitivity and magnitude of crucial parameters related to willow for energy from an integrated life-cycle perspective, namely dLUC, iLUC and the fossil energy substituted. We challenge the assumption of large available land estimations remaining marginal (and thus “iLUC free”) after large-scale, bioenergy friendly frameworks and incentives are on place. We claim that a carbon negative bioenergy system that compensates for potential iLUC emissions and changes in SOC is needed, combined with an effective regulation to ensure bioenergy species being planted in marginal lands, or in conjunction with food crops and not in competition with them. This approach did not consider impacts on other environmental aspects, and therefore gasification biochar does not compensate for the deterioration of other ecosystem services and biodiversity, which are deemed to be rather significant for iLUC.

References

1. European Environment Agency (EEA), “EEA scientific committee on GHG accounting on bioenergy,” no. September, pp. 1–10, 2011.
2. T. W. Hertel, A. a. Golub, A. D. Jones, M. O’Hare, R. J. Plevin, and D. M. Kammen, “Effects of US Maize Ethanol on Global Land Use and Greenhouse Gas Emissions: Estimating Market-

- mediated Responses,” *Bioscience*, vol. 60, no. 3, pp. 223–231, Mar. 2010.
3. U. Fritsche, R. Sims, and A. Monti, “Direct and indirect land-use competition issues for energy crops and their sustainable production—an overview,” *Biofuels, Bioprod. Bioref.*, vol. 4, pp. 692–704, 2010.
4. D. Tilman, J. Hill, and C. Lehman, “Carbon-negative biofuels from low-input high-diversity grassland biomass,” *Science*, vol. 314, no. 5805, pp. 1598–600, Dec. 2006.
5. I. Gelfand, R. Sahajpal, X. Zhang, R. C. Izaurralde, K. L. Gross, and G. P. Robertson, “Sustainable bioenergy production from marginal lands in the US Midwest,” *Nature*, vol. 493, no. 7433, pp. 514–7, Jan. 2013.
6. P. Pointereau, F. Coulon, P. Girard, M. Lambotte, T. Stuczynski, V. Sánchez Ortega, and A. Del Rio, “Analysis of farmland abandonment and the extent and location of agricultural areas that are actually abandoned or are in risk to be abandoned,” *Inst. Environ. Sustain. (Joint Res. Centre)*, 2008.
7. D. Strijker, “Marginal lands in Europe—causes of decline,” *Basic Appl. Ecol.*, vol. 6, no. 2, pp. 99–106, Apr. 2005.
8. C. Keenleyside, G. Tucker, and A. McConville, “Farmland Abandonment in the EU: an Assessment of Trends and Prospects,” *London WWF IEEP*, no. November, 2010.
9. L. Hamelin, U. Jørgensen, B. M. Petersen, J. E. Olesen, and H. Wenzel, “Modelling the carbon and nitrogen balances of direct land use changes from energy crops in Denmark: a consequential life cycle inventory,” *GCB Bioenergy*, vol. 4, no. 6, pp. 889–907, Nov. 2012.
10. D. Tonini, L. Hamelin, H. Wenzel, and T. Astrup, “Bioenergy production from perennial energy crops: a consequential LCA of 12 bioenergy scenarios including land use changes,” *Environ. Sci. Technol.*, vol. 46, no. 24, pp. 13521–30, Dec. 2012.

**Anders Schlaikjer**

Phone: +45 4525 2869
E-mail: andsh@kt.dtu.dk
Discipline: Engineering Thermodynamics

Supervisors: Georgios Kontogeorgis
Kaj Thomsen

PhD Study

Started: June 2014
To be completed: June 2017

Development of the Electrolyte Cubic-Plus-Association Equation of State

Abstract

Electrolytes have a significant effect in many industrial processes. In the oil and gas industry salts have many either beneficial or harmful effects, while electrolytes have many applications in the chemical industry. The objectives of this project are to parameterize an electrolyte extension to the Cubic-Plus-Association Equation of State, as well as test the capabilities of the model on a range of industrially relevant systems. Estimating a three-parameter temperature dependence to osmotic and mean ionic activity coefficients yield low deviations, and accurate prediction of the freezing point depression, while unsuccessful to represent solubility. Including solubility data in the parameter estimation improves this significantly; however the deviations of the osmotic and activity coefficients will increase, when doing so.

Introduction

Electrolytes have a significant effect in many industrial processes. In the oil and gas industry salts can increase the inhibitory effect of methanol, ethanol and glycols on the formation of gas hydrates, and have an effect of the gas solubility in water-hydrocarbon mixtures. Salts may enhance corrosion of pipelines and also precipitation of salts (scaling) may occur, due to the change in temperature, pressure and composition from reservoir to surface[1].

Salts also play a role in many chemical industries, for instance for separation purposes as salts may induce liquid-liquid separation for some otherwise miscible liquids. Water-Acetone is such a system which is miscible under normal conditions, but when adding specific salts a phase separation occurs. Also electrolytes are important in the energy industry both with regard to energy storage, as well as flue gas cleaning.

Accurate prediction of thermodynamic properties is important in the design and operation of processes, especially for complex mixtures. For many complex mixtures there are typically very little to none experimental data, and therefore it is needed to use trusted thermodynamic models.

Electrolyte systems are typically modeled with activity coefficient models such as the e-NRTL, and extended-UNIQUAC, however such models have difficulty handling high pressures, in which case there is a need for an Equation of State (EoS).

Several Equations of State for electrolytes have been developed over the year, but relatively few that can handle mixtures of both hydrogen bonding compounds as well as electrolytes have been proposed. Also only very few have been developed to a stage where it can be considered ready for implementation in industry.

Specific Objectives

The overall objective of the e-CPA project is to develop an electrolyte EoS, such that the model in absence of electrolytes reduces to the Cubic Plus Association (CPA) EoS. The initial focus for this model is implementation in the oil and gas industry, and it is developed with engineering problems in mind.

The Current PhD study directly succeeds a completed PhD study, from which a model equation has already been proposed [2]. This provides a strong baseline to work from, and thus the focus of the study will, at least initially, be on validation and parameterization.

Parameters for the currently proposed model will be estimated with several different approaches in order to determine optimal parameters, but also to investigate what type of data should be included in estimation.

The relation between salt specific and ion specific parameters will be investigated in order to work towards the use of ion specific parameters.

Finally the model, with optimized parameters, will be tested on a wide range of industrially relevant systems, in order to evaluate the performance of the

model. Based on this evaluation the model equation will be revisited if necessary.

Electrolyte-CPA Equation of State.

A new model for electrolytes has been proposed as an extension to the CPA EoS. The electrolyte-CPA (e-CPA) reduces to the CPA in the absence of electrolytes, while the CPA in turn reduces to the Soave-Redlich-Kwong (SRK) cubic EoS in the absence of associating compounds. [2]

A major difference between electrolytes and most other compounds are the long-range electrostatic interactions. The CPA EoS cannot account for such interactions and therefore extra terms should be added to the model, to account for these interactions. For electrostatic interactions the Debye-Hückel term is added to the model, while a Born term is added to the model to account for ion-solvation [2, 3]. With these additions the contributions to the model will be as shown in Figure 1, where the first three contributions are what the CPA EoS covers. The full model equation can be viewed in [2].

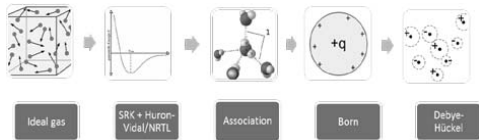


Figure 1: Contributions to the Electrolyte CPA EoS. [2]

It has been found that a key property for the accuracy of the electrostatic contributions is the static permittivity of the solvent. Therefore a need for accurate estimation of this is needed, and a model for the static permittivity of associating fluids has been proposed and further extended to fluids containing electrolytes. A more detailed description of this can be found in the graduate year book of 2013 by Bjørn Maribo-Mogensen and in [4, 5].

The typical parameters of the CPA EoS is the co-volume, b_0 , and the two energy parameters, Γ and c_1 , which together can be viewed as a temperature dependent energy parameter $a(T)$, for the physical part (SRK), the association volume, β , and the association energy, ϵ , for the associating part. For e-CPA, no additional parameters are added as all properties in the electrostatic part can be found in literature or by prediction. No association for the electrolytes is considered and thus the association parameters should not be estimated at all. Typically CPA EoS is implemented with the van der Waals one fluid mixing rule (vdW1f) for the co-volume and energy parameters, which is seen in eq. 1, and eq. 2.

$$b = \sum_i \sum_j x_i x_j \left(\frac{b_i + b_j}{2} \right) \quad (1)$$

$$a = \sum_i \sum_j x_i x_j \sqrt{a_i a_j} (1 - k_{ij}) \quad (2)$$

For the electrolyte-solvent interaction, however, these mixing rules are not suitable and therefore the Huron-Vidal mixing rule (HV) is used instead, which is shown in eq 3.

$$\frac{a}{b} = \sum_i x_i \frac{a_i}{b_i} - \frac{g^{E,\infty}}{\ln 2} \quad (3)$$

The excess Gibbs energy is found from the modified Huron Vidal/NRTL equation. Simplifying the expression by stating that no interaction between ions should be taken into account and by setting the NRTL non-randomness parameter, α , to zero, the relation will look as in eq. 4.

$$\frac{g^{E,\infty}}{RT} = \frac{1}{b} \sum_i \sum_j x_i x_j b_j \frac{\Delta U_{ji}}{RT} \quad (4)$$

Setting the CPA energy parameter, $a(T)$ to 1 per default for all ions and by predicting the co-volume from eq. 5, the number of adjustable parameters pr. ion-solvent mixture is reduced to 1, being the ΔU_{ij} parameter. In eq. 5 σ is the hard-sphere diameter.

$$b = \frac{2}{3} \pi N_A \sigma^3 \quad (5)$$

This single parameter does, however, not capture temperature dependence very well, and a temperature dependence of this parameter is introduced as seen in eq. 6.

$$\frac{\Delta U_{ij}}{R} = \frac{\Delta U_{ij}^{ref}}{R} + \alpha_i \left[\left(1 - \frac{T}{T_\alpha} \right)^2 - \left(1 - \frac{T_{ref}}{T_\alpha} \right)^2 \right] \quad (6)$$

Here the ΔU_{ij}^{ref} is a parameter estimated at a reference temperature T_{ref} typically 298.15K, while T_α and α are additional parameters.

Finally, instead of considering the parameters as ion specific, it is chosen to have salt specific parameters by adding the constrain, that both ions in a salt must have the same parameter values.

Results and Discussion

Model parameters have been estimated for a range of salts consisting of alkali and alkaline-earth cations and halogen, nitrate or sulfate anions, with water as a solvent. Thus for each salt three parameters are estimated for the interaction between the salt and water. The parameters are estimated by regression to osmotic – and mean ionic activity coefficient data, which is available from [6]. Initially only the reference interaction parameter was fitted to data at 298.15K in order to obtain a suitable initial guess for ΔU_{ij}^{ref} . Following this, data at all temperatures were included

and all three parameters were estimated. The deviations of selected salts and an average for all 50 salts are found in table 1, and the mean ionic activity coefficient and the osmotic coefficient for NaCl is presented graphically in figure 2 and 3. The deviations are generally satisfying as they are within the expected experimental uncertainty.

Table 1: Relative average deviation (RAD) for osmotic and mean ionic activity coefficients of selected salts and the average over 50 salts.

	RAD Φ %	RAD γ %
NaCl	1.34%	1.78%
NaBr	1.73%	1.83%
KCl	0.58%	0.37%
KBr	0.72%	0.72%
MgCl ₂	1.83%	4.85%
MgBr ₂	2.07%	6.48%
Average (50)	1.77%	2.71%

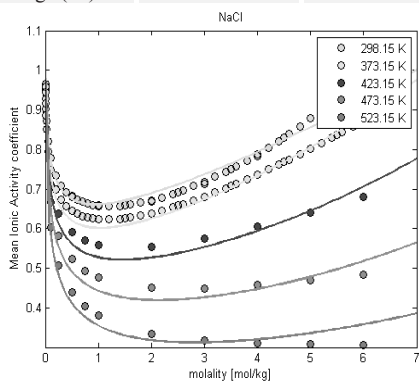


Figure 2: Mean Ionic activity coefficients of NaCl at different temperatures modelled with e-CPA. Solid line is model calculations, while dots are experimental data. Data from [6].

After parameterization it was tested if other properties could be predicted. One such property is the freezing point depression, for which good agreement with experimental data was found. For a range of chloride salts the freezing point depression predictions and experimental data are illustrated in figure 4. The accurate prediction of the freezing point depression is, however, expected as it is closely related to the water activity, which is directly related to the osmotic coefficient. Therefore it would be expected that accurate representation of the osmotic coefficient would also result in accurate representation of the freezing point depression.

Another key property of electrolytes is the salt solubility. Modelling Solid-Liquid-Equilibrium (SLE) require the use of standard states. While such standard states are available for some salts through for example

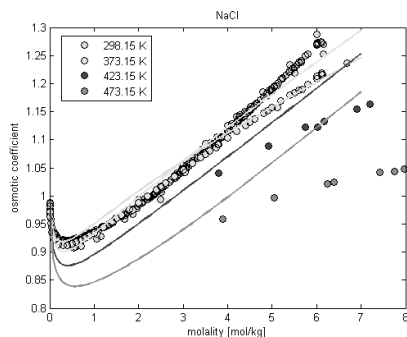


Figure 3: Osmotic coefficients of NaCl at different temperatures modelled with e-CPA. Solid line is model, while dots are experimental data, Data from [6].

NIST [7], especially for hydrated salts no standard states are available. Instead standard states for the hydrated salts are chosen to be those used in the extended-UNIQUAC model, at least as an initial estimate [8]. Using these standard states and the parameters fitted to osmotic and activity coefficient data will, however, not yield very satisfying results. This is illustrated in figure 5, where the prediction of the solubility of NaBr is presented along with experimental data. This salt shows one of the better representations of the solubility.

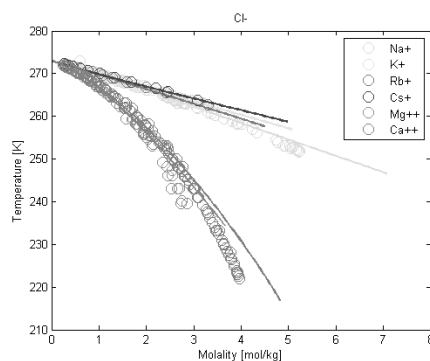


Figure 4: Freezing point depression of chloride salts. Solid lines are model predictions, while dots are experimental data. Data from [6].

Table 2: Relative average deviation (RAD) for osmotic and mean ionic activity coefficients as an average for 22 salts, with parameters fitted to data both including and excluding solubility data

	RAD Φ %	RAD γ %
Average, No solubility data	1.24%	2.74%
Average, With solubility data	2.66%	6.03%

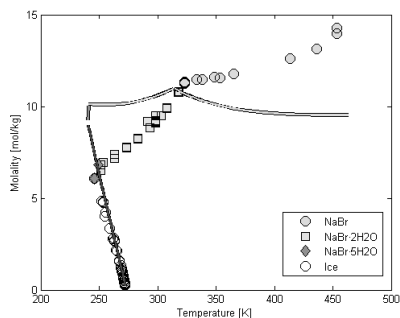


Figure 5: Solubility of NaBr, predicted with e-CPA using parameters fitted to osmotic and activity coefficient data. Solid line is model prediction, while dots are experimental data. Data from [6]

In order to improve the solubility representation it was chosen to include the solubility data in the parameter estimation, while still keeping the standard states from extended UNIQUAC. Viable standard states covering all relevant hydrated and pure salts were available for 22 of the pure salts and thus for these 22 salts new parameters were estimated, where both osmotic and activity coefficient data as well as solubility data were included. This clearly improved the representation of the solubility as seen in Figure 6, however it does have an effect on the accuracy of the model in terms of osmotic and activity coefficients as the relative average deviation compared to the parameters without solubility in the estimation roughly doubles, as can be seen in table 2. This could indicate that the use of extended UNIQUAC fitted standard states is not the best choice for the standard states and that the standard states should be fitted to this model. Also only 22 of the 50 salts investigated in this study have reasonable standard states, and thus it is not possible to investigate solubility for the remaining salts without also determining or estimating the standard states for the salts.

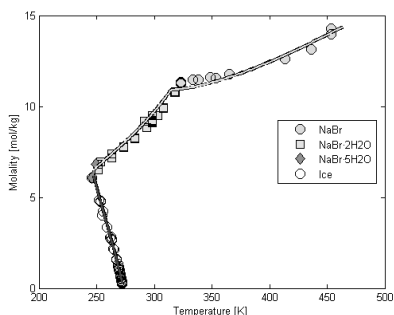


Figure 6: Solubility of NaBr, calculated with e-CPA using parameters fitted to both osmotic and activity coefficient data as well as solubility data. Solid line is model prediction, while dots are experimental data. Data from [6]

Conclusions

The e-CPA model has been parameterized with a three parameter, non-linear temperature dependence. Initially only osmotic and mean ionic activity coefficient data were included in the estimation, in order to investigate if it would be enough to describe all key properties of the salts. The model could for all salts describe the osmotic and mean ionic activity coefficients with acceptable deviations.

It was found that the solubility was not represented with satisfaction, and thus solubility data were also included in the solubility. Including the solubility data in the parameter-estimation yielded much more accurate descriptions of the solubility, however, the deviations for osmotic and activity coefficients roughly doubled.

It is noted for many of the salts investigated in this study, that standard states are not available, neither from databases nor from extended UNIQUAC. Also it is questionable to use standard states in e-CPA, which was fitted to a different model (extended UNIQUAC). This suggests that new standard states should be estimated both where none are available, but also the standard states which were fitted to the extended UNIQUAC.

Acknowledgements

The author wishes to thank the industrial partners in the CHIGP (Chemicals in Gas Processing) consortium and DTU for financial support.

References

1. G. M. Kontogeorgis, G. K. Folas. *Thermodynamic Models For Industrial Applications : From Classical and Advanced Mixing Rules To Association Theories*. John Wiley & Sons Ltd, 2010.
2. B. Maribo-Mogensen, (2014). *Development of an Electrolyte CPA Equation of state for Applications in the Petroleum and Chemical Industries*. PhD thesis, Department of chemical and Biochemical Engineering Technical University of Denmark
3. B. Maribo-Mogensen, G. M. Kontogeorgis, and K. Thomsen, *Journal of Physical Chemistry B* 117(12) (2013): 3389-3397
4. B. Maribo-Mogensen, G. Kontogeorgis, and K. Thomsen, *Journal of Physical Chemistry B* 117(36)(2013): 10523-10533.
5. K. Thomsen, *Cere electrolyte database*, www.cere.dtu.dk/Expertise/Data_bank/Search
6. NIST chemistry webbook, <http://webbook.nist.gov/chemistry>
7. K. Thomsen, P. Rasmussen, *Chemical Engineering Science*, 54(12):1787-1802, 1999



Rasmus Seerup
Phone: +45 45 25 28 53
Email: rasee@kt.dtu.dk
Discipline: CHEC Research Center

Supervisor: Kim Dam-Johansen
Weigang Lin

PhD study
Started: November 2013
To be completed: October 2016

Modelling of Gasification of Biomass in Dual Fluidized Beds

Abstract

During biomass gasification, tar are formed from the biomass, which can be problematic for downstream processing. Controlling the properties of the tars may make the cleaning of the gas easier, and help to run at optimal conditions. This project investigates the formations of tars from biomass under gasification conditions in the dual fluidised bed, by modelling the development of tar in a particle scale and reactor scale.

Introduction

There is a great focus on the utilization of biomass as a renewable source for energy. The advantage of the dual fluidised bed is the possibility of producing synthetic gas with high hydrogen content and a high LHV (lower heating value). Since biomass ashes have a high tendency of agglomeration at elevated temperature, the production of the syngas in fluidised beds is usually conducted at relatively low temperatures, which lead to the formation of tars. In some process using syngas, tars may be troublesome (catalytic conversion of syngas and fuel cells), because of condensation and fouling. Tar may also be regarded as a valuable by-product that may increase the feasibility of gasification. The understanding of tar formation and properties becomes important for optimizing the downstream cleaning or separation.

Specific Objective

The objective is to understand the tar development under gasification conditions found in a dual fluidised bed, by modelling. Both at a particle scale and at reactor scale.

Tar properties

Tar contains a lot of different organic compound. Therefore, tar are often not listed as individual components but by their properties. Tar properties is often divided into 5 different classes [1].

1. GC-undetactable: heavy tars that cannot be detected by GC.
2. Heterocyclic: highly water soluble tars that is often among the primary tars released from biomass.

3. Light aromatic (1 ring): easily condensable and can be dissolved in water
4. Light PAH (2-3 rings): condense at low temperatures even at low concentrations
5. Heavy PAH (4-7 rings): Condense at high temperatures

With biomass being a complex material it is not all tar that are equal troublesome. The tar with highest amount come from cellulose and hemicelluloses, which can be easily degraded. The amount of Tar from lignin is low but is hard to degrade and often repolymerised at high temperatures to even heavier tars. Thus, the modelling of tar during gasification will be focused on those from lignin.

Modelling approach

Tar development at the reactor level is dependent on the primary tar (class 2 and 3) that is released during the devolatilisation of the biomass, and thus the modelling start with biomass devolatilisation. Devolatilisation is dependent on biomass composition, (ash, cellulose, hemicellulose, lignin), heating rate, particle size, and pressure primarily. Setting up a model for heat and mass transfer and reaction is important for accurate prediction of tar release.

Further development of tar (to class 4, 5 and 1) in the reactor is dependent on temperature, residence time, gasification agent concentration, hydrodynamic condition, feeding position, presence of catalyst, and pressure, besides the primary release of tar. Modelling of the tar development at the reactor scale will be done at a simplified system, by compartmentalising the system to account for changing hydrodynamics.

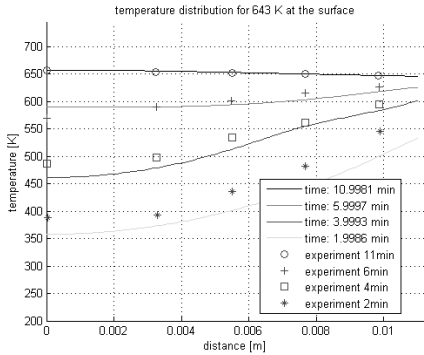


Figure 1: Temperature prediction compared to experimental data from [2].

Present status of study

At present, the heat transfer inside a particle is modelled as an infinite cylinder to accommodate the biomass geometry. Giving a heat transport equation of:

$$C_p \frac{d\rho T}{dt} = \lambda \left(\frac{d^2 T}{dr^2} + \frac{1}{r} \frac{dT}{dr} \right) + (-\Delta H) \frac{d\rho}{dt} \quad (1)$$

With the boundary conditions

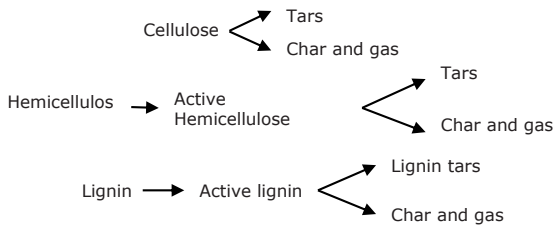
$$\frac{dT}{dr} = 0 \text{ for all } t \text{ and } r = 0 \quad (2)$$

$$-\lambda \frac{dT}{dr} = h(T_R - T_{bulk}) + \epsilon\sigma(T_R^4 - T_{bulk}^4) \quad (3)$$

for all t and $r = R$

$$T = T_0 \text{ for all } r \text{ and } t = 0 \quad (4)$$

The density change is evaluated from the reaction of the individual components:



Evaluation of this system give relative good results for the temperature profile as shown in Figure 1 when a small heat release is related to the pyrolysis. The reactions need to be extended to include more detailed information for the primary tars.

Challenges

The major challenge for tar models is often the lack of reactions kinetics, which leads to models that can only

be used to predict tar formation for specific systems/conditions or types of biomass.

Many models focus on predicting the tar under flash conditions, which is used for bio-oil production. For these systems, the amount of tar from lignin is a relative low and is often of less interest. The secondary reactions are often neglected because of small particles and quenching of the gas. The effect of inorganics is seldom considered. These facts indicate that information of the role of lignin in gasification is needed for the modelling of tar formation under gasification conditions. Increasing information on the composition of the primary tar will be a key for better understanding the tar properties during gasification.

Future work

The further work is based on investigating how inorganic combines with torrefaction may influence the primary tar release from lignin. This will lead to a different combination of side groups, which may affect the primary tar composition.

The particle modelling will be further extended to include more information on the primary tar composition. Including how secondary reaction with inorganics inside the particle may influence the composition.

At the end, the particle model should be integrated with a reactor scale model to understand the tar development.

Acknowledgements

This project is part of DANCNGAS. Financial support provided by Sino-Danish Centre for education and research and the Technical University of Denmark are gratefully acknowledged.

References

1. S. Anis and Z. a. A. Zainal, "Tar reduction in biomass producer gas via mechanical, catalytic and thermal methods: A review," *Renew. Sustain. Energy Rev.*, vol. 15, no. 5, pp. 2355–2377, Jun. 2011.
2. D. L. Pyle and C. A. Zaror, "Heat transfer and kinetics in the low temperature pyrolysis of solids," *Chem. Eng. Sci.*, vol. 39, no. 1, pp. 147–158, 1984.



Catarina Seita

Phone: +45 4525 2926
E-mail: casse@kt.dtu.dk

Supervisors: John Woodley, DTU
Mathias Nordblad, DTU
Jessica Rehdorf, BRAIN AG

PhD Study

Started: December 2013
To be completed: December 2016

Bioprocess Evaluation Tools

Abstract

This project is developing a systematic framework for sustainable process design of bioprocesses, where applying adequate evaluation tools from an early stage of development can guide research and development. This approach is illustrated with a case-study – the biocatalytic synthesis of R-(+)-perillic acid by *Pseudomonas putida* DSM 12264. Perillic-acid is a monoterpenoic acid with a broad growth-inhibitory effect on bacteria, yeast and moulds, thus its production process faces several challenges, namely product inhibition. Process simulation tools allowed the identification of key parameters for process development and targets for process metrics, such as product concentration (g_{product}/L) and space-time yield ($g_{\text{product}}/L_{\text{reactor}}/h$). This can provide a set of guidelines for biocatalyst and process development that will assist research and support decision-making.

Introduction

During the last few years considerable progress has been made in the production of organic compounds by means of fermentation or biocatalysis [1].

Biocatalytic processes have a number of features that make them into alternatives with great potential for “green” and selective processes and its application is steadily increasing at an industrial scale [2].

However, most biocatalytic processes at an early development stage do not fulfill the economic requirements for industrial operation [4] [5].

Many of these under-developed biocatalytic processes often show low product concentrations (g_{product}/L), which compromises downstream processing cost; low space-time yield ($g_{\text{product}}/L_{\text{reactor}}/h$) which will increase capital costs (CAPEX) and energy requirements during the reaction; low reaction yield ($g_{\text{product}}/g_{\text{substrate}}$) and finally low biocatalyst yield ($g_{\text{product}}/g_{\text{biocatalyst}}$). All these process metrics are critical for an economically competitive process at an industrial scale.

This PhD project aims to evaluate the feasibility of 3-5 case studies and establish a set of tools that can be used to evaluate processes in several stages of development and to provide guidance for research and development.

Case-study 1

The first case study to be evaluated is the production of R-(+)-perillic acid via biotransformation of R-(+)-limonene using a whole-cell biocatalyst (see Figure 1) [3].

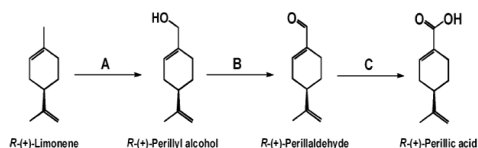


Figure 1: Bioconversion of R-(+)-limonene to R-(+)-perillic acid by *P. putida* DSM 12264: (A) monooxygenase; (B) alcohol dehydrogenase; (C) aldehyde dehydrogenase [3].

Perillic acid is a monoterpenoic acid present in the plants *Perilla mint* and *Perilla frutescens*, which has a broad growth-inhibitory effect on bacteria, yeast and moulds. Thus it is an attractive candidate to be used in substitution of conventional preservatives, particularly in cosmetic industry [3].

However, the bioprocess faces numerous challenges, namely substrate and product inhibition, low biocatalyst activity, low water solubility of limonene and its derivatives and high volatility of limonene.

To overcome product inhibition limitations, *in situ* product removal (ISPR) is necessary. Figure 2 shows the scheme of the integrated bioprocess, where the culture broth is continuously recirculated through a recovery loop containing a column with a fluidized bed of anion exchanger.

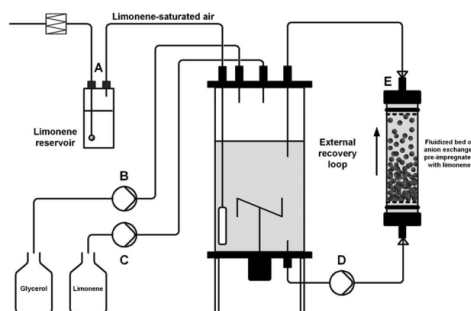


Figure 2: Scheme of the integrated bioprocess [3].

In order to determine the process bottlenecks, an initial feasibility analysis of perillic acid production process was done. Mass balances and process simulations were made, which allowed the determination of values for a set of process metrics (product concentration, reaction yield and space-time yield) which can be used to provide targets associated with the economic demands of the process. These metrics can then be used to help define a suitable development strategy.

From the *in silico* analysis, it was observed that the metrics are still far from the required targets to achieve the economic goals of this process.

Further analysis, allowed the identification of the main bottlenecks of the process – the specific productivity ($g_{\text{product}}/g_{\text{cell}}/h$) of the selected strain is low; product inhibition; and substrate volatility.

This allowed the identification of a set of intensification technologies that can improve the process – e.g. two-liquid phase operation, an adequate strategy for substrate feeding or alternative approaches for *in situ* product removal; and a set of tools for biocatalyst improvement, namely genetic engineering tools (improved expression of the enzymes of interest or selection of different host organisms).

All the options for process and biocatalyst improvement will be included in a suitable development strategy, which can result in a reduced process development time.

Conclusions

It is still a challenge to develop bioprocesses given the complexity of the systems. However, the determination of process metrics from an early stage of development provides a valuable tool for better understanding of the systems limitations and to help define the introduction of intensification technologies, such as substrate feeding, or two-liquid phase operation; or alternatively genetic or protein engineering for biocatalyst improvement.

Acknowledgements

The project is part of the strategic alliance NatLifE 2020 coordinated by BRAIN AG. The financial support from BMBF (grant no. 031A206-B) is acknowledged.

References

1. B. G. Hermann, M. Patel, Today's and tomorrow's bio-based bulk chemicals from white biotechnology, *Appl. Biochem. Biotechnol.* 136 (2007) 361–388.
2. P. Tufvesson, J. Lima-Ramos, M. Nordblad, J. M. Woodley, Guidelines and cost analysis for catalyst production in biocatalytic processes, *Org. Process Res. Dev.* 15 (2011) 266-274.
3. M. A. Mirata, D. Heerd, J. Schrader, Integrated bioprocess for the oxidation of limonene to perillic acid with *Pseudomonas putida* DSM 12264, *Process Biochemistry* 44 (2009) 764-771.
4. P. Tufvesson, J. Lima-Ramos, N. Al Haque, K. V. Gearney, J. M. Woodley, Advances in the Process Development of Biocatalytic Processes, *Org. Process Res. Dev.* 17 (2013) 1233-1238.
5. J. Lima-Ramos, W. Neto, J. M. Woodley, Engineering of Biocatalysis and Biocatalytic Processes, *Top Catal* (2014) 57:301-320.



Daria Semenova

Phone: +45 4525 2958
E-mail: dsem@kt.dtu.dk

Supervisors: Krist V. Gernaey
Ulrich Krühne

PhD Study
Started: August 2014
To be completed: August 2017

Development of advanced mathematical data interpretation methods for application in microbioreactors

Abstract

During the last decade significant research within industrial biotechnology has been directed to downscaling, and channeled in the development and further implementation of small scale bioreactors. Recently studied microbioreactors (MBRs) with parallel operation hold the promise of enabling faster, less labor intensive bioprocess development, with significantly reduced reagent usage and waste generation. However, the successful application of MBR technology will only be possible if it can rely on appropriate software and automated data interpretation of the MBR experiments. Thus, the software and data interpretation tools should allow maximizing the exploitation of the flexibility and the capabilities of the MBR platform to deliver information-rich experiments on the one hand, and on extracting as much information as possible from the obtained experimental data on the other hand. In practice, this can be achieved by coupling advanced mathematical data interpretation to the MBR experiments.

Introduction

Industrial biotechnology processes rely on screening programs for achieving high yields and volumetric productivities, which are crucial to economic viability. High-throughput screening is a feasible approach to identify interesting, refined production strain candidates. However, a significant problem – both in screening and in large scale biotechnological processes – is state estimation. The design of model based state and parameters estimators that could provide reliable on-line information on the biological variables and model parameters has always been under discussion. Thus, there is a clear need for systems that enable rapid testing, optimization, control and bioprocess development in low sample volumes, allowing parallel cultivations with setup and run-time efforts, both in terms of time and resource consumption, that remain nearly independent of the number of bioreactors. MBR technology with integrated sensors is an adequate solution for rapid, high-throughput, and cost-effective screening. It allows, in principle, continuous measurement and control of various fermentation parameters, despite the low volumes.

Methodology

Performing experiments at microscale will generate a considerable amount of data, and in the end operating such a microscale system with multiple functions in

parallel will cause difficulties to interpret all generated data using traditional tools such as a spreadsheet program. Therefore, this project will be focused on streamlining the data interpretation. The first part of the work will be based on describing cultivations and biocatalytic processes at microscale by mechanistic models of reactor systems, either based on ordinary differential equations (ODEs) or partial differential equations (PDEs), and will specifically work on the modeling of *Saccharomyces cerevisiae* batch and continuous cultivations. Based on an existing Matlab™ toolbox developed at DTU, the work will be continued for the further application of uncertainty and sensitivity analysis for this model with the aim to use the analysis results for proposing targeted new experiments in order to collect informative experiments with the experimental microbioreactor set-up using as few experiments as possible. Furthermore, software sensors have to be developed as well for the MBR platforms, to extend the number of variables for which on-line information is available. The two chemometric methods principal component analysis (PCA) and partial least squares (PLS) regression are commonly applied together with spectroscopic data and process data, and will be used to predict variables such as biomass concentration and substrate concentration which are usually difficult to measure on-line. The last part of the project will be focused on automating experiments,

coupling simulations with a model with techniques like Design of Experiments, Monte Carlo simulation or optimization methods on the one hand, and then transforming results into new experiments that are to be performed in a MBR.

Mechanistic model

In order to propose a model both the bioreactor performance and the microbial kinetics have to be considered. Description of the bioreactor performance includes the modelling of the mass transfer effects in both gas and liquid phases and the microbial kinetics. The microbial kinetics can be described either with an unstructured model (no intracellular components considered) or with a structured model (intracellular components considered). At the level of the individual cell, the population model may be unstructured (all cells in the whole population assumed to be identical, i.e. only one morphological form), or morphologically structured (with an infinite number of morphological forms the term segregated population model is often used) [1].

Sonnleitner and Käppeli [2] proposed a classical mechanistic model describing the aerobic growth of budding yeast. The model is based on the fact that glucose degradation proceeds via two pathways under conditions of aerobic ethanol formation. One part is metabolized oxidatively, and the other part reductively, with ethanol being the end product of reductive energy metabolism. Thus, their model describes the glucose-limited growth of *Saccharomyces cerevisiae* and it is able to account for the overflow metabolism, and to predict the concentrations of biomass, glucose, ethanol, and oxygen throughout an aerobic cultivation in a stirred tank reactor. It has been shown that this mechanistic model is quite generic [3] and in principle could be applied in the case of MBR technology as well. Furthermore, the workflow for a systematic model analysis shown in Figure 1 is rather common and could be used in this project as well.

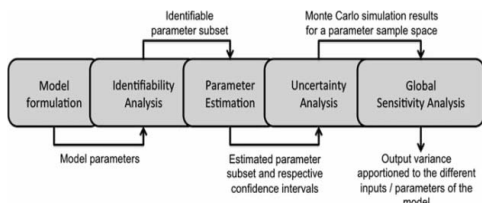


Figure 1: Schematic workflow for the model analysis [3].

Software sensors

In the last decade numerous ‘software sensors’ have been tested in biotechnological processes, mainly in lab-scale. The concept ‘software sensor’ associates two terms: a sensor and a software part that could be defined as a hardware and an estimation algorithm respectively (Figure 2). The development of reliable sensors for relevant cultivation parameters leads to on-line

estimation of the unmeasurable variables and kinetic parameters. Thus, it makes the software sensors an important and potentially very useful tool in bioprocess monitoring and control.

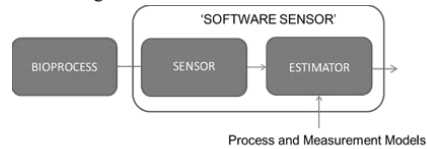


Figure 2: Principle of a ‘software sensor’.

The key tools in software sensor design are mathematical models. The model properties settle an appropriate estimation algorithm, and the quality and validity of the model affects the performance of the resulting ‘software sensor’. Usually, mechanistic bioprocess models are based on mass balance equations, which can be used as software sensors [4]. Being difficult to define and to validate functions, the kinetic parameters values could be settled as unknown and time varying parameters. Thus, applying the adaptive methods based on models with time varying parameters is one of the most reliable techniques for bioprocesses software sensors [5]. However, in case of lack of knowledge about the reaction kinetics an alternative solution would be an asymptotic estimator design, which is based on General Dynamic Model (GDM) of the process, developed on the basis of a corresponding General Reaction Scheme (GRS) - a qualitative description of the main metabolic reactions. Such estimators are simpler in comparison with the exponential estimators, based on the Kalman filtering method and full knowledge of the process kinetics [6].

Acknowledgements

The research project has received funding from the People Programme (Marie Curie Actions) of the European Union's Seventh Framework Programme FP7/2007-2013/ under REA grant agreement n° 608104 (EUROMBR). The article represents only the authors’ views and European Union is not liable for any use of the information presented here.

References

1. J. Nielsen, J. Villadsen, Chem. Eng. Science 47 (1992), 4225-4270.
2. B. Sonnleitner, O. Käppeli, Biotech. Bioeng. 28 (1986), 927-937.
3. R. L. Fernandes, V. K. Bodla, M. Carlquist, A. L. Heins, A. E. Lantz, G. Sin, K. V. Gernaey, Adv. Biochem. Eng. Biotechnol. 132 (2013), 137-166.
4. S. T. F. C. Mortier, K. V. Gernaey, T. De Beer, I. Nopens, Eur. J. Pharm. Biopharm., 86 (2014), 532-543.
5. A. Chéruey, J. Biotechnol. 52 (1997), 193-199.
6. T. Patarinska, V. Trenev, S. Popova, Int. J. BIOautomation 14 (2) (2010), 99-118.



Aamir Shabbir

Phone: +45 45256195
E-mail: aash@kt.dtu.dk
Discipline: Chemical and Biochemical engineering

Supervisors: Ole Hassager
Anne Ladegaard Skov

PhD Study
Started: October 2013
To be completed: September 2016

The influence of hydrogen bonding on nonlinear extensional rheology of supramolecular poly(n-butyl acrylate)

Abstract

Supramolecular polymers are used in many fields as adhesives, coatings, cosmetics and in printing. Understanding the dynamics of such transient systems is essential for tailoring user defined properties. Unlike linear viscoelasticity, only few extensional rheology data exists for supramolecular polymers. They indicate that they are very promising for tailoring the appearance of strain hardening. On the other hand, such data is also needed to develop sophisticated multi-scale models that can later be used for predicting the flow behavior and molecular dynamics of supramolecular networks. We investigate rheological properties of well-defined linear supramolecular polymers based on Poly (n-butyl acrylate) (PBA). Systems with varying hydrogen bonding made via hydrolysis of PBA were studied. While systems with moderate degree of hydrolyzation exhibit pure reptation based relaxation in the linear regime, they exhibit significant strain hardening behavior compared to the untreated PBA. Furthermore, at a critical percentage of hydrolyzation, the supramolecular PBA exhibits rubber like characteristics. The extensional rheology experiments were performed on an updated filament stretching rheometer

Introduction

Hydrogen bonding is the most employed non-covalent reversible interaction to create supramolecular polymeric assemblies [1]. The dynamics of hydrogen bonded transient networks can be significantly altered by changing the exchange rate between two hydrogen bonding motifs via external stimuli such as temperature. At high temperatures molecular chains can release stress at a fast rate because of decrease of hydrogen bond life time which can lead to low viscosity melts. This remarkable property thus allows easy processing of such materials for various applications [2]. Alternatively, at low temperatures the hydrogen bond life can be significantly larger than the experimental time scales leading to transient networks [3]. Hydrogen bonded supramolecular polymers can be represented as shown in Figure 1.



Figure 1: Cartoon representation of hydrogen bonded supramolecular polymer assembly. Red triangles symbolize the hydrogen bonding moieties

Majority of work in the field of hydrogen bonded supramolecular networks exists for small deformations or linear viscoelasticity (LVE) [3,4]. To the best of our knowledge, mostly un-entangled systems have been investigated to study the linear rheological response of hydrogen bonded supramolecular polymers primarily due to the ease of practicality involved with them and importantly such systems offer isolating the dynamics of entanglements from the dynamics of association/disassociation. This however, still leaves out room for the study of entangled hydrogen bonded supramolecular polymer, albeit the complexity involved. Surprisingly, no literature exists on the non-linear elongational behaviour of such hydrogen bonded supramolecular polymers which provided us the incentive for this research.

Experimental Details

Materials

We used pure Polybutyl-n-acrylate (PnBA) and three of its hydrolyzed variants mentioned here in increasing amount of hydrogen bonding content. These include samples: AA6, AA12, AA38. The numbers used in this nomenclature denote the percentage of acrylic acid groups. Pure PnBA was obtained from Polymer

source, Inc. and had a polydispersity index, PDI, of 1.38. Hence polydispersity may have an effect on the data reported hereafter, albeit small.

Non-linear viscoelasticity

The extensional stress growth coefficient as a function of time was measured by a filament stretching rheometer (DTU-FSR). Measurements were performed at a constant Hencky strain rate imposed at the mid-filament diameter using an online control scheme [5]. All experiments were performed at 21.5°C. The imposed strain rates were varied from 0.0006s^{-1} to 1s^{-1} .

Results

The non-linear rheology measured using the DTU-FSR is shown in Figure 1. The strain rates increase from right to left in Figure 1. The solid lines represent the LVE envelop obtained from a multi-mode Maxwell fit to the linear rheology data.

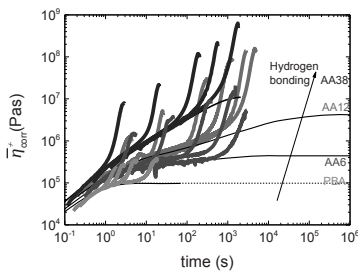


Figure 2: Stress growth coefficients at various strain rates for PnBA and its hydrolyzed derivatives as a function of time.

Typically for monodisperse entangled linear melts no deviation from the LVE envelop (often termed as strain hardening) is observed for imposed strain rates less than the inverse of longest relaxation time. However, strain hardening is observed for our samples as evident from Figure 1 despite the fact that the strain rates were well less than the inverse of longest relaxation time. This deviation is attributed to the presence of acrylic acid groups in the hydrolyzed samples thus representing hydrogen bonding. The amount of strain hardening increases with amount of acrylic acid group density to almost four orders of magnitude for AA38 containing 38% acrylic acid groups.

When the stress is plotted as a function of Hencky strain, the curves show a tendency to come closer as opposed to what one would expect for a pure monodisperse linear melt where each curve is distinct and separated. This is shown in Figure 3. The black line represents the stress prediction of Neo-hookean model.

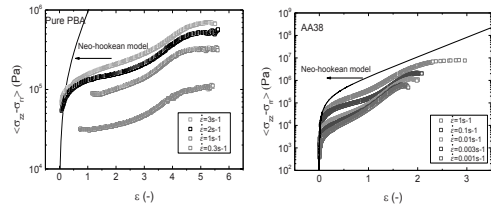


Figure 3: Extensional stress as function of Hencky strain at different strain rates for pure PnBA and 38% hydrolyzed PnBA.

Discussion

We interpret the increase of strain hardening behaviour with increasing acrylic acid group density, as an increase of life time of hydrogen bonds causing more extension of sticky rouse modes thus resulting in an increased strain hardening. This reasoning correlates well to the slope of 0.5 observed in the linear rheology data for AA38. Deviation from Neo-hookean prediction becomes relatively less for hydrolyzed PnBA suggesting that the hydrogen bonds are relatively long lived yet still transient because of absence of a unique stress-strain curve.

Conclusions

The incorporation of acrylic acid groups resulted in significant increase in strain hardening behaviour of hydrolyzed PnBA melts indicating that the life of hydrogen bonds increases with increasing concentration. These results suggest a potential in utilizing hydrogen bond transient networks in melt rheology to tailor strain hardening behaviour.

References

1. Nair, Kamlesh P. and Breedveld, Victor and Weck, Marcus 41 (10) (2008) 3429-3438.
2. Yan, Xuzhou and Wang, Feng and Zheng, Bo and Huang, Feihe 41 (18) (2012) 6042-65.
3. Lewis, Christopher L and Stewart, Kathleen and Anthamatten, Mitchell 47 (2014) 729-740.
4. Feldman, Kathleen E. and Kade, Matthew J. and Meijer, E. W. and Hawker, Craig J. and Kramer, Edward J. 42 (22) (2009) 9072-9081.
5. Roman Marin, Jose Manuel and Husom, Jakob Kjølsted and Alvarez, Nicolas Javier and Huang, Qian and Rasmussen, Henrik Koblitiz and Bach, Anders and Skov, Anne Ladegaard and Hassager, Ole. 194 (2013) 14-22.

Acknowledgments

This project is a part of SUPOLEN, funded under the Initial Training Network in the Seventh Framework Marie Curie Program.



Laura Snip
Phone: +45 4525 2990
E-mail: lasn@kt.dtu.dk

Supervisors: Krist V. Gernaey
Ulf Jeppsson, Lund University
Xavier Flores-Alsina
Benedek Plósz, Environmental Engineering
Ulrich Krühne

PhD Study
Started: May 2012
To be completed: April 2015

Practical Application of Models in the Urban Water System: Simulation Based Scenario Analysis

Abstract

Nowadays a wastewater treatment plant is challenged to not only provide clean water but also to take its carbon footprint into account. Another 'new' challenge is the removal of so called micropollutants. In order to further optimize the performance of the wastewater treatment plant a good understanding of the production of greenhouse gases and the removal of micropollutants is required. Modeling these processes contributes to the development of a proper understanding of the main mechanisms involved, and enables to test different plant operation scenarios on their efficiency *in silico*. As a result new evaluation tools can be developed concerning the production of greenhouse gases and the removal of micropollutants.

Introduction

With the increasing awareness of global warming also wastewater treatment plants (WWTPs) have to monitor and if possible reduce their production of greenhouse gases (GHGs). In a WWTP, three different GHGs are produced, namely CO_2 , CH_4 and N_2O . The global warming potential (a measure to compare the effect of different chemicals on the global warming) of CH_4 is 34 kg equivalent CO_2 and that of N_2O is 298 kg equivalent CO_2 [1]. This shows that a small production of N_2O will have a higher impact compared to a small production of CO_2 and therefore it is important to take those emissions into account.

Besides GHG emissions, a WWTP has a relatively new challenge. Indeed, the development of methods to measure chemicals at low concentrations has resulted in a growing awareness of the presence of low concentrations of the so-called micropollutants in the aquatic environment. These micropollutants can originate from medication, illicit drugs and personal care products. Recent studies have shown that these chemicals can influence aquatic life by inducing sex reversal and/or intersexuality [2], or that the reproductive behavior is reduced [3]. WWTPs are traditionally not designed to remove micropollutants; however a change in operational conditions such as increasing the sludge retention time can increase the removal of certain micropollutants in a WWTP [4].

In order to face these challenges the Benchmark Simulation Model 2 (BSM2) will be extended to include the processes concerning GHGs and micropollutants.

The BSM2 is a general plant wide model of a WWTP that was developed with the purpose of comparing different control strategies [5]. The model includes a plant layout, shown in Figure 1, a simulation model, influent loads, test procedures and evaluation criteria. When using the same plant layout, influent loads, test procedures and evaluation criteria, the outcome of different control strategies will be comparable in an objective way.

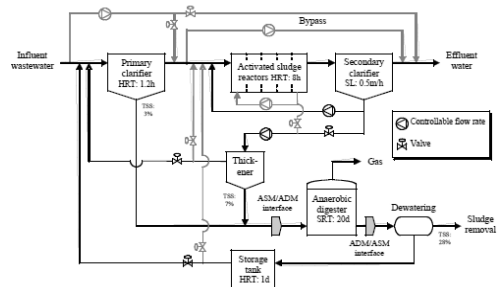


Figure 1: A schematic overview of the plant layout of BSM2.

Objective of PhD study

The objective of this PhD study is to extend the BSM2 with processes involving the GHG production and processes concerning the micropollutants. Once this extension is made different operating scenarios will be compared *in silico* according to newly developed evaluation tools. These evaluation tools should include

criteria concerning GHG emissions and micropollutants besides the current effluent quality index and operational cost index.

Carbon footprint of the WWTP

Nitrous oxide is being produced in a WWTP as an intermediate in the anoxic zones during heterotrophic denitrification. It can also be produced in the aerobic zones by ammonia oxidizing bacteria. This can happen during nitrifier denitrification and by chemical reactions; however it is not yet known precisely how these processes work and to what extent they contribute to the overall production of N₂O [6]. Ni *et al.* [7] have developed four different mathematical models that can describe the N₂O production. These models were implemented into the BSM1 in order to account for N₂O production by ammonia oxidizing bacteria (AOB). The dynamic simulation results of the different models are shown in table 1.

Table 1: The dynamic results of the four different models published by Ni *et al.* [7] with the BSM1.

* Concentration taken from last reactor

	AOB denitrification		Incomplete oxidation of hydroxylamine (NH ₂ OH)		Units
	Model	Model	Model	Model	
	A	B	C	D	
S _{O2}	2.51	3.96	5.42	2.52	g O ₂ .m ⁻³
S _{NH4}	2.86	0.042	2.31	3.35	g N.m ⁻³
S _{NO3}	14.34	2.99	23.82	13.96	g N.m ⁻³
S _{NO2}	1.81	1.98	0.0030	1.10	g N.m ⁻³
S _{NO}	0.019	0.33	0.0010	0.0020	g N.m ⁻³
S _{N2O}	0.026	0.098	0.069	0.046	g N.m ⁻³
X _{AOB*}	102.7	95.16	48.53	81.25	g COD.m ⁻³
X _{NOB*}	30.38	13.20	29.22	30.52	g COD.m ⁻³
G _{N2O}	68.42	175.20	70.13	56.70	kg N ₂ O-N.d ⁻¹
	6.8%	17.5%	7.0%	5.7%	% N ₂ O produced of N-influent

As can be seen in the table, the different models predict a different percentage of N₂O produced with model B having the highest percentage (17.5%) and model D the lowest of 5.7%. This indicates that more research is needed to establish the pathways involved in N₂O production. With N₂O data obtained at different WWTPs in Sweden, calibrations will be performed with the available models in order to select the most realistic model.

For now the CO₂ production is mainly calculated by conversion factors and the CH₄ production by the anaerobic digester is already calculated in the BSM2. The emissions that are taken into account when calculating the carbon footprint are emissions during: i) treatment, namely biological treatment, endogenous respiration, BOD oxidation, nitrification (CO₂ credit

and nitrogen removal; ii) energy use of the plant; iii) sludge digestion; iv) sludge disposal; v) power credit by use of biogas; and, vi) chemical usage. The emissions during the building of the WWTP are not taken into account as those are not controllable. Once the BSM2 is extended with the production of the three GHGs, different control strategies can be compared in order to decrease the carbon footprint of the plant during operation.

Micropollutants

There are many different micropollutants present in the wastewater with each compound having its own characteristics. Therefore every compound has to be modeled with different parameters. However, the same processes are responsible for the removal of the micropollutants in WWTPs. The dominant processes removing the micropollutants are sorption and biotransformation [8]. Other processes that also occur with the micropollutants are desorption and retransformation into parent compound. These processes can take place in the aerobic and in the anoxic phase; however there are different parameters for the aerobic and anoxic phase. These processes will lead to three different forms of the micropollutant in the wastewater, namely the liquid form, C_{LI}, the sorbed form, C_{SL}, and the conjugated form, C_{CI}. There is then also a fraction of the micropollutants that can not be removed because it is sequestered (C_{SLI}). These are just the processes concerning the micropollutants in the activated sludge reactors. To model the fate of the micropollutants in an urban water system context, also the behavior in the sewer system, the settlers, the anaerobic digester and the receiving waters should be taken into account.

There are different studies on the removal of micropollutants in a WWTP, however not all include a mathematical model, and the published models differ largely. For this study the framework published by Plósz *et al.* [8, 9] was chosen. This framework takes the above-mentioned processes and variables into account, has been tested in lab scale and full scale and is easily added to the activated sludge model. With this framework, the occurrence, transport and fate of different pharmaceuticals could be simulated. The occurrence of the pharmaceuticals was modeled by extending the influent generator of the BSM2 [10]. This generator consists of a model block calculating the flow rate, a block calculating the pollutant loads and a block calculating the temperature. These calculations are put together to define concentration profiles and passed through a transport block where the sewer system is defined. This is schematically shown in figure 3. To calculate the loads of pollutants a daily profile is combined with a weekly and a seasonal profile, which is multiplied with the number of Person Equivalent (PE) that are in the catchment (figure 3).

The occurrence of micropollutants is generated with two different approaches. Daily, weekly and seasonal influent dynamics for micropollutant with a regular pattern are generated following a phenomenological approach based on user-defined pollutant profiles.

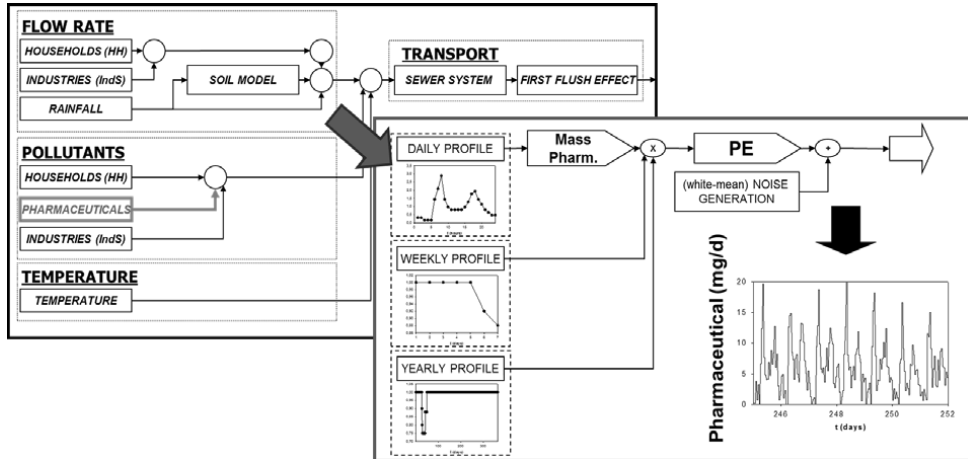


Figure 3: Schematic representation of the influent pollutant disturbance scenario modelling approach with the addition of micropollutants

For compounds which are known to have more random patterns/dynamics in the influent, a stochastic approach based on Markov Chains is used. Drug administration patterns, bioavailability, half-time and total annual consumption rates are the basis to generate the user defined profiles, while the Markov Chains are constructed assuming a set of transition probabilities. As mentioned before, the daily, weekly and seasonal variation is combined and multiplied with the PE. Zero-mean white noise can be added to give more realism to the generated time series using the noise variance as a tuning parameter [11].

The generation of the occurrence of the micropollutants is calibrated with data provided during an external stay at the University of Girona, Spain. High frequency data of the occurrence of micropollutants during three days was available. The occurrences of three different micropollutants, ibuprofen (IBU), sulfamethoxazole (SMX) and carbamazepine (CMZ) are generated (figure 4).

IBU and SMX present a high correlation with ammonium, which clearly indicates the impact of human urine (figure 4 a,b). The estimated total pollution loads are 60.58 g/day for IBU and 2.11 g/day for SMX. It is important to highlight that to correctly describe the dynamics of SMX the parameter *subarea* had to be reduced. There could be two possible explanations to this situation. First of all, one must notice that SMX is several orders of magnitude lower in concentration than IBU and consequently more sensitive to the error of the sampling method [12]. Secondly, due to the sparsely distributed catchment, the authors assume that the compound that can be measured is consumed in the closest urban area. Here the shorter hydraulic residence time prevents complete mixing of SMX and therefore the concentrations remains above detection limits.

Indeed, the sources of NH_4 and IBU are higher and more plausible with a wide geographical distribution. The last studied compound (CMZ) is correlated with the

occurrence of total suspended solids (TSS). This is attributed to the fact that CMZ is excreted for only 1% in the urine and 28% in the faeces [13]. However, the metabolites of CMZ are correlated with the occurrence of ammonium and therefore two different user defined profiles were used (Fig. 3 e,f). The estimated pollution load for CMZ is 1.55 g/d.

In order to evaluate the different control strategies of a WWTP regarding the removal of micropollutants, the traditional performance evaluation criteria have to be extended. This can be done by including removal indexes based on percentages of micropollutant removed, or sorbed, but also by including a receiving water model. With a receiving water model, concentrations of the micropollutant after discharge can be calculated and compared with concentration limits of toxic compounds.

Conclusion

The extension of the BSM2 with processes concerning GHGs is ongoing as there is no consensus on the dominant pathway(s) for N_2O production by AOB. The extension with processes concerning micropollutants has been focused on pharmaceuticals. The occurrence, transport and fate of different micropollutants has been modeled with the extended BSM2 and the occurrence model has been successfully calibrated with high frequency data from the University of Girona, Spain.

The extended BSM2 will make it possible to objectively compare different operational/control strategies by evaluating their operational costs, effluent quality, GHG emissions and micropollutant removal.

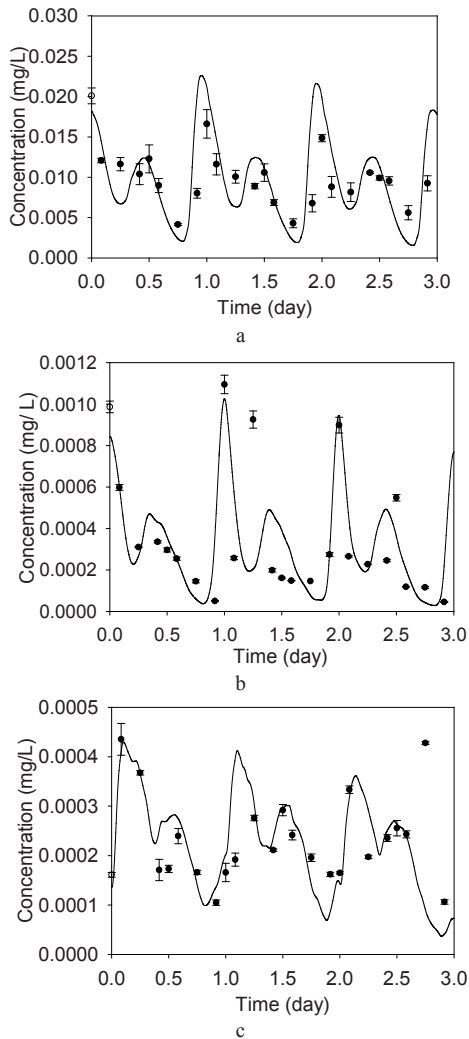


Figure 4: Dynamic occurrence of IBU (a) measured (dots with uncertainty error bars) and simulated (line), SMX (b) measured (dots with uncertainty error bars) and simulated (line), and CMZ (c) measured (dots with uncertainty errorbars) and simulated (line), during a week generated with the extended BSM2 influent generator.

Acknowledgements

Laura Snip acknowledges the People Program (Marie Curie Actions) of the European Union's Seventh Framework Programme FP7/2007-2013 under REA agreement 289193 (SANITAS). This article reflects only the authors' views and the European Union is not liable for any use that may be made of the information contained therein.

References

1. IPCC, *Climate Change 2013: The Physical Science Basis*, Cambridge University Press, 2013, chapter 8.
2. A. Lange, G.C. Paull, T.S. Coe, Y. Katsu, H. Urushitani, T. Iguchi, C.R. Tyler, *Environmental Science and Technology*, 43 (4) (2009) 1219-1225.
3. T.S. Coe, P.B. Hamilton, D. Hodgson, G.C. Paull, J.R. Stevens, K. Sumner, C.R. Tyler, *Environmental Science and Technology*, 42 (13) (2008) 5020-5025.
4. M. Clara, N. Kreuzinger, B. Strenn, O. Gans, H. Kroiss, *Water Research*, 39 (1) (2005) 97-106.
5. Gernaey, K.V., Jeppsson, U., Vanrolleghem, P.V. and Copp, J.B. (eds.) (2014). IWA Publishing, London, UK.
6. M.J. Kampschreur, H. Temmink, R. Kleerebezem, M.S. Jetten, M.C. van Loosdrecht, *Water Research*, 43 (2009) 4093-4103.
7. B.-J. Ni, Z. Yuan, K. Chandran, P.A. Vanrolleghem, S. Murthy, *Biotechnology and Bioengineering*, 110 (1), (2013) 153-163
8. B.Gy. Plósz, K.H. Langford, K.V. Thomas, *Biotechnology and Bioengineering*, 109 (11) (2012) 2757-2769
9. B.Gy. Plósz, H. Leknes, and K.V. Thomas, *Environmental Science and Technology*, 44 (2) (2010) 734-742.
10. K.V. Gernaey, X. Flores-Alsina, C. Rosen, L. Benedetti, and U. Jeppsson, *Environmental Modelling & Software*, 26 (11) (2011) 1255-1267.
11. Snip, L., Flores-Alsina X., Plósz B.G., Jeppsson U. and Gernaey, K.V. *Environmental Modelling & Software*, 62, (2014) 112-127.
12. Ort, C., Gujer, W. *Water Science & Technology*, 54, (2006) 169-176.
13. Zhang, Y., Geissen, S.-U., Gal, C., *Chemosphere* 73, (2008) 1151-61.

List of Publications

Flores-Alsina, X., Arnell, M., Amerlinck, Y., Corominas, L.I., Gernaey, K.V., Guo, L., Lindblom, E., Nopens, I., Porro, J., Shaw, A., Snip, L., Vanrolleghem, P.A. and Jeppsson, U. (2014). Balancing effluent quality, economic cost and greenhouse gas emissions during the evaluation of (plant-wide) control/operational strategies in WWTPs. *Science of the Total Environment*, 466-467, 616-624.

Snip, L.J.P., Boiocchi, R., Flores-Alsina X., Jeppsson U. and Gernaey, K.V. (2014). Challenges encountered when expanding activated sludge models: A case study based on N₂O production. *Water Science and Technology*, 70(7) 1251-1260.

Snip, L., Flores-Alsina X., Plósz B.G., Jeppsson U. and Gernaey, K.V. (2014). Modelling the occurrence, transport and fate of micropollutants in urban wastewater systems. *Environmental Modelling & Software*, 62, 112-127.



Tobias Pape Thomsen

Phone: +45 2235 4425
 E-mail: ttho@kt.dtu.dk
 Discipline: Thermal gasification and pyrolysis

Supervisors: Jesper Ahrenfeldt, DTU KT
 Ulrik B. Henriksen, DTU KT
 Henrik Hauggaard-Nielsen, RUC
 Jens Kai Holm, DONG Energy

PhD Study
 Started: September 2013
 To be completed: December 2016

Low Temperature Thermal Gasification of marginal biomass and waste resources – coproduction of energy and fertilizer

Abstract

This work aims at identifying new potential fuels for CHP systems encompassing pretreatment of marginal biomass resources by low temperature gasification. The first part of the project has been development and application of an easy-to-apply screening method for identification of promising new fuels. The subsequent parts of the work will include pilot plant conversion of selected fuels and development of strategies to find optimal process balances between output of high efficiency energy products and high quality ash fertilizer.

Introduction

The global biomass resources are limited, and especially the high quality biomass resources – i.e. woody biomasses, are stressed by increased utilization in small and large scale energy and material systems around the world. To facilitate a significant substitution of coal and other fossil fuels with renewable biomass on a global scale, suitable conversion systems need to be introduced that can handle biomass resources of lower quality.

The Low Temperature Circulating Fluidized Bed (LT-CFB) Gasifier is such a system. A simple process diagram of the process is provided in Figure 1 below.

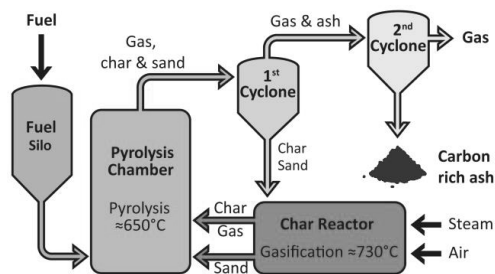


Figure 1: Process diagram of the LT-CFB gasification process.

The LT-CFB technology is highly fuel flexible, robust and relatively inexpensive [1].

The current commercial application of the LT-CFB gasification technology is as pretreatment and thermal separation unit for biomass and waste fuels in coal-

based co-firing systems. After treatment in the LT-CFB gasifier, 95% of the heating value potential of the fuel and 5% of the inorganics are present in a hot, combustible gas product and the remaining 5% of the heating value potential is left as residual carbon along with 95% of the inorganics in the solid fraction extracted from the bottom of the secondary cyclone. The gas product is used to substitute coal in large scale utility boilers and the solid product is applicable as ash fertilizer and soil enhancer [1]–[3]. An illustration of integration of LT-CFB gasification and existing coal based power plant infrastructure is provided in Figure 2.

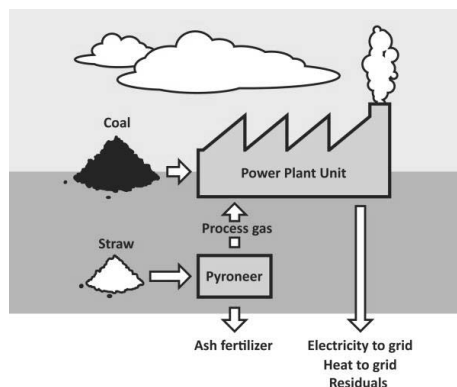


Figure 2: Illustration of the integration of LT-CFB gasifiers and existing coal-based power plant infrastructure.

Specific Objectives

A pilot LT-CFB facility with a thermal feed capacity of 100 kW exists at DTU Risø Campus and is used within the project to test selected new promising fuels and produce ashes for subsequent characterization and plant growth experiments in related work packages. Through pilot plant operation and subsequent char characterization and system assessment, it is the goal to identify process settings for optimal system operation. It is the hypothesis that for each LT-CFB fuel systems there is an optimal balance between stability of operation, energetic efficiency of the system and char quality.

As the project includes pilot scale testing of very few fuels only, the initial screening and selection process applied to pinpoint and select these fuels is a very important part of the project. Identification of new marginal biomasses is based on the following fuel characteristics – or a mix hereof:

- The resource has a significant, unfulfilled energy potential due to e.g. severe ash melting or sintering tendencies
- The resource has a significant, unfulfilled fertilizer potential due to e.g. severe risks or toxicity issues related to its use and application
- The resource poses a significant waste problem

After identifying, selecting and testing new promising fuels for the LT-CFB conversion platform, and collecting data about the conversion of the fuel and the characteristics of the produced products, it is also a minor part of the project to conduct a sustainability analysis on one or more of the fuels.

Results and Discussion

The main results from the project at the current state are related to the findings of the fuel screening and identification process. The focus of the work was on development of a suitable, fast and easy-to-apply screening method and the subsequent identification and characterization of multiple new marginal biomass resources. The assessment included 4 references, 9 residues from vegetable production, 4 residues from animal production and 5 sludge- and waste fractions. The technical assessment was conducted by comparing the results from a series of physical-mechanical and thermochemical experiments to those of already proven references. The technical assessment was supplemented by an evaluation of practical application and overall energy balance.

The assessment yielded a long list of results including:

- Bulk energy density per weight and volume
- Energy use for transport, drying and grinding
- Fuel proximate composition
- Char reactivity in reducing atmosphere, 750 °C
- The ratio between energy content in char and volatiles from pyrolysis
- Agglomeration/char-sticking issues in pyrolysis at 650 °C
- Ash sintering issues in steam/air at 750 °C

- Ash volatilization at 750 °C
- Char and ash densities
- Potential production of electricity and heat from the thermal conversion system (including power plant block)?

Based on the screening, many fuels were identified as promising for LT-CFB conversion, and sewage sludge from waste water treatment was selected as the first to test in pilot scale conversion. This resource has a global perspective within all three selection criteria - energy potential, fertilizer potential and waste issues.

Conclusions

Low temperature gasification has a unique potential to co-produce electricity, heat and fertilizer from marginal biomass resources inapplicable in other thermal conversion systems. An initial fuel screening process has identified numerous promising new fuels for the platform, and sewage sludge has been selected as the first of these resources for subsequent pilot scale testing, product characterization and system assessment.

Acknowledgements

I would like to acknowledge Energistyrelsen and the EUDP project funding as well as all project partners for realizing the project. I would also like to thank everyone contributing to collection of samples for the initial fuel screening. Finally, I would like to thank master student Giulia Ravenni for participating in the experimental work related to the fuel screening.

References

1. J. Ahrenfeldt, T. P. Thomsen, U. Henriksen, and L. R. Clausen, *Appl. Therm. Eng.*, 50 (2) (2013) 1407–1417.
2. R. G. Nielsen, *Optimering af Lav Temperatur Cirkulerende Fluid Bed forgasningsprocessen til biomasse med højt askeindhold*, DTU, 2007.
3. K. Kuligowski, *Utilization of ash from thermal gasification of pig manure as p-fertilizer and soil amendment*, Aalborg University, 2009.

List of Publications

1. T. P. Thomsen, G. Ravenni, J. K. Holm, J. Ahrenfeldt, H. Hauggaard-Nielsen, U. B. Henriksen, *Screening New Marginal Biomass and Waste Resources for Low Temperature Gasification – Method Development and Application*, Biomass Bioenergy, In Review.
2. T. P. Thomsen, G. Ravenni, J. K. Holm, J. Ahrenfeldt, H. Hauggaard-Nielsen, U. B. Henriksen, *New Marginal Biomass Resources for Medium and Large Scale Low Temperature Gasification in Denmark - Characterization and Feasibility Assessment*, 22nd European Biomass Conference and Exhibition, ETA-Florence Renewable Energies 2014.



Asbjørn Toftgaard Pedersen

Phone: +45 4525 2992

E-mail: astp@kt.dtu.dk

Supervisors: John M. Woodley
Ulrich Krühne
Gustav Rehn

PhD Study

Started: April 2014

To be completed: March 2017

Biooxidation – Reactor and Process Design

Abstract

Oxidation reactions are a cornerstone in the fine chemical industry, but the reactions often suffer from low selectivity and excessive waste generation. Biocatalysis can potentially solve these problems, however, it requires that the technology is developed further to ensure industrially relevant product concentration, yield and productivity. This PhD project will investigate how process and reaction engineering principles can help to solve the challenges encountered in oxidative biocatalysis.

Introduction

Oxidation reactions are a key part of organic chemistry, and perhaps the most frequently employed reaction type in the chemical industry. Oxidation reactions enable the formation of important functional groups such as alcohols, aldehydes, epoxides and carboxylic acids, from which various other functionalities can be incorporated to produce the compound of interest. Traditionally the oxidation chemistry is conducted with stoichiometric amounts of transition metal based oxidants (e.g. permanganate and dichromate) in the fine chemical industry. These processes often generate large amounts of waste, and most often require chlorinated organic solvents. Much work have been carried out to develop metal catalysts that enable highly selective oxidation using simple oxidants such as O_2 or H_2O_2 , however, there are still significant requirements for improvements in order to develop processes complying with the principles of green chemistry [1].

Biocatalytic oxidation (biooxidation) can potentially solve many of the problems encountered with chemocatalysis, as enzymes offer high regio- and stereoselectivity and high turnover rates at mild reaction conditions using simple oxidants (O_2) [2]. Industrial applications of biooxidation do exist, but are limited to few specialty chemicals employing mainly whole-cell biocatalysis (growing or resting cells) [3]. A main reason for the low level of industrial implementation is that many of the most industrially relevant enzymes have poor stability even in the environment of a cell. The stability is further challenged by the need for

processing unnatural substrates, which typically are both inhibitory to the enzymes and increase deactivation. Furthermore, the enzymes require molecular oxygen, which traditionally is supplied by bubbling air through the reaction mixture. Enzyme deactivation at gas-liquid interfaces is a well-established phenomenon; the air bubbles may therefore furthermore decrease the enzyme stability [4].

There is a need for further research to develop new biocatalysts, to improve activity and stability of existing biocatalysts, to develop suitable reactor technology, to perform economic and environmental assessments, and to demonstrate process robustness at bench and pilot scale in order to facilitate the implementation of the biooxidation technology in the chemical industry. These challenges are investigated in the European project BIOOX, which this PhD project is part of [5].

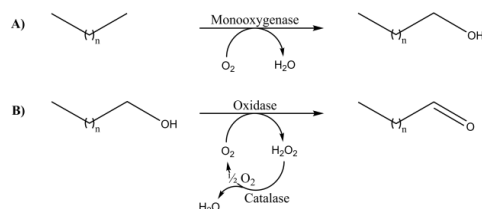


Figure 1: Examples of biooxidation reactions: Terminal hydroxylation of alkane to alcohol (A) and oxidation of alcohol to aldehyde (B).

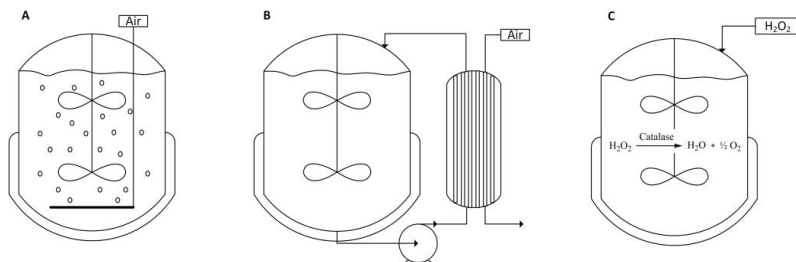


Figure 2: Oxygen supply methods to be investigated: A) bubble aeration, B) membrane aeration, and C) hydrogen peroxide decomposition by catalase.

Specific Objectives

This PhD project aims to investigate how process and reaction engineering principles can improve the productivity of alcohol synthesis and transformation using oxygen dependent enzymes.

The project will focus on two types of reactions – terminal hydroxylation of alkanes to alcohols (Figure 1A) and oxidation of alcohols to aldehydes (Figure 1B). The hydroxylation reaction is carried out using a P450 monooxygenase in the form of a whole-cell biocatalyst, i.e. using enzymes situated inside a cell, because the enzyme requires NADH co-factor that is regenerated by cell metabolism. The oxidation of alcohols is catalyzed by a soluble oxidase, whereby molecular oxygen is reduced to hydrogen peroxide, which is decomposed by catalase. Both reaction systems represent specific challenges, such as limited enzyme stability, substrate/product inhibition, and low substrate/product solubility.

A major challenge is to ensure that the reaction rate is not limited by the oxygen supply rate, while minimizing enzyme deactivation. Soluble enzymes tend to unfold at the gas-liquid interface hereby increasing the risk of irreversible deactivation of the enzyme either by oxidation of amino acid residues or protein aggregation. A key part of this project will therefore be to study the deactivation of enzymes at gas-liquid interfaces, and how this can be avoided. To do so the enzyme stability will be studied at different aeration rates and oxygen concentrations in a reactor with bubble aeration. Furthermore, alternative strategies for supplying oxygen will be investigated (Figure 2), such as membrane aeration, where oxygen is supplied to the reaction medium via a membrane. Hereby the gas-liquid interface can be avoided, therefore potentially reducing enzyme deactivation. Oxygen can also be supplied by adding hydrogen peroxide which is decomposed to oxygen and water by catalase. The method also avoids a gas-liquid interface in the reactor. However, hydrogen peroxide can also damage the enzymes (or cells) and it is therefore important to ensure a low concentration of hydrogen peroxide at all times. This might become a limitation in an industrial scale reactor, where spatial heterogeneity is unavoidable due to imperfect mixing.

Another focus in this project will be to investigate the oxygen consumption of biocatalysts. The oxygen consumption rate of soluble enzymes follows directly

from the stoichiometry of the oxidation reaction. However, for living whole-cell biocatalysts the oxygen consumption rate is determined not only by the oxidation reaction, but also by the metabolism of the cell. Flux balancing can be used to predict the oxygen requirements of cells. This requires knowledge of the energy requirements for cellular maintenance and growth, which is known for most organisms at typical growth conditions. However, during biocatalysis the cells are typically nitrogen limited to avoid growth and exposed to unnatural substrates, which might substantially change energy requirements and hence the oxygen consumption rate. An objective in this project is therefore to design experiments to determine the required energetic parameters and oxygen consumption at relevant conditions.

The last part of the PhD project will focus on the development of a simple process flowsheets for a bio-oxidation process, which will enable the identification of process bottlenecks and economic and environmental evaluation of the process, hereby identifying where further development is required to facilitate industrial implementation.

Acknowledgements

The research leading to these results has received funding from the European Union's Seventh Framework Programme for research, technological development and demonstration under grant agreement n° 613849.

References

1. T. Punniyamurthy, S. Velusamy, J. Iqbal, *Chem. Rev.* 105 (2005) 2329-2363.
2. N. Turner, *Chem. Rev.* 111 (2011) 4073-4087.
3. A. Liese, K. Seelbach, A. Buchholz, J. Haberland, in: A. Liese, K. Seelbach, C. Wandrey (Eds.), *Industrial Biotransformations*, Wiley-VCH Verlag, Weinheim, 2006, p. 148.
4. A. Bommarius, A. Karau, *Biotechnol. Prog.* 21 (2005) 1663-1672.
5. www.BIOOX.eu

**Jon Trifol Guzman**

Phone: +45 4525 6196
E-mail: jotg@kt.dtu.dk

Supervisors: Peter Szabo
Anders Daugaard
Ole Hassager

Started: September 2012
To be completed: August 2015

Novel Clay/Nanocellulose Biocomposite Films and Coatings in the Context of New Packaging Materials

Abstract

During recent years several efforts have been made into bio-based and renewable resources. Among all the resources the packaging and more specifically the packaging for food application has started to awake the interest of the scientific community. Although currently there are biopolymers available at the market, there is still some work to do in the optimization of some technical properties, such as mechanical properties and barrier properties. The addition of novel nanoreinforcements as nanocellulose, cellulose nanofibers or whiskers, organically modified layered silicates or other kind of nanoreinforcements could promote the properties of the biopolymers enough to have the right technical parameters for this application.

Introduction

The use of petroleum-based products for packaging applications represents a serious global environmental problem, not only from the point of view of the raw material but also due to the lack of biodegradability of the most part of the petroleum-based products. In recent years novel bio-based materials have been exploited to develop edible and biodegradable materials.

However, the use of edible and biodegradable polymers as PLA has been limited because of challenges related to material performance (such as brittleness, poor gas and moisture barrier), processing (such as low heat distortion temperature) and cost¹. The addition of some nanoreinforcements such as nanocellulose², nanoclays³ and others⁴ could possibly enhance enough the biomaterials properties for these applications. Nowadays a big effort is being made into the field of reinforced composites for food packaging applications⁵

During recent years several researches into cellulose nanofibers reinforced polymers have been done⁶. There are several publications reporting the influence of the nanocellulose into the mechanical properties of the polymers. Apart from the mechanical properties an improvement on barrier properties has been reported⁹.

There is no uniformity of results in cellulose nanofibers based composites since there are several factors which can affect the result of the composites: a) the aspect ratio and nature of the cellulose nanofiber, b)

the compatibility, dispersion and load of the reinforcing agent and c) the nature of the matrix, among others.

The first nanoclay composite was obtained by Toyota in 1993 but improvement in nanocomposite properties has not been reported until 2002. The addition of small amounts of nanoclays in the polymeric matrix has been reported to improve some properties such as the barrier properties (up to 60%), mechanical properties especially at low clay loading that also gives fire retardant behavior. The barrier properties especially for oxygen are key parameters to develop edible films for food packaging applications since the permeability to oxygen is related to the shelf life of the food.

Recently novel nanoclay/nanofibers nanopapers have been developed which are reported to have great mechanical and gas barrier properties. This material has been reported to have fire retardant effect.

Specific Objectives

The research will be focused on the development of nanoclay/cellulose nanofiber reinforced films for food packaging applications. The cellulose nanofibers could enhance the mechanical properties of the films meanwhile the nanoclays could improve the barrier properties.

Results

In previous works we proved that the CNF was a better nanofiller than the C30B in order to improve the thermomechanical and barrier properties. Moreover it

was found that the combination of both fillers was leading to enhanced barrier and thermomechanical properties.

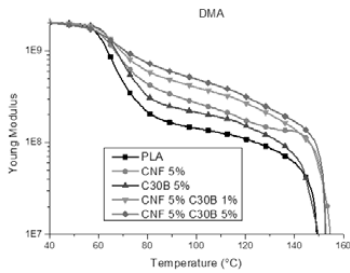


Figure 1: DMA of the nanocomposites

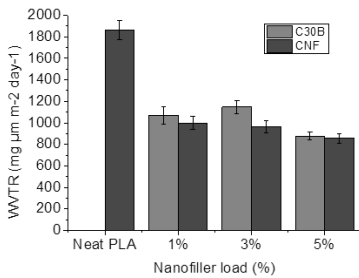


Figure 2: WVTR of single nanocomposites

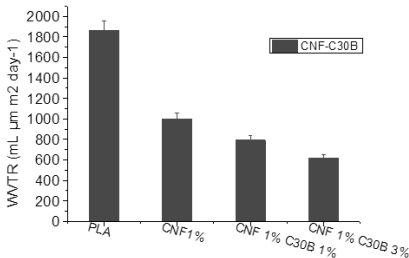


Figure 3: WVTR of hybrid nanocomposites

Apart from those improvements on properties which are critical for food packaging it was found that the combination of CNF and C30B was enhancing the crystallization speed of the nanocomposites.

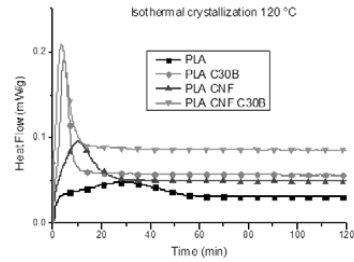


Figure 4: Isothermal crystallization of the nanocomposites

Conclusions

The combination of even small quantities of CNF and C30B reinforces the PLA making it suitable for the food packaging industry.

Acknowledgements

The author wants to thank the Marie Curie Initial Training Network for funding the research. The PhD fellow is very grateful to Professor Iñaki Mondragón Egaña whom dedication to science during his life is an example for everybody.

References

1. Madhavan Nampoothiri, K., Nair, N. R., & John, R. P.. An overview of the recent developments in polylactide (PLA) research. *Bioresource technology*, 101(22) (2010) 8493–501.
2. Eichhorn, S. J., Dufresne, A., Aranguren, M., Marcovich, N. E., Capadona, J. R., Rowan, S. J., Weder, C., et al. Review: current international research into cellulose nanofibres and nanocomposites. *Journal of Materials Science* (45) (2009) 1–33.
3. Sinha Ray, S., & Okamoto, M., Polymer/layered silicate nanocomposites: a review from preparation to processing. *Progress in Polymer Science* 28(11) (2003) 1539–1641.
4. Aider, M., Chitosan application for active bio-based films production and potential in the food industry: Review. *LWT - Food Science and Technology*, 43(6) (2010) 837–842.
5. Azeredo, H. M. C. D., Nanocomposites for food packaging applications. *Food Research International*, 42(9) (2009) 1240–1253.

List of Publications

Trifol, J., Plackett, D., Sillard, C., Bras, J., Hassager, O., Daugaard, A., Szabo, P., Improved properties of PLA based nanocomposites. *TAPPI NANO* (2014)



Anna Trubetskaya
Phone: +45 4525 2952
E-mail: atru@kt.dtu.dk
Discipline: Reaction and Transport Engineering

Supervisors: Peter Glarborg
Peter Arendt Jensen
Anker Degn Jensen

PhD Study
Started: April 2012
To be completed: March 2015

Single Biomass Particle Combustion and Fuel Characterization

Abstract

Coal fired power plants contribute significantly to greenhouse gas emissions, particularly CO₂. An attainable way to reduce CO₂ emissions is to replace coal with biomass in power plants. Biomass has traditionally been fired in grate and fluidized bed boilers, while experience with pure pulverized biomass combustion is limited. The objective of this PhD research is to establish accurate simplified one-dimensional mathematical models, which will be possible to use for the prediction of main combustion processes for biomass particles of different sizes and shapes. The accuracy of these models will be validated against the experimental data provided by the measurements on the wire-mesh reactor and entrained flow reactor.

Introduction

Biomass as an environmentally friendly and CO₂ neutral fuel is increasingly used for power production. On the global scale biomass contributes currently roughly 10 % to the primary energy demand [1].

Biomass combusted in boiler can be used for the production of heat, power and electricity. There are a variety of biomass residues available around the world. The most abundant of these are crops, forestry and livestock residues [2].

The most common ways of biomass combustion in power plants are grate firing and pulverized wood combustion. Suspension firing of pulverized fuel has been used for coal combustion for many decades. One of the challenges in the pulverized biomass combustion is to keep the power plant production energy efficient and stable in operation. The reactivity of the chars produced in the pyrolysis stage influences significantly the power plant production.

The nature of the virgin fuel and the reaction conditions during the pyrolysis stage have a strong impact on the char reactivity [3]. The impacts of pyrolysis reaction conditions on the char reactivity have been studied by many researchers. However, only limited amount of work is available to relate the pyrolysis conditions and char reactivity.

Another challenge by using biomass in a suspension firing plant is the presence of large top size biomass particles (0.5-2 mm) where the coal particles size are maximum 0.1-0.3 mm, causing problems with the flame stability and burnout. The research dealing with the char

reactivity and biomass particles larger 0.5 mm at the pyrolysis conditions has not been carried out in a larger extent.

Objectives

A major focus of this work is to investigate the different stages of a single particle biomass combustion behavior (ignition, pyrolysis and char oxidation) for particles of different type, size and shape. The char reactivity and burnout will be studied on fuels with the various ash contents and on different particle size fractions to relate the pyrolysis conditions with the char reactivity through the structural evolution and morphological changes of the char.

The accurate simplified one-dimensional mathematical single-particle model for biomass fast pyrolysis will be developed for thermally thin and thermally thick particles based on conservation of mass, energy and momentum. The developed model will additionally include influences of heating rate, final temperature and organic/inorganic composition on the char formation and yield.

The accuracy of the model will be validated against the experimental data provided by measurements on the wire-mesh reactor and entrained-flow reactor.

Results and discussion

The experimental setup has been designed and used at TU Muenchen. The reactor is presented schematically in figure 1:

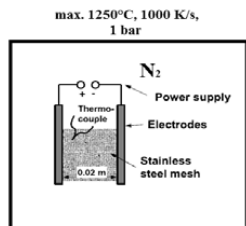


Figure 1: Wire mesh reactor setup

The wire mesh reactor can be operated at temperatures up to 1250°C and pressure up to 50bar. The heating rate is controllable up to 3000K/s. The heating rates and end temperature of the wire mesh are controlled until the end of each run by LabView. The mesh is constantly swept by nitrogen to remove any pyrolysis products and to prevent the re-condensation of tars. After the heating period the mesh is cooled down by thermal radiation and the nitrogen sweep stream.

The experimental work is carried out to investigate the influence of the heating rate, final temperature and organic/inorganic content on the char yield and char formation. In all experiments a sample mass of 10mg is used. In the reference measurements the sample mass of 10mg is verified to be low enough to ensure uniform distribution of biomass particles between wire meshes. The final temperatures of 600, 1000 and 1250°C and heating rates 10, 100, 300, 600, 1000 and 3000K/s with the additional holding time 1.0s, which is found sufficient to completed devolatilization process of 50-200µm biomass particles. Several different biomasses were used in this experimental work: pinewood (0.26%, ash), beechwood (1.3%, ash), wheat straw (3.8%, ash), washed wheat straw (1.5%) and rice husks (19.7%, ash). The result of this investigation in terms of the

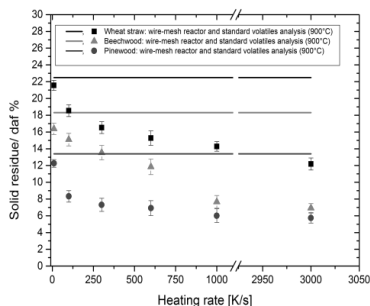


Figure 2: Influence of heating rate on char yield

heating rate influence on the char yield is shown in figure 2. The increase in the char yield is observed for all three samples when the heating rate steps up from 10K/s to 3000K/s.

In figure 3, a significant influence of the final pyrolysis temperature is noticed.

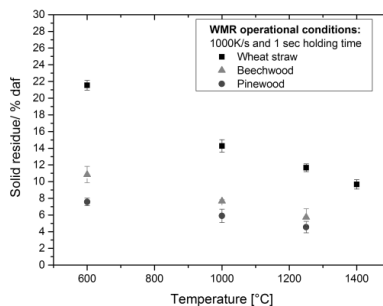


Figure 3: Influence of final temperature on char yield

Based on the conducted experiments, it can be concluded that the final pyrolysis temperature has stronger influence on the char yield than the heating rate. The results at 600°C and 1000°C, measured on the wire-mesh reactor, are compared with the flash TGA data.

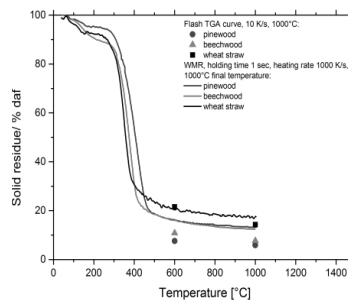


Figure 4: Comparison of flash TGA results with the wire-mesh reactor in terms of char yield

In comparison to the measurements on the fast TGA (10K/s, 1000°C, N₂), the WMR data shows 4-7% more of yielded char.

The influence of temperature on the particle size is studied on the wire-mesh reactor, where pinewood and wheat straw samples are sieved to such particle size fractions as 50-200µm, 250-355µm, 355-425µm, 425-600µm, 600-850µm and 850-1000µm. The results of this study are summarized in figures 5 and 6.

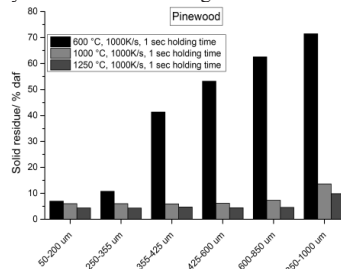


Figure 5: Influence of particle size on pinewood char yield

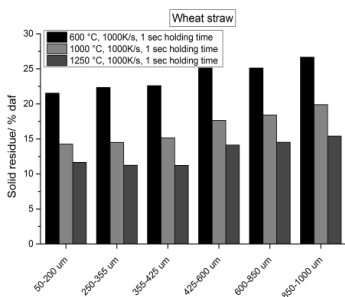


Figure 6: Influence of particle size on wheat straw char yield

The results in figures 5 and 6 indicate increasing char yield with the increasing particle size for pinewood and wheat straw. The char yield for the pinewood and wheat straw at 1250°C is nearly constant, while the char yield for 600°C and 1000°C decreases with the increasing temperature. Additionally, the nearly constant char yield is observed for the wheat straw at all three temperatures. The influence of particle size on the char yield, based on the results in figures 5 and 6, shows how the differences in particle form can influence biomass char yield. Original pinewood particles are cylindrical in shape with the larger characteristic length than the wheat straw particle, which are quite elongated and flat. The differences in shape cause very high char yield for the pinewood particle size fraction > 425μm, indicating importance of intra-particle temperature gradients for larger particles. However, from the results in figures 5 and 6, the isothermal assumption for particle size < 425μm is considered to be valid in 1D modelling.

In figures 7 and 8, particle size fractions are shown over different holding times on the wire-mesh. The choice of maximal holding time of 4 sec for the study comes from Werkelin's investigation [5] on low-ash containing pellets.

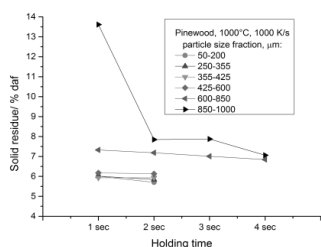


Figure 7: Influence of holding time on pinewood char yield in dependency on the particle size fraction

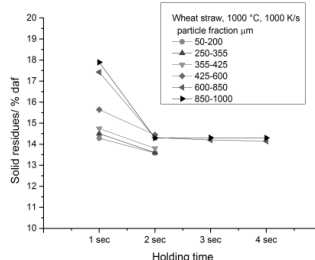


Figure 7: Influence of holding time on wheat straw char yield in dependency on the particle size fraction

The results, shown in figures 6 and 7, indicate strong influence of holding time on the complete conversion of larger particles (>425μm). For the complete conversion of smaller particle size fractions (<425μm) the holding time of 1 sec is sufficient. The pinewood particles > 425 μm show nearly constant char yield after holding sample on the mesh 4sec, while for the wheat straw particles from 50μm to 1mm no significant changes in the char yield are observed after 2sec holding. The differences in char yield of pinewood and wheat straw particles > 425μm are due to the differences in the heat transfer, indicating importance of particle size and shape representation in 1D and CFD models.

The char of beechwood and wheat straw from the wire-mesh reactor measurements is collected and analyzed by using elementary analysis instrument, scanning-electron microscope, FTIR and Near-Raman instrument.

Investigations carried out on chars, prepared on the wire-mesh reactor and oven at 1000°C, show that by application of fast heating rates (10-3000K/s) and slow heating rate (10K/min) melting of the cell structure occurs. The SEM images of pinewood at 1000°C with the fast heating rate of 1000K/s indicate completely molten particles with small cavities on the surface, while the wheat straw particles retain their original shape with the slight melting on the surface and formation of bubbles.

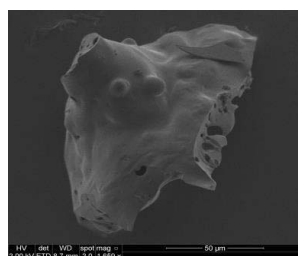


Figure 8: SEM image of a molten pinewood particle

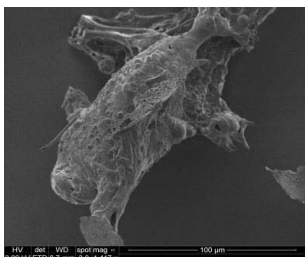


Figure 9: SEM image of a partially molten wheat straw particle

The plastic transformation of char particles could be related to the influence of organic and inorganic components of biomass, described by Solomon model [7]. This model assumes that during pyrolysis depolymerisation, repolymerisation and cross-linking of metaplast fragments occur with the transport of lighter molecules away from the particle surface and with the internal transport of lighter molecules by gas bubbles. These phenomena are simultaneous at low heating rate, but consecutive at high heating rates, where repolymerisation starts after depolymerisation, leading to the formation of a highly molten particle during pyrolysis. Additionally, it was found that small differences in the cross-linking rate affects drastically the fluidity of the resulting char and that oxygen favors cross-linking thereby preventing fluidity of the char [7]. This observation can be supported by results from the elementary analysis, shown in figure 8.

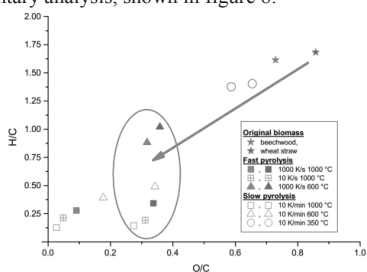


Figure 9: CHNO-S analysis of beechwood and wheat straw samples.

The measurements show decrease in O/C and H/C ratios with the temperature increase from 600°C to 1000°C and decrease in heating rate from 1000K/s to 10K/min, indicating an increase in aromatization. Based on the conducted measurements, the nearly constant O/C ratio is observed for the wheat straw. This result may indicate differences, coming from graphitizing and non-graphitizing carbons. Franklin [6] investigated graphitization and non-graphitization phenomena in the coal thermo-chemical processes. The pinewood and beechwood samples change its porosity from 250°C to 1000°C significantly and contain probably more graphitizing carbon with carbon nuclei remaining more mobile after pyrolysis, while wheat straw does not show

any differences in porosity and retains shape of original biomass. It is possible that the wheat straw char mostly consists of non-graphitizing carbon, characterized by stronger cross-linking, where crystallites-neighbors hold with the increasing temperature during pyrolysis apart by showing random orientation with respect to each other, or, in other words, hindering coalescence. The differences in the graphitizing tendency could influence morphological changes of biomasses.

Conclusion and future work

From the investigations on the wire-mesh reactor, it can be concluded that the final temperature has more significant influence on the char yield than the heating rate. However, the influence of holding time, temperature and heating rate on the different particle size fractions depends on the biomass type. The morphological transformations of char are related to the repolymerization, depolymerization and cross-linking reactions, which are more consecutive during fast pyrolysis than during slow heating rate pyrolysis. For the future work the 1D mathematical model will be established.

Acknowledgements

This PhD project is a part of the GREEN Research Center (Center for Power Generation from Renewable Energy) financed by the Danish Strategic Research Council.

References

1. M. Kaltschmitt, Biomass for energy in Germany: status, perspectives and lessons learned, Journal of Sustainable Energy and Environ. Special Issue (2011) 481-490.
2. M. Balat, G. Ayar, Biomass Energy in the World, Use of biomass and Potential Trends, Energy Sources, 27 (10) (2006) 931-940.
3. E. Cetin, B. Moghtaderi, R. Gupta, T.F. Wall, Influence of pyrolysis conditions on the structure and gasification reactivity of biomass chars, Fuel, 83 (2004) 2139-2150.
4. K. Umeki, K. Kirtania, L. Chen, S. Bhattacharya, Fuel Particle Conversion of Pulverized Biomass during Pyrolysis in an Entrained Flow Reactor, Industrial & Engineering Chemistry Research, 51 (2012) 13973-13979.
5. J. Werkelin, M. Hupa, Release of ash-forming matter of a woody biomass during fast pyrolysis in a wire mesh reactor, Proceedings: Impacts of Fuel Quality on Power Production and Environment, August 30 – September 3, 2010, Saariselkä
6. R. Franklin, Crystallite Growth in Graphitizing and Non-Graphitizing Carbons, Proceedings of the Royal Society of London. Series A, Mathematical and Physical Sciences, 209 (1097) (1951), 196-218
7. M. A. Serio, S. Charpenaz, R. Basilakis, P.R. Solomon, Measurement and modeling of lignin pyrolysis, Biomass and Bioenergy, 7 (1-6) (1994), 107-124



Anjan Kumar Tula

Phone: +45 4525 2817

E-mail: antu@kt.dtu.dk

Supervisors: Prof. Rafiqul Gani
Gurkan Sin

PhD Study

Started: December 2013

To be completed: December 2016

Process synthesis and design using process group contribution methodology

Abstract

Process synthesis implies the investigation of chemical reactions needed to produce the desired product, selection of the separation techniques needed for downstream processing, as well as making decisions on sequencing the involved reaction and separation operations. For an effective, efficient and flexible design approach, what is needed is a systematic way to identify the types of tasks/operations that need to be performed, the corresponding design of the operation/equipment, their configuration, mass/energy flows, etc., resulting in an optimal flowsheet. This work highlights the development of computer aided methodology for fast, reliable and consistent generation of process flowsheets and rank them based on various flowsheet performance indices. The methodology is based on the group contribution principles to solve the synthesis-design problem of chemical processes, where, chemical process flowsheets could be synthesized in the same way as atoms or groups of atoms are synthesized to form molecules in computer aided molecular design (CAMD) techniques. As in CAMD the generated molecules are quickly evaluated with respect to target molecular properties using GC property models, the generated flowsheet alternatives are also evaluated for properties like energy consumption, atom efficiency, environmental impact, etc.

Introduction

In a group contribution method for estimating pure component/mixture properties of a molecule, the molecular identity is described by means of a set of functional groups of atoms bonded together to form a molecular structure. Once the molecular chemical structure is uniquely represented by the functional groups, the specific properties can be estimated from regressed contributions of the functional groups representing the molecule. Having the groups, their contributions and their interactions together with governing rules to combine the groups into a molecule, allows us to synthesize molecules and/or mixtures. This is known as CAMD, computer aided molecular design. Let us now imagine that each group used to represent a fraction of a molecule could also be used to represent a chemical process operation or a set of operations in a chemical process flowsheet. A functional process-group would represent either a unit operation (such as a reactor, or a distillation column), or a set of unit operations (such as, two distillation columns in extractive distillation). The bonds among the process-groups represent the streams connecting the unit operations, similar to the bonds combining (molecular) functional groups. In the same way as CAMD method applies connectivity rules to combine the molecular

functional groups to form feasible molecular structures, functional process-groups would have connectivity rules to combine process-groups to form structurally feasible process alternatives. Finally with flowsheet property model and corresponding process-group contributions it would be possible to predict various flowsheet properties which can be used as performance indicators for screening of alternatives.

Computer Aided Flowsheet Design (CAFD) Methodology

The CAFD Framework, as shown in figure 1 is composed of seven main steps:

Step 1: Problem definition. In this step the user provides the necessary information of the inlet and outlet stream data (for example, pressure, temperature, compositions and individual flow rates) along with the property (process) targets for optimization.

Step 2: Problem analysis. The objective of this step is to further define the problem through analysis of available knowledge and physical insights.

- *Reaction Analysis:* This analysis identifies the reaction tasks needed to produce the desired product. A database search is performed to find the set of chemical reactions yielding the desired product. All new reactants or by-products from the

matched reaction mechanisms are added to the synthesis problem.

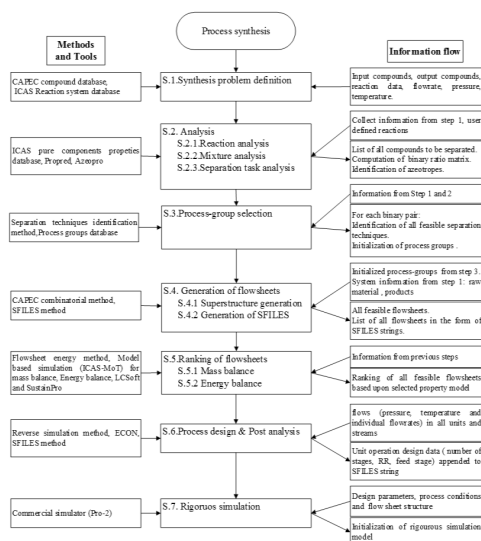


Figure 1: Computer Aided Flowsheet Design (CAFD) Methodology

- Mixture analysis:** This analysis is carried out in two tasks. First the pure component analysis is performed by retrieving a list of 22 pure component properties from the ICAS database. For compounds missing data/new compounds, the properties are calculated using ProPred (property prediction tool box) which is part ICAS [1]. Second the mixture property analysis is made in terms of the binary pairs of all the chemical species identified in the problem. For each binary component pair identified, analysis is performed to identify possible azeotropes, eutectic points or potential mass separation agents.

- Separation task analysis:** In this task feasible process operation tasks are identified for each binary component pair using the physical insights based method for flowsheet synthesis developed by Jaksland and Gani [2].

Step 3: Process-group selection. The objective of this step is to select and initialize the process groups representing all the combinations possible for each of the separation task identified in the previous step.

Step 4: Generation of flowsheets. The objective in this step is to combine the process-groups selected in step 3 according to a set of connectivity rules and specifications to generate feasible flowsheet structures.

- Superstructure generation:** In this task a combinatorial algorithm is employed to generate the superstructure of all flowsheet alternatives from the initialized process-groups. The combinatorial algorithm generates new flowsheet alternatives by

combining process-groups according to a set of connectivity rules.

- Generation of SFILES:** Having a process flowsheet represented by process groups provides the possibility to employ simple notation systems for efficient storage of structural information of all the process alternatives generated. The SFILES method for flowsheets is similar to SMILES (Simplified Molecular Input Line Entry System) developed by David Weininger [3].

Step 5: Ranking of flowsheets. In this step, benchmarking of all the feasible alternatives generated is performed. For this flowsheet energy consumption index property model developed by d' Anterrosches [4] is used to predict the energy consumption of a given flowsheet from contributions of corresponding process groups employed in the processing route.

Step 6: Process design & Post analysis. This step of the framework has three tasks: i) the resolution of the mass balance through each process-group in the selected alternative, ii) calculation of flowsheet design parameters of the process unit operations in the flowsheet structure through reverse simulation using driving force concept [5], and iii) post analysis of the selected alternatives to further screen the alternatives based on various indicators related to environmental impact, process safety and efficiency.

Step 7: Rigorous simulation. At this step of the methodology, all the necessary information to perform the final verification through rigorous simulation is available. Rigorous simulators like PROII or ICASSim [1] are used to further refine the most promising process flowsheet and to perform optimization of the design parameters.

Conclusions

A novel systematic approach based on the group contribution concept has been presented. One important feature of the method is its versatility, since it can be extended by adding new process-groups representing all types of process unit operations. Thus, it is possible to simultaneously model, design, and synthesize novel products and processes. On the other hand, the ability to predict a flowsheet property (energy consumption) without the need for rigorous simulation offers a lot of advantages as it opens the possibility to screen a lot of process options very quickly and with high accuracy.

References

- R. Gani, 2002, ICAS documentation. CAPEC, Technical University Of Denmark
- C. Jaksland, PhD Thesis, Department of Chemical and Biochemical Engineering, DTU, Denmark, 1996.
- D. Weininger, Journal of Chemical Information and Computer Sciences, 1988
- L. d' Anterrosches, R. Gani, Fluid Phase Equilib, 228-229 (2005) 141-146.
- E. Bek-Pedersen, R. Gani, Chem. Eng. Process. 43 (2004) 251.



Fragkiskos Tzirakis
Phone: +45 4525 2821
E-mail: frtz@kt.dtu.dk

Supervisors: Georgios Kontogeorgis
Nicholas von Solms
Christophe Coquelet, MINES ParisTech
Paolo Stringari, MINES ParisTech

PhD Study
Started: June 2013
To be completed: June 2016

An experimental and theoretical study of CO₂ hydrate formation systems

Abstract

CO₂ capture and sequestration (CCS) is nowadays an important area of research for alleviating CO₂ emissions worldwide. According to literature, CO₂ is globally the largest pollutant to which the global warming is attributed. Consequently, hydrate technology may become an alternative post combustion solution of CO₂ capture from flue gases (hydrate crystallisation). A main disadvantage of hydrate process is the high pressure it needs and, therefore, several chemicals (promoters) are currently under examination which lessen hydrate equilibrium pressure. In this study hydrate experimental results with several promoters are presented which were produced in MINES ParisTech. Different CO₂ and N₂ gas mixtures were used with presence of promoters such as tetra butyl ammonium bromide (TBAB), tetra butyl ammonium fluoride (TBAF), cyclopentane (CP) and mixtures of TBAB/F with CP.

Introduction

The capture of CO₂ and sequestration (CCS) has become an important area of research for treating CO₂ emissions. The effort is to develop energy efficient and environmental friendly technologies to capture the CO₂ produced in large scale power-plants, where flue gas typically contains mostly CO₂ and N₂ [1]. One novel approach to separate CO₂ from combustion flue gas is via gas hydrate crystallization technique [4], [1]. This technique allows hydrate crystals to be formed from a mixture of CO₂+gases and CO₂ is captured. Then the hydrate crystals dissolve through imposition of increased temperature and CO₂ is concentrated in one stream. [4]

Project objectives

This project aims to close the gap of experimental and theoretical knowledge on CO₂ hydrates concentrating mainly on promoters. Two research groups, one from DTU and one from MINES ParisTech, are working on closely, developing a new theory for the thermodynamic treatment of CO₂ hydrates (DTU) as well as producing new experimental data (France) for enhancing hydrate formation literature. More particularly, the project core is the execution of equilibrium experiments on gas hydrate-formation systems e.g. for mixtures of CO₂+N₂+H₂O+promoter. The chosen promoters were tetra butyl ammonium bromide (TBAB), tetra butyl ammonium fluoride (TBAF), cyclopentane (CP) and mixtures TBAB/F with CP. The combination of TBA halides with CP was inspired by [15] as it was revealed

synergetic effect between TBAB and CP. This work was conducted in collaboration with the Center of Thermodynamic of Processes in MINES ParisTech, where the experimental work was undertaken. The results obtained are to be modeled using an extension of van der Waals-Platteeuw's theory along with an association model for fluid phases.

Carbon dioxide hydrates

CO₂ hydrates are solid non-stoichiometric inclusion compounds formed by a lattice structure, composed of water molecules (named *host* molecules) linked together by hydrogen bonding, and stabilized by encapsulating CO₂ molecules (named *guest* molecules). The most common gas hydrates belong to the three crystal structures: cubic structure I (sI), cubic structure II (sII) and hexagonal structure H (sH). CO₂ forms sI structure.

Hydrate promoters

Currently various promoters (or formers) and mixtures of them are under examination. Thermodynamic promoters extend the hydrate formation region in a *P,T* diagram. Thermodynamic promoters are considered as kinds of ionic liquids (ILs). The most well experimentally examined example is the cyclic aliphatic ether: tetrahydrofuran (THF). THF in water forms nonideal mixture which shows high immiscibility at low-temperatures and complex liquid-phase behavior at high temperature [5]. Some tetra-alkylammonium halides, which are water-soluble, such as tetrabutyl ammonium bromide (TBAB), of fluoride (TBAF), of

chloride (TBAC) and some tetra-alkylphosphonium halides like tetra-butylphosphonium bromide (TBPB) have also been proposed as promoters of gas hydrates as well as water immiscible cyclic hydrocarbon such as cyclopentane (CP). Especially, the TBAB is generally considered as promising material for various innovating processes.

Equipment description

A brief sketch of the experimental equipment as used in MinesParisTech is presented in Figure 1. At first, two cylinders one of nitrogen and one of CO₂ and N₂ are used. The first is used for cleaning the cell and the last for providing the gas mixture in desirable pressure. Then there is a vacuum pump in order to avoid contamination of the tube and also to help cleaning the cell. The procedure was as follows. The cell was immersed in a water bath for controlling the temperature and three transducers were attached to it; two of temperature (on the top and bottom of the cell) and one of pressure on the top. All of them were connected after acquisition units to personal computer. The acquisition results were obtained by the temperature transducer of the top and pressure transducer of the bottom.

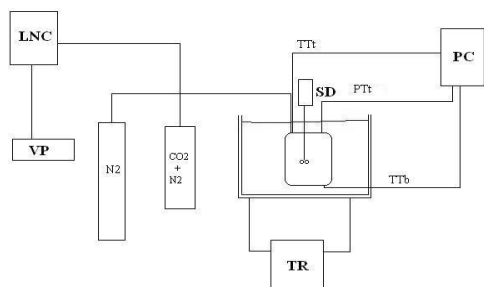


Figure 1: Simplified schematic diagram of equilibrium cell equipment. LNC: liquid nitrogen container. VP: vacuum pump. SD:stirring device. TR: temperature regulator. TTt: temperature transducer top. TTb: temperature transducer bottom. PTt: pressure transducer top. PC: personal computer.

Temperature of the cell was controlled using a thermostatic water bath (LAUDA PROLine RP3530). One platinum temperature probe (Pt100) inserted in the cell interior was used to measure the temperature inside the cell within measurement uncertainties, which are estimated to be less than 0.02K with a second order polynomial calibration equation. The data acquisition units (Agilent 34970A, HP 34970A) were coupled with a personal computer to measure -and automatically record- pressure, temperature and time data. The data acquisition software also allowed adjusting the rate of data acquisition. Continuous recording of pressures and temperatures allowed detecting any subtle changes in the system and true equilibrium conditions. A motor-driven turbine agitation system (Top Industrie, France) enabled to stir the cell contents at a speed up to 1100 rpm to increase the fluids contact and enhance water conversion into hydrate.

Experimental part

The four gas mixtures used in this work were produced with the use of a cylinder in which different concentrations of CO₂ and N₂ were mixed. The CO₂ and N₂ gas bottles used in this work were supplied by Air Liquide. The molar fractions of CO₂ gas mixture were app. 0.15, 0.11, 0.07 and 0.005. The exact concentrations were measured by a gas chromatograph. TBAB solutions with mass fractions of (0.05, 0.10 and 0.20) and TBAF solutions with mass fractions of (0.03, 0.05 and 0.10) were prepared by gravimetric method using an accurate analytical balance (Mettler, AT200), with mass uncertainty of ± 0.0001 g. Double-distilled and deionized water from Direct-Q5 Ultrapure Water Systems (MilliporeTM), was used in all experiments. When needed, cyclopentane was added in TBAB and TBAF solutions with use of proper syringes. The results for different CO₂/N₂ mixture concentration for TBAB promoter are summarised in Figure 2. In general, it is observed very good agreement with the literature for similar systems of 5%, 10% and 20% w/w TBAB solutions which correspond to 0.29%, 0.62% and 1.38% mol respectively.

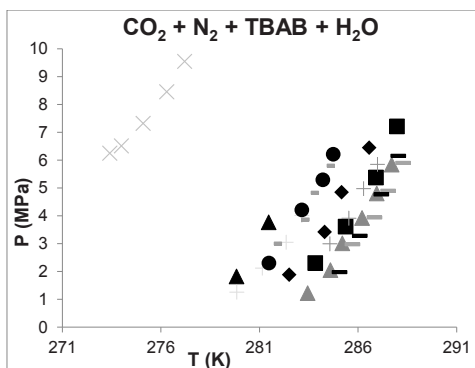


Figure 2 Hydrate equilibrium points for different CO₂+N₂ systems with TBAB promoter. X: CO₂ (20%mol)+N₂, Olsen et al., 1999 [2]; \blacktriangle : CO₂ (11.24%mol)+N₂+TBAB (0.29%mol), this work; \bullet : CO₂ (14.92%mol)+N₂+TBAB (0.29%mol), this work; \circ : CO₂ (13.70%mol)+N₂+TBAB (0.29%mol), Chen et al., 2014 [13]; \ominus : CO₂ (20%mol)+N₂ TBAB (0.29%mol), Meysel et al, 2011 [3]; \blacklozenge : CO₂ (6.87%mol)+N₂+TBAB (0.62%mol), this work; \blacksquare : CO₂ (14.92%mol)+N₂+TBAB (0.62%mol), this work; $+$: CO₂ (20%mol)+N₂ TBAB (0.62%mol), Meysel et al, 2011 [3]; \blacktriangle : CO₂ (15.90%mol)+N₂+TBAB (1.00%mol), Lu et al., 2009 [7]; $-$: CO₂ (20%mol)+N₂ TBAB (1.38%mol), Meysel et al, 2011 [3]; \times : CO₂ (6.87%mol)+N₂+TBAB (1.38%mol), this work.

More specifically, the results of similar promoter and gas mixture concentrations are in excellent agreement, namely CO₂ (6.87% mol)+N₂+TBAB (20% w/w or 1.38% mol) of this work, CO₂ (15.9% mol)+N₂+TBAB (15.9% w/w or 1.00% mol) of Lu et al., 2009 and CO₂ (20% mol)+N₂+TBAB (20% w/w) of Meysel et al., 2011 [3]. In addition, the same behavior applies for CO₂ (14.92% mol)+N₂+TBAB (5% w/w or 0.29% mol) of this work, CO₂ (20% mol)+N₂+TBAB (0.29% mol) of Meysel et al., 2011 [3] and CO₂ (13.70% mol)+N₂+TBAB (0.29% mol) of Chen et al., 2014 [13].

Another observation is that the system of CO₂ (6.87% mol)+N₂+TBAB (10% w/w or 0.62% mol) of this work is well placed on the left of CO₂ (14.92% mol)+N₂+TBAB (0.62% mol) of this work and CO₂ (20%mol)+N₂+TBAB (0.62% mol) of Meysel et al., 2011 [3]. It intensifies the rational notion that the higher CO₂ concentration in the mixture the easier the promotion occurs. Similarly, CO₂ (11.24%mol)+N₂+TBAB (0.29% mol) of this work is weaker promoted compared to CO₂ (14.92% mol)+N₂+TBAB (0.29% mol) of this work because of the lower CO₂ content.

From the literature, there is mismatch of CO₂ (13.70% mol)+N₂+TBAB (0.29% mol) of Chen et al., 2014 [13] with the system CO₂ (15.9%mol)+N₂+TBAB (0.29% mol) of Lu et al., 2009 [7] respectively as shown in Figure 1. Moreover, there is very good agreement in CO₂ (6.87% mol)+N₂+TBAB (20% w/w or 1.38% mol) of this work and CO₂ (20%mol)+N₂+TBAB (1.38% mol) of Meysel et al., 2011 [3].

Similar procedure was followed for the system CO₂+N₂+CP+H₂O. For CO₂/N₂ mixture (6.87/93.13), 15 ml of low CP concentration (6.03% mol or 20% w/w) was used, purchased by Acros Organics (purity ≥98%). According to Galfré et al., 2014 [12], concentration of CP above 27.8% w/w produces emulsion which means better mixing. Therefore, higher CP concentration (22.15% mol or 52.57% w/w) was used from which emulsion was obtained. Figure 3 summarises the results.

In Figure 3, there is a region in which CO₂+N₂ mixture dissociation points should exist according to Tohidí et al., 1997 [10]; Zhang and Lee, 2009 [8] and Mohammadi and Richon, 2009 [9]. These are the boundaries of pure CO₂ and pure N₂ with CP+H₂O system respectively. The results of this work are well included in these boundaries. Moreover, the CP concentration does not have any impact on thermodynamic equilibrium, in contrast to TBAB, most likely due to water insolubility. This fact results, in other words, results in excellent matching among the systems of different CP concentrations.

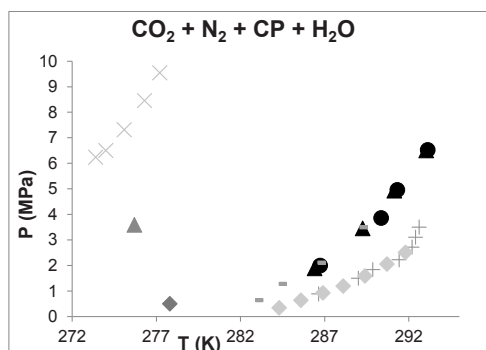


Figure 3 Hydrate equilibrium points for different systems. ∇ : CO₂ (20%mol)+N₂, Olsen et al., 1999 [2]; \blacktriangle : CO₂+CP (1.33%mol), Galfré et al., 2011 [11]; \blacklozenge : CO₂+CP (6.03%mol), Galfré et al., 2011 [11]; $-$: N₂+CP (20.42%mol), Tohidí et al., 1997 [10]; \blacktriangle : CO₂

(6.87%mol)+N₂+CP (22.15%mol), this work; \bullet : CO₂ (6.87%mol)+N₂+CP (6.03%mol), this work; $+$: CO₂+CP (17.39%mol), Zhang and Lee, 2009 [8]; \blacklozenge : CO₂+CP (16.16%mol), Mohammadi and Richon, 2009 [9].

For CO₂/N₂ mixture (0.48/99.52), 30 ml of TBAB promoter were used, purchased by Sigma-Aldrich (75% w/w in H₂O). In Figure 4 the results are presented together with three systems from literature. [14], [15] [16], [17], [18]. The pressure range of Li et al., 2010 [14] is more narrow than of this work but anyhow there is nice coverage between similar systems.

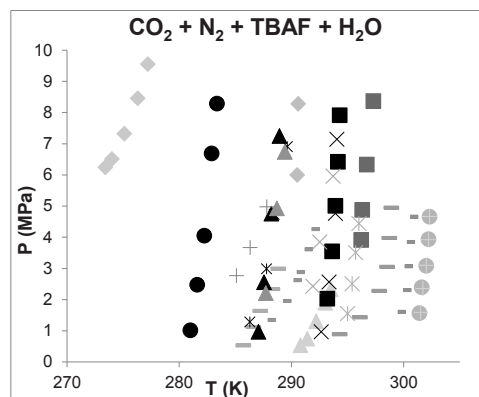


Figure 3 Hydrate equilibrium points for different systems. \blacklozenge : CO₂ (20%mol)+N₂, Olsen et al., 1999 [2]; \bullet : CO₂ (0.48%mol)+N₂+TBAB (0.23%mol), this work; $+$: CO₂+TBAB (0.14%mol), Mohammadi et al., 2013 [16]; \blacklozenge : CO₂ (0.48%mol)+N₂+TBAB (0.36%mol)+CP (5% v/v), this work; \blacktriangle : CO₂ (0.48%mol)+N₂+TBAB (0.36%mol), this work; \blacktriangle : CO₂ (30%mol)+N₂+TBAB (0.36%mol), Sfaxi et al., 2014 [17]; $-$: CO₂+TBAB (0.29%mol), Li et al., 2010 [14]; \blacklozenge : N₂+TBAB (0.36%mol), Mohammadi et al., 2013 [16]; $-$: CO₂+TBAB (0.36%mol), Mohammadi et al., 2013 [16]; \times : CO₂ (30%mol)+N₂+TBAB (0.68%mol), Sfaxi et al., 2014 [17]; \times : CO₂ (0.48%mol)+N₂+TBAB (0.76%mol)+CP (5% v/v), this work; \blacksquare : CO₂ (0.48%mol)+N₂+TBAB (0.76%mol), this work; \blacktriangle : CO₂+TBAB (0.62%mol), Li et al., 2010 [14]; \blacklozenge : CO₂+TBAB (0.80%mol), Lee et al., 2012 [18]; \blacklozenge : N₂+TBAB (1.20%mol), Mohammadi et al., 2013 [16]; $-$: CO₂+TBAB (1.20%mol), Mohammadi et al., 2013 [16]; $-$: CO₂+TBAB (5.30%mol), Lee et al., 2012 [18]; \blacklozenge : CO₂+TBAB (3.00%mol), Lee et al., 2012 [18]; $+$: CO₂+TBAB (3.30%mol), Lee et al., 2012 [18];

The w/w TBAB results for 3.20% (0.23%mol), 5% (0.36%mol) and 10% (0.76%mol) seem well placed in the figure in comparison with literature. The gas mixture, which is 99.52% mol N₂, produced more steepen results than with higher CO₂ concentration. But nonetheless, the difference in steepness even with pure CO₂ is negligible. In addition, 0.23% and 0.36%mol TBAB are in very good agreement with similar solutions from literature as well as with gas mixtures with 30% mol CO₂ results. [17] Moreover, there is consistency between the results of N₂+TBAB (1.20%mol), Mohammadi et al., 2013 [16] and CO₂ (0.48%mol)+N₂+TBAB (0.76%mol), this work. Finally, the use of CP for 0.76% mol TBAB has no effect in the results while for 0.36% mol TBAB the behavior is ambiguous. For low pressures (<30 bar), inhibition effect is observed while for higher pressures (>30 bar)

promotion effect appears. In Figure 5 all hydrate equilibrium points of this work are presented.

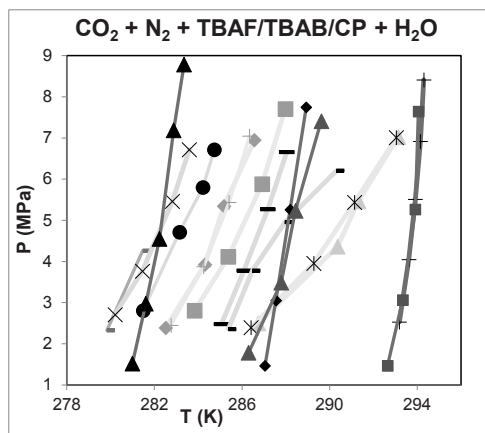


Figure 5 Hydrate equilibrium points for different systems. -: CO₂ (11.24%mol)+N₂+TBAB (0.29%mol), this work; ●: CO₂ (14.92%mol)+N₂+TBAB (0.29%mol), this work; X: CO₂ (6.87%mol)+N₂+TBAB (0.29%mol)+CP (5% v/v), this work; ▲: CO₂ (0.48%mol)+N₂+TBAF (0.23%mol), this work; ◆: CO₂ (6.87%mol)+N₂+TBAB (0.62%mol), this work; +: CO₂ (6.87%mol)+N₂+TBAB (0.62%mol)+CP (5% v/v), this work; ■: CO₂ (14.92%mol)+N₂+TBAB (0.62%mol), this work; -: CO₂ (6.87%mol)+N₂+TBAB (1.38%mol), this work; -: CO₂ (6.87%mol)+N₂+TBAB (1.38%mol)+CP (5% v/v), this work; ▲: CO₂ (0.48%mol)+N₂+TBAF (0.36%mol)+CP (5% v/v), this work; ◆: CO₂ (0.48%mol)+N₂+TBAF (0.36%mol), this work; ✖: CO₂ (6.87%mol)+N₂+CP (22.15%mol), this work; ▲: CO₂ (6.87%mol)+N₂+CP (6.03%mol), this work; ■: CO₂ (0.48%mol)+N₂+TBAF (0.76%mol)+CP (5% v/v), this work; +: CO₂ (0.48%mol)+N₂+TBAF (0.76%mol).

Conclusions – Future work

The simultaneous use of TBAB (0.29% mol) with CP (5% v/v) induced inhibition effect. For the system, TBAB (0.62% mol) with CP (5% v/v) the results are virtually identical. On the contrary, the use of higher TBAB concentration (1.38% mol) and CP (5% v/v) revealed promotion effect and also as the pressure rises, this phenomenon becomes more intense. In addition, the higher the CO₂ concentration, the stronger the promotion is for every TBAB solution. However, this fact is not easily observable for low CO₂ concentration differences in mixtures. Consequently, it came out that the factor of gas mixture concentration has moderate impact on hydrate equilibrium compared to promoter's concentration.

The use of CP solution (even though virtually water insoluble) proved to be stronger promoter than TBAB maybe because of the different hydrate structure it induces. According to the promotion trend of TBAB, for 42% w/w TBAB, above of which it acts as inhibitor, the promotion results may become similar to CP results. In addition, there is slightly inhibition effect when higher CP concentration is used, e.g. 22.15% mol.

Finally, TBAF proves to be by far much stronger promoter than TBAB and CP, especially for lower pressures. This is not easily observable because of the

almost pure N₂ mixture it was used. The use of TBAF concentration (10% w/w) with CP (5% v/v) revealed promotion effect above 30bar and also as the pressure raises it becomes more intense.

The results obtained will be then modeled using an extension of van der Waals-Platteeuw's theory along with an association model (CPA EoS) for fluid phases so that a more comprehensive insight can be acquired.

Acknowledgments

The project is part of "CO₂ Hydrates – Challenges and possibilities" (Project ID: 50868) and is financed by 2/3 through Danish Research Council for Independent Research and by 1/3 through DTU.

Reference

1. Belandria V., Eslamimanesh A., Mohammadi A.H., Richon D., *Ind. Eng. Chem. Res.* 50 (2011) 4722–4730.
2. Olsen M.B., Majumdar A. and Bishnoi P.R., *Int. J. of The Soc. of Mat. Eng. For Resources* 7 (1999) 17–23.
3. Meysel P., Oellrich L., Bishnoi P.R., Clarke M.A., *J. Chem. Thermodyn.* 43 (2011) 1475–1479.
4. Mohammadi A.H., Eslamimanesh A., Belandria V., Richon D., *J. Chem. Eng. Data* 56 (2011) 3855–3865.
5. Ricaurte M., Torré J.-P., Asbai A., Broseta D., Dicharry C., *Ind. Eng. Chem. Res.* 51 (2012) 3157–3169.
6. Deschamps J., Dalmazzone D., *J. Therm. Anal. Calorim.* 98 (2009) 113–118.
7. Lu T., Zhang Y., Li X.-S., Chen Z.-Y., Yan K.-F., *The Chinese J. of P. Eng.* 9 (2009) 541-544. (in chinese)
8. Zhang J., Lee J.W., *J. Chem. Eng. Data* 54 (2009) 659–661.
9. Mohammadi A.H., Richon D., *Chem. Eng. Science* 64 (2009) 5319–5322.
10. Tohidi B., Danesh A., Todd A.C., Burgass R.W., Ostergaard K.K., *Fluid Phase Equilibria*, 138 (1997), 241-250.
11. Galfré A., Fezoua A., Ouabbas Y., Cameirao A., Herri J.-M., 2011, 7th International Conference on Gas Hydrates, Edinburg, UK
12. Galfré A., Kwaterski M., Brântuas P., Cameirao A., Herri J.-M., *J. Chem. Eng. Data* 59 (2014) 592–602.
13. Chen C., Li X.-S., Chen Z.-Y., Xia Z.-M., Yan K.-F., Cai J., *J. Chem. Eng. Data*, 59 (2014) 103–109.
14. Li S., Fan S., Wang J., Lang X., Wang Y., *J. Chem. Eng. Data* 55 (2010) 3212–3215.
15. Li X.-S., Xia Z.-M., Chen Z.-Y., Wu H.-J., *Energy Fuels* 25 (2011) 1302–1309.
16. Mohammadi A., Manteghian M. and Mohammadi A.H., *J. Chem. Eng. Data* 58 (2013) 3545–3550.
17. Sfaxi I., Durand I., Lugo R., Mohammadi A., Richon D., *International Journal of Greenhouse Gas Control* 26 (2014) 185–192.
18. Lee S., Lee Y., Park S., Kim Y., Lee J.-D. and Seo Y., *J. Phys. Chem. B* 116 (2012) 9075–9081.



Sara Lindeblad Wingstrand

Phone: +45 4525 XXXX
E-mail: saliwi@kt.dtu.dk
Discipline: Polymer Materials

Supervisors: Ole Hassager
Peter Szabo

PhD Study
Started: September 2014
To be completed: September 2017

On the Correlation Between Youngs Modulus and Melt Flow in Fiber Spinning Operations

Abstract

Polymers in extensional flow is encountered in a wide range of polymer processing techniques, among others fiber spinning. The purpose of this project is to investigate the correlation between extensional flow in fiber spinning operations and the final elastic properties of the quenched fibers. This has, until very recently, been impossible due to difficulties in obtaining a constant strain rate throughout the entire course of elongation. Consequently very little is known quantitatively about the relation between extensional rate and final strength of the polymer.

Introduction

Polymer fibers are known to have extraordinary strength. In fact, expressed in terms of strength-to-weight ratio, polymer fibers outperform steel [1]. Thus ultrahigh molar mass polyethylene (Dyneema by DSM) has a strength-to-weight ratio in the range 8-15 times that of steel.

The extraordinary properties are believed to be tied to molecular orientation in the solid fibers [2]. This, again, is believed to be due to the extensional flow in the processing operation for fiber spinning [3]. However to the best of our knowledge, there has never been a systematic investigation of the relation between extensional melt flow, cooling rate, frozen molecular orientation and ultimate fiber strength.

The strength of semi-crystalline polymers and their corresponding morphology are closely related. It has long been known, that molecular orientation, can be altered upon shearing of the molten polymer prior to quenching. This changes the morphology in terms of degree of crystallization, orientation of crystals and in some case even the type of crystal structure [4].

A vast body of work, connecting strength of polymers and shear-induced crystallization, exists. Despite the fact that extensional deformation is of just as great interest, the extent of research in the field is very limited. Results from one of the few exceptions are shown in Figure 2. Here it is seen that the morphology changes with the Hencky strain rate ($\dot{\epsilon}$).

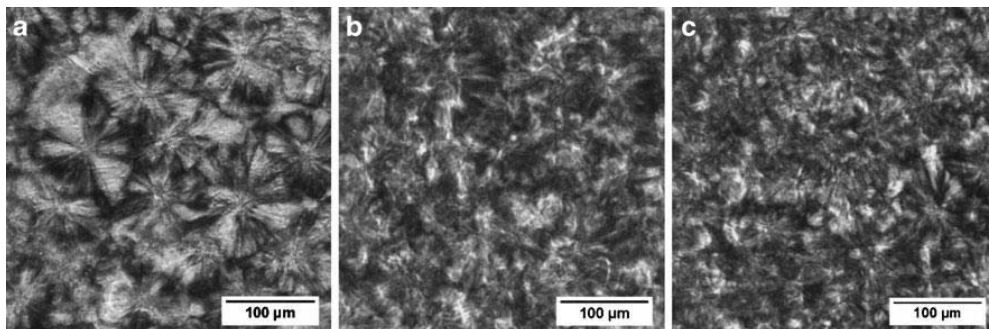


Figure 1: Polarized micrographs of final morphology in isotactic poly propylene (iPP) showing the size of spherulites in samples crystallized at $T_c = 146\text{ }^\circ\text{C}$, and (a) at quiescent conditions, (b) $\dot{\epsilon} = 0.10\text{ s}^{-1}$ and (c) $\dot{\epsilon} = 0.25\text{ s}^{-1}$ [3].

The absence of literature is due to the great challenge in obtaining a constant Hencky strain rate ($\dot{\epsilon}$) during the entire course of deformation [5]. In order to obtain a constant $\dot{\epsilon}$, the diameter (D) needs to decay logarithmically in time:

$$\dot{\epsilon} = -2 \ln \left(\frac{D(t)}{D_0} \right) \quad (1)$$

Recent advances in extensional rheometry have made it possible to maintain a controlled mid-filament diameter [6] using a filament stretching rheometer (FSR) (see Figure 1).

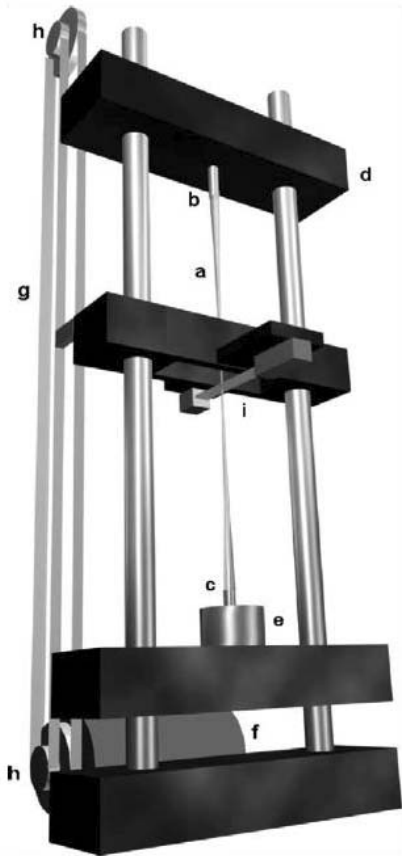


Figure 1: Sketch of the filament stretching rheometer at DPC. (a) filament, (b) top plate, (c) bottom plate, (d) movable support for top plate, (e) weighing cell (f) motor, (g) timing belts, (h) gearing and (i) laser. [7]

The FSR is capable of producing well-defined extensional kinematics and temperature up to 300 Centigrade. As depicted in Figure 2, the DTU-FSR

consists of two parallel plates that can be separated in a controlled fashion. The polymer sample to be investigated is placed between the plates and allowed to reach the equilibrium temperature of the intended measurement. Once the sample has reached equilibrium, the plates are separated whereby a polymer filament is formed between the plates. The constant extensional rate is achieved by combination of a laser micrometer that monitors the filament diameter and a control loop that controls the plate separation as function of time. The up-graded DTU-FSR has the ability to quench polymer filaments by simply opening the oven in a fast manner.

Specific Objectives

The first part of the project will be devoted to the fabrication of a number of quenched polymer filaments that have been subjected to known stretch ratios at controlled stretch rates. Initially this will most likely be made with a polymer material for which experience with melt rheology is already available. These could be either polystyrene, polyethylene, polypropylene or poly(methyl methacrylate).

The second part of the project will concern the design and fabrication of sample holders to enable the measurement of Young's modulus and Poisson's ratio for quenched polymer filaments.

After the quenching technique and the solids characterization holders have been developed for a model polymer more systematic mapping of polymers subjected to large elongational deformations prior to quenching will take place. Combining characterization using the FSR to evaluate strength, with instrumentation able to reveal molecular orientation and crystal structure (e.g. electron microscopy, X-ray diffraction, and small angle neutron scattering), a systematic quantitative characterization of polymers in extension is possible.

References:

1. F. X. Kromm, T. Lorriot, B. Coutand, R. Harry, J. M. Quenisset, *Polymer Testing* 22 (4) (2003) 463–470.
2. B. Zhang, J. Chen, X. Zhang, C. Shen, *Polymer* 52(9) (2011) 2075–2084.
3. B. E. White, H.H. Winter, J. P. Rothstein, *Rheologica Acta*, 51(4) (2011), 303–314.
4. J.A. Kornfield, G. Kumaraswamy, A.M. Issaian, *Industrial and Engineering Chemistry Research* 41 (2002) 6383–6392.
5. R. Séguéla, *Macromolecular Materials and Engineering* 292 (3) (2007) 235–244.
6. J. M. Román Marín, J. K. b. Huusom, N. J. Alvarez, Q. Huang, H. K. Rasmussen, A. Bach, A. L. Skov, O. Hassager, *Journal of Non-Newtonian Fluid Mechanics* 194 (2013) 14–22.
7. A. Bach, H. Koblitz, P. Longin, and O. Hassager, *Journal of Non-Newtonian Fluid Mechanics* 108 (2002) 163–186.



Zakaria, Shamsul

Phone: +45 4525 6817
E-mail: shaza@kt.dtu.dk
Discipline: Chemical Engineering

Supervisors: Anne Ladegaard Skov

PhD Study

Started: January 2013

To be completed: January 2016

The electrical breakdown strength of prestretched elastomers with and without sample volume conservation

Abstract

In this study, two experimental configurations were used to determine the stretch dependence of the breakdown strength of polydimethylsiloxane (PDMS) elastomers. The breakdown strength was determined for samples with and without volume conservation. The breakdown strength is found to depend strongly on both the stretch ratio and on how the experiment was performed. The breakdown strength of samples with volume conservation was found to be significantly smaller than that of samples with a reduction of the volume.

Introduction

The effects of prestretch on the electrical breakdown strength of DEAPs have been studied previously [1][2]. For instance, one of the most commonly studied dielectric elastomers, the electrical breakdown strength of the acrylic elastomer VHB produced by 3M Corporation has been reported to increase from 18 to 218 V/ μm when prestretched 6 times biaxially[1]. However, the mechanisms by which prestretching improves the electrical breakdown strength of DEAP are still not fully understood.

The variation in thickness in response to prestretching poses a challenge on how to measure the electrical breakdown strength accurately. Tröls and coworkers [2] investigated the effect of different configurations of electrodes on the breakdown strength of acrylic VHB elastomers supplied by 3M prestretched up to 5 times. Stretched elastomer films were sandwiched between compliant carbon grease electrodes or rigidly clamped between two stamp electrodes for breakdown measurements. The breakdown strength was increased from 100 to 163 V/ μm for rigid electrodes, and from 25 to 143 V/ μm for compliant electrodes at 5 times biaxial prestretching. It was also found that the breakdown strength depends on the surface area of the electrodes. The normalized thickness (h/H) was reduced from 1.0 to 0.028 upon 5 times prestretching and thus the sample volumes were not conserved during the measurements. For this reason, in the present study the effect of volume conservation on the breakdown strength was investigated as a function of prestretch for four types of PDMS specimens. The sample volumes were conserved

by enlarging the surface area of the applied electrodes according to the prestretch. Subsequently, the results of the breakdown voltage measurements were compared to those obtained on samples without volume conservation. Thereby, reliable and consistent data are produced which then can be used for further interpretation of the favorable effects of prestretch.

Methodology

Four different types of silicone elastomers with different loadings of silica (within the commercial silicone elastomer) and permittivity enhancing fillers (titanium dioxide) have been studied; i.e., XLR630, filled XLR630, RT625 and filled XLR630. The elastomers are commercially available elastomers of type liquid silicone rubber (LSR) or room-temperature vulcanizing (RTV). The thin films were prepared and were characterized for the breakdown strength and the Young's modulus.

Results and discussions

Two experimental techniques for measuring breakdown strength as a function of prestretch were applied and are illustrated in figure 1.

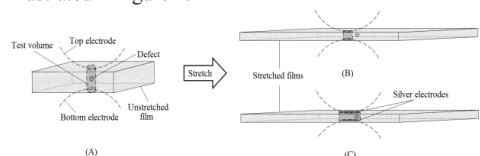


Figure 1: Breakdown measurements were performed on films before stretching (A) and after stretching: (B)

without volume conservation and (C) with volume conservation.

In figure 2 the breakdown strengths as a function of the stretch ratio for different experimental configurations on several types of PDMS can be seen. The breakdown strengths for the 4 different unstretched elastomers are of the order of 79-103 V/ μm (volume conservation technique, configuration (C) in figure 6) and 100-120 V/ μm without. For stretched samples (at $\lambda=2$) the breakdown strength varies between 227-296 V/ μm and 247-320 V/ μm . The discrepancies between the two methods in the unstretched state ($\lambda=1$) are due to different sample volumes as well as the variation in electrodes. The samples with volume conservation are measured with 5 mm radius electrodes in the unstretched state whereas the samples without volume conservation are just contacted by the electrodes and thus the sample volumes are significantly smaller. The strong influence of sample volume on breakdown strength is furthermore confirmed by the consistent deviation between identical samples at identical prestretches measured by the two methods. There is an apparent improvement of breakdown strength of approximately 10 V/ μm when the sample volume is not conserved upon prestretching.

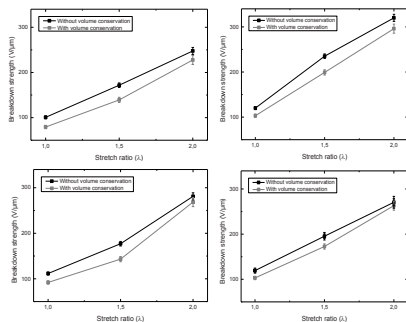


Figure 2: Breakdown strength as a function of the stretch ratio for several PDMS films.

In order to evaluate the effect of Young's modulus on breakdown strengths, quasi-static uniaxial tensile tests were performed on the samples. Figure 3 shows the breakdown strengths as function of Young's moduli derived from the stress-strain curves of several PDMS films at different stretch ratios. The results indicate that the resistance of the elastomers to electrical breakdown is certainly enhanced with the increase of Young's modulus for pure XLR630 and filled XLR630 films. On the other hand, the Young's modulus for RT625 (room temperature vulcanization PDMS) are inversely proportional to the increasing of breakdown strength upon prestretching which demonstrate the incoherent relation between the breakdown strength and the Young's modulus. Therefore, upon comparison with previous studies as well, the improved breakdown strengths are not solely due to the increased Young's

moduli since the increase of breakdown strengths with Young's modulus is significantly larger than previously reported for silicones as well as for the more commonly investigated acrylic VHB[3].

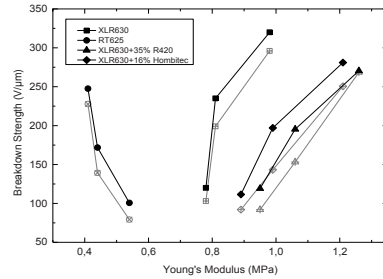


Figure 3: Breakdown strength as function of Young's modulus for different PDMS materials. The black curves indicate the samples without volume conservation and grey curves indicate the samples with volume conservation.

Conclusion

A method for measuring the breakdown strength of prestretched films with constant sample volume was presented. The method was compared to a traditional experiment where the sample volume was significantly reduced upon prestretching. The breakdown strengths of the prestretched elastomers were shown to be over-estimated if the reduction of volume upon prestretching was not taken into consideration. It was furthermore shown that the breakdown strengths were proportional to the Young's moduli of the samples but that the Young's moduli played a coupled role with the alignment of polymer chains as well as defects.

Acknowledgement

The authors gratefully acknowledge the financial support from the Ministry of Education of Malaysia and Universiti Malaysia Pahang. Danfoss PolyPower A/S is also acknowledged for financial support to Z. Shamsul.

References

1. G. Kofod, P. Sommer-Larsen, R. Kornbluh, and R. Pelrine, "Actuation Response of Polyacrylate Dielectric Elastomers," in *Journal of Intelligent Materials Systems and Structures* **14**, pp. 787–793 (2003)
2. A. Tröls, A. Kogler, R. Baumgartner, R. Kaltseis, C. Keplinger, R. Schwödauer, I. Graz, and S. Bauer, "Stretch dependence of the electrical breakdown strength and dielectric constant of dielectric elastomers," *Smart Materials and Structures* **22**(10), 104012 (2013).
3. L. Yu, S. Vudayagiri, S. Zakaria, M. Y. Benslimane, and A. L. Skov, "Filled liquid silicone rubbers: possibilities and challenges," Y. Bar-Cohen, Ed., 90560S (2014)



Guofeng Zhou

Phone: +45 4525 2853
E-mail: guzho@xx.dtu.dk

Supervisors: Anker Degn Jensen
Peter Arendt Jensen
Niels Ole Knudsen, DONG Energy

PhD Study
Started: October 2012
To be completed: September 2015

Fast Pyrolysis of Lignin and Direct Upgrading of the Pyrolysis Vapor via H-ZSM-5

Abstract

Lignin fast pyrolysis and direct upgrading of pyrolysis vapor via H-ZSM-5 is studied using a Pyrolysis Centrifuge Reactor. Lignin fast pyrolysis is feasible and it produces about 45 wt%_{daf} bio-oil yield (26wt%_{daf} organic yield). Direct upgrading of lignin derived pyrolysis vapor can be done to yield a reduced amount of organics (<10wt%_{daf}), which has a narrow distribution of aromatics, such as benzene and toluene. The upgrading step is favored at high temperature, such as 600°C. At low catalyst temperature, it is found that zeolite effectively traps the pyrolysis vapor.

Introduction

Lignin is the second most abundant biomass component found in the nature [1]. The estimated lignin production is 50 million tons/year from pulp and paper industry [2]. This number will increase with the development of new biomass utilizations, such as second generation bio-ethanol production. Hence the potential of lignin as a renewable source for chemicals and fuels should not be overlooked. By fast pyrolysis, lignin can be converted into a liquid fuel, known as pyrolysis oil or bio-oil [3]. Due to its high oxygen content, a subsequent upgrading step is essential for using pyrolysis oil as an engine fuel. In this study, lignin, obtained as a by-product from a second generation bio-ethanol plant, is pyrolyzed in a Pyrolysis Centrifuge Reactor. The pyrolysis vapor is directly upgraded catalytically using a zeolite (HZSM-5) before product condensation.

Materials and Methods

The lignin particles are fed tangentially to the horizontally oriented reactor cylinder where the centrally mounted arch-shaped rotor pushes the particles against the reactor wall. The reactor is kept at 500°C. While circulating on the wall, the particles simultaneously move axially towards the tangential reactor outlet. External to the reactor, the flow of gas and particles are first directed to a simple change-in flow-direction separator (460°C), a cyclone (440°C) and then a hot gas filter (300°C) to remove solid chars. The char free gas then passes through a catalytic reactor. The liquid product is condensed in a series of condensers placed in a cooling bath and a dry ice/ethanol bath. A

carrier gas, 4 Nl/min N₂ preheated to 450 °C is introduced to the reactor, which provides a gas residence time inside the reactor of 1.8 seconds. A typical run lasts 25 minutes. For each experiment, 30 g H-ZSM-5 (SiO₂/Al₂O₃=25) is used and about 30 g of biomass is fed.

Results and Discussion

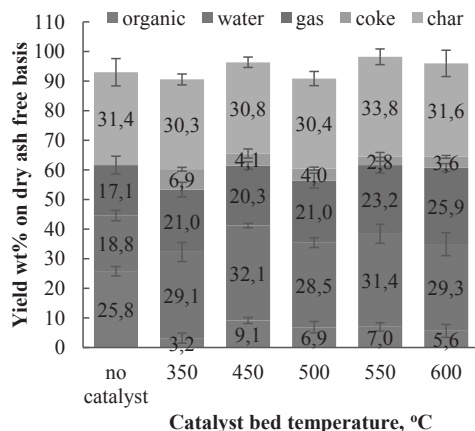


Figure 1: Overall yields from fast pyrolysis of lignin and direct upgrading of pyrolysis vapor at temperatures from 350°C to 600°C

As shown in figure 1, fast pyrolysis of lignin produces about 26 wt%_{daf} (weight percent on dry ash free lignin basis) organic, 30 wt%_{daf} char, 18 wt%_{daf} reaction water and 17 wt%_{daf} gas. In the presence of the zeolite, the organic yield decreases significantly to less than 10 wt%_{daf}. The organic yield reaches a peak at 450°C catalyst temperature and then decreases again at higher catalyst temperature. Surprisingly, lower catalyst temperature than 450 °C does not give more organics, but high coke deposit is observed. The coke yield decreases with increasing catalyst temperature. Reaction water yield increases at the presence of H-ZSM-5 and it does not follow a clear trend when the catalyst temperature increases from 350 °C to 600 °C. Gas yield increases with increasing catalyst temperature.

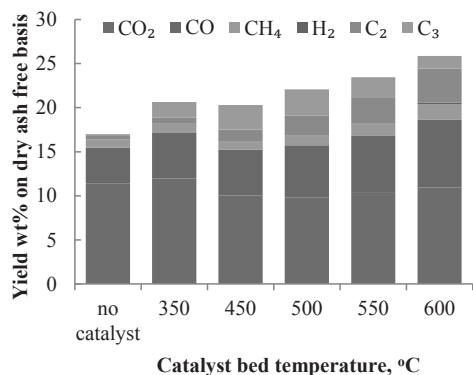


Figure 2: Gas components from fast pyrolysis of lignin and direct upgrading of pyrolysis vapor at temperatures from 350°C to 600°C

As shown in figure 2, among the produced gases, CO and CO₂ are the major components. In the presence of the catalyst, the CO yield increases more than CO₂ with increasing catalyst temperature. The CO yield increases from 4.1 wt% without catalytic upgrading of pyrolysis vapor to 7.7 wt% at 600°C catalyst temperature. The yields of methane, hydrogen and C₂ increase as well from 350°C to 600°C catalyst temperature. Hydrogen production accounts for a negligible amount on weight basis. The increasing yield of methane could be from demethylation reactions. The C₃ yield reaches a peak at 500°C catalyst temperature and decreases again. The selectivity of C₂-C₃ is towards ethene with increasing catalyst temperature. The total olefin yield (including ethene and propene) is 4.3 wt%_{daf} at 600°C catalyst temperature.

The target products of zeolite upgrading are aromatics. As shown in figure 3, the aromatic production increases with increasing catalyst temperature. The highest aromatic yield is about 3.7 wt% at 600°C catalyst temperature. This indicates that aromatics formation is favored at high reaction temperature. At high catalyst temperature, the yield of aromatics with two methyl substituents decreases and the aromatics selectivity is towards benzene and

toluene. This is also consistent with increasing yield of methane at high catalyst temperature.

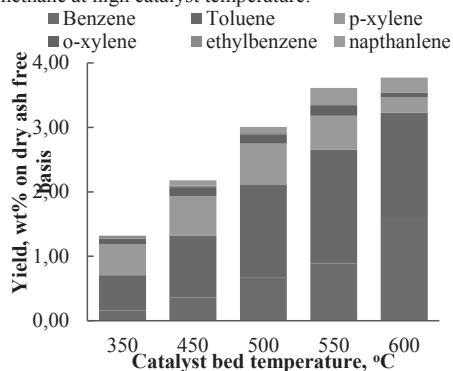


Figure 3: Aromatic yields from direct upgrading of pyrolysis vapor at temperatures from 350°C to 600°C

Surprisingly, after the experiments, the catalyst weight increases significantly when the catalyst temperature is low, such as 350°C. The spent catalysts are investigated by thermogravimetric analysis under nitrogen flow. When the spent catalyst is heated up to > 400°C, a weight loss is observed for all the catalysts. The catalyst spent at 350°C, shows the most significant weight loss (about 5 wt%). It indicates that the zeolite efficiently traps the pyrolysis vapor at low catalyst temperature. The trapped pyrolysis vapor does not form a graphite coke. Instead it is still reactive at elevated temperature such as >400°C.

Conclusion

It is feasible to convert lignin into a bio-oil and achieve 45 wt% bio-oil yield (26 wt% organic yield) using fast pyrolysis. In the presence of H-ZSM-5 as catalyst for pyrolysis vapor conversion, the production of aromatics, such as benzene and toluene, is increased. The aromatic formation favored at high catalyst temperature. The highest yield of olefins and aromatics is 4.3 wt% and 3.7 wt% respectively at 600°C catalyst temperature. At low catalyst temperature, such as 350°C, H-ZSM-5 effectively traps the pyrolysis vapor. However, the trapped reactant is still reactive at temperature >400°C. H-ZSM-5 rejects oxygen from lignin derived pyrolysis vapor mainly through the formation of H₂O and CO, which is less efficient than decarboxylation forming CO₂.

References

1. D.J. Nowakowski, A.V. Bridgwater, D.C. Elliott, D. Meier, P. de Wild, Journal of analytical and applied pyrolysis 88 (2010) 53-72.
2. R. J. A. Gosselink, E. De Jong, B. Guran, A. Abächerli, Industrial Crops and Products 20 (2) (2004) 121-129.
3. T.N. Trinh, P.A. Jensen, K. Dam-Johansen, N.O. Knudsen, H.R. Sørensen, S. Hvilsted, Energy & Fuel 27 (2013) 1399-1409.



Andreas Åberg

Phone: +45 4525 2912
E-mail: aben@kt.dtu.dk

Supervisors: Jens Abildskov
Jakob Kjøbsted Huusom
Anders Widd, Haldor Topsøe A/S

PhD Study
Started: August 2013
To be completed: July 2016

Modeling the Automotive SCR system

Abstract

Diesel engine exhaust gases contain amongst other things nitrous gases such as NO and NO₂. Reducing the amount of these gases is of great importance due to new legislation, and because of the effect they have on urban air quality. A promising and widely used technology for this is based on selective catalytic reduction (SCR) of the gases, with ammonia as a reducing agent. A model for the SCR catalyst was derived based on first principles. The kinetic model was calibrated with bench-scale equipment and validated using full-scale equipment. The project is in collaboration with Haldor Topsøe A/S.

Introduction

Heavy duty diesel (HDD) vehicles handle a substantial part of the world's transport and logistics. Harmful pollutants are however formed, such as nitrogen oxides (NO_x), hydrocarbons (HC), particulate matter (PM), and carbon monoxide (CO) [1]. The diesel exhaust after treatment (DEA) system has been developed to treat the pollutants in the exhaust gas. Figure 1 illustrates the current standard DEA system consisting of a series of catalytic units. The Diesel Oxidation Catalyst (DOC) oxidizes CO and HC to CO₂ and H₂O, as well as generates NO₂ from NO. The Diesel Particulate Filter (DPF) is a wall-flow filter, entraining PM in its monolith walls. The DPF can be regenerated actively by increasing the exhaust gas temperature using post-injection of fuel, or passively using a catalyst. NO₂ generated by the DOC also assists regeneration. NO_x is treated through Selective Catalytic Reduction (SCR) using ammonia (NH₃) as the reducing agent. NH₃ is supplied to the system through urea dosing, regulated by the onboard control unit. Excess NH₃ is controlled with the Ammonia Slip Catalyst (ASC). Upon exiting the DEA system, the emissions should meet the restrictions imposed by the Euro VI regulations [2].

The DEA system is very complex, requiring efficient exhaust treatment for a wide range of operating conditions, corresponding to cold start, stop-and-start driving (inner city), and high speed driving (highways). As a result, DTU Chemical Engineering and Haldor Topsøe A/S are collaborating on the development of the next generation DEA system, with funding from Innovation Fund Denmark. The underlying PhD

projects concern the development of new DOC and ASC formulations (Thomas Klint Hansen, pg. 87-88), the combination of the DPF and SCR components (Kasper Linde, pg. 117-118), and the development of the control unit for efficient regulation of urea dosing in this project.

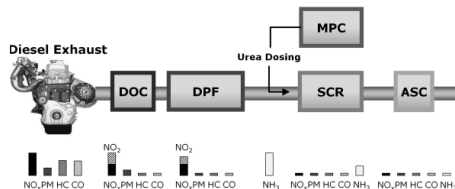


Figure 1: Example of a standard design of the DEA system, consisting of the DOC, DPF, SCR component, urea dosing control unit, and the ASC.

Specific Objectives

The overall objective of this project is to develop models and model based control structures to control the urea injection to the catalyst demanded by enhanced legislation. Since a new catalyst design most likely will be developed by the other PhD-students in the overall project, it is important that the results in this project are generic and can be used for a new system as well. Therefore, the project will focus on developing a methodology on a currently used catalyst, to be able to tackle similar problems. Developing the methodology will involve several steps:

- Develop high fidelity simulation model based on first principles, parameter estimation and validation of the model
- Develop lower accuracy models, parameter estimation and validation of the models
- Quantify information loss in different models to understand the needed model complexity
- Develop and investigate several model based control schemes
- Validate the chosen control structure with full-scale engine tests using standardized test driving cycles.

Results and Discussion

The physical phenomena inside the catalyst resulted in the model described by Eqs. (1) through (4). The equations describe the concentration of the relevant species and temperature in the bulk phase and the washcoat phase of the catalyst. It is assumed that no diffusion occur in the washcoat, thus it is only treated as a surface where the reactions take place. The kinetic expressions are based on findings in literature [3]. The kinetic parameters were calibrated using isothermal steady state data produced with small-scale monolith supplied with simulated exhaust gases. The objective function for the calibration results for the NH₃ can be seen in Fig. 2, with the model fit represented as crosses and the data as circles. The residuals are small, and the fit was considered satisfactory.

$$\frac{\partial c_{b,i}}{\partial t} = -u \frac{\partial c_{b,i}}{\partial z} - \frac{4k_g}{b} (c_{b,i} - c_{wc,i}) \quad (1)$$

$$\frac{\partial c_{wc,i}}{\partial t} = \frac{4k_g}{b} (c_{b,i} - c_{wc,i}) + \sum_i r_i \quad (2)$$

$$\frac{\partial T_b}{\partial t} = -u \frac{\partial T_b}{\partial z} - \frac{4h_{heat}}{b\rho_b c_{p,b}} (T_b - T_{wc}) \quad (3)$$

$$\frac{\partial T_{wc}}{\partial t} = \frac{4h_{heat}}{b\rho_b c_{p,b}} (T_b - T_{wc}) + \sum_i \Delta H_{r,i} r_i \quad (4)$$

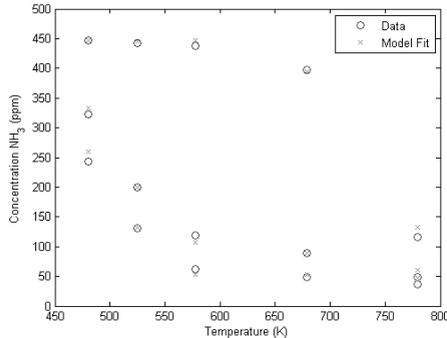


Figure 2: Calibration results for NH₃. The circles represent the data and the crosses the model fit.

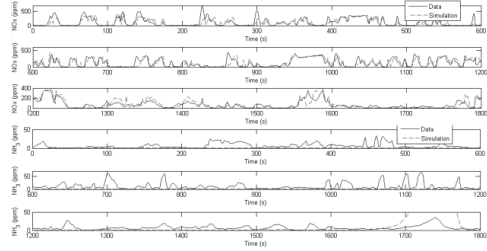


Figure 3: Validation results for the full-scale data. Three top figures are NOx results and three bottom pictures are NH₃ results. The dotted line is the model prediction and the full line is the data.

Figure 3 shows a simulation of a full-scale monolith with real truck engine exhaust gases as input to the catalyst. The full line shows the output measurement taken after the gases have passed through the catalyst, and the dotted line shows the model prediction. The NOx prediction is in good agreement with the data, especially in time but also in absolute value. The NH₃ simulation does not agree with data. The model predicts no NH₃-slip, except for a big peak at the end of the test. Using isothermal data has likely not contained enough information to calibrate the kinetic reactions properly.

Conclusions and Future Work

The developed first principles model was combined together with a kinetic model and calibrated with steady-state small-scale monolith data at isothermal conditions. The model was validated using full-scale monolith data with exhaust gases produced by a real diesel truck engine. The results showed that the model is capable of accurately predict the NOx output from the catalyst, but not the NH₃-slip. Future work will include improving the models predictive capabilities regarding NH₃. Possibly this will require using non-isothermal data. Control structures will be developed that will be used together with the model.

Acknowledgement

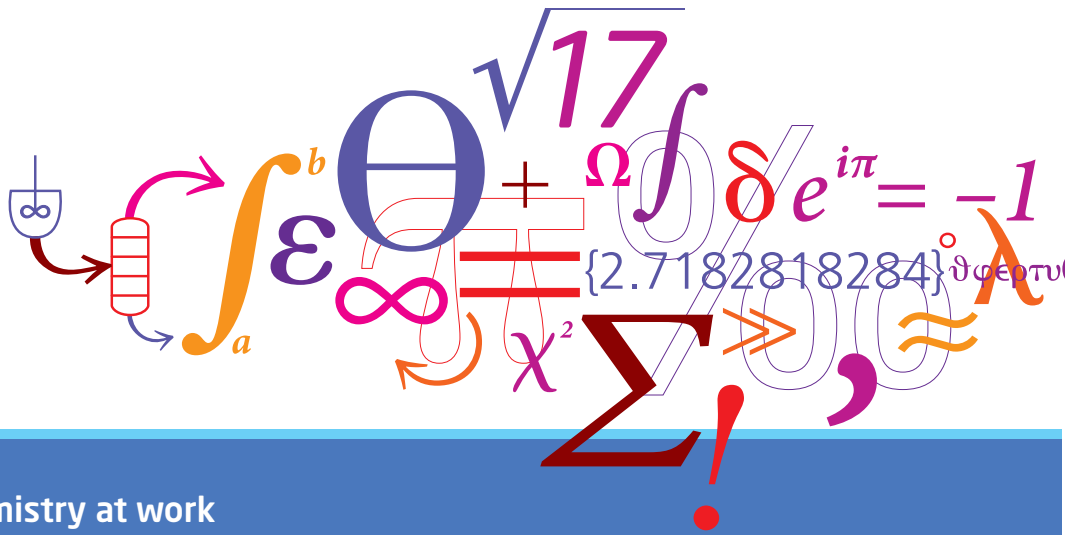
This project is a collaboration between the CAPEC research center of DTU Chemical Engineering, Haldor Topsøe A/S and Innovation Fund Denmark.

References

1. A. Fritz, V. Pitchon. The current state of research on automotive lean NOx catalysts, Appl. Catal. B 13 (1997).
2. W. A. Majewski, M. K. Khair, Diesel Emissions and Their Control, SAE International (2006)
3. L. Olsson, H. Sjövall, R. J. Blint, A kinetic model for ammonia selective catalytic reduction over Cu-ZSM-5. Appl. Catal. B 81 (2008)



Group photo: Klaus Holsting



Chemistry at work

Bio Engineering

Catalysis

Combustion and Environmental Engineering

Ecosystem Modelling and Sustainability

Engineering Thermodynamics

Enzyme Technology

Petroleum Engineering

Polymer Technology

Process Technology and Unit Operations

Product Design

Reaction and Transport Engineering

Systems Engineering

Department of Chemical
and Biochemical Engineering

DTU Building 229
Søltofts Plads
DK-2800 Kgs. Lyngby
www.kt.dtu.dk